

Four new species of the genus *Yunguirius* (Araneae, Agelenidae) from China

Mian Wei^{1,2}, Jie Liu^{1,2,3}, Kai Wang^{1,2}

¹ Hubeiate Key Laboratory of Regional Development and Environmental Response, Faculty of Re-sources and Environmental Science, Hubei University, Wuhan 430062, China

² The State Key Laboratory of Biocatalysis and Enzyme Engineering of China, School of Life Sciences, Hubei University, Wuhan 430062, Hubei, China

³ School of Nuclear Technology and Chemistry and Biology, Hubei University of Science and Technology, Xianning 437100, Hubei, China

Corresponding author: Kai Wang (Kai_wang@hubu.edu.cn)

Abstract

Four new species of *Yunguirius* B. Li, Zhao & S.Q. Li, 2023 are described from China, namely: *Yunguirius parvus* Wei & Liu, **sp. nov.** (♀), *Yunguirius trigonus* Wei & Liu, **sp. nov.** (♀), *Yunguirius wangqiqiae* Wei & Liu, **sp. nov.** (♀), and *Yunguirius xiannushanensis* Wei & Liu, **sp. nov.** (♀).

Key words: Biodiversity, coelotine spiders, description, morphology, taxonomy

Introduction

Coelotinae F.O. Pickard-Cambridge, 1893, the most diverse subfamily of Agelenidae C.L. Koch, 1837, is endemic to the Northern Hemisphere. To date, 806 species across 40 genera have been described (WSC 2024). In recent years, there has been frequent reporting of new taxa as well as taxonomic revisions of previously described species, particularly those in the genera *Coelotes* Blackwall, 1841 and *Draconarius* Ovtchinnikov, 1999 (Chen et al. 2016; Chen 2017; Li et al. 2018a, 2018b, 2019, 2023; Okumura 2020; Okumura et al. 2021; Okumura and Zhao 2022; Hoang et al. 2023; Luo et al. 2023). The genus *Yunguirius*, was recently described by Li et al. (2023) based on *Draconarius ornatus* (Wang, Yin, Peng & Xie, 1990) and includes two newly described species along with two others transferred from *Draconarius*: *Y. duoge* B. Li, Zhao & S.Q. Li, 2023, *Y. subterebratus* (Zhang, Zhu & Wang, 2017), *Y. terebratus* (Peng & Wang, 1997) and *Y. xiangding* B. Li, Zhao & S.Q. Li, 2023. According to previous studies, all five described *Yunguirius* species predominantly occur along the northern edge of the Yunnan-Guizhou Plateau.

While examining our specimens, four undescribed species of *Yunguirius* collected from the northern edge of the Yunnan-Guizhou Plateau were discovered. We report these new species in the current paper, the descriptions, detailed colour illustrations, and distributional maps of new species are provided.



Academic editor: Dragomir Dimitrov

Received: 29 April 2024

Accepted: 13 July 2024

Published: 2 September 2024

ZooBank: <https://zoobank.org/16DBAD49-A3D7-40F4-A1A1-FB221AB008BD>

Citation: Wei M, Liu J, Wang K (2024) Four new species of the genus *Yunguirius* (Araneae, Agelenidae) from China. ZooKeys 1211: 1–15. <https://doi.org/10.3897/zookeys.1211.126487>

Copyright: © Mian Wei et al.
This is an open access article distributed under terms of the Creative Commons Attribution License (Attribution 4.0 International – CC BY 4.0).

Materials and methods

All specimens were preserved in 75% ethanol and examined with an Olympus SZX7 stereomicroscope. Male palps and female genitalia were dissected from the spider bodies to be examined and photographed. Epigynes were cleared with Proteinase K to study their inner structures. Photographs were taken with a Canon EOS 90D wide zoom digital camera (8.5 megapixels) mounted on an Olympus BX 43 compound microscope. The images were montaged using Helicon Focus 7.0.2 image stacking software. Left palps are illustrated. Leg measurements are given as total length (coxa, trochanter, femur, patella, tibia, metatarsus, tarsus). Only the structures on the left (e.g., pedipalpus, legs) were measured. All specimens have been deposited at the Centre for Behavioural Ecology and Evolution, College of Life Sciences, Hubei University, Wuhan, China (CBEE).

Abbreviations used. Morphological characters:

ALE	anterior lateral eye;
AME	anterior median eye;
AME–ALE	distance between AME and ALE;
AME–AME	distance between AME and AME;
ALE–PLE	distance between ALE and PLE;
AME–PME	distance between AME and PME;
PLE	posterior lateral eye;
PME	posterior median eye;
PME–PLE	distance between PME and PLE;
PME–PME	distance between PME and PME;

Taxonomy

Family Agelenidae C.L. Koch, 1837

Subfamily Coelotinae F.O. Pickard-Cambridge, 1893

Genus *Yunguirius* B. Li, Zhao & S.Q. Li, 2023

***Yunguirius parvus* Wei & Liu, sp. nov.**

<https://zoobank.org/E2FDC5CF-C53D-47F2-9DA3-83F9C6AD20A1>

Figs 2, 3, 10

Type material. *Holotype* ♀ (HBU-WM-24-001), 1 ♀ *paratype* (HBU-WM-24-002): CHINA: Yunnan Province, Honghe Hani and Yi Autonomous, Gejiu County, Gejia Forest Park, 23.3893°N, 103.1254°E, elevation: 2045 m, 23.VIII.2020, M. Wei leg.

Etymology. The specific epithet is taken from the Latin word *parvus*, meaning “small”, referring to the relatively small body type of new species; an adjective.

Diagnosis. The females of *Yunguirius parvus* sp. nov. resemble those of *Y. duoge* in 1) the atrium is subrounded with a complete anterior margin (Fig. 2A; fig. 2A in Li et al. 2023); 2) the openings of the copulatory ducts are wide, approximately half the circumference of the atrium (Fig. 2B; fig. 2B in Li et al. 2023); 3) the blind sacs of the copulatory ducts are extremely short, symmetrical, and separate (Fig. 2B; fig. 2B in Li et al. 2023). In other *Yunguirius* species, the atrium is non-subrounded (except in *Y. terebratus*) with an incomplete

anterior margin (Figs 1A, 4A, 6A, 8A; fig. 245A in Zhu et al. 2017; figs 3A, 4A in Li et al. 2023), the copulatory openings are equal to or less than the length of the lateral margin of the atrium, and the blind sacs are asymmetrical and overlapping (Figs 1B, 4B, 6B, 8B; fig. 245B in Zhu et al. 2017; figs 3B, 4B in Li et al. 2023). However, *Y. parvus* sp. nov. can be differentiated from *Y. duoge* by 1) the absence of the fold (Fig. 2A), versus being present in the latter (Fig. 2A in Li et al. 2023); 2) the blind sac is shorter than the spermathecal stalk (Fig. 2B), versus being longer in the latter (Fig. 2B in Li et al. 2023); 3) the spermathecal stalk has a conch-shaped distal tip (Fig. 2B), versus being nearly round in the latter (Fig. 2B in Li et al. 2023).

Description. Female (holotype) (Fig. 3). Carapace reddish brown. Cervical and radial groove distinct. Cephalic region moderately raised and wide, lateral margin with distinct furrows. Chelicerae with 3 promarginal teeth and 2 retro-marginal teeth, condyle red. Sternum longer than wide. Abdomen pale yellow, with 5 chevron-shaped patterns, covered by hairs. Legs red. Total length 10.41. Carapace 5.85 long, 3.54 wide, cephalic region 3.12 wide. Abdomen 4.69 long, 3.10 wide. Eye size and interdistance: AME 0.19, ALE 0.23, PME 0.22, PLE 0.25; AME–AME 0.09, AME–ALE 0.14, AME–PME 0.09, ALE–PLE 0.05, PME–PME 0.06, PME–PLE 0.32. Leg measurements: Leg I 14.02 (1.80, 0.70, 3.53, 1.63, 2.78, 2.46, 1.39), leg II 12.40 (1.52, 0.69, 3.04, 1.48, 2.44, 2.23, 1.33), leg III 10.35 (1.38, 0.67, 2.43, 1.32, 1.68, 1.95, 1.08), leg IV 14.42 (1.66, 0.61, 3.50, 1.59, 2.91, 2.84, 1.41). Epigyne (Fig. 2). Epigynal teeth absent. Atrium centrally situated, subrounded, anterior margin complete. Epigynal sclerite small. Hoods weak, vertically oriented, situated laterally. Fold absent. Copulatory ducts openings broad, subequal to $\frac{1}{2}$ the circumference of atrium, laterally originated, blind

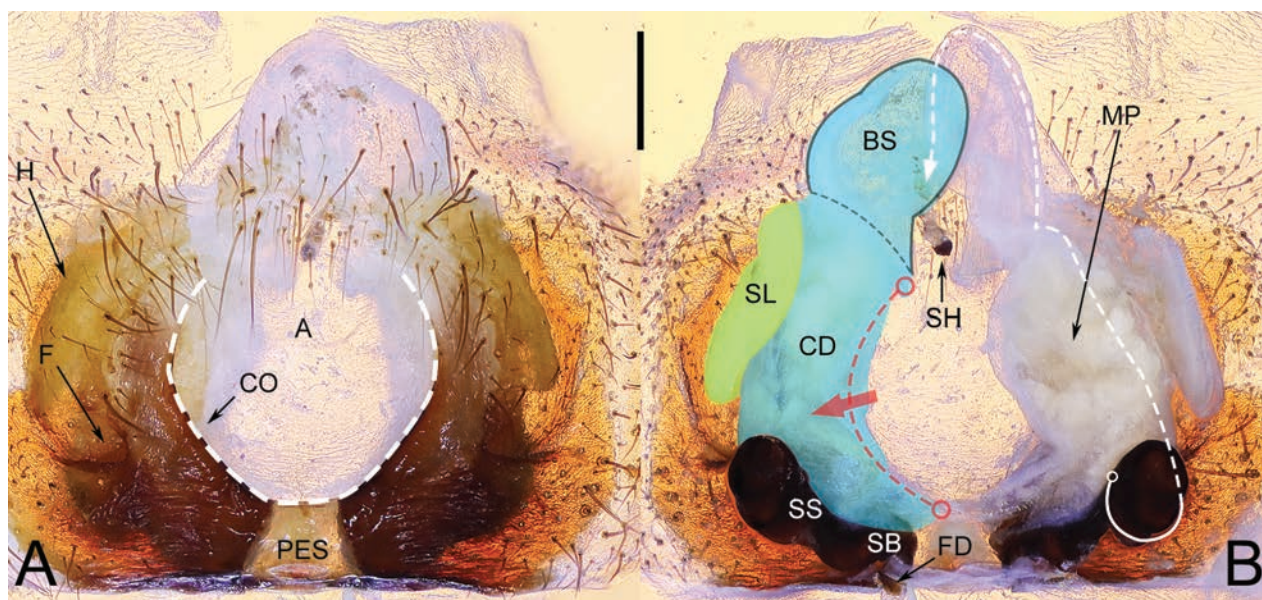


Figure 1. Epigyne and vulva of *Yunguirius terebratus* **A** epigyne, ventral view **B** vulva, dorsal view. Abbreviations: A = atrium; BS = blind sac; CD = copulatory duct; CO = copulatory opening; F = fold; FD = fertilization duct; H = hood; MP = mating plug; PES = posterior epigynal sclerite; SB = spermathecal base; SH = spermathecal head; SL = the secondary layer of copulatory duct; SS = spermathecal stalk. The white dashed line in A represents the margin of atrium and in B represents the spermathecal head. The black outline B shows the blind sac of the copulatory duct. The red dashed line and arrow in B indicate the opening of copulatory duct. The blue area indicates the copulatory duct, and the yellow area indicates the secondary layer of the copulatory duct. Scale bar: 0.50 mm.

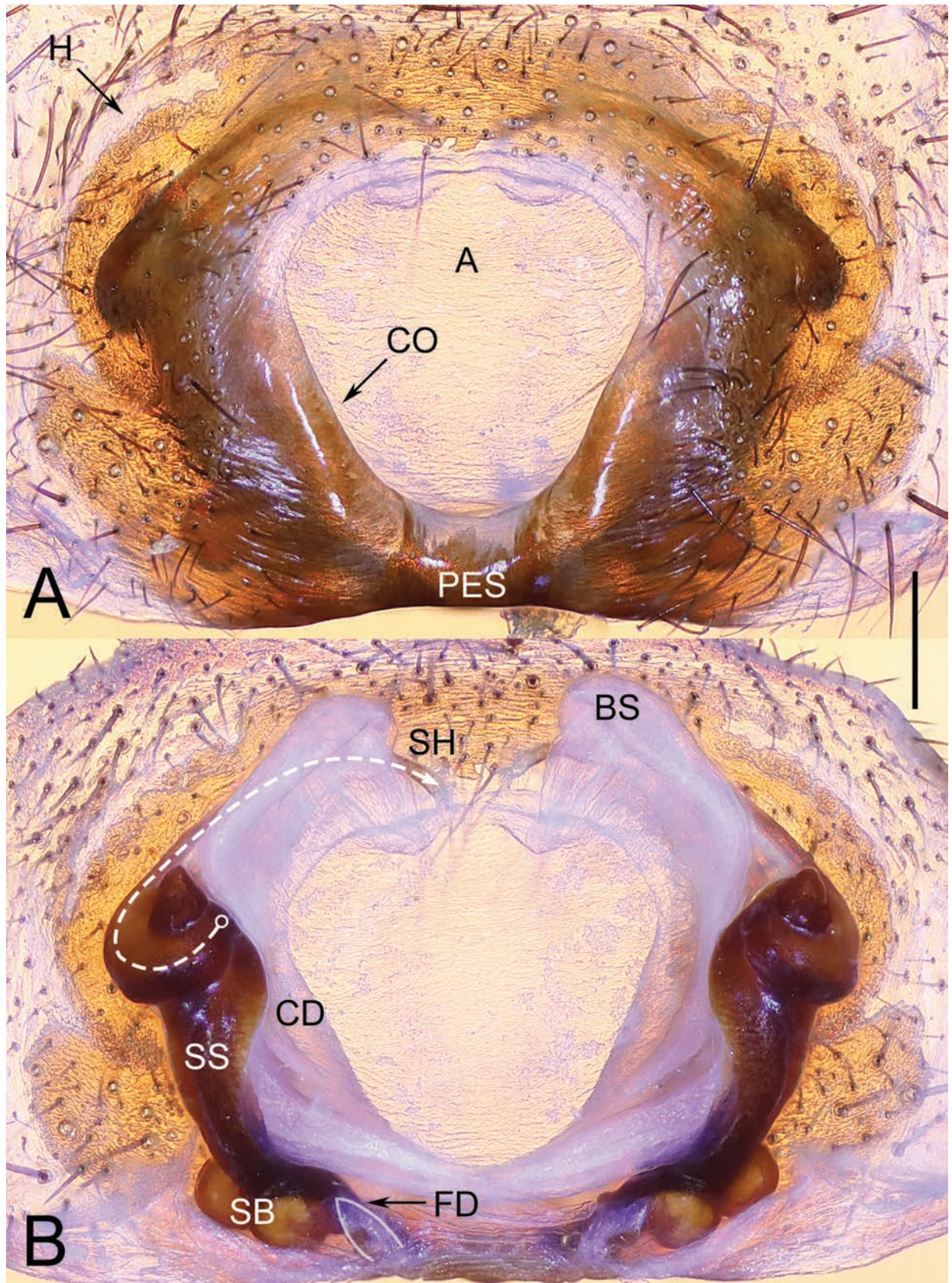


Figure 2. Epigyne of *Yunguirius parvus* sp. nov. **A** epigyne, ventral view **B** vulva, dorsal view. Abbreviations: A = atrium; BS = blind sac; CD = copulatory duct; CO = copulatory opening; FD = fertilization duct; H = hood; PES = posterior epigynal sclerite; SB = spermathecal base; SH = spermathecal head; SS = spermathecal stalk. The white dashed line B indicates the spermathecal head, the white outline B indicates the fertilization duct. Scale bar: 0.50 mm.

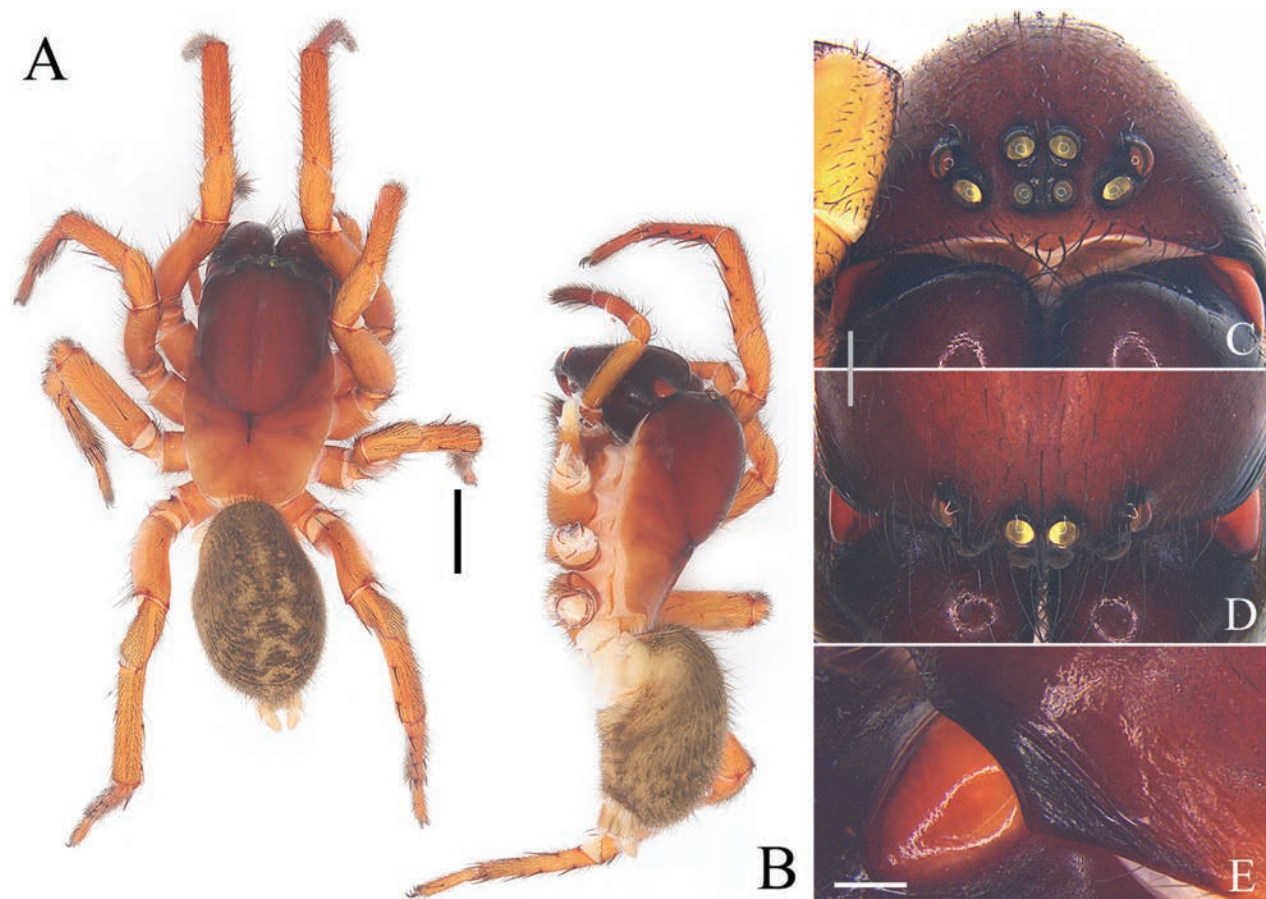


Figure 3. Characters of the female of *Yunguirius parvus* sp. nov. **A** habitus, dorsal view **B** habitus, prolateral view **C** eye area, frontal view **D** eye area, dorsal view **E** cephalic region, lateral view. Scale bars: 2.00 mm (**A**, **B**); 0.50 mm (**C**, **D**); 0.25 mm (**E**).

sacs short, symmetric, and untouched. Spermathecal bases consisted of 2 spherical chambers, spermathecal stalks long, with distal tips conch-shaped, spermathecal heads anteriorly originated, long and sclerotized. Fertilization ducts posteriorly situated.

Male. Unknown.

Distribution. China (Yunnan).

***Yunguirius trigonus* Wei & Liu, sp. nov.**

<https://zoobank.org/8854F835-A7BA-448B-B3B2-B0921CB9E1A6>

Figs 4, 5, 10

Type material. *Holotype* ♀ (HBU-WM-24-003): CHINA: Chongqing City, Nanchuan District, Jinfo Mountain, 29.0489°N, 107.1279°E, elevation: 681 m, 30.IX.2021, T.X. Gu leg.

Etymology. The specific epithet is derived from the Greek word “trigon”, meaning triangular and referring to the atrium and the posterior epigynal sclerite of the new species forming into a subtriangular pattern; an adjective.

Diagnosis. The females of *Yunguirius trigonus* sp. nov. resemble those of *Y. subterebratus* and *Y. wangqiqiae* sp. nov. in having a trapezoidal atrium, with the width longer than the length and the width at the widest point being three

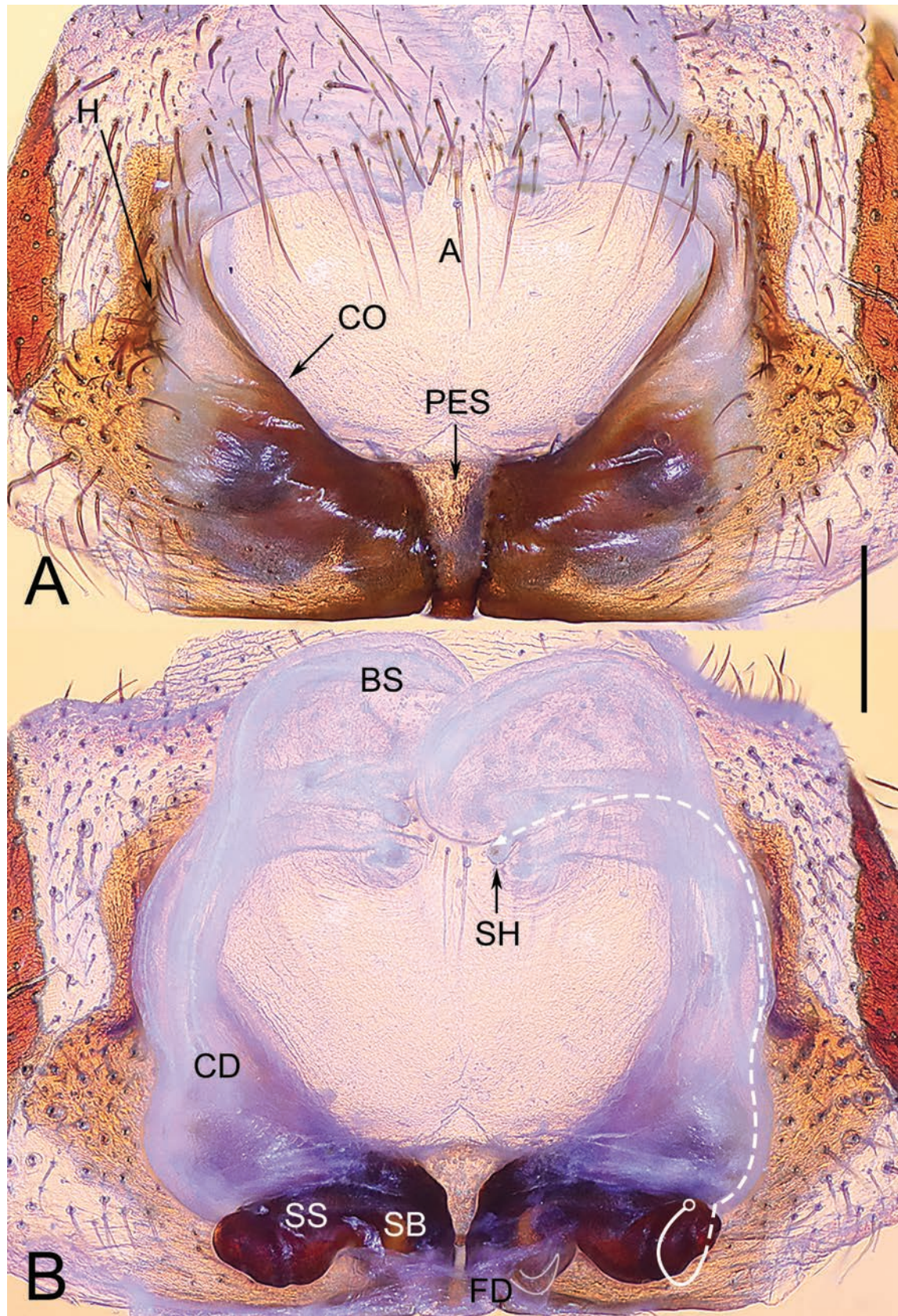


Figure 4. Epigyne of *Yunguirius trigonus* sp. nov. **A** epigyne, ventral view **B** vulva, dorsal view. Scale bars: 1.00 mm. Abbreviations: A = atrium; BS = blind sac; CD = copulatory duct; CO = copulatory opening; FD = fertilization duct; H = hood; PES = posterior epigynal sclerite; SB = spermathecal base; SH = spermathecal head; SS = spermathecal stalk. The white dashed line B indicates the spermathecal head, the white outline B indicates the fertilization duct. Scale bar: 0.50 mm.

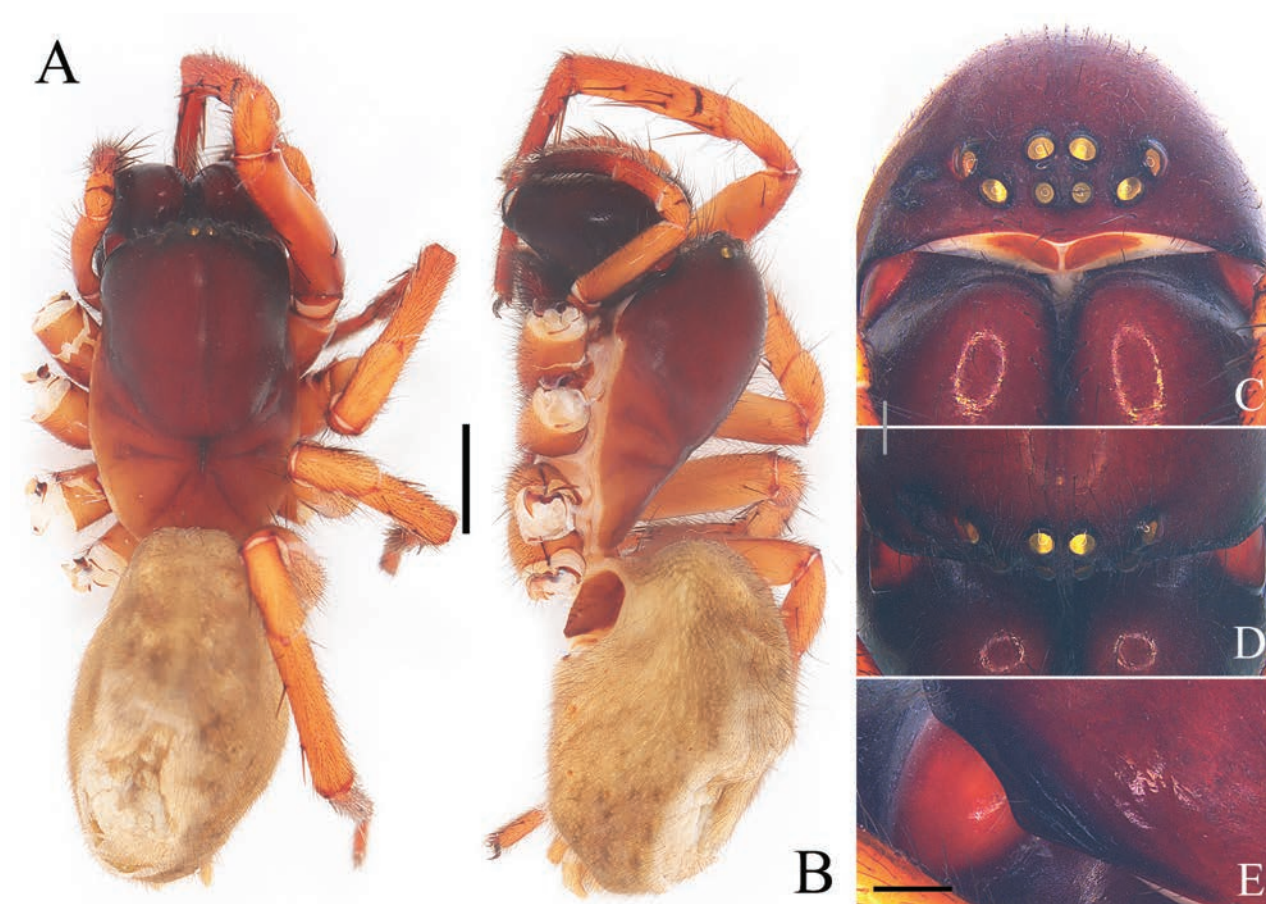


Figure 5. Characters of the female of *Yunguirius trigonus* sp. nov. **A** habitus, dorsal view **B** habitus, prolateral view **C** eye area, frontal view **D** eye area, dorsal view **E** cephalic region, lateral view. Scale bars: 2.00 mm (**A**, **B**); 0.50 mm (**C**, **D**); 0.25 mm (**E**).

times longer than the narrowest point (Figs 4A, 6A; fig. 245A in Zhu et al. 2017), compared to being trapezoidal but with the width being shorter than the length, and the width of the widest point approximately being twice that of the narrowest point in *Y. ornatus* (Fig. 3A in Li et al. 2023), and being heart-shaped, pentagonal or subrounded in other *Yunguirius* species (Figs 1A, 2A, 8A; figs 2A, 4A in Li et al. 2023). However, *Y. trigonus* sp. nov. can be distinguished from the latter by the following characteristics: 1) the presence of a pair of long and linear hoods (Fig. 4A), versus having a pair of triangular hoods in the latter (Fig. 6A; fig. 245A in Zhu et al. 2017); 2) the short and slightly overlapping blind sacs of the copulatory ducts (Fig. 4B), versus being long and obviously overlapped in the latter (Fig. 6B; fig. 245B in Zhu et al. 2017); 3) the spermathecal stalks are relatively short and thick (Fig. 4B), versus being reduced in *Y. subterebratus* (fig. 245B in Zhu et al. 2017) or being subequal to half the width of the atrium in *Y. wangqiqiae* Wei & Liu, sp. nov. (Fig. 6B).

Description. Female (holotype) (Fig. 5). Carapace reddish brown. Cervical and radial groove distinct. Cephalic region wide, moderately raised and wide, lateral margin with indistinct furrows. Chelicerae with 3 promarginal teeth and 2 retromarginal teeth, condyle red. Sternum longer than wide. Abdomen pale yellow, covered by hairs. Legs red. Total length 12.31. Carapace 5.83 long, 3.99 wide, cephalic region 3.49 wide. Abdomen 6.48 long, 3.68 wide. Eye size and interdistance: AME 0.18, ALE 0.27, PME 0.22, PLE 0.25; AME–AME 0.10, AME–ALE 0.17, AME–PME 0.16, ALE–PLE 0.10, PME–PME 0.11, PME–PLE 0.42. Leg

measurements: Leg I 16.00 (2.12, 0.81, 3.97, 1.71, 3.39, 2.86, 1.57), leg II 14.71 (1.82, 0.82, 3.61, 1.66, 2.68, 2.74, 1.65), leg III 12.33 (1.55, 0.80, 2.99, 1.41, 1.94, 2.35, 1.45), leg IV 16.90 (1.87, 0.93, 4.13, 1.82, 3.41, 3.33, 1.61). Epigyne (Fig. 4). Epigynal teeth absent. Atrium centrally situated, trapezoidal, anterior margin incomplete, posterior margin short. Epigynal sclerite longer than wide. Hoods long, vertically oriented, situated laterally. Fold absent. Copulatory ducts broad, laterally originated, blind sacs short, distal tips slightly overlapped. Spermathecal bases normal, spermathecal stalks extended laterally, with distal tips conch-shaped, spermathecal heads reduced and membranous, distal tips visible. Fertilization ducts posteriorly situated.

Male. Unknown.

Distribution. China (Chongqing).

***Yunguirius wangqiqiae* Wei & Liu, sp. nov.**

<https://zoobank.org/161CD48B-7C1E-4F46-BB59-0587C2B20AE0>

Figs 6, 7, 10

Type material. *Holotype* ♀ (HBU-WM-24-004), 1 ♀ *paratype* (HBU-WM-24-005): CHINA: Yunnan Province, Zhaotong City, Weixin County, Houshan mountain, 27.8147°N, 104.8050°E, elevation: 1363 m, 1.X.2018, C.F. Tao and H.Y. Chen leg.

Etymology. The specific name is dedicated to Ms Qiqi Wang, at the desire of Caifu Tao, who provided the holotype; a noun (name) in genitive case.

Diagnosis. The females of *Yunguirius wangqiqiae* sp. nov. resemble those of *Y. subterebratus* and *Y. terebratus* in that they have long blind sacs of the copulatory ducts, approximately equal to the length of the openings of the copulatory ducts, while the copulatory ducts are ventrally connected with the spermathecae (Figs 1B, 6B; fig. 245B in Zhu et al. 2017). In contrast, other species such as *Y. duoge*, *Y. parvus* sp. nov., *Y. trigonus* sp. nov. and *Y. xiangding* have short blind sacs, shorter than the length of the openings of the copulatory ducts (Fig. 2B, 4B; figs 2B, 4B in Li et al. 2023), or have long blind sacs but the copulatory ducts are dorsally connected with the spermathecae such as *Y. ornatus* and *Y. xian-nushanensis* sp. nov. (Fig. 8; fig. 3B in Li et al. 2023). However, *Y. wangqiqiae* sp. nov. can be distinguished from the latter by the following characteristics: 1) the atrium is bowl-shaped, wider than long, and lacks the fold (Fig. 6A), versus being trapezoidal in *Y. subterebratus* (fig. 245A in Zhu et al. 2017) or being subrounded, with the width roughly equal to the length, and presenting the fold in *Y. terebratus* (Fig. 1A); 2) the copulatory ducts featuring only the prototype of the secondary layers (Fig. 6B), versus possessing advanced secondary layers in *Y. terebratus* (Fig. 1B); 3) the spermathecal stalks are long and extend laterally with conch-shaped distal ends (Fig. 6B), versus being extremely short in *Y. subterebratus* (fig. 245B in Zhu et al. 2017), and in *Y. terebratus*, they are long but extend obliquely upward, with large and round distal ends (Fig. 1B).

Description. Female (holotype) (Fig. 7). Carapace reddish brown. Cervical and radial groove distinct. Cephalic region moderately raised and wide, lateral margin with distinct furrows. Chelicerae with 3 promarginal teeth and 2 retromarginal teeth, condyle red. Sternum longer than wide. Abdomen pale yellow, with 5 chevron-shaped patterns, covered by hairs. Legs red. Total length

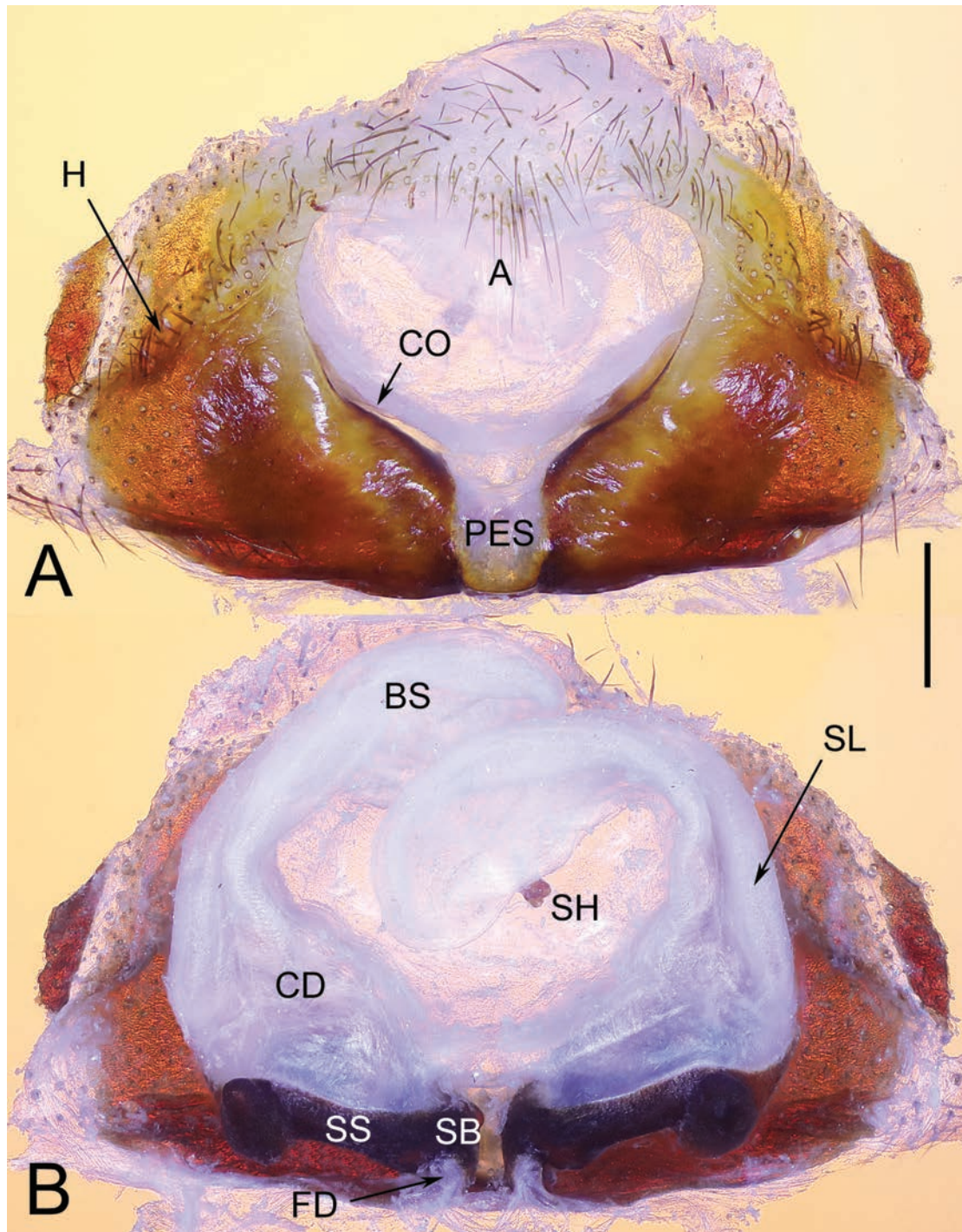


Figure 6. Epigyne of *Yunguirius wangqiqiae* sp. nov. **A** epigyne, ventral view **B** vulva, dorsal view. Abbreviations: A = atrium; BS = blind sac; CD = copulatory duct; CO = copulatory opening; FD = fertilization duct; H = hood; PES = posterior epigynal sclerite; SB = spermathecal base; SH = spermathecal head; SL = the secondary layer of copulatory duct; SS = spermathecal stalk. Scale bar: 0.50 mm.

14.48. Carapace 7.51 long, 5.03 wide, cephalic region 4.28 wide. Abdomen 7.95 long, 4.80 wide. Eye size and interdistance: AME 0.22, ALE 0.31, PME 0.32, PLE 0.38; AME–AME 0.16, AME–ALE 0.20, AME–PME 0.19, ALE–PLE 0.11, PME–PME 0.09, PME–PLE 0.45. Leg measurements: Leg I 19.71 (2.53, 0.93, 4.98, 2.11, 4.08, 3.47, 1.96), leg II 17.82 (2.21, 0.86, 4.44, 1.93, 3.23, 3.28, 2.11), leg III 14.82 (2.00, 0.92, 3.67, 1.73, 2.44, 2.85, 1.61), leg IV 19.73 (2.31,



Figure 7. Characters of the female of *Yunguirius wangqiqiae* sp. nov. **A** habitus, dorsal view **B** habitus, prolateral view **C** eye area, frontal view **D** eye area, dorsal view **E** cephalic region, lateral view. Scale bars: 2.00 mm (**A**, **B**); 0.50 mm (**C**, **D**); 0.25 mm (**E**).

1.11, 4.87, 1.87, 3.84, 4.13, 1.84). Epigyne (Fig. 6). Epigynal teeth absent. Atrium large, bowl-shaped, anterior margin incomplete. Posterior epigynal sclerite weakly sclerotized and opalescent. Hoods weak, situated laterally. Fold absent. Copulatory ducts broad, laterally originated, slightly folded, with the prototype of the secondary layers; blind sacs long and with distal tips overlapped. Spermathecal base small; spermathecal stalk long, with distal tip conch-shaped and extended laterally; spermathecal head only remaining a sclerotized end. Fertilization ducts posteriorly situated.

Male. Unknown.

Distribution. China (Guizhou, Yunnan).

***Yunguirius xiannushanensis* Wei & Liu, sp. nov.**

<https://zoobank.org/40CEC348-B43B-4EB1-9491-103172F2690E>

Figs 8, 9, 10, 11

Type material. *Holotype* ♀ (HBU-WM-24-006): CHINA: Chongqing City, Wulong District, Xiannu Mountain, 29.4508°N, 107.7280°E, elevation: 1951 m, 15.IX.2021, T.X. Gu leg.

Etymology. The new species is named after the type locality, Xiannu Mountain; an adjective.

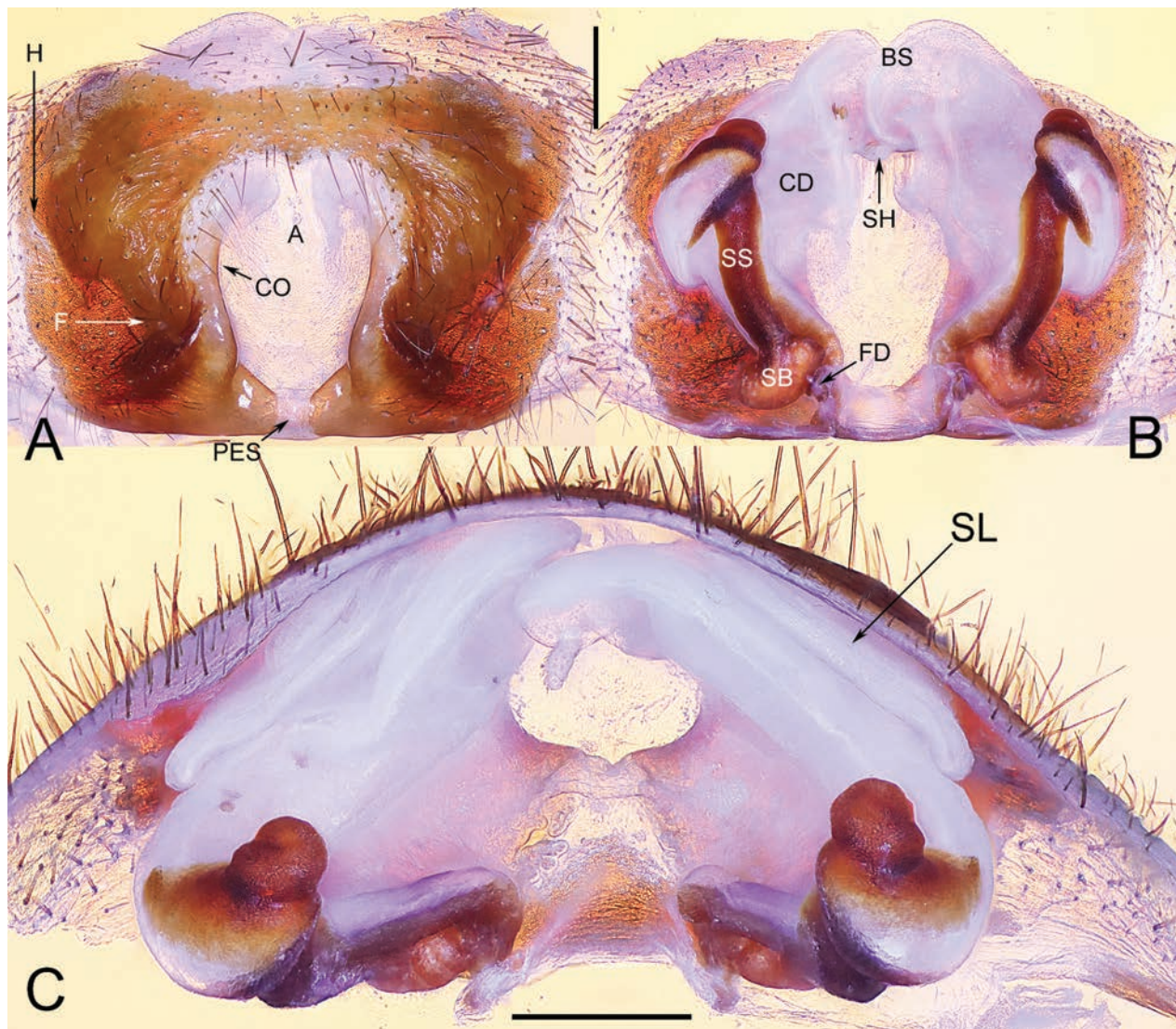


Figure 8. Epigyne of *Yunguirius xiannushanensis* sp. nov. **A** epigyne, ventral view **B** vulva, dorsal view **C** vulva, apical view. Abbreviations: A = atrium; BS = blind sac; CD = copulatory duct; CO = copulatory opening; F = fold; FD = fertilization duct; H = hood; PES = posterior epigynal sclerite; SB = spermathecal base; SH = spermathecal head; SL = the secondary layer of copulatory duct; SS = spermathecal stalk. Scale bars: 0.50 mm.

Diagnosis. The females of *Yunguirius xiannushanensis* sp. nov. resemble those of *Y. ornatus* in 1) the atrium is relatively small, less than 1/3 the width of the epigyne, with a reduced anterior margin (Fig. 8A; fig. 3A in Li et al. 2023); 2) the connection of the copulatory duct and the spermatheca presents dorsally (Fig. 8B; fig. 3B in Li et al. 2023). While in other *Yunguirius* species, the atrium exceeding 1/3 the width of the epigyne, with the anterior margin complete (*Y. duoge* and *Y. parvus* sp. nov., fig. 2A; fig. 2A in Li et al. 2023) or incomplete (*Y. subterebratus*, *Y. terebratus*, *Y. trigonus* sp. nov., *Y. wangqiqiae* sp. nov. and *Y. xiangding*, figs 1A, 4A, 6A; fig. 245A in Zhu et al. 2017; fig. 4A in Li et al. 2023), and the connection of the copulatory duct and the spermatheca presents ventrally (Figs 1B, 2B, 4B, 6B; fig. 245B in Zhu et al. 2017; figs 2B, 4B in Li et al. 2023). *Y. xiannushanensis* sp. nov. can be distinguished from *Y. ornatus* by the following characteristics: 1) the atrium is pentagonal (Fig. 8A), versus being trapezoidal in *Y. ornatus* (Fig. 3A in Li et al. 2023); 2) the posterior epigynal

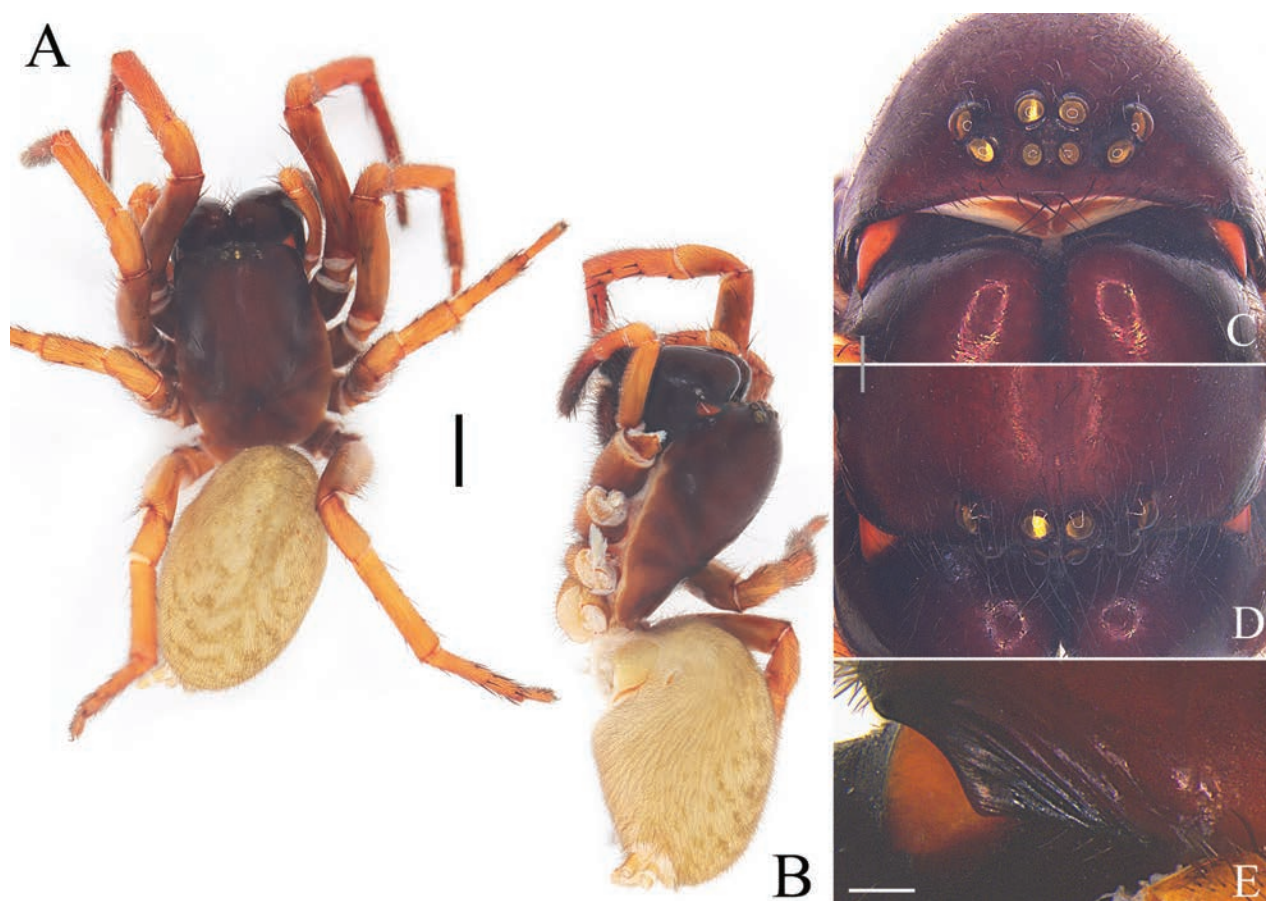


Figure 9. Characters of the female of *Yunguirius xiannushanensis* sp. nov. **A** habitus, dorsal view **B** habitus, prolateral view **C** eye area, frontal view **D** eye area, dorsal view **E** cephalic region, lateral view. Scale bars: 2.00 mm (**A**, **B**); 0.50 mm (**C**, **D**); 0.25 mm (**E**).

sclerite is reduced and thin, roughly a quarter of the width of the atrium (Fig. 8A), versus being more substantial and about equal to the width of atrium in *Y. ornatus* (Fig. 3A in Li et al. 2023); 3) the copulatory ducts are folded, and with distinct secondary layer (Fig. 8B), versus being monolayered in *Y. ornatus* (Fig. 3B in Li et al. 2023); 4) the spermathecal bases are large, twice as wide as the stalks, the spermathecal stalks have conch-shaped distal tips, and the spermathecal heads are membranous and only the distal tips are visible (Fig. 8B); in contrast, in *Y. ornatus*, the spermathecal bases are relatively small, slightly wider than the stalks, the distal tips of the stalks are normal, and the spermathecal heads are long and sclerotized (Fig. 3B in Li et al. 2023).

Description. Female (holotype) (Fig. 9). Carapace reddish brown. Cervical and radial groove distinct. Cephalic region moderately raised and wide, lateral margin with distinct furrows. Chelicerae with 3 promarginal teeth and 2 retromarginal teeth, condyle red. Sternum longer than wide. Abdomen pale yellow, with 5 chevron-shaped patterns, covered by hairs. Legs red. Total length 13.20. Carapace 6.40 long, 4.25 wide, cephalic region 3.70 wide. Abdomen 7.14 long, 4.36 wide. Eye size and interdistance: AME 0.19, ALE 0.25, PME 0.25, PLE 0.28; AME–AME 0.12, AME–ALE 0.18, AME–PME 0.10, ALE–PLE 0.05, PME–PME 0.13, PME–PLE 0.34. Leg measurements: Leg I 17.18 (2.26, 0.75, 4.27, 1.91, 3.57, 3.20, 1.69), leg II 15.25 (1.94, 0.74, 3.79, 1.70, 3.02, 2.79, 1.67), leg III 12.68 (1.64, 0.79, 3.15, 1.45, 2.10, 2.39, 1.40), leg IV 17.77 (1.94, 0.95, 4.40, 1.88, 3.57, 3.49, 1.70).

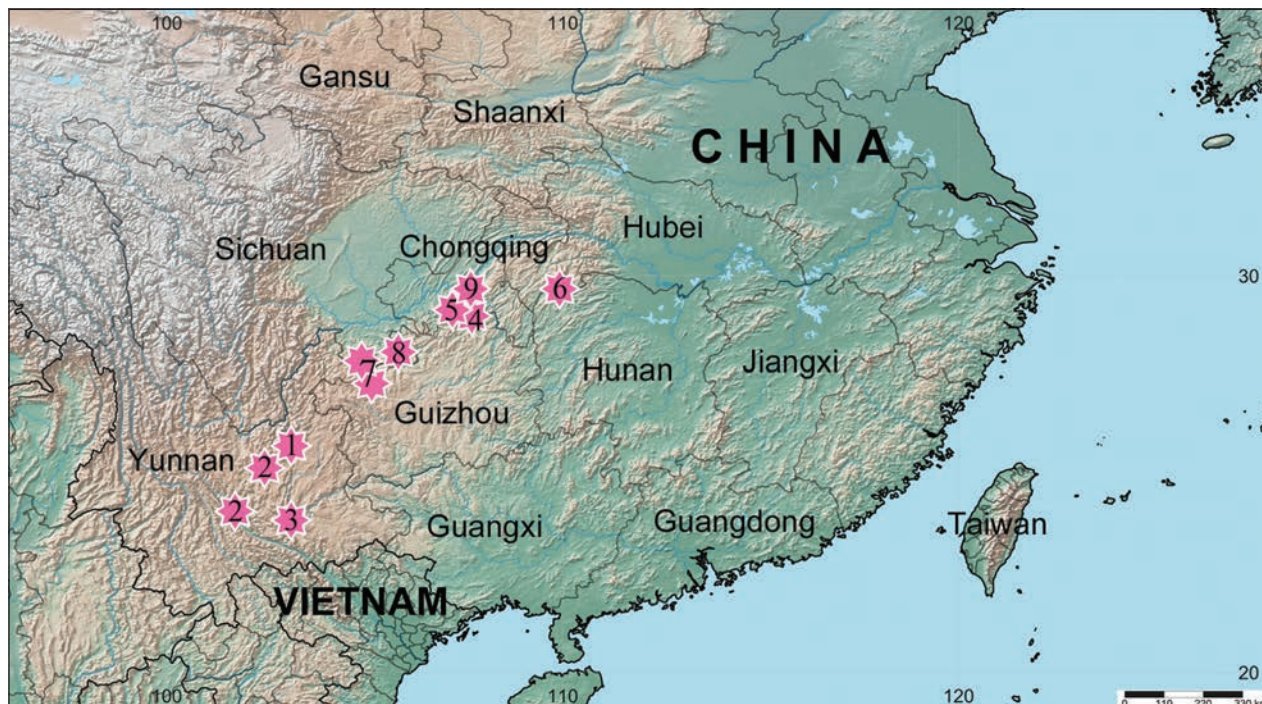


Figure 10. Distributions of the species of *Yunguirius*. 1 *Y. duoge* 2 *Y. ornatus* 3 *Y. parvus* sp. nov. 4 *Y. subterebratus* 5 *Y. terebratus* 6 *Y. trigonus* sp. nov. 7 *Y. wangqiqiae* sp. nov. 8 *Y. xiangding* 9 *Y. xiannushanensis* sp. nov.



Figure 11. Photos of the nest and the living female of *Yunguirius xiannushanensis* sp. nov. **A** opening of the tube nest **B** living female.

Epigyne (Fig. 8). Epigynal teeth absent. Atrium relatively small, pentagonal, anterior margin reduced. Epigynal sclerite small, opalescent. Hoods weak, vertically oriented, situated laterally. Fold distinct, triangular. Copulatory ducts broad, laterally originated, folded into 2 layers, and connected with spermathecae ventrally; blind sacs broad and short. Spermathecal base bean-shaped and twice wider than width of spermathecal stalk; spermathecal stalk long, with distal tip conch-shaped; spermathecal head reduced, only remaining a membranous tip on the distal tip of blind sac. Fertilization ducts posteriorly situated.

Male. Unknown.

Distribution. China (Chongqing).

Notes. Our fieldwork indicates that these new *Yunguirius* species inhabit tube nests with round openings dug into soil, moss, or rotten wood of high humidity, rather than constructing funnel webs beneath rocks or crevices like some other common agelenid spiders. A further study may be required to determine the origins of the burrowing behavior of these spiders.

Acknowledgements

We thank Hongyu Chen, Tianxuan Gu, Caifu Tao for their great help in collecting the specimens. The manuscript benefited greatly from comments by Dragomir Dimitrov (editor) and two anonymous reviewers.

Additional information

Conflict of interest

The authors have declared that no competing interests exist.

Ethical statement

No ethical statement was reported.

Funding

This study was financially supported by the Science & Technology Fundamental Resources Investigation Program of China (2023FY100200).

Author contributions

Writing - original draft: MW. Writing - review and editing: JL, KW.

Author ORCIDs

Mian Wei  <https://orcid.org/0000-0001-7348-8885>

Kai Wang  <https://orcid.org/0000-0002-9877-5140>

Data availability

All of the data that support the findings of this study are available in the main text.

References

- Chen J (2017) A new synonym of *Prochora praticola* (Bösenberg & Strand, 1906) (Araneae: Miturgidae). *Acta Arachnologica Sinica* 26(1): 45.
- Chen L, Zhao Z, Li SQ (2016) *Sinocoelotes* gen. n., a new genus of the subfamily Coelotinae (Araneae, Agelenidae) from Southeast Asia. *ZooKeys* 614: 51–86. <https://doi.org/10.3897/zookeys.614.8663>
- Hoang QD, Tran HMT, Le STT (2023) A new synonymy and combination in Vietnamese agelenids (Araneae: Agelenidae: Coelotinae), supported by both morphology and DNA barcoding. *Zootaxa* 5389(3): 393–395. <https://doi.org/10.11646/zootaxa.5389.3.7>
- Koch CL (1837) Übersicht des Arachnidensystems. Nürnberg, Heft 1, 39 pp. <https://doi.org/10.5962/bhl.title.39561>

- Li B, Zhao Z, Zhang CT, Li SQ (2018a) *Sinodraconarius* gen. n., a new genus of Coelotinae spiders from southwest China (Araneae, Agelenidae). *ZooKeys* 770: 117–135. <https://doi.org/10.3897/zookeys.770.22470>
- Li B, Zhao Z, Zhang CT, Li SQ (2018b) *Nuconarius* gen. n. and *Hengconarius* gen. n., two new genera of Coelotinae (Araneae, Agelenidae) spiders from southwest China. *Zootaxa* 4457(2): 237–262. <https://doi.org/10.11646/zootaxa.4457.2.2>
- Li B, Zhao Z, Zhang CT, Li SQ (2019) *Troglocoelotes* gen. n., a new genus of Coelotinae spiders (Araneae, Agelenidae) from caves in south China. *Zootaxa* 4554(1): 219–238. <https://doi.org/10.11646/zootaxa.4554.1.7>
- Li B, Zhao Z, Okumura K, Meng K, Li SQ, Chen HF (2023) *Yunguirius*, a new genus of Coelotinae (Araneae, Agelenidae) spiders from southwest China. *ARPHA Preprints*. <https://doi.org/10.3897/arphapreprints.e100836>
- Luo B, Lu F, Zhang ZS, Wang LY (2023) A further study on the spider genus *Baiyueries* Zhao, Li & Li, 2023, from China (Agelenidae, Coelotinae). *ZooKeys* 1184: 91–102. <https://doi.org/10.3897/zookeys.1184.107931>
- Okumura KI (2020) Three new genera with taxonomic revisions of the subfamily Coelotinae (Araneae: Agelenidae) from Japan. *Acta Arachnologica* 69(2): 77–94. <https://doi.org/10.2476/asjaa.69.77>
- Okumura KI, Zhao Z (2022) Taxonomic revision of six species of the subfamily Coelotinae (Araneae: Agelenidae) from Japan accompanied with the description of *Nesiocoelotes* gen. n. *Acta Arachnologica* 71(2): 93–103. <https://doi.org/10.2476/asjaa.71.93>
- Okumura KI, Koike N, Nakano T (2021) First description of the male of *Aeolocoelotes cornutus* (Nishikawa, 2009) n. comb. (Araneae, Agelenidae) from Japan. *Bulletin of the National Museum of Nature and Science Tokyo (A)* 47(3): 117–122. https://doi.org/10.50826/bnmnszool.47.3_117
- Peng XJ, Wang JP (1997) Seven new species of the genus *Coelotes* (Araneae: Agelenidae) from China. *Bulletin - British Arachnological Society* 10: 327–333.
- Pickard-Cambridge FO (1893) Handbook to the study of British spiders (Drassidae and Agelenidae). *British Naturalist* 3: 117–170.
- Wang JF, Yin CM, Peng XJ, Xie L (1990) New species of the spiders of the genus *Coelotes* from China (Araneae: Agelenidae). In: *Spiders in China: One Hundred New and Newly Recorded Species of the Families Araneidae and Agelenidae*. Hunan Normal University Press, Hunan, 172–253.
- World Spider Catalog (2024) World Spider Catalog. Natural History Museum Bern. Version 25.5. <http://wsc.nmbe.ch/> [accessed on 22th July, 2024]
- Zhu MS, Wang XP, Zhang ZS (2017) *Fauna Sinica: Invertebrata Vol. 59: Arachnida: Araneae: Agelenidae and Amaurobiidae*. Science Press, Beijing, 727 pp.

Further notes on the genus *Eurhaphidophora* Gorochov, 1999 (Orthoptera, Rhaphidophoridae) with description of a new species from China

Qidi Zhu¹, Fuming Shi²

¹ College of Agronomy, Jiangxi Agricultural University, Nanchang 330045, China

² Key Laboratory of Zoological Systematics and Application of Hebei Province, College of Life Sciences, Hebei University, Baoding 071002, China

Corresponding author: Fuming Shi (shif_m@126.com)

Abstract

This paper revises the genus *Eurhaphidophora* from China and describes a new species, i.e., *Eurhaphidophora dulongjiangensis* Zhu & Shi, **sp. nov.** The females of *Eurhaphidophora tarasovi doitungensis* Dawwrueng, Gorochov & Suwannapoom, 2020 and *Eurhaphidophora fossa* Lu, Huang & Bian, 2022 are described for the first time. Moreover, *Eurhaphidophora curvata* Lu, Huang & Bian, 2022, **syn. nov.** is considered as a new synonym of *Eurhaphidophora pawangkhananti* Dawwrueng, Gorochov & Suwannapoom, 2020. Images illustrating the morphology of these species are provided.

Key words: Cave crickets, morphology, new species, new synonymy, taxonomy



Academic editor: Jun-Jie Gu

Received: 25 May 2024

Accepted: 14 July 2024

Published: 2 September 2024

ZooBank: <https://zoobank.org/B8B0712C-99B6-439B-B9B4-DAA489817F70>

Citation: Zhu Q, Shi F (2024) Further notes on the genus *Eurhaphidophora* Gorochov, 1999 (Orthoptera, Rhaphidophoridae) with description of a new species from China. ZooKeys 1211: 17–28. <https://doi.org/10.3897/zookeys.1211.128308>

Copyright: © Qidi Zhu & Fuming Shi.
This is an open access article distributed under terms of the Creative Commons Attribution License (Attribution 4.0 International – CC BY 4.0).

Introduction

Gorochov (1999) established the genus *Eurhaphidophora* Gorochov, 1999 and assigned *Eurhaphidophora nataliae* Gorochov, 1999 from Vietnam as type species. Thereafter, nine species were described from China, Vietnam, Laos, Thailand and Malaysia (Gorochov 2010, 2011, 2012). Later, *E. truncata* Bian & Shi, 2016, *E. curvata* Lu, Huang & Bian, 2022 and *E. fossa* Lu, Huang & Bian, 2022 were published from China (Bian and Shi 2016; Lu et al. 2022), while *E. pawangkhananti* Dawwrueng, Gorochov & Suwannapoom, 2020, *E. tarasovi doitungensis* Dawwrueng, Gorochov & Suwannapoom, 2020 and *E. apicoexcisa* Dawwrueng, Gorochov, Pinkaew & Vitheepradit, 2023 were discovered from Thailand (Dawwrueng et al. 2020, 2023).

Up to now, the genus *Eurhaphidophora* includes fifteen species, four of which are recorded from China. Here, we describe a new species *E. dulongjiangensis* Zhu & Shi, sp. nov. from China, describe the females of *E. tarasovi doitungensis* Dawwrueng, Gorochov & Suwannapoom, 2020 and *E. fossa* Lu, Huang & Bian, 2022 for the first time, and propose *E. curvata* Lu, Huang & Bian, 2022, syn. nov. to become a new synonym of *Eurhaphidophora pawangkhananti* Dawwrueng, Gorochov & Suwannapoom, 2020.

Materials and methods

Specimens were collected by hand at night and preserved in 75% ethanol. The genitalia were dissected with an insect needle and then put in 10% KOH solution to clean the tissue. Images were taken with a Zeiss AxioCam ICc5 digital camera attached to a Zeiss Stereo Discovery V12 microscope and edited with ADOBE PHOTOSHOP 2022. With regard to the scheme of arrangement of spines on the tibiae and hind basitarsus we follow Gorochov and Storozhenko (2015) and for measurements we follow Zhu et al. (2022). The type specimen is deposited in the Museum of Hebei University, Baoding, China (**HBU**).

Results

Genus *Eurhaphidophora* Gorochov, 1999

Type species. *Eurhaphidophora nataliae* Gorochov, 1999, by original designation.

Diagnosis. Body medium-sized in Rhabdiphorinae. Seventh and eighth abdominal tergites of male with a small posterior median projection that is nearly rounded or angular. Posterior margin of ninth abdominal tergite of male provided with a large median process. Male epiproct simple. Male genitalia membranous. Lateral lobes of dorso-median blade large, almost entirely covering central lobe of this blade.

Distribution. China, Laos, Malaysia, Thailand and Vietnam.

Eurhaphidophora dulongjiangensis Zhu & Shi, sp. nov.

<https://zoobank.org/FAE6DAB0-1028-40DD-A5A2-1F8BA6D2411A>

Figs 1, 2A, B

Type material. Holotype. ♂, CHINA: Yunnan Province, Gongshan County, Dulongjiang Town, Bapo Village, 27.7418°N, 98.3561°E, alt. 1610 m, 9.VII.2021, Shengchuan Yang leg.

Diagnosis. The new species can be distinguished from other congeneric species by the shape of the male epiproct and the ninth abdominal tergite. The ninth abdominal tergite of the male has a long posteromedian process, basal half narrow with a longitudinal median furrow, lateral sides raised into ridges; apical half slightly broadened and curved downwards, with a carina in midline, apex truncate. Male epiproct linguiform, concave on ventral side, apical area slightly protruding.

Description. Male. Body medium-sized. Fastigium verticis with rostral tubercles, pressed to each other and divided by a narrow and deep furrow, pointing forwards. Eyes ovoid, protruding forwards; lateral ocelli large and circular, occupying basal 2/3 of lateral surface of rostral tubercles; median ocellus slightly smaller, oval, located between antennal sockets. Pronotum long, anterior margin straight, posterior margin arcuate; lateral lobe longer than high, ventral margin arc-shaped. Mesonotum and metanotum short, posterior margin of mesonotum arcuate, posterior margin of metanotum straight. Fore coxa with one small spine. Internal genicular lobe of fore femur with one long spine; internal and external genicular lobes of mid femur each with one long spine; hind femur with

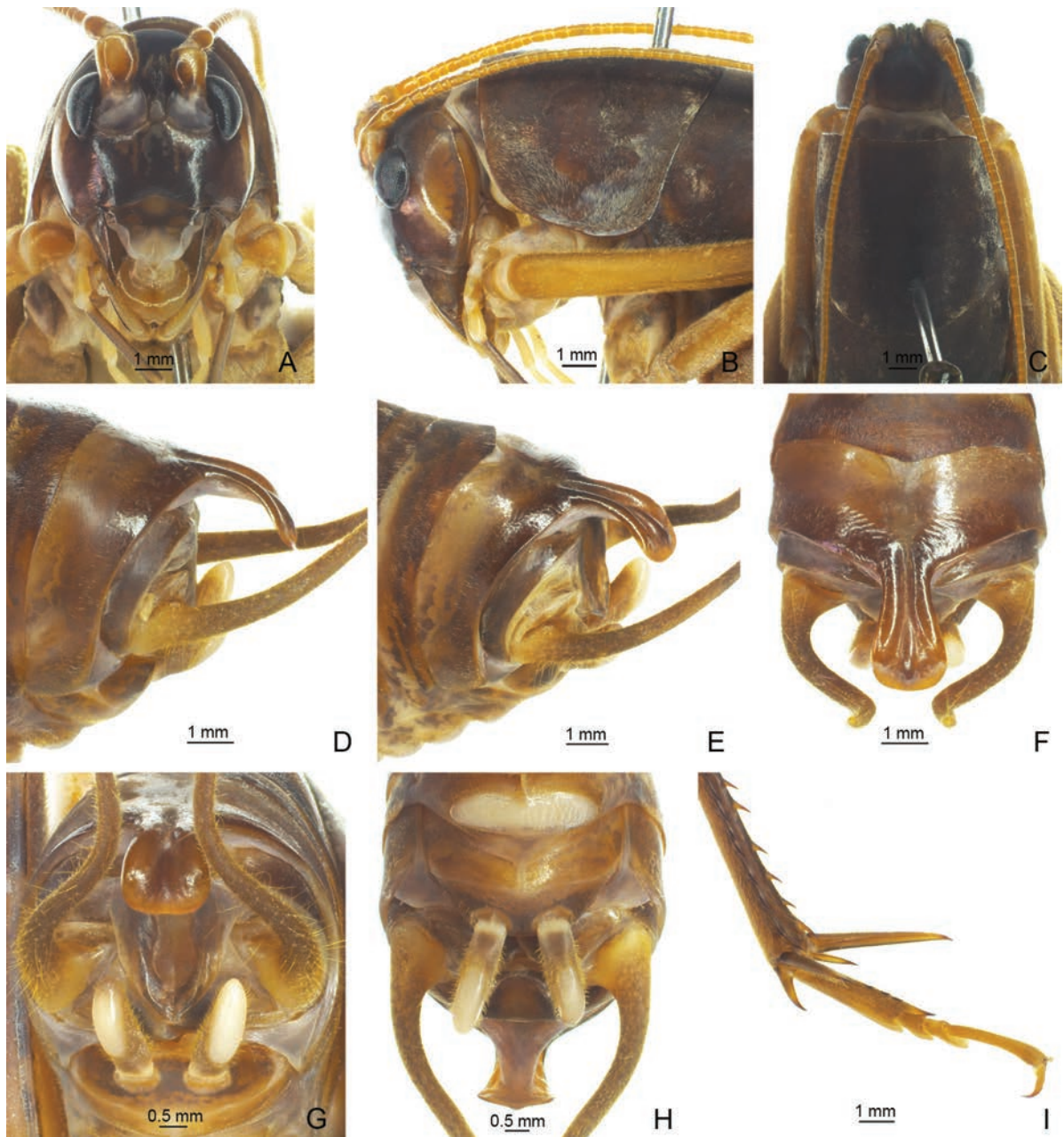


Figure 1. *Eurhaphidophora dulongjiangensis* Zhu & Shi, sp. nov. **A–I** ♂ **A–C** head and pronotum **A** frontal view **B** lateral view **C** dorsal view **D–H** apex of abdomen **D** lateral view **E** apico-lateral view **F** dorsal view **G** apical view **H** ventral view **I** hind tarsus in lateral view.

one inner spine on ventral surface, internal genicular lobe with one small spine. Tibia and hind basitarsus with following armament – ve, vi, ve, v2a / de, d~2, d2a, ve, ve, v2a / d20e–18i (d22e–20i), d2sa, 6a / d3c, dac. Posterior margin of eighth abdominal tergite angularly projecting. Ninth abdominal tergite with long posteromedian process, basal half narrow with a longitudinal median furrow, lateral sides raised into ridges; apical half slightly broadened and curved downwards, with a carina in midline, apex truncate. Epiproct linguiform, concave ventrad, apical area slightly protruding; paraproct nearly triangular in lateral view. Cercus narrow, conical, apex acute. Subgenital plate transverse and broad, posterior margin straight. Stylus cylindrical, apex rounded, inserted on postero-lateral area of subgenital plate. Genitalia membranous. **Female.** Unknown.

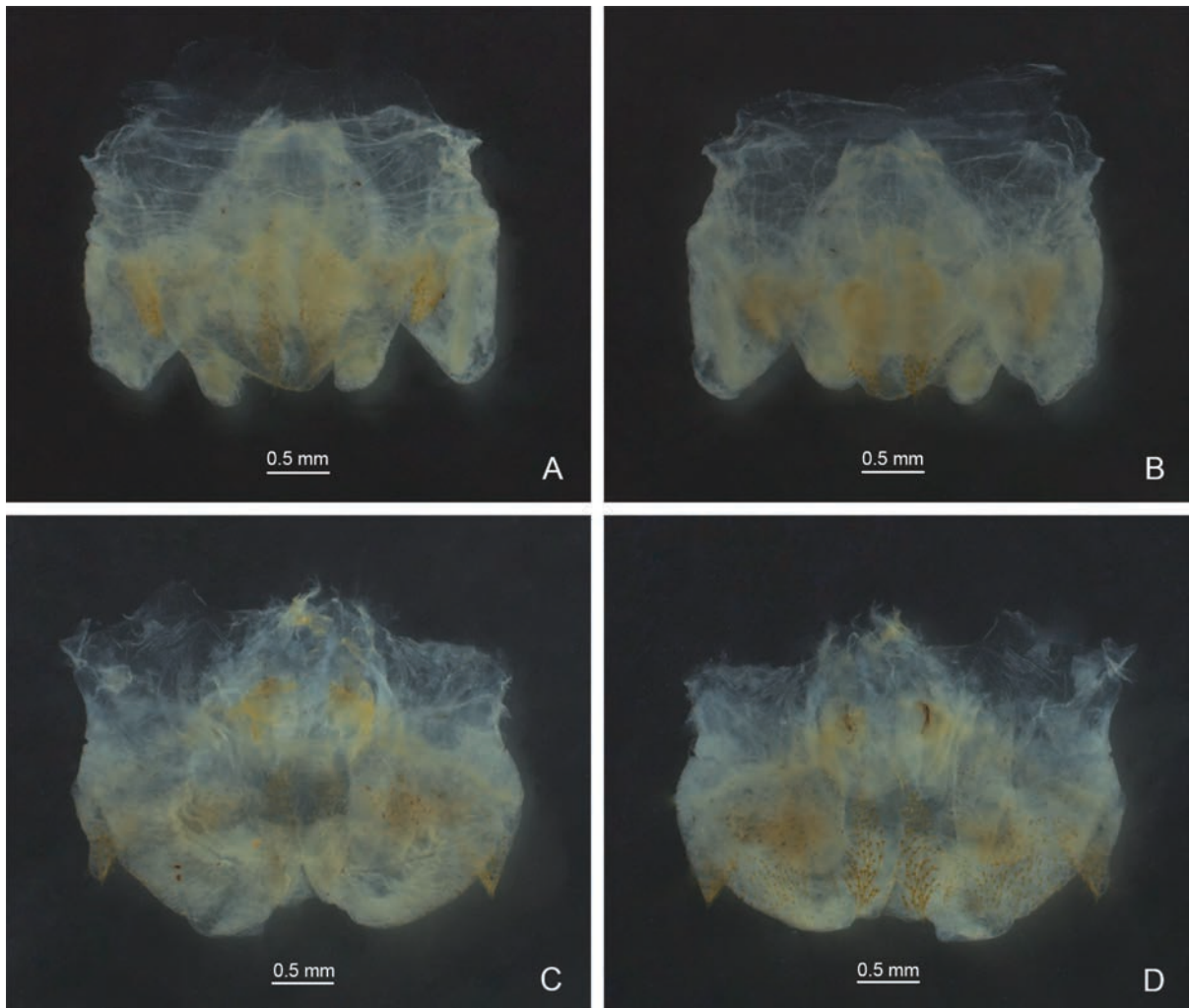


Figure 2. Male genitalia of *Eurhaphidophora* spp. **A, C** dorsal view **B, D** ventral view **A, B** *Eurhaphidophora dulongjiangensis* Zhu & Shi, sp. nov. **C, D** *Eurhaphidophora tarasovi doitungensis* Dawwrueng, Gorochov & Suwannapoom, 2020.

Coloration. Body light brown. Face, fastigium verticis and eyes black; ocelli pale. Thoracic tergites brown.

Measurements (mm). Body length: ♂29.60; length of pronotum: ♂7.44; length of fore femur: ♂9.36; length of hind femur: ♂20.18; length of hind tibia: ♂18.34; length of hind basitarsus: ♂3.50.

Etymology. The name of the new species derives from the type locality.

Distribution. China (Yunnan).

***Eurhaphidophora tarasovi doitungensis* Dawwrueng, Gorochov & Suwannapoom, 2020**

Figs 2C, D, 3

Eurhaphidophora tarasovi doitungensis Dawwrueng, Gorochov & Suwannapoom, 2020. In: Dawwrueng, Gorochov, Tanomtong and Suwannapoom 2020: 240.

Material examined. 1♂1♀, CHINA: Yunnan Province, Lvchun County, Banpo Town, 22.6517°N, 102.1236°E, alt. 1073 m, 17.VIII.2023, Mengjia Zheng leg.

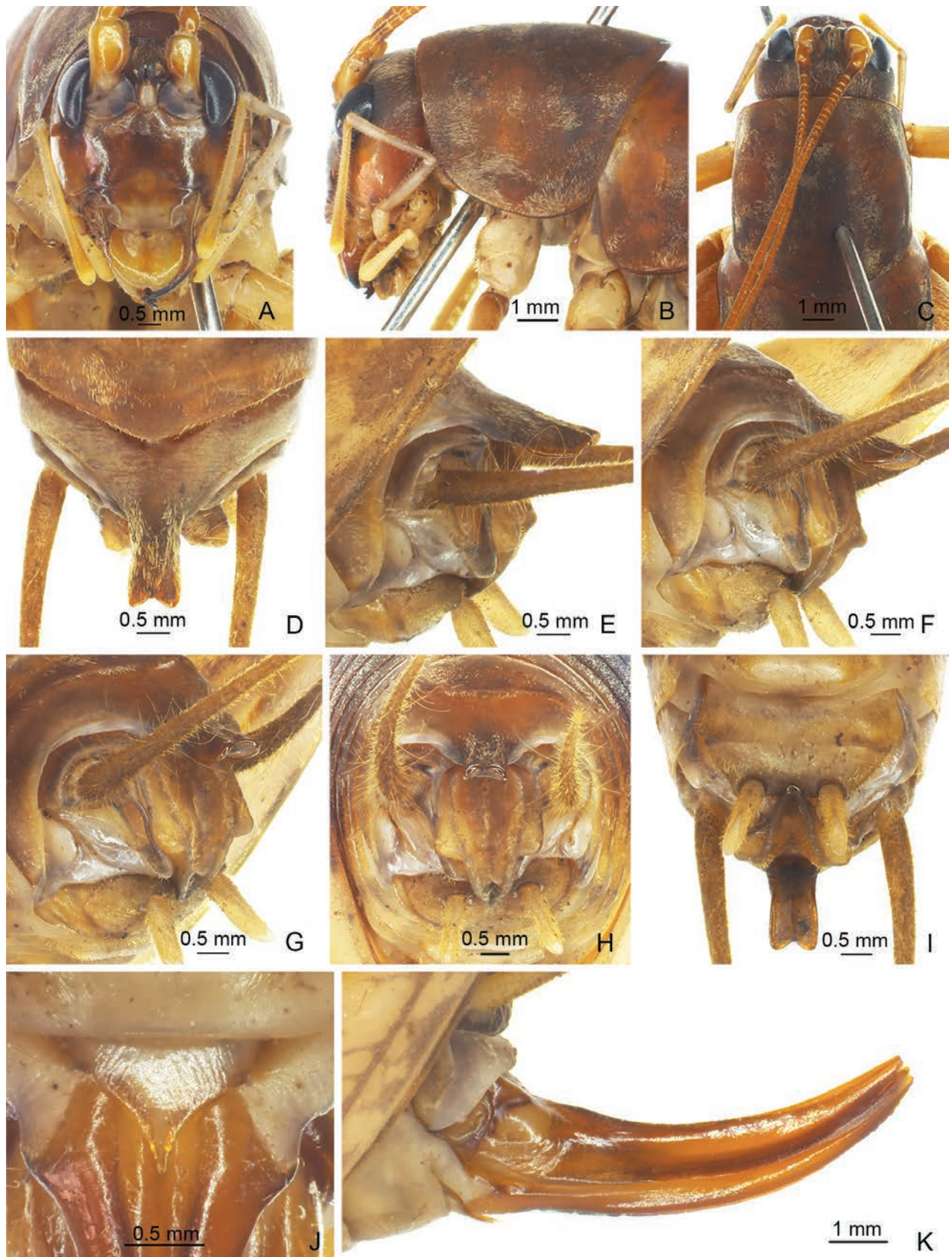


Figure 3. *Eurhaphidophora tarasovi doitungensis* Dawwrueng, Gorochoy & Suwannapoom, 2020 **A–I** ♂ **A–C** head and pronotum **A** frontal view **B** lateral view **C** dorsal view **D–I** apex of abdomen **D** dorsal view **E** lateral view **F, G** apico-lateral view **H** apical view **I** ventral view **J, K** ♀ **J** subgenital plate **K** ovipositor in lateral view.

Description. Male. Body medium-sized. Fastigium verticis with rostral tubercles, pressed to each other and divided by a narrow and deep furrow, pointing forwards. Eyes ovoid, protruding forwards; lateral ocelli large and circular, occupying basal 2/3 of lateral surface of rostral tubercles; median ocellus slightly smaller, oval, located between antennal sockets. Pronotum long, anterior margin straight, posterior margin arcuate; lateral lobe longer than high, ventral margin arc-shaped. Mesonotum and metanotum short, posterior margin of mesonotum arcuate, posterior margin of metanotum straight. Fore coxa with one small spine. Internal genicular lobe of fore femur with one long spine; internal and external genicular lobes of mid femur each with one long spine; internal genicular lobe of hind femur with one small spine. Tibia and hind basitarsus with following armament – ve, vi, ve, v2a / d~2, d2a, ve, ve, v2a / d17e–17i (d21e–19i), d2sa, 6a / d2c (d3c), dac. Posterior margin of eighth abdominal tergite angularly projecting. Ninth abdominal tergite with long posteromedian process, parallel on both sides, lateral margin bent downwards, apical area with a wide notch. Epiproct with longitudinal median concavity on dorsal surface, basal half with a pair of angular lateral lobes, apical half linguiform, curved downwards and forwards; paraproct nearly triangular in lateral view. Cercus slender, conical, apex acute. Subgenital plate transverse and broad, posterior margin straight. Stylus cylindrical, apex rounded, inserted on posterolateral area of subgenital plate. Genitalia membranous. **Female.** Posterior margin of ninth abdominal tergite slightly convex. Epiproct linguulate. Ovipositor short, slightly curved upwards, apical area of ventral margin denticulate. Subgenital plate triangular, apex acute.

Coloration. Body light brown. Face, fastigium verticis and thoracic tergites brown. Eyes black, ocelli pale.

Measurements (mm). Body length: ♂23.70, ♀18.10; length of pronotum: ♂6.48, ♀6.48; length of fore femur: ♂7.60, ♀7.44; length of hind femur: ♂18.26, ♀17.66; length of hind tibia: ♂16.86, ♀15.90; length of hind basitarsus: ♂2.66, ♀2.96; length of ovipositor: 8.26.

Distribution. China (Yunnan); Thailand.

Remarks. The species is newly recorded from China and the female is described for the first time.

***Eurhaphidophora pawangkhananti* Dawwrueng, Gorochov & Suwannapoom, 2020**
Figs 4, 5, 6A, B

Eurhaphidophora pawangkhananti Dawwrueng, Gorochov & Suwannapoom, 2020. In: Dawwrueng, Gorochov, Tanomtong and Suwannapoom 2020: 242.
Eurhaphidophora curvata Lu, Huang & Bian, 2022, syn. nov.

Material examined. CHINA: • Yunnan Province, 1♂1♀, Puer City, Meizihu Park, 22.7594°N, 100.9963°E, alt. 1302 m, 20.VIII.2019, Qidi Zhu leg.; • 4♂♂2♀♀, Puer City, Yixiang Town, 22.7487°N, 101.0563°E, alt. 1470 m, 22.VIII.2019, Qidi Zhu leg.; • 12♂♂20♀♀, Puer City, Meizihu Park, 22.7594°N, 100.9963°E, alt. 1302 m, 19.VIII.2023, Jie Su leg.

Description. Male. Body medium-sized. Fastigium verticis with rostral tubercles, pressed to each other and divided by a narrow and deep furrow, pointing forwards.

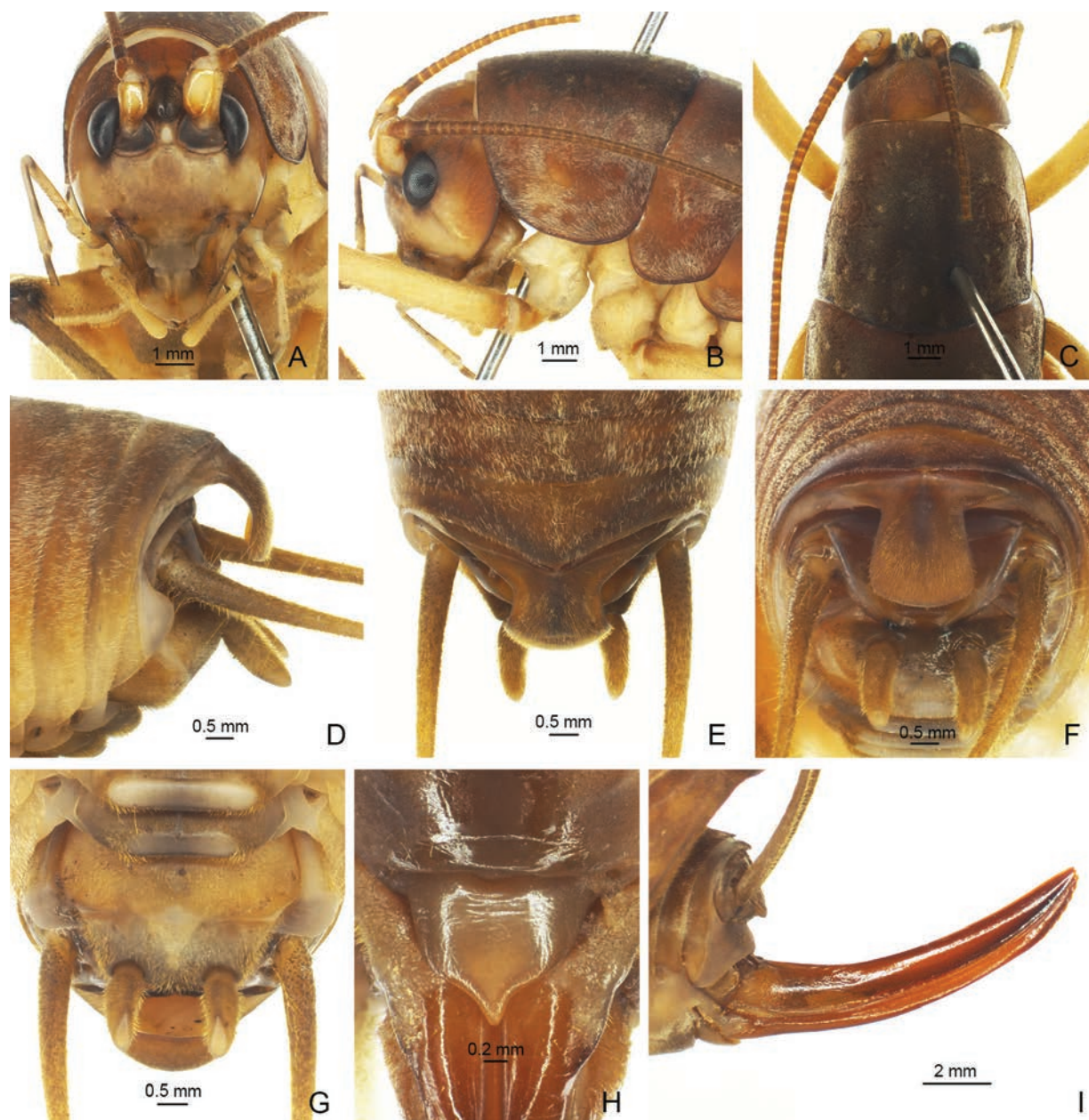


Figure 4. *Eurhaphidophora pawangkhananti* Dawwrueng, Gorochov & Suwannapoom, 2020 **A–G** ♂ **A–C** head and pronotum **A** frontal view **B** lateral view **C** dorsal view **D–G** apex of abdomen **D** lateral view **E** dorsal view **F** apical view **G** ventral view **H, I** ♀ **H** subgenital plate **I** ovipositor in lateral view.

Eyes ovoid, protruding forwards; lateral ocelli large and circular, occupying basal 2/3 of lateral surface of rostral tubercles; median ocellus slightly smaller, oval, located between antennal sockets. Pronotum long, anterior margin straight, posterior margin arcuate; lateral lobe longer than high, ventral margin arc-shaped. Mesonotum and metanotum short, posterior margin of mesonotum arcuate, posterior margin of metanotum straight. Fore coxa with one small spine. Internal genicular lobe of fore femur with one long spine; internal and external genicular lobes of mid femur each with one long spine; internal genicular lobe of hind femur with one small spine. Tibia and hind basitarsus with following armament – ve, (vi), ve, v2a / d~2, d2a, ve, ve, v2a / d18e–18i (d20e–19i), d2sa, 6a / d1c (d4c), dac. Posterior margin of eighth abdominal tergite angularly projecting. Ninth abdominal tergite

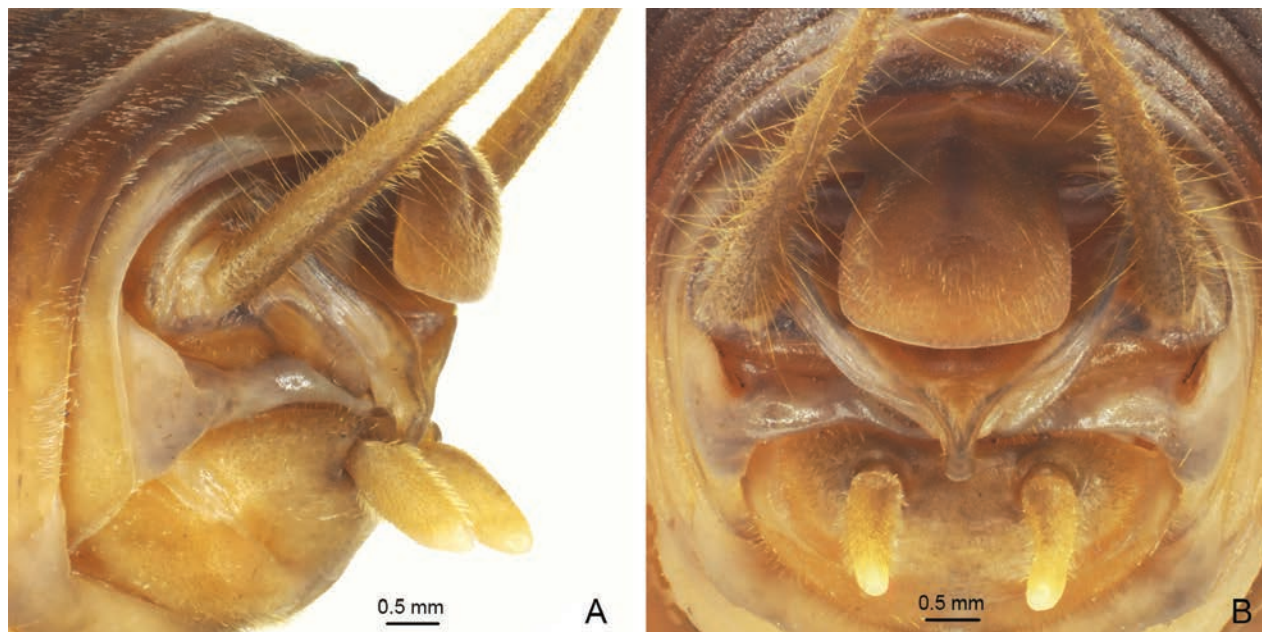


Figure 5. *Eurhaphidophora pawangkhananti* Dawwrueng, Gorochov & Suwannapoom, 2020 **A, B** apex of male abdomen **A** apico-lateral view **B** apical view.

long and wide, strongly curved downwards, basal half with a short dorso-median ridge, apex nearly truncate. Epiproct cup-shaped, basal half wide, nearly semicircular, apical process narrow, curved downwards and forwards. Cercus slender, conical, apex acute. Subgenital plate transverse and broad, posterior margin straight. Stylus cylindrical, apex rounded, inserted on posterolateral area of subgenital plate. Genitalia membranous. **Female.** Posterior margin of ninth abdominal tergite with small projection. Epiproct lingulate. Ovipositor slightly curved upwards, apical area of ventral margin denticulate. Subgenital plate nearly triangular, apex acute.

Coloration. Body light brown. Eyes black, ocelli pale.

Measurements (mm). Body length: ♂25.50–26.8, ♀24.68–25.40; length of pronotum: ♂6.54–6.90, ♀6.58–6.60; length of fore femur: ♂7.52–7.80, ♀7.50–7.76; length of hind femur: ♂17.06–17.66, ♀17.38–17.96; length of hind tibia: ♂15.58–15.90, ♀15.02–15.50; length of hind basitarsus: ♂3.22–3.26, ♀2.96–3.20; length of ovipositor: 12.02–12.80.

Distribution. China (Yunnan); Thailand.

Remarks. Dawwrueng et al. (2020) described *E. pawangkhananti* from Thailand. Then, Lu et al. (2022) published *E. curvata* from China and thought it was close to *E. ampla* Gorochov, 2010 and *E. orlovi* Gorochov, 2010. Dawwrueng et al. (2023) compared *E. curvata* to *E. pawangkhananti*, which is very similar to *E. curvata*. The two species can be distinguished by the characteristics of the male epiproct and the subgenital plate. However, the male epiproct of *E. curvata* is also greatly similar to that of *E. pawangkhananti*, which is cup-shaped, broad and rather short with an apical process that is very narrow and slightly curved forward in lateral view (Fig. 5). When the apical part is not fully exposed, the posterior margin of the epiproct appears to be widely rounded (Fig. 4F). Moreover, it is not obvious whether the posterior margin of the male subgenital plate between its styli is convex or almost straight, so it cannot be used as the main distinguishing character. Therefore, we consider *E. curvata* Lu, Huang & Bian, 2022, syn. nov. to be a new synonym of *E. pawangkhananti* Dawwrueng, Gorochov & Suwannapoom, 2020.

***Eurhaphidophora fossa* Lu, Huang & Bian, 2022**

Figs 6C, D, 7

Eurhaphidophora fossa Lu, Huang & Bian, 2022: 394.

Material examined. CHINA: • Yunnan Province, 5♂♂4♀♀, Jinghong City, Gasa Town, 21.9589°N, 100.7678°E, alt. 1340 m, 11.VIII.2019, Qidi Zhu leg.; • 1♂3♀♀, Menghai County, Guomenshan, 22.0610°N, 100.5682°E, alt. 1770 m, 11.VIII.2023, Jie Su and Sheng Gao leg.; • 4♂♂6♀♀, Lvchun County, Banpo Town, 22.6517°N, 102.1236°E, alt. 1073 m, 17.VIII.2023, Mengjia Zheng, Xiaolong Tong and Tianshuo Han leg.

Description. Male. Body medium-sized. Fastigium verticis with rostral tubercles, pressed to each other and divided by a narrow and deep furrow, pointing forwards. Eyes ovoid, protruding forwards; lateral ocelli large and circular, occupying basal 2/3 of lateral surface of rostral tubercles; median ocellus slightly smaller, oval, located between antennal sockets. Pronotum long, anterior margin straight, posterior margin arcuate; lateral lobe longer than high, ventral margin arc-shaped. Mesonotum and metanotum short, posterior margin of mesonotum arcuate, posterior margin of metanotum straight. Fore coxa with one small spine.

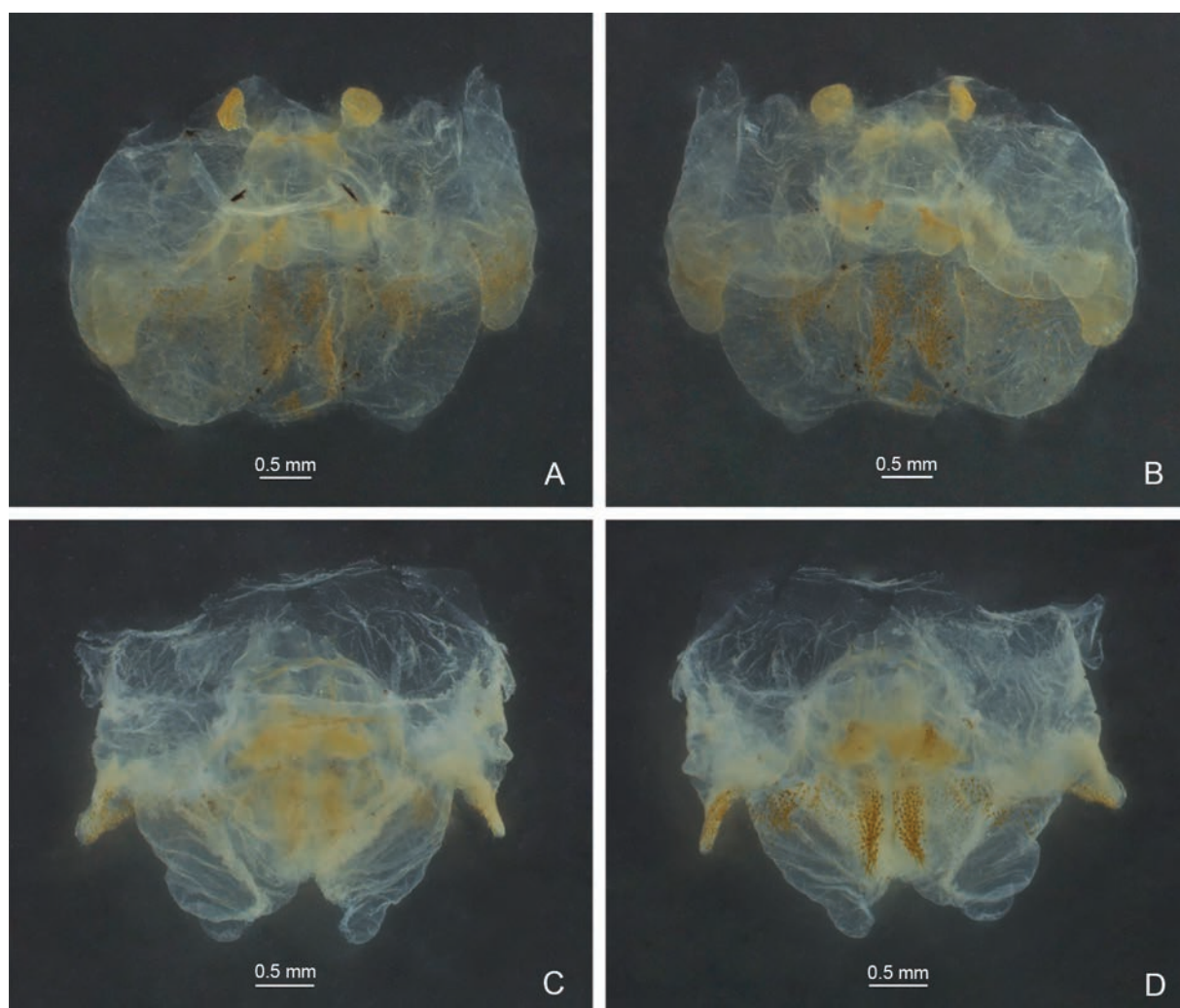


Figure 6. Male genitalia of *Eurhaphidophora* spp. **A, C** dorsal view **B, D** ventral view **A, B** *Eurhaphidophora pawangkhananti* Dawwrueng, Gorochoch & Suwannapoom, 2020 **C, D** *Eurhaphidophora fossa* Lu, Huang & Bian, 2022.

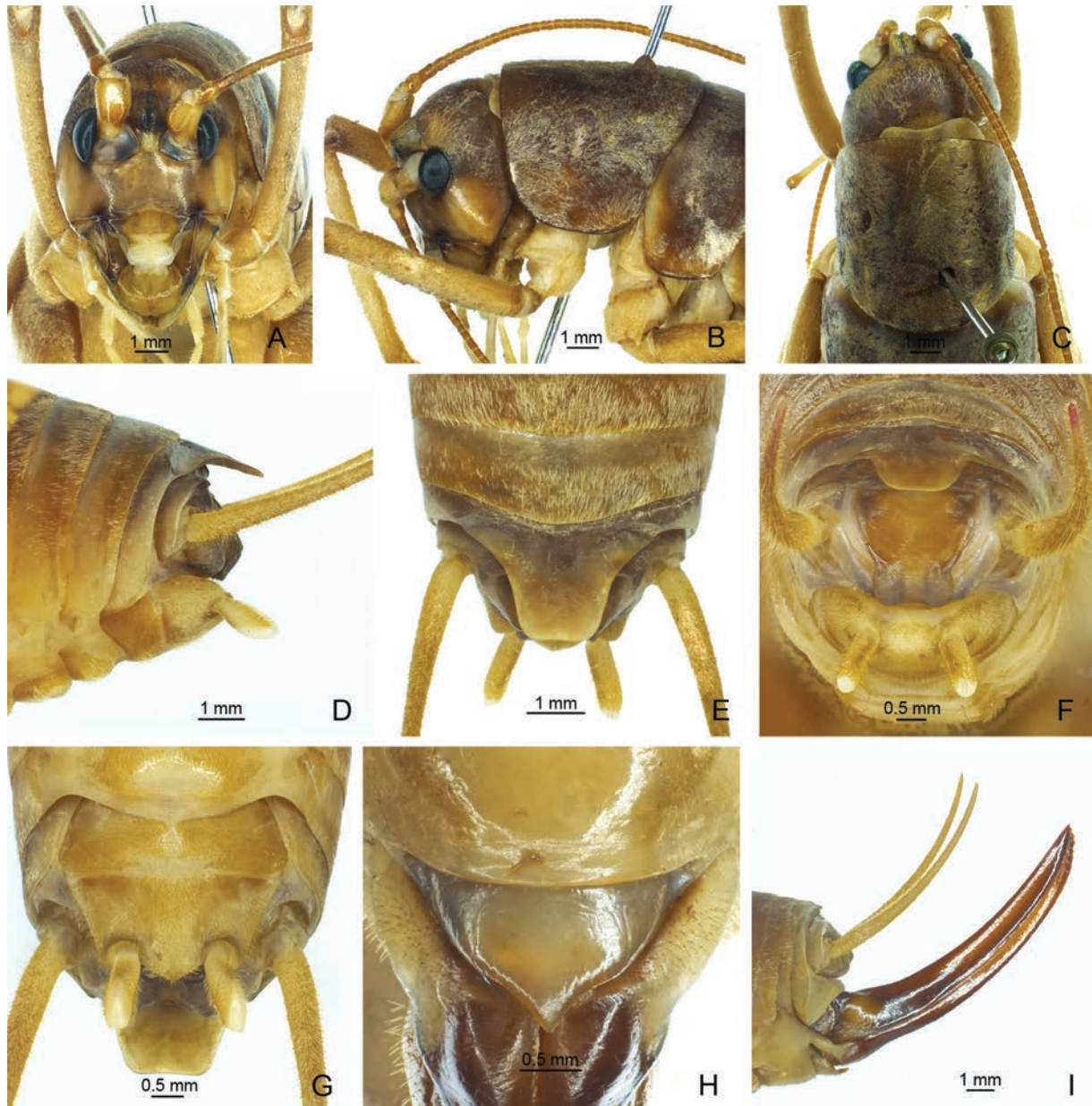


Figure 7. *Eurhaphidophora fossa* Lu, Huang & Bian, 2022 **A–G** ♂ **A–C** head and pronotum **A** frontal view **B** lateral view **C** dorsal view **D–G** apex of abdomen **D** lateral view **E** dorsal view **F** apical view **G** ventral view. **H, I** ♀ **H** subgenital plate **I** ovipositor in lateral view.

Internal genicular lobe of fore femur with one long spine; internal and external genicular lobes of mid femur each with one long spine; internal genicular lobe of hind femur with one small spine. Tibia and hind basitarsus with following armament – ve, vi, ve, v2a / d~2, d2a, ve, ve, v2a / d17e–16i (d19e–19i), d2sa, 6a / d1c (d5c), dac. Posterior margin of eighth abdominal tergite rounded. Ninth abdominal tergite long, trapezoid. Basal 2/3 of epiproct trapezoid, apical 1/3 rectangular, curved downwards; paraproct nearly triangular in lateral view. Cercus narrow, conical, apex acute. Subgenital plate transverse and broad. Stylus cylindrical, apex rounded, inserted in posterolateral area of subgenital plate. Genitalia membranous. **Female.** Posterior margin of ninth abdominal tergite with small projection. Epiproct lingulate. Ovipositor slightly curved upwards, apical area of ventral margin denticulate. Subgenital plate nearly triangular, apex acute.

Coloration. Body light brown. Eyes black, ocelli pale.

Measurements (mm). Body length: ♂27.76–27.94, ♀28.00–28.60; length of pronotum: ♂6.68–7.20, ♀7.40–7.68; length of fore femur: ♂7.72–7.80, ♀7.80–8.38; length of hind femur: ♂18.26–19.38, ♀20.26–21.00; length of hind tibia: ♂16.30–16.40, ♀17.2–18.4; length of hind basitarsus: ♂3.20–3.92, ♀3.78–4.00; length of ovipositor: 13.44–14.20.

Distribution. China (Yunnan).

Remarks. The female of *E. fossa* Lu, Huang & Bian, 2022 is described for the first time.

Discussion

The subfamily Rhabdophorinae includes eight genera (Cigliano et al. 2024). The genus *Eurhaphidophora* can be distinguished from other genera by the structure of the ninth abdominal tergite and the male genitalia (Gorochov 1999; Lu et al. 2022; Dawwrueng et al. 2023). The other genera differ in the form of the male epiproct or the abdominal tergites (Bian and Shi 2016; Qin et al. 2018). However, the classification of some species remains controversial, such as *Neorhaphidophora longispinula* (Bian, Zhu & Shi, 2017). Up to now, the classification of the subfamily Rhabdophorinae is based on morphological characteristics, without molecular evidence. We cannot judge whether the distinguishing characters of the classification system for the genera are appropriate. Moreover, the phylogenetic relationship between genera is still unclear. Further studies on the subfamily Rhabdophorinae based on more evidence are needed.

Acknowledgments

We are thankful to Shengchuan Yang, Jie Su, Sheng Gao, Mengjia Zheng, Xiaolong Tong and Tianshuo Han for collecting specimens.

Additional information

Conflict of interest

The authors have declared that no competing interests exist.

Ethical statement

No ethical statement was reported.

Funding

This research was supported by the National Natural Science Foundation of China (No. 31872268) and the doctoral research start-up fund of Jiangxi Agricultural University (No. 9232310345).

Author contributions

All authors have contributed equally.

Author ORCIDs

Qidi Zhu  <https://orcid.org/0000-0001-8187-1286>

Fuming Shi  <https://orcid.org/0000-0002-4885-9012>

Data availability

All of the data that support the findings of this study are available in the main text.

References

- Bian X, Shi FM (2016) Contribution to the Chinese subfamily Rhaphidophorinae Walker, 1869 (Orthoptera: Rhaphidophoridae: Rhaphidophorinae): new additions to the genera *Eurhaphidophora* and *Stonychophora*. *Zootaxa* 4109(1): 46–58. <https://doi.org/10.11646/zootaxa.4109.1.4>
- Cigliano MM, Braun H, Eades DC, Otte D (2024) Orthoptera Species File. Version 5.0/5.0 <http://Orthoptera.SpeciesFile.org> [Accessed on 20 May 2024]
- Dawwrueng P, Gorochov AV, Tanomtong A, Suwannapoom C (2020) Contribution to the knowledge of Rhaphidophorinae (Orthoptera: Ensifera: Rhaphidophoridae) from Thailand: three genera *Neorhaphidophora*, *Eurhaphidophora* and *Minirhaphidophora*. *Zootaxa* 4853(2): 235–253. <https://doi.org/10.11646/zootaxa.4853.2.5>
- Dawwrueng P, Gorochov AV, Pinkaew N, Vitheepradit A (2023) Review of the genus *Eurhaphidophora* Gorochov, 1999 (Orthoptera: Ensifera: Rhaphidophoridae) from Thailand, with description of a new species. *Zootaxa* 5278(2): 351–362. <https://doi.org/10.11646/zootaxa.5278.2.7>
- Gorochov AV (1999) Data on fauna and taxonomy of Stenopelmatoidea (Orthoptera) from Indochina and some other territories: II. *Entomological Review* 79(3): 262–278.
- Gorochov AV (2010) New species of the families Anostostomatidae and Rhaphidophoridae (Orthoptera: Stenopelmatoidea) from China. *Far Eastern Entomologist* 206: 1–16.
- Gorochov AV (2011) Contribution to the fauna and systematics of the Stenopelmatoidea (Orthoptera) of Indochina and some other territories: IX. *Entomological Review* 91(1): 71–89. <https://doi.org/10.1134/S0013873811010064>
- Gorochov AV (2012) Contribution to the knowledge of the fauna and systematics of the Stenopelmatoidea (Orthoptera) of Indochina and some other territories: X. *Entomological Review* 92(7): 747–772. <https://doi.org/10.1134/S0013873812070032>
- Gorochov AV, Storozhenko SY (2015) New and little-known taxa of the tribe Diestramimini (Orthoptera: Rhaphidophoridae: Aemodogryllinae) from Southeast Asia. Part 1. *Zoosystematica Rossica* 24(1): 48–84. <https://doi.org/10.31610/zsr/2015.24.1.48>
- Lu X, Huang X, Bian X (2022) Contribution to the Chinese subfamily Rhaphidophorinae Walker, 1869 (Orthoptera: Rhaphidophoridae) V: two new species of *Eurhaphidophora*. *Zootaxa* 5093(3): 392–396. <https://doi.org/10.11646/zootaxa.5093.3.7>
- Qin YY, Jiang H, Liu XW, Li K (2018) A new genus of Rhaphidophorinae (Orthoptera, Rhaphidophoridae) from China. *Zootaxa* 4500(2): 179–194. <https://doi.org/10.11646/zootaxa.4500.2.2>
- Zhu QD, Shi FM, Zhou ZJ (2022) Notes on the genus *Microtachycines* Gorochov, 1992 and establishment of a new genus from China (Rhaphidophoridae: Aemodogryllinae). *European Journal of Taxonomy* 817: 1–10. <https://doi.org/10.5852/ejt.2022.817.1757>

Taxonomic diversity of amphibians (Amphibia, Anura) and reptiles (Reptilia, Testudines, Squamata) in a heterogeneous landscape in west-central Mexico: a checklist and notes on geographical distributions

Verónica Carolina Rosas-Espinoza¹, Eliza Álvarez-Grzybowska¹, Arquímedes Alfredo Godoy González¹, Ana Luisa Santiago-Pérez², Karen Elizabeth Peña-Joya³, Fabián Alejandro Rodríguez-Zaragoza¹, Leopoldo Díaz Pérez¹, Francisco Martín Huerta Martínez⁴

- 1 *Laboratorio de Ecología Molecular, Microbiología y Taxonomía (LEMITAX), Departamento de Ecología Aplicada,, Centro Universitario de Ciencias Biológicas y Agropecuarias, Universidad de Guadalajara, Camino Ramón Padilla Sánchez 2100, CP 45200, Zapopan, Jalisco, Mexico*
 - 2 *Departamento de Producción Forestal, Centro Universitario de Ciencias Biológicas y Agropecuarias, Universidad de Guadalajara, Camino Ramón Padilla Sánchez 2100, CP 45200, Zapopan, Jalisco, Mexico*
 - 3 *Laboratorio de Ecología, Paisaje y Sociedad, Centro Universitario de la Costa, Universidad de Guadalajara, Puerto Vallarta 48280, Jalisco, Mexico*
 - 4 *Centro de Estudios en Interacciones Ecológicas, Departamento de Ecología, Centro Universitario de Ciencias Biológicas y Agropecuarias, Universidad de Guadalajara, Camino Ramón Padilla Sánchez 2100, CP 45200, Zapopan, Jalisco, Mexico*
- Corresponding author: Francisco Martín Huerta Martínez (martin.huerta@academicos.udg.mx)



Academic editor: Uri García-Vázquez
Received: 8 March 2024
Accepted: 18 July 2024
Published: 2 September 2024

ZooBank: <https://zoobank.org/6B1977D8-A2B0-4CCA-A3BE-76E876AE0C38>

Citation: Rosas-Espinoza VC, Álvarez-Grzybowska E, Godoy González AA, Santiago-Pérez AL, Peña-Joya KE, Rodríguez-Zaragoza FA, Díaz Pérez L, Huerta Martínez FM (2024) Taxonomic diversity of amphibians (Amphibia, Anura) and reptiles (Reptilia, Testudines, Squamata) in a heterogeneous landscape in west-central Mexico: a checklist and notes on geographical distributions. ZooKeys 1211: 29–55. <https://doi.org/10.3897/zookeys.1211.122565>

Copyright:

© Verónica Carolina Rosas-Espinoza et al.
This is an open access article distributed under terms of the Creative Commons Attribution License (Attribution 4.0 International – CC BY 4.0).

Abstract

In Mexico, land use changes have significantly impacted the diversity of amphibians and reptiles in a negative way. In light of this, we evaluate the alpha and beta components of the taxonomic diversity of amphibians and reptiles in a heterogeneous landscape in west-central Mexico. Additionally, we provide a checklist of amphibian and reptile species recorded over nine years of observations within the studied landscape and surrounding areas. The land cover/use types with the highest species richness and alpha taxonomic diversity differed between amphibians and reptiles. Overall beta taxonomic diversity was high for both groups, but slightly higher in reptiles. This taxonomic differentiation mainly corresponded to a difference in the turnover component and was greater in pristine habitats compared to disturbed ones. The checklist records 20 species of amphibians (ten of which are endemic) and 48 of reptiles (30 endemics). Additionally, the study expands the known geographical distribution range of one species of frog and three species of snakes. Our findings suggest that heterogeneous landscapes with diverse land cover/use types can provide essential habitats for the conservation of amphibian and reptile species.

Key words: Crops, herpetofauna, Jalisco state, native vegetation, range extension

Introduction

Amphibians and reptiles are abundant and diverse components of terrestrial and freshwater ecosystems, serving various ecological functions (Pough et al. 2004; Wells 2007). Mexico harbors 418 species of amphibians (AmphibiaWeb

2023; Ramírez-Bautista et al. 2023) and 1,044 of reptiles (Ramírez-Bautista et al. 2023; Uetz 2024), which account for 4.9% of the world's amphibians and 8.9% of its reptiles. Besides, 65% of the amphibians and 57% of the reptiles are endemic to Mexico, occurring predominantly in the Trans-Mexican Volcanic Belt and the Balsas Depression (Ochoa-Ochoa and Flores-Villela 2006).

Human pressure on natural environments has been intensifying mainly with agricultural landscapes becoming increasingly dominant. Land-use changes threaten biodiversity, primarily through habitat loss and degradation (Fischer and Lindenmayer 2007; Sayer et al. 2013; Davison et al. 2021). Amphibians and reptiles have very distinct physiologies, biologies, and ecological traits (Pough et al. 2004; Wells 2007). As a result, they tend to differ in their responses to environmental disturbances (Koleff and Guyer 2008). Particularly amphibians are often more susceptible to these changes due to their permeable skin, and their communities can show significant shifts in taxonomic and functional diversity (Ernst et al. 2006; Ernst and Rödel 2008). In disturbed environments, amphibian and reptile communities are less diverse than in pristine or protected ones mainly due to microhabitat loss, lack of food (Gardner et al. 2007; Trimble and Aarde 2014; Thompson et al. 2015) competition, predation, spread of diseases from invasive species (Bucciarelli et al. 2014; Kraus 2015; Falaschi et al. 2020), in addition to habitat alteration and hybridization (Falaschi et al. 2020). Also, disturbed habitats can lead to significant species turnover at the landscape scale, favoring generalist or invasive species while also sustaining a few native species (Wanger et al. 2010).

One approach used to quantify the taxonomic complexity of species assemblages at the local level and to evaluate the response of organisms to spatial gradients and differentiation at the regional level has been to analyze the alpha (local) and beta (turnover) diversity of these assemblages (Baselga 2010; Jost et al. 2011). The more traditional diversity measures (e.g., species richness, Shannon index, Jaccard index, etc.) of alpha and beta diversity (often referred to as ecological) assume that all species carry the same weight (Magurran 2004; Chao et al. 2010), and thus fail to consider taxonomic diversity of species and their evolutionary past (Gaston and Spicer 2004). As a result, methods have been developed to add this dimension (Warwick and Clarke 1995). Alpha and beta diversity can be assessed by incorporating supra-specific levels associated with each species (e.g., genus, family, and order) to capture information on their phylogenetic diversity and their ecological and evolutionary histories (Warwick and Clarke 1998; Nipperess et al. 2010; Carvalho et al. 2012). This approach can even be used with large assemblages that lack species-level phylogenies (Izsak and Price 2001; Carvalho et al. 2012).

The alpha component of taxonomic diversity consists in the distinctiveness of taxa which measures the degree of taxonomic relatedness of species present in each sample, a reflection of the ecological and evolutionary mechanisms that have contributed to taxonomic composition (Warwick and Clarke 1998). Beta taxonomic diversity can be divided into turnover (replacement) and differences in richness (loss or gain) components (Baccaro et al. 2007; Carvalho et al. 2012). The measure of differences in richness is useful to understand how habitat conditions affect communities and, when assessing highly heterogeneous landscapes, the patchiness of the species that inhabit them (Melo et al. 2009; Ochoa-Ochoa et al. 2014).

Our understanding of taxonomic diversity of amphibians and reptiles in Mexico has been enriched by several studies. Cruz-Elizalde et al. (2014) showed that the richest environments for reptile species in the Chihuahuan Desert were not taxonomically diverse. Hernández-Salinas et al. (2023), who measured taxonomic and functional diversity in amphibian and reptile communities in six vegetation types in Durango, found that vegetation types that had more complex family and genera networks differed between the two groups. Díaz de la Vega-Pérez et al. (2019) recorded high amphibian and reptile dissimilarities between habitats at La Malinche National Park. Many have reported high overall values of taxonomic beta diversity for amphibians and reptiles compared to other vertebrate groups (Koleff et al. 2008; Ochoa-Ochoa et al. 2014; Calderón-Patrón et al. 2016). However, between these two groups Calderón-Patrón et al. (2016) recorded higher beta diversity (species) and beta taxonomic diversity (species and associated taxonomic levels) for reptiles and Ochoa-Ochoa et al. (2014) obtained this same result particularly for the central and northwest regions of Mexico.

Although in Mexico amphibians and reptile species have been documented as disappearing because of human activity such as habitat fragmentation, pollution, pet trade, invasive species, emerging diseases, and global warming, they are still the less well-studied vertebrate groups (Ceballos et al. 2015). In this study, we report on 1) the spatial variation of alpha (Warwick and Clarke 1998) and beta (Carvalho et al. 2012) taxonomic diversity of amphibians and reptiles in a heterogeneous landscape in west-central Mexico, and 2) a checklist including some species' geographic range extensions. We first hypothesized that species richness and alpha taxonomic diversity of amphibians and reptiles would be highest in the same habitats across the heterogeneous landscape. Secondly, we predicted a lower species richness and taxonomic diversity in the land use types of corn and sugarcane crops for both groups and, for amphibians, higher species richness, and alpha taxonomic diversity in the riparian habitat surrounded by tropical dry forest (RH-TDF). We made these predictions because habitat complexity, the presence of permanent water (especially for amphibians), and less habitat disturbance encourage patterns of higher species richness and taxonomic distinctiveness. Thirdly, we expected beta diversity to be high for both groups due to the heterogeneity of the landscape, and for it to be higher for amphibians than reptiles with a strong turnover component due to their lower mobility as reported in previous work. Finally, we predicted higher dissimilarities between the land use types and the land cover types for both groups.

Materials and methods

Study area

The study area consisted of different land cover/use types within the municipalities of Aqualulco de Mercado (main population 20°42'6.84"N, 103°58'24.96"W) and Teuchitlán (20°40'59.88"N, 103°50'51.72"W), both located in the west-central state of Jalisco, México (Fig. 1). The territory of Aqualulco de Mercado ranges in elevation between 1280 and 2600 m a.s.l. The weather is semi-warm / semi-humid, with a mean annual temperature of 20.5 °C and average minimum

and maximum temperatures of 7.9 °C and 33.3 °C, respectively. The average annual precipitation is 900 mm, with a cumulative average of 643.27 mm (IIEG 2023a). In Teuchitlán, the elevation ranges between 1247 and 2392 m a.s.l. The weather is semi-dry / semi-warm, with a mean annual temperature of 21.2 °C and average maximum and minimum temperatures of 33.5 °C and 8.4 °C, respectively (IIEG 2023b). Mean annual precipitation is 948 mm, with an average accumulated precipitation of 634.56 mm; rain occurs mainly in the summer, and dry periods happen during spring and winter (IIEG 2023b). We selected the following ten main land cover/use types (sampling sites): sugar cane field (SCF), riparian habitat surrounded by crops (RH-C), cornfield (C), highly perturbed tropical dry forest (HPTDF), tropical dry forest (TDF), riparian habitat surrounded by tropical forest (RH-TDF), riparian habitat surrounded by temperate forest (RH-TF), secondary vegetation surrounded by temperate forest (SV-TF), oak forest (OF) and pine-oak forest (POF) (Fig. 1).

The municipalities of Ahualulco de Mercado and Teuchitlán have similar territorial areas of 235.25 and 211.18 square kilometers, respectively. The two neighboring municipalities share a broad valley. The predominant land use types are agricultural and livestock activity, covering 60% of its surface, followed by secondary vegetation at 17% (IIEG 2023a, 2023b). The SCF land use type was located between 1258 and 1390 m a.s.l. Both municipalities are important for sugarcane production in Jalisco (SIAP 2018). The C was found on the lower slopes of the mountains between 1250 and 1440 m a.s.l. Clearing events for agriculture have occurred in these areas since pre-Columbian times. The predominant crops are rainfed corn, *Zea mays*, and *Agave tequilana* (Santiago-Pérez 2023).

The RH-C land cover type is found between 1265 and 1270 m a.s.l. along a stretch of the Teuchitlán River. The dominant tree species were *Salix humboldtiana*, *Fraxinus uhdei*, *Ficus insipida*, *Lysiloma acapulcense*, *Baccharis salicifolia*, *Salix taxifolia*, *Arundo donax* and *Scirpus californicus*. One riverbank is used for crops, the other for recreational activities. HPTDF, with a high disturbance level, was found between 1200 and 1500 m a.s.l., and the dominant tree species were *Acacia farnesiana*, *A. pennatula*, *Prosopis laevigata*, and *Pithecellobium dulce*. The TDF was found between 1200 and 1700 m a.s.l. and included *Bursera bipinnata*, *Ipomoea murucoides*, *L. acapulcense*, *Opuntia fuliginosa*, and *Tecoma stans* as dominant species (García-Martínez and Rodríguez 2018). The TDF had both temporary and permanent water bodies, but some areas were deforested, so C and SCF were established instead (Rosas-Espinoza et al. 2022). The TDF in the archaeological zone of Guachimontones (1300 to 1482 m a.s.l.) had frequent *Bursera fagaroides*, *B. bipinnata*, *B. palmeri*, *Ipomoea intrapilosa*, *Heliocarpus terebinthinaceus*, *Guazuma ulmifolia*, *Eysenhardtia polystachya*, and *Leucaena leucocephala* (Santiago-Pérez 2023).

The RH-TDF had permanent streams. It was found between 1450 and 1750 m a.s.l. and was dominated by *L. acapulcense*, *Lippia umbellata*, *Eysenhardtia polystachya* and *I. intrapilosa*. The RH-TF had both permanent and temporal streams. It was located between 1500 and 1800 m a.s.l., and the dominant tree species were *Salix bonplandiana*, *Quercus magnoliifolia*, *Q. splendens*, *Q. obtusata*, *Aiouea pachypoda*, and *Oreopanax peltatus* (García-Martínez and Rodríguez 2018). The dominant tree species in SV-TF (1550–1750 m a.s.l.) were *I. intrapilosa*, *T. stans*, *A. farnesiana*, *Verbesina greenmanii*, *Solanum madrense*,

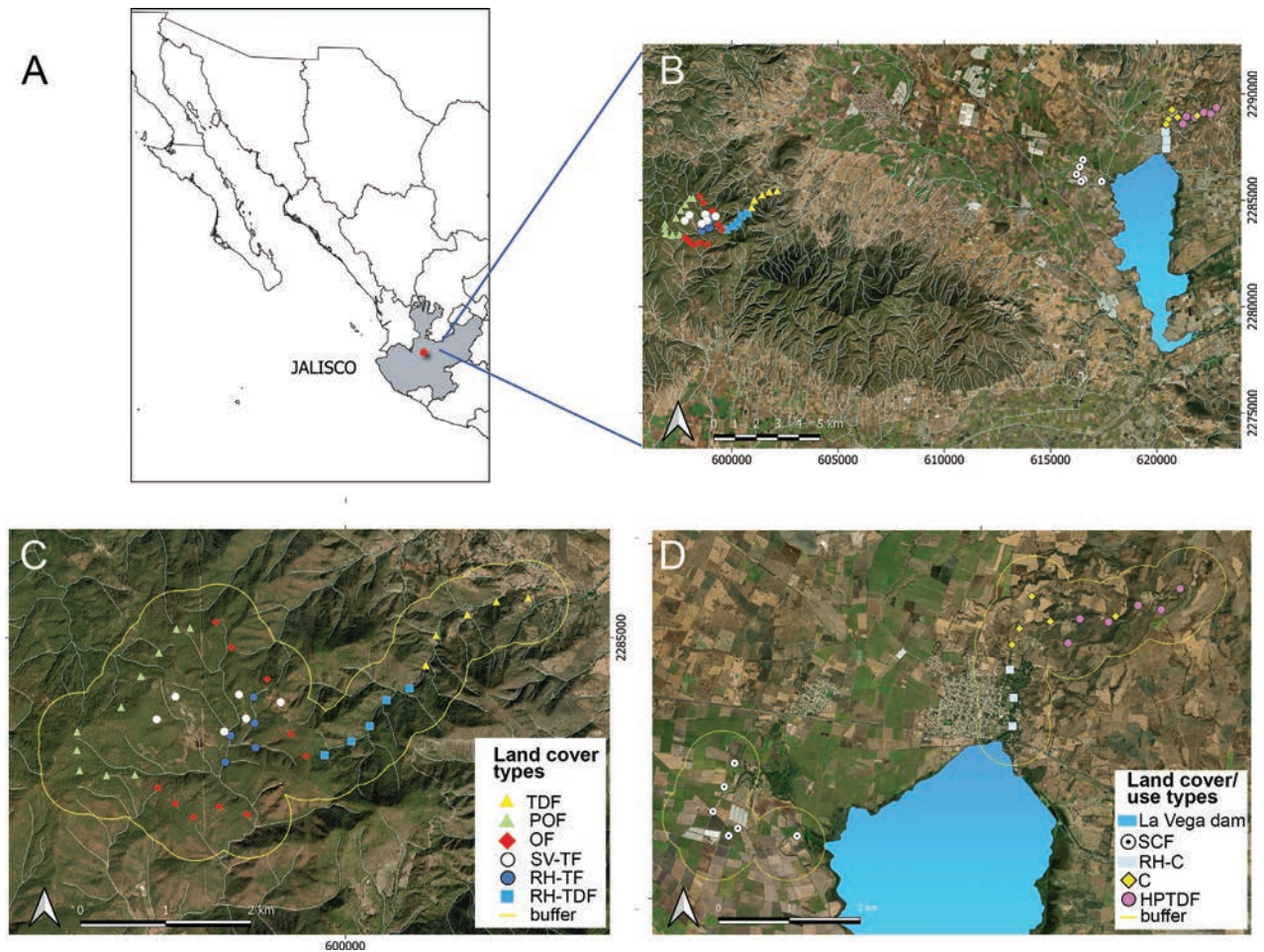


Figure 1. A study area in Jalisco, Mexico B sampling points in the landscape. Sampling plots (C, D). Codes: sugar cane field (SCF), riparian habitat surrounded by crops (RH-C), cornfield (C), highly perturbed tropical dry forest (HPTDF), tropical dry forest (TDF), riparian habitat surrounded by tropical dry forest (RH-TDF), riparian habitat surrounded temperate forest (RH-TF), secondary vegetation surrounded by temperate forest (SV-TF), oak forest (OF) and pine-oak forest (POF) (modified after Rosas-Espinoza et al. 2022).

and *Senna foetidissima* (García-Martínez and Rodríguez 2018). An artificial pond had water yearly (Rosas-Espinoza et al. 2022). The OF was found between 1500 and 1900 m a.s.l., with *Quercus resinosa*, *Q. magnoliifolia*, *Q. castanea*, and *Q. gentry* as the dominant tree species. The POF was found between 1800 and 2590 m a.s.l. The predominant tree species were *Q. resinosa*, *Pinus oocarpa*, *P. devoniana*, and *P. lumholtzii* (García-Martínez and Rodríguez 2018).

Amphibian and reptile surveys for taxonomic diversity measurements

We established circular diurnal (500 m² each one) and rectangular nocturnal (10,000 m²) survey plots in each land cover/use type. The diurnal plots were separated 400 m of distance from each one. At each plot an intensive unrestricted visual search was carried out on the microhabitats preferred by these reptile species in each point count (i.e., logs and rocks). We recorded all individuals observed, and when possible, measured and photographed them. They were later released at the capture site. We conducted nine, monthly, samplings of the amphibian and reptile communities from July 2011 to August 2012 in

TDF, RH-TDF, RH-TF, SV-TF, OF, and POF. Additionally, we surveyed both groups of taxa for eight months from September 2012 to September 2013 in SCF, RH-C, C, and HPTDF. Once a month during the day, we surveyed 12,500 m² in TDF, RH-TDF, and RH-TF; 15,000 m² in SCF, C, and HPTDF; 17,500 m² in SV-TF; 25,000 m² in OF and POF; and 22,500 m² in RH-C. And at night we surveyed 10,000 m² in each land cover/use type.

Amphibian and reptile checklist and distribution extensions

We included in the checklist all species whose presence within the study area or surroundings was confirmed by direct observation between August 2011 and December 2020. To corroborate a species' identity, we took and deposited photographs in the Colección Herpetológica of the Museo de Zoología in the Facultad de Estudios Superiores Zaragoza, Universidad Autónoma de México. We followed Frost (2023) for the taxonomy of amphibians, Uetz (2024) and Zaher et al. (2019) for that of the reptiles, and CONABIO (2023) for common names. We considered various scientific sources to determine the endemism of amphibians and reptiles (e.g., Cruz-Sáenz et al. 2017; Johnson et al. 2017; Frost 2023; AmphibiaWeb 2023; Ramírez-Bautista et al. 2023). We consulted the Mexican government threatened species list NOM-059 (SEMARNAT 2019), IUCN (2024) and Environmental Vulnerability Score (EVS; Wilson et al. 2013a, 2013b) to establish each species' conservation status. We used the species distribution maps published by the Red List of Threatened Species of the IUCN (2024) and records from Global Biodiversity Information Facility (GBIF). We measured the distance of our records to the closest observations in the region. We determined a species range extension when an observation was made at least 20 km in a straight line from the nearest record.

Statistical analysis of the taxonomic diversity

We generated monthly matrices of presence-absence of amphibian and reptile species. We determined sampling effort in each land/use type and the whole study area using sample-based rarefaction curves using the non-parametric estimators Chao 2, Jackknife 1, and Jackknife 2. All rarefaction curves were built using 10,000 randomizations without replacement. We performed these analyses using EstimateS 9.1.0 (Colwell 2013).

Alpha taxonomic diversity

We measured the alpha component of taxonomic diversity by computing taxonomic distinctness. It takes into consideration the degree of taxonomic relatedness among species in each sample as a reflection of the ecological and evolutionary mechanisms that contribute to taxonomic composition (Warwick and Clarke 1998). To quantify the degree of taxonomic relatedness among species in the various land covers/use types, we calculated the average taxonomic distinctness (Delta, Δ^+) and its variation (Lambda, Λ^+) (Warwick and Clarke 1995; Clarke et al. 2014) per land cover/use type for all amphibians and reptiles' assemblages. We built a five-level taxonomic aggregation matrix that included species, genus, family, order, and phylum. We used the same weight

for all taxonomic levels ($\omega = 1$). We created the models with a 95% confidence interval by carrying out 10,000 permutations and with a ratio of 1.2 species (Clarke and Warwick 1998). All analyses ($\Delta +$ and $\Lambda +$) were performed using PRIMER 7.0.21 and PERMANOVA +1 (Clarke and Gorley 2015).

Beta taxonomic diversity

We measured the beta component of taxonomic diversity by calculating and partitioned taxonomic beta into turnover ($\beta.3$) and differences in richness ($\beta.rich$) components following Baccaro et al. (2007) and Carvalho et al. (2012). Bcc represents the total dissimilarity ($1 - \text{Jaccard's similarity coefficient}$) split between the components of dissimilarity ($\beta.3$) and dissimilarity due to differences in richness ($\beta.rich$). We considered four supra-specific levels (species, genus, family, and order) for both groups. We assessed taxonomic beta diversity and partitioning of components using the "BAT" package (Cardoso et al. 2024) and Carvalho et al. (2012) script. We performed these analyses using the R studio program R-project 4.1.1 (R Development Core Team 2022).

Results

We recorded 20 species of amphibians and 39 of reptiles in the study area between August 2011 and September 2013. The average sampling effort for amphibians was 81.8% of representativity for the study area and that for reptiles, 80.5% (Fig. 2). The average sampling effort varied between 61% and 95.6% of representativity between all land cover/use types for amphibians, and between 65.3% and 97.6% for reptiles (Suppl.material 1: table S1).

Alpha taxonomic diversity

Numerically, we recorded the lowest amphibian species richness in POF (three species) compared to the highest richness in HPTDF (eight), RH-C (nine), and RH-TDF (ten). Medium species richness was recorded in OF (five), TDF (five), RH-TF (six), CO (six), SCF (seven), and SV-TF (seven). In contrast, we recorded the lowest species richness for reptiles in RH-TF (five), CA (seven), C (seven), and POF (nine). SV-TF (18) had the highest richness. Medium species richness was registered in RH-TDF (10), OF (12), HPTDF (12), RH-C (13), and TDF (14).

The average taxonomic distinctness for amphibians and reptiles had all the $\Delta +$ and $\Lambda +$ values within the probability funnels ($p > 0.05$) (Fig. 3), which indicates that the alpha taxonomic richness of amphibians and reptiles was within the model's expectations.

Beta taxonomic diversity

The taxonomic beta diversity of amphibians and reptiles was high overall in both groups, being slightly higher in reptiles ($\beta_{multi} = 0.70$) than in amphibians ($\beta_{multi} = 0.60$). The turnover component ($\beta.3 = 0.43$ and $\beta.3 = 0.32$, respectively) was the most significant contributor to taxonomic differentiation in all comparisons. In turn, the two groups had a low contribution from the differences in richness component ($\beta.rich = 0.27$ for reptiles and $\beta.rich = 0.27$ for amphibians) (Fig. 4A, C).

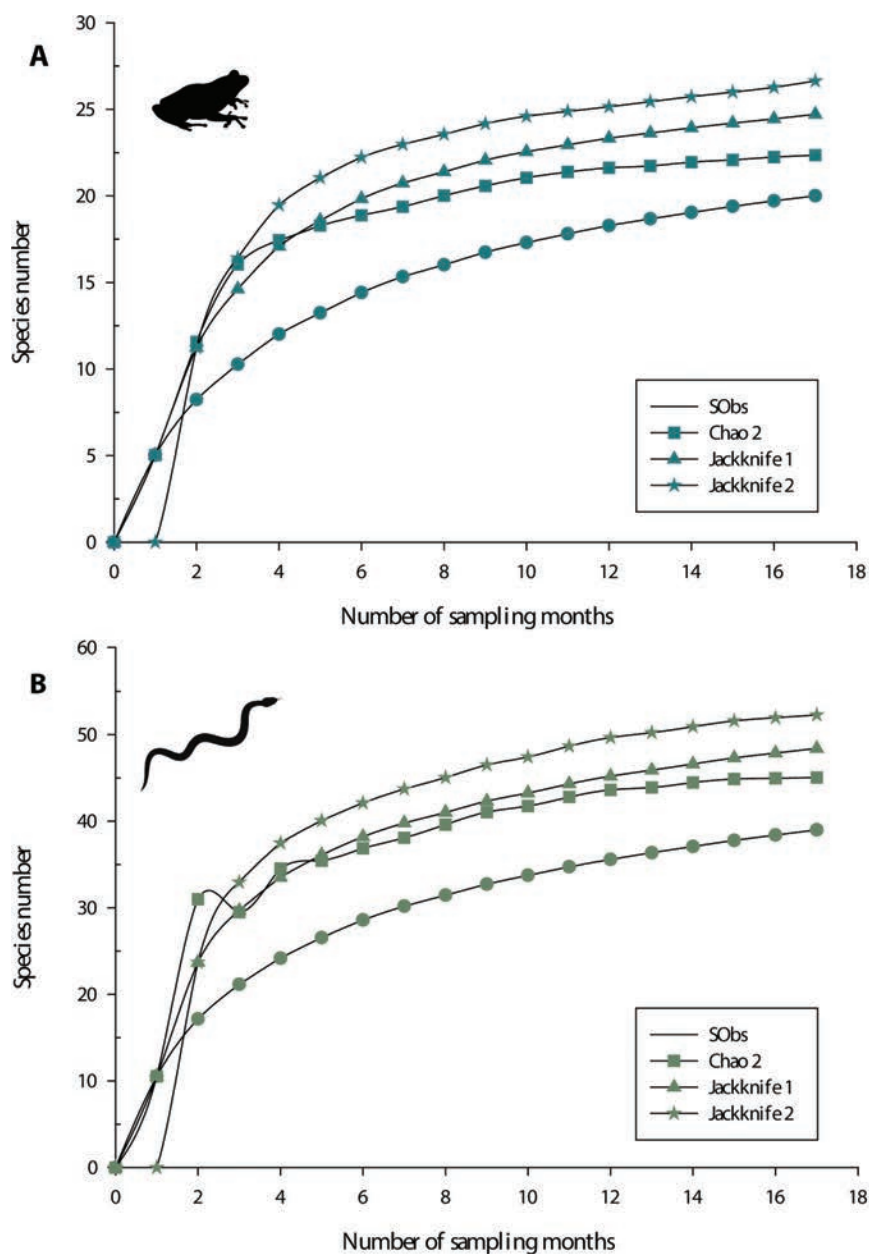


Figure 2. Sample-based rarefaction curves for amphibians and reptiles generated using presence-absence data, showing observed and expected species for the different land cover/use types using non-parametric estimators. Codes: sugar cane field (SCF), riparian habitat surrounded by crops (RH-C), cornfield (C), highly perturbed tropical dry forest (HPTDF), tropical dry forest (TDF), riparian habitat surrounded by tropical forest (RH-TDF), riparian habitat surrounded temperate forest (RH-TF), secondary vegetation surrounded by temperate forest (SV-TF), oak forest (OF), pine-oak forest (POF), and number of species observed (Sobs).

In contrast, amphibians and reptiles had divergent patterns in regard to beta diversity (both turnover and richness differences) in pairwise comparisons between land cover/use types. Only POF and OF showed differences in richness in amphibians and reptiles without the turnover component (Fig. 4B, D).

For amphibians, the pairwise comparisons with the highest beta taxonomic diversity were between POF and SCF (0.92), POF and RH-C (0.86), and TDF and SCF (0.82), while the lowest were between RH-C and SCF (0.19), SV-TF and

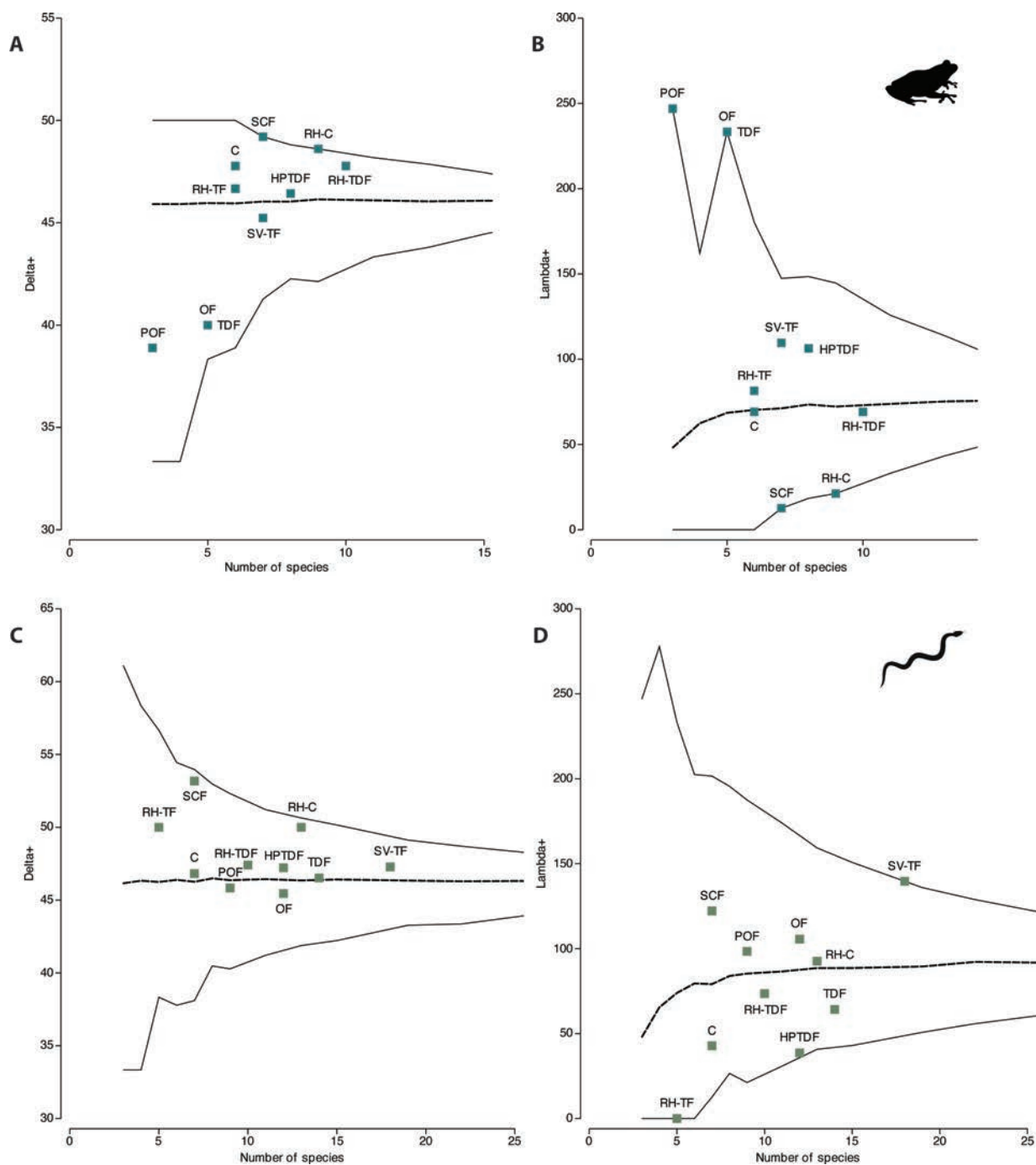


Figure 3. Average taxonomic distinctness ($\Delta+$) and its variance ($\Lambda+$) by land cover/use type of **A** amphibians and **B** reptiles in a heterogeneous landscape at west-central Mexico.

RH-TF (0.26), and RH-TF and TDF (0.35). The comparisons with the highest turnover were between SV-TF and C (0.69), SV-TF and SCF (0.81), RH-TF and SCF, and SV-TF and HPTDF (0.77 respectively) (Fig. 4B). In these comparisons the component with the greatest contribution to differentiation was differences in richness in POF and RH-TDF (0.77), POF and RH-C (0.86), and POF and HPTDF (0.73). Some of the comparisons consisted only in the replacement component, like HPTDF and SCF (0.60), SV-TF and C (0.69), and OF and TDF (0.50). Likewise, RH-C and SCF (0.19), POF and OF (0.33), POF-SV-TF (0.52), and POF and RH-TDF (0.77) were only represented by differences in richness.

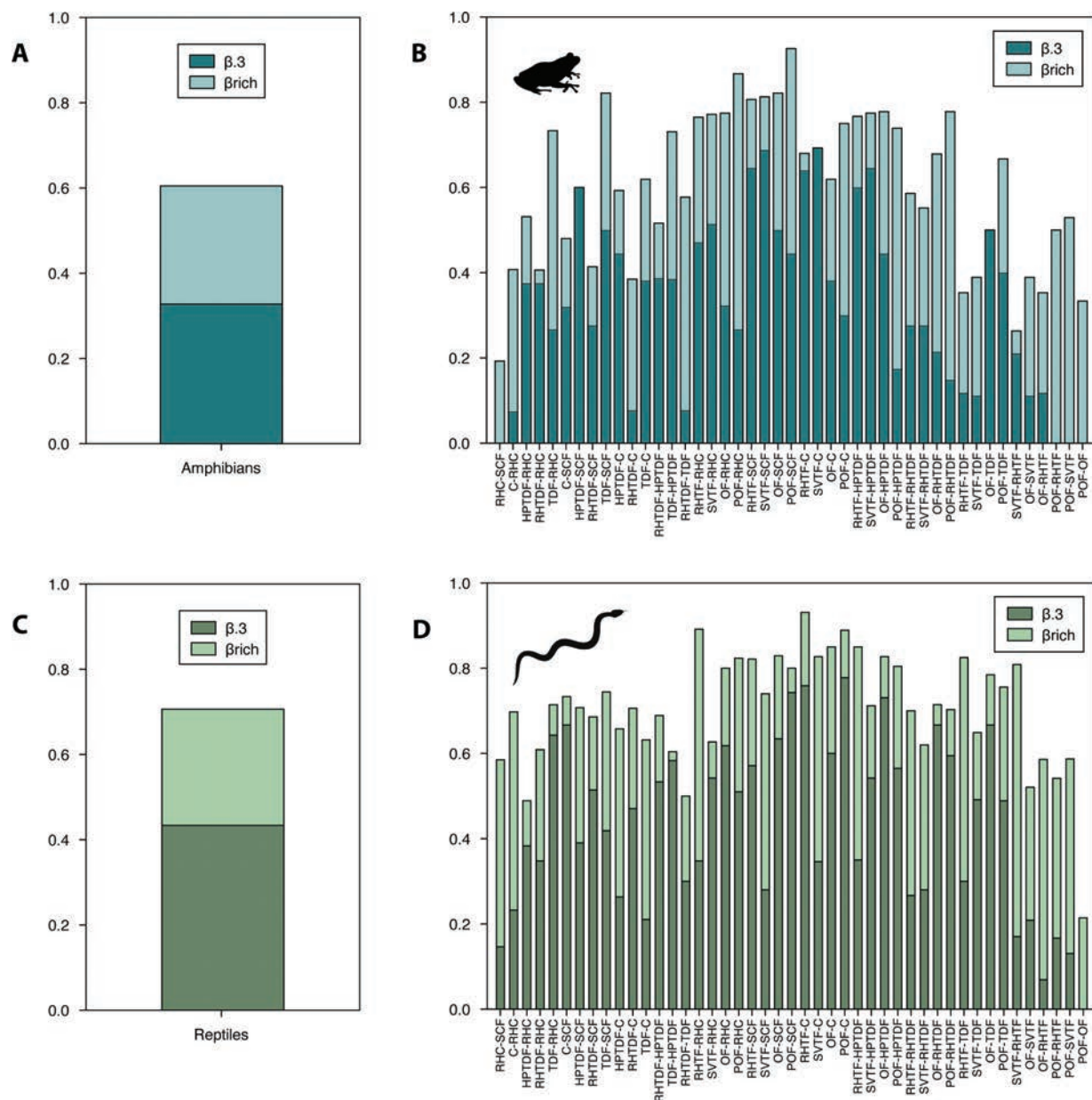


Figure 4. Taxonomic beta diversity of amphibians and reptiles considering the turnover ($\beta.3$) and differences in richness ($\beta.rich$) components by land cover/use types **A** total and **B** paired beta diversity of amphibians; and **C** total and **D** paired beta diversity of reptiles. Codes: sugar cane field (SCF), riparian habitat surrounded by crops (RH-C), cornfield (C), highly perturbed tropical dry forest (HPTDF), tropical dry forest (TDF), riparian habitat surrounded by tropical forest (RH-TDF), riparian habitat surrounded temperate forest (RH-TF), secondary vegetation surrounded by temperate forest (SV-TF), oak forest (OF) and pine-oak forest (POF).

In relation to land cover/use types taxonomic beta diversity among reptiles was highest when comparing RH-TF and C (0.17), RH-TF and RH-C (0.54), and POF-C (0.11). The comparisons with the lowest values were POF-OF (0.21), HPTDF and RH-C (0.10), RH-TDF and TDF (0.20). The comparisons with the highest contribution of turnover component were between POF-C (0.11), RH-TF and C (0.17), and POF-SCF (0.05) comparisons, and for differences in richness component were between SV-TF and RH-TF (0.63), RH-TF and RH-C (0.54), and RH-TF-TDF (0.52). Similarly to amphibians, the comparison between POF-OF (0.21) was uniquely represented by differences in richness (Fig. 4D).

Amphibian checklist and geographic expansion distributions

During nine years of observations, we recorded 20 species of amphibians belonging to 14 genera, nine families, and one order. The families with the highest species richness were Hylidae (seven species), Craugastoridae (three species) and Ranidae (three species). Ten of these species are endemic and under some protection category. Four species are under the Special Protection category, and one is under the Threatened category (SEMARNAT 2019). IUCN threat categories included two species that are considered Endangered and one, Vulnerable (IUCN 2024). With respect to the Environmental Vulnerability Score (EVS), ten species are classified under low (L) vulnerability, seven species under medium (M), and one under high (H) vulnerability categories (Table 1).

We documented extensions in the known distribution range of *Sarcohyala hapsa* (Suppl.material 1: fig. S1A). *Sarcohyala hapsa* is endemic to western Mexico (Campbell et al. 2018). It was observed in September 2011 in the RH-TF at 1842 m a.s.l. (20°38,58'N, 104°3,14'W). This species was recently split from the widespread Mexican hylid *Sarcohyala bistincta* (Campbell et al. 2018). This extends the known distribution by 38 km from its closest record, base La Ciénega, Sierra de Quila (Rosas-Espinoza et al. 2013; GBIF 2023a) (Suppl.material 1: fig. S2).

Reptile checklist and geographic expansion distributions

We recorded 48 species of reptiles belonging to 34 genera, 17 families, and two orders (Table 1). The families with the highest species richness were Colubridae (11 species), Phrynosomatidae (eight species), Dipsadidae (seven species) and Natricidae (five species). More than half of these species are endemic to Mexico (62.5%). All the species are native to Mexico except *Hemidactylus frenatus* and *Indotyphlops braminus*, which are native to the Eastern Hemisphere. According to the Mexican species protection list, 21 species are in a category of risk, of which 13 are under Special protection and eight are Threatened (SEMARNAT 2019). IUCN threat categories classify two species as Endangered, one as Vulnerable, and two as Near Threatened (IUCN 2024). According to the EVS (Wilson et al. 2013a), 12 species are under low (L) vulnerability, 18 species under medium (M), and 14 are below the high (H) vulnerability categories (Table 1).

We documented extensions in the known distribution range of three species of reptiles. *Lampropeltis ruthveni* was observed in September 2011 in SV-TF (20°40'01"N, 103°52'23"W) (Suppl.material 1: fig. S1B). There are a few records of this species in the Trans-Mexican Volcanic Belt. Its distribution is extended by at least 44 km from its closest known record near Sierra de Quila, Jalisco (GBIF 2023b) (Suppl.material 1: fig. S3A).

Thamnophis copei is endemic to Mexico (Suppl.material 1: fig. S1C). It was observed in September 2012 at HPTDF (20°41,52'N, 103°49,35'W). This extends the known distribution range of the species by 39 km from La Quemada, Jalisco (GBIF 2023c) (Suppl.material 1: fig. S3B).

Imantodes gemmistratus was observed in September 2012 in HPTDF (20°41',41"N, 103°50'33"W) (Suppl.material 1: fig. S1D). This extends its known distribution by 36 km from 2.3 km presa El Texcalame, (GBIF 2023d) (Suppl. material 1: fig. S3C).

Table 1. Checklist of amphibians and reptiles (August 2011 to December 2020) present in the various land/use types in a heterogeneous landscape in west-central Mexico. Codes: sugar cane field (SCF), riparian habitat surrounded by crops (RH-C), cornfield (C), highly perturbed tropical dry forest (HPTDF), tropical dry forest (TDF), riparian habitat surrounded by tropical forest (RH-TDF), riparian habitat surrounded temperate forest (RH-TF), secondary vegetation surrounded by temperate forest (SV-TF), oak forest (OF), pine-oak forest (POF), endemic to Mexico (E), exotic (F), Special Protection (Pr), Threatened (A), Least Concern (LC), Near Threatened (NT), Vulnerable (VU), Endangered (EN), Low (L), Medium (M), High (H), records with distribution range extensions (*).

Taxonomic hierarchies and species	Common name	Endemism	Conservation status	SCF	RH-C	C	HPTDF	TDF	RH-TDF	RH-TF	SV-TF	OF	POF	Other land cover/use
AMPHIBIA														
Order Anura														
Craugastoridae														
<i>Craugastor cf. hobarthsmithi</i> (Taylor, 1937)	Smith's pigmy tropical frog	E	EN, LC, L		X	X	X	X						
<i>Craugastor occidentalis</i> (Taylor, 1941)	Taylor's Barking Frog	E	LC, M			X		X	X	X	X	X	X	
<i>Craugastor augusti</i> (Dugès, 1879)	Barking Frog		LC, L				X	X	X	X	X	X	X	
Eleutherodactylidae														
<i>Eleutherodactylus sp.</i>				X	X	X	X		X	X				
Bufonidae														
<i>Incilius occidentalis</i> (Camerano, 1879)	Pine Toad	E	LC, M								X	X	X	
<i>Rhinella horribilis</i> (Wiegmann, 1833)	Giant Marine Toad		L	X		X	X		X					
Hylidae														
<i>Exerodonta smaragdina</i> (Taylor, 1940)	Emerald Tree Frog	E	Pr, LC, M								X			
<i>Dryophytes arenicolor</i> (Cope, 1866)	Canyon Tree Frog		LC, L				X	X	X	X	X			
<i>Dryophytes eximius</i> (Baird, 1854)	Mountain Tree Frog	E	LC, M						X	X	X			
<i>Sarcohylla hapsa</i> * Campbell, Brodie, Caviedes-Solis, Nieto-Montes de Oca, Luján, Flores-Villela, García-Vázquez, Sarker & Wostl, 2018	Northern Streamside Tree Frog	E	Pr, LC, L							X				
<i>Smilisca baudinii</i> (Duméril & Bibron, 1841)	Common Mexican treefrog		LC, L											
<i>Smilisca fodiens</i> (Boulenger, 1882)	Lowland Burrowing Tree Frog		LC, L											
<i>Tlalocohyla smithii</i> (Boulenger, 1902)	Dwarf Mexican Tree Frog	E	LC, M											
Leptodactylidae														
<i>Leptodactylus melanonotus</i> (Hallowell, 1861)	Black Jungle-Frog		LC, L	X	X				X					
Microhylidae														
<i>Hypopachus variolous</i> (Cope, 1866)	Mexican Nar-row-mouthed Toad		LC, L						X					

Taxonomic hierarchies and species	Common name	Endemism	Conservation status	SCF	RH-C	C	HPTDF	TDF	RH-TDF	RH-TF	SV-TF	OF	POF	Other land cover/use
Phyllomedusidae														
<i>Agalychnis daenicolor</i> (Cope, 1864)	Mexican Giant Tree Frog	E	LC, M		X									
Ranidae														
<i>Rana cf. forreri</i> (Boulenger, 1883)	Forrer's leopard frog		Pr, LC, L						X					
<i>Rana neovolcanica</i> Hillis & Frost, 1985	Transverse Volcanic Leopard Frog	E	A, NT, M	X	X				X		X			
<i>Rana megapoda</i> Taylor, 1942	Big-footed Leopard Frog	E	Pr, VU, H											X
Scaphiropodidae														
<i>Spea multiplicata</i> (Cope, 1863)	Mexican Spadefoot		LC, L				X							
REPTILIA														
Orden Squamata														
Anguidae														
<i>Elgaria kingii</i> Gray, 1838	Arizona Alligator Lizard		Pr, LC, M				X			X		X	X	
Anolidae														
<i>Anolis nebulosus</i> (Wiegmann, 1834)	Clouded Anole	E	LC, M		X	X	X	X	X	X	X	X	X	
Geckonidae														
<i>Hemidactylus frenatus</i> Duméril & Bibron, 1836	Asian House Gecko	F												X
Iguanidae														
<i>Ctenosaura pectinata</i> (Wiegmann, 1834)	Mexican Spinytail Iguana	E	A, H	X	X		X	X	X		X			
Phrynosomatidae														
<i>Sceloporus dugesii</i> Bocourt, 1874	Duges' Spiny Lizard	E	LC, M			X	X							
<i>Sceloporus heterolepis</i> Boulenger, 1895	Dorsalkeel Spiny Lizard	E	LC, H				X	X	X	X	X	X	X	
<i>Sceloporus horridus</i> Wiegmann, 1834	Horrible Spiny Lizard		LC, M				X	X	X		X	X	X	
<i>Sceloporus nelson</i> Cochran, 1923	Nelson's Spiny Lizard	E	LC, M			X								
<i>Sceloporus torquatus</i> Wiegmann, 1828	Torquate Lizard	E	LC, M				X							
<i>Sceloporus spinosus</i> Wiegmann, 1828	Eastern Spiny Lizard	E	LC, M						X					
<i>Sceloporus utiformis</i> Cope, 1864	Antesator	E	LC, H						X	X	X	X	X	
<i>Urosaurus bicarinatus</i> (Duméril, 1856)	Tropical tree lizard	E	LC, M	X			X	X						

Taxonomic hierarchies and species	Common name	Endemism	Conservation status	SCF	RH-C	C	HPTDF	TDF	RH-TDF	RH-TF	SV-TF	OF	POF	Other land cover/use
Phyllodactylidae														
<i>Phyllodactylus lanei</i> Smith, 1935	Lane's Leaf-toed Gecko	E	LC, H				X							
Scincidae														
<i>Plestiodon dugesii</i> (Thomiot, 1883)	Duges' Skink	E	Pr, VU, H						X	X	X	X	X	
<i>Plestiodon callicephalus</i> (Bocourt, 1879)	Mountain Skink		LC, M				X	X						
Teiidae														
<i>Aspidoscelis costatus</i> (Cope, 1878)	Western Mexico Whiptail	E	Pr	X	X	X	X							
<i>Aspidoscelis communis</i> (Cope, 1878)	Colima Giant Whiptail	E	Pr, LC, M					X						
Boidae														
<i>Boa sigma</i> (Smith, 1943)	Boa		A, LC, M				X	X						
Colubridae														
<i>Masticophis mentovarius</i> (Duméril, Bibron & Duméril, 1854)	Neotropical Whip Snake	E	LC, L	X	X		X	X	X					
<i>Drymarchon melanurus</i> (Duméril, Bibron & Duméril, 1854)	Blacktail Cribo		LC, L	X	X		X			X				
<i>Lampropeltis ruthveni</i> * Blanchard, 1920	Ruthvens Kingsnake		A, NT, H		X		X				X		X	
<i>Leptophis diplotropis</i> (Günther, 1872)	Pacific Coast Parrot Snake	E	A, LC, H					X						
<i>Masticophis bilineatus</i> (Jan, 1863)	Sonoran Whipsnake		LC, M			X								
<i>Oxybelis aeneus</i> (Wagler, 1824)	Mexican Vine Snake		L			X		X						
<i>Pituophis deppei</i> (Duméril, 1853)	Mexican Bull Snake	E	A, LC, H				X	X						
<i>Senticolis triaspis</i> (Cope, 1866)	Green Rat Snake		LC, L	X			X							
<i>Sonora mutabilis</i> Stickel, 1943	Mexican Groundsnake	E	LC, H				X							
<i>Tantilla bocourti</i> (Günther, 1895)	Bocourt's Black-headed Snake	E	LC, L	X	X	X								
<i>Trimorphodon tau</i> Cope, 1870	Mexican Lyre Snake	E	LC, M				X	X						
Dipsadidae														
<i>Diadophis punctatus</i> (Linnaeus, 1766)	Ring-necked snake		LC, L		X		X							
<i>Hypsiglena torquata</i> (Günther, 1860)	Sinaloa Nightsnake		Pr, LC, L					X						
<i>Imantodes gemmistratus</i> * (Cope, 1861)	Central American Tree Snake		Pr, L				X							

Taxonomic hierarchies and species	Common name	Endemism	Conservation status	SCF	RH-C	C	HPTDF	TDF	RH-TDF	RH-TF	SV-TF	OF	POF	Other land cover/use	
<i>Leptodeira maculata</i> (Hallowell, 1861)	Southwestern Cat-eyed Snake	E	Pr, LC, L								X				
<i>Leptodeira splendida</i> Günther, 1885	Splendid Cat-eyed Snake	E	Pr, LC, H		X			X							
<i>Rhadinaea hesperia</i> Bailey, 1940	Western Graceful Brown Snake	E	LC, M				X				X				
<i>Rhadinaea taeniata</i> (Peters, 1863)	Pine-Oak Snake	E	LC, M								X				
Elapidae															
<i>Micrurus distans</i> * Kennicott, 1860	West Mexican Coral Snake	E	Pr, LC, H				X				X		X		
Leptotyphlopidae															
<i>Rena humilis</i> Baird & Girard, 1853	Western Blind Snake		LC, L				X	X							
Natricidae															
<i>Thamnophis copei</i> * (Dugès, 1879)	Cope's mountain meadow snake	E	Pr, VU, H				X								
<i>Storeria storerioides</i> (Cope, 1866)	Mexican Brown Snake	E	LC, M								X	X	X		
<i>Thamnophis eques</i> (Reuss, 1834)	Mexican Garter Snake		A		X				X						
<i>Thamnophis melanogaster</i> (Peters, 1864)	Blackbelly Garter Snake	E	A, LC, L											X	
<i>Thamnophis cyrtopsis</i> (Kennicott, 1860)	Black-necked Garter Snake		A, LC, L				X				X		X		
Typhlopidae															
<i>Indotyphlops braminus</i> (Daudin, 1803)	Boottace Snake	F			X	X		X							
Viperidae															
<i>Agkistrodon bilineatus</i> Günther, 1863	Cantil Viper		Pr, NT, M		X	X		X							
<i>Crotalus basiliscus</i> (Cope, 1864)	Basilisk Rattlesnake	E	Pr, LC, H	X	X					X					
<i>Crotalus triseriatus</i> Wagler, 1830	Western Dusky Rattlesnake	E	H										X		
Order Testudines															
Kinosternidae															
<i>Kinosternon integrum</i> Le Conte, 1854	Mexican Mud Turtle	E	Pr, M	X	X						X				

Discussion

We achieved high sampling efforts for both amphibians and reptiles at all sites, so the samples can be considered representative of both groups. Support for this assessment comes also from having recorded the same number of species of amphibians in another seven years of non-systematic surveys and species observations within the study area. In contrast, the number of species of reptiles increased from 39 to 48 species, the earlier systematic survey (August 2011 to September 2013) detected 81% of the reptile species present there.

Alpha taxonomic diversity

Monitoring taxonomic diversity has been proposed as a tool to develop ecosystem management plans, ecological restoration projects, and the creation of protected areas (Somerfield et al. 2008), and guide conservation strategies in areas where biodiversity loss is occurring at an accelerated rate (Hernández-Salinas et al. 2023). In the present work, we obtained sound estimates of the alpha taxonomic diversity of amphibians and reptiles in the different land cover/use types. This may have been helped by the fact that the study area consists of a heterogeneous landscape with different land cover types with temperate and tropical native vegetation. Although, the HPTDF had a high level of disturbance, it is known that secondary TDF in human-dominated landscapes can support substantial amphibian diversity (Suazo-Ortuño et al. 2015). Moreover, animals can move between patches with native vegetation and crops to seek shelter (when there is vegetation cover), food, or to reproduce (during the rainy season). Iglesias-Carrasco et al. (2023) reported that monocultures and poly-specific plantations affect the conservation and ecological value of these habitats to both amphibian and reptile communities detrimentally and alter the evolutionary processes shaping these communities. In contrast, forests with lower impact disturbances can, to some extent, serve as reservoirs of species. Another important factor to consider is the resilience of species to disturbance, since some species populations do not seem to be affected as markedly as others.

Only the RH-C (five species) had higher taxonomic distinctiveness of amphibians than expected from the model. RH-TDF (ten species) and SCF (four species) had the highest alpha taxonomy diversity within the model. TDF did not have the highest alpha taxonomic richness against what we expected, even though it is recognized as a neotropical ecosystem with an important amphibian richness (23% of Mexican amphibians) (Ceballos and García 1995). Suazo-Ortuño et al. (2011) and Álvarez-Grzybowska et al. (2020) reported that TDF in western Mexico sheltered a high amphibian richness but only during the rainy season. Hromada et al. (2021) highlighted the importance of water for amphibians. Even when water quality was reduced, they found that amphibian diversity was higher in ponds surrounded by low-intensity agricultural areas influenced by the surrounding forest and pasture. Our alpha taxonomic results for amphibians are consistent with the observation that amphibians are highly associated with water (Wells 2007). Additionally, it has been reported that diversity is higher in tropical ecosystems compared to temperate ones. The high taxonomic diversity in the SCF may be assisted by its proximity to the RH-TDF and the fact that amphibians can move between land cover/use types, especially during the rainy season.

Almost all the land cover/use types used by reptiles had a higher alpha taxonomic distinctiveness than the average within the model. These results suggest that reptiles can maintain high alpha taxonomic diversity even in heterogeneous landscapes. SCF (nine species), RH-C (14 species), and RH-TF (seven species) had the highest alpha taxonomic diversity within the model, and RH-TDF (eight species) and HPTDF medium ones (24 species). Agricultural systems can vary greatly in structure; uniform agroecosystems like monocultures exhibit shallow levels of biodiversity (Altieri and Nicholls 2004), while more complex agroecosystems shelter high biodiversity (Isbell et al. 2017). However, in a landscape context, certain cultivated areas can function as buffer zones at natural edges (Gascon et al. 2004) or as corridors between native habitat fragments (García et al. 2006). SCF had high alpha taxonomic diversity probably because this crop provides continuous cover for years (approximately six years) and shelters a high population of rodents and other prey such as lizards, frogs, and toads that can serve as food for snakes. RH-C, RH-TF, and RH-TDF also provided habitat, water, and food availability for different species. It has been reported that TDF shelters 34% of Mexican reptiles (Ceballos and García 1995), and even secondary TDF harbors high reptile' diversity (Suazo-Ortuño et al. 2015), as we found in HPTDF.

Beta taxonomic diversity

Factors that contribute to different components of beta diversity in amphibians and reptiles include the physiological limits of the species (*βrich*) and speciation processes (*β.3*), especially in taxa with low mobility (Baselga et al. 2012). The heterogeneous mosaic arrangement with patches of arable areas, forest remnants, and the temperate-tropical configuration in the study area helps explain high beta diversity values for both groups (Ceballos and García 1995; Baselga 2010). Additionally, elevation has been considered a strong promoter of beta taxonomic diversity because it promotes contrasting characteristics within the gradient of vegetation types that change with elevation (Baselga et al. 2012; Ochoa-Ochoa et al. 2014).

For the region evaluated, the turnover component (*β.3*) contributed the most to taxonomic differentiation because of the configuration with abrupt changes in patches mentioned earlier. Because of the narrow distribution ranges of amphibians and reptiles, this is consistent with previous work (Baselga et al. 2012; Ochoa-Ochoa et al. 2014; Rodríguez et al. 2019). However, it has been observed that differences in richness component (*βrich*) can be major in groups with low mobility not only with respect to nesting, but also gain or loss of species among the sites evaluated (Carvalho et al. 2012; Calderón-Patrón et al. 2016), as was the case with amphibians where both components contributed almost equally to diversity of taxonomic differentiation.

Taxonomic beta diversity can also be expected to differ between groups with different evolutionary histories; notably, it has been reported that amphibians show higher taxonomic beta diversity due to dispersal limitations and their dependence on water bodies (Ochoa-Ochoa et al. 2014; Calderón-Patrón et al. 2016). However, we observed the opposite pattern, with reptiles showing the highest taxonomic beta diversity of the two groups. This could be due to the study area being a highly heterogeneous region with disturbed areas promoting greater spatial differentiation for reptiles.

The relationship between alpha and beta taxonomic diversity remains poorly understood (Ochoa-Ochoa et al. 2014). In the present study, the reptiles had the highest species richness and beta diversity. However, amphibians showed the highest average taxonomic distinctiveness (at the 90% level) because of the inclusion of members of different orders and families. In contrast, the supra-specific levels of reptiles differed at a 70% level at the genus and family level.

Although paired comparisons between the two groups reveal differences in beta diversity, we also documented common responses. In amphibians, the highest beta diversity occurred between conserved (POF, TDF) and disturbed (SCF, RHC) habitats. This reflects a high sensitivity to local disturbance, especially considering that this group was strongly influenced by the differences in richness component of beta diversity, as in the case of the comparison of POF with RH-C (one of the comparisons with the highest beta diversity). This indicates that despite shared taxa, supra-specific levels are aggregated to cause differences in richness between the paired comparisons. In the same way, in reptiles, we found that the comparisons with the highest beta diversity occurred between conserved (RH-TF, POF) and disturbed (C, RH-C) habitats, showing a consistent pattern with a predominance of the turnover component. This resulted from changes in the taxa set between these habitats. These results suggest that disturbance could become more important for taxonomic beta diversity of amphibians and reptiles than temperate vs. tropical conditions, given its high potential to threaten species and populations, acting more aggressively than the evolutionary history of species (Ochoa-Ochoa et al. 2014).

Amphibians and Reptiles checklist and geographic range extensions

Our work found that the study area shelters 40.4% and 28.1% of Jalisco's state amphibians (52 species) and reptiles (171 species), respectively (Cruz-Sáenz et al. 2017). This finding highlights the region's significance for conserving amphibians and reptiles. The 68 species (20 and 48 amphibians and reptiles, respectively) observed in this study were higher than in nearby natural areas with similar land cover types, for example La Primavera Forest (with the presence of POF, OF, RH, and TDF) with 56 species (17 amphibians and 39 reptiles) (Reyna-Bustos et al. 2007) and Tequila Volcano (pine forest, POF, OF, RH, TDF, Mountain cloud forest, grassland) with 32 species (10 amphibians and 22 reptiles) (Rojo-Gutiérrez et al. 2022). Conversely, the species richness was comparable to that of Sierra de Quila (oak pine forest, OF, RH, and TDF), with 69 species (23 amphibians and 46 reptiles) (Santiago-Pérez et al. 2012). Salcido-Rodríguez et al. (2023) reported 18 amphibians and 47 reptile species (65 species total) for Sierra de Tesistán with land cover types POF, OF, and secondary vegetation in the ecotone between OF and TDF. Finally, Flores-Covarrubias et al. (2012) reported 20 amphibians and 40 reptiles (61 species) for the TDF, Thorn scrub, OF, POF, grassland, secondary vegetation, and agricultural lands in Hostotipaquillo. The diversity of amphibians and reptiles observed in this study underlines the richness of the herpetofauna in the area, even though it is a heterogeneous landscape with crops.

Many of the recorded species (56.5%) in this heterogeneous landscape are endemic to Mexico. This was true for more than half of the species of reptiles, highlighting the area's role in conserving existing native biodiversity. This could be due to its geographical position and the influence of the Trans-Mexican Volcanic Belt which, through the complexity of the landscape, promotes pro-

cesses of speciation and endemism and is considered one of the most diverse zones in the country (Flores-Villela 1993). We observed two exotic species in the study area: the snake *I. braminus* and the lizard *H. frenatus*. According to CONABIO (2020), exotic species are Mexico's third most significant threat to biodiversity. The dangers associated with their presence in the study area remain unknown (Farr 2011). Also, according to NOM-059 (2019), IUCN (2024) and Wilson (2013a, 2013b), 73% of the species (11 amphibians and 39 reptiles) are under some protection status, highlighting the importance of the existing matrix of different habitats (especially different native vegetation types) to shelter endemic amphibians and reptiles or those with conservation concerns.

Knowing the local distribution of species is essential to monitor and manage local wildlife (Pisanty et al. 2016) as well as the first step in biodiversity conservation. In this study, we found species with a wide distribution in Mexico (e.g., *A. nebulosus*, *Pituophis deppei*, and *Kinosternon integrum*) or in west-central Mexico (e.g., *Phyllodactylus lanei*, *Sceloporus dugesii*, and *Sonora mutabilis*), as well as others with very restricted ones, like *S. hapsa*, *L. ruthveni*, and *T. copei*. Extensions in the distribution range of one amphibian and three reptile species shows that Mexico's west-central region has not been studied enough towards the mountain areas within the Trans-Mexican Volcanic Belt and the Sierra Madre Occidental.

Conclusions

We found that the amphibian and reptile taxonomic diversity in the studied landscape results from i) remnants of native vegetation, even with some level of disturbance, ii) the existence of a heterogeneous matrix with different land cover/use types, albeit with a higher number of land cover types, iii) availability of water during the whole year in some of the land cover types, iv) connectivity between areas allowing the animals to move between different land cover/use types. Finally, the proximity of the study area to mountainous areas like La Primavera or Tequila Volcano is probably another factor to consider. These mountains are natural areas that harbor wildlife and that might act as species pools that could disperse to the study area.

Recommendations

Knowing the distribution of species at different spatial scales, having complete checklists, and analyzing diversity in its various facets at both alpha and beta levels are essentials for species management and conservation. Variation in alpha and beta taxonomic diversity presents a challenge for conservation strategies and management plans as they need to consider differences between sites. It is vital to consider endemic species, particularly those under conservation categories or those associated with native vegetation cover types with low disturbance, so management practices can encourage their presence and abundance. In this sense, preserving remaining natural forests and those with different levels of disturbance is necessary for conserving amphibian and reptile communities. Moreover, this study highlights the need for specific conservation strategies and recommendations to be integrated into broader landscape-level conservation planning. Nowadays, the great rate of land cover changes highlights the need to promote the existence of a connected heterogeneous landscape with different land cover/use

types, thus enhancing the ability to conserve amphibians and reptiles. The other patches can offer shelter, water, and food permanently or temporarily. Even more, encouraging the connection among different land cover/use types will ensure that amphibians and reptiles can move between patches of this matrix.

Acknowledgments

We thank Uri Omar García Vázquez and Matias Domínguez Laso for helping as with the digital deposits of the species photographs in the Museo de Zoología in the Facultad de Estudios Superiores Zaragoza, UNAM. We are grateful to Leobardo Padilla Miranda and Ericka Blanco Morales (Centro Interpretativo Guachimontones Phil Weigand), Mónica Ureña Díaz (Ayuntamiento de Teuchitlán 2012–2015), Ricarda Orozco Wences (Restaurant Soky) and Edgar Lucke Gracián (Hacienda Labor de Rivera). We thank Jachar Aguirre, Alvaro Urzúa, Héctor Franz, Jesús Navarro, and Ramón Vázquez for their field assistance. We are grateful to Robert Cushman, Jocelyn Hudon, and the anonymous reviewers for their valuable comments and reviews which significantly improved the manuscript's quality.

Additional information

Conflict of interest

The authors have declared that no competing interests exist.

Ethical statement

No ethical statement was reported.

Funding

Funding support for this research project were provided through Leobardo Padilla Miranda and Ericka Blanco Morales (Centro Interpretativo Guachimontones Phil Weigand), Mónica Ureña Díaz (Ayuntamiento de Teuchitlán 2012-2015), Ricarda Orozco Wences (Restaurant Soky) and Edgar Lucke Gracián (Hacienda Labor de Rivera).

Author contributions

Conceptualization: VCRE, FARZ, ALSP. Data curation: VCRE, AAGG, EAG, ALSP. Formal analysis: VCRE, EAG, ALSP. Investigation: VCRE, ALSP, EAG, AAGG. Methodology: FARZ, VCRE, ALSP, EAG, KEPJ, FMHM, LDP. Project administration: VCRE, ALSP. Writing-review and editing: VCRE, FMHM, KEPJ, FARZ.

Author ORCIDs

Verónica Carolina Rosas-Espinoza  <https://orcid.org/0000-0001-8595-3203>

Eliza Álvarez-Grzybowska  <https://orcid.org/0000-0003-3580-3869>

Arquímedes Alfredo Godoy González  <https://orcid.org/0000-0002-6313-0238>

Ana Luisa Santiago-Pérez  <https://orcid.org/0000-0001-7494-9129>

Karen Elizabeth Peña-Joya  <https://orcid.org/0000-0002-7237-5894>

Fabián Alejandro Rodríguez-Zaragoza  <https://orcid.org/0000-0002-0066-4275>

Leopoldo Díaz Pérez  <https://orcid.org/0000-0003-0271-9257>

Francisco Martín Huerta Martínez  <https://orcid.org/0000-0001-6923-3425>

Data availability

All of the data that support the findings of this study are available in the main text or Supplementary Information.

References

- Altieri MA, Nicholls CI (2004) An agroecological basis for designing diversified tropical cropping systems. *Journal of Crop Improvement* 11(1–2): 81–103. https://doi.org/10.1300/J411v11n01_05
- Álvarez-Grzybowska E, Urbina-Cardona N, Córdova-Tapia F, García A (2020) Amphibian communities in two contrasting ecosystems: Functional diversity and environmental filters. *Biodiversity and Conservation* 29(8): 2457–2485. <https://doi.org/10.1007/s10531-020-01984-w>
- AmphibiaWeb (2023) AmphibiaWeb. <https://amphibiaweb.org> [accessed 23 May 2023]
- Baccaro G, Ricotta C, Mazzoleni S (2007) Measuring beta-diversity from taxonomic similarity. *Journal of Vegetation Science* 18: 793–798. <https://doi.org/10.1111/j.1654-1103.2007.tb02595.x>
- Barrett K, Guyer C (2008) Differential responses of amphibians and reptiles in riparian and stream habitats to land use disturbances in western Georgia, USA. *Biological Conservation* 141(9): 2290–2300. <https://doi.org/10.1016/j.biocon.2008.06.019>
- Baselga A (2010) Partitioning the turnover and nestedness components of beta diversity. *Global Ecology and Biogeography* 19(1): 134–143. <https://doi.org/10.1111/j.1466-8238.2009.00490.x>
- Baselga A, Gómez-Rodríguez C, Lobo JM (2012) Historical legacies in world amphibian diversity revealed by beta diversity's turnover and nestedness components. *PLoS ONE* 7(2): e32341. <https://doi.org/10.1371/journal.pone.0032341>
- Bucciarelli GM, Blaustein AR, Garcia TS, Kats LB (2014) Invasion complexities: The diverse impacts of nonnative species on amphibians. *Copeia* 2014(4): 611–632. <https://doi.org/10.1643/OT-14-014>
- Calderón-Patrón JM, Goyenechea I, Ortiz-Pulido R, Castillo-Cerón J, Manriquez N, Ramírez-Bautista A, Rojas-Martínez AE, Sánchez-Rojas G, Zuria I, Moreno CE (2016) Beta Diversity in a Highly Heterogeneous Area: Disentangling Species and Taxonomic Dissimilarity for Terrestrial Vertebrates. *PLoS ONE* 11(8): e0160438. <https://doi.org/10.1371/journal.pone.0160438>
- Campbell JA, Brodie ED, Caviades-Solis IW, Nieto-Montes de Oca A, Luja VH, Flores-Villela O, García-Vázquez UO, Sarker GC, Wostl E (2018) Systematics of the frogs allocated to *Sarcohyala bistrincta* sensu lato (Cope, 1877), with description of a new species from Western Mexico. *Zootaxa* 4422(3): 366–384. <https://doi.org/10.11646/zootaxa.4422.3.3>
- Cardoso P, Mammola S, Rigal F, Carvalho J (2024) Biodiversity Assessment Tools. <https://cran.r-project.org/web/packages/BAT/BAT.pdf>
- Carvalho JC, Cardoso P, Gomes P (2012) Determining the relative roles of species replacement and species richness differences in generating beta-diversity patterns. *Global Ecology and Biogeography* 21(7): 760–771. <https://doi.org/10.1111/j.1466-8238.2011.00694.x>
- Ceballos G, García A (1995) Conserving neotropical biodiversity: The role of dry forests in Western Mexico. *Conservation Biology* 9(6): 1349–1353. <https://doi.org/10.1046/j.1523-1739.1995.09061349.x>

- Ceballos G, Ehrlich PR, Barnosky AD, García A, Pringle RM, Palmer TM (2015) Accelerated modern human-induced species losses: Entering the sixth mass extinction. *Science Advances* 1(5): 1–5. <https://doi.org/10.1126/sciadv.1400253>
- Chao A, Chiu CH, Jost L (2010) Phylogenetic diversity measures based on Hill numbers. *Philosophical Transactions of the Royal Society B Biological Science* 27: 365 (1558): 3599–3609. <https://doi.org/10.1098/rstb.2010.0272>
- Clarke KR, Gorley RN (2015) PRIMER v7: user manual/tutorial. PRIMER-E Ltd., Plymouth, United Kingdom, 296 pp.
- Clarke KR, Warwick RM (1998) A taxonomic distinctness index and its statistical properties. *Journal of Applied Ecology* 35(4): 523–531. <https://doi.org/10.1046/j.1365-2664.1998.3540523.x>
- Colwell R (2013) EstimateS 9.1.0: Statistical Estimation of Species Richness and Shared Species from Samples. <https://www.robertkcolwell.org/pages/estimates>
- CONABIO (2020) Comisión Nacional para el Conocimiento y Uso de la Biodiversidad, Sistema de Información sobre especies invasoras. <https://www.biodiversidad.gob.mx/especies/Invasoras>
- CONABIO (2023) Comisión Nacional para el Conocimiento y Uso de la Biodiversidad, enciclovida. <https://enciclovida.mx/explora-por-clasificacion>
- Cruz-Elizalde R, Ramírez-Bautista A, Johnson JD, Moreno CE (2014) Community structure of reptiles from the southern portion of the Chihuahuan Desert Region, Mexico. *North-Western Journal of Zoology* 10(1): 173–182.
- Cruz-Sáenz D, Muñoz-Nolasco F, Mata-Silva V, Johnson J, García-Padilla E, Wilson L (2017) The herpetofauna of Jalisco, Mexico: Composition, distribution, and conservation. *Mesoamerican Herpetology* 4: 23–118.
- Davison C, Rahbek W, Morueta-Holme N (2021) Land-use change and biodiversity: Challenges for assembling evidence on the greatest threat to nature. *Global Change Biology* 27(21): 5414–5429. <https://doi.org/10.1111/gcb.15846>
- Díaz de la Vega-Pérez AH, Jiménez-Arcos VH, Centenero-Alcalá E, Méndez-de la Cruz FR, Ngo A (2019) Diversity and conservation of amphibians and reptiles of a protected and heavily disturbed forest of central Mexico. *ZooKeys* 830: 111–125. <https://doi.org/10.3897/zookeys.830.31490>
- Ernst R, Rödel MO (2008) Patterns of community composition in two tropical tree frog assemblages: Separating spatial structure and environmental effects in disturbed and undisturbed forests. *Journal of Tropical Ecology* 24(2): 111–120. <https://doi.org/10.1017/S0266467407004737>
- Ernst R, Linsenmair KE, Rödel MO (2006) Diversity erosion beyond the species level: Dramatic loss of functional diversity after selective logging in two tropical amphibian communities. *Biological Conservation* 133(2): 143–155. <https://doi.org/10.1016/j.biocon.2006.05.028>
- Falaschi M, Melotto A, Manenti R, Ficetola GF (2020) Invasive species and amphibian conservation. *Herpetologica* 76(2): 216–227. <https://doi.org/10.1655/0018-0831-76.2.216>
- Farr WL (2011) Distribución de *Hemidactylus frenatus* en México. *The Southwestern Naturalist* 56(2): 265–273. <https://doi.org/10.1894/N06-FJRR-01.1>
- Fischer J, Lindenmayer DB (2007) Landscape modification and habitat fragmentation: A synthesis. *Global Ecology and Biogeography* 16(3): 265–280. <https://doi.org/10.1111/j.1466-8238.2007.00287.x>
- Flores-Covarrubias E, Lazcano D, Cruz-Sáenz D (2012) Notes on the Herpetofauna of Western Mexico 6: Amphibians and Reptiles of Hostotipaquillo, Jalisco, Mexico. *Bulletin Chicago Herpetological Society* 47(2): 21–26.

- Flores-Villela O (1993) Herpetofauna of Mexico: distribution and endemism. In: Ramamoorthy TP, Bye R, Lot A, Fa J (Eds) Biological diversity of Mexico: origins and distributions. Oxford University Press, New York, 253–280.
- Frost DR (2023) Amphibian Species of the World: An Online Reference. <https://amphibiansoftheworld.amnh.org/index.php>
- García EC, Damon A, Sánchez HC, Soto PL, Ibarra NG (2006) Bat diversity in montane rainforest and shaded coffee under different management regimes in southeastern Chiapas, Mexico. *Biological Conservation* 132(3): 351–361. <https://doi.org/10.1016/j.biocon.2006.04.027>
- García-Martínez MA, Rodríguez A (2018) Vegetación y flora fanerogámica del área natural protegida Piedras Bola, Jalisco, México. *Polibotánica* 46: 71–90. <https://doi.org/10.18387/polibotanica.46.4>
- Gardner TA, Barlow J, Peres CA (2007) Paradox, presumption and pitfalls in conservation biology: The importance of habitat change for amphibians and reptiles. *Biological Conservation* 138(1–2): 166–179. <https://doi.org/10.1016/j.biocon.2007.04.017>
- Gascon C, da Fonseca GAB, Sechrest W, Billmark KA, Sanderson J (2004) Biodiversity conservation in deforested and fragmented tropical landscapes: an overview. In: Schroth G, da Fonseca GAB, Harvey CA, Gascon C, Vasconcelos HL, Izac AMN (Eds) *Agroforestry and biodiversity conservation in tropical landscapes*. Washington DC, Island Press, 15–32.
- Gaston KJ, Spicer JI (2004) *Biodiversity: An Introduction*. 2nd edn. Blackwell Science Ltd, Australia.
- GBIF [Global Biodiversity Information Facility] (2023a) *Sarcohyla hapsa* Campbell, Brodie, Caviedes-Solis, Nieto-Montes de Oca, Luja, Flores-Villela et al. 2018. GBIF Backbone Taxonomy. Checklist dataset. <https://doi.org/10.15468/39omei> [accessed via GBIF.org on 11 January 2024]
- GBIF [Global Biodiversity Information Facility] (2023b) *Lampropeltis ruthveni* GBIF Backbone Taxonomy. Checklist dataset. <https://doi.org/10.15468/39omei> [accessed via GBIF.org on 11 January 2024]
- GBIF [Global Biodiversity Information Facility] (2023c) *Adelophis copei* GBIF Occurrence Download. <https://doi.org/10.15468/dl.mnav6c> [accessed 06 February 2024]
- GBIF [Global Biodiversity Information Facility] (2023d) *Imantodes gemmistratus* (Cope, 1861) GBIF Backbone Taxonomy. Checklist dataset. <https://doi.org/10.15468/39omei> [accessed via GBIF.org 11 January 2024]
- Hernández-Salinas U, Cruz-Elizalde R, Ramírez-Bautista A, Wilson LD, Berriozabal-Islas C, Johnson JD, Mata-Silva V (2023) Taxonomic and functional diversity of the amphibians and reptile communities of the state of Durango, Mexico. *Community Ecology* 24(2): 229–242. <https://doi.org/10.1007/s42974-023-00145-7>
- Hromada SJ, Iacchetta MG, Beas BJ, Flaherty J, Fulbright MC, Wild KH, Scott AF, Gienger CM (2021) Low-Intensity Agriculture Shapes Amphibian and Reptile Communities: Insights from a 10-Year Monitoring Study. *Herpetologica* 77(4): 294–306. <https://doi.org/10.1655/Herpetologica-D-20-00007.1>
- Iglesias-Carrasco M, Medina I, Ord TJ (2023) Global effects of forest modification on herpetofauna communities. *Conservation Biology* 37(1): e13998. <https://doi.org/10.1111/cobi.13998>
- IIEGa (2023a) Instituto de Información Estadística y Geográfica de Jalisco. Ahualulco de Mercado, Diagnóstico del municipio. <https://iieg.gob.mx/ns/wp-content/uploads/2023/08/Ahualulco-de-Mercado.pdf>

- IIEG (2023b) Instituto de Información Estadística y Geográfica de Jalisco. Teuchitlán Diagnóstico del municipio. <https://iieg.gob.mx/ns/wp-content/uploads/2023/08/Teuchitl%C3%A1n.pdf>
- Isbell F, Adler PR, Eisenhauer N, Fornara D, Kimmel K, Kremen K, Letourneau DK, Liebman M, Polley HW, Quijas S, Scherer-Lorenzen M (2017) Benefits of increasing plant diversity in sustainable agroecosystems. *Journal of Ecology* 105(4): 871–879. <https://doi.org/10.1111/1365-2745.12789>
- IUCN (2024) The IUCN Red List of Threatened Species. Version 2023-1. <https://www.iucnredlist.org>
- Iszak C, Price ARG (2001) Measuring β -diversity using a taxonomic dissimilarity index, and its relation to spatial scale. *Marine Ecology Progress Series* 215: 69–77. <https://doi.org/10.3354/meps215069>
- Johnson JD, Wilson LD, Mata-Silva V, García-Padilla E, DeSantis DL (2017) The endemic herpetofauna of Mexico: Organisms of global significance in severe peril. *Mesoamerican Herpetology* 4: 544–620.
- Jost L, Chao A, Chazdon RL (2011) Compositional similarity and β (beta) diversity. In: Magurran A, McGill BJ (Eds) *Biological diversity: frontiers in measurement and assessment*. Oxford University Press, New York, 66–87.
- Koleff P, Soberón J, Arita HT, Dávila P, Flores-Villela O, Golubov J, Halffter G, Lira-Noriega A, Moreno CE, Moreno E, Munguía M, Murguía M, Navarro-Sigüenza A, Téllez O, Ochoa-Ochoa L, Peterson AT, Rodríguez P (2008) Patrones de diversidad espacial en grupos selectos de especies. In: Sarukhán J (Ed.) *Capital natural de México, Vol. I, Conocimiento actual de la biodiversidad*. Conabio, México, D. F., 323–364.
- Kraus F (2015) Impacts from invasive reptiles and amphibians. *Annual Review of Ecology, Evolution, and Systematics* 46(1): 75–97. <https://doi.org/10.1146/annurev-ecolsys-112414-054450>
- Magurran AE (2004) *Measuring Biological Diversity*. Blackwell Publishing, Oxford, 256 pp.
- Melo AS, Rangel TFLVB, Diniz-Filho JAF (2009) Environmental drivers of beta-diversity patterns in New-World birds and mammals. *Ecography* 32(2): 226–236. <https://doi.org/10.1111/j.1600-0587.2008.05502.x>
- Nipperess DA, Faith DP, Barton K (2010) Resemblance in phylogenetic diversity among ecological assemblages. *Journal of Vegetation Science* 21(5): 809–820. <https://doi.org/10.1111/j.1654-1103.2010.01192.x>
- Nyelele C, Murwira A, Shekede MD, Mugabe PH (2014) Woodland fragmentation explains tree species diversity in an agricultural landscape of Southern Africa. *Tropical Ecology* 55: 365–374.
- Ochoa-Ochoa LM, Flores-Villela O (2006) Áreas de diversidad y endemismo de la herpetofauna mexicana. UNAM-CONABIO, DF, México, 211 pp.
- Ochoa-Ochoa L, Munguía M, Lira-Noriega A, Sánchez-Cordero V, Flores-Villela O, Navarro-Sigüenza A, Rodríguez P (2014) Spatial scale and beta diversity of terrestrial vertebrates in México. *Revista Mexicana de Biodiversidad* 85(3): 918–930. <https://doi.org/10.7550/rmb.38737>
- Pisanty I, Urquiza-Haas E, Vargas-Mena AA, Ruiz GSP, Urquiza-Hass T, García MG (2016) Instrumentos de conservación in situ en México: logros y retos. In: Sarukhán J, Pisanty I (Eds) *Capital natural de México, vol. IV: Capacidades humanas e institucionales*. CONABIO, México, 245–302.
- Pough FH, Andrews R, Cadle JE, Crump ML, Savitzki AH, Wells KD (2004) *Herpetology*. Prentice Hall, New Jersey, USA, 726 pp.

- R Development Core Team (2022) R: A language and environment for statistical computing. R Foundation for Statistical Computing, Vienna, Austria. <https://www.R-project.org/>
- Ramírez-Bautista A (1994) Manual y claves ilustradas de los anfibios y reptiles de la región de Chamela, Jalisco, México. Cuadernos 23, Instituto de Biología, UNAM, DF, México, 127 pp.
- Ramírez-Bautista A, Torres-Hernández LA, Cruz-Elizalde R, Berriozabal-Islas C, Hernández-Salinas U, Wilson LD, Johnson JD, Porras LW, Balderas-Valdivia CJ, González-Hernández AJX, Mata-Silva V (2023) An updated list of the Mexican herpetofauna: With a summary of historical and contemporary studies. *ZooKeys* 1166: 287–306. <https://doi.org/10.3897/zookeys.1166.86986>
- Reyna-Bustos OF, Ahumada CIT, Vazquez HO (2007) Anfibios y reptiles del bosque La Primavera: guía ilustrada. Universidad de Guadalajara, Guadalajara, Jalisco, México, 125 pp.
- Rodríguez P, Ochoa-Ochoa LM, Munguía M, Sánchez-Cordero V, Navarro-Sigüenza AG, Flores-Villela OA, Nakamura M (2019) Environmental heterogeneity explains coarse-scale β -diversity of terrestrial vertebrates in Mexico. *PLoS ONE* 14(1): e0210890. <https://doi.org/10.1371/journal.pone.0210890>
- Rojo-Gutiérrez JR, Salcido-Rodríguez I, Amaral-Medrano DA, Cruz-Sáenz D, Rodríguez-López A, Lazcano D, Fuckso LA, Wilson LD (2022) Notes on the Herpetofauna of Western Mexico 27: Amphibians and Reptiles of Palo Gordo, Sierra de Tesistán, Zapopan, Jalisco, Mexico. *Bulletin of the Chicago Herpetological Society* 57(6): 109–113.
- Rosas-Espinoza VC, Rodríguez-Canseco JM, Santiago-Pérez AL, Ayón-Escobedo A, Domínguez-Laso M (2013) Distribution of some amphibians from central western Mexico: Jalisco. *Revista Mexicana de Biodiversidad* 84(2): 690–696. <https://doi.org/10.7550/rmb.31945>
- Rosas-Espinoza VC, Peña-Joya KE, Álvarez-Grzybowska E, Godoy-González AA, Santiago-Pérez AL, Rodríguez-Zaragoza FA (2022) Amphibian Taxonomic and Functional Diversity in a Heterogeneous Landscape of West-Central Mexico. *Diversity* 14(9): 738. <https://doi.org/10.3390/d14090738>
- Salcido-Rodríguez I, Hernández-Valadez FI, Castillo-Franco AE, Cruz-Sáenz D, Hernández-Juárez EE, Lazcano D, Fucsko LA and Wilson LD (2023) Notes on the Herpetofauna of Western Mexico 31: Herpetofauna from Sierra de Tesistán, Zapopan, Jalisco, Mexico. *Bulletin of the Chicago Herpetological Society* 58(10):165–171.
- Santiago-Pérez AL (2023) El hábitat del sitio arqueológico Guachimontones. In: Alvarez-Gryzbowska E, Rosas-Espinoza VC, Santiago-Pérez AL (coords.) *Los Anfibios y reptiles de Jalisco: Guachimontones y alrededores de Teuchitlán*. Universidad de Guadalajara, Guadalajara, México, 27–31.
- Santiago-Pérez AL, Domínguez-Laso M, Rosas-Espinoza VC, Rodríguez-Canseco JM (2012) *Anfibios y Reptiles de las montañas de Jalisco: Sierra de Quila*. Orgánica Editores, CONABIO, México, 228 pp.
- Sayer J, Sunderland T, Ghazoul J, Pfund JL, Sheil D, Meijaard E, Venter M, Boedhihartono AK, Day M, Garcia C, Oosten CV, Buck LE (2013) Ten principles for a landscape approach to reconciling agriculture, conservation, and other competing land uses. *Proceedings of the National Academy of Sciences of the United States of America* 110(21): 8349–8356. <https://doi.org/10.1073/pnas.1210595110>
- SEMARNAT (2019) Lista de especies en riesgo de la Norma Oficial Mexicana NOM-059-SEMARNAT-2010. https://www.dof.gob.mx/nota_detalle.php?codigo=5578808&fecha=14/11/2019

- SIAP [Servicio de Alimentación Agropecuaria y Pesquera] (2018) Atlas agroalimentario 2012–2018. https://nube.siap.gob.mx/gobmx_publicaciones_siap/pag/2018/Atlas-Agroalimentario-2018
- Somerfield PJ, Clarke KR, Warwick RM, Dulvy NK (2008) Average functional distinctness as a measure of the composition of assemblages. –. *ICES Journal of Marine Science* 65(8): 1462–1468. <https://doi.org/10.1093/icesjms/fsn118>
- Suazo-Ortuño I, Alvarado-Díaz J, Martínez-Ramos M (2011) Riparian areas and conservation of herpetofauna in a tropical dry forest in western Mexico. *Biotropica* 43(2): 237–245. <https://doi.org/10.1111/j.1744-7429.2010.00677.x>
- Suazo-Ortuño I, Alvarado-Díaz J, Mendoza E, López-Toledo L, Lara-Urbe N, Márquez-Carmargo C, Paz-Gutiérrez JG, Rangel-Orozco JD (2015) High resilience of herpetofaunal communities in a human-modified tropical dry forest landscape in western Mexico. *Tropical Conservation Science* 8(2): 396–423. <https://doi.org/10.1177/194008291500800208>
- Taylor E (1942) Mexican snakes of the genera *Adelophis* and *Storeria*. *Herpetologica* 2(4): 75–79.
- Thompson ME, Nowakowski AJ, Donnelly MA (2015) The importance of defining focal assemblages when evaluating amphibian and reptile responses to land use. *Conservation Biology* 30(2): 249–258. <https://doi.org/10.1111/cobi.12637>
- Trimble MJ, Aarde RJ (2014) Amphibian and reptile communities and functional groups over a land-use gradient in a coastal tropical forest landscape of high richness and endemism. *Animal Conservation* 17(5): 441–453. <https://doi.org/10.1111/acv.12111>
- Uetz P (2024) The Reptile Database. www.reptile-database.org
- Wanger TC, Iskandar DT, Motzke I, Brook BW, Sodhi NS, Clough Y, Tschardt T (2010) Effects of land-use change on community composition of tropical amphibians and reptiles in Sulawesi, Indonesia. *Conservation Biology* 24(3): 795–802. <https://doi.org/10.1111/j.1523-1739.2009.01434.x>
- Warwick RM, Clarke KR (1995) New biodiversity measures reveal a decrease in taxonomic distinctness with increasing stress. *Marine Ecology Progress Series* 129: 301–305. <https://doi.org/10.3354/meps129301>
- Warwick RM, Clarke KR (1998) Taxonomic distinctness and environmental assessment. *Journal of Applied Ecology* 35: 532–543. <https://doi.org/10.1046/j.1365-2664.1998.3540532.x>
- Wells KD (2007) *The Ecology and Behavior of Amphibians*. University of Chicago Press, Chicago, USA, 1400 pp.
- Wilson LD, Mata-Silva V, Johnson JD (2013a) A conservation reassessment of the reptiles of Mexico based on the EVS measure. *Special Mexico Issue. Amphibian & Reptile Conservation* 7: 1–47.
- Wilson LD, Mata-Silva V, Johnson JD (2013b) A conservation reassessment of the amphibians of Mexico based on the EVS measure. *Special Mexico Issue. Amphibian & Reptile Conservation* 7: 97–127.
- Zaher H, Murphy RW, Arredondo JC, Graboski R, Machado-Filho PR, Mahlow K, Montingelli GG, Quadros AB, Orlov NL, Wilkinson M, Zhang YP, Grazziotin FG (2019) Large-scale molecular phylogeny, morphology, divergence-time estimation, and the fossil record of advanced caenophidian snakes (Squamata: Serpentes). *PLoS ONE* 14(5): e0216148. <https://doi.org/10.1371/journal.pone.0216148>

Supplementary material 1

Supplementary information

Authors: Verónica Carolina Rosas-Espinoza, Eliza Álvarez-Grzybowska, Arquímedes Alfredo Godoy González, Ana Luisa Santiago-Pérez, Karen Elizabeth Peña-Joya, Fabián Alejandro Rodríguez-Zaragoza, Leopoldo Díaz Pérez, Francisco Martín Huerta Martínez

Data type: docx

Explanation note: **table S1**. Sample-based rarefaction curves generated using presence-absence data for both amphibians and reptiles. We report observed and expected species by land cover/use type using non-parametric estimators. Codes: sugar cane field (SCF), riparian habitat surrounded by crops (RH-C), cornfield (C), highly perturbed tropical dry forest (HPTDF), tropical dry forest (TDF), riparian habitat surrounded by tropical forest (RH-TDF), riparian habitat surrounded temperate forest (RH-TF), secondary vegetation surrounded by temperate forest (SV-TF), oak forest (OF), pine-oak forest (POF) and number of species observed (Sobs). **fig. S1**. Species with the documented range extensions. **A** *Sarcohyla hapsa* **B** *Lampropeltis ruthveni* **C** *Thamnophis copei* **D** *Imantodes gemmistratus* in a heterogeneous landscape in west-central Mexico. All photos by Eliza Álvarez-Grzybowska, except B) by Aldo Dávalos Martínez. **fig. S2**. Records of *Sarcohyla hapsa* in Jalisco state (black triangles, GBIF 2023a). The red star shows our record of range extension for *S. hapsa*. **fig. S3**. Records of **A** *Lampropeltis ruthveni* **B** *Thamnophis copei*, and **C** *Imantodes gemmistratus* in Jalisco state (black triangles, GBIF 2023). The red stars show our records of range extension for these different species. The colored areas are published distributions (IUCN 2024).

Copyright notice: This dataset is made available under the Open Database License (<http://opendatacommons.org/licenses/odbl/1.0/>). The Open Database License (ODbL) is a license agreement intended to allow users to freely share, modify, and use this Dataset while maintaining this same freedom for others, provided that the original source and author(s) are credited.

Link: <https://doi.org/10.3897/zookeys.1211.122565.suppl1>

Review of the genus *Salicarus* (Hemiptera, Heteroptera, Miridae)

Fedor V. Konstantinov^{1,2}, Reza Hosseini³

1 Zoological Institute, Russian Academy of Sciences, Universitetskaya nab. 1, St. Petersburg 199034, Russia

2 National Museum of Natural History, Bulgarian Academy of Sciences, 1 Tsar Osvoboditel Blvd, 1000 Sofia, Bulgaria

3 Department of Plant Protection, Faculty of Agricultural Sciences, University of Guilan, Rasht, 41635–1314, Iran

Corresponding author: Fedor V. Konstantinov (fkonstantinov@gmail.com)

Abstract

The genus *Salicarus* Kerzhner, 1962 is revised, with differential diagnoses and redescrptions provided for nine species. Three distinct species groups were recognized within the genus: *S. nitidus* group (*S. cavinotum*, *S. genistae*, *S. nitidus*, *S. perpusillus*), *S. roseri* group (*S. concinnus*, *S. roseri*, *S. urnammu*), and *S. fulvicornis* group (*S. halimodendri*, *S. fulvicornis*). A key to species, illustrations of dorsal habitus, male and female genitalia, and selected diagnostic structures are included. Additionally, available host information and distributional records are summarized. *Phoenicocoris qiliananus* Zheng, 1996 is synonymized with *Salicarus halimodendri* V. G. Putshkov, 1977.

Key words: Distribution, hosts, new synonymy, Palearctic, phylogeny, taxonomy

Introduction

Salicarus Kerzhner, 1962 belongs to the subfamily Phylinae of the hyperdiverse family Miridae, or plant bugs, the second largest family of insects with incomplete metamorphosis (Cassis et al. 2007). Phylines are, in turn, the second largest subfamily of plant bugs, predominantly host specific, with many taxa still lacking adequate diagnoses. The genus has a convoluted taxonomic history, with most species now treated within *Salicarus* being previously placed in several different genera. Kerzhner (1962) erected the genus *Salicarus* for the single species, *S. roseri* (Herich-Schaeffer, 1839), in an effort to create monophyletic groupings within the wide array of species previously assigned to *Sthenarus* Fieber, 1858. Wagner (1975a) considered *Salicarus* (incorrectly spelt *Salicarius*) as a subgenus within *Sthenarus* but included a wide assemblage of species, all of which except the type species were subsequently transferred to *Campylomma* Reuter, 1878 (Kerzhner and Matocq 1997; Konstantinov 2023) or *Psallus* Fieber, 1858 (Wagner 1975b). Putshkov (1977) described two new species of *Salicarus* and updated the concept of the genus without commenting on the Mediterranean species. Stonedahl (1990) and Schwartz and Stonedahl (2004) published revisions of the genera *Atractotomus* Fieber, 1858 and *Phoenicocoris* Reuter, 1875, respectively, providing important insights into the taxonomy of these and related genera, including *Salicarus* and *Heterocapillus* Wagner, 1960. The latter genus was considered non-monophyletic and consisting of several unrelated groups of species (Stonedahl 1990; Konstantinov



Academic editor: Nikolay Simov

Received: 13 June 2024

Accepted: 29 July 2024

Published: 2 September 2024

ZooBank: <https://zoobank.org/OD172F1C-B539-497C-BC62-17FE910EC512>

Citation: Konstantinov FV, Hosseini R (2024) Review of the genus *Salicarus* (Hemiptera, Heteroptera, Miridae). ZooKeys 1211: 57–100. <https://doi.org/10.3897/zookeys.1211.129660>

Copyright: © F. V. Konstantinov & R. Hosseini
This is an open access article distributed under terms of the Creative Commons Attribution License (Attribution 4.0 International – CC BY 4.0).

2008). Konstantinov (2023) performed a morphology-based phylogenetic analysis of the group in question, showing the low taxonomic utility of many characters of external morphology traditionally used in the generic taxonomy of these genera. He updated the diagnosis and species composition of *Salicarus*, particularly by transferring to it four species previously assigned to *Heterocapillus*.

The present paper serves as a supplement to the mentioned revision by Konstantinov (2023) and aims to summarize current knowledge about *Salicarus*, including species delimitation, distributional ranges, and host plant associations. Consequently, a key to all nine species and standardized species re-descriptions with detailed illustrations are provided.

Materials and methods

Microscopy, illustrations, and terminology

Observations, measurements, and habitus images were made using a Zeiss Stemi 508 stereomicroscope equipped with a Canon EOS 2000D digital SLR camera. Partially focused images of each specimen or structure were stacked using Helicon Focus software. Images of the selected structures, including male and female genitalia, were taken with a Keyence VHX–500F digital microscope at the University of Hamburg. Illustrated structures were macerated in potassium hydroxide, cleared in distilled water, and then transferred to glycerin jelly for proper orientation. Scanning electron micrographs of selected structures were taken using a Quanta 250 scanning electron microscope.

Unless otherwise stated, all measurements are in millimeters. Measurements shown in Table 1 include body length, clypeus to apex of cuneus length, width of head, interocular distance, length of antennal segments I and II, and pronotum length and width. The morphological terminology follows Schuh and Weirauch (2020), except for genitalia, which follows Konstantinov (2003, 2019) for males and Schwartz (2011) for females.

Specimens and collections

The material examined for this study is retained in the following collections:

- HNHM** Hungarian Natural History Museum, Budapest (András Orosz);
- NMWC** National Museum of Wales, Cardiff (Mike Wilson);
- SNSB** Zoologische Staatssammlung München (Tanja Kothe);
- UGNHM** Natural History Museum of the University of Guilan, Rasht;
- ZISP** Zoological Institute, Russian Academy of Sciences, St. Petersburg;
- ZMUH** Zoological Museum, University of Hamburg (Frank Wieland, Martin Husemann).

Bar code labels, uniquely identifying each specimen, were attached to all examined specimens listed in the “Material examined” sections. Further information, such as additional photographs of habitus and genitalia structures, geo-referenced coordinates, specimens dissected, notes, and collecting methods, can be obtained from the Heteroptera Species Pages (<http://research.amnh.org/pbi/heteropteraspeciespage/>), which assembles available data from a

Table 1. Measurements (mm). Abbreviations. Cun–Clyp – distance between apex of clypeus and apex of corium in dorsal view, Head Length – distance between apex of clypeus and the highest point of vertex, AntSeg1, AntSeg2 – length of antennal segments I and II, InterOcDi – width of vertex between inner margins of eyes in dorsal view.

Species		Length					Width		
		Body	Cun–Clyp	Pronotum	Tibia3	AntSeg2	Head	InterOcDi	Pronotum
<i>Salicarus cavinotum</i>									
♂♂ (n = 5)	Mean	2.16	1.86	0.37	0.98	0.49	0.65	0.36	0.83
	SD	0.25	0.27	0.03	0.05	0.03	0.03	0.02	0.05
	Range	0.60	0.70	0.06	0.14	0.07	0.07	0.05	0.10
	Min	2.00	1.60	0.34	0.90	0.46	0.61	0.34	0.78
	Max	2.60	2.30	0.40	1.04	0.53	0.68	0.39	0.88
♀♀ (n = 5)	Mean	2.15	1.91	0.39	1.02	0.49	0.68	0.40	0.89
	SD	0.09	0.08	0.03	0.07	0.03	0.03	0.01	0.04
	Range	0.23	0.22	0.09	0.15	0.07	0.06	0.04	0.09
	Min	2.05	1.83	0.35	0.95	0.45	0.65	0.38	0.85
	Max	2.28	2.04	0.44	1.10	0.52	0.71	0.41	0.94
<i>Salicarus concinnus</i>									
♂♂ (n = 5)	Mean	3.21	2.78	0.62	1.51	0.71	0.80	0.42	1.25
	SD	0.33	0.21	0.03	0.04	0.04	0.02	0.01	0.07
	Range	0.75	0.50	0.08	0.13	0.10	0.05	0.01	0.18
	Min	2.95	2.63	0.58	1.45	0.65	0.78	0.41	1.18
	Max	3.70	3.13	0.65	1.58	0.75	0.83	0.43	1.35
♀♀ (n = 5)	Mean	3.24	2.79	0.59	1.56	0.71	0.81	0.44	1.25
	SD	0.18	0.11	0.06	0.11	0.09	0.03	0.01	0.09
	Range	0.45	0.25	0.15	0.20	0.20	0.06	0.03	0.23
	Min	3.00	2.70	0.53	1.45	0.65	0.79	0.43	1.15
	Max	3.45	2.95	0.68	1.65	0.85	0.85	0.45	1.38
<i>Salicarus fulvicornis</i>									
♂♂ (n = 5)	Mean	3.82	3.08	0.57	1.54	0.85	0.80	0.40	1.20
	SD	0.10	0.07	0.05	0.06	0.05	0.02	0.00	0.12
	Range	0.25	0.15	0.10	0.18	0.10	0.05	0.00	0.30
	Min	3.70	3.00	0.53	1.45	0.80	0.78	0.40	1.00
	Max	3.95	3.15	0.63	1.63	0.90	0.83	0.40	1.30
♀♀ (n = 5)	Mean	3.29	2.82	0.53	1.41	0.73	0.84	0.45	1.18
	SD	0.14	0.10	0.02	0.01	0.05	0.02	0.02	0.05
	Range	0.35	0.25	0.05	0.03	0.10	0.04	0.05	0.13
	Min	3.15	2.70	0.50	1.40	0.68	0.83	0.43	1.13
	Max	3.50	2.95	0.55	1.43	0.78	0.86	0.48	1.25
<i>Salicarus genistae</i>									
♂♂ (n = 5)	Mean	2.36	2.10	0.46	1.18	0.58	0.75	0.39	1.04
	SD	0.11	0.08	0.02	0.03	0.02	0.02	0.01	0.01
	Range	0.28	0.22	0.04	0.06	0.04	0.05	0.02	0.04
	Min	2.20	2.00	0.44	1.14	0.56	0.72	0.38	1.02
	Max	2.48	2.22	0.48	1.20	0.60	0.77	0.40	1.06
♀♀ (n = 5)	Mean	2.72	2.43	0.49	1.27	0.59	0.79	0.43	1.06
	SD	0.09	0.10	0.01	0.03	0.03	0.02	0.01	0.03
	Range	0.20	0.24	0.03	0.08	0.08	0.05	0.02	0.06
	Min	2.60	2.30	0.47	1.22	0.54	0.76	0.42	1.04
	Max	2.80	2.54	0.50	1.30	0.62	0.81	0.44	1.10
<i>Salicarus halimodendri</i>									
♂♂ (n = 5)	Mean	3.71	3.11	0.57	1.42	0.78	0.89	0.45	1.32
	SD	0.17	0.11	0.05	0.02	0.02	0.03	0.02	0.05
	Range	0.33	0.25	0.10	0.05	0.05	0.05	0.05	0.13
	Min	3.55	2.95	0.50	1.40	0.75	0.85	0.43	1.25
	Max	3.88	3.20	0.60	1.45	0.80	0.90	0.48	1.38

Species	Length						Width		
		Body	Cun–Clyp	Pronotum	Tibia3	AntSeg2	Head	InterOcDi	Pronotum
♀♀ (n = 5)	Mean	3.34	2.96	0.58	1.41	0.69	0.92	0.49	1.36
	SD	0.15	0.12	0.02	0.03	0.03	0.03	0.01	0.03
	Range	0.35	0.33	0.05	0.08	0.08	0.08	0.03	0.08
	Min	3.13	2.83	0.55	1.38	0.65	0.88	0.48	1.33
	Max	3.48	3.15	0.60	1.45	0.73	0.95	0.50	1.40
<i>Salicarus nitidus</i>									
♂♂ (n = 2)	Min	2.30	2.00	0.40	1.06	0.52	0.74	0.40	0.94
	Max	2.60	2.28	0.46	1.22	0.53	0.75	0.42	0.96
♀♀ (n = 2)	Min	2.18	1.98	0.42	1.07	0.56	0.70	0.40	0.96
	Max	2.40	2.16	0.44	1.14	0.57	0.74	0.40	0.98
<i>Salicarus perpusillus</i>									
♂♂ (n = 3)	Mean	2.24	1.88	0.40	1.09	0.50	0.69	0.38	0.87
	Min	2.14	1.84	0.38	1.02	0.49	0.66	0.37	0.84
	Max	2.37	1.95	0.41	1.14	0.52	0.71	0.39	0.88
♀♀ (n = 5)	Mean	2.27	1.97	0.42	1.04	0.53	0.70	0.39	0.90
	SD	0.11	0.14	0.02	0.02	0.01	0.03	0.01	0.03
	Range	0.24	0.33	0.04	0.04	0.03	0.07	0.02	0.07
	Min	2.16	1.83	0.40	1.02	0.51	0.66	0.38	0.86
	Max	2.40	2.16	0.44	1.06	0.54	0.73	0.40	0.93
<i>Salicarus roseri</i>									
♂♂ (n = 5)	Mean	3.80	3.31	0.68	1.65	0.74	0.86	0.41	1.40
	SD	0.16	0.20	0.02	0.10	0.04	0.03	0.02	0.06
	Range	0.38	0.50	0.05	0.25	0.10	0.08	0.05	0.15
	Min	3.58	3.13	0.65	1.58	0.68	0.83	0.39	1.33
	Max	3.95	3.63	0.70	1.83	0.78	0.90	0.44	1.48
♀♀ (n = 5)	Mean	3.76	3.25	0.67	1.61	0.71	0.89	0.41	1.42
	SD	0.22	0.21	0.06	0.07	0.07	0.02	0.05	0.07
	Range	0.55	0.50	0.15	0.20	0.18	0.05	0.13	0.18
	Min	3.38	2.88	0.58	1.50	0.60	0.85	0.33	1.30
	Max	3.93	3.38	0.73	1.70	0.78	0.90	0.45	1.48
<i>Salicarus urnammu</i>									
♂♂ (n = 3)	Mean	3.61	3.04	0.67	1.53	0.73	0.85	0.43	1.28
	Min	3.45	2.88	0.63	1.50	0.70	0.83	0.43	1.25
	Max	3.75	3.20	0.73	1.55	0.75	0.89	0.43	1.35
♀♀ (n = 3)	Mean	3.34	2.94	0.63	1.48	0.66	0.85	0.43	1.29
	Min	3.20	2.83	0.60	1.45	0.60	0.83	0.40	1.25
	Max	3.45	3.08	0.65	1.53	0.70	0.88	0.45	1.38

specimen database (Konstantinov and Namyatova 2019). Refer to Suppl. material 1 for unique specimen identifiers of illustrated specimens. Original locality data are given in square brackets if it differs from currently existing toponyms.

Taxonomic account

Salicarus Kerzhner, 1962

Salicarus Kerzhner, 1962: 381. Type species by original designation: *Capsus roseri* Herrich-Schaeffer, 1838.

Salicarus: Putshkov (1977): 365 (revision); Kerzhner (1964): 996 (key, figures).

Salicarius [sic!]: Wagner (1975a): 99 (key, descriptions, figures).

Diagnosis. Body broadly oval, with short appendages (Figs 1–3); head vertical, clypeus barely visible in dorsal view, posterior margin of vertex attenuate,

covering anterior margin of pronotum (Figs 4, 5, 6E); dorsum and/or thoracic pleura clothed with scale-like setae and simple setae (Figs 4, 5, 6C); parempodium apically spatulate; pulvillum small, not reaching midpoint of claw (Fig. 6A, D); vesica large, strongly coiled at middle, apically with two long and thin, gradually tapering blades tightly fused along almost entire length (Figs 7A–D, 8), or slightly dilate apically (Fig. 7G–J); secondary gonopore large, located close to middle of vesica, equipped with gonopore sclerite; vestibulum of bursa copulatrix S-shaped, contrastingly long and thin (Fig. 10). Refer to Konstantinov (2023) for additional discussion.

Redescription. Male. Coloration. Dorsum and venter uniformly chestnut to dark brown with whitish antennal segments III and IV in *S. nitidus* species group (Fig. 3E–L), in other species ranging from uniformly dark brown to pale yellow, often exhibiting significant polymorphism within a species (Figs 1, 2).

Surface and vestiture. Dorsum shiny to moderately shiny, head and pronotum usually smooth, scutellum and hemelytron weakly rugose. Vestiture composed of dense simple setae intermixed with one of two types of scale-like setae: wide, apically serrate, densely covering dorsum, thoracic pleura, abdomen, and sometimes appendages (*S. nitidus* species group, Fig. 5) or narrow, apically acuminate, always located on thoracic pleura and usually also on dorsum or hemelytron only (other species, Figs 4, 6C). Thoracic pleurites devoid of simple setae and densely clothed exclusively with scale-like setae located above metathoracic scent gland evaporatory area, with no vestiture in ventral half (Fig. 6E). Simple setae usually adpressed, sometimes semierect, ranging from as long as to almost twice as long as scale-like setae; in addition, in *S. nitidus* species group, pronotum laterally and hemelytron proximally with robust, dark, contrastingly long, erect to semierect bristle-like simple setae. Appendages with simple, adpressed to semierect, usually pale setae; antennal segments I and II in *S. nitidus* species group with contrastingly dense, dark and robust simple setae (Fig. 5); head and fore coxa ventrally with contrastingly long simple silver setae; pronotum with a pair of black erect bristle-like setae at anterior corners; femora with several similar black setae dorso-apically; tibial spines dark brown to black.

Structure. Body elongate-oval to oval, total length 2.0–4.0. **Head:** Flattened and strongly sloping, barely protruding beyond anterior margin of eyes (Figs 4, 5, 6E); eyes occupying almost entire height of head in lateral view, posterolateral margins of eyes contiguous with anterolateral margins of pronotum; vertex flat, with attenuate posterior margin covering anterior margin of pronotum, frons vertical, clypeus not visible or barely visible in dorsal view; antenna inserted near ventral margin of eye; segment I either short, swollen, widest at apex, about twice as long as width at apex (*S. nitidus* species group, Fig. 5), or cylindrical, thin (other species, Fig. 4); segment II shorter than head width, in *S. nitidus* species group swollen along entire length, usually distinctly fusiform, in other species rod-shaped, slightly dilated distally; segments III and IV filiform; labium reaching meso- or metacoxa. **Thorax:** Pronotum trapezoidal, about twice as broad as long, calli indistinct; mesonotum only slightly exposed; metathoracic scent gland evaporatory area broadly triangular, peritreme oval, broadly rounded apically. Metathoracic spiracle with well-developed sculpture dorsally (Fig. 6E, F). Cuneal fracture deeply incised at base. **Legs:** Comparatively short, femora swollen, broader medially, tibia cylindrical, second and third tarsal segments of nearly equal length, claw (Fig. 6A, B) with relatively narrow base, strongly bent at

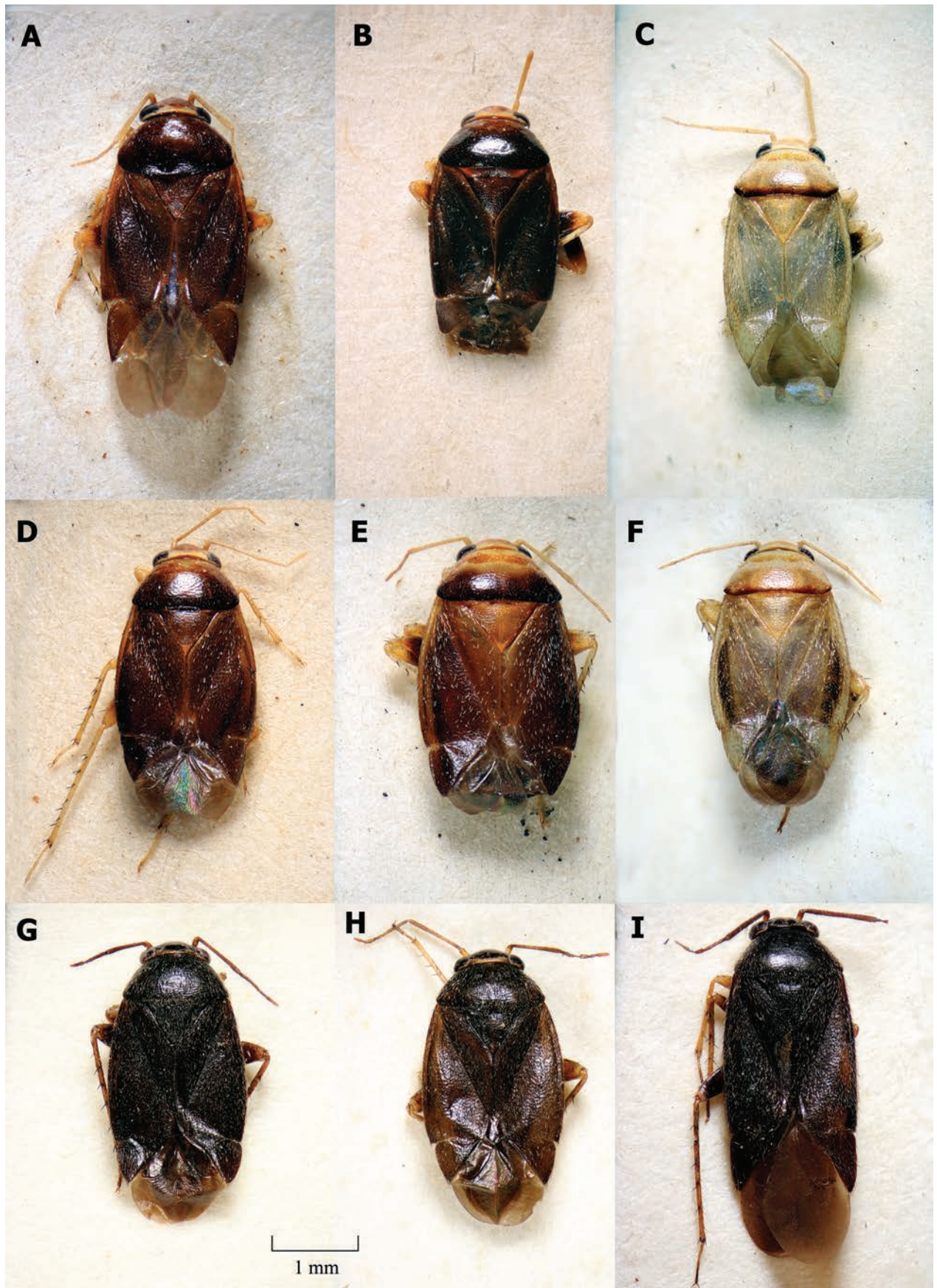


Figure 1. Dorsal habitus **A–C** ♂ paratype of *Salicarus concinnus* **D–F** ♀ paratype of *S. concinnus* **G, H** ♀ *S. fulvicornis* **I** ♂ *S. fulvicornis*.

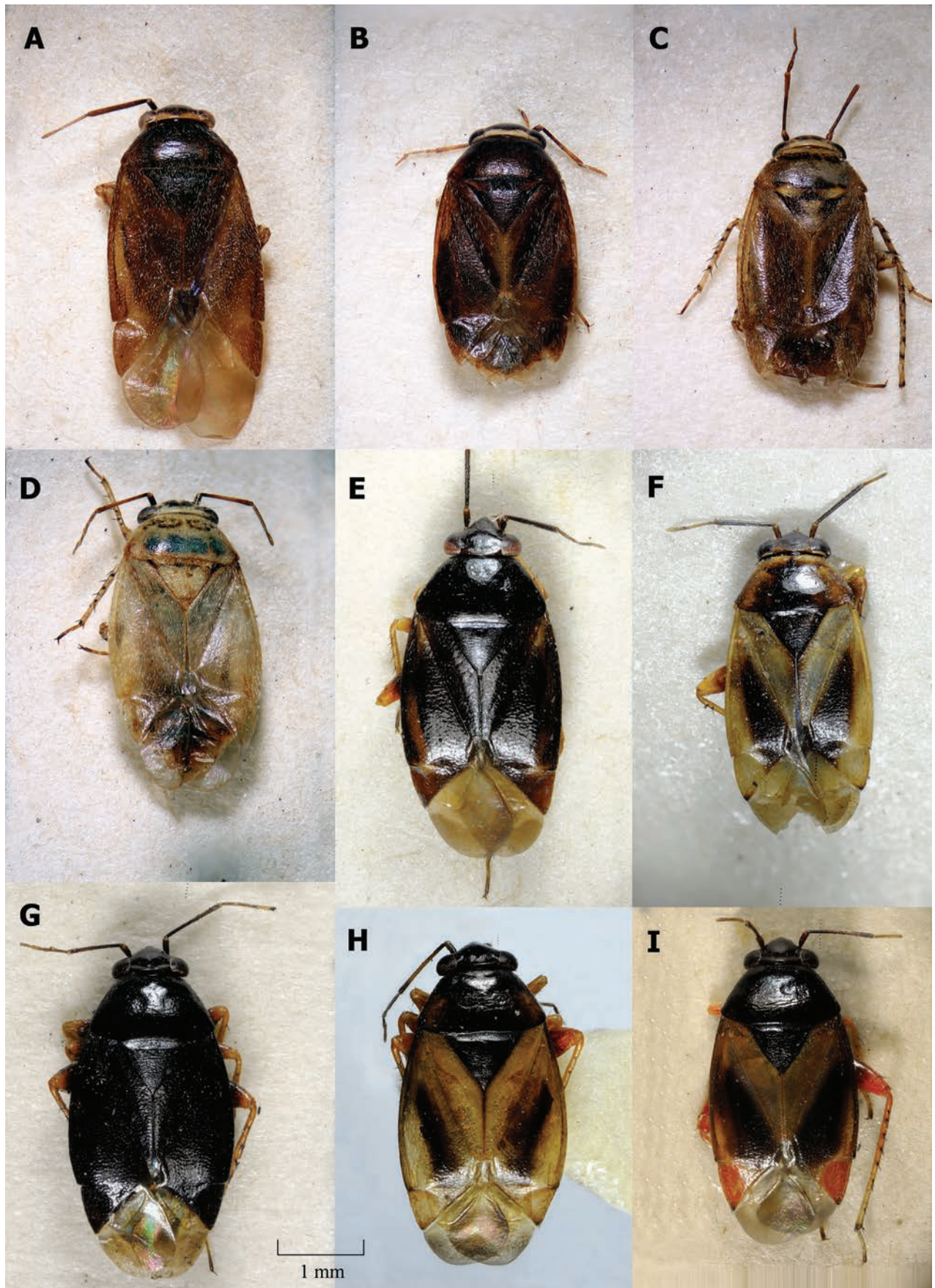


Figure 2. Dorsal habitus A ♂ *Salicarus halimodendri* B–D ♀ *S. halimodendri* F, G ♂ *S. roseri* H, I ♀ *S. roseri*.

midpoint, pulvillus small, not reaching or barely reaching midpoint of claw, attached to the claw along entire length; parempodia apically spatulate.

Genitalia. Genital capsule cone-shaped, without distinctive ornamentation, as long as or slightly longer than wide at base. Sclerotized apical part of phalotheca narrow, beak-shaped, somewhat constricted at base (Fig. 9C, F, I, L, O, R, U). Right paramere oval to elongate-oval, usually basally broadly rounded, and well expanded proximally beyond basal process, with contrastingly long, straight, apical process (Fig. 9A, D, G, J, M, P, S). Left paramere of typical phylina shape, with straight apical process and triangular, sensory lobe (Fig. 9B, E, H, K, N, Q, T). Vesica large, strongly coiled at middle, with two long and thin, gradually tapering apical blades tightly fused along most length; secondary gonopore large, located close to middle of vesica, with small gonopore sclerite (Figs 7, 8).

Female. Coloration, surface, and vestiture. As in male. **Structure.** Similar to male, usually smaller on average (Table 1). Antennal segment II in *S. nitidus* species group somewhat shorter and more strongly swollen, distinctly fusiform.

Genitalia. Dorsal labiate plate with large and wide, broadly oval or apically tapering sclerotized rings (Fig. 10A–C, G). Posterior wall membranous, with indistinctly bordered longitudinal sclerotized bands at sides (Fig. 10D, F). Sclerites encircling vulva triangular, symmetrical (Fig. 10 E, H). Vestibulum characteristically long and thin, S-shaped (Fig. 10B, E, H).

Species groups. Three distinct groups of species can be recognized within *Salicarus*, and the species treatments below are arranged alphabetically within each group:

***Salicarus nitidus* species group.** This group includes *S. cavinotum*, *S. genistae*, *S. nitidus*, and *S. perpusillus*. Species in this group are characterized by their uniformly dark color, dorsum densely covered with wide, apically serrate scale-like setae (scales type 2 sensu Stonedahl 1990), small size with a stumpy body, and total length ranging from 2.0 to 2.8. They have strongly swollen antennal segments I and II, with segment II distinctly fusiform. Species of this group have a Euro-Mediterranean distribution and utilize legumes (Fabaceae) of the tribe Genisteae (*Genista*, *Calicotome*, *Echinopartum*) as hosts.

***Salicarus roseri* species group.** This group includes *S. concinnus*, *S. roseri*, and *S. urnammu*. Species in this group are characterized by their highly variable color pattern, relatively large, oval body with a total length of 3.0–4.0. The dorsum vestiture consists of short, adpressed simple setae, while narrow, apically acuminate scale-like setae (scales type 1 sensu Stonedahl 1990) are scarce and limited to the hemelytron (if present). The vesica in these species is relatively large, with short and robust, knife-shaped apical blades. Species in this group feed on *Salix* spp. and tend to have a wide distribution: Palearctic in the case of *S. roseri*, Central Asia for *S. concinnus*, and western Asia for *S. urnammu*.

***Salicarus fulvicornis* species group.** This group includes *S. halimodendri* and *S. fulvicornis*. Species in this group are variable in coloration, with elongate males (3.6–4.0) and more ovoid females (3.5–3.9). The entire dorsum, except the head, is clothed with a mixture of silvery narrow, apically acuminate scale-like setae, and dense, comparatively long simple setae that are approximately 1.5× as long as the scales. The apical blades of the vesica are very long, thin, gradually curved, and abruptly furcate. Species of this group feed exclusively on *Caragana* spp. (Fabaceae: Hedysareae) and are mainly distributed in Central Asia and Mongolia.

Key to species

- 1 Smaller than 2.8. Antennal segment II distinctly swollen, fusiform. Dorsum and venter, including head, pronotum and abdomen, with dense, wide, apically serrate scales (Fig. 5).....**2**
- Larger than 3.0. Antennal segment II thin. Scale-like setae on dorsum, if present, narrow and apically acuminate (Fig. 4)**5**
- 2 Femora with scale-like setae**3**
- Femora without scale-like setae.....**4**
- 3 Apical blades of vesica long, gradually curving, closely located but separate, not adjoining each other (Fig. 8D, E, I). Southern Spain, southern France, southern Italy ***S. nitidus***
- Apical blades of vesica gradually curved and tightly adjoining each other along their entire length (Fig. 8F, G). Spain, southern France, Greece ***S. perpusillus***
- 4 Antennal segment II distinctly fusiform in both sexes, 1.6–1.8× as wide at midpoint as segment I at apex (Fig. 5A, B). Apical blades of vesica comparatively long, with length of larger blade distinctly exceeding distance between its base and secondary gonopore (Fig. 8A). Greece..... ***S. cavinotum***
- Antennal segment II in male swollen along entire length, slightly fusiform, with midpoint width subequal to apical width of segment I (Fig. 5G). In female segment II fusiform 1.5–1.6× as wide at midpoint as segment I at apex (Fig. 5C). Apical blades of vesica comparatively short, with length of larger blade subequal to distance between its base and secondary gonopore (Fig. 8B, C). Cyprus ***S. genistae***
- 5 Hemelytron without scale-like setae, clothed with short, strongly adpressed, simple silvery setae only (Fig. 2F–I). Vesica with straight, short and robust, diverging apical blades (Fig. 7G, H). Widely distributed in the Palearctic. On *Salix* spp. ***S. roseri***
- Hemelytron clothed with a mixture of simple setae and narrow, apically acuminate scale-like setae (Fig. 3C, F, I).....**6**
- 6 Dorsum clothed with short, subequal in length to scale-like setae on hemelytron, adpressed simple setae; narrow scale-like setae scarce and present on hemelytron only (Fig. 4C, O). Vesica with straight, short and robust apical blades (Fig. 7A, B, I, J). On *Salix* spp. **7**
- Pronotum, scutellum, and hemelytron clothed with a mixture of silvery narrow scale-like setae and dense, long, simple setae ~ 1.5× as long as scales (Fig. 4 D–I). Vesica with long and thin apical blades (Fig. 7C–F). On *Caragana* spp. **8**
- 7 Vesica with almost parallel apical blades (Fig. 7A, B). Color-pattern of dorsum variable, ranging from entirely or largely brown to pale yellow with darkened basal margin of pronotum (Fig. 1A–F). Central Asia ***S. concinnus***
- Vesica with gradually diverging apical blades (Fig. 7I, J). Dorsum yellow, frequently with orange tinge, sometimes with partly brown pronotum, scutellum, and endocorium (Fig. 3A–D). Southwest Asia ***S. urnammu***
- 8 Coloration of dorsum variable, ranging from almost entirely dark brown to pale yellow, but vertex always dirty to whitish yellow along posterior

margin (Fig. 2A–D). Body in male elongate-oval, 2.7–2.9× as long as posterior width of pronotum. Apical blades of vesica abruptly furcate, with one being distinctly smaller than the other (Fig. 7E, F). Central Asia and Mongolia ***S. halimodendri***

- Dorsum uniformly dark brown to brown (Fig. 1G–I). Body in male elongate, almost parallel-sided, 3.1–3.6× as long as width of pronotum at base. Both blades of vesica long, slightly diverging (Fig. 7C, D). Mongolia and adjacent regions of Russia and China ***S. fulvicornis***

***Salicarus nitidus* species group**

***Salicarus cavinotum* (Wagner, 1973)**

Figs 3E, F, 5A, B, 8A

Heterocapillus cavinotum Wagner, 1973: 121.

Heterocapillus cavinotum: Wagner (1975a): 128 (key, description, figures); Linnavuori (1999): 58 (figures, updated diagnosis); Kment et al. (2005): 12 (new record).

Salicarus cavinotum: Konstantinov (2023): 861 (phylogenetic placement, figures, discussion).

Material examined. Holotype: ♂ GREECE • **Dodecanese Islands:** Petaloudes, Rhodos, 36.444°N, 28.222°E, 01 Jun 1972, Eckerlein (AMNH_PBI 00184018) (ZMUH). **Paratypes:** GREECE • **Dodecanese Islands:** Petaloudes, Rhodos, 36.444°N, 28.222°E, 01 Jun 1972, Eckerlein, 1♂ (AMNH_PBI 00184019), 1♀ (AMNH_PBI 00336963) (ZMUH).

Other specimens examined: GREECE • **Dodecanese Islands:** Petaloudes, Rhodos, 36.444°N, 28.222°E, 01 Jun 1972, Eckerlein, 1♂ (AMNH_PBI 00240965) (ZISP) • **Peloponnese: Corinth (Korinthia):** nr Kehries, 37.885°N, 22.9875°E, 26 May 1989, R. Linnavuori, 2♂ (AMNH_PBI 00338309, AMNH_PBI 00338310) (NMWC) • Karitena, 37.46667°N 22.03333°E, 02 Jul 2007, A. Matocq, 7♀ (ZISP_ENT 00011853, ZISP_ENT 00011852), 4♂ (ZISP_ENT 00011853) (ZISP) • **Thessalia:** Magnesia Co.: nr Goritsa, 39.35389°N, 22.97694°E, 03 Jun 1989, R. Linnavuori, 3♀ (ZISP_ENT 00011721), 3♂ (ZISP_ENT 00011721) (NMWC).

Diagnosis. Recognized by the small size, body length 2.0–2.6; antennal segment II fusiform in both sexes, wider in female; dorsum uniformly dark brown, with dense, wide and apically serrate silvery scale-like setae (Figs 3E, F, 5A, B); legs and antennae without scales; apical blades of vesica gradually curved and tightly adjoining each other along their entire length, comparatively long, with length of larger blade distinctly exceeding distance between its base and secondary gonopore (Fig. 8A).

Salicarus cavinotum is most similar to *S. perpusillus* in general appearance, size, and vesica structure, which appear indistinguishable between these species (Fig. 8A, F, G). However, the latter species can be distinguished from *S. cavinotum* by the presence of dense scale-like setae on all femora, the bases of tibiae, antennal segment I, and the base of segment II (Fig. 5D–F). Additionally, in *S. perpusillus*, antennal segment II in males is 4.3–4.6× as long as wide at the midpoint and appears only slightly narrower than in

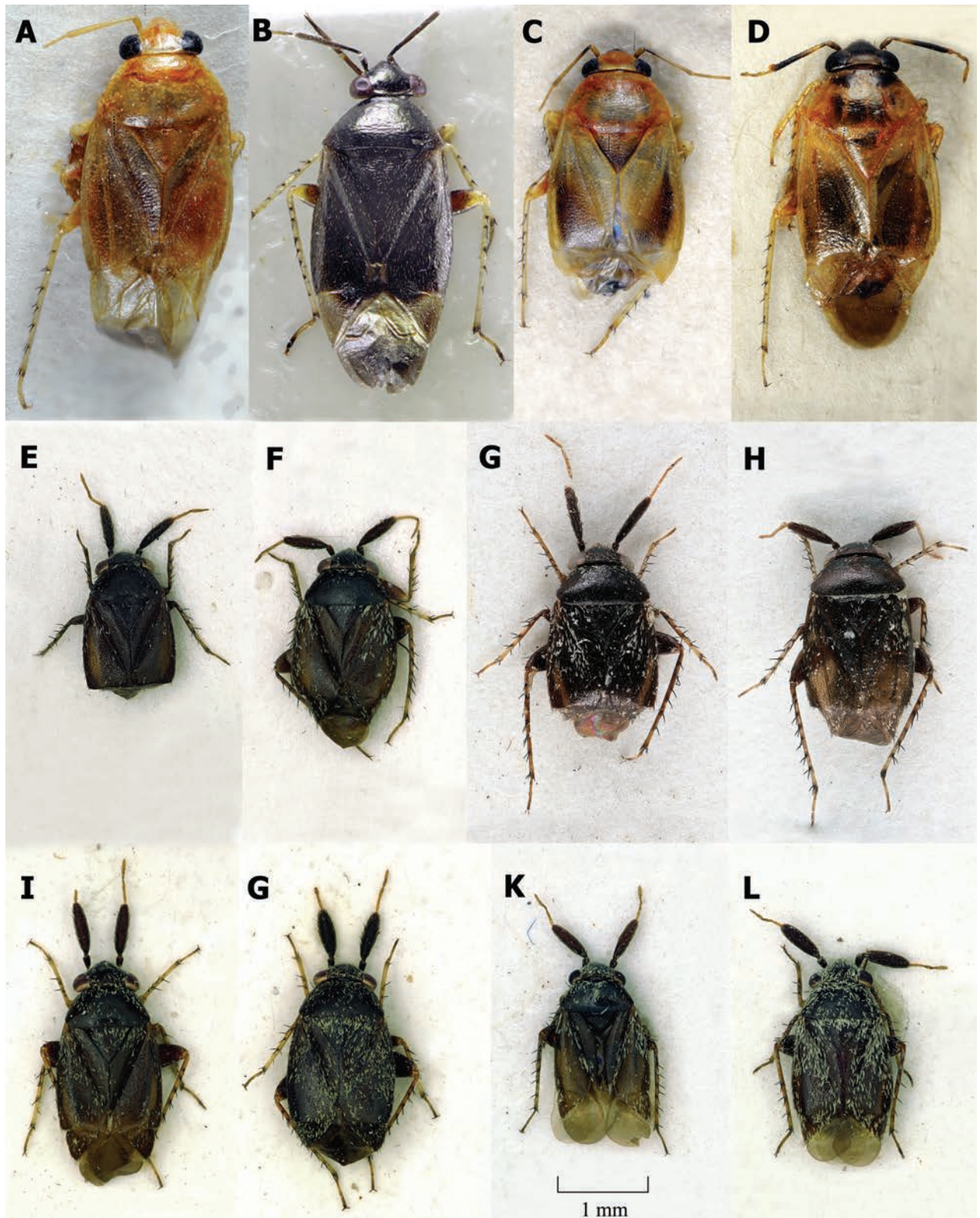


Figure 3. Dorsal habitus **A, B** ♂ *Salicarus urnammu* **C, D** ♀ *S. urnammu* **E** ♂ paratype of *S. cavinotum* **F** ♀ paratype of *S. cavinotum* **G** ♂ *S. genistae* **H** ♀ *S. genistae* **I** ♂ *S. nitidus* **G** ♀ *S. nitidus* **K** ♂ holotype of *S. perpusillus* **L** ♀ *S. perpusillus*.

females, while in *S. cavinotum* this segment in male is less fusiform, 4.9–5.3× as long as wide at the midpoint. Refer to the diagnosis of *S. genistae* for additional discussion.

Redescription. Male. Coloration. Dorsum and venter uniformly brown to dark brown (Fig. 3E). **Head:** Brown to dark brown, apices of labial segments I and II usually pale brown; antennal segments III and IV uniformly pale yellow. **Thorax:** Uniformly brown to dark brown, extreme apices of fore and middle femora pale brown to dirty yellow, tibiae dirty yellow, with small but distinct round spots at bases of tibial spines; tarsi pale yellow, with darkened apices; membrane and veins uniformly brown. **Abdomen:** Uniformly dark brown.

Surface and vestiture. Smooth, moderately shiny; dorsum, thoracic pleura, and abdomen with dense, silvery, broad and apically serrate scale-like setae and adpressed to semierect, long, almost twice as long as scales, simple setae, dark on cuneus and apex of corium, yellowish elsewhere; legs and antennae without scale-like setae; sides of pronotum and hemelytron at base with robust, long, erect to semierect, black bristle-like setae.

Structure. Body 2.4–3.0× as long as posterior width of pronotum; total length 2.0–2.6; vertex 2.3–2.7× as wide as eye; antennal segment I short, swollen, widest at apex, about twice as long as width at apex; segment II fusiform, 1.6× as wide at midpoint as segment I at apex, 4.9–5.3× as long as wide, 0.6× as long as posterior width of pronotum, 0.7–0.8× as long as width of head; segments III and IV filiform; pronotum 2.1–2.4× as wide as long, 1.2–1.3× as wide as head.

Genitalia. Right paramere with oval body about twice as long as wide, basally broadly rounded and expanded well proximally beyond basal process, apical process long and straight, apically rounded. Left paramere similar to those of *S. genistae* (Fig. 9E) and *S. nitidus* (Fig. 9H), with comparatively short and straight apical process and gradually narrowing towards apex, broadly rounded sensory lobe. Apical blades of vesica gradually curved, tightly adjoining each other along their entire length, comparatively long, with length of larger blade distinctly exceeding distance between its base and secondary gonopore (Fig. 8A).

Female. Coloration, surface, and vestiture. As in male (Fig. 3F).

Structure. Body 2.2–2.5× as long as posterior width of pronotum; total length 2.1–2.3; vertex 2.5–2.9× as wide as eye; antennal segment I short, swollen, widest at apex, about twice as long as width at apex; segment II fusiform, wider than in male, 1.7–1.8× as wide at midpoint as segment I at apex, 4.1–4.3× as long as wide, 0.5–0.6× as long as posterior width of pronotum, 0.7–0.8× as long as width of head; pronotum 2.1–2.4× as wide as long, 1.3× as wide as head.

Genitalia. Dorsal labiate plate with large and wide, broadly oval, but apically tapering sclerotized rings.

Distribution. Currently this species is documented exclusively in Greece, spanning Thessaly, the Peloponnese and Attic peninsulas, as well as Crete and Rhodes Island (Wagner 1973; Linnavuori 1999; Kment et al. 2005)

Hosts. *Genista* sp. (Wagner 1975a), *Genista acanthoclada* DC (Linnavuori 1999).

Discussion. Wagner (1973, 1975a) highlighted the significance of paired rounded pits on the pronotum as the primary distinguishing feature of *S. cavinotum*, effectively distinguishing it from closely related species. Upon examination of the holotype of this species, we discovered the absence of cavities on the pronotum as described originally, albeit the designated holotype being teneral specimen with a slightly deformed pronotum, as correctly noted by Linnavuori (1999). Other specimens from the type series are in good condition and exhibit no signs of pits on pronotum (Fig. 5A, B).

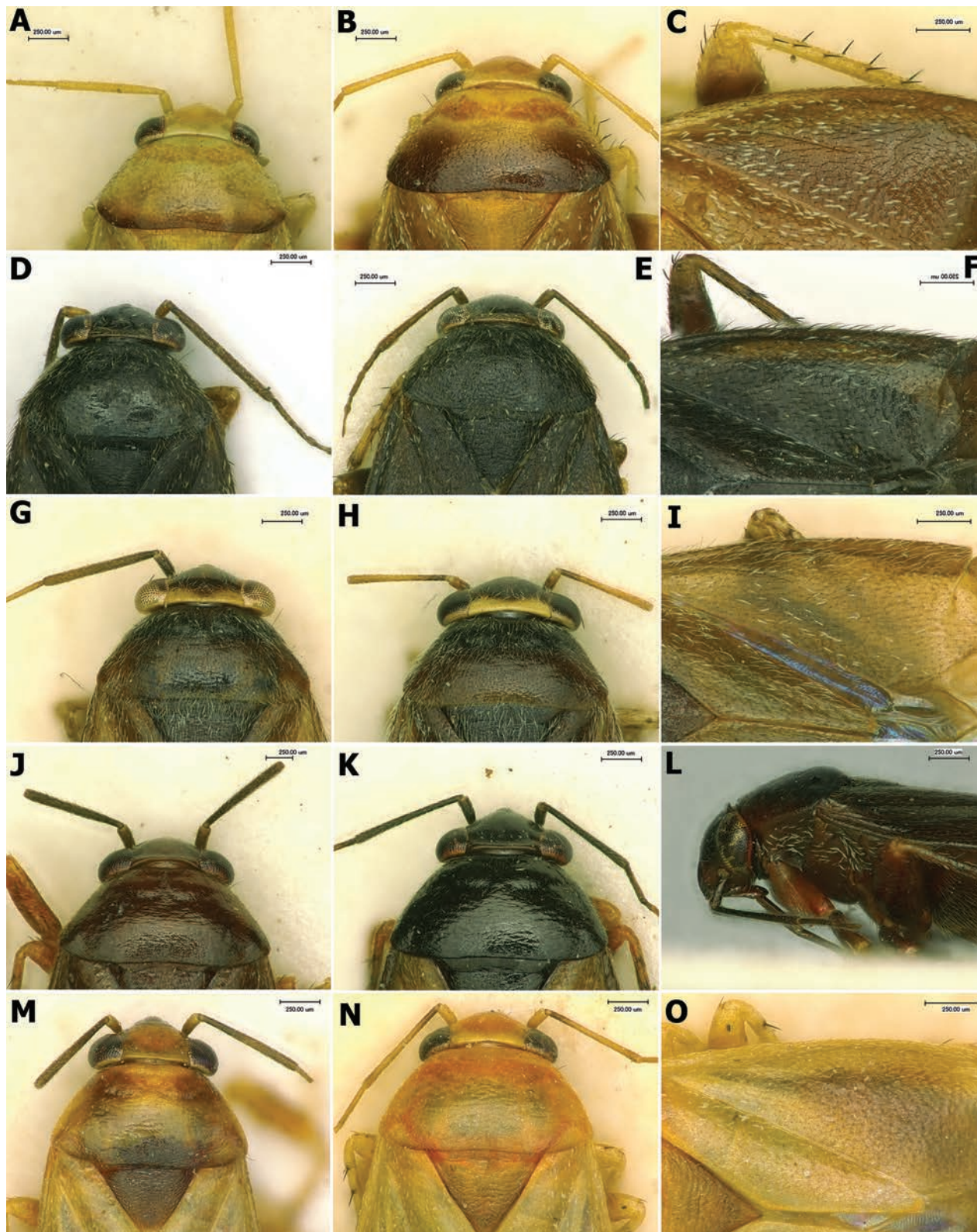


Figure 4. Head, pronotum, and vestiture **A–C** *Salicarus concinnus* in dorsal view: **A** ♂ paratype, head and pronotum **B** ♀ paratype, head and pronotum **C** ♀ paratype, vestiture on hemelytron **D–F** *S. fulvicornis* in dorsal view: **D** ♂ head and pronotum **E** ♀ head and pronotum **F** ♂ vestiture on hemelytron **G–I** *S. halimodendri* in dorsal view: **G** ♂ paratype **H** ♀ paratype **I** ♂ paratype, vestiture on hemelytron **J–L** *S. roseri*: **J** ♂ head and pronotum **K** ♀ head and pronotum **L** head and thoracic pleura in lateral view **M–O** *S. urnammu* in dorsal view: **M** ♂ head and pronotum **N** ♀ head and pronotum **O** ♀ vestiture on hemelytron.

***Salicarus genistae* (Lindberg, 1948)**

Figs 3G, H, 5C, G, 8B, C, H, 9D–F, 10C, E

Atractotomus genistae Lindberg, 1948: 53.

Heterocapillus genistae: Wagner (1975a): 126 (key, description, figures);

Linnavuori (1999): 58 (figures of antennae and vesica, discussion).

Salicarus genistae: Konstantinov (2023): 861 (phylogenetic placement, figures, discussion).

Material examined. Paralectotypes: **CYPRUS** • Ayios Hilarion, 35.3125°N, 33.28333°E, 07 Jun 1939, Hakan Lindberg, 1♂ (AMNH_PBI 00336958) (ZMUH) • Troodos Mesopotamos, 34.896°N, 32.908°E, 21 Jun 1939, Hakan Lindberg, 1♀ (AMNH_PBI 00336965) (ZMUH).

Otherspecimens examined: **CYPRUS** • Kakomallis Mt., 34.83333°N, 33.03333°E, 914 m, 13 Jun 1965, G. Mavromoustakis, 2♂ (AMNH_PBI 00336959, AMNH_PBI 00336960), 2♀ (AMNH_PBI 00336966, AMNH_PBI 00336967) (ZMUH) • Kalokhorio, 34.845°N, 33.034°E, 762 m, 29 Jun 1956, Unknown collector, 1♀ (AMNH_PBI 00240953), 2♂ (AMNH_PBI 00240954, AMNH_PBI 00240946) (ZISP) • Pano Lefkara, 34.869°N, 33.302°E, 28 May 1972, Eckerlein, 6♂ (AMNH_PBI 00240947–AMNH_PBI 00240952), 1♀ (AMNH_PBI 00240955) (ZISP).

Diagnosis. Recognized by the relatively small, stumpy, dark brown body, total length male 2.2–2.5, female 2.6–2.8 (Fig. 3G, H); dorsum with dense, wide and apically serrate white scales; legs and antennae without scales; antennal segment II in male swollen, somewhat fusiform, subequal in width at midpoint to apical width of segment I, 6.4–6.7× as long as wide, in female distinctly fusiform, 1.5–1.6× as wide at midpoint as segment I at apex, 4.9–5.2× as long as wide (Fig. 5C, G); apical blades of vesica tightly adjoining each other along their entire length, comparatively short, with length of larger blade subequal to distance between its base and secondary gonopore (Fig. 8B, C, H).

Salicarus genistae is most similar in habitus, coloration, size, and male genitalia structure to *S. cavinotum*, *S. nitidus*, and *S. perpusillus*. It differs habitually from these species by its sexually dimorphic antennal segment II: in males it is slightly fusiform with the width at the midpoint being subequal to the apical width of segment I; in females it is distinctly fusiform, being 1.5–1.6× as wide at the midpoint as segment I at the apex. Consequently, antennal segment II is 6.4–6.7× as long as wide in males of *S. genistae*, being 4.9–5.2× as long as wide in female. In other three closely related species this ratio ranges 4.1–5.3× in males and 3.9–4.3× in females. However, these ratios should be used with caution due to observed polymorphism and the extremely dense vestiture of antennal segment II, which can affect the measurements. *Salicarus genistae* further differs from both *S. nitidus* and *S. perpusillus* in the absence of scales on femora. In vesica structure, with the apical blades tightly adjoining each other, it is most similar to *S. cavinotum* (Fig. 8A) and *S. perpusillus* (Fig. 8F, G), whereas in *S. nitidus* blades are apically separated. However, the vesica in *S. genistae* is slightly larger than in both *S. cavinotum* and *S. perpusillus*, and differs by having shorter apical blades, with the length of the larger blade subequal to the distance between its base and the secondary gonopore.

Redescription. Male. Coloration. Dorsum and venter uniformly chestnut to dark brown (Fig. 3G). **Head:** Brown to dark brown, buccula and apices of labial

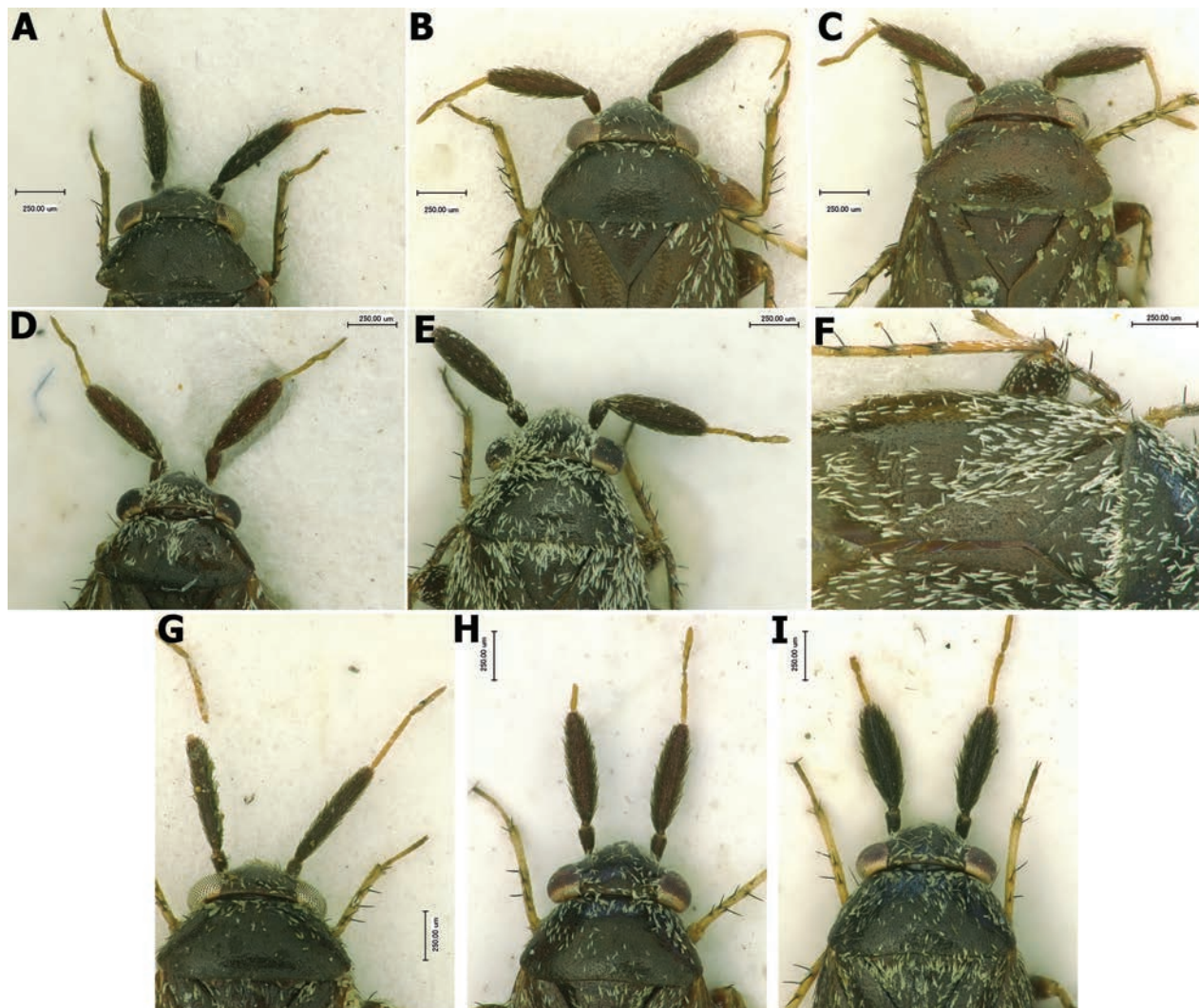


Figure 5. Head, pronotum, and vestiture **A, B** paratype of *Salicarus cavinotum*, head and pronotum in dorsal view: **A** ♂ **B** ♀ **C, G** *S. genistae*, head and pronotum in dorsal view: **C** ♂ **G** ♀ **D–F** paratypes of *S. perpusillus*: **D** ♂ head and pronotum in dorsal view **E** ♀ head and pronotum in dorsal view **F** ♀ vestiture on dorsum and legs **H–I** *S. nitidus*, head and pronotum in dorsal view: **H** ♂ **I** ♀.

segments I and II usually paler; antennal segments III and IV uniformly pale yellow. **Thorax:** Uniformly brown to dark brown, tibiae dirty yellow, rarely somewhat darkened basally, with small, sometimes indistinct round spots at bases of tibial spines; tarsi pale yellow, with darkened apices; membrane and veins uniformly brown. **Abdomen:** Uniformly dark brown.

Surface and vestiture. Smooth, moderately shiny; dorsum, thoracic pleura, and abdomen with dense, silvery, broad and apically serrate scale-like setae and adpressed to semierect, long, almost twice as long as scales, simple setae, dark on cuneus and extreme apex of corium and goldish yellow elsewhere (Fig. 5G); in addition, sides of pronotum and hemelytron at base with robust dark contrastingly long, erect to semierect simple setae; appendages with simple, adpressed to semierect pale setae, contrastingly dense, dark and robust on antennal segments I and II; tibial spines dark brown to black.

Structure. Body stumpy, oval, 2.1–2.4× as long as posterior width of pronotum; total length 2.2–2.5; vertex flat, 2.0–2.2× as wide as eye; segment I

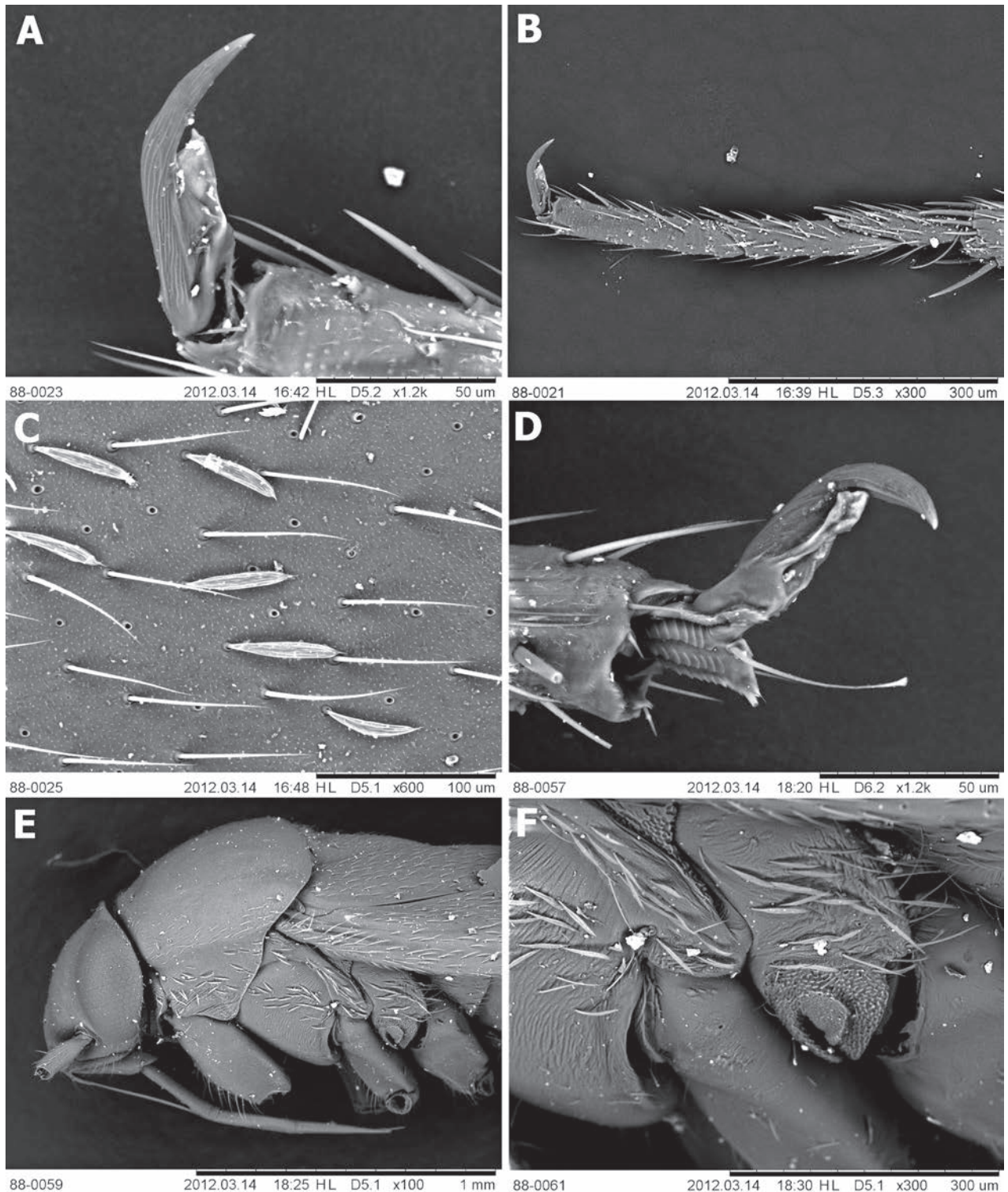


Figure 6. Scanning electron images of selected structures **A–C** *Salicarus fulvicornis*: **A** pretarsus in lateral view **B** hind tarsus in lateral view **C** vestiture on hemelytron **D–F** *S. roseri*: **D** pretarsus in lateral view **E** head and thoracic pleura in lateral view **F** metathoracic spiracle and scent gland evaporative area.

short, swollen, widest at apex, about twice as long as width at apex; segment II swollen along entire length, somewhat fusiform, with midpoint width subequal to apical width of segment I, 6.4–6.7× as long as wide, 0.5–0.6× as long as basal width of pronotum, 0.7–0.8× as long as width of head; segments III

and IV filiform; labium reaching metacoxa; pronotum 2.2–2.4× as wide as long, 1.4–1.5× as wide as head; mesonotum only slightly exposed.

Genitalia. Right paramere oval, approximately twice as long as wide, basally broadly rounded, and well expanded proximally beyond basal process, with long, straight, gradually tapering apical process (Fig. 9D). Left paramere with short and straight apical process and triangular, apically broadly rounded sensory lobe (Fig. 9E). Vesica with comparatively short apical blades tightly adjoining each other along their entire length, larger blade subequal in length to distance between its base and secondary gonopore (Fig. 8B, C).

Female. Coloration, surface, and vestiture. As in male (Fig. 3H).

Structure. Body 2.5–2.7× as long as posterior width of pronotum; total length 2.6–2.8; vertex 2.2–2.6× as wide as eye; antennal segment I short, swollen, widest at apex, about twice as long as width at apex; segment II somewhat shorter than in male, strongly swollen, fusiform, 1.5–1.6× as wide at midpoint as segment I at apex, 4.9–5.2× as long as wide, 0.5–0.6× as long as posterior width of pronotum, 0.7–0.8× as long as width of head; pronotum 2.1–2.2× as wide as long, 1.3–1.4× as wide as head.

Genitalia. Dorsal labiate plate with large and wide, broadly oval, but apically tapering sclerotized rings (Fig. 10C). Posterior wall membranous, somewhat strongly sclerotized at sides (Fig. 10D). Vestibulum long and thin, S-shaped (Fig. 10E).

Distribution. Originally described and still known from Cyprus. A record from Manavgat (Antalya province of Turkey) based on a single specimen of unknown sex (Lodos et al. 2003) requires confirmation.

Host. *Genista fasselata* Decne. (Lindberg 1948, as *G. sphacelata*). An indication of *Onopordum* sp. (Asteraceae) as host (Lodos et al. 2003) certainly represents a sitting record.

Discussion. Refer to the corresponding section in the redescription of *S. nitidus*.

***Salicarus nitidus* (Horváth, 1905)**

Figs 3I, G, 5H, I, 8D, E, I, 9G–I

Atractotomus nitidus Horváth, 1905: 275.

Heterocapillus nitidus: Wagner (1975a): 127 (key, description, figures); Heckmann et al. (2015): 95 (figure of vesica).

Salicarus nitidus: Konstantinov (2023): 861 (phylogenetic placement, figures, discussion).

Material examined. Holotype: SPAIN • *Castile-La Mancha*: ♀ Pozuelo de Calatrava 38.91°N, 3.84°W, Collection date unknown, José María de la Fuente (HNHM) (not seen; pictures of the head and habitus in dorsal and lateral views were examined).

Other specimens examined: FRANCE • *Corse (Corsica)*: Costa, 42.0333°N, 8.95°E, 19 Jul 1963, Unknown collector, 1 ♀ (AMNH_PBI 00336969) (ZMUH) • Tiuccia, 42.06566°N, 8.73889°E, 10 m, 19 Jun 1961, J. Péricart, *Calicotome villosa* (Fabaceae), 1 ♂ (AMNH_PBI 00336961), 1 ♀ (AMNH_PBI 00336968) (ZMUH) • *Midi-Pyrenees*: Vernet, 43.18305°N, 1.6°E, 700 m, 06 Jun 1962, J. Péricart, 1 ♂ (AMNH_PBI 00336964) (ZMUH).

Diagnosis. Recognized by the small, stumpy, uniformly dark brown body, total length male 2.3–2.6, female 2.2–2.4; dorsum with dense, wide, and apically serrate scale-like setae, femora also clothed with scales (Fig. 3I, G); antennal segment II distinctly fusiform, at midpoint male 1.4–1.5 \times , female 1.6–1.7 \times as wide as segment I at apex (Fig. 5H, I); apical blades of vesica long, gradually curving, closely located but separate, not adjoining each other (Fig. 8D, E, I).

Most similar to *S. perpusillus* in size, body proportions, and the distinctly fusiform antennal segment II in both sexes, as well as the presence of scale-like setae on femora (although scales are absent on the bases of tibiae and antennae). However, it differs from this species, as well as from *S. cavinotum* and *S. genistae* in the vesica structure with apical blades that are not tightly adjoining. Additionally, *S. nitidus* is the only one of the closely related species mentioned above that feeds on *Calicotome* rather than *Genista* spp. Refer to the diagnosis of *S. genistae* for additional discussion.

Redescription. Male. Coloration. Dorsum and venter uniformly brown to dark brown (Fig. 3I). **Head:** Brown to dark brown, apices of labial segments I and II usually pale brown; antennal segments III and IV uniformly pale yellow. **Thorax:** Brown to dark brown, tibiae dirty yellow, with round spots at bases of tibial spines, very small on fore and middle tibiae, distinct on hind tibia; tarsi pale yellow, with darkened apices; membrane and veins uniformly brown. **Abdomen:** Uniformly dark brown.

Surface and vestiture. Smooth, moderately shiny; dorsum, thoracic pleura, femora, and abdomen with dense, silvery, broad and apically serrate scale-like setae and adpressed to semierect, long, almost twice as long as scales, simple setae, dark on cuneus and apex of corium, yellowish elsewhere; series of long simple setae on fore coxa silver; sides of pronotum and hemelytron at base with robust, long, erect to semierect, black bristle-like setae.

Structure. Body 2.5–2.7 \times as long as posterior width of pronotum; total length 2.3–2.6; vertex 2.3–2.6 \times as wide as eye; antennal segment II distinctly fusiform, 1.4–1.5 \times as wide at midpoint as segment I at apex, 4.1–4.3 \times as long as wide, 0.5–0.6 \times as long as posterior width of pronotum, 0.7 \times as long as width of head; pronotum 2.1–2.3 \times as wide as long, 1.3 \times as wide as head.

Genitalia. Right paramere spoon-shaped, with long, straight, and blunt apical process (Fig. 9G). Right paramere with thin, short, and straight apical process and broadly rounded sensory lobe (Fig. 9H). Vesica with very long, gradually curving, apical blades, closely located but separate, not adjoining each other (Fig. 8D, E, I).

Female. Coloration, surface, and vestiture. As in male (Fig. 3G).

Structure. Body 2.3–2.5 \times as long as posterior width of pronotum; total length 2.2–2.4; vertex 2.4–2.6 \times as wide as eye; antennal segment II somewhat wider than in male, 1.6–1.7 \times as wide at midpoint as segment I at apex, 4.0–4.1 \times as long as wide, 0.6 \times as long as posterior width of pronotum, 0.7 \times as long as width of head; pronotum 2.2–2.3 \times as wide as long, 1.3–1.4 \times as wide as head.

Genitalia. Dorsal labiate plate with large and wide, broadly oval at base, apically tapering sclerotized rings.

Distribution. Ciudad Real province of Spain (Wagner 1975a: Pozuelo de Calatrava), southern France (Wagner 1975a: Corsica), southern Italy (Carapezza 1984: Sardinia; Carapezza 1993: Aeolian Islands).

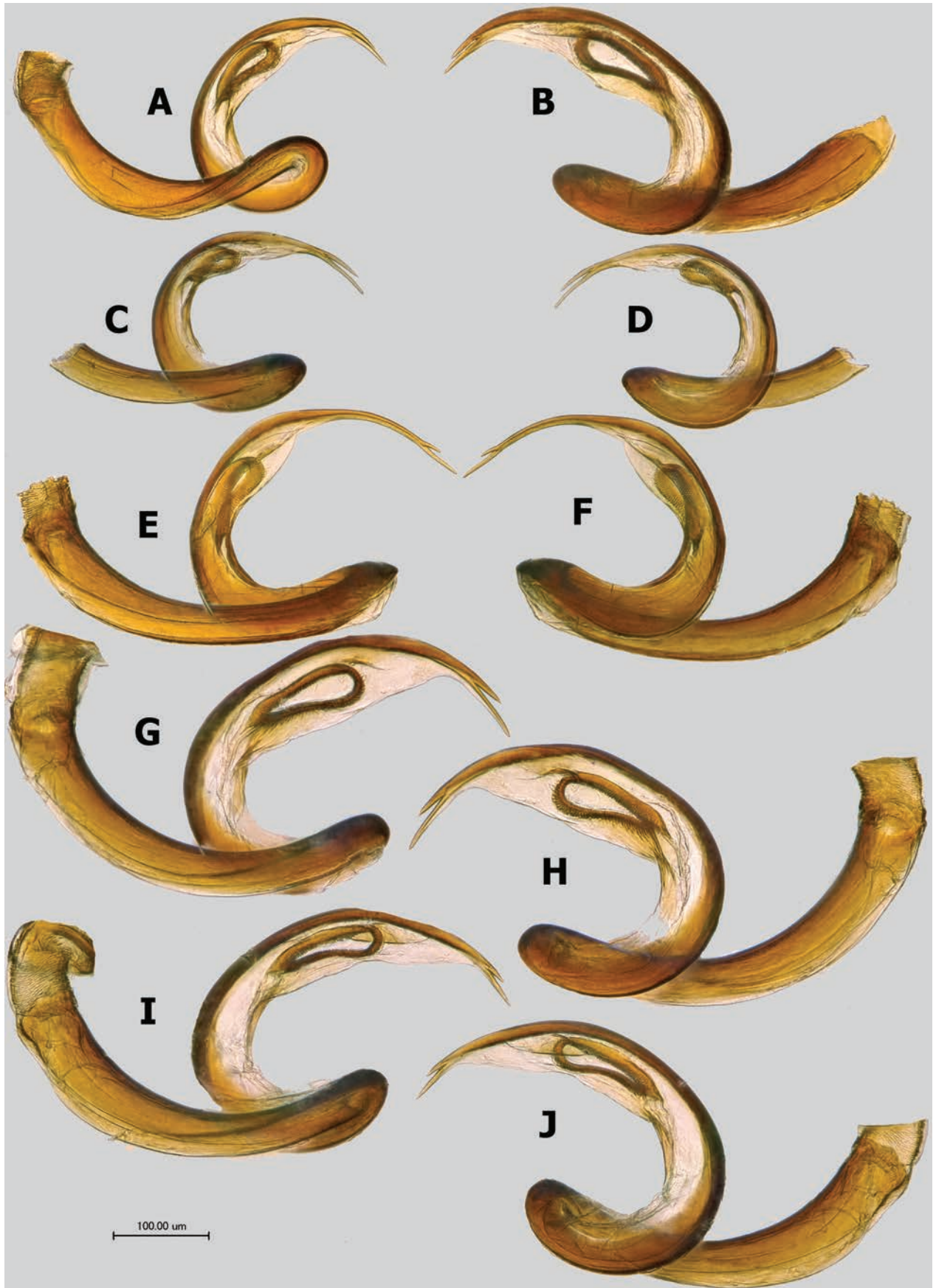


Figure 7. Vesica in left and right lateral views (left and right columns, respectively) **A, B** paratypes of *Salicarus concinnus* **C, D** *S. fulvicornis* **E, F** paratype of *S. halimodendri* **G, H** *S. roseri* **I, J** *S. urnammu*.

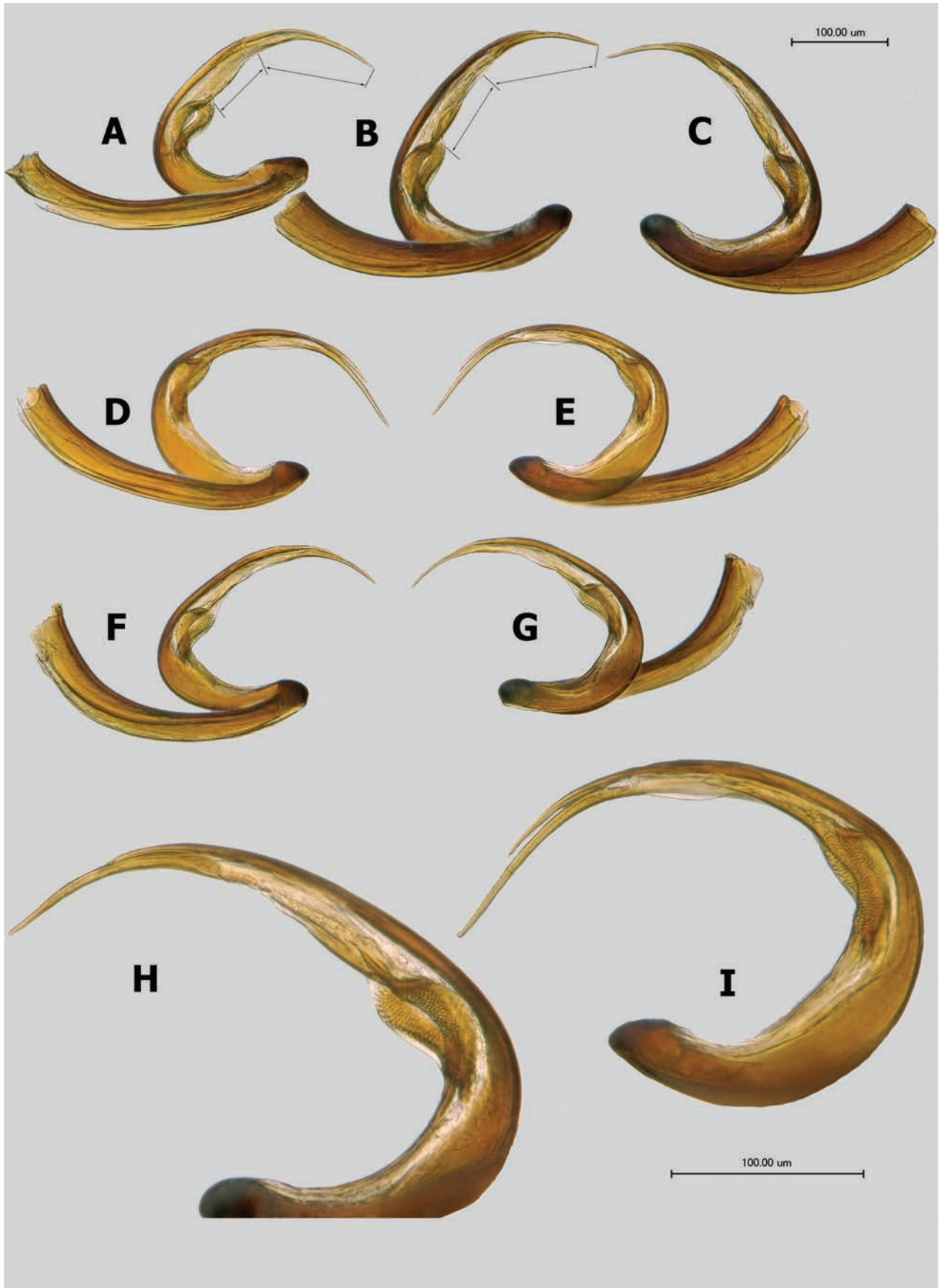


Figure 8. Vesica **A** *Salicarus cavinotum*, paratype **B, C** *S. genistae* **D, E** *S. nitidus* **F, G** *S. perpusillus*, paratype **H, I** apical part of vesica enlarged: **H** *S. genistae* **I** *S. nitidus*.

Host. *Calicotome villosa* (Poir.) Link. (Wagner 1975a). *Genista corsica* (Loisel.) DC was reported as a host from Sardinia (Carapezza 1984) and *Genista ephedroides* DC. from Aeolian Islands (Carapezza 1993). However, the last two records may pertain to *S. perpusillus* and require further confirmation (Carapezza 1995).

Discussion. *Salicarus nitidus* (Horváth, 1905) belongs to a group of four hardly distinguishable species with a complex taxonomic history, which also includes *S. cavinotum* (Wagner, 1973), *S. genistae* (Lindberg, 1948), and *S. perpusillus* (Wagner, 1960). These species inhabit the North Mediterranean, from central Spain in the West to Cyprus in the East. Horváth (1905) described *Atractotomus nitidus* based on a single female from central Spain and noted its similarity with *Atractotomus* (currently *Heterocapillus*) *tigripes* (Mulsant & Rey, 1852) due to its overall appearance and coloration, as well as the presence of large dark spots at bases of tibial spines. He distinguished *A. nitidus* by its much smaller size (2.25 mm), less fusiform antennal segment II, and tibiae not darkened ventrally.

Lindberg (1948) described *A. genistae* from a series of specimens collected in two localities in Cyprus. He emphasized the similarity of the new species to *Atractotomus mali* (Meyer-Dur, 1843) due to the spindle-shaped antennal segment II in both sexes. According to the original description, the new species differs in having a dark-colored membrane, dark spots at the bases of tibial spines, smaller size, and a shorter segment II, which is distinctly shorter than the head width. Lindberg (1948) did not mention *A. nitidus* in his diagnosis and was apparently unaware of this species.

Wagner (1960) described *Atractotomus perpusillus* from Sierra Nevada (southern Spain) as the smallest species of the genus (2.1–2.4 mm), most similar to *A. parvulus* Reuter, 1878, but differing from that species in having wide scale-like setae, a spindle-shaped antennal segment II, and a long and thin apical process of the vesica. Wagner also noted that the dorsal vestiture of *A. perpusillus*, with three types of setae, separates it from all congeners except *A. tigripes*. To accommodate these two species and *A. putoni* Reuter, 1878 (subsequently synonymized with *A. validicornis* Reuter, 1876), he erected the subgenus *Heterocapillus* Wagner, 1960 which was later upgraded to a valid genus by Kerzhner (1962). The last species of this group, *Heterocapillus cavinotum*, was described by Wagner (1973) from Rhodos Island (Greece). According to the original description, this species is most similar to *H. nitidus* and *H. perpusillus* but differs from both in having a pair of rounded pits on the pronotum, and a set of minor distinctions some of which, such as body length, appear to contradict with provided measurements.

In his monographic treatment of Mediterranean plant bugs Wagner (1975a) formulated the species concepts of these four closely related species as follows:

Heterocapillus genistae (Cyprus, on *Genista* sp.): relatively large, body length male 2.5 mm, female 3.0 mm, antennal segment II slightly spindle-shaped in male, distinctly spindle-shaped in female.

Heterocapillus cavinotum (Rhodos Island, on *Genista* spp.): body length male 2.35 mm, female 1.9 mm, pronotum with a pair of pits, antennal segment II distinctly spindle-shaped in both sexes, 3.8–4.0× as long as wide at middle.

Heterocapillus nitidus (central Spain, Corsica, on *Calicotome villosa*): body length male 2.5 mm, female 2.2–2.3 mm, antennal segment II spindle-shaped in both sexes, male 4×, female 3.9× as long as wide at middle.

Heterocapillus perpusillus (southern Spain, southern France, on *Genista* sp.): body length male 2.1 mm, female 2.3–2.4 mm, antennal segment II spindle-shaped in both sexes, male 4.2×, female 4.0× as long as wide at middle.

Since then, *H. cavinotum* was additionally reported from Peloponnese peninsula and Crete (Linnavuori 1999; Kment et al. 2005), while the presence of pits on the pronotum in this species was refuted (Linnavuori 1999). *Heterocapillus nitidus* was additionally indicated from Sardinia and Aeolian Islands (Italy, Carapezza 1984, 1993), while *H. perpusillus* from Laconia (Greece, Rieger 2012) and Crete (Heckmann et al. 2015). A synonymy of *H. perpusillus* with *H. nitidus* was suspected by Goula and Ribes (1995), but Heckmann et al. (2015) noted slight distinctions in the size and shape of the vesica between these two species. Konstantinov (2023) transferred all these species to *Salicarus*. Examination of all available material allows us to conclude that despite the notable similarity, all four species could be distinguished from each other by the combination of characters provided in the key to species and diagnoses. Molecular data are desirable for elucidating the status of these species. Pending such a study, we refrain from nomenclatorial changes.

***Salicarus perpusillus* (Wagner, 1960)**

Figs 3K, L, 5 D–F, 8F, G

Atractotomus (*Heterocapillus*) *perpusillus* Wagner, 1960: 81.

Heterocapillus perpusillus: Wagner (1975a): 128 (key, description, figures); Heckmann et al. (2015): 95 (figures of dorsal habitus and vesica).

Salicarus perpusillus: Konstantinov (2023): 861 (phylogenetic placement, figures, discussion).

Material examined. Holotype: SPAIN • Andalu**cia:** ♂ Northern Slopes of Veleta Peak [Veleta -Nordhang], Sierra Nevada, 37.07°N, 3.37°W, 2500 m, 03 Aug 1959, E. Wagner, (AMNH_PBI 00184020) (ZMUH). **Paratypes: SPAIN • Andalu****cia:** Northern Slopes of Veleta Peak [Veleta -Nordhang], Sierra Nevada, 37.07°N, 3.37°W, 2500 m, 02 Aug 1959, E. Wagner, 1 ♀ (AMNH_PBI 00336976) (ZMUH); 03 Aug 1959, E. Wagner, 1 ♂ (AMNH_PBI 00336979), 3 ♀ (AMNH_PBI 00336974, AMNH_PBI 00336975, AMNH_PBI 00336978) (ZMUH) • Sierra Nevada Veleta, 37.08333°N, 3.16667°W, 25 Jul 1959–04 Aug 1959, H. H. Weber, 2 ♀ (AMNH_PBI 00126474, AMNH_PBI 00126475) (ZSMC).

Other specimens examined: SPAIN • Catalonia: Campllong, Bergueda, 41.88333°N, 2.81667°E, 15 Jul 1984, E. Ribes, 1 ♂ (ZISP_ENT 00011719), 1 ♀ (ZISP_ENT 00011719) (NMPC) • Seros, Segria, 41.462°N, 0.412°E, 27 Jun 1971, J. Ribes, *Ulex* sp. (Fabaceae), 1 ♂ (AMNH_PBI 00338308) (NMWC) • Sonadell, Lleida, 02 Jun 1963, J. Ribes, 1 ♂ (AMNH_PBI 00338307) (NMWC).

Diagnosis. Recognized by the small and stumpy body, total length 2.1–2.4; dorsum uniformly dark brown with dense, wide and apically serrate scale-like setae (Fig. 3K); femora, bases of tibiae, segment I and base of segment II with also covered with wide silvery scales (Fig. 5F); antennal segment II distinctly fusiform, at middle male 1.3–1.5×, female 1.6–1.7× as wide as segment I at apex (Fig. 5D, E); apical blades of vesica gradually curved and tightly

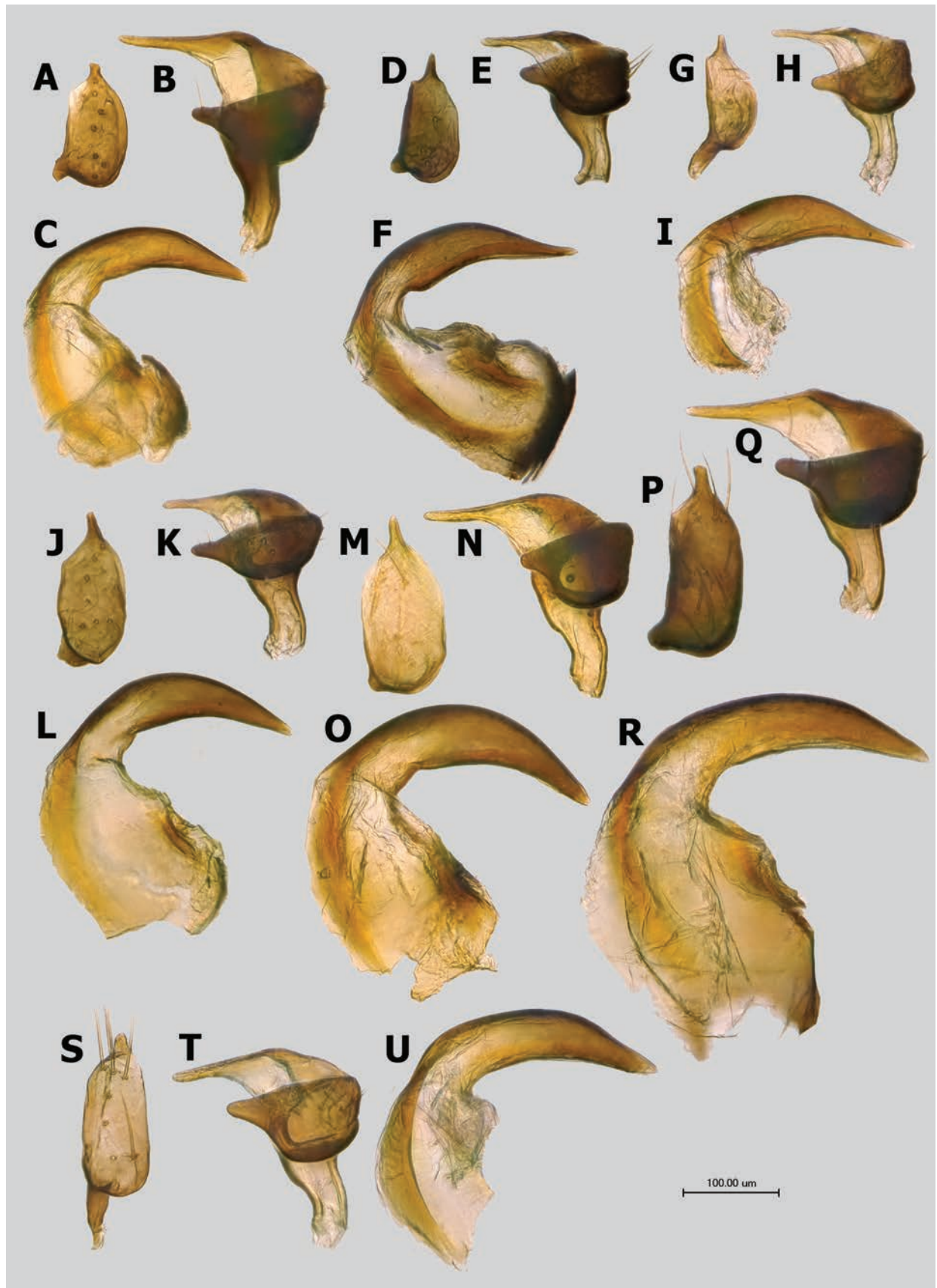


Figure 9. Male genitalia **A–C** *Salicarus concinnus*, paratype **D–F** *S. genistae* **G–I** *S. nitidus* **J–L** *S. fulvicornis* **M–O** *S. halimodendri*, paratype **P–R** *S. roseri* **S–U** *S. urnammu* **A D G J M P S**: right paramere **B E H K N Q U**: left paramere **C F I L O R U**: apex of phallosome.

adjoining each other along their entire length, comparatively long, with length of larger blade distinctly exceeding distance between its base and secondary gonopore (Fig. 8F, G).

Salicarus perpusillus is habitually most similar to *S. nitidus* in body proportions, the distinctly fusiform antennal segment II in both sexes, and the presence of scale-like setae on the femora. However, the latter species differs from *S. perpusillus* in its distinctive vesica structure with separate, not tightly adjoining apical blades. Indistinguishable from *S. cavinotum* in vesica structure but differs from that species by the presence of dense scale-like setae on the femora.

Redescription. Male. Coloration. Dorsum and venter uniformly brown to dark brown (Fig. 3K). **Head:** Brown to dark brown, apices of labial segments I and II usually pale brown; antennal segments III and IV uniformly pale yellow. **Thorax:** Uniformly brown to dark brown, tibiae dirty yellow, with small round spots at bases of tibial spines, less distinct on fore and middle tibiae; tarsi pale yellow, with darkened segment III; membrane and veins uniformly brown. **Abdomen:** Uniformly dark brown.

Surface and vestiture. Smooth, moderately shiny; dorsum, thoracic pleura, and abdomen with very dense, silvery, broad and apically serrate scale-like setae and adpressed to semierect, long, almost twice as long as scales, simple setae, dark on cuneus and apex of corium, yellowish elsewhere; antennal segments I and II, all femora and basal parts of tibiae clothed with scale-like setae; sides of pronotum and hemelytron at base with robust, long, erect to semierect, black bristle-like setae.

Structure. Body 2.1–2.3× as long as posterior width of pronotum; total length 2.1–2.4; vertex 2.2–2.5× as wide as eye; segment II distinctly fusiform, 1.3–1.5× as wide at midpoint as segment I at apex, 4.3–4.6× as long as wide, 0.5–0.6× as long as posterior width of pronotum, 0.7–0.8× as long as width of head; pronotum 2.1–2.2× as wide as long, 1.2–1.3× as wide as head.

Genitalia. Right paramere spoon-shaped, with long, straight apical process. Right paramere with short and straight apical process and broadly rounded sensory lobe. Vesica with gradually curved and comparatively long apical blades tightly adjoining each other along their entire length, with length of larger blade distinctly exceeding distance between its base and secondary gonopore (Fig. 8F, G).

Female. Coloration, surface, and vestiture. As in male (Fig. 3L).

Structure. Body 2.4–2.6× as long as posterior width of pronotum; total length 2.2–2.4; vertex 2.3–2.7× as wide as eye; segment II distinctly somewhat wider than in male, 1.6–1.7× as wide at midpoint as segment I at apex, 3.9–4.2× as long as wide, 0.6× as long as posterior width of pronotum, 0.7–0.8× as long as width of head; pronotum 2.1–2.2× as wide as long, 1.3× as wide as head.

Genitalia. Dorsal labiate plate with large and wide, broadly oval at base, apically tapering sclerotized rings.

Distribution. Spain (Wagner 1960: Sierra Nevada; Ehanno 1987: Navarre; Ribes et al. 2004: Catalonia; Pagola-Carte and Zabalegui 2007: Araba and Navarre), southern France (Wagner 1975a: Corsica; Ehanno 1987: Pyrénées-Orientales), Greece (Rieger 2012: Laconia; Heckmann et al. 2015: Peloponnese, Western Thrace, Crete). An indication from Italy (Faraci and Rizzotti Vlach 1995) was based on specimens collected by A. Melber in Saltino and Montemignaio, Tuscany from *Cytisus scoparius* L. (Melber 1993) and partly retained at the Museum of Verona. Franco Faraci kindly provided us with pictures of one

specimen from Secchieta Mt. which may belong to *S. genistae* and requires further confirmation of the species identity.

Host. *Genista versicolor* Boiss. (Wagner 1975a, as *Genista baetica* Spach.), *Genista scorpius* (L.) DC. (Ribes et al. 2004; Pagola-Carte and Zabalegui 2007), *Echinopartum horridum* (Vahl) Rothm. (Ehanno 1987, as *Genista horrida*).

Discussion. Goula and Ribes (1995), followed by Kerzhner and Josifov (1999) suspected that *S. perpusillus* is a junior synonym of *S. nitidus*. Heckmann et al. (2015) argued that these species can be distinguished based on their sizes, antennal proportions, and the shape of the vesica. Our observations indicate that distinctions in size and antennal segment II are not reliable diagnostic features, but these species can be differentiated by distinctions in the mutual arrangement of their apical blades (see Diagnosis).

***Salicarus roseri* species group**

***Salicarus concinnus* V. G. Putshkov, 1977**

Figs 1A–F, 4A–C, 7A, B, 9 A–C, 10A, B

Salicarus (Salicarus) concinnus V. G. Putshkov, 1977: 365.

Salicarus concinnus: Konstantinov (2023): 874 (phylogenetic placement, figures, discussion).

Material examined. Holotype: TAJIKISTAN • ♂ Kondara Canyon, Valley of Varzob River, 38.83333°N, 68.83333°E, 1100 m, 08 Jul 1955, Lopatin, (AMNH_PBI 00233863) (ZISP). **Paratypes:** KAZAKHSTAN • **South Kazakhstan Prov.:** Daubabana Tyul'kubas, Shimkent Dist., 42.46666°N, 70.26666°E, 18 Jun 1966, Unknown collector, *Salix* sp. (Salicaceae), 1♂ (AMNH_PBI 00233874) (ZISP). **KYRGYZSTAN** • Gava, 41.26666°N, 72.83333°E, 03 Aug 1937, A. N. Kiritshenko, 2♂ (AMNH_PBI 00233872, AMNH_PBI 00233873) (ZISP). TAJIKISTAN • Kondara Canyon, Valley of Varzob River, 38.83333°N, 68.83333°E, 1100 m, 19 Jun 1937, Gussakovskiy, 1♀ (AMNH_PBI 00233768) (ZISP) • 30 Jun 1943, A. N. Kiritshenko, 2♂ (AMNH_PBI 00233866, AMNH_PBI 00233867), 4♀ (AMNH_PBI 00233761-AMNH_PBI 00233764) (ZISP) • 05 Jul 1943, A. N. Kiritshenko, 1♀ (AMNH_PBI 00233760) (ZISP) • 10 Jun 1955, Zakieva, 1♀ (AMNH_PBI 00233769) (ZISP) • 16 Jun 1955, Lopatin, 1♀ (AMNH_PBI 00233758) (ZISP) • 08 Jul 1955, Lopatin, 1♂ (AMNH_PBI 00233864), 2♀ (AMNH_PBI 00233756, AMNH_PBI 00233757) (ZISP) • 09 Jul 1955, Lopatin, 1♂ (AMNH_PBI 00233865), 1♀ (AMNH_PBI 00233759) (ZISP) • 13 Jun 1956, Denisova and Ivanova, 3♀ (AMNH_PBI 00233765-AMNH_PBI 00233767) (ZISP) • 28 Jun 1956, Kiriyanova, 2♀ (AMNH_PBI 00233770, AMNH_PBI 00233771) (ZISP). **UZBEKISTAN** • Angren River, 15 km NO Angren, 41.1°N, 70.3°E, 18 Jun 1966, I. M. Kerzhner, 4♀ (AMNH_PBI 00233868-AMNH_PBI 00233871), 8♂ (AMNH_PBI 00233868-AMNH_PBI 00233871) (ZISP) • Karzhantau Mt. Ridge, 41.73333°N, 70.03333°E, 01 Jul 1939, Obukhova, *Salix wilhelmsiana* (Salicaceae), 1♀ (AMNH_PBI 00233773) (ZISP) • Tugay Ugama, Karzhantau Mt. Ridge, 41.73333°N, 70.03333°E, 17 Jul 1939, Obukhova, *Salix* sp. (Salicaceae), 4♂ (AMNH_PBI 00233875-AMNH_PBI 00233878), 1♀ (AMNH_PBI 00233772) (ZISP).

Other specimens examined: TAJIKISTAN • 6 km W Kuibyshevsk, Valley of Vakhsh River, 37.96666°N, 68.75°E, 14 Jul 1943, A. N. Kiritshenko, 1♀

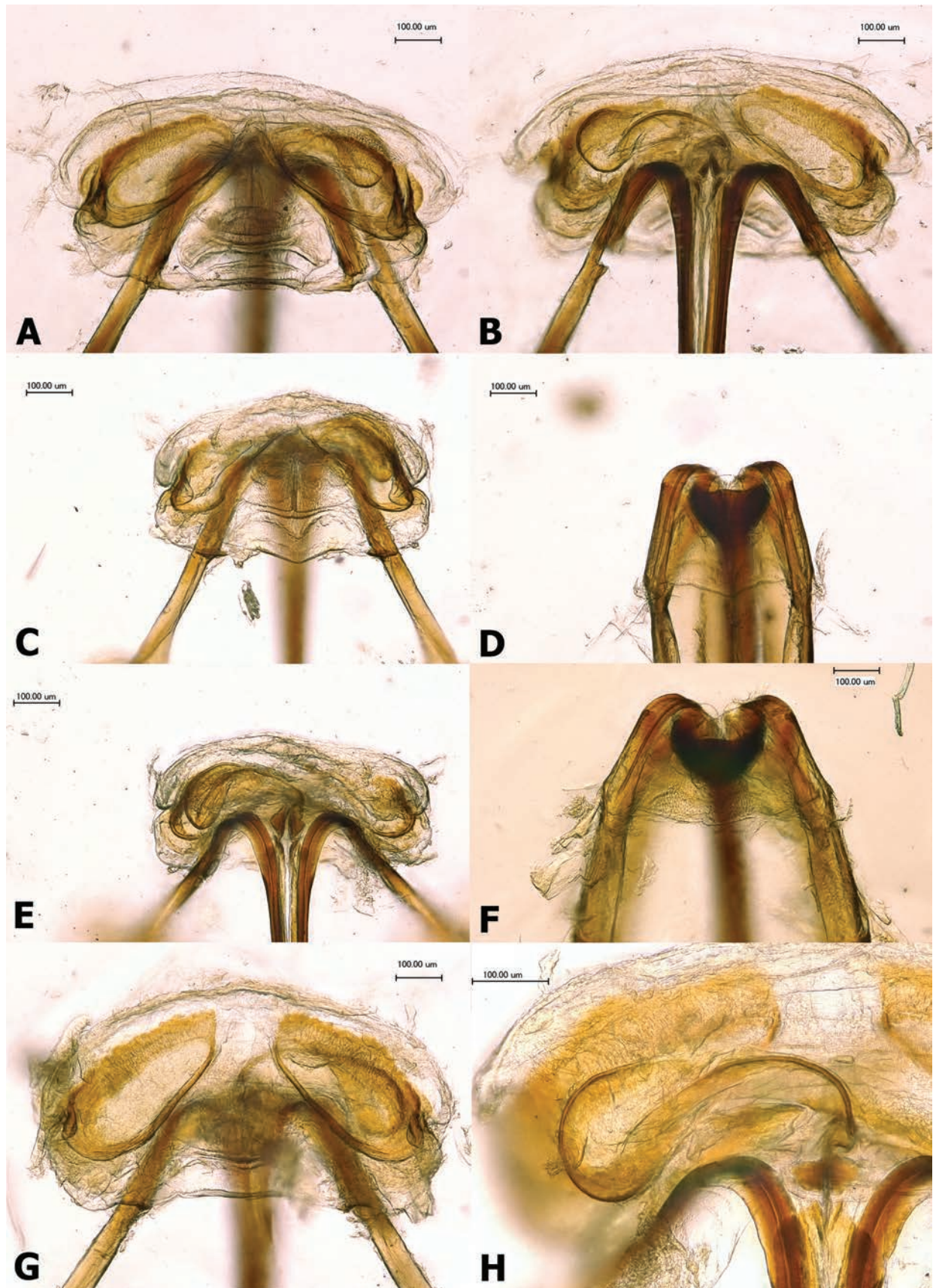


Figure 10. Female genitalia **A, B** *Salicarus concinnus*, paratype: **A** dorsal labiate plate **B** vestibulum **C–E** *S. genistae*: **C** dorsal labiate plate **D** posterior wall **E** vestibulum **F** *S. halimodendri*, posterior wall **G, H** *S. roseri*: **G** dorsal labiate plate **H** vestibulum.

(AMNH_PBI 00233774) (ZISP). **TURKMENISTAN** • Charshanga, 30 km W Kelif, 37.5°N, 66.015°E, 07 Jun 1934, Bregetova, 2♀ (AMNH_PBI 00233775, AMNH_PBI 00233776) (ZISP). **UZBEKISTAN** • Karzhantau Mt. Ridge, 41.73333°N, 70.03333°E, 01 Jul 1939, Obukhova, *Salix wilhelmsiana* (Salicaceae), 1♂ (AMNH_PBI 00233879) (ZISP).

Diagnosis. Recognized by the following combination of characters: Body oval, total length 3.0–3.7; antenna uniformly pale yellow, with thin segment II (Fig. 4A, B), coloration of dorsum variable, ranging from entirely or largely brown to pale yellow with darkened basal margin of pronotum (Fig. 1A–F); hemelytron clothed with a mixture of short adpressed simple setae and scarce, narrow, apically acuminate, silvery scale-like setae (Fig. 4C); pronotum and scutellum with short simple setae only; apical blades of vesica robust, almost straight, and parallel each other (Fig. 7A, B).

Salicarus concinnus is most similar in size, body proportions, vestiture, and vesica structure to *S. roseri* and *S. urnammu*. The vestiture of the dorsum in all three species is mainly composed of short, adpressed simple setae, with the addition of scarce, narrow, apically acuminate scale-like setae on the hemelytron in the case of *S. concinnus* and *S. urnammu*. In *S. roseri*, scale-like setae are present on the thoracic pleura only. The color pattern of the dorsum in these species is highly variable, although in *S. concinnus*, it tends to be more uniform, frequently being either dark brown with a yellowish vertex or whitish yellow with a darkened posterior margin of the pronotum. In contrast, in dark specimens of *S. urnammu* and pale specimens of *S. roseri*, the anterior part of the pronotum is most frequently darkened, and the hemelytron usually has a more or less darkened endocorium (Figs 2F–I, 3A–D). The vesica in these species is relatively large, with short and robust, knife-shaped apical blades. However, in both *S. roseri* and *S. urnammu*, the apical blades of the vesica are apically diverging (Fig. 7G–J), while they are parallel to each other in *S. concinnus* (Fig. 7A, B).

Redescription. Male. Coloration. Variable, ranging from entirely or largely brown to pale yellow with darkened basal margin of pronotum (Fig. 1A–C). **Head:** Brown, with narrow whitish edging along eyes gradually expanding towards vertex to whitish yellow, with large brown spot on frons, sometimes uniformly whitish yellow; vertex always whitish entirely or along posterior margin; antenna uniformly pale yellow; labrum dirty yellow; entire labium brown even in pale specimens, with dark brown segment IV. **Thorax:** Pronotum dorsally ranging from brown, darker towards base, to pale yellow, with narrowly brown posterior margin; lateral sides of pronotum uniformly brown to pale yellow with narrow brown edging; exposed part of mesonotum and scutellum from uniformly brown to pale yellow, sides of mesonotum sometimes with orange tinge. Hemelytron uniformly brown, pale brown or whitish yellow; membrane pale brown, semi-transparent. Coxae entirely or basally brown; femora always brown in basal two-thirds, with pale yellow apices; tibiae and tarsi uniformly pale yellow. Thoracic pleura always brown to dark brown. **Abdomen:** Uniformly brown to dark brown.

Surface and vestiture. Dorsum smooth, shiny. Pronotum, scutellum, and hemelytron with short, subequal in length to scale-like setae on hemelytron, adpressed simple setae, usually dark brown, sometimes yellowish; hemelytron additionally with silver scale-like setae; thoracic pleurites clothed with dense scale-like setae only (Fig. 4A–C); appendages and abdomen with thin and short, adpressed, whitish simple setae; tibial spines black.

Structure. Body oval, 2.4–2.8× as long as posterior width of pronotum, total length 3.0–3.7; head vertical, rather wide, slightly protruding beyond eyes anteriorly and ventrally; vertex flat, posteriorly attenuate and covering anterior margin of pronotum, 2.1–2.3× as wide as eye; frons weakly convex; clypeus flat, not visible in dorsal view; antennal segment II thin and short, 0.5–0.6× as long as posterior width of pronotum, 0.9× as long as width of head; pronotum with broadly rounded anterior and posterior corners, 1.9–2.1× as wide as long, 1.5–1.6× as wide as head.

Genitalia. Right paramere oval, ~ 1.9× as long as wide, with basal part broadly rounded and expanded proximally beyond basal process; apical process comparatively short, subrectangular (Fig. 9A). Left paramere with long, thin, and straight apical process and relatively thin, apically broadly rounded sensory lobe (Fig. 9B). Vesica relatively large, with almost straight, robust and parallel subapical blades (Fig. 7A, B).

Female. Coloration, surface and vestiture. As in male (Fig. 1D–F). **Structure.** Similar to male, body 2.3–2.6× as long as posterior width of pronotum; total length 3.0–3.5; vertex 2.3–2.6× as wide as eye; antennal segment II 0.5× as long as posterior width of pronotum, 0.8–0.9× as long as width of head; pronotum 2.0–2.2× as wide as long, 1.5–1.7× as wide as head.

Genitalia. Dorsal labiate plate with large and broadly oval sclerotized rings (Fig. 10A). Vestibulum S-shaped, thin (Fig. 10B).

Distribution. Central Asia. Known from Southern Kazakhstan, Kyrgyzstan, Tajikistan, Turkmenistan, and Uzbekistan (Putshkov 1977).

Hosts. Feeds on fructiferous *Salix* spp. (Putshkov 1977).

***Salicarus roseri* (Herrich-Schaeffer, 1838)**

Figs 2F–I, 4J–L, 6D–F, 7G, H, 9D–F, 10G, H

Capsus roseri Herrich-Schaeffer, 1838: 78.

Capsus geniculatus Stål, 1858: 355 (synonymized by Thomson 1871: 449).

Capsus saliceticola Stål, 1858: 355 (synonymized by Thomson 1871: 449).

Sthenarus vittatus Fieber, 1858: 339 (synonymized by Puton 1875: 44).

Sthenarus roseri: Fieber (1861): 309 (description); Reuter (1878): 47 (description, key); Southwood and Leston (1959): 233 (description, key).

Plagiognathus (Sthenarus) roseri: Reuter (1875): 178 (description).

Lygus roseri: Vollenhoven (1875): 93 (description).

Sthenarus (Phoenicocoris) roseri: Wagner (1958): 412 (description, figures); Wagner and Weber (1964): 437 (description, figures, key).

Salicarus roseri: Kerzhner (1962): 381 (new combination, description, figures); Kerzhner (1964): 996 (key, figures); Schwartz and Stonedahl (2004): 12 (discussion, figures, SEM); Konstantinov (2023): 874 (figures, discussion).

Sthenarus (Salicarius (sic!)) roseri: Wagner (1975a): 101 (description, figures, key).

Material examined. **BELARUS** • Korolevo nr Vitebsk, 55.13333°N, 30.5°E, 08 Jul 1905, Birulya, 1♂ (AMNH_PBI 00233591) (ZISP). **BULGARIA** • Srouma River Valley, Topolnitsa Vill., 41.41607°N, 23.31772°E, 07 Jun 2014, Simov N., 1♂ (AMNH_PBI 00341036) (ZISP). **GEORGIA** • Benara, 19 km W Akhaltsykh, 41.65°N, 42.815°E, 10 Jun 1949, A. N. Kiritshenko, *Salix* sp. (Salicaceae), 1♂ (AMNH_PBI 00233544)

(ZISP) • 14 Jun 1949, A. N. Kiritshenko, 1♂ (AMNH_PBI 00233545), 1♀ (AMNH_PBI 00233472) (ZISP) • 17 Jun 1949, A. N. Kiritshenko, 4♂ (AMNH_PBI 00233546-AMNH_PBI 00233549), 4♀ (AMNH_PBI 00233473-AMNH_PBI 00233476) (ZISP) • 18 Jun 1949, A. N. Kiritshenko, 3♀ (AMNH_PBI 00233477-AMNH_PBI 00233479), 4♂ (AMNH_PBI 00233550-AMNH_PBI 00233553) (ZISP) • 19 Jun 1949, A. N. Kiritshenko, 3♂ (AMNH_PBI 00233554-AMNH_PBI 00233556), 6♀ (AMNH_PBI 00233480-AMNH_PBI 00233485) (ZISP) • 20 Jun 1949, A. N. Kiritshenko, 6♀ (AMNH_PBI 00233486-AMNH_PBI 00233491), 11♂ (AMNH_PBI 00233557-AMNH_PBI 00233567) (ZISP) • 22 Jun 1949, A. N. Kiritshenko, 1♂ (AMNH_PBI 00233568), 1♀ (AMNH_PBI 00233492) (ZISP) • 23 Jun 1949, A. N. Kiritshenko, 4♀ (AMNH_PBI 00233493-AMNH_PBI 00233496), 3♂ (AMNH_PBI 00233569-AMNH_PBI 00233571) (ZISP) • 25 Jun 1949, A. N. Kiritshenko, 3♀ (AMNH_PBI 00233497-AMNH_PBI 00233499) (ZISP) • Borzhomi [Borzhom] Tiflis Dist., 41.83333°N, 43.36666°E, 1867, A. Brandt, 1♀ (AMNH_PBI 00233913) (ZISP). **MONGOLIA** • **Central Aimak**: Toola river, between Gachurin and Khuantey, NE of Ulaanbaator [Urga], 47.933°N, 107.165°E, 04 Jul 1897, Klements, 1♀ (AMNH_PBI 00233916) (ZISP) • **South Govi Aimak**: Nr Muna-Ula Mt., Jun 1871, Przhevalskiy, 2♀ (AMNH_PBI 00233918, AMNH_PBI 00233919) (ZISP) • **South Hangay Aimak**: Lamyn-gegen, SE Khangay, 22 Jul 1926, A. N. Kiritshenko, 1♀ (AMNH_PBI 00233928) (ZISP). **POLAND** • Khabirov, Kalish Dist., 51.75°N, 18.08333°E, 19 Jun 1908, Yachevskiy, 1♂ (AMNH_PBI 00233837), 1♀ (AMNH_PBI 00233990) (ZISP) • 31 Jul 1908, Yachevskiy, 2♂ (AMNH_PBI 00233835, AMNH_PBI 00233836) (ZISP). **RUSSIAN FEDERATION** • **Altai Terr.**: Tigirekskiy National Reserve, 51.05°N, 82.98333°E, 26 Jun 2005, A. Namyatova, 2♀ (AMNH_PBI 00233941, AMNH_PBI 00233942) (ZISP) • 03 Jul 2005, A. Namyatova, 1♂ (AMNH_PBI 00233823) (ZISP) • **Amur Prov.**: Klimoutsy, 40 km W of Svobodnyi, 51.4667°N, 127.5833°E, 242 m, 13 Jul 1959, I. M. Kerzhner, 1♂ (AMNH_PBI 00233931) *Salix* spp. (Salicaceae), 1♂ (AMNH_PBI 00233932) (ZISP) • 14 Jul 1959, I. M. Kerzhner, *Salix* spp. (Salicaceae), 1♂ (AMNH_PBI 00233816) (ZISP) • 15 Jul 1959, I. M. Kerzhner, 1♂ (AMNH_PBI 00233933) (ZISP) • Korsakovo on Amur River, 51.33333°N, 126.95°E, 25 Jul 1959, I. M. Kerzhner, 1♂ (AMNH_PBI 00233934) (ZISP) • **Arkhangelsk Prov.**: Left bank of Severnaya Dvina River, oppos. Kotlas, 61.25°N, 46.51666°E, 06 Aug 1942, Stark, 1♂ (AMNH_PBI 00233818) (ZISP) • 14 Aug 1942, Stark, 1♀ (AMNH_PBI 00233937) (ZISP) • **Chelyabinsk Prov.**: Tract nr Troitsk Region, Magnitogorsk Distr., 54.108°N, 61.568°E, 07 Jun 1927, Shelud'ko, 1♀ (AMNH_PBI 00233917) (ZISP) • **Irkutsk Prov.**: Irkutsk, 52.31666°N, 104.23333°E, Yakovlev, 3♀ (AMNH_PBI 00233962, AMNH_PBI 00233513, AMNH_PBI 00233514), 1♂ (AMNH_PBI 00233578) (ZISP) • 18 Jul 1961, Kulik, *Salix* sp. (Salicaceae), 20♀ (AMNH_PBI 00233969-AMNH_PBI 00233972, AMNH_PBI 00233510-AMNH_PBI 00233512), 7♂ (AMNH_PBI 00233575-AMNH_PBI 00233577) (ZISP) • Padun on Verkhnyaya Tunguska River, 56.28333°N, 101.71667°E, 1867, A. Czekanowski, 1♀ (AMNH_PBI 00233924) (ZISP) • **Kamchatka Terr.**: Klyuchevskoe on the Kamchatka River, 56.3°N, 160.83333°E, 09 Jul 1908, Bianchi, 1♀ (AMNH_PBI 00233910) (ZISP) • **Khabarovsk Terr.**: Troitskoe, bank of Amur river, Primor'e, 49.43333°N, 136.55°E, 10 Jun 1909, Efremov, 1♀ (AMNH_PBI 00233940) (ZISP) • **Krasnodar Terr.**: Slavyansk-na-Kubani [Slavyanskaya], lower course of Kuban river, 45.23333°N, 38.11666°E, 12 Jul 1937, Rysakov, 1♀ (AMNH_PBI 00233979), 1♂ (AMNH_PBI 00233819) (ZISP) • Tuapse, 44.1°N, 39.08333°E, 13 Jul 1911, W. Pliginskiy, 1♂ (AMNH_PBI 00233822) (ZISP) • **Krasnoyarsk Terr.**: Krasnoyarsk, 56.00972°N,

92.79167°E, 03 Aug 1924, Vinogradov, 1♀ (AMNH_PBI 00233912) (ZISP) • **Lenin-grad Prov.:** Bank of Tosna River nr Sablino, 59.62°N, 30.81°E, 12 Aug 1922, A. N. Kiritshenko, 1♂ (AMNH_PBI 00233814) (ZISP) • Bolshie Izhory [Bol'shiye Izori], 58.7986°N, 30.0786°E, 57 m, 16 Jun 1917, Bianchi, 1♀ (AMNH_PBI 00233980), 1♂ (AMNH_PBI 00233593) (ZISP) • Ivanovskoe on Neva River, 59.75°N, 30.76666°E, 20 Jul 1931, Lyubishchev, 1♀ (AMNH_PBI 00233976) (ZISP) • Novyy Petergof [Petrodvorets], 59.86666°N, 29.91666°E, 09 Jul 1896, Chekini, 1♂ (AMNH_PBI 00233587) (ZISP) • Shuvalovo, 60.05°N, 30.3°E, 25 May 1897, Jakobson, 1♀ (AMNH_PBI 00233921) (ZISP) • 05 Jun 1897–08 Jun 1897, Jakobson, 1♀ (AMNH_PBI 00233922) (ZISP) • 04 Jul 1897, Jakobson, 1♀ (AMNH_PBI 00233961) (ZISP) • St.-Petersburg [Petrograd, Leningrad], 59.935°N, 30.31°E, 1869, Sol'skiy, 8♀ (AMNH_PBI 00233964, AMNH_PBI 00233966, AMNH_PBI 00233590) (ZISP) • Udel'naya, 60.016°N, 30.318°E, 20 Jun 1916, Knyazhetskiiy, 1♀ (AMNH_PBI 00233923) (ZISP) • **Moscow Prov.:** Belye Kolodezi, Kolomna distr., 54.91889°N, 38.69139°E, 08 Jun 1903, G.A. Kozhevnikov, 1♀ (AMNH_PBI 00233963) (ZISP) • **Nizhegorod Prov.:** Pamyati Parizhskoi Kommuny inlet, 56.099°N, 44.516°E, 12 Jul 1979, Khrynova, 1♂ (AMNH_PBI 00233820) (ZISP) • **North Ossetia Rep.:** Vladikavkaz, 43.01666°N, 44.66666°E, 11 Jul 1925, A. N. Kiritshenko, 1♀ (AMNH_PBI 00233929), 1♂ (AMNH_PBI 00233930) (ZISP) • **Orenburg Prov.:** Nr Orenburg, 51.76666°N, 55.1°E, 18 Jun 1924, A.I. Ivanov, 1♂ (AMNH_PBI 00233821) (ZISP) • **Perm Terr.:** Perm, 58.01666°N, 56.3°E, 1925, Lubischev, 1♀ (AMNH_PBI 00233977) (ZISP) • **Primorsky Terr.:** Tal'bomogi, Tumen'-Ula, Russia-Korean boundary, 42.4144°N, 130.6486°E, 07 Jul 1913, Cherskiy, 1♂ (AMNH_PBI 00233586), 1♀ (AMNH_PBI 00233914) (ZISP) • Vinogradovka, 46.2°N, 134.4°E, 05 Jul 1929, A. N. Kiritshenko, 1♀ (AMNH_PBI 00233926) (ZISP) • 07 Jul 1929, A. N. Kiritshenko, 1♂ (AMNH_PBI 00233813) (ZISP) • 09 Jul 1929, A. N. Kiritshenko, 1♀ (AMNH_PBI 00233927) (ZISP) • Yakovlevka, 44.4°N, 133.45°E, 28 Jun 1926, Dyakonov & Filip'ev, 1♀ (AMNH_PBI 00233939) (ZISP) • **Rostov Prov.:** Rostov-na-Donu, 47.21666°N, 39.7°E, 29 Jun 1928, Unknown collector, 1♀ (AMNH_PBI 00233960) (ZISP) • **Samara Prov.:** Krasnaya Glinka, 25 km of Samara, 53.33333°N, 50.18333°E, 08 Jul 1928, Lubischev, 3♀ (AMNH_PBI 00233973-AMNH_PBI 00233975), 2♂ (AMNH_PBI 00233588, AMNH_PBI 00233589) (ZISP) • **Tambov Prov.:** Michurinsk [Kozlov], 52.88333°N, 40.46666°E, W. H. Lange, 6♂ (AMNH_PBI 00233831, AMNH_PBI 00233584, AMNH_PBI 00233585), 2♀ (AMNH_PBI 00233831) (ZISP) • **Volgograd Prov.:** Krasnoarmeysk [former Sarepta], 48.5°N, 44.48333°E, V. Jakovlev coll., 2♀ (AMNH_PBI 00233515, AMNH_PBI 00233516) (ZISP) • **Voronezh Prov.:** Nr Ramon', 51.91666°N, 39.31666°E, 15 Jun 1984, Golub, 1♀ (AMNH_PBI 00233938) (ZISP) • **Yakutia Rep.:** Balagannakh, 30 km ESE of Ust'-Nera, 64.498°N, 143.857°E, 04 Jul 1974, N.N. Vinokurov, 3♀ (AMNH_PBI 00233507-AMNH_PBI 00233509) (ZISP) • Batagay on Yana river, NE Yakutia (80 km E Verkhoyansk), 67.65°N, 134.63333°E, 12 Jul 1957, Semenov, 1♂ (AMNH_PBI 00233817), 2♀ (AMNH_PBI 00233935, AMNH_PBI 00233936) (ZISP) • Khokhur-terde on Amga river, 60.7°N, 131.6°E, 05 Aug 1925, Bianchi, 1♀ (AMNH_PBI 00233911) (ZISP) • Left bank of Yana River nr Verkhoyansk, 67.55°N, 133.36666°E, 21 Jul 1974, N.N. Vinokurov, 3♂ (AMNH_PBI 00233572-AMNH_PBI 00233574), 7♀ (AMNH_PBI 00233500-AMNH_PBI 00233506) (ZISP) • **Yamalo-Nenets Distr.:** Tal'bey on Adz'va River, 68.086°N, 72.048°E, Zhuravskiiy, 1♀ (AMNH_PBI 00233915) (ZISP) • **Yaroslavl Prov.:** Nizhniy Isl., Yaroslavl' distr., 57.482°N, 40.1°E, 19 Jun 1896, Unknown collector, 7♂ (AMNH_PBI 00233830,

AMNH_PBI 00233580-AMNH_PBI 00233582), 6♀ (AMNH_PBI 00233830, AMNH_PBI 00233957, AMNH_PBI 00233958, AMNH_PBI 00233582) (ZISP) • Zhukov Isl., Jaroslavl' distr., 57.482°N, 40.1°E, 05 Jul 1896, Unknown collector, 1♀ (AMNH_PBI 00233956), 1♂ (AMNH_PBI 00233583) (ZISP). **UKRAINE** • Pyatikhatka, Oktyabr'skiy Dist., 45.3°N, 34.26666°E, 28 Jun 1952, Loginova, 9♂ (AMNH_PBI 00233824, AMNH_PBI 00233825, AMNH_PBI 00233806-AMNH_PBI 00233812), 11♀ (AMNH_PBI 00233943-AMNH_PBI 00233950, AMNH_PBI 00233981-AMNH_PBI 00233983) (ZISP) • Near Salgir river, 44.95°N, 34.08333°E, 22 Jun 1924, A. N. Kiritschenko, 1♀ (AMNH_PBI 00233986) (ZISP) • 24 Jun 1924, A. N. Kiritschenko, 3♂ (AMNH_PBI 00233827-AMNH_PBI 00233829), 1♀ (AMNH_PBI 00233951) (ZISP) • 14 Jul 1924, A. N. Kiritschenko, 1♂ (AMNH_PBI 00233826), 2♀ (AMNH_PBI 00233984, AMNH_PBI 00233985) (ZISP) • Cherkasy, 49.436°N, 32.084°E, 18 Jun 1931, Lubischev, 1♂ (AMNH_PBI 00233843) (ZISP) • Izmail, Bessarabiya, 45.35°N, 28.83333°E, 09 Jun 1911, Chernavin, 1♀ (AMNH_PBI 00233925) (ZISP) • Kamyshany [Arnautka] nr Kherson, 46.61666°N, 32.48333°E, 18 May 1939, Nikolaev, 1♂ (AMNH_PBI 00233592) (ZISP) • Korobov on Donets river, 7 km of Zmiev, 49.5889°N, 36.3428°E, 06 Jul 1955–07 Jul 1955, L.V. Arnoldi, 1♀ (AMNH_PBI 00233959) (ZISP) • Korsunskiy monastery', cursus inf. fl. Dnepr., 46.7167°N, 33.2167°E, 02 Aug 1928, S. I. Medvedev, 1♀ (AMNH_PBI 00233978) (ZISP) • Kozin [Koncha-Zaspa] nr Kiev, 50.21666°N, 30.63333°E, 12 Jul 1932, S. I. Medvedev, 2♀ (AMNH_PBI 00233988, AMNH_PBI 00233989), 1♂ (AMNH_PBI 00233842) (ZISP) • Odessa, Khadzhib liman, 46.46666°N, 30.71666°E, 09 Jun 1920, A. N. Kiritschenko, 4♀ (AMNH_PBI 00233952-AMNH_PBI 00233954, AMNH_PBI 00233815) (ZISP) • Provalye, 48.16666°N, 39.83333°E, 01 Jul 1947, S. I. Medvedev, 1♂ (AMNH_PBI 00233838) (ZISP) • Stanitsa Luganskaya nr Lugansk, 48.65°N, 39.48333°E, 26 Jul 1927, F.K. Lukjanovitsh, 1♀ (AMNH_PBI 00233992) (ZISP) • Verkhovka [former Mahilyow uezd], 48.9°N, 27.65°E, 10 Jun 1901, Chekini, 1♀ (AMNH_PBI 00233967) (ZISP) • Vilkovo, Izmail Distr., Bessarabiya, 45.406°N, 29.589°E, 30 May 1911, Chernavin, 1♀ (AMNH_PBI 00233987) (ZISP).

Diagnosis. Recognized by the following characters: body oval, total length 3.4–4.0; antennal segment I brown, segment II thin, brown or at least with darkened base and apex (Fig. 4G, K); Color-pattern variable, ranging from uniformly dark brown to pale yellow, with more or less darkened head, pronotum, and endocorium (Fig. 2E–I); dorsum devoid of scale-like setae, clothed exclusively with short, strongly adpressed slivery simple setae (Figs 4L, 6E); apical blades of vesica short and robust, straight, apically diverging (Fig. 7G, H).

Salicarus roseri easily differs from congeners by the absence of scale-like setae on dorsum. It further differs by having short, robust, straight, and slightly diverging apical blades of the vesica, being most similar to *S. urnammu* in this respect, although the blades in the latter species are shorter.

Redescription. Male. Coloration. Highly variable, dorsum ranging from uniformly dark brown to pale yellow, with somewhat darkened head (Fig. 2E, F); pale specimens typically with widely darkened endocorium and partly or entirely dark brown pronotum and scutellum, rarely without any dark markings on dorsum. **Head:** Entirely dark brown to brown, sometimes with yellow or orange vertex and edging along inner margins of eyes; antennal segment I dark brown to yellow, segment II dark brown to yellow with darkened apex, segments III and IV usually dirty yellow, sometimes brown; labium usually dark brown, pale brown to dirty yellow in the palest specimens. **Thorax:** Pronotum from uniformly dark

or chestnut brown to whitish yellow, frequently with reddish tinge, in pale specimens usually with dark markings on calli and darkened posterior margin, rarely uniformly whitish; scutellum usually dark brown, rarely dirty yellow or orange; hemelytron ranging from uniformly dark brown to whitish yellow, pale specimens typically with entirely yellow or whitish clavus, partly or entirely yellow exocorium, largely darkened endocorium, and yellow or orange cuneus, membrane uniformly dark to pale brown, semitransparent; thoracic pleura usually dark brown, rarely dorsally or entirely yellow; coxae dark brown to brown, femora in dark specimens brown with yellowish apical halves or at least extreme apices, in pale specimens entirely yellow, frequently with reddish tinge, tibiae yellow, tarsi yellow or apically darkened. **Abdomen:** Dark brown to yellow.

Surface and vestiture. Dorsum shiny, head and pronotum smooth, scutellum and hemelytron weakly rugose (Fig. 4J–L); clothed with short, strongly adpressed, simple silvery setae, sparse on vertex and pronotum, dense on scutellum and hemelytron; antenna, legs, and abdomen with similar but somewhat longer simple setae; thoracic pleurites with dense, narrow, apically acuminate silvery scale-like setae above scent gland evaporatory area; pronotum with a pair of black erect bristle-like setae at anterior corners; femora with several similar black setae dorso-apically; tibial spines black.

Structure. Body oval, 2.6–2.9× as long as width of pronotum at base, total length 3.6–4.0; head vertical, rather wide, slightly protruding beyond eyes anteriorly and ventrally; vertex flat, posteriorly attenuate and covering anterior margin of pronotum, 1.8–1.9× as wide as eye; antennal segment II at base distinctly thinner than segment I, slightly dilating apically, comparatively short, 0.5–0.6× as long as basal width of pronotum, 0.8–0.9× as long as width of head; pronotum with broadly rounded anterior and posterior corners, 2.0–2.2× as wide as long, 1.5–1.7× as wide as head.

Genitalia. Right paramere elongate-oval, ~ 2.5× as long as wide, with long, straight and apically blunt apical process (Fig. 9P). Left paramere with long and straight apical process, and elongate, comparatively thin, slightly upturned sensory lobe (Fig. 9Q). Vesica large and strongly sclerotized, with straight, short and robust, diverging apical blades (Fig. 7G, H).

Female. Coloration, surface and vestiture. As in male (Fig. 2G–I). **Structure.** Similar to male, body 2.5–2.8× as long as posterior width of pronotum; total length 3.4–3.9; vertex 1.8–2.0× as wide as eye; antennal segment II 0.4–0.5× as long as posterior width of pronotum, 0.7–0.9× as long as width of head; pronotum 2.0–2.3× as wide as long, 1.5–1.6× as wide as head.

Genitalia. Sclerotized rings of dorsal labiate large, broadly oval (Fig. 10G). Vestibulum thin, S-shaped (Fig. 10H).

Distribution. Widely distributed in the Palearctic, including almost the entire Europe, extending eastward to the Khabarovsk and Kamchatka territories in Russia, and southward to Spain, Italy, Greece, Turkey, Transcaucasia, Iran, Turkmenistan, Kazakhstan, Mongolia, and Inner Mongolia of China. To the north, it extends to the central Fennoscandia, Karelia, Arkhangelsk and Komi Provinces, the southern Yamalo-Nenets district, southern Krasnoyarsk Territory, southern and central Yakutia, and Magadan Territory (Vinokurov et al. 2010; Aukema 2024).

Host. Confined to *Salix* spp. (Southwood and Leston 1959; Kerzhner 1962; Göllner-Scheiding 1974).

***Salicarus urnammu* Linnavuori, 1984**

Figs 3A–D, 4 M–O, 7I, J, 9S–U

Salicarius [sic!] *urnammu* Linnavuori, 1984: 51.

Salicarus urnammu: Konstantinov (2023): 874 (figures, discussion).

Material examined. **ARMENIA** • Aralykh, 40.11722°N, 44.27055°E, 07 Jun 1911, K. Satunin, 3♂ (AMNH_PBI 00233861, AMNH_PBI 00233862, AMNH_PBI 00233858) (ZISP). **AZERBAIJAN** • Arpa-chay River, 39.4675°N, 44.93444°E, 03 Jul 1937–05 Jul 1937, Ryabov, 1♂ (AMNH_PBI 00233755) (ZISP). **IRAN** • **Ardabil Prov.:** 10 km W Khalkhal, 37.6179°N, 48.522°E, 08 Jul 2002–09 Jul 2002, R. & S. Linnavuori, 2♀ (ZISP_ENT 00011858, ZISP_ENT 00011859) (NMWC) • Ask-estan-Site, 1 37°28'N, 48°39'E, 11 Jul 2022, R. Hosseini 4♂ 2♀ (UGNHM) • Givi-Khalkhal-Site, 2 37°41'N, 48°30'E, 9 Jul.2022, R. Hosseini, 7♂ 5♀ (UGNHM) • Majareh-Site 3, 37°33'N, 48°36'E, 23 Jul 2022, R. Hosseini 1♀ (UGNHM) • Poonel Khalkhal-Site 3, 37°34'N, 48°39'E 27 Jun 2022, R. Hosseini, 6♂ 3♀ (UGNHM) • **Guilan Prov.:** Lur-Site 5, 36°51'N, 49°53'E, 13 Jun 2022, R. Hosseini, 1♀ (UGNHM) • Malumeh-Site 1, 36°51'N, 49°55'E, 11 Jun 2022, R. Hosseini, 14♂ 5♀ (UGNHM) • Malumeh-Site 3, 36°51'N, 49°55'E, 11 Jun 2022, R. Hosseini, 8♂ 10♀ (UGNHM) • **Tehran Prov.:** Shahrestanak, 60 km NE Karaj, 34.8508°N, 50.4544°E, 2100 m, 10 Jul 2005–12 Jul 2005, R. Linnavuori, 2♂ (ZISP_ENT 00011863), 2♀ (ZISP_ENT 00011863) (NMWC). **IRAQ** • Sulaymaniyah nr Halabja, 35.555°N, 45.479°E, 11 Jun 1980, R. Linnavuori, 3♂ (ZISP_ENT 00011857, ZISP_ENT 00011860, ZISP_ENT 00011862), 1♀ (ZISP_ENT 00011861) (NMWC), 1♀ (AMNH_PBI 00233754) (ZISP). **TURKMENISTAN** • Garrygala [Kara-Kala], 38.41666°N, 56.25°E, 20 May 1952, Kryzhanovskij, 1♂ (AMNH_PBI 00233859) (ZISP).

Diagnosis. Recognized by the oval body, total length male 3.5–3.8; female 3.2–3.5; antenna typically yellow, in dark specimens segments I and II partly brown, segment II thin (Fig. 4M, N); Dorsum yellow, frequently with orange tinge, sometimes with partly brown pronotum, scutellum, and endocorium (Fig. 3A–D); vestiture composed of short, strongly adpressed simple silvery setae, dense on scutellum and hemelytron but scarce on vertex and pronotum; hemelytron additionally with scarce, narrow, apically acuminate scale-like setae (Fig. 4O); apical blades of vesica short and robust, straight, apically diverging (Fig. 7I, J).

Salicarus urnammu is most similar to *S. concinnus* and *S. roseri* but can usually be distinguished from these species by the color pattern. It further differs from *S. roseri* by the presence of scale-like setae on the hemelytron, and from *S. concinnus* by the diverging apical blades of the vesica. Refer to the diagnoses of these species for additional discussion.

Redescription. Male. Coloration. Variable, ranging from yellow, frequently with orange tinge, sometimes with partly brown pronotum, scutellum, and endocorium to almost uniformly dark brown, with yellow base of hemelytron and cuneus (Fig. 3A, B). **Head:** Orange-yellow, usually with whitish vertex and somewhat darkened clypeus (Fig. 4M, N); in dark specimens dirty yellow, with dark brown clypeus, brown mandibular and maxillary plate, and largely brown frons, sometimes uniformly dark brown; antenna typically yellow, in dark specimens segment I partly or entirely brown, segment II basally and/or apically, sometimes entirely brown; labium orange-yellow to brown, apex of segment IV dark brown. **Thorax:** Pronotum from yellow to uniformly dark brown, frequently yellow with reddish tinge and brown

diffuse spots on calli and darkened posterior margin; scutellum usually orange-yellow, entirely brown in dark specimens; hemelytron usually whitish yellow, usually with large wedge-shaped brown spot occupying entire exocorium except base, in dark specimens entire clavus and corium except base dark brown, cuneus dirty yellow; membrane pale brown, semitransparent; thoracic pleura orange-yellow to dark brown; legs typically orange-yellow, without any color pattern, in dark specimens femora more or less brown, with yellow apices, tibiae with minute spots at bases of tibial spines. **Abdomen:** Orange-yellow, sometimes with darkened stripes along apical margins of pregenital segments, or uniformly dark brown.

Surface and vestiture. Dorsum shiny, head and pronotum smooth, scutellum and hemelytron weakly rugose; clothed with short, subequal in length to scale-like setae on hemelytron, strongly adpressed, simple silvery setae, scarce on vertex and pronotum, dense on scutellum and hemelytron; hemelytron additionally with scarce, silvery, narrow, apically acuminate scale-like setae (Fig. 40); thoracic pleurites with scarce silvery scale-like setae above scent gland evaporative area; pronotum with a pair of brown erect bristle-like setae at anterior corners; femora with several similar brown setae dorso-apically; tibial spines black.

Structure. Body oval, 2.8–2.9× as long as posterior width of pronotum, total length 3.5–3.8; head vertical, rather wide, slightly protruding beyond eyes anteriorly and ventrally; vertex flat, posteriorly attenuate and covering anterior margin of pronotum, 1.8–2.1× as wide as eye; antennal segment II at base distinctly thinner than segment I, slightly dilating apically, comparatively short, 0.5–0.6× as long as posterior width of pronotum, 0.8–0.9× as long as width of head; pronotum with broadly rounded anterior and posterior corners, 1.9–2.0× as wide as long, 1.5× as wide as head.

Genitalia. Right paramere elongate-oval, ~ 2.4× as long as wide, with straight, comparatively short, and blunt apical process (Fig. 9S). Right paramere with thin straight apical process and triangular, apically broadly rounded sensory lobe (Fig. 9T). Vesica large, with straight, short and robust, gradually diverging apical blades (Fig. 7G, H).

Female. Coloration, surface and vestiture. As in male (Fig. 3C, D). **Structure.** Similar to male, body 2.5–2.7× as long as posterior width of pronotum; total length 3.2–3.5; vertex 1.9–2.2× as wide as eye; antennal segment II 0.5–0.6× as long as posterior width of pronotum, 0.7–0.9× as long as width of head; pronotum 2.0–2.1× as wide as long, 1.5–1.6× as wide as head.

Genitalia. Sclerotized rings of dorsal labiate plate large, broadly oval.

Distribution. Originally described from Iraq, this species was subsequently found in Turkey, Transcaucasia, Iran, and Turkmenistan (Linnavuori 2007; Konstantinov and Namyatova 2008).

Host. *Salix* spp. (Linnavuori 1984, 2007)

***Salicarus fulvicornis* species group**

***Salicarus fulvicornis* (Jakovlev, 1889)**

Figs 1G–I, 4D–F, 6A–C, 7C–D, 9J–L

Agalliaestes fulvicornis Jakovlev, 1889: 348.

Chlamydatus fulvicornis: Oshanin (1910): 932 (new comb., catalogue).

Phoenicocoris flagellatus Wagner (1967): 71 (syn. by Kerzhner 1997: 247).

Salicarus fulvicornis: Vinokurov and Kanyukova (1995): 58 (new comb.); Schwartz and Stonedahl (2004): 42, figs. 2, 26 (disc., SEM, MG, host); Lu et al. (2011): 500, fig. 1 (descr., figs); Konstantinov (2023): 874 (phylogenetic placement, figures, discussion).

Material examined. Lectotype of *Agalliaestes fulvicornis* Jakovlev, 1889 • ♀ **MONGOLIA: Selenge Aimak**: Between Khara and Boroii [Boro], 48.83°N, 106.195°E, Yakovlev coll. (AMNH_PBI 00233377) (ZISP).

Paratypes of *Phoenicocoris flagellatus* Wagner 1967: MONGOLIA • Bayan Olgii Aimak: Chovd-gol, ~ 15 km E of Ulgij, 49.06666°N, 90.2°E, 1650 m, 28 Jul 1964–29 Jul 1964, Mongolisch - Deutsche Biolog. Exped., 3♂ (AMNH_PBI 00184011, AMNH_PBI 00340326, AMNH_PBI 00340327) (ZMUH).

Other specimens examined: MONGOLIA • Central Aimak: Nr Songiin [Songino], SW of Ulaanbaatar, steppe, 47.81666°N, 106.66666°E, 18 Jun 1967, I. M. Kerzhner, *Caragana bungei* (Fabaceae), 7♂ (AMNH_PBI 00233373-AMNH_PBI 00233376), 8♀ (AMNH_PBI 00233374, AMNH_PBI 00233447-AMNH_PBI 00233450) (ZISP) • 18 Jun 1967, Zaytsev, 3♂ (AMNH_PBI 00233520, AMNH_PBI 00233521) (ZISP) • 01 Jul 1967, Zaytsev, 3♂ (AMNH_PBI 00233363-AMNH_PBI 00233365), 1♀ (AMNH_PBI 00233432) (ZISP) • 01 Jul 1967, I. M. Kerzhner, *Caragana bungei* (Fabaceae), 13♂ (AMNH_PBI 00233352-AMNH_PBI 00233362, AMNH_PBI 00266431, AMNH_PBI 00266433), 6♀ (AMNH_PBI 00233427-AMNH_PBI 00233431, AMNH_PBI 00266432) (ZISP) • 01 Jul 1967, Emeljanov, 3♂ (AMNH_PBI 00233366-AMNH_PBI 00233368), 5♀ (AMNH_PBI 00233433-AMNH_PBI 00233437) (ZISP) • Nothern mountainside of Bogdo Ula, nr Ulan Bator, 47.81667°N, 107°E, 29 Jun 1967, I. M. Kerzhner, 4♂ (AMNH_PBI 00233369-AMNH_PBI 00233372), 9♀ (AMNH_PBI 00233438-AMNH_PBI 00233446) (ZISP) • **South Hangay Aimak**: Tuin-Gol river, middle Khalkhin-Gol [Khalkha] river, 45.796°N, 100.807°E, 01 Aug 1926, A. N. Kiritshenko, 7♂ (AMNH_PBI 00233537-AMNH_PBI 00233543), 11♀ (AMNH_PBI 00233456-AMNH_PBI 00233466) (ZISP) • **Suhbaatar Aimak**: 40 km SE of Barun-Urt, 46.426°N, 113.644°E, 14 Jul 1971, I. M. Kerzhner, 4♂ (AMNH_PBI 00233534, AMNH_PBI 00233535), 4♀ (AMNH_PBI 00233535, AMNH_PBI 00233453) (ZISP) • Dzutol-Khan-Ula Mt., 45.83333°N, 114.66667°E, 12 Jul 1971, I. M. Kerzhner, 1♂ (AMNH_PBI 00233536), 6♀ (AMNH_PBI 00233454, AMNH_PBI 00233455) (ZISP) • Lun-Ula Mt., 30 km WNW of Ovoot [Dariganga], 45.393°N, 113.516°E, 07 Jul 1971, Emeljanov, 6♂ (AMNH_PBI 00233523-AMNH_PBI 00233526), 4♀ (AMNH_PBI 00233524, AMNH_PBI 00233526, AMNH_PBI 00233452) (ZISP) • Mt. Dzun-Nert, 20 km NE of Dariganga, 45.47°N, 114°E, 09 Jul 1971, Emeljanov, 1♂ (AMNH_PBI 00233522), 1♀ (AMNH_PBI 00233451) (ZISP) • Ongon-Els Sands, 15 km SSE Hongor, 45.664°N, 112.819°E, 05 Jul 1971–06 Jul 1971, I. M. Kerzhner, *Caragana* sp. (Fabaceae), 1♂ (AMNH), *Caragana* sp. (Fabaceae), 19♂ (AMNH_PBI 00233527-AMNH_PBI 00233533), 2♀ (AMNH_PBI 00233528, AMNH_PBI 00233529) (ZISP). **RUSSIAN FEDERATION • Altai Rep.**: Kosh-Agach, 49.98333°N, 88.63333°E, 08 Jun 1907, N. W. Rodd, 1♀ (AMNH_PBI 00233471) (ZISP) • 05 Jul 1964, I. M. Kerzhner, 25♂ (AMNH_PBI 00233318-AMNH_PBI 00233342), 34♀ (AMNH_PBI 00233385-AMNH_PBI 00233397, AMNH_PBI 00233399-AMNH_PBI 00233419) *Caragana spinosa* (Fabaceae), 2 larvae (AMNH_PBI 00233343, AMNH_PBI 00233344), 1♀ (AMNH_PBI 00233398) (ZISP) • 10 Jul 1964, I. M. Kerzhner, 2♂ (AMNH_PBI 00233349, AMNH_PBI

00233350), 3♀ (AMNH_PBI 00233423, AMNH_PBI 00233424, AMNH_PBI 00233426) *Caragana spinosa* (Fabaceae), 1♂ (AMNH_PBI 00233351), 1♀ (AMNH_PBI 00233425) (ZISP) • 22 Jul 1964, I. M. Kerzhner, *Caragana bungei* (Fabaceae), 6♂ (AMNH_PBI 00233312-AMNH_PBI 00233317), 7♀ (AMNH_PBI 00233378-AMNH_PBI 00233384) (ZISP) • 31 Jul 1964, I. M. Kerzhner, 4♂ (AMNH_PBI 00233345-AMNH_PBI 00233348), 3♀ (AMNH_PBI 00233420-AMNH_PBI 00233422) (ZISP) • **Buryatia Rep.:** Kyakhta [former Troitskosavsk], 50.3508°N, 106.44939°E, 757 m, 27 Jul 1928, F.K. Lukjanovitsh, 4♀ (AMNH_PBI 00233467-AMNH_PBI 00233470) (ZISP).

Diagnosis. Recognized by the following combination of characters: Body in male elongate, almost parallel sized, 3.1–3.6× as long as posterior width of pronotum, total length 3.7–4.0 (Fig. 1I), female more stumpy, 2.4–2.5× as long as posterior width of pronotum, total length 3.1–3.5 (Fig. 1G, H); dorsum uniformly dark brown to brown; antenna pale brown to brown, segment I frequently dirty yellow, segment II thin, rod-shaped; entire dorsum except head clothed with a mixture of narrow, apically acuminate silvery scales and dense, long, ~ 1.5× as long as scales, adpressed simple setae (Fig. 4D–F); vesica small, with long, thin, gradually curving and slightly diverging distally apical blades (Fig. 7C, D).

Salicarus fulvicornis is a distinctive species that can be easily distinguished from its congeners. Females of this species may be confused with dark specimens of *S. concinnus* and *S. roseri*. However, *S. fulvicornis* is easily differentiated by the presence of flattened scales on the pronotum and scutellum, as well as by the contrastingly long simple vestiture. It further differs from both species by having long and thin apical blades of the vesica that slightly diverge from each other.

Redescription. Male. Coloration. Uniformly dark brown to brown (Fig. 1I). **Head:** Dark brown; antenna pale brown to brown, segment I frequently dirty yellow; labium dark brown with black segment IV. **Thorax:** Pronotum, scutellum, thoracic pleurites, and hemelytron uniformly dark brown to brown, membrane pale brown, semitransparent; coxae dark brown, femora brown, sometimes with pale brown apices; tibiae pale brown to dirty yellow, with minute dark brown spots at bases of tibial spines; tarsi dirty yellow, apically darkened. **Abdomen:** Uniformly dark brown.

Surface and vestiture. Dorsum smooth; pronotum, scutellum, and hemelytron clothed with a mixture of silvery, narrow, apically acuminate scale-like setae and dense, long, ~ 1.5× as long as scales, adpressed, goldish yellow simple setae, these setae on corium sometimes dark brown (Fig. 6C); thoracic pleurites densely clothed exclusively with scale-like setae, while vertex antenna, legs, and abdomen covered with goldish yellow simple setae only; tibial spines black.

Structure. Body elongate, almost parallel-sided, 3.1–3.6× as long as posterior width of pronotum; total length 3.7–4.0; head vertical, slightly protruding beyond eyes anteriorly and ventrally; vertex flat, posteriorly distinctly attenuate and covering anterior margin of pronotum, 1.9–2.1× as wide as eye; frons weakly convex; clypeus flat, barely visible in dorsal view; antennal segment II rod-shaped, slightly thinner than segment I, comparatively long, 0.7–0.8× as long as posterior width of pronotum, 1.0–1.1× as long as width of head; pronotum with broadly rounded anterior and posterior corners, 2.0–2.4× as wide as long, 1.5–1.6× as wide as head.

Genitalia. Right paramere elongate-oval, not expanded proximally beyond basal process, with long, straight, apically blunt apical process (Fig. 9J). Right

paramere with straight, comparatively short apical process and thin, gradually narrowing, and apically rounded sensory lobe (Fig. 9K). Vesica small, with long, thin, gradually curving and slightly diverging distally apical blades (Fig. 7C, D).

Female. Coloration, surface and vestiture. As in male (Fig. 1G, H). **Structure.** Similar to male but body shorter, oval, 2.7–3.0× as long as posterior width of pronotum, total length 3.2–3.5; head with slightly more convex frons and clypeus, and with smaller eyes, vertex 2.1–2.4× as wide as eye; antennal segment II distinctly thinner than segment I, shorter than in male, 0.5–0.7× as long as posterior width of pronotum, 0.8–0.9× as long as width of head; pronotum 2.1–2.3× as wide as long, 1.3–1.5× as wide as head.

Genitalia. Dorsal labiate plate with large and broadly oval sclerotized rings.

Distribution. Known from Mongolia, adjacent steppe regions of Russia (Altai Rep., Buryatia Rep., Zabaykalsky Terr.), and Inner Mongolia in China (Kulik 1974; Lu et al. 2011).

Hosts. Feeds on *Caragana* spp. (Fabaceae), including *Caragana bungei* Ledeb. and *Caragana spinosa* (L.) Vahl ex Hornem.

***Salicarus halimodendri* V. G. Putshkov, 1977**

Figs 2A–D, 4G–I, 7E, F, 9M, O, 10F

Salicarus (*Salicarus*) *halimodendri* V. G. Putshkov 1977: 367.

Salicarus halimodendri: Konstantinov (2023): 874 (phylogenetic placement, figures, discussion).

Phoenicocoris qiliananus Zheng, 1996 in Zheng and Li (1996: 101). New synonym.

Salicarus qiliananus: Schwartz and Stonedahl (2004): 42 (new combination, discussion, suspected synonymy).

Material examined. Holotype: KAZAKHSTAN • **East Kazakhstan Prov.:** ♂ Bazariskiy Picket, Zaysan, 47.45°N, 84.86666°E, 22 Jun 1930, F.K. Lukjanovitsh, (AMNH_PBI 00233844) (ZISP).

Paratypes: KAZAKHSTAN • **Almaty Prov.:** Iliyskiy on Ili River, 43.52194°N, 76.82972°E, 05 Jun 1969, Seitova, 2♂ (AMNH_PBI 00233855) (ZISP) • **East Kazakhstan Prov.:** Bazariskiy Picket, Zaysan, 47.45°N, 84.86666°E, 22 Jun 1930, F.K. Lukjanovitsh, 3♂ (AMNH_PBI 00233845-AMNH_PBI 00233847), 3♀ (AMNH_PBI 00233993-AMNH_PBI 00233995) (ZISP) • Buran, Mouth of Kaldzhir, 48.01666°N, 85.2°E, 26 Jun 1930, F.K. Lukjanovitsh, *Halimodendron halodendron* (Fabaceae), 1♀ (AMNH_PBI 00233997) (ZISP) • Burkhatka Picket, Zaysan, 47.45°N, 84.86666°E, 22 Jun 1930, F.K. Lukjanovitsh, 1♀ (AMNH_PBI 00233996) (ZISP) • **Karaganda Prov.:** 12 km E Balqash [Balkhash], 46.83333°N, 75.1°E, 18 Jun 1962, I. M. Kerzhner, *Halimodendron halodendron* (Fabaceae), 1♂ (AMNH_PBI 00233854) (ZISP) • **Kostanay Prov.:** 200 km SO Qyzylorda, nr Tyshkanbay [Akkum], Syt-Darya, 50.06666°N, 62.13333°E, 30 Jun 1966, I. M. Kerzhner, 1♀ (AMNH_PBI 00234005) (ZISP) • **Kyzylorda Prov.:** 40 km NW of Turkistan, Karatau Mts. Range, 43.562°N, 67.921°E, I. M. Kerzhner, *Halimodendron halodendron* (Fabaceae), 1♀ (AMNH_PBI 00234000) (ZISP); 18 May 1966–19 May 1966, I. M. Kerzhner, *Halimodendron halodendron* (Fabaceae), 5♂ (AMNH_PBI 00233848-AMNH_PBI 00233851), 3♀ (AMNH_PBI 00233998, AMNH_PBI 00233999) (ZISP) • 29 May 1966, I. M. Kerzhner, *Halimodendron halodendron*

(Fabaceae), 2♂ (AMNH_PBI 00233852, AMNH_PBI 00233853), 6♀ (AMNH_PBI 00233853, AMNH_PBI 00234001-AMNH_PBI 00234004) (ZISP). **MONGOLIA** • **Hovd Aimak**: 15 km S of Bulgan, 45.952°N, 91.564°E, 29 Jul 1970, Narchuk, *Halimodendron halodendron* (Fabaceae), 1♀ (AMNH_PBI 00234013) (ZISP) • Elhon, 20 km SE Altai on Bodonchi River, 45.68333°N, 92.48333°E, 27 Jul 1970, I. M. Kerzhner, 14♀ (AMNH_PBI 00233856, AMNH_PBI 00234006-AMNH_PBI 00234008, AMNH_PBI 00234010-AMNH_PBI 00234012), 3♂ (AMNH_PBI 00233856, AMNH_PBI 00233857) *Halimodendron halodendron* (Fabaceae), 3♀ (AMNH_PBI 00234009) (ZISP).

Other specimens examined: **KAZAKHSTAN** • **Zhambul Prov.**: Karatau Mts., 4 km S of Karabastau, 42.88722°N, 70.80667°E, 557 m, 18 May 2015, F. Konstantinov & N. Simov, 1♀ (AMNH_PBI 00343015) (ZISP).

Diagnosis. Recognized by the oval body, total length: male 3.6–3.9, female 3.1–3.5; antennal segment I brown, segment II thin, basally or entirely darkened, remaining segments dirty yellow (Fig. 4G, H); coloration of dorsum variable, ranging from almost entirely dark brown to pale yellow; dorsum except head with a mixture of narrow, apically acuminate scale-like setae and dense, comparatively long, ~ 1.5× as long as scales, adpressed, silvery simple setae (Fig. 4I); apical blades of vesica very long and thin, gradually curved, abruptly furcate (Fig. 7E, F).

Dark specimens of *Salicarus halimodendri* are somewhat similar to *S. fulvicornis* in having long simple setae and the arrangement of flattened scale-like setae on the dorsum. However, the latter species can be distinguished by the exceptionally long and thin, subapically bifurcate apical blades (Fig. 7C, D).

Redescription. Male. Coloration. Variable, ranging from almost entirely dark brown to pale yellow (Fig. 2A–D). **Head:** In dark specimens almost entirely dark brown, with midline on frons and mandibular plate somewhat paler and with vertex always dirty to whitish yellow along posterior margin; in pale specimens head whitish yellow, with a series of brown, frequently confluent lines radiating from midline on frons, entirely or apically brown clypeus, and brown maxillary plate; antennal segment I dark brown to brown, segment II entirely brown to dirty yellow with brown basal one-fourth, remaining segments dirty yellow; labium dirty yellow, with dark brown segment IV. **Thorax:** Pronotum, scutellum, and hemelytron from uniformly dark brown to whitish yellow, hemelytron in dark specimens usually paler than pronotum; membrane uniformly pale brown to almost colorless; pronotum and scutellum in pale specimens typically with brown markings on calli and on suture between scutellum and mesonotum, sometimes uniformly whitish yellow; coxae usually yellow, rarely paler brown, femora dirty to whitish yellow, with two or three series of large rounded maculae on ventral surfaces and anterior margins, sometimes confluent in dark specimens, and several dark markings at apices of dorsal surfaces; tibiae yellow with minute dark brown spots at bases of tibial spines; thoracic pleurites brown to pale yellow. **Abdomen:** Brown to pale yellow.

Surface and vestiture. Dorsum weakly rugose, head smooth, shiny. Pronotum, scutellum, and hemelytron with a mixture of silvery scale-like setae and dense, comparatively long, ~ 1.5× as long as scales, adpressed, silvery simple setae; mesopleuron clothed with scale-like setae alone, while vertex, antenna, legs, metapleuron, and abdomen covered exclusively with adpressed silvery simple setae; tibial spines black to dark brown.

Structure. Body oval, 2.7–2.9× as long as posterior width of pronotum; total length 3.6–3.9; head vertical, slightly protruding beyond eyes anteriorly and ventrally; vertex flat, posteriorly distinctly attenuate and covering anterior margin of pronotum, 2.0–2.2× as wide as eye; frons weakly convex; clypeus flat, barely visible in dorsal view; antennal segment II rod-shaped, slightly thinner than segment I, 0.5–0.6× as long as posterior width of pronotum, 0.8–0.9× as long as width of head; pronotum with broadly rounded anterior and posterior corners, 2.3–2.5× as wide as long, 1.4–1.5× as wide as head.

Genitalia. Right paramere elongate-oval, ~ 1.7× as long as wide, with long, slightly narrowing and apically rounded apical process (Fig. 9M). Left paramere with thin and straight apical process and comparatively short, broadly rounded sensory lobe (Fig. 9N). Vesica comparatively large, with very long and thin, gradually curved, abruptly furcate apical blades (Fig. 7E, F).

Female. Coloration, surface and vestiture. As in male. **Structure.** Similar to male but body smaller and more stumpy, 2.4–2.5× as long as posterior width of pronotum, total length 3.1–3.5; head with slightly more convex frons and clypeus, vertex 2.2–2.4× as wide as eye; antennal segment II distinctly thinner than segment I, 0.5× as long as posterior width of pronotum, 0.7–0.8× as long as width of head; pronotum 2.3–2.4× as wide as long, 1.4–1.5× as wide as head.

Genitalia. Sclerotized rings of dorsal labiate plate large, broadly oval. Posterior wall weakly sclerotized, with indistinctly bordered longitudinal sclerotized bands at sides (Fig. 10F).

Distribution. This species inhabits plains and foothills of Central Asia within the area of its host plant, spanning from Uzbekistan and southwestern and southern Kazakhstan to Mongolia.

Hosts. *Salicarus halimodendri* is known to feed exclusively on *Caragana halimodendron* (Pall.) Dum. Cours. (Fabaceae), commonly known as the common salt tree. This distinctive shrub is primarily found in saline deserts and semideserts and was long classified within the monotypic genus *Halimodendron*.

Remarks. *Phoenicocoris qiliananus* Zheng, 1996 was described in Zheng and Li (1996) from Mati in Gansu province, Northwestern China. Schwartz and Stonedahl (2004) transferred this species to *Salicarus* due to the claw and vesica structure and suspected its possible synonymy with *S. halimodendri*, referring to personal communication from I. M. Kerzhner. However, they refrained from formal synonymization pending examination of additional material. Indeed, the coloration of the dorsum, antenna, and legs of *S. qiliananus*, the vestiture composed of short simple setae and narrow, apically acuminate scale-like setae (which are not exclusively restricted to the hemelytron), the structure of both parameres (Zheng and Li 1996: figs 4, 5), and body proportions suggest that this taxon is conspecific with *S. halimodendri*. The only notable distinction is the presence of a single apical blade of the vesica postulated in the original description. However, all *Salicarus* and *Phoenicocoris* species without exception have a twin-coned vesica, while in *S. halimodendri*, the shorter blade is exceptionally short and thin (Fig. 7E, F), and could have been easily overlooked in the aspects chosen by the authors of the original description for making drawings (Zheng and Li 1996: figs 8, 9). Based on the foregoing discussion, we synonymize *Salicarus qiliananus* (Zheng, 1996) with *Salicarus halimodendri* V. G. Putshkov, 1977.

Acknowledgments

Frank Wieland (Zoological Museum, University of Hamburg) and Mike Wilson (National Museum of Wales, Cardiff) provided access to collections and a supportive environment during the stay of the first author in these museums. Attilio Carapezza (Università degli Studi di Palermo) and Franco Faraci (Bardolino, Verona) offered helpful comments on the relevant literature and specimens. We are also indebted to András Orosz (Hungarian Natural History Museum) for sending pictures of the holotype of *S. nitidus* from the collection of HHNM. The constructive comments of Petr Kment (National Museum, Prague) and Artur Tazsakowski (University of Silesia in Katowice) resulted in substantial improvements to the original manuscript. The Heteroptera collection of the Zoological Institute, Russian Academy of Sciences (ZISP), heavily used in this study, is financially supported by the state research project 122031100272-3. We acknowledge the Core Facility Center “Taxon” at the Zoological Institute, St. Petersburg, for access to SEM equipment and technical assistance.

Additional information

Conflict of interest

The authors have declared that no competing interests exist.

Ethical statement

No ethical statement was reported.

Funding

This research was funded by the Russian Foundation for Basic Research (RFBR) (grant 20-54-56011) and the Iran National Science Foundation (INSF) (grant 98025845).

Author contributions

Conceptualisation: FK. Data curation: FK and RH. Formal analysis: FK. Writing-original draft: FK. Visualisation:FK and RH. Funding acquisition: FK and RH. Writing-review and editing: FK and RH.

Author ORCIDs

Fedor V. Konstantinov  <https://orcid.org/0000-0002-7013-5686>

Reza Hosseini  <https://orcid.org/0000-0002-6556-8401>

Data availability

All of the data that support the findings of this study are available in the main text or Supplementary Information.

References

- Aukema B (2024) Catalogue of the Palaearctic Heteroptera. <https://catpalhet.linnaeus.naturalis.nl/> [Accessed 05.05.2024]
- Carapezza A (1984) Eterotteri nuovi o poco noti per la fauna Sarda. *Bollettino della Società Sarda di Scienze Naturale* 23: 155–159.

- Carapezza A (1993) Eterotteri nuovi per le Isole Eolie, Ustica e le Isole Egadi, con nuove sinonimie. *Naturalista Siciliano* (4) 17: 291–303.
- Carapezza A (1995) Heteroptera. In: Massa B (Ed.) *Arthropoda di Lampedusa, Linosa e Pantelleria (Canale di Sicilia, Mar Mediterraneo)*. *Naturalista Siciliano* (4) 19 Suppl., 199–278.
- Cassis G, Wall M, Schuh R (2007) Insect biodiversity and industrializing the taxonomic process: a case study with the Miridae (Heteroptera). In: Hodkinson T, Parnell J (Eds) *Towards the Tree of Life: taxonomy and systematics of large and species rich clades*. Boca Raton, FL: CRC, 193–212. <https://doi.org/10.1201/9781420009538.ch13>
- Ehanno B (1987) *Les hétéroptères mirides de France*. Tome 2A: Inventaire et synthèses écologiques. *Inventaires de Faune et de Flore*, Paris.
- Faraci F, Rizzotti Vlach M (1995) Heteroptera. In: Minelli A, Ruffo S, La Posta S (Eds) *Checklist della specie della fauna italiana*, vol. 41, Calderini, Bologna, 1–56.
- Fieber FX (1861) *Die europäischen Hemipteren. Halbflügler (Rhynchota Heteroptera)*. Gerold's Sohn, Wien, 113–444. <https://doi.org/10.5962/bhl.title.15204>
- Göllner-Scheiding U (1974) Beiträge zur Heteropterenfauna Brandenburgs. 3. Die Heteropterenfauna der Oderwiesen und- hänge bei Lebus/Oder (Hemiptera, Heteroptera). *Faunistische Abhandlungen* 5: 181–198.
- Goula M, Ribes J (1995) Lista de especies de los Miridae de Cataluna (Insecta, Heteroptera). *Boletín de la Asociación Española de Entomología* 19: 175–217.
- Heckmann R, Strauß G, Rietschel S (2015) Die Heteropterenfauna Kretas. *Carolinea* 7: 83–130.
- Herrich-Schaeffer GAW (1838) *Die wanzenartigen Insecten*. C. H. Zeh, Nurnberg 4: 33–92.
- Horváth G (1905) Descripciones de algunos Hemipteros nuevos del centro de España. *Boletín de la Real Sociedad Espanola de Historia Natural* 5: 272–277.
- Jakovlev BE (1889) Zur Hemipteren-Fauna Russlands un der angrenzenden Lander. *Horae Societatis Entomologicae Rossicae* 24: 311–348. [In Russian and German]
- Kerzhner IM (1962) Materials on the taxonomy of capsid bugs (Hemiptera - Miridae) in the fauna of the USSR. *Entomologicheskoe Obozrenie* 41: 372–387. [In Russian]
- Kerzhner IM (1964) Family Isometopidae. Family Miridae (Capsidae). In: Bei-Bienko GY (Ed.) *Opredelitel' nasekomykh evropeiskoi chasti SSSR [Keys to the Insects of the European part of the USSR]*. Vol. 1. Apterygota, Palaeoptera, Hemimetabola. Nauka, Moskova and Leningrad, 700–765. [In Russian; English translation: 1967, Israel Program for Scientific Translation, Jerusalem: 913–1003]
- Kerzhner IM (1997) Notes on taxonomy and nomenclature of Palearctic Miridae (Heteroptera). *Zoosystematica Rossica* 5: 245–248.
- Kerzhner IM, Josifov M (1999) Miridae Hahn, 1833. In: Aukema B, Rieger C (Eds) *Catalogue of the Heteroptera of the Palaeartic Region*, Vol. 3. The Netherlands Entomological Society, Amsterdam, 1–576.
- Kerzhner IM, Matocq A (1997) On some Mediterranean Miridae (Heteroptera). *Zoosystematica Rossica* 6: 191–192.
- Kment P, Bryja J, Jindra Z (2005) New records of true bugs (Heteroptera) of the Balkan peninsula. *Acta Entomologica Slovenica* 13: 9–20.
- Konstantinov FV (2003) Male genitalia in Miridae (Heteroptera) and their significance for suprageneric classification of the family. Part I: general review, Isometopinae and Psallopinae. *Belgian Journal of Entomology* 5: 3–36.

- Konstantinov FV (2008) Revision of *Phaeochiton* Kerzhner, 1964 (Heteroptera: Miridae: Phylini). *European Journal of Entomology* 105: 771–781. <https://doi.org/10.14411/eje.2008.102>
- Konstantinov FV (2019) Revision of *Agraptocoris* Reuter (Heteroptera: Miridae: Phylinae), with description of five new species and a review of aedeagal terminology. *Arthropod Systematics & Phylogeny* 77: 87–124. <https://doi.org/10.26049/ASP77-1-2019-05>
- Konstantinov FV (2023) Plant bugs with swollen antennae: a morphology-based phylogenetic analysis of *Heterocapillus* Wagner, 1960 and related genera (Hemiptera: Miridae: Phylinae). *Arthropod Systematics & Phylogeny* 81: 845–879. <https://doi.org/10.3897/asp.81.e104396>
- Konstantinov FV, Namyatova AA (2008) New records of Phylinae (Hemiptera: Heteroptera: Miridae) from the Palaearctic Region. *Zootaxa* 1870(1): 24–42. <https://doi.org/10.11646/zootaxa.1870.1.2>
- Konstantinov FV, Namyatova AA (2019) Taxonomic revisions and specimen databases in the internet age: dealing with a species rich insect taxon. *Entomological Review* 99: 340–362. <https://doi.org/10.1134/S0013873819030072>
- Kulik SA (1974) Terrestrial true bugs (Heteroptera) of Eastern Siberia and the Far East. *Insect fauna of Eastern Siberia and the Far East*. Irkutsk, 3–41. [In Russian]
- Lindberg H (1948) On the insect fauna of Cyprus. Results of the expedition of 1939 by Harald, Hakan and P. H. Lindberg, I–II. *Societatis Scientiarum Fennica, Commentationes Biologicae* 10(7): 23–175.
- Linnavuori RE (1984) New species of Hemiptera Heteroptera from Iraq and the adjacent countries. *Acta Entomologica Fennica* 44: 1–59.
- Linnavuori RE (1999) Studies on the Miridae fauna of Greece (Hemiptera, Heteroptera). *Biologica Gallo-Hellenica* 25: 25–68.
- Linnavuori RE (2007) Studies on the Miridae (Heteroptera) of Gilan and the adjacent provinces in northern Iran. II. List of species. *Acta Entomologica Musei Nationalis Pragae* 47: 17–56.
- Lodos N, Önder F, Pehlivan E, Atalay R, Erkin E, Karsavuran Y, Tezcan S, Aksoy S (2003) Faunistic Studies on Miridae (Heteroptera) of Western Black Sea, Central Anatolia and Mediterranean Regions of Turkey. *Meta Basmevi*, İzmir, 85 pp.
- Lu X, Cui L, He Y (2011) Description of two species of genus *Salicarus* from Inner Mongolia, China. *Journal of Jilin Agricultural University* 33(5): 500–502.
- Melber A (1993) Beitrag zur Kenntnis der Heteropterenfauna des toskanischen Apennins (Insecta, Heteroptera). *Bollettino del Museo Civico Storia naturale di Verona* 17: 293–356.
- Oshanin V (1910) Verzeichnis der palaearktischen Hemipteren mit besonderer Berücksichtigung ihrer Verteilung im russischen Reiche. Vol. 1(3). *Ezhagodnik Zoologicheskago Muzeya Imperatorskoj Akademii Nauk* 14(suppl.): 587–1087.
- Pagola-Carte S, Zabalegui I (2007) Nuevos e interesantes registros de Miridae (Hemiptera: Heteroptera) en el País Vasco (norte de la Península Ibérica). *Heteropterus Revista de Entomología* 7(1): 33–56.
- Puton A (1875) *Catalogue des Hémiptères (Hétéroptères, Cicadines et Psyllines) d'Europe et du bassin de la Méditerranée*. Deyrolle, Paris, 155 pp. <https://doi.org/10.1002/mmnd.48018750242>
- Putshkov VG (1977) New and little-known mirid bugs (Heteroptera, Miridae) from Mongolia and Middle Asia. *Entomologicheskoe Obozrenie* 56: 360–374. [In Russian; English translation: *Entomological Review* 56(2): 91–100]

- Reuter OM (1875) Revisio critica Capsinarum praecipue Scandinaviae et Fenniae. Akademisk Afhandling, Helsingfors, [101 +] 190 pp.
- Reuter OM (1878) Hemiptera Gymnocerata Europae. Hémiptères Gymnocérates d'Europe, du bassin de la Méditerranée et de l'Asie russe. I. Acta Societatis Scientiarum Fennicae 13: 1–188[8 pls].
- Ribes J, Serra A, Goula M (2004) Catàleg dels heteròpters de Catalunya (Insecta, Hemiptera, Heteroptera). Institut d'Estudis Catalans, Barcelona.
- Rieger C (2012) Notes on the distribution of some Palearctic Heteroptera. Entomologische Zeitschrift Stuttgart 122(3): 133–134.
- Schuh RT, Weirauch C (2020) True bugs of the world (Hemiptera: Heteroptera). Siri Scientific Press, Manchester, UK, 800 pp.
- Schwartz MD (2011) Revision and phylogenetic analysis of the north American genus *Slaterocoris* Wagner with new synonymy, the description of five new species and a new genus from Mexico, and a review of the genus *Scalponotatus* Kelton (Heteroptera: Miridae: Orthotylinae). Bulletin of the American Museum of Natural History 354: 1–290. <https://doi.org/10.1206/354.1>
- Schwartz MD, Stonedahl GM (2004) Revision of *Phoenicocoris* Reuter with descriptions of three new species from North America and a new genus from Japan (Heteroptera: Miridae: Phylinae). American Museum Novitates 3464: 1–55. [https://doi.org/10.1206/0003-0082\(2004\)464%3C0001:ROPRWD%3E2.0.CO;2](https://doi.org/10.1206/0003-0082(2004)464%3C0001:ROPRWD%3E2.0.CO;2)
- Southwood TRE, Leston D (1959) Land and Water Bugs of the British Isles. Frederick Warne and Co., London, 436 pp.
- Stål C (1858) Nya svenska Hemiptera. Öfversigt af Kongliga Vetenskapsakademiens Förhandlingar 15: 355–357.
- Stonedahl GM (1990) Revision and cladistic analysis of the Holarctic genus *Atractotomus* Fieber (Heteroptera: Miridae: Phylinae). Bulletin of the American Museum of Natural History 198: 1–88. <http://hdl.handle.net/2246/889>
- Thomson CG (1871) Öfversigt af de i Sverige fauna arter af gruppen Capsina. Opuscula Entomologica 4: 410–452.
- Vinokurov NN, Kanyukova EV (1995) Conspect of the Fauna of Heteroptera of Siberia: Contribution to the Catalogue of Palaearctic Heteroptera. Yakutian Scientific Centre, Yakutsk, 62 pp. [In Russian]
- Vinokurov NN, Kanyukova EV, Golub VB (2010) Katalog poluzhestkokrylykh nasekomykh (Heteroptera) Aziatskoy chasti Rossii [Catalogue of Heteroptera of the Asian part of Russia]. Novosibirsk, Nauka, 1–323. [In Russian]
- Vollenhoven SC, Snellen van (1875) De inlandsche Hemipteren, beschreven en meerendeels ook afgebeeld. Tijdschrift voor Entomologie 18: 150–185. [In Dutch]
- Wagner E (1958) Zur Gattung *Sthenarus* Fieber 1858 (Hem. Het. Miridae). Acta Entomologica Musei Nationalis Pragae 32: 405–421.
- Wagner E (1960) Beitrag zur Systematik der Gattung *Atractotomus* Fiber 1858 (Hem. Het. Miridae). Trabajos del Museo de Zoología, Barcelona 2: 2–4.
- Wagner E (1967) Die Heteropteren-Ausbeute der Mongolisch-Deutschen Biologischen Expeditionen 1962 und 1964. Ergebnisse der Zoologischen Museum Berlin 43: 53–76. <https://doi.org/10.1002/mmz.19670430105>
- Wagner E (1973) Drei neue Miriden-Arten von Rhodos (Hemiptera, Heteroptera). Nachrichtenblatt der Bayerischen Entomologen 22: 121–125.
- Wagner E (1975a) Die Miridae Hahn, 1831, des Mittelmeerraumes und der Makaronesischen Inseln (Hemiptera, Heteroptera). Teil 3. Entomologische Abhandlungen 40 Suppl., [ii +] 483 pp. <https://doi.org/10.1515/9783112653241>

- Wagner E (1975b) Über *Asthenarius* Kerzhner, 1962 (Hemiptera, Heteroptera, Miridae). Reichenbachia 15: 233–244.
- Wagner E, Weber HH (1964) Héteroptères Miridae. Faune de France 67. Fédération Française des Sociétés de Sciences Naturelles, Paris, 592 pp.
- Zheng L, Li X (1996) A new species of the genus *Phoenicocoris* Reuter (Hemiptera: Miridae) from China. Entomotaxonomia 18(2): 101–104. [In Chinese with description repeated in English]

Supplementary material 1

USI numbers of figured specimens

Authors: Fedor V. Konstantinov

Data type: pdf

Explanation note: Label data.

Copyright notice: This dataset is made available under the Open Database License (<http://opendatacommons.org/licenses/odbl/1.0/>). The Open Database License (ODbL) is a license agreement intended to allow users to freely share, modify, and use this Dataset while maintaining this same freedom for others, provided that the original source and author(s) are credited.

Link: <https://doi.org/10.3897/zookeys.1211.129660.suppl1>

A new species of karst-dwelling bent-toed gecko of the *Cyrtodactylus intermedius* group (Squamata, Gekkonidae) from eastern Thailand and the phylogenetic placement of *C. intermedius*

Natee Ampai¹, Attapol Rujirawan^{2,3}, Siriporn Yodthong⁴, Korkhwan Termprayoon⁵, Bryan L. Stuart⁶, Anchalee Aowphol^{2,3}

1 Department of Biology, Faculty of Science, Srinakharinwirot University, Bangkok, 10110 Thailand

2 Animal Systematics and Ecology Speciality Research Unit, Department of Zoology, Faculty of Science, Kasetsart University, Bangkok, 10900 Thailand

3 Biodiversity Center, Kasetsart University, Bangkok, 10900, Thailand

4 Department of Biological Science, Faculty of Science, Ubon Ratchathani University, Ubon Ratchathani 34190, Thailand

5 School of Science, Walailak University, Nakhon Si Thammarat, 80161, Thailand

6 Section of Research & Collections, North Carolina Museum of Natural Sciences, Raleigh, NC, USA

Corresponding author: Anchalee Aowphol (fsciac@ku.ac.th)



Academic editor: Johannes Penner

Received: 8 March 2024

Accepted: 21 July 2024

Published: 3 September 2024

ZooBank: <https://zoobank.org/991B836A-7F5B-497E-A57C-1591D18EAE43>

Citation: Ampai N, Rujirawan A, Yodthong S, Termprayoon K, Stuart BL, Aowphol A (2024) A new species of karst-dwelling bent-toed gecko of the *Cyrtodactylus intermedius* group (Squamata, Gekkonidae) from eastern Thailand and the phylogenetic placement of *C. intermedius*.

ZooKeys 1211: 101–130. <https://doi.org/10.3897/zookeys.1211.122563>

Copyright: © Natee Ampai et al.

This is an open access article distributed under terms of the Creative Commons Attribution License (Attribution 4.0 International – CC BY 4.0).

Abstract

A new karst-dwelling bent-toed gecko of the *Cyrtodactylus intermedius* group is described from Khlong Hat District, Sa Kaeo Province, eastern Thailand, based on an integrative taxonomic analysis of genetic data and morphological characteristics. Phylogenetic analyses using the mitochondrial NADH dehydrogenase subunit 2 (ND2) gene revealed that topotypes of *C. intermedius* were sister to a clade containing *C. kulenensis* from Cambodia, an unnamed lineage from Sakaerat Biosphere Reserve in Nakhon Ratchasima Province, Thailand, and the Khlong Hat lineage described here as *Cyrtodactylus khlonghatensis* **sp. nov.** Multivariate analyses of morphometric and meristic characters showed that *C. khlonghatensis* **sp. nov.** is morphologically distinct from all other species in the group by having the combination of SVL 76.5–82.8 mm in adult males and 88.5 mm in an adult female; eight supralabial and nine infralabial scales; 30–32 paravertebral tubercles; 20 or 21 longitudinal rows of dorsal tubercles; 43 or 44 ventral scales; seven or eight expanded subdigital lamellae on the 4th toe; 12 unmodified subdigital lamellae on the 4th toe; 19 or 20 total subdigital lamellae on the 4th toe; 31 or 32 total number of enlarged femoral scales; enlarged femoral and precloacal scales continuous; 6–8 pore-bearing precloacal scales in males; three or four rows of enlarged post-precloacal scales; 1–3 postcloacal tubercles; proximal femoral scales less than one-half the size of distal femoral scales; absence of interdigital pocketing between digits of forefeet and hindfeet; and posterior border of the nuchal loop rounded. Uncorrected pairwise genetic divergences (*p*-distances) between the new species and other species of the *intermedius* group ranged from 4.73–22.55%. The discovery of this new species exclusively in isolated karst formations from the Thai-Cambodia border suggests that there may be further undiscovered *Cyrtodactylus* in unexplored karst landscapes along the border of eastern Thailand and western Cambodia.

Key words: Distribution, Gekkota, integrative taxonomy, ND2 gene, multivariate analysis

Introduction

The bent-toed gecko genus *Cyrtodactylus* Gray, 1827, is one of the most diverse among reptiles and the third-largest vertebrate genus globally (Grismer et al. 2021a), with 354 recognized species to date (Uetz et al. 2024). This genus exhibits a wide-ranging geographic distribution across various regions and is predominantly found in Southeast Asia, with their distribution extending from South Asia through the Indo-Australian Archipelago (Oliver et al. 2008, 2016; Wood et al. 2012; Luu et al. 2016; Agarwal et al. 2018; Neang et al. 2020; Chan et al. 2023; Grismer et al. 2015; 2021a, 2021b, 2022; Nugraha et al. 2023; Riyanto et al. 2022). *Cyrtodactylus* species have successfully adapted and evolved to occupy a variety of environments and ecological niches within this extensive range, including terrestrial, arboreal, cave-dwelling, and various substrate specialists (Ngo et al. 2008; Geissler et al. 2019; Grismer et al. 2020a, 2020b; Riyanto et al. 2022; Yodthong et al. 2022). In Thailand, 48 nominal species of *Cyrtodactylus* occur throughout the mainland and adjacent offshore islands (Uetz et al. 2024). Their presence in such diverse regions underscores their adaptability to thrive in a range of habitats and implies a complex evolutionary history for the genus (Chomdej et al. 2022; Grismer et al. 2018a, 2018b, 2020b, 2021b, 2023a; Termprayoon et al. 2021a, 2021b, 2023; Yodthong et al. 2022).

Cyrtodactylus intermedius (Smith, 1917) was originally described from Khao Sebab (= Namtok Phlio National Park), Chanthaburi Province, eastern Thailand. Additional populations were later reported from throughout eastern and southern Thailand, extending through the Cardamom Mountains of Cambodia and southward to southern Vietnam (Taylor, 1963; Stuart and Emmet 2006; Geissler et al. 2019; Murdoch et al. 2019; Grismer et al. 2020a, 2021b). *Cyrtodactylus intermedius* is now considered to represent a complex of species (Ngo et al. 2010; Murdoch et al. 2019; Grismer et al. 2015, 2020a, 2023a) known as the *C. intermedius* group (Grismer et al. 2021b). The group is monophyletic and comprises 13 recognized species (Murdoch et al. 2019; Grismer et al. 2020a, 2021b, 2023a; Uetz et al. 2024). These species include *C. auralensis* Murdoch, Grismer, Wood, Neang, Poyarkov, Tri, Nazarov, Aowphol, Pauwels, Nguyen & Grismer, 2019; *C. bokorensis* Murdoch, Grismer, Wood, Neang, Poyarkov, Tri, Nazarov, Aowphol, Pauwels, Nguyen & Grismer, 2019; *C. cardamomensis* Murdoch, Grismer, Wood, Neang, Poyarkov, Tri, Nazarov, Aowphol, Pauwels, Nguyen & Grismer, 2019; *C. disjunctus* Grismer, Pawangkhanant, Idi-iatullina, Trofimets, Nazarov, Suwannapoom & Poyarkov, 2023; *C. hontreensis* Ngo, Grismer & Grismer, 2008; *C. intermedius* (Smith, 1917); *C. kohrongensis* Grismer, Onn, Oaks, Neang, Sokun, Murdoch, Stuart & Grismer, 2020; *C. kulenensis* Grismer, Geissler, Neang, Hartmann, Wagner & Poyarkov, 2021; *C. laangensis* Murdoch, Grismer, Wood, Neang, Poyarkov, Tri, Nazarov, Aowphol, Pauwels, Nguyen & Grismer, 2019; *C. phuquocensis* Ngo, Grismer & Grismer, 2010; *C. regicavernicolus* Chhin, Neang, Chan, Kong, Ou, In, Samorn, Sor, Lou, Sin, Chhim, Stuart & Grismer, 2024; *C. septimontium* Murdoch, Grismer, Wood, Neang, Poyarkov, Tri, Nazarov, Aowphol, Pauwels, Nguyen & Grismer, 2019; and *C. thylacodactylus* Murdoch, Grismer, Wood, Neang, Poyarkov, Tri, Nazarov, Aowphol, Pauwels, Nguyen & Grismer, 2019. Of these 13 species, only two species occur in Thailand, *C. disjunctus* (southern Thailand) and *C. intermedius* (eastern Thailand). Members of the *C. intermedius* group are highly adaptable to different habitats, including karst formations, granitic montane areas, sandstone, and other non-elevated terrestrial habitats (Grismer

et al. 2020a, 2021b). This adaptability is likely due to their ecological versatility and ability to thrive in a variety of environmental settings (Murdoch et al. 2019; Grismer et al. 2023a). Other divergent mitochondrial lineages have been reported, suggesting that additional species diversity might exist within the *C. intermedius* group (Grismer et al. 2021a, 2021b, 2023a). One major hindrance to delimiting species in the *C. intermedius* group has been the lack of topotypic genetic material from the type locality of the nominate species *C. intermedius*.

During fieldwork from 2022–2023, we conducted surveys for *Cyrtodactylus* at Chanthaburi and Sa Kaeo Provinces in eastern Thailand. An integrative taxonomic approach, combining morphological characters, mitochondrial DNA analysis, and ecological data, was employed to compare the specimens to other members of the *C. intermedius* group and determine their taxonomic status. Additionally, samples were obtained from the type locality of *C. intermedius*. Herein, a distinct population from Khlong Hat District, Sa Kaeo Province is described as a new species.

Materials and methods

Sampling and specimen collection

Field sampling was carried out through visual encounter surveys conducted both during the daytime (1000–1700 h) and at night (1900–2200 h) from July 2022 to February 2023 in two locations of eastern Thailand: (1) Khlong Hat District, Sa Kaeo Province and (2) Namtok Phlio National Park, Mueang Chanthaburi District, Chanthaburi Province (Fig. 1). Geographical coordinates and elevation for each locality were recorded using a Garmin GPSMAP 64s. Environmental factors (ambient temperature and relative humidity) were collected using a Kestrel 400 Weather Meter. Data on habitat, including microhabitat preferences, habitat use, and substrate type were also recorded for each specimen. Specimens were hand-collected and kept individually in bags for photographing prior to their euthanization. Specimens were humanely euthanized with tricaine methanesulfonate (MS-222) solution. The MS-222 solution was freshly prepared on the day of its use for euthanasia (Conroy et al. 2009; Simmons 2015; American Veterinary Medical Association 2020). Liver tissue was removed from each euthanized specimen, preserved in 95% ethanol, and stored at -20 °C for molecular study.

Voucher specimens were initially preserved in 10% formalin solution and subsequently transferred to 70% ethanol for morphological study and long-term storage. All specimens and tissue samples are deposited in the herpetological collection at the Zoological Museum of Kasetsart University, Bangkok, Thailand (ZMKU). Additional data were obtained from the original species descriptions of the *C. intermedius* group (Smith, 1917, 1935; Ngo et al. 2008; 2010; Murdoch et al. 2019; Grismer et al. 2020a, 2021b, 2023a; Chhin et al. 2024).

Mitochondrial DNA analyses

Genomic DNA of the seven newly collected specimens (*C. intermedius* from the type locality, $n = 4$, and the Khlong Hat population, $n = 3$) was isolated from liver tissue samples using the Qiagen DNAeasy™ Blood & Tissue Kit (Qiagen, Germany). A partial fragment of the mitochondrial NADH dehydrogenase subunit 2 (ND2) gene and its flanking tRNAs were amplified by polymerase chain reaction (PCR)

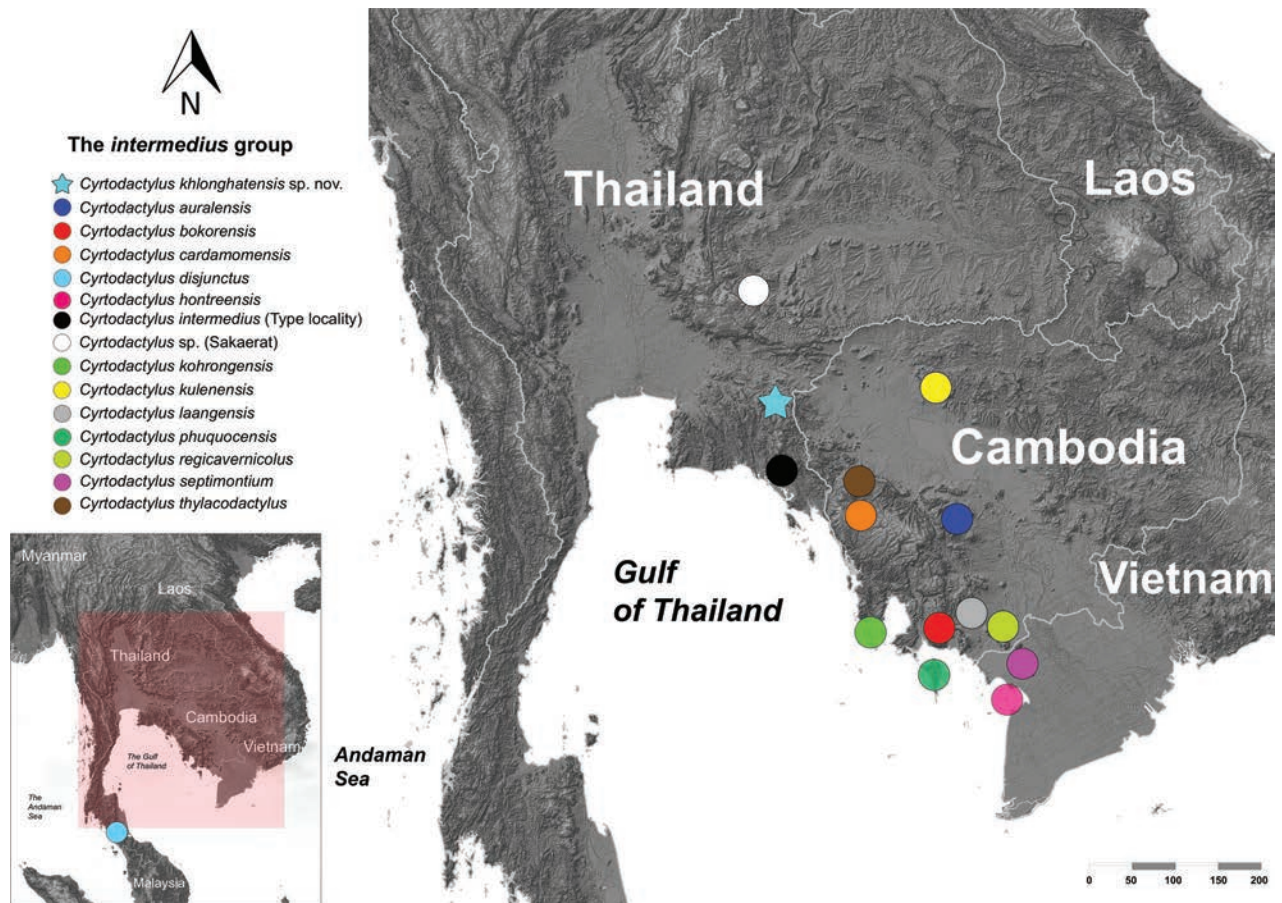


Figure 1. Map illustrating the distribution of the species of the *Cyrtodactylus intermedius* group using QGIS 3.34.8 (QGIS Development Team 2024). The elevation background data was derived from NASA LP DAAC (2013).

under the following conditions: initial denaturation (95 °C, 2 min) followed by 31 cycles of a second denaturation (95 °C, 35 s), annealing (56 °C, 35 s), extension (72 °C, 35 s), and a final extension (72 °C, 10 min) using the light strand primer, L4437b (5'-AAGCAGTTGGGCCCATACC-3'; Macey et al. 1997) and the heavy strand primer, H5934 (5' -AGRGTGCCAATGTCTTTGTGRTT-3'; Macey et al. 1997). All PCR products were purified using the QIAquick PCR Purification Kit (Qiagen Ltd., Hilden, Germany) and sequenced using the amplifying primers on an ABI 3730XL automatic sequencers (Applied Biosystems, CA, USA) with BigDye version 3 chemistry and the amplifying primers (Applied Biosystems, CA, USA). DNA sequences were edited and manually checked in Geneious Prime 2022.2.1 (Biomatters Ltd., Auckland, New Zealand). All newly generated sequences were deposited in GenBank under accession numbers PP444475–PP444481. All 42 sequences of *C. intermedius* group species and the five outgroups *C. oldhami* (Theobald, 1876), *C. trigroides* Bauer, Sumontha & Pauwels, 2003, *C. zebraicus* Taylor, 1962, *Dixonius siamensis* (Boulenger, 1898), and *Hemidactylus frenatus* Duméril & Bibron, 1836 were downloaded from GenBank (Suppl. material 1) following Ngo et al. (2010), Murdoch et al. (2019), Grismer et al. (2020a, 2021b), and Yodthong et al. (2022). The recently described species *C. regicavernicolus* was not included in the analyses but is closely related to *C. laangensis* (see Chhin et al. 2024). All downloaded sequences were aligned to the newly generated sequences using the MUSCLE plug-in as implemented in Geneious Prime 2022.2.1. The aligned dataset was partitioned by ND2 codon position and the flanking tRNAs.

Maximum Likelihood (ML) and Bayesian Inference (BI) analyses were used to estimate the phylogenetic relationships within the *C. intermedius* group. ModelFinder function within IQ-TREE (Kalyaanamoorthy et al. 2017) was used to select the best partitions for the ND2 gene and tRNAs for both ML and BI analyses. The selection was based on the Bayesian Information Criterion (BIC). For the ML analysis, TIM+F+G4 was identified as the best-fit model for codon partitions, and TN+F+G4 for the flanking tRNAs partitions. The ML analysis was conducted by the IQ-TREE webserver (Trifinopoulos et al. 2016) with 10,000 bootstrap pseudo-replicates employing the ultrafast bootstrap approximation algorithm (UFB; Minh et al. 2013; Hoang et al. 2018) to construct a final consensus ML phylogenetic tree. Nodes with ultrafast bootstrap supported values of 95 and above were considered strongly supported (Minh et al. 2013).

The BI analysis was conducted using MrBayes v. 3.2.7a on XSEDE (Ronquist et al. 2012) through the CIPRES Science Gateway (Miller et al. 2010). The BI analysis used default prior and GTR+I+ Γ model of evolution for the codon partitions and flanking tRNAs. Two simultaneous runs were performed with four chains per run (three heated chains and one cold chain), using the default priors setting, a chain temperature set to 0.1, and 20 million generations sampled every 2,000 generations from the Markov Chain Monte Carlo (MCMC) chains. The first 25% of each run was discarded as burn-in using the “sumt” command. The stationary states of each parameter based on the standard deviation of split frequencies < 0.01 and the effective sample size (ESS) score above 200 for all parameters were assessed in Tracer v. 1.7.1 (Rambaut et al. 2018). The 50% majority-rule consensus of sampled tree from the post burn-in tree of the BI analysis and the most likely tree in the ML analysis were visualized and edited in FigTree v. 1.4.4 (Rambaut 2018). Nodes with Bayesian posterior probabilities support (BPP) of 0.95 and above were considered strongly supported (Huelsenbeck and Ronquist 2001; Wilcox et al. 2002). Uncorrected pairwise genetic divergences (*p*-distances) were estimated in MEGA11 (Tamura et al. 2021) using bootstrap method with 1,000 replications and the complete deletion option to remove missing data.

Voucher abbreviations are the School of Agriculture and Natural Resources, University of Phayao (**AUP**), Aaron M. Bauer field series (**AMB**), Chulalongkorn University Museum of Zoological Records, Bangkok, Thailand (**CUMZR**), the Field Museum of Natural History, Chicago, Illinois, USA (**FMNH**), Institut Royal des Sciences Naturelles de Belgique, Belgium (**IRSNB**), the Institute of Tropical Biology Collection of Zoology in Ho Chi Minh City, Vietnam (**ITBCZ**), La Sierra University Herpetological Collection (**LSUHC**), the Zoological Research Museum Alexander Koenig, Bonn, Germany (**ZFMK**), the Zoological Museum of Kasetart University (**ZMKU**), the corresponding Sabira S. Idiatullina field number of the Zoological Museum of Moscow State University (**ZMMU ISS**) and the corresponding Nikolay A. Poyarkov field numbers of the Zoological Museum of Moscow State University (**ZMMU NAP**).

Morphological analyses

Coloration and patterns in life were assessed through digital images of individuals across all available age groups prior to preservation, taken by AR. Mensural, meristic, and qualitative characters were recorded by the first author on

the left side of specimens for symmetrical traits using digital Mitutoyo CD-6" ASX Digimatic Calipers to the nearest 0.1 mm under a Nikon SMZ 745 dissecting stereomicroscope. Only adult individuals, determined by the presence of secondary sexual characteristics such as the presence of large pore-bearing precloacal scales or hemipenial swelling in males, or visible eggs on the ventral side of the body in females, were included for morphological measurements and analyses. A total of 32 morphological characters (16 mensural characters and 16 meristic characters) were modified from previous studies of the *C. intermedius* group (Murdoch et al. 2019; Grismer et al. 2020a, 2021b).

Mensural measurements were as follows:

- SVL** snout to vent length, taken from tip of snout to the anterior margin of vent;
- TW** tail width, taken at the base of the tail immediately posterior to the postcloacal swelling;
- TL** tail length, taken from the vent to the tip of the tail, original or regenerated;
- FL** forearm length, taken on the dorsal surface from the posterior margin of the elbow while flexed 90° to the inflection of the flexed wrist;
- TBL** tibia length, taken on the ventral surface from the posterior surface of the knee while flexed 90° to the base of the heel;
- HL** head length, distance from the posterior margin of the retroarticular process of the lower jaw to the tip of the snout;
- HW** head width, measured at the angle of the jaws;
- HD** head depth, the maximum height of head from the occiput to the throat;
- AG** axilla to groin length, taken from the posterior margin of the forelimb at its insertion point on the body to the anterior margin of the hind limb at its insertion point on the body;
- ED** eye diameter, the maximum horizontal diameter of the eyeball;
- EE** eye-ear distance, measured from the anterior margin of the ear opening to the posterior edge of the eyeball;
- EL** ear length, taken from the greatest vertical distance of the ear opening;
- EN** eye to nostril distance, measured from the anterior most margin of the eyeball to the posterior margin of the external nares;
- ES** eye to snout distance, measured from the anterior margin of the eyeball to the tip of snout;
- IN** internarial distance, measured between the nares across the rostrum;
- IO** interorbital distance, measured between the anterior edges of the orbit.

Meristic characters were as follows:

- SL** the number of supralabial scales, counted from the largest scale immediately below the middle of the eyeball to the rostral scale;
- IL** the number of infralabial scales, counted from the mental to the termination of enlarged scales just after the upturn of the mouth;
- PVT** the number of paravertebral tubercles between limb insertions, counted in a straight line immediately left of the vertebral column;
- LRT** the number of longitudinal rows of body tubercles, counted transversely across the center of the dorsum from one ventrolateral fold to the other;

- VS** the number of longitudinal rows of ventral scales, counted transversely across the center of the abdomen from one ventrolateral fold to the other;
- 4SLU** the number of small, unmodified subdigital lamellae distal to the digital inflection on the 4th toe, counted from the digital inflection to the claw;
- 4SLE** the number of expanded subdigital lamellae proximal to the digital inflection on the 4th toe, counted from the base of the first phalanx where it contacts the body of the foot to the largest scale on the digital inflection;
- 4SLT** the total number of subdigital lamellae beneath the 4th toe;
- FS** The total number of enlarged femoral scales from each thigh combined as a single metric;
- PS** the number of enlarged precloacal scales;
- PP** the number of precloacal pores in males;
- PPS** the number of rows of post-precloacal scales on the midline between the enlarged precloacal scales and the vent;
- PCT** the number of postcloacal tubercles on either side of the base of the tail;
- BB** the number of dark body bands between limb insertions;
- LCB** the number of light caudal bands on the original tail;
- DCB** the number of dark caudal bands on the original tail.

Additional categorical characters examined were enlarged femoral and cloacal scales continuous or separated by a diastema at the base of the femora; proximal femoral scales were less than one-half the size of the distal femoral scales; and the presence or absence of a pocket in the skin webbing between the digits of the hind and forefeet. Color pattern characters examined were the nuchal loop being continuous from eye to eye or separated medially into paravertebral sections; the posterior border of the nuchal loop rounded or chevron-shaped to a point; the presence or absence of dark pigmented blotches on the top of the head; light-colored caudal bands encircling tail or not; regenerated tail bearing a pattern of dark spots or not. Morphological comparisons were based on examination of the original descriptions of species in the literature (Ngo et al. 2010; Murdoch et al. 2019; Grismer et al. 2015, 2020a, 2021b, 2023a).

Thirteen morphometric variables were size-adjusted for differences in ontogenetic composition by the allometric equation: $X_{adj} = \log[X \pm \beta(SVL \pm SVL_{mean})]$, where X_{adj} is the adjusted value of the morphometric variable; X is the unadjusted value of dependent variable; β = unstandardized regression coefficient for each species; SVL is snout to vent length; and SVL_{mean} is overall mean of SVL of each allometry species (Thorpe 1975, 1983; Turan 1999; Leonart et al. 2000) using the R package "GroupStruct" (Chan and Grismer 2021) in the software R v.4.0.1 (R Core Team, 2020). Three morphological variables, including TL (tail length), TW (tail width), and EL (ear length), were excluded from the analyses due to differences in their conditions. Thirteen size-adjusted morphometric variables (SVL_{adj} , FL_{adj} , TBL_{adj} , AG_{adj} , HL_{adj} , HW_{adj} , HD_{adj} , ED_{adj} , EE_{adj} , EN_{adj} , ES_{adj} , IN_{adj} , and IO_{adj}) were tested for normality using the Shapiro-Wilk test ($p \geq 0.05$). Normality of data was confirmed for homogeneity of variances using Levene's test ($p \geq 0.05$) through the Paleontological statistics software (PAST version 4.11; Hammer et al. 2001).

Statistical analyses were performed to compare differences in morphological characteristics, body size, and shape within the *intermedius* group ($n = 58$), including populations from Khlong Hat samples ($n = 4$) and nine congener species: *C. auralensis* ($n = 6$), *C. bokorensis* ($n = 7$), *C. cardamomensis* ($n = 6$), *C. intermedius* (topotypes; $n = 5$), *C. kohrongensis* ($n = 6$), *C. kulenensis* ($n = 9$), *C. laangensis* ($n = 5$), *C. septimontium* ($n = 7$), *C. thylacodactylus* ($n = 3$) (Suppl. material 2). Due to lack of available measurements and small sample size, four species in the *intermedius* group (*C. disjunctus*, *C. hontreensis*, *C. phuquocensis* and *C. regicavernicolus*) were not included in the morphological analyses. Multivariate analyses employed 13 morphometric characters (SVL_{adj} , FL_{adj} , TBL_{adj} , AG_{adj} , HD_{adj} , HL_{adj} , HW_{adj} , ED_{adj} , EE_{adj} , EN_{adj} , ES_{adj} , IN_{adj} , and IO_{adj}) and 10 meristic characters data (SL, IL, PVT, LRT, VS, 4SLU, 4SLE, 4SLT, FS, and PS). Femoral and precloacal pores were omitted from the multivariate analyses due to their presence only in males. Morphometric and meristic characters were concatenated into a single dataset and analyzed by principal component analysis (PCA) using the built in R functions: “prcomp” (R Core Team, 2020) and “ggplot2” (Wickham 2016) to find the best low-dimensional space character variation in data set and to reduce noise and the potential of overfitting. A discriminant analysis of principal components (DAPC) was performed using the “adeget” package in R (Jombart 2008) to characterize clustering and distance separation in the morphospace of new groups, defined in the PCA, in comparison to nine congeners of the *intermedius* group. It was also used to generate linear combinations of centroids with the highest between-group variance (Jombart et al. 2010). Prior to plotting, dimension reduction in the DAPC involves preserving the initial set of principal components (PCs) that collectively explain approximately 90% of the variation within the dataset (Jombart and Collins 2015), a determination derived from a scree plot generated during the analysis. Maintaining an excessive number of PCs may introduce artificial structure into the data, whereas retaining too few run the risk of overlooking genuine structure (Cangelosi and Goriely 2007).

Results

Molecular analyses

The total aligned dataset contained 1,227 characters of 49 individuals of the *C. intermedius* group and five individuals of the outgroup species (Fig. 2). The maximum likelihood value of the best ML tree was $\ln L = -26,799.981$. The standard deviation of split frequencies was 0.002503 between the two simultaneous BI runs and the ESS values were $\geq 14,230$ for all parameters. The results of ML and BI phylogenetic analyses recovered identical topologies (Fig. 2). The Khlong Hat samples represented a well-supported monophyletic lineage (100 UFB, 1.0 BPP) nested within the *C. intermedius* group (Fig. 2). The Khlong Hat population was strongly supported for BI (0.95 BPP) but not in ML (79 UFB) as the sister lineage to the clade containing *C. kulenensis* and *Cyrtodactylus* sp. from Sakaerat Biosphere Reserve, Nakhon Ratchasima Province (Fig. 2). The Khlong Hat population had uncorrected p -distances of 4.73–5.09% from *C. intermedius* (topotypes), 6.71–6.96% from *C. intermedius* (Khao Khitchakut), 5.82% from *Cyrtodactylus* sp. (Sakaerat) and 4.73–22.55% from other species

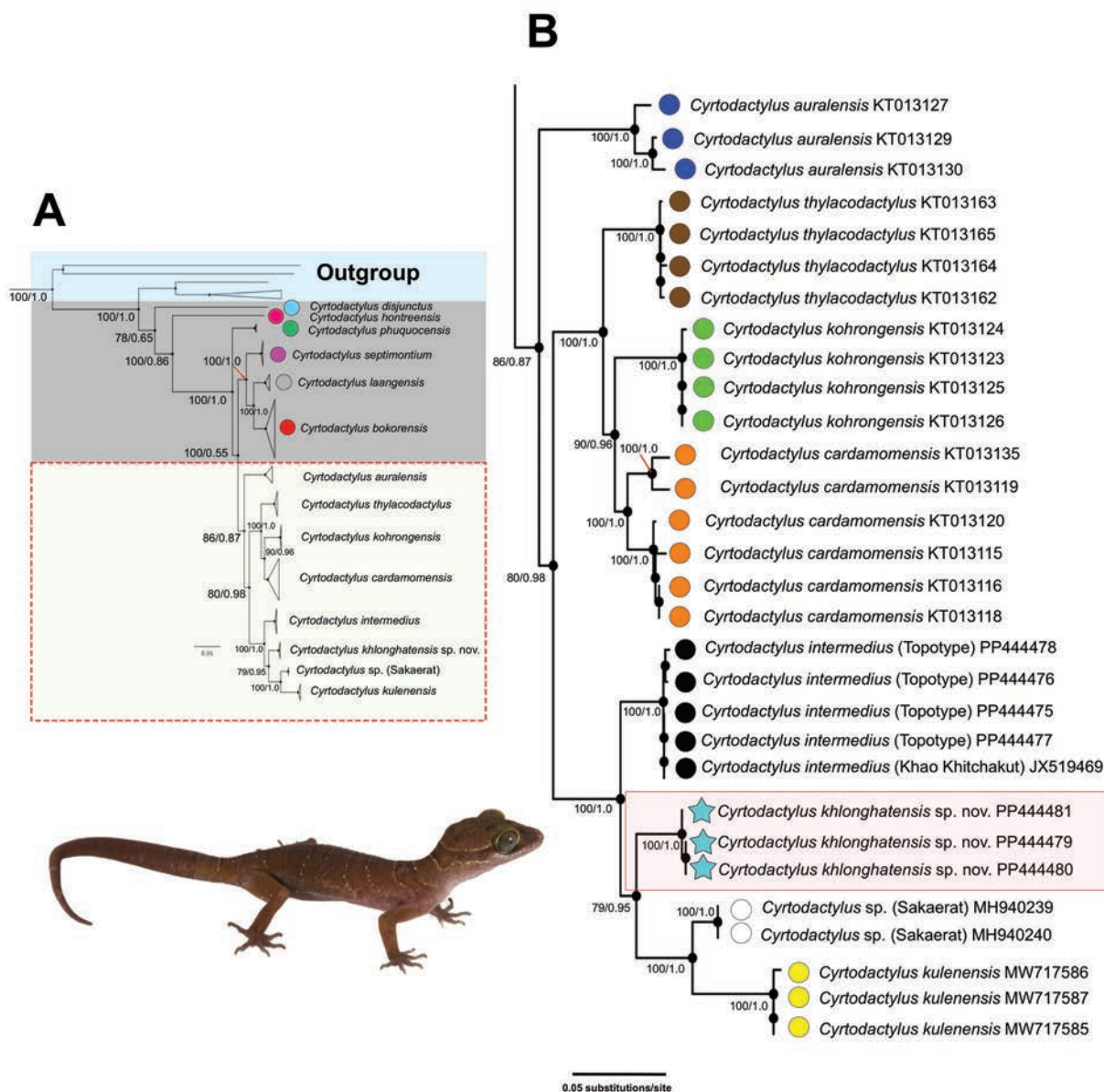


Figure 2. A best maximum likelihood topology illustrating the relationships of the *Cyrtodactylus intermedius* group and other related species based on 1,227 bp of the ND2 gene and flanking tRNAs **A** shown in full view **B** relevant clades of the *intermedius* group in close-up view. Nodal support values are ultrafast bootstrap values (UFB) from maximum likelihood analysis followed by posterior probabilities (BPP) of Bayesian analysis.

in the *intermedius* group (Suppl. material 3). The within population uncorrected *p*-distances of the Khlong Hat population was 0.00%.

Cyrtodactylus intermedius samples from Namtok Phlio National Park (topotypes) and Khao Khitchakut, Chanthaburi Province, were recovered as a well-supported lineage (100 UFB, 1.0 BPP) and are the well-supported (100 UFB, 1.0 BPP) sister taxon to a clade comprised of *C. kulenensis*, *Cyrtodactylus* sp. from Sakaerat Biosphere Reserve and the Khlong Hat samples. *Cyrtodactylus intermedius* had uncorrected *p*-distance of 4.73–22.91% from other species in the *C. intermedius* group. The intraspecific uncorrected *p*-distances of *C. intermedius* was 0.00–1.87% (0.00–1.09% within the type locality; 1.75–1.87% between the type locality and Khao Khitchakut).

Morphological analyses

Multivariate analyses using PCA and DAPC of Khlong Hat samples and nine species in the *C. intermedius* group revealed morphospacial differences along the ordination of the first two components and accounted for 50.31% of the variation (Fig. 3). The first six components of the PCA with eigenvalues > 1.0 accounted for 80.47% of the variation in the dataset (Table 1). PC1 explained for 36.78% of the variation and was heavily loaded with body size and head size (SVL_{adj}, HL_{adj}, HW_{adj}). PC2 accounted for 13.53% of the variation and was heavily loaded on VS, 4SLE, 4SLU, and 4SLT. PC3–PC6 accounted for 11.76%, 7.09%, 6.50% and 4.81% of the variation, respectively and were heavily loaded on IO_{adj}, SL, IL, 4SLE, 4SLU, LRT, FS, and PS (Table 1). The ordination of the first two components showed that the Khlong Hat samples clustered separately from all other species except *C. intermedius* (overlapped with one specimen). Factor loadings for each component of the morphometric and meristic characters data are provided in Table 1. The DAPC (76.89% of cumulative variance) showed strong separation of the Khlong Hat samples from all other species in the *C. intermedius* group (Fig. 3B).

Table 1. Summary of eigenvalues, standard deviation, percentage of variance, and factor loadings from the first six principal components (PC) of 13 size-adjusted morphometric and ten meristic characters of *Cyrtodactylus khlonghatensis* sp. nov., and nine congeners of the *intermedius* group including *C. auralensis*, *C. bokorensis*, *C. cardamomensis*, *C. intermedius*, *C. kohrongensis*, *C. kulenensis*, *C. laangensis*, *C. septimontium*, and *C. thylacodactylus*. Values highlighted in bold represent those with the greatest contribution (factor loading ≥ 0.300) to the first six PCs with eigenvalue > 1.0. Measurement abbreviations are defined in the text.

	PC1	PC2	PC3	PC4	PC5	PC6
Eigenvalue	8.458	3.112	2.704	1.629	1.496	1.107
Standard deviation	2.908	1.764	1.644	1.277	1.223	1.052
% of variance	36.78	13.53	11.76	7.09	6.50	4.81
SVL _{adj}	-0.303	0.055	-0.189	0.049	-0.125	0.050
FL _{adj}	-0.280	0.134	-0.037	0.271	0.011	-0.011
TBL _{adj}	-0.287	0.084	-0.006	0.278	0.009	-0.162
AG _{adj}	-0.209	0.226	-0.249	0.187	-0.157	0.224
HL _{adj}	-0.300	-0.129	-0.168	-0.021	-0.080	-0.078
HW _{adj}	-0.305	-0.025	-0.161	-0.029	-0.099	0.079
HD _{adj}	-0.284	0.119	0.149	-0.121	0.197	0.065
ED _{adj}	-0.267	0.100	0.155	-0.023	-0.219	-0.127
EE _{adj}	-0.262	-0.125	-0.160	-0.161	0.166	0.045
ES _{adj}	-0.292	-0.113	0.063	-0.025	0.280	-0.036
EN _{adj}	-0.281	-0.151	0.002	-0.077	0.213	-0.008
IN _{adj}	-0.088	0.163	-0.173	0.284	0.287	-0.118
IO _{adj}	-0.183	0.038	0.355	0.010	0.122	0.269
SL	-0.138	-0.265	0.183	-0.210	-0.207	-0.370
IL	-0.055	0.274	-0.046	-0.008	-0.447	-0.537
PVT	-0.205	0.170	0.181	-0.248	-0.243	0.159
LRT	-0.017	-0.103	-0.232	-0.527	-0.142	0.029
VS	-0.079	-0.305	-0.237	-0.104	-0.033	0.131
4SLE	-0.125	-0.341	0.358	-0.024	0.035	-0.107
4SLU	0.046	-0.325	-0.064	0.424	-0.382	0.223
4SLT	-0.058	-0.446	0.203	0.270	-0.223	0.090
FS	0.013	-0.201	-0.481	-0.100	-0.020	0.077
PS	-0.042	0.248	0.180	-0.161	-0.296	0.505

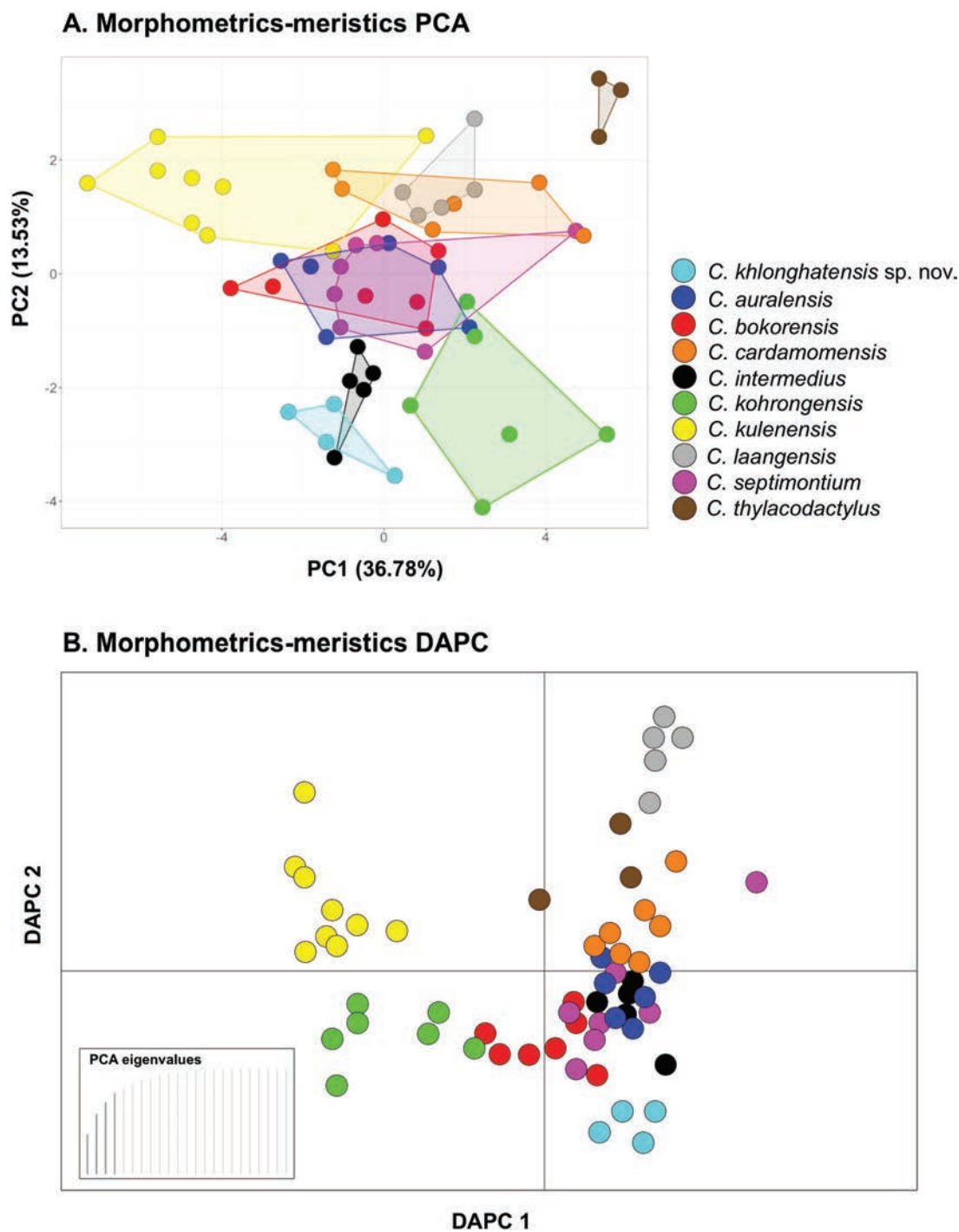


Figure 3. Multivariate analysis results of principal component analysis (PCA) and discriminant analysis of principal component (DAPC) of 23 morphological variables for ten species ($n = 59$ individuals) of the *intermedius* group **A** PCA scatterplot showing morphospacial differentiation among ten species in the *intermedius* group **B** DAPC plot based on the retention of 4 PC axes and discriminant eigenvalues showing morphospacial variation among ten species in the *intermedius* group.

Taxonomic hypotheses

The Khlong Hat population is clearly distinct from all other members of the *C. intermedius* group, as evidenced by the convergence of multiple analyses, including the phylogeny, multivariate analyses, and discrete diagnostic morphological characters (see “Comparison” below). Therefore, we hypothesize that the Khlong Hat population represents a distinct species that is described below as new.

Systematics

Cyrtodactylus khlonghatensis sp. nov.

<https://zoobank.org/595F31AB-E56F-436B-951A-633B3703EE40>

Figs 4–6

Suggested common name: Khlong Hat Bent-toed Gecko

Type material. *Holotype* • ZMKU R 01068, adult male (Figs 4, 5B, 6) from Thailand, Sa Kaeo Province, Khlong Hat District, Khlong Hat Subdistrict, Tham (= cave) Phet Pho Thong (13°25.116'N, 102°19.690'E, 246 m elevation), collected on 28 July 2022 by Attapol Rujirawan. *Paratypes*. Five paratypes (three adults and two sub-adults) • Two adult males (ZMKU R 01067, ZMKU R 01069) and one adult female (ZMKU R 01070), same data as holotype • One sub-adult female (ZMKU R 01071), same data as holotype • One sub-adult male (ZMKU R 01072), same data as holotype, except from Khlong Kai Thuean Subdistrict, Tham Nam Khao Phra Siwa (13°19.258'N, 102°19.661'E, 178 m elevation), collected on 29 July 2022.

Diagnosis. *Cyrtodactylus khlonghatensis* sp. nov. can be distinguished from all other species of the *intermedius* group by having the following combination of characters: (1) SVL of 76.5–82.8 mm (mean 80.5 ± 3.5 mm, $n = 3$) in adult males and 88.5 mm in an adult female ($n = 1$); (2) eight supralabial and nine infralabial scales; (3) 30–32 paravertebral tubercles; (4) 20 or 21 longitudinal rows of dorsal tubercles; (5) 43 or 44 ventral scales; (6) seven or eight expanded subdigital lamellae on the 4th toe; (7) 12 unmodified subdigital lamellae on the 4th toe; (8) 19 or 20 total subdigital lamellae on the 4th toe; (9) 31 or 32 total number of enlarged femoral scales; (10) enlarged femoral and precloacal scales continuous; (11) 6–8 pore-bearing precloacal scales in males; (12) three or four rows of enlarged post-precloacal scales; (13) 1–3 postcloacal tubercles; (14) proximal femoral scales < 1/2 the size of distal femoral scales; (15) absence of interdigital pocketing between digits of forefeet and hindfeet; and (16) posterior border of the nuchal loop rounded.

Description of holotype. Adult male in good state of preservation with 82.8 mm SVL; head relatively moderate in length (HL/SVL 0.30), wide (HW/HL 0.64), slightly flattened (HD/HL 0.36), distinct from the neck, and triangular in dorsal profile; lores concave anteriorly, inflated posteriorly; frontal region flattened, prefrontal region concave; canthus rostralis rounded; snout rather elongate (ES/HL 0.40), rounded in the rostral region, eye to snout distance slightly greater than head depth; eye large (ED/HL 0.21), eyeball slightly protuberant, pupil vertical, the eye to ear distance greater than eye diameter; ear opening elliptical, obliquely oriented, moderate in size (EL/HL 0.07); rostral large, subrectangular, wider (3.3 mm) than high (1.8 mm), partially divided by a dorsal furrow, posteriorly bordered by left and right supranasals and smaller three internasal scales, laterodorsally bordered by nostril opening and 1st supralabial; external nares anteriorly bordered by rostral, dorsally by large supranasal, posteriorly by two small postnasals, ventrally bordered by 1st supralabial; 8L/8R subrectangular supralabials extending to below the center of the eye, 10L/10R to the posterior margin of the eyeball, subrectangular anteriorly, elliptical shape posteriorly; 2nd to 6th supralabials slightly larger than 1st supralabial; 6L/6R infralabials extending to below center of the eye, 9L/9R to below the posterior margin of the eyeball, larger than supralabials, tapering smoothly posteriorly; scales of frontonasal, prefrontal and lores small, domed,

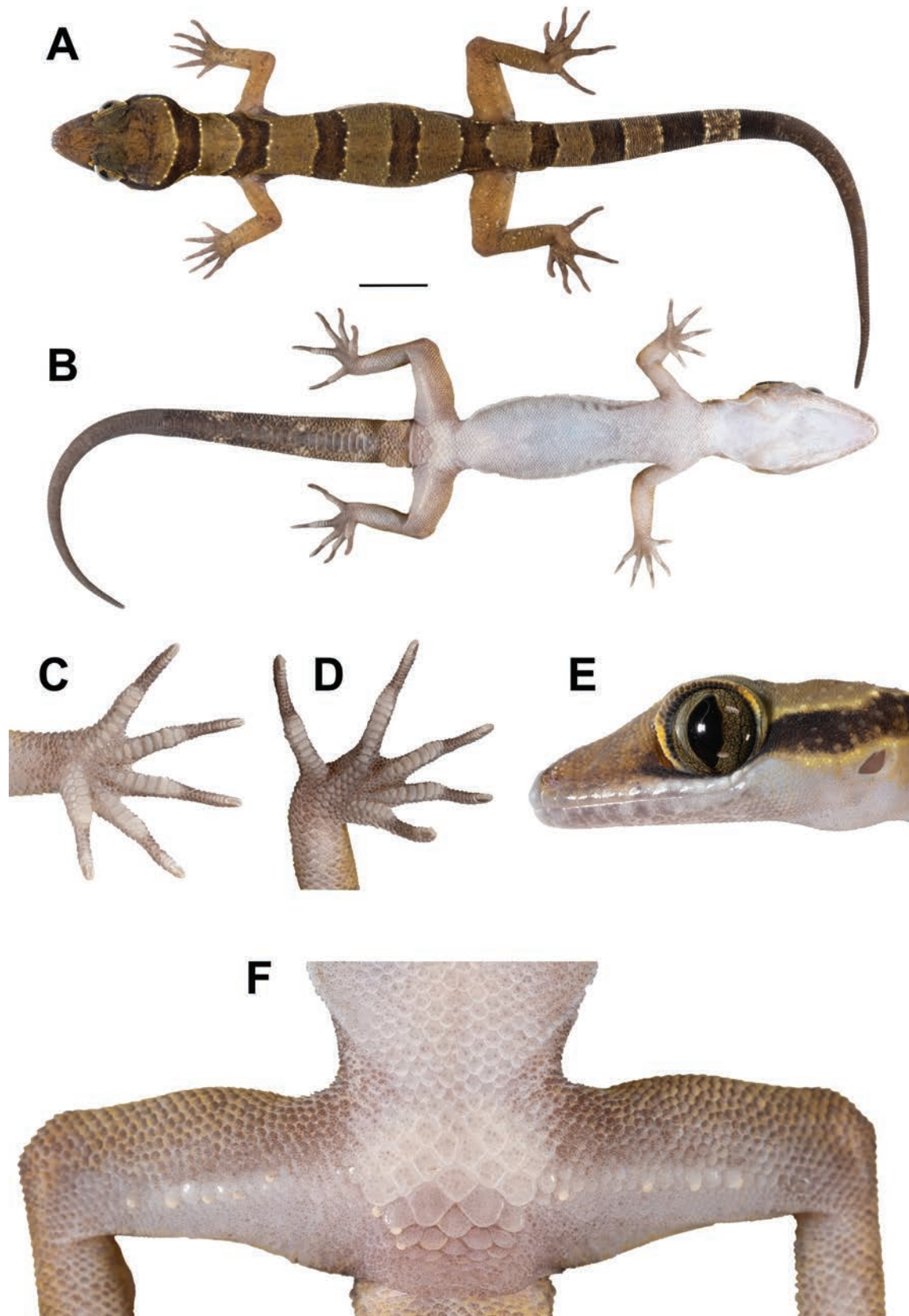


Figure 4. Adult male holotype of *Cyrtodactylus khlonghatensis* sp. nov. (ZMKU R 01068) from Tham Phet Pho Thong, Khlong Hat Subdistrict, Khlong Hat District, Sa Kaeo Province, Thailand, prior to preservation **A** dorsal view **B** ventral view **C** palmar view of the right hand **D** plantar view of the right foot **E** lateral view of left side of head, and **F** precloacal region showing distribution of enlarged femeropreloacal scales. Scale bar in dorsal and ventral views: 10 mm.

relatively raise, slightly larger than granular scales on top of head and occiput; scales of occiput and top of head intermixed with scattered, distinct, enlarged tubercles, more prominent tubercles between occiput and ear opening; dorsal supraciliaries smooth, not elongate; mental large, triangular, 3.2 mm in width, 2.4 mm in length, laterally bordered by 1st infralabial and posteriorly by large, left and right trapezoidal postmentals which contact medially for 50% of their length posterior to mental; one row of slightly enlarged, elongate sub-labials extending posteriorly to 7th infralabials for both side; and gular and throat scales small, granular, grading posteriorly into larger, smooth, flat, imbricate, pectoral and ventral scales.

Body slender, relatively short (AG/SVL 0.41), with poorly-defined ventrolateral folds posteriorly; dorsal scales small, homogenous, granular, interspersed with relatively large, conical, semi-regularly arranged, slightly prominent trihedral keeled tubercles; tubercles extending from occipital region onto base of tail but end at regenerated tail, smaller at the anterior portion of body and increasing in size posteriorly; tubercles on occiput, nape and upper body at the level above shoulder smaller, subconical; mid-dorsally, on the posterior section of the body and tail larger, more dense, slightly more prominently keeled, semi-regularly arranged; approximately 21 longitudinal rows of dorsal tubercles between ventrolateral body folds at midbody; 32 paravertebral tubercles; 44 longitudinal rows of flat, imbricate smooth ventral scales between ventrolateral body fold much larger than dorsal scales; one row of 16L/15R enlarged femoral scales continuous with enlarged precloacal scales, enlarged femoral scales extending along 2/3 of the femora; proximal femoral scales < 1/2 size of distal femoral scales; femoral pores absent; seven enlarged, pore-bearing precloacal scales, smooth, approximately twice the size of femoral scales; precloacal groove or depression absent; three rows of enlarged post-precloacal scales.

Forelimbs rather slender, relatively short (FL/SVL 0.14); granular scales on forearm slightly larger than those on body, interspersed with enlarged, subconical smooth tubercles; dorsal scales of wrist and palm slightly rounded, flat, smooth, imbricate, slightly raise; ventral scales of palm flat, weakly rounded, smaller than those on body, slightly raised; 18L/18R total subdigital lamellae on 4th finger; 7L/7R proximal subdigital lamellae rectangular with rounded, wide, transversely expanded proximal to joint inflection on 4th finger, 11L/11R unmodified lamellae distal to inflection, gradually more expanded near the claw; digits narrower distal to inflections; interdigital pocketing absent on the forefeet; claws well-developed, relatively short, claw base sheathed by a dorsal and ventral scales; hindlimbs more robust than forelimbs, moderate in length (TBL/SVL 0.17); dorsal scales slightly rounded, granular, subconical, interspersed with enlarged subconical, smooth tubercles, and anteriorly by flat, slightly larger scales; ventral scales of femora flat, imbricate, smooth, larger than dorsals; ventral scales of tibia and subtibia flat, smooth, imbricate; 20L/20R total subdigital lamellae on 4th toe, 8L/8R proximal subdigital lamellae, rectangular with rounded, wide, transversely expanded proximal to joint inflection on 4th toe, 12L/12R unmodified lamellae distal to inflection, gradually more expanded near the claw; digits narrower distal to inflections; interdigital pocketing absent on the hindfeet; claws well-developed, short, claw base sheathed by a dorsal and ventral scales.

Tail regenerated, 100.5 mm in length, longer than SVL (TL/SVL 1.21), moderate in proportions, cylindrical, segmented, wide anteriorly, 7.7 mm in width at the base, tapering to a point, becoming slender toward the tip; dorsal scales of

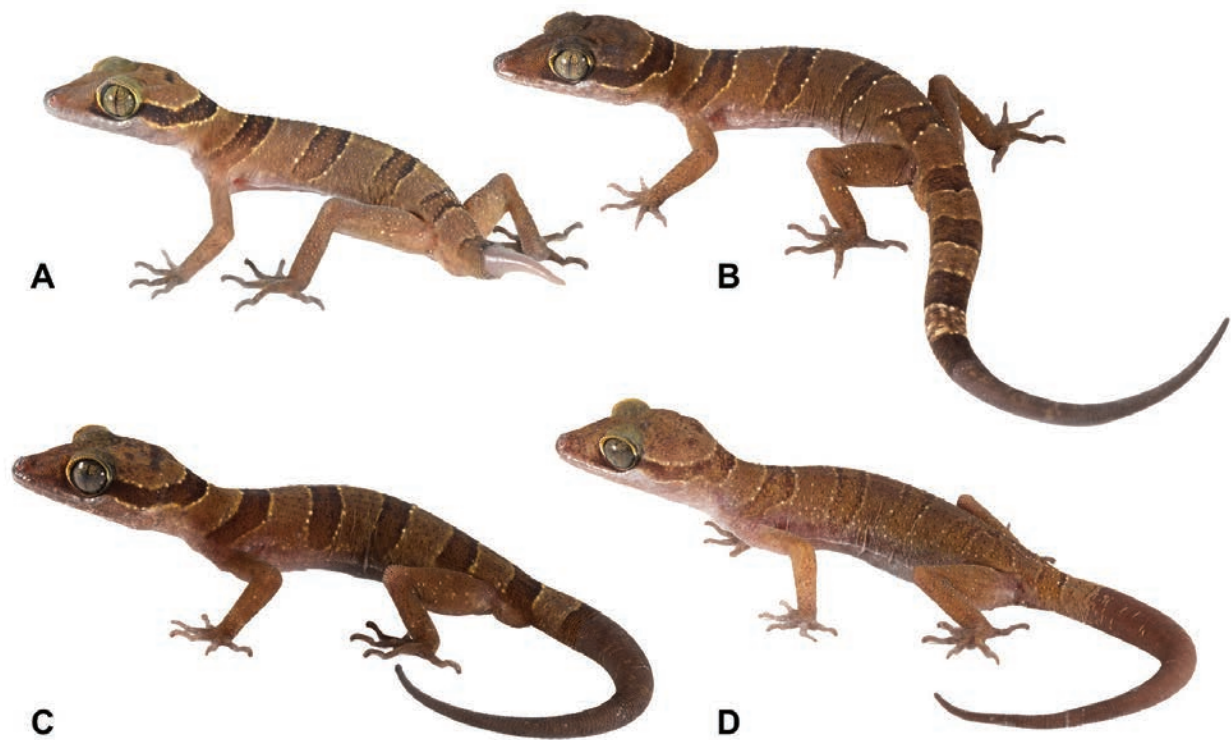


Figure 5. Variation in color pattern of *Cyrtodactylus khlonghatensis* sp. nov. Tham Phet Pho Thong, Khlong Hat Subdistrict, Khlong Hat District, Sa Kaeo Province, Thailand, in life **A** adult male paratype (ZMKU R 01067) **B** adult male holotype (ZMKU R 01068) **C** adult male paratype (ZMKU R 01069), and **D** adult female paratype (ZMKU R 01070).

the original portion of tail small, flat, squared; dorsal scales of tail base granular, rounded, regenerated portion covered by small, smooth subcircular scales, grading posteriorly into larger, flatter; trihedral keeled tubercles forming paravertebral rows on tail base extending to posterior margin of 1/2 of tail; subcaudal scale rows enlarge, smooth; median row of transversely expanded subcaudal scales present, significantly larger than dorsal caudal scales; well-defined narrow ventrolateral subcaudal furrow present; tail base bearing hemipenial swellings; 3L/3R smooth, conical, flat, imbricate postcloacal tubercles on either side of hemipenial swellings; and postcloacal tubercles approximately equal in size.

Coloration of holotype in life. (Figs 4, 5B). Dorsal ground color of head, body, and limbs light-brown; indistinct dark-brown markings on top of head; superciliary scales pale yellow anteriorly and posteriorly; iris brown with dark brown vermiculations; rostral and loreal regions dark brown; rostral, mental, supralabial and infralabial scales creamy-white with scattered dark brown pigment; dark brown nuchal loop with rounded posterior border extends from posterior margin of orbit to posterior margin of the other orbit; nuchal loop edged with thin, pale lines and creamy white tubercles; four similar dark brown body bands, edged in creamy white tubercles with slightly paler centers occur between limb insertion; first body band terminates at shoulders near anterior margin of forelimb insertion; second and third body bands terminate at dorsal to ventrolateral fold on flanks; fourth body band terminates at anterior margin of hindlimb insertion; limbs lighter brown; dorsal portion of forelimbs bearing scattered dark brown markings; dorsal portion of hindlimbs bearing pale yellow spots; four wide dark brown caudal bands encircling the original tail edged in creamy white

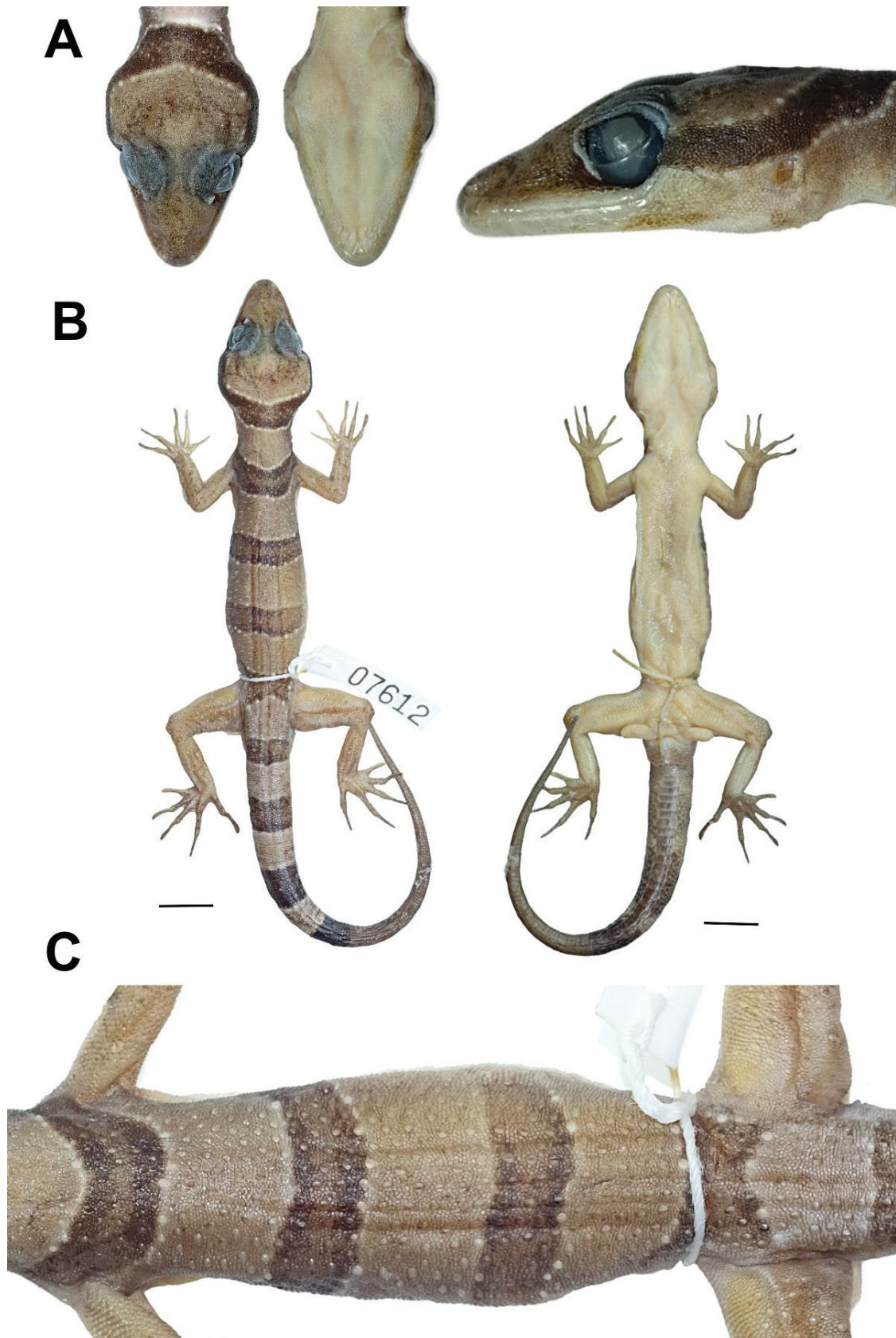


Figure 6. Adult male holotype of *Cyrtodactylus khlonghatensis* sp. nov. (ZMKU R 01068; field number AA 07612) from Tham Phet Pho Thong, Khlong Hat Subdistrict, Khlong Hat District, Sa Kaeo Province, Thailand, in preservation **A** head dimensions showing dorsal, ventral, and lateral views **B** dorsal and ventral views **C** dorsal view of trunk. Scale bars in dorsal and ventral views: 10 mm.

tubercles; three wide pale caudal bands brown encircling tail; regenerated tail, uniformly brown with small, scattered creamy white markings dorsally; regenerated tail extending from posterior margin of 4th dark caudal band.

Ventral surfaces of head, body, and limbs dull white to beige, stippled; ventral surfaces of fingers and toes with dark pigmentation; subdigital lamellae on fingers and toes off-white; palmar surface dark brown; hemipenial swelling dark brown with scattered pale yellow; subcaudal region darkened with fine mottling anteriorly.

Coloration in preservative. (Fig. 6). Overall color pattern of head, body, limbs, flanks, and tail remains similar to that observed in life; dorsal ground color became pale brown in hue; all creamy white tubercles and scales on both dorsal and ventral surfaces faded to an off-white; dark body bands and dark caudal bands appear lighter than observed in life; entire ventral surfaces changed to greyish white with small, refined dark mottling; regenerated tail turned pale brown.

Variation. All paratypes closely resemble the holotype in coloration (Fig. 5). Morphometric, meristic and color pattern characters of the type series of *C. khlonghatensis* sp. nov. are presented in Tables 2, 3. ZMKU R 01067 (adult male), ZMKU R 01069 (adult male), ZMKU R 01070 (adult female), ZMKU R 01071 (subadult female), and ZMKU R 01072 (subadult male) bear dark brown blotches on the top of the head. The adult female (ZMKU R 01070) exhibits a pale-colored nuchal loop, body, and caudal bands edged with creamy white tubercles. All paratypes have regenerated tails, except for two subadult specimens (ZMKU R 01071–01072), which retain their original tails with a caudal band encircling the tail edge. Posterior portion of tail in juveniles (not collected) white.

Distribution. *Cyrtodactylus khlonghatensis* sp. nov. is currently known from only two localities: (1) Tham Phet Pho Thong (type locality) in Khlong Hat District, Sa Kaeo Province, Thailand; and (2) Tham Nam Khao Phra Siwa, Khlong

Table 2. Descriptive measurements of the type series (adult) of *Cyrtodactylus khlonghatensis* sp. nov. in millimeters. Abbreviations are defined in Materials and methods. Key: *n* = number.

Characters	Holotype male	Holotype and paratypes males		Paratype females
	<i>n</i> = 1	<i>n</i> = 3		<i>n</i> = 1
		Min–Max	Mean ± SD	
SVL	82.8	76.5–82.8	80.5 ± 3.5	88.5
AG	33.8	33.7–33.9	33.8 ± 0.1	38.4
ED	5.2	5.1–5.3	5.2 ± 0.1	5.7
EE	7.1	6.9–7.2	7.1 ± 0.1	7.4
EL	1.7	1.6–1.8	1.7 ± 0.1	1.7
EN	7.7	7.4–7.9	7.7 ± 0.2	7.7
ES	9.8	9.6–9.9	9.7 ± 0.2	9.5
FL	11.7	11.6–11.7	11.7 ± 0.1	12.0
HD	9.0	8.3–9.0	8.8 ± 0.4	9.2
HL	24.7	23.4–24.7	24.1 ± 0.6	25.4
HW	15.9	15.2–15.9	15.6 ± 0.4	16.1
IN	2.4	2.2–2.4	2.3 ± 0.1	2.2
IO	3.5	3.2–3.5	3.4 ± 0.2	3.2
TBL	14.1	13.9–14.2	14.1 ± 0.2	14.4
TL (original)	–	–	–	–
TL (regenerated)	100.5	20.8–100.5	69.2 ± 42.6	86.5
TW	7.7	7.2–7.7	7.4 ± 0.2	7.4

Table 3. Morphological data for the type series of *Cyrtodactylus khlonghatensis* sp. nov. Abbreviations are defined in Materials and methods. Key: re = regenerated tail; L = left; R = right; NA = not applicable.

Characters	ZMKU R 01068	ZMKU R 01067	ZMKU R 01069	ZMKU R 01070	ZMKU R 01071	ZMKU R 01072
Type	Holotype	Paratype	Paratype	Paratype	Paratype	Paratype
Sex	Male	Male	Male	Female	Subadult-female	Subadult-male
SVL	82.8	76.5	82.2	88.5	65.9	64.2
TL	100.5re	20.8re	86.3re	86.5re	85.5	80.1
TW	7.7	7.2	7.3	7.4	5.2	6.1
FL	11.7	11.6	11.6	12.0	9.3	9.4
TBL	14.1	13.9	14.2	14.4	10.4	10.9
AG	33.8	33.7	33.9	38.4	27.3	29.0
HL	24.7	23.4	24.2	25.4	19.2	18.9
HW	15.9	15.2	15.8	16.1	11.9	12.7
HD	9.0	8.3	8.9	9.2	6.9	7.1
ED	5.2	5.1	5.3	5.7	3.9	4.2
EE	7.1	6.9	7.2	7.4	5.8	5.6
ES	9.8	9.6	9.9	9.5	7.5	7.4
EN	7.7	7.4	7.9	7.7	5.7	5.5
EL	1.7	1.6	1.8	1.7	1.4	1.1
IN	2.4	2.2	2.3	2.2	1.9	1.9
IO	3.5	3.2	3.4	3.2	2.7	2.7
supralabials	8L/8R	8L/8R	8L/8R	8L/8R	8L/8R	8L/8R
infralabials	9L/9R	9L/9R	9L/9R	9L/9R	9L/9R	9L/9R
paravertebral tubercles	32	31	31	30	30	31
longitudinal rows of tubercles	21	21	20	21	20	20
ventral scales	44	44	44	43	43	43
expanded subdigital lamellae on 4 th toe	8	8	7	8	8	8
unmodified subdigital lamellae on 4 th toe	12	12	12	12	12	12
total subdigital lamellae on 4 th toe	20	20	19	20	20	20
sum of enlarged femoral scales	31 (16L/15R)	32 (16L/16R)	32 (16L/16R)	32 (16L/16R)	32 (16L/16R)	32 (16L/16R)
precloacal scales	7	6	8	8	8	7
precloacal pores	7	6	8	7 pits	8 pits	7
post-precloacal scales rows	3	4	3	4	4	3
postcloacal tubercles	3L/3R	2L/2R	3L/3R	2L/2R	1L/1R	2L/3R
body bands	4	4	4	4	4	4
femoral and precloacal scales continuous (yes or no)	yes	yes	yes	yes	yes	yes
proximal femoral scales < 1/2 size of distal femorals	yes	yes	yes	yes	yes	yes
pocketing between digits of hindfeet	no	no	no	no	no	no
pocketing between digits of forefeet	no	no	no	no	no	no
dark pigmented blotches on top of the head	no	yes	yes	yes	yes	yes
posterior border of the nuchal loop rounded or pointed	rounded	rounded	rounded	rounded	rounded	rounded
no. of dark caudal bands	NA	NA	NA	NA	10	10
no. of light caudal bands	NA	NA	NA	NA	9	9
dark caudal bands wider than light caudal bands	NA	NA	NA	NA	yes	yes

Kai Thuean Subdistrict, Khlong Hat District, Sa Kaeo Province, Thailand, approximately 10 km from the type locality.

Natural history. The type locality is an isolated karstic formation mountain surrounded by karstic outcrops in dry deciduous forest at an elevation of 246 m. The type series of *C. khlonghatensis* sp. nov. was found during both day (1400–1530 h) and night (1900–2000 h) in various microhabitats of the Tham Phet Pho Thong karstic area (Fig. 7), including karstic boulders, karstic wall, cracks, and crevices; shrubs; vines and other vegetations. The male holotype was found at night (1950 h), perched on a dry vine near a karstic wall, approximately 20 cm above the ground. The male paratype (ZMKU R 01067) was found during the day on a karstic wall in a cave, approximately 5 m from the entrance, with air temperatures of 26.3 °C and a relative humidity of 93.3%. Another male paratype (ZMKU R 01069) was found at night on a karstic wall in a cave. The female paratype (ZMKU R 01070) was found perched on a dry log along a trail in a karstic habitat. A subadult male (ZMKU R 01071) was found perched upside down on a shrub, approximately 50 cm above ground level. At Tham Nam Khao Phra Siwa, a subadult female (ZMKU R 01072) was found on crevices of a karstic wall near a cave entrance, approximately 50 cm

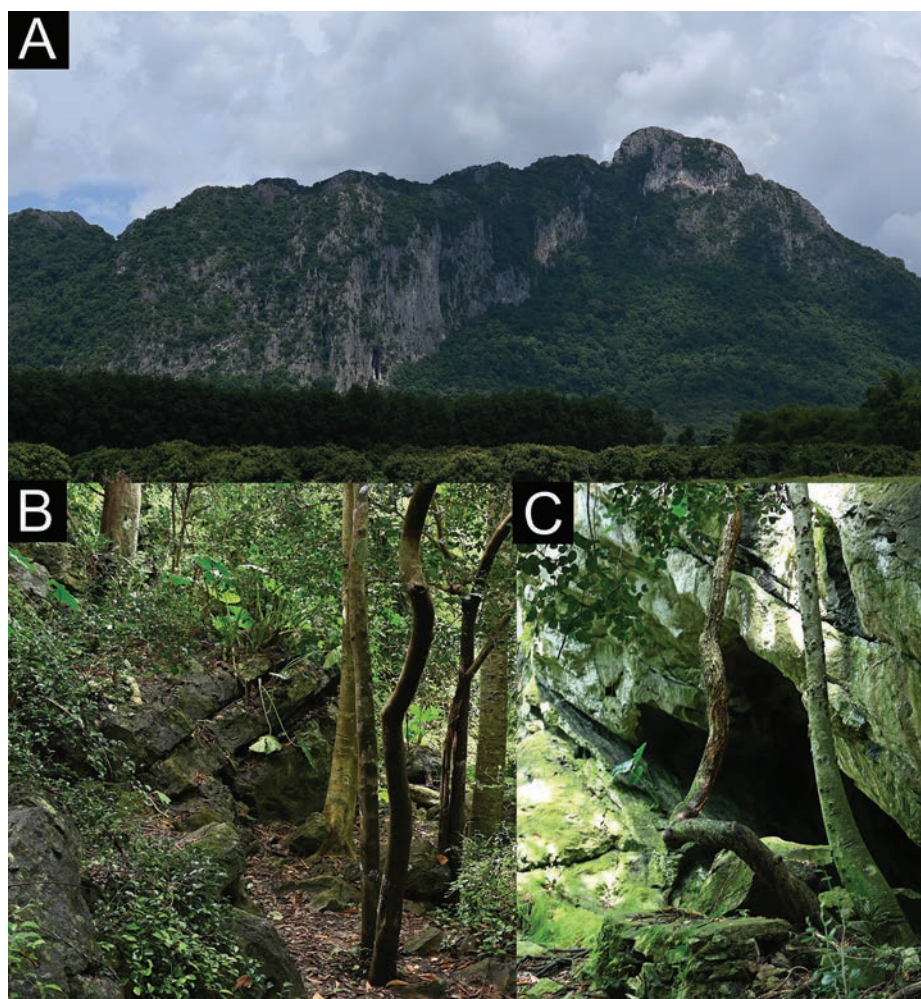


Figure 7. Habitats of *Cyrtodactylus khlonghatensis* sp. nov. at the type locality of Tham Phet Pho Thong, Khlong Hat Subdistrict, Khlong Hat District, Sa Kaeo Province, Thailand **A** the isolated karstic mountain surrounded by karstic outcrops with dry deciduous forest **B** karstic trail **C** karst boulders.

above the ground. *Cyrtodactylus khlonghatensis* sp. nov. is likely a nocturnal species that inhabits karstic environments. During the day, individuals were found to be inactive in shaded areas with cracks, while at night, they were active both on the karstic terrain and in vegetation. In this survey, the smaller nocturnal gekkonid *Gehyra mutilata* (Wiegmann, 1834) was found in sympatry on karstic boulders, karstic outcrops and vegetations such as tree trunks and dry shrubs.

Comparisons. (Suppl. materials 3, 4). *Cyrtodactylus khlonghatensis* sp. nov. is differentiated from 13 recognized species of the *intermedius* group by having a unique combination of morphological characteristics and uncorrected pairwise sequence divergences of mtDNA (ND2) of 4.73–22.55%.

Cyrtodactylus khlonghatensis sp. nov. is distinguished from *C. auralensis* by having a larger maximum SVL of 88.5 mm (vs 84.3 mm); 20 or 21 longitudinal rows of body tubercles (vs 17 or 18 rows); and 31 or 32 total number of enlarged femoral scales (vs 23–28 scales).

Cyrtodactylus khlonghatensis sp. nov. is distinguished from *C. bokorensis* by having a smaller maximum SVL of 88.5 mm (vs 93.0 mm); 31 or 32 total number of enlarged femoral scales (vs 26–30 scales); and posterior border of the nuchal loop rounded (vs pointed).

Cyrtodactylus khlonghatensis sp. nov. is distinguished from *C. cardamomensis* by having a larger maximum SVL of 88.5 mm (vs 84.1 mm); 7 or 8 expanded subdigital lamellae proximal to the digital inflection on the 4th toe (vs 5 or 6 lamellae); 31 or 32 total number of enlarged femoral scales (vs 23–28 scales); 6–8 precloacal pores (vs 9 or 10 pores); proximal femoral scales < 1/2 size of distal femoral scales present (vs absent); and dark pigmented blotches on top of the head varies (vs absent).

Cyrtodactylus khlonghatensis sp. nov. is distinguished from *C. disjunctus* by having a larger maximum SVL of 88.5 mm (vs 66.7 mm); 8 supralabial scales (vs 12 scales); 9 infralabial scales (vs 11 scales); 30–32 paravertebral tubercles between limb insertions (vs 41 tubercles); 20 or 21 longitudinal rows of body tubercles (vs 11 rows); 43 or 44 longitudinal rows of ventral scales (vs 36 rows); 12 unmodified subdigital lamellae distal to the digital inflection on the 4th toe (vs 9 lamellae); 19 or 20 total number of subdigital lamellae beneath the 4th toe (vs 17 lamellae); 31 or 32 total number of enlarged femoral scales (vs 21 scales); 6–8 precloacal scales (vs 10 scales); 6–8 precloacal pores (vs 9 pits); 3 or 4 rows of post-precloacal scales (vs 1 row); enlarged femoral and precloacal scales continuous (vs discontinuous); 4 body bands (vs 3 bands); and dark pigmented blotches on top of the head varies (vs absent).

Cyrtodactylus khlonghatensis sp. nov. is distinguished from *C. hontreensis* by having 8 supralabial scales (vs 11–13 scales); 30–32 paravertebral tubercles between limb insertions (vs 20–24 tubercles); 20 or 21 longitudinal rows of body tubercles (vs 14 rows); 43 or 44 longitudinal rows of ventral scales (vs 40–42 rows); 31 or 32 total number of enlarged femoral scales (vs 4–9 scales); enlarged femoral and precloacal scales continuous (vs discontinuous); and 4 body bands (vs 3 bands).

Cyrtodactylus khlonghatensis sp. nov. is distinguished from *C. intermedius* by having 31 or 32 total number of enlarged femoral scales (vs 23–26 scales); and dark pigmented blotches on top of the head varies (vs absent).

Cyrtodactylus khlonghatensis sp. nov. is distinguished from *C. kohrongensis* by having a larger maximum SVL of 88.5 mm (vs 76.1 mm); 43 or 44 longitudinal

rows of ventral scales (vs 38–42 rows); 31 or 32 total number of enlarged femoral scales (vs 14–26 scales); enlarged femoral and precloacal scales continuous (vs discontinuous); and dark pigmented blotches on top of the head varies (vs absent).

Cyrtodactylus khlonghatensis sp. nov. is distinguished from *C. kulenensis* by having 30–32 paravertebral tubercles between limb insertions (vs 33–38 tubercles); 20 or 21 longitudinal rows of body tubercles (vs 17–19 rows); 31 or 32 total number of enlarged femoral scales (vs 10–21 scales); 6–8 precloacal scales (vs 9 or 10 scales); and dark pigmented blotches on top of the head varies (vs absent).

Cyrtodactylus khlonghatensis sp. nov. is distinguished from *C. laangensis* by having a larger maximum SVL of 88.5 mm (vs 82.2 mm); 9 infralabial scales (vs 10–11 scales); 20 or 21 longitudinal rows of body tubercles (vs 17 or 18 rows); 43 or 44 longitudinal rows of ventral scales (vs 37–40 rows); and 31 or 32 total number of enlarged femoral scales (vs 0–16 scales).

Cyrtodactylus khlonghatensis sp. nov. is distinguished from *C. phuquocensis* by having a larger maximum SVL of 88.5 mm (vs 85.8 mm); 8 supralabial scales (vs 9–13 scales); 20 or 21 longitudinal rows of body tubercles (vs 16–18 rows); 7 or 8 expanded subdigital lamellae proximal to the digital inflection on the 4th toe (vs 5 or 6 lamellae); 31 or 32 total number of enlarged femoral scales (vs 21–28 scales); and dark pigmented blotches on top of the head varies (vs absent).

Cyrtodactylus khlonghatensis sp. nov. is distinguished from *C. regicavernicolus* by having a larger maximum SVL of 88.5 mm (vs 80.7 mm); 20 or 21 longitudinal rows of body tubercles (vs 15–18 rows); 31 or 32 total number of enlarged femoral scales (vs 8–23 scales); and enlarged femoral and precloacal scales continuous (vs discontinuous).

Cyrtodactylus khlonghatensis sp. nov. is distinguished from *C. septimontium* by having a smaller maximum SVL of 88.5 mm (vs 90.4 mm); 20 or 21 longitudinal rows of body tubercles (vs 16–19 rows); 43 or 44 longitudinal rows of ventral scales (vs 38–42 rows); and 31 or 32 total number of enlarged femoral scales (vs 24–28 scales)

Cyrtodactylus khlonghatensis sp. nov. is distinguished from *C. thylacodactylus* by having a larger maximum SVL of 88.5 mm (vs 74.6 mm); 8 supralabial scales (vs 7 scales); 43 or 44 longitudinal rows of ventral scales (vs 36–42 rows); 7 or 8 expanded subdigital lamellae proximal to the digital inflection on the 4th toe (vs 5 or 6 lamellae); 19 or 20 total number of subdigital lamellae beneath the 4th toe (vs 15–18 lamellae); 31 or 32 total number of enlarged femoral scales (vs 17–22 scales); proximal femoral scales < 1/2 size of distal femoral scales present (vs absent); interdigital pocketing between digits of forefeet and hindfeet absent (vs present); and dark pigmented blotches on top of the head varies (vs absent).

Etymology. The specific epithet *khlonghatensis* is named after the type locality of Khlong Hat Subdistrict, Khlong Hat District, Sa Kaeo Province, Thailand.

Discussion

In recent decades, there has been a notable increase in research focusing on the taxonomy and systematics of *Cyrtodactylus*, especially in Southeast Asia (Welton et al. 2010; Johnson et al. 2012; Oliver et al. 2014; Grismer et al. 2020a, 2021a, 2021b, 2022, 2023a, 2023b; Chan et al. 2023; Ngo et al. 2022; Termprayoon et al. 2023; Uetz et al. 2024). Grismer et al. (2015) first noted that *C. intermedius* represented a species complex with ecomorphologically diverse characteristics.

An integrative taxonomic approach, combining morphological, molecular data, and ecology, has played a crucial role in unveiling the hidden diversity within the *intermedius* group (Murdoch et al. 2019; Grismer et al. 2020a, 2021b, 2023a).

The discovery of *Cyrtodactylus khlonghatensis* sp. nov. further highlights the remarkable endemism of gekkonids in the isolated hilly karstic regions of the Indo-Burma Hotspot (e.g., Grismer et al. 2014, 2018b; Murdoch et al. 2019; Rujirawan et al. 2019; Nguyen et al. 2020; Luu et al. 2023), while also demonstrating the adaptability of habitat preferences within the *C. intermedius* group. The discovery of this new species increases the total number of species in the *C. intermedius* group to 14, of which three occur in Thailand. These findings also suggest that additional members of the *C. intermedius* group may exist in Thailand, where vast unexplored karst landscapes remain. Further surveys are warranted to delineate the geographic distribution of *C. intermedius* in eastern and northeastern Thailand.

This study provides the first genetic data for *C. intermedius* from its type locality at Khao Sebab (= Namtok Phlio National Park, Mueang Chanthaburi District), Chanthaburi Province. We identified an error in the reported sampling locality of *C. intermedius* (LSUHC 9513) that was incorrectly listed as “Khao Soi Dao, Chanthaburi, Thailand” (see Murdoch et al. 2019: table 1), rectified here to the sampling locality of “Khao Khitchakut, Chanthaburi Province, Thailand” (Suppl. material 1). Our results support the hypotheses of Murdoch et al. (2019) that *C. intermedius* from Khao Khitchakut, located 30 km north of the type locality, is conspecific with true *C. intermedius*. This confirmation is also based on morphological comparisons between syntypes (UMMZ 78687, MCZ R 39040, and FMNH 215981; see Murdoch et al. 2019), the newly collected topotypic specimens from this study (ZMKU R 01037–01038 and ZMKU R 01044–01045), and the Khao Khitchakut population (LSUHC 9513; see Murdoch et al. 2019). The phylogenetic position of *C. intermedius* from the type locality was recovered as the sister species to a clade composed of three species: *C. khlonghatensis* sp. nov. from Khlong Hat District, Sa Kaeo Province, *Cyrtodactylus* sp. from Sakaerat Biosphere Reserve, Wang Nam Khiao District, Nakhon Ratchasima Province, and *C. kulenensis* from Phnom Kulen National Park, Phnom Kbal, Benteay Srei District, Siem Reap Province, Cambodia. The eastern-southern division of the *C. intermedius* group shown here is concordant with previous studies (Murdoch et al. 2019; Grismer et al. 2015, 2020a, 2021b, 2023a).

Thailand’s complex geological history is evident in the abundance of limestone and granite formations found in the eastern and northeastern regions (Day and Urich 2000; Morley et al. 2011). These karstic regions and granitic outcrops are revealing a rich diversity of reptiles, particularly species with limited ranges (Bauer and Das 1998; Bauer et al. 2002; Wood et al. 2010; Murdoch et al. 2019; Vogel and Patrick 2019; Grismer et al. 2019). To enhance our understanding of the taxonomy, ecology, distribution, biogeography, and conservation of *C. intermedius* group in eastern and northeastern Thailand, further research and additional field surveys in unexplored regions are imperative.

Acknowledgments

Department of National Parks, Wildlife and Plant Conservation, Thailand provided permission to conduct the research in Namtok Phlio National Park. Tawat Jenkarn (superintendent of Namtok Phlio National Park) and the Namtok Phlio

National Park's staffs for facilitating the fieldwork. Taksin Artchawakom (Sakaerat Environmental Research Station) for scientific support. We thank L. Lee Grismer, Jesse L. Grismer, Evan S.H. Quah, and Mohd Abdul Muin for their valuable suggestions, which greatly improved the manuscript.

Additional information

Conflict of interest

The authors have declared that no competing interests exist.

Ethical statement

This research was approved by the Institutional Animal Care and Use Committee of Srinakharinwirot University (permit no. COA/ AE-015-2565).

Funding

This work was financially supported by Office of the Permanent Secretary, Ministry of Higher Education, Science, Research and Innovation (Grant No. RGNS 65-191).

Author contributions

Conceptualization, Aowphol A., Ampai N., Rujirawan, A.; Methodology and Investigation, Ampai N., Rujirawan A., Aowphol A., Yodthong S., Termprayoon, T., Stuart B.L.; Writing original draft, Ampai N., Rujirawan, A., Aowphol A.; Editing, Ampai N., Rujirawan A., Aowphol A., Yodthong S., Termprayoon, T., Stuart, B.L.; Supervision, Aowphol A., Rujirawan, R.

Author ORCIDs

Natee Ampai  <https://orcid.org/0000-0001-8562-299X>

Attapol Rujirawan  <https://orcid.org/0000-0001-9179-6910>

Siriporn Yodthong  <https://orcid.org/0000-0001-6577-5358>

Korkhwan Termprayoon  <https://orcid.org/0000-0003-1903-3040>

Bryan L. Stuart  <https://orcid.org/0000-0003-4719-1951>

Anchalee Aowphol  <https://orcid.org/0000-0001-9504-4601>

Data availability

All of the data that support the findings of this study are available in the main text or Supplementary Information.

References

- Agarwal I, Mahony S, Giri VB, Chaitanya R, Bauer AM (2018) Six new *Cyrtodactylus* (Squamata: Gekkonidae) from northeast India. *Zootaxa* 4524(5): 501–535. <https://doi.org/10.11646/zootaxa.4524.5.1>
- American Veterinary Medical Association (2020) AVMA guidelines for the euthanasia of animals: 2020 edition. <https://www.avma.org/sites/default/files/2020-02/Guidelines-on-Euthanasia-2020.pdf> [Accessed 16 July 2024]
- Bauer AM, Das I (1998) A new *Cnemaspis* (Reptilia: Gekkonidae) from Southeastern Thailand. *Copeia*: 439–444. <https://doi.org/10.2307/1447438>
- Bauer AM, Pauwels OSG, Chanhom L (2002) A new species of cave-dwelling *Cyrtodactylus* (Squamata: Gekkonidae) from Thailand. *Tropical Natural History* 2(2): 19–29.

- Cangelosi R, Goriely A (2007) Component retention in principal component analysis with application to cDNA microarray data. *Biology direct* 2: 2. <https://doi.org/10.1186/1745-6150-2-2>
- Chan KO, Grismer LL (2021) A standardized and statistically defensible framework for quantitative morphological analyses in taxonomic studies. *Zootaxa* 5023(2): 293–300. <https://doi.org/10.11646/zootaxa.5023.2.9>
- Chan KO, Grismer LL, Santana F, Pinto P, Loke FW, Conaboy N (2023) Scratching the surface: a new species of Bent-toed gecko (Squamata, Gekkonidae, *Cyrtodactylus*) from Timor-Leste of the *darmandvillei* group marks the potential for future discoveries. *ZooKeys* 1139: 107–126. <https://doi.org/10.3897/zookeys.1139.96508>
- Chhin S, Neang T, Chan S, Kong K, Ou R, Samorn V, Sor R, Lou V, Sin S, Chhim M, Stuart BL, Grismer LL (2024) A new species in the *Cyrtodactylus intermedius* (Squamata: Gekkonidae) group from an isolated limestone karst formation in southwestern Cambodia. *Zootaxa* 5474(1): 1–20. <https://doi.org/10.11646/zootaxa.5474.1.1>
- Chomdej S, Pradit W, Pawangkhanant P, Kuensaen C, Phupanbai A, Naiduangchan M, Piboon P, Nganvongpanit K, Yuan Z, Zhang Y, Che J, Sucharitakul P, Suwannapoom C (2022) A new *Cyrtodactylus* species (Reptilia: Gekkonidae) from Nan Province, Northern Thailand. *Asian Herpetological Research* 13(2): 96–108. <https://doi.org/10.16373/j.cnki.ahr.210055>
- Conroy CJ, Papenfuss T, Parker J, Hahn N (2009) Use of tricaine methanesulfonate (MS-222) for euthanasia of reptiles. *Journal of the American Association for Laboratory Animal Science* 48: 28–32.
- Day M, Urich P (2000). An assessment of protected karst landscapes in Southeast Asia. *Cave and Karst Science* 27: 61–70.
- Geissler P, Hartmann T, Ihlow F, Neang T, Seng R, Wagner P, Böhme W (2019) Herpetofauna of the Phnom Kulen National Park, northern Cambodia – an annotated checklist. *Cambodian Journal of Natural History* 2019(1): 40–63.
- Grismer LL, Wood Jr PL, Shahrul A, Awal R, Norhayati A, Muin M, Sumontha M, Grismer J, Chan K, Quah ESH, Pauwels OSG (2014) Systematics and natural history of Southeast Asian Rock Geckos (genus *Cnemaspis* Strauch, 1887) with descriptions of eight new species from Malaysia, Thailand, and Indonesia. *Zootaxa* 3880(1): 1–147. <https://doi.org/10.11646/zootaxa.3880.1.1>
- Grismer LL, Wood Jr PL, Ngo VT, Murdoch ML (2015) The systematics and independent evolution of cave ecomorphology in distantly related clades of Bent-toed Geckos (Genus *Cyrtodactylus* Gray, 1827) from the Mekong Delta and islands in the Gulf of Thailand. *Zootaxa*, 3980(1): 106–126. <https://doi.org/10.11646/zootaxa.3980.1.6>
- Grismer LL, Wood Jr PL, Quah ESH, Murdoch ML, Grismer MS, Herr MW, Espinoza RE, Brown RM, Lin A (2018a) A phylogenetic taxonomy of the *Cyrtodactylus peguensis* group (Reptilia: Squamata: Gekkonidae) with descriptions of two new species from Myanmar. *PeerJ* 6: e5575. <https://doi.org/10.7717/peerj.5575>
- Grismer LL, Wood Jr PL, Thura MK, Zin T, Quah ESH, Murdoch ML, Grismer MS, Lin A, Kyaw H, Lwin N (2018b) Twelve new species of *Cyrtodactylus* Gray (Squamata: Gekkonidae) from isolated limestone habitats in east-central and southern Myanmar demonstrate high localized diversity and unprecedented microendemism. *Zoological Journal of the Linnean Society* 182(4): 862–959. <https://doi.org/10.1093/zoolinnean/zlx057>
- Grismer LL, Wood Jr PL, Quah ESH, Anuar S, Poyarkov NA, Thy N, Orlov NL, Thammachoti P, Seiha H (2019). Integrative taxonomy of the Asian skinks *Sphenomorphus stellatus* (Boulenger, 1900) and *S. praesignis* (Boulenger, 1900) with the resurrection of *S. annamiticus*

- (Boettger, 1901) and the description of a new species from Cambodia. *Zootaxa* 4683(3): zootaxa.4683.3.4. <https://doi.org/10.11646/zootaxa.4683.3.4>
- Grismer LL, Chan KO, Oaks JR, Neang T, Sokun L, Murdoch ML, Stuart BLS, Grismer JL (2020a) A new insular species of the *Cyrtodactylus intermedius* (Squamata: Gekkonidae) group from Cambodia with a discussion of habitat preference and ecomorphology. *Zootaxa* 4830(1): 75–102. <https://doi.org/10.11646/zootaxa.4830.1.3>
- Grismer LL, Wood Jr PL, Le MD, Quah ES, Grismer JL (2020b) Evolution of habitat preference in 243 species of Bent-toed geckos (Genus *Cyrtodactylus* Gray, 1827) with a discussion of karst habitat conservation. *Ecology and Evolution* 10(24): 13717–13730. <https://doi.org/10.1002/ece3.6961>
- Grismer LL, Wood Jr PL, Poyarkov NA, Le MD, Kraus F, Agarwal I, Oliver PM, Nguyen SN, Nguyen TQ, Karunarathna S, Welton LJ, Stuart BL, Luu VQ, Bauer AM, O’Connell KA, Quah ESH, Chan KO, Ziegler T, Ngo H, Nazarov RA, Aowphol A, Chomdej S, Suwannapoom C, Siler CD, Anuar S, Tri NV, Grismer JL (2021a) Phylogenetic partitioning of the third-largest vertebrate genus in the world, *Cyrtodactylus* Gray, 1827 (Reptilia; Squamata; Gekkonidae) and its relevance to taxonomy and conservation. *Vertebrate Zoology* 71: 101–154. <https://doi.org/10.3897/vertebrate-zoology.71.e59307>
- Grismer LL, Geissler P, Neang T, Hartmann T, Wagner P, Poyarkov, NA (2021b) Molecular phylogenetics, PCA, and MFA recover a new species of *Cyrtodactylus* (Squamata: Gekkonidae) from an isolated sandstone massif in northwestern Cambodia. *Zootaxa* 4949(2): 261–288. <https://doi.org/10.11646/zootaxa.4949.2.3>
- Grismer LL, Aowphol A, Yodthong S, Ampai N, Termprayoon K, Aksornneam A, Rujirawan A (2022) Integrative taxonomy delimits and diagnoses cryptic arboreal species of the *Cyrtodactylus brevipalmatus* group (Squamata, Gekkonidae) with descriptions of four new species from Thailand. *ZooKeys* 1129: 109–162. <https://doi.org/10.3897/zookeys.1129.90535>
- Grismer LL, Pawangkhanant P, Idiitullina SS, Trofimets AV, Nazarov RA, Suwannapoom C, Poyarkov NA (2023a) A new species of *Cyrtodactylus* Gray, 1827 (Squamata: Gekkonidae) from the Thai-Malay Peninsula and the independent evolution of cave ecomorphology on opposite sides of the Gulf of Thailand. *Zootaxa* 5352(1): 109–136. <https://doi.org/10.11646/zootaxa.5352.1.4>
- Grismer LL, Rujirawan A, Chomdej S, Suwannapoom C, Yodthong S, Aksornneam A, Aowphol A (2023b) A new species of the *Cyrtodactylus brevipalmatus* group (Squamata, Gekkonidae) from the uplands of western Thailand. *ZooKeys* 1141: 93–118. <https://doi.org/10.3897/zookeys.1141.97624>
- Hammer Ø, Harper DAT, Ryan PD (2001) PAST: Paleontological Statistics Software Package for Education and Data Analysis. *Palaeontologia Electronica* 4: 1–9.
- Hoang DT, Chernomor O, von Haeseler A, Minh BQ, Vinh LS (2018) UFBoot2: Improving the ultrafast bootstrap approximation. *Molecular Biology and Evolution* 35(2): 518–522. <https://doi.org/10.1093/molbev/msx281>
- Huelsenbeck JP, Ronquist F (2001) MRBAYES: Bayesian inference of phylogenetic trees. *Bioinformatics* 17(8): 754–755. <https://doi.org/10.1093/bioinformatics/17.8.754>
- Johnson CB, Quah ESH, Anuar S, Muin MA, Wood Jr PL, Grismer JL, Onn CK, Ahmad N, Bauer AM, Grismer LL (2012) Phylogeography, geographic variation, and taxonomy of the Bent-toed Gecko *Cyrtodactylus quadrivirgatus* Taylor, 1962 from Peninsular Malaysia with the description of a new swamp dwelling species. *Zootaxa* 3406: 39–58. <https://doi.org/10.11646/zootaxa.3406.1.3>

- Jombart T (2008) ADEGENET: A R package for the multivariate analysis of genetic markers. *Bioinformatics* 24(11): 1403–1405. <https://doi.org/10.1093/bioinformatics/btn129>
- Jombart T, Collins C (2015) A tutorial for discriminant analysis of principal components (DAPC) using adegenet 2.0.0. *Rvignette*: 1–37.
- Jombart T, Devillard S, Balloux F (2010) Discriminant analysis of principal components: A new method for the analysis of genetically structured populations. *BMC Genetics* 11(1): e94. <https://doi.org/10.1186/1471-2156-11-94>
- Kalyaanamoorthy S, Minh BQ, Wong TK, von Haeseler A, Jermini LS (2017) ModelFinder: Fast model selection for accurate phylogenetic estimates. *Nature Methods* 14(6): 587–589. <https://doi.org/10.1038/nmeth.4285>
- Lleonart J, Salat J, Torres GJ (2000) Removing allometric effects of body size in morphological analysis. *Journal of Theoretical Biology* 205(1): 85–93. <https://doi.org/10.1006/jtbi.2000.2043>
- Luu VQ, Bonkowski M, Nguyen TQ, Le MD, Schneider N, Ngo HT, Ziegler T (2016) Evolution in karst massifs: Cryptic diversity among bent-toed geckos along the Truong Son Range with descriptions of three new species and one new country record from Laos. *Zootaxa* 4107(2): 101–140. <https://doi.org/10.11646/zootaxa.4107.2.1>
- Luu VQ, Nguyen TH, Do QH, Pham CT, Hoang TT, Nguyen TQ, Le MD, Ziegler T, Grismer JL, Grismer LL (2023) A new species of *Hemiphyllodactylus* (Squamata, Gekkonidae) from Ha Giang Province, Vietnam. *ZooKeys* 1167: 353–382. <https://doi.org/10.3897/zookeys.1167.103713>
- Macey JR, Larson A, Ananjeva NB, Papenfuss TJ (1997) Evolutionary shifts in three major structural features of the mitochondrial genome among iguanian lizards. *Journal of Molecular Evolution* 44(6): 660–674. <https://doi.org/10.1007/PL00006190>
- Miller MA, Pfeiffer W, Schwartz T (2010) Creating the CIPRES Science Gateway for inference of large phylogenetic trees. 2010 Gateway Computing Environments Workshop (GCE): 1–8. <https://doi.org/10.1109/GCE.2010.5676129>
- Minh Q, Nguyen M, von Haeseler AA (2013) Ultrafast approximation for phylogenetic bootstrap. *Molecular Biology and Evolution* 30(5): 1188–1195. <https://doi.org/10.1093/molbev/mst024>
- Morley CK, Charusiri P, Watkinson IM (2011) Structural geology during the Cenozoic. In: Ridd, MF, Barber AJ, Crow MJ (Eds) *Geology of Thailand*. Geological Society, London: 273–333. <https://doi.org/10.1144/GOTH.11>
- Murdoch ML, Grismer LL, Wood Jr PL, Neang T, Poyarkov NA, Ngo VT, Nazarov RA, Aowphol A, Pauwels OSG, Nguyen HN, Grismer JL (2019) Six new species of the *Cyrtodactylus intermedius* complex (Squamata: Gekkonidae) from the Cardamom Mountains and associated highlands of Southeast Asia. *Zootaxa* 4554(1): 1–62. <https://doi.org/10.11646/zootaxa.4554.1.1>
- NASA LP DAAC (2013) NASA Shuttle Radar Topography Mission (SRTM) Version 3.0 (SRTM Plus) Product Release. Land Process Distributed Active Archive Center, National Aeronautics and Space Administration.
- Neang T, Henson A, Stuart BL (2020) A new species of *Cyrtodactylus* (Squamata, Gekkonidae) from Cambodia's Prey Lang Wildlife Sanctuary. *ZooKeys* 926: 133–158. <https://doi.org/10.3897/zookeys.926.48671>
- Ngo VT, Grismer LL, Grismer JL (2008) A new endemic cave dwelling species of *Cyrtodactylus* Gray, 1827 (Squamata: Gekkonidae) in Kien Giang Biosphere Reserve, southwestern Vietnam. *Zootaxa* 1967: 53–62. <https://doi.org/10.11646/zootaxa.1967.1.3>

- Ngo VT, Grismer LL, Grismer JL (2010) A new species of *Cyrtodactylus* Gray, 1827 (Squamata: Gekkonidae) in Phu Quoc National Park, Kien Giang Biosphere Reserve, Southwestern Vietnam. *Zootaxa* 2604: 37–51. <https://doi.org/10.11646/zootaxa.2604.1.3>
- Ngo HT, Do QH, Pham CT, Luu VQ, Grismer L, Ziegler T, Nguyen VTH, Nguyen TQ, Le MD (2022) How many more species are out there? Current taxonomy substantially underestimates the diversity of bent-toed geckos (Gekkonidae, *Cyrtodactylus*) in Laos and Vietnam. *ZooKeys* 1097: 135–152. <https://doi.org/10.3897/zookeys.1097.78127>
- Nguyen TQ, Do QH, Ngo HT, Pham AV, Pham CT, Le MD, Ziegler T (2020) Two new species of *Hemiphyllodactylus* (Squamata: Gekkonidae) from Hoa Binh Province, Vietnam. *Zootaxa* 4801(3): 513–536. <https://doi.org/10.11646/zootaxa.4801.3.5>
- Nugraha FAD, Ahda Y, Tjong DH, Kurniawan N, Riyanto A, Fauzi MA, Lin SM (2023) Common but ignored: a new species of *Cyrtodactylus* (Chordata, Reptilia, Squamata, Gekkonidae) from lowland Sumatra Barat, Indonesia. *ZooKeys* 1169: 47–64. <https://doi.org/10.3897/zookeys.1169.98681>
- Oliver PM, Richards SJ, Mumpuni, Rösler H (2016) The Knight and the King: two new species of giant bent-toed gecko (*Cyrtodactylus*, Gekkonidae, Squamata) from northern New Guinea, with comments. *ZooKeys* 562: 105–130. <https://doi.org/10.3897/zookeys.562.6052>
- Oliver PM, Tjaturadi B, Mumpuni, Krey K, Richards S (2008) A new species of large *Cyrtodactylus* (Squamata: Gekkonidae) from Melanesia. *Zootaxa* 1894: 59–68. <https://doi.org/10.11646/zootaxa.1894.1.5>
- Oliver PM, Skipwith P, Lee MS (2014) Crossing the line, increasing body size in a trans-Wallacean lizard radiation (*Cyrtodactylus*, Gekkota). *Biology Letters* 10(10): 20140479. <https://doi.org/10.1098/rsbl.2014.0479>
- QGIS Development Team (2024) QGIS Geographic Information System. QGIS Software. <https://www.qgis.org>
- R Core Team (2020) R: A Language and Environment for Statistical Computing. R Foundation for Statistical Computing, Vienna. <https://www.R-project.org>
- Rambaut A (2018) FigTree: tree figure drawing tool (Version 1.4.4). <http://tree.bio.ed.ac.uk/software/figtree>
- Rambaut A, Drummond AJ, Xie D, Baele G, Suchard MA (2018) Posterior summarization in Bayesian phylogenetics using Tracer 1.7. *Systematic Biology* 67(5): 901–904. <https://doi.org/10.1093/sysbio/syy032>
- Riyanto A, Faz FH, Amarasinghe, AAT, Munir M, Fitriana YS, Hamidy A, Kusri MD, Oliver PM (2022) A new bent-toed gecko of the *Cyrtodactylus marmoratus* group (Reptilia: Gekkonidae) from Obi Island, Indonesia. *Herpetologica* 78(1): 30–39. <https://doi.org/10.1655/Herpetologica-D-21-00028.1>
- Ronquist F, Teslenko M, Van Der Mark P, Ayres DL, Darling A, Höhna S, Larget B, Liu L, Suchard MA, Huelsenbeck JP (2012) MrBayes 3.2: Efficient Bayesian phylogenetic inference and model choice across a large model space. *Systematic Biology* 61(3): 539–542. <https://doi.org/10.1093/sysbio/sys029>
- Rujirawan A, Fong JJ, Ampai N, Yodthong S, Termprayoon K, Aowphol A (2019) A new karst-dwelling gecko of the *Gekko petricolus* group (Reptilia: Gekkonidae) from Phitsanulok Province, central Thailand. *Journal of Natural History* 53: 557–576. <https://doi.org/10.1080/00222933.2019.1597937>
- Simmons JE (2015) *Herpetological Collecting and Collections Management*, 3rd ed. Society for the Study of Amphibians and Reptiles Herpetological Circular No. 42. Salt Lake City, UT, 191 pp.

- Smith MA (1917) Descriptions of new reptiles and a new batrachian from Siam. The journal of the Natural History Society of Siam 2: 221–225.
- Smith MA (1935) The fauna of British India, including Ceylon and Burma. Reptiles and Amphibia, Vol. II. Sauria. Taylor and Francis, London, 440 pp.
- Stuart BL, Emmet DA (2006) A Collection of amphibians and reptiles from the Cardamom Mountains, southwestern Cambodia. Zoology 109: 1–17. [https://doi.org/10.3158/0015-0754\(2006\)109\[1:ACOAAR\]2.0.CO;2](https://doi.org/10.3158/0015-0754(2006)109[1:ACOAAR]2.0.CO;2)
- Tamura K, Stecher G, Kumar S (2021) MEGA11: Molecular Evolutionary Genetics Analysis Version 11. Molecular Biology and Evolution 38(7): 3022–3027. <https://doi.org/10.1093/molbev/msab120>
- Taylor EH (1963) The lizards of Thailand. The University of Kansas science bulletin 44: 687–1077.
- Termprayoon K, Rujirawan A, Ampai N, Wood Jr PL, Aowphol A (2021a) A new insular species of the *Cyrtodactylus pulchellus* group (Reptilia, Gekkonidae) from Tarutao Island, southern Thailand revealed by morphological and genetic evidence. ZooKeys 1070: 101–134. <https://doi.org/10.3897/zookeys.1070.73659>
- Termprayoon K, Rujirawan A, Grismer LL, Wood Jr PL, Aowphol A (2021b) Taxonomic reassessment and phylogenetic placement of *Cyrtodactylus phuketensis* (Reptilia, Gekkonidae) based on morphological and molecular evidence. ZooKeys 1040: 91–121. <https://doi.org/10.3897/zookeys.1040.65750>
- Termprayoon K, Rujirawan A, Grismer LL, Wood Jr PL, Aowphol A (2023) Two new karst-adapted species in the *Cyrtodactylus pulchellus* group (Reptilia, Gekkonidae) from southern Thailand. ZooKeys 1179: 313–352. <https://doi.org/10.3897/zookeys.1179.109712>
- Thorpe RS (1975) Quantitative handling of characters useful in snake systematics with particular reference to interspecific variation in the Ringed Snake *Natrix natrix* (L.). Biological Journal of the Linnean Society. Linnean Society of London 7(1): 27–43. <https://doi.org/10.1111/j.1095-8312.1975.tb00732.x>
- Thorpe RS (1983) A review of the numerical methods for recognized and analysing racial differentiation. In: Felsenstein J (Ed.) Numerical taxonomy. Berlin Heidelberg, Springer, 404–423. https://doi.org/10.1007/978-3-642-69024-2_43
- Trifinopoulos J, Nguyen LT, von Haeseler A, Minh BQ (2016) W-IQ-TREE: A fast online phylogenetic tool for maximum likelihood analysis. Nucleic Acids Research 44(W1): 232–235. <https://doi.org/10.1093/nar/gkw256>
- Turan C (1999) A note on the examination of morphometric differentiation among fish populations: The truss system. Turkish Journal of Zoology 23: 259–263.
- Uetz P, Freed P, Hošek J [Eds] (2024) The Reptile Database. <http://www.reptiledatabase.org> [Accessed 15 January 2024]
- Vogel G, Patrick D (2019) A new species of the *Lycodon fasciatus* complex from the Khorat Plateau, eastern Thailand (Reptiles, Squamata, Colubridae). Zootaxa 4577(3): 515–528. <https://doi.org/10.11646/zootaxa.4577.3.6>
- Welton LJ, Siler CD, Linkem CW, Diesmos AC, Brown RM (2010) Philippine bent-toed geckos of the *Cyrtodactylus agusanensis* complex: multilocus phylogeny, morphological diversity, and descriptions of three new species. Herpetological Monographs 24: 55–85. <https://doi.org/10.1655/HERPMONOGRAPHS-D-10-00005.1>
- Wickham H (2016) ggplot2: Elegant Graphics for Data Analysis. Springer-Verlag New York, 216 pp. https://doi.org/10.1007/978-3-319-24277-4_9

- Wilcox TP, Zwickl DJ, Heath TA, Hillis DM (2002) Phylogenetic relationships of the dwarf boas and a comparison of Bayesian and bootstrap measures of phylogenetic support. *Molecular Phylogenetics and Evolution* 25(2): 361–371. [https://doi.org/10.1016/S1055-7903\(02\)00244-0](https://doi.org/10.1016/S1055-7903(02)00244-0)
- Wood Jr PL, Grismer LL, Grismer JL, Neang T, Chav T, Holden J (2010) A new cryptic species of *Acanthosaura* Gray, 1831 (Squamata: Agamidae) from Thailand and Cambodia. *Zootaxa* 2488(1): 22–38. <https://doi.org/10.11646/zootaxa.2488.1.2>
- Wood Jr PL, Heinicke MP, Jackman TR, Bauer AM (2012) Phylogeny of bent-toed geckos (*Cyrtodactylus*) reveals a west to east pattern of diversification. *Molecular Phylogenetics and Evolution* 65(3): 992–1003. <https://doi.org/10.1016/j.ympev.2012.08.025>
- Yodthong S, Rujirawan A, Stuart BL, Grismer LL, Aksornneam A, Termprayoon K, Ampai N, Aowphol A (2022) A new species in the *Cyrtodactylus oldhami* group (Squamata, Gekkonidae) from Kanchanaburi Province, western Thailand. *ZooKeys* 1103: 139–169. <https://doi.org/10.3897/zookeys.1103.84672>

Supplementary material 1

Material examined in the molecules, locality, collection numbers, GenBank accession numbers and references

Authors: Natee Ampai, Attapol Rujirawan, Siriporn Yodthong, Korkhwan Termprayoon, Bryan L. Stuart, Anchalee Aowphol

Data type: xlsx

Explanation note: Material examined, including locality, collection numbers, GenBank accession numbers, and references for the specimens used in the phylogenetic analyses.

Copyright notice: This dataset is made available under the Open Database License (<http://opendatacommons.org/licenses/odbl/1.0/>). The Open Database License (ODbL) is a license agreement intended to allow users to freely share, modify, and use this Dataset while maintaining this same freedom for others, provided that the original source and author(s) are credited.

Link: <https://doi.org/10.3897/zookeys.1211.122563.suppl1>

Supplementary material 2

Data for multivariate analyses of the *Cyrtodactylus intermedius* group

Authors: Natee Ampai, Attapol Rujirawan, Siriporn Yodthong, Korkhwan Termprayoon, Bryan L. Stuart, Anchalee Aowphol

Data type: xlsx

Explanation note: Dataset of morphological and meristic characters for multivariate analyses of the *Cyrtodactylus intermedius* group.

Copyright notice: This dataset is made available under the Open Database License (<http://opendatacommons.org/licenses/odbl/1.0/>). The Open Database License (ODbL) is a license agreement intended to allow users to freely share, modify, and use this Dataset while maintaining this same freedom for others, provided that the original source and author(s) are credited.

Link: <https://doi.org/10.3897/zookeys.1211.122563.suppl2>

Supplementary material 3

Mean uncorrected p-distances (%) within the *Cyrtodactylus intermedius* group based on the mitochondrial ND2 gene and flanking tRNAs

Authors: Natee Ampai, Attapol Rujirawan, Siriporn Yodthong, Korkhwan Termprayoon, Bryan L. Stuart, Anchalee Aowphol

Data type: xlsx

Explanation note: Mean (minimum–maximum) uncorrected p-distances (%) within the *Cyrtodactylus intermedius* group based on 1,227 bp of the mitochondrial ND2 gene and flanking tRNAs. Numbers in bold are within species divergence. n = number of individuals.

Copyright notice: This dataset is made available under the Open Database License (<http://opendatacommons.org/licenses/odbl/1.0/>). The Open Database License (ODbL) is a license agreement intended to allow users to freely share, modify, and use this Dataset while maintaining this same freedom for others, provided that the original source and author(s) are credited.

Link: <https://doi.org/10.3897/zookeys.1211.122563.suppl3>

Supplementary material 4

Summary of morphological characters, meristic characters, and color pattern data of the *Cyrtodactylus intermedius* group

Authors: Natee Ampai, Attapol Rujirawan, Siriporn Yodthong, Korkhwan Termprayoon, Bryan L. Stuart, Anchalee Aowphol

Data type: xlsx

Explanation note: Summary of morphological characters, meristic characters, and color pattern data of the *Cyrtodactylus intermedius* group. Abbreviations are defined in Materials and methods. Key: NA = no data or not applicable.

Copyright notice: This dataset is made available under the Open Database License (<http://opendatacommons.org/licenses/odbl/1.0/>). The Open Database License (ODbL) is a license agreement intended to allow users to freely share, modify, and use this Dataset while maintaining this same freedom for others, provided that the original source and author(s) are credited.

Link: <https://doi.org/10.3897/zookeys.1211.122563.suppl4>

Species groups, subgroups, and key to world species of the genus *Schizotetranychus* Trägårdh, 1915 (Acari, Prostigmata, Tetranychidae)

Muhammad Kamran¹, Abdul Hafeez², Fahad Jaber Alatawi¹, Carlos Holger Wenzel Flechtmann³

¹ Department of Plant Protection, College of Food and Agriculture Sciences, King Saud University, Riyadh, Saudi Arabia

² Department of Plant Protection, Ghazi University, Dera Ghazi Khan, Punjab, Pakistan

³ Departamento de Entomologia e Acarologia, Escola Superior de Agricultura "Luiz de Queiroz", Universidade de São Paulo, São Paulo, Brazil

Corresponding author: Muhammad Kamran (murafique@ksu.edu.sa)

Abstract

After a comprehensive taxonomic assessment of descriptions/ illustrations of all known (118) species of the spider mite genus *Schizotetranychus* Trägårdh (Acari: Prostigmata: Tetranychidae), five species groups are proposed based on the number of tactile setae on tibia II in female, i.e., *vermiculatus* with four setae (four spp.), *schizopus* with five setae (52 spp.), *spireaefolia* with six setae (10 spp.), *asparagi* with seven setae (20 spp.), and *bambusae* with eight setae on tibia II (22 spp.). The species group *schizopus* is further divided into three species subgroups based on tactile setae on tibia I: *schizopus* with eight/ nine setae (21 spp.), *andropogoni* with seven setae (26 spp.), and *taquarae* with six tactile setae excluding the solenidion on tibia I (five spp.). Eight *Schizotetranychus* species were not assigned to any species group because of brief descriptions and/ or illustration and without information on the number of tactile setae on tibiae I and II. Moreover, two *Schizotetranychus* species, *S. gausus* Baker & Pritchard and *S. luculentus* Tseng that have six setae/ structures including a spinneret and a solenidion on the palp tarsus, are provisionally transferred to the genus *Stigmaeopsis* Banks. Finally, keys to species groups and subgroups of the world species of *Schizotetranychus* are provided.

Key words: *Asparagi*, *schizopus*, tactile setae, *taquarae*, *vermiculatus*



Academic editor: Vladimir Pesic

Received: 23 May 2024

Accepted: 8 July 2024

Published: 4 September 2024

ZooBank: <https://zoobank.org/F1E24C8D-23B5-444C-8526-91EF52BF27DC>

Citation: Kamran M, Hafeez A, Alatawi FJ, Flechtmann CHW (2024) Species groups, subgroups, and key to world species of the genus *Schizotetranychus* Trägårdh, 1915 (Acari, Prostigmata, Tetranychidae). ZooKeys 1211: 131–150. <https://doi.org/10.3897/zookeys.1211.127353>

Copyright: © Muhammad Kamran et al.
This is an open access article distributed under terms of the Creative Commons Attribution License (Attribution 4.0 International – CC BY 4.0).

Introduction

The genus *Schizotetranychus* Trägårdh (Acari, Prostigmata, Tetranychidae) was erected by Trägårdh (1915) based on the shape of leg empodia, i.e., divided deeply into two claw-like structures and having ten pairs of dorsal hysterosomal setae. It is one of the largest genera of spider mites containing 118 species, widely distributed in the world (Migeon and Dorkeld 2006–2024). *Schizotetranychus* species are phytophagous on different plant species and some species are considered as pests of agricultural crops, i.e., *Schizotetranychus andropogoni* (Hirst) and *Schizotetranychus asparagi* (Oudemans, 1928) are widespread in United States and Europe causing serious infestations to pineapple plants (Jeppson et al. 1975; Hoy 2011).

Schizotetranychus species identity has been challenging due to the inadequate number of diagnostic characters, minute differences in male aedeagus morphology, and interspecific similarities in females of many species. Specimens of both sexes are usually required for accurate identification of *Schizotetranychus* species (Pritchard and Baker 1955; Meyer 1974, 1987; Jeppson et al. 1975; Flechtmann 2012). Pritchard and Baker (1955) and Meyer (1974, 1987) provided only diagnostic keys of *Schizotetranychus* species occurring in some regions. Lastly, Flechtmann (2012) arbitrarily organized the *Schizotetranychus* species into 17 groups only based on female morphology; however, the identification characters used are confusing. Additionally, a diagnostic key to world *Schizotetranychus* species is not available. The present study aimed to classify the species of the genus *Schizotetranychus* into species group and subgroups based on consistent diagnostic morphological characters, and to develop diagnostic keys to species groups and subgroups of world species of the genus *Schizotetranychus*.

Materials and methods

The taxonomic literature of all known *Schizotetranychus* species were critically studied, and the diagnostic characters were compared. The generic characters of *Schizotetranychus* and *Stigmaeopsis* were carefully analyzed for possible new combinations. The strength of each morphological character was evaluated for its suitability at the specific level. The consistency of tibia I and II setal counts were carefully evaluated for the construction of species and sub-species group. The key to species of the genus *Schizotetranychus* is provided based on persistent and fixed characteristics.

Results and discussion

Subfamily Tetranychinae Berlese

Tribe Tetranychini Reck

Genus *Schizotetranychus* Trägårdh

Type species. *Tetranychus schizopus* Zacher, 1913.

Diagnosis. Dorsal hysterosoma with ten pairs of setae (c_{1-3} , d_{1-2} , e_{1-2} , f_{1-2} , and h_1), setae h_2 and h_3 present on ventral opisthosoma, empodial claw divided deeply into two claw-like structures, palp tarsus with seven structures/ setae (one spinneret, two eupathidia, one solenidion, three setiform setae); dorsal hysterosoma medially usually with transverse striations, but may be longitudinal or irregular between d_1 and e_1 ; two sets of duplex setae on tarsus I present distally, nearly adjacent to each other.

Background and taxonomic review of the genus *Schizotetranychus*

The genus *Schizotetranychus* was erected by Trägårdh (1915) based on *Tetranychus schizopus* Zacher, 1913 and distinguished from the genus *Tetranychus* by having the leg empodia divided deeply into two claw-like structures. Two years later, Banks (1917) erected the genus *Stigmaeopsis* and designated *St. celarius* Banks its type species. Banks (1917) described the genus *Stigmaeopsis* very

briefly and did not provide any diagnostic characters which could separate it from the closely related genus *Schizotetranychus*. Later, McGregor (1950) synonymized the monospecific genus *Stigmaeopsis* with *Schizotetranychus*. This synonymy was accepted and followed by Pritchard and Baker (1955), Baker and Pritchard (1960), Tuttle and Baker (1968), Gutierrez (1968), Meyer (1974, 1987), Tuttle et al. (1976), Bolland et al. (1998), and Ehara (1999).

For the first time, Ehara (1999) introduced species groups in the genus *Schizotetranychus* by dividing the nine *Schizotetranychus* species reported from Japan into two species groups: *schizopus* (six species) with transverse striations in the anterior portion of dorsocentral area on dorsal opisthosoma and *celarius* (three species) with longitudinal striations in the anterior portion of dorsocentral area on dorsal opisthosoma.

Later, Saito et al. (2004) reinstated the genus *Stigmaeopsis* and distinguished it from *Schizotetranychus* and other genera of Tetranychidae by having six setae/structures on the palp tarsus in the female (instead of seven); dorsal striations between c_1 and d_1 , clearly longitudinal, forming a trapezoidal shape instead of having mostly transverse or longitudinal irregular without forming a trapezoidal shape in *Schizotetranychus*. Also, the bases of setae e_1 , d_1 , and c_1 gradually become further apart than the bases of f_1 setae; if hypothetical lines connecting their bases are drawn, they form a V-shaped pattern vs these lines being almost parallel in *Schizotetranychus* and related genera, as described by Saito et al. (2004). Based on these characteristics, Flechtmann (2012) transferred two *Schizotetranychus* species, *S. malkovskii* Wainstein, 1956 and *S. meghalensis* (Gupta & Gupta, 1994) to *Stigmaeopsis*. Although *S. meghalensis* has transverse striations between setae c_1 , d_1 , and e_1 , and does not satisfy several characters of *Stigmaeopsis*, despite the fact that Saito et al. (2016, 2018, 2019) provisionally included this species in *Stigmaeopsis* because of its six setae/structures on the palp tarsus.

Morphological diagnostic features previously used for grouping *Schizotetranychus* species

Flechtmann (2012) categorized world 106 *Schizotetranychus* species into 17 groups based on following female morphological characters: body length: width ratio, dorsal setal length, shape of peritremes, number of tactile setae on tibia I. As a result, numerous species groups in the genus *Schizotetranychus* based on variable morphological characters are causing confusion and misunderstanding in species identification.

1. Peritremes distally are variously developed in *Schizotetranychus* species, straight in most species, and either making a U-shape, ring, or looped distally others. Peritremes distally are anastomosing in two species *S. cajani* Gupta, 1996, *S. prosopis* Tuttle, Baker & Abbatiello, 1976. Flechtmann (2012) used this character to arbitrarily propose different groups for *Schizotetranychus* species. We consider the shape of the peritreme at species level a misleading character because it is variously developed distally even in different specimens of the same species, and described and illustrated differently for one species by various authors. Also, this character was already causing confusion while attempting to separate the species groups of *Schizotetranychus* created by Flechtmann (2012).

2. Mite body shape is either oval (longer than wide in most of species), or orbicular (as long as wide in few species), or elongate (more than 2× longer than width of body in few species). This character was used by Flechtmann (2012) to develop groups in *Schizotetranychus*. However, it caused confusion in the identification of those groups because some species lie on the borderline in length and width ratios. Also, the length and width ratios could be affected by the mounting of specimens on glass slides.
3. Dorsal and ventral idiosoma is entirely striated in almost all *Schizotetranychus* species, either widely or closely spaced, except *S. reticulatus* Baker & Pritchard, 1960 with reticulations on the propodosoma medially, and the hysterosoma is entirely striated and rugose. The dorsal hysterosoma between setae c_1 , d_1 , e_1 , and f_1 with transverse striations entirely in all *Schizotetranychus* species except six, namely *S. hidayahae* Yusof & Zhang, 2003, *S. baltazarae* Rimando, 1962, *S. spiculus* Baker & Pritchard, 1960, *S. brevisetosus* Ehara, 1989, *S. rhodanus* Baker & Pritchard, 1960, and *S. colocasiae* Ehara, 1988 (as in Ehara & Tho, 1988), in which the striations between setae e_1 and d_1 form a V-shaped pattern or is irregular.

Dorsal body setae are usually setiform in *Schizotetranychus* species. However, few species have awl-shaped dorsal setae with slightly expanded bases. Flechtmann (2012) used this character to develop species groups in *Schizotetranychus*. However, dorsal setae were not properly illustrated or described in detail for many *Schizotetranychus* species, so for those species it is very difficult to discern the exact shape (awl or setiform) of the dorsal setae. This character can be considered as supporting species level character.

Taxonomic notes about two *Schizotetranychus* species having six setae/ structures on the palp tarsus as in the genus *Stigmaeopsis*

As mentioned earlier, the genus *Stigmaeopsis* differs from *Schizotetranychus* by having six setae/ structures on the palp tarsus in females instead of seven; dorsal striations lie between c_1 and d_1 are clearly longitudinal and forming a trapezoidal shape instead of being mostly transverse or irregularly longitudinal between setae d_1 and e_1 in six *Schizotetranychus* species, namely, *S. hidayahae*, *S. baltazarae*, *S. spiculus*, *S. brevisetosus*, *S. rhodanus* and *S. colocasiae* without forming a trapezoidal shape. Also, the bases of setae e_1 , d_1 , and c_1 gradually widen further apart than the bases of f_1 setae if hypothetical lines connecting their bases are drawn. They form a V-shaped pattern vs almost parallel lines are in *Schizotetranychus* and related genera, as described by Saito et al. (2004).

In the present study, it was found that two *Schizotetranychus* species, *S. gausus* Baker & Pritchard, 1960 and *S. luculentus* (Tseng, 1990) have six setae/ structures including spinneret and solenidion on palp tarsus. The original description of these species lacking information of palp setae. So, relying on the original illustrations, these two *Schizotetranychus* species having six setae on palp tarsus are provisionally transferred to *Stigmaeopsis*. Also, dorsum is entirely reticulated in *S. luculentus* (Tseng, 1990). However, dorsum with transverse striations between setae c_1 , d_1 and irregular longitudinal between setae e_1 and d_1 in *S. gausus*. Moreover, 16 known species of *Stigmaeopsis* have five tactile setae on tibia II except *S. gausus* having seven setae on tibia II.

Furthermore, bases of length dorsal setae c_1 , d_1 which is $\sim 2\times$ more widely spaced to the bases of e_1 and f_1 (bases of c_1 , d_1 , e_1 , f_1 forming a V-shaped pattern) in *S. Attiah*, 1967 as in all known 16 *Stigmaeopsis* species. Few other *Schizotetranychus* species have a similar pattern of dorsal setal bases. So, the supporting diagnostic character that hypothetical lines connecting the bases of setae c_1 , d_1 , e_1 , and f_1 forming a V-shaped taken by Saito et al. (2004) for *Stigmaeopsis* while reinstating this genus to separate it from *Schizotetranychus* becomes impractical.

Hence it is understood from the above discussion that genus *Stigmaeopsis* is different from *Schizotetranychus* by only one character, the presence of six setae/ structures on palp tarsus vs seven in *Schizotetranychus*. All other supporting characters (longitudinal striations between setae c_1 and d_1 , bases of setae c_1 , d_1 , e_1 , and f_1 forming a V-shaped pattern) of *Stigmaeopsis* taken by Saito et al. (2004, 2018) as a generic character could be considered as species level characters.

Species groups and subgroups of *Schizotetranychus* developed in the current study

In the present research, after comprehensive taxonomic assessment of descriptions and illustrations of all known (116) species of the genus *Schizotetranychus*, species grouping in this genus is reconsidered based on females using only the number of tactile setae on tibia II and species subgroups based on only the number of tactile setae on tibia I. The number of tactile setae on tibia II is found to be a consistent diagnostic character in *Schizotetranychus* species and described in 110 *Schizotetranychus* species, even those which were very briefly described. Flechtmann (2012) used tactile setae on tibia I to separate some *Schizotetranychus* groups. Pritchard and Baker (1955) and Mushtaq et al. (2021) also used tactile setae on tibia I to develop species groups in the genus *Oligonychus*. Based on tibial setal counts, species groups of *Schizotetranychus* can easily be recognized.

In the present study, the genus *Schizotetranychus* can be divided into five species groups based on the number of tactile setae on tibia II in the female: *schizopus* group (52 spp.) with five setae, *asparagi* group with seven setae (20 spp.), *bambusae* group with eight setae (22 spp.), *spireaefolia* group with six setae (10 spp.) and *vermiculatus* group with four setae on tibia II (four spp.). Also, keys to the world *Schizotetranychus* species, species groups, and subgroups are developed for the first time. Eight *Schizotetranychus* species were not assigned any species group because these have been described and illustrated very briefly without information on the number of setae on tibia I and II.

1. Species group *schizopus*

Diagnosis. Female: Tibia II with five setae (52 species).

Exemplar species. *Schizotetranychus schizopus* (Zacher, 1913)

Species group *schizopus* is further divided into three species subgroups based on number of tactile setae excluding solenidion on tibia I.

i) Species subgroup *schizopus*

Diagnosis. Female. Tibia I with eight/ nine setae (21 species).

Exemplar species. *Schizotetranychus schizopus*

ii) Species subgroup *andropogoni*

Diagnosis. Female. Tibia I with seven setae (26 species).

Exemplar species. *Schizotetranychus andropogoni* (Hirst, 1926)

iii) Species subgroup *taquarae*

Diagnosis. Female. Tibia I with six setae (5 species).

Exemplar species. *Schizotetranychus taquarae* Paschoal, 1971

2. Species group *asparagi*

Diagnosis. Female. Tibia II with seven setae (20 spp.)

Exemplar species. *Schizotetranychus asparagi* (Oudemans, 1928)

3. Species group *bambusae*

Diagnosis. Female. Tibia II with eight setae (22 spp.).

Exemplar species. *Schizotetranychus bambusae* Reck, 1941

4. Species group *spireaefolia*

Diagnosis. Female. Tibia II with six setae (10 spp.).

Exemplar species. *Schizotetranychus spireaefolia* Garman, 1940

5. Species group *vermiculatus*

Diagnosis. Female. Tibia II with four setae (04 spp.).

Exemplar species. *Schizotetranychus vermiculatus* Ehara & Wongsiri, 1975

Ungrouped species

The following eight species were not assigned any species group because these have been described and illustrated very briefly without information of number of tactile setae on tibiae I and II. *Schizotetranychus setariae* Meyer, 1987 was not assigned to any species group/ subgroup because it was only described/ known from the male.

1. *S. graminicola* Goux, 1949
2. *S. glabrisetus* (Ugarov & Nikolskii, 1937)
3. *S. tuberculatus* (Ugarov & Nikolski, 1937)
4. *S. guatemalae-novae* (Stoll, 1886)
5. *S. hindustanicus* (Hirst, 1924)
6. *S. mustafaii* Mustafa & Chaudri, 1972 (as in Mustafa et al. 1972)
7. *S. oudemansi* Reck, 1948
8. *S. setariae* Meyer, 1987

Moreover, two *Schizotetranychus* species, *S. gausus* and *S. luculentus*, that have six setae/ structures including spinneret and a solenidion on the palp tarsus based

on original illustrations, are provisionally transferred to *Stigmaeopsis*. Further studies are required to confirm the clear taxonomic status of these two species.

1. *Schizopus* species group (52 species)

I- *Schizopus* species subgroup (21 species)

(Female: tibia II with 5 setae, tibia I with 8 or 9 tactile setae excluding solenidion)

Key to species of *schizopus* species subgroup of *schizopus* species group

- 1 Propodosoma dorsomedially with reticulate pattern..... **S. reticulatus Baker & Pritchard, 1960**
- Propodosoma dorsomedially striated..... **2**
- 2 Peritremes distally curved U- or ring-shaped/ looped..... **3**
- Peritremes distally straight or slightly hooked **7**
- 3 Tibia I with 9 tactile setae and 1 sensory seta ... *S. australis* Gutierrez, 1968
- Tibia I with 8 tactile setae and 1 sensory seta **4**
- 4 Dorso-opisthosomal setae c_1, d_1, e_1 at least reaching 1/2 to 2/3 of the setae next in line..... **S. pennamontanus Meyer, 1987**
- Dorso-opisthosomal setae c_1, d_1, e_1 almost reaching or crossing the setae next in line..... **5**
- 5 Male aedeagus upturned part not sigmoid, distal part not projecting posteriorly..... **S. russeus Davis, 1969**
- Male aedeagus upturned part sigmoid, distal part projecting posteriorly **6**
- 6 In male: tarsus I with 3 and tibia I with 1 spindle-shaped setae; in female: setae c_1, d_1, e_1 at least reaching the setae next in line **S. eremophilus McGregor, 1950**
- In male: tarsus I and tibia I without spindle-shaped setae; in female: setae c_1, d_1, e_1 crossing the setae next in line **S. elymus McGregor, 1950**
- 7 Tibia I with 9 tactile setae and 1 solenidion **8**
- Tibia I with 8 tactile setae and 1 solenidion **10**
- 8 Male: aedeagus upturned part almost sigmoid, without anterior projection, tibia I with 7 tactile setae and 2 solenidia..... **S. mansonii Gupta, 1980**
- Male: aedeagus upturned part, not sigmoid, with anterior projection, tibia I with 9 tactile setae and 3 or 4 solenidia **9**
- 9 Male: tibia I with 9 tactile setae and 3 solenidia, tibia II with 5 tactile setae. **S. schizopus (Zacher, 1913)**
- Male: tibia I with 9 tactile setae and 4 solenidia, tibia II with 6 tactile setae. **S. lechrius Rimando, 1962**
- 10 Female: genu III with 4 tactile setae..... **11**
- Female: genu III with 3 tactile setae..... **14**
- 11 Female: setae c_1, d_1, e_1 far behind the bases of setae next in line..... **S. agropyron Tuttle & Baker, 1976**
- Female: setae c_1, d_1, e_1 crossing the bases of setae next in line..... **12**
- 12 Male: aedeagus upturned part at right or acute angle to the shaft, does not project posteriorly..... **S. nesbitti Meyer, 1965**
- Male: aedeagus upturned part making obtuse angle to the shaft, projecting posteriorly **13**

- 13 Male: aedeagus not sigmoid, upturned part gradually narrowing toward distal end, 1.5× longer than max. width of shaft.....
..... **S. cynodonis** McGregor, 1950
- Male: aedeagus almost sigmoid, upturned part abruptly narrowing toward distal end, less than max. width of shaft.....
..... **S. paezi** Alvarado & Freitez, 1976
- 14 Female: femur I with 7 or 8 setae..... 15
- Female: femur I with 9 or 10 setae..... 17
- 15 Female: genu IV with 2 setae..... **S. echinulatus** Mitrofanov, 1978
- Female: genu IV with 3 setae..... 16
- 16 Dorso-central hysterosomal setae shorter than distance/interval to base of seta immediately behind..... **S. saba-sulchani** Reck, 1956
- Dorso-central hysterosomal setae as long as or longer than distance/interval to base of seta immediately behind **S. yoshimekii** Ehara & Wongsiri, 1975
- 17 Femur I with 9 setae..... 18
- Femur I with 10 setae..... 19
- 18 Female: tibia III with 5 setae. Male: aedeagus upturned part with knob, prominent neck, and anterior projection **S. hilariae** Tuttle & Baker, 1968
- Female: tibia III with 5 setae. Male: aedeagus upturned part without knob, neck, or anterior projection **S. tuttleii** Zaher, Gomaa & El-Enany, 1982
- 19 Female: femur III with 2 setae, peritremes L-shaped distally. Male: aedeagus upturned part length of shaft less than max. width of shaft.....
..... **S. kochummeni** Ehara, 1988 (as in Ehara and Tho 1988)
- Female: femur III with 3 setae, peritremes straight distally. Male: aedeagus upturned part of shaft length > 2× the max. width of shaft..... 20
- 20 Female: femur IV with 2 setae. Male: aedeagus upturned part almost at right angle to the shaft, not projecting posteriorly.....
..... **S. tbilisiensis** Reck, 1959
- Female: femur IV with 3 setae. Male: aedeagus upturned part making obtuse angle (120°) to the shaft, projecting posteriorly.....
..... **S. tumidus** Wang, 1981

II- *andropogoni* species subgroup (26 species)

(Female: tibia II with 5 setae, tibia I with 7 tactile setae excluding solenidion)

Key to species of *andropogoni* species subgroup

- 1 Peritremes distally hooked, branched, or looped 10
- Peritremes distally simple (bulb-like)..... 2
- Peritremes distally anastomosing..... **S. cajani** Gupta, 1996
- 2 Dorsal setae comparatively shorter in length, setae c_1 reaching at least 2/3 the distance c_1-d_1 3
- Dorsal setae comparatively long, setae c_1 reaching/ crossing the bases of d_1 , almost equal to/ longer than the distance c_1-d_1 7
- 3 Idiosoma elongate, ratio of body length (not including rostrum): width > 2..
..... 4
- Idiosoma oval/ orbicular, ratio of body length (not including rostrum): width < 2 5

- 4 Tarsus I with 3 tactile setae and 1 solenidion proximal to proximal duplex setae..... **S. lycurus Tuttle & Baker, 1964**
- Tarsus I with 1 tactile seta and 1 solenidion proximal to proximal duplex setae.....**S. boutelouae Tuttle & Baker, 1968**
- 5 Femur I with 7 setae, area anterior to genital flap with transverse striations, tarsus I with 2 tactile setae and 7 solenidion proximal to proximal duplex setae..... **S. celtidis Tuttle & Baker, 1968**
- Femur I with 9 setae, area anterior to genital flap with longitudinal striations, tarsus I with 3 tactile setae and 1 solenidion proximal to proximal duplex setae..... **6**
- 6 Genu III with 2 setae, genu IV with 1 seta, area on hysterosoma between d_1 and e_1 with longitudinal striations **S. hidayahae Yusof & Zhang, 2003**
- Genua III and IV each with 3 setae, hysterosoma dorsomedially with transverse striations entirely**S. montanae Tuttle & Baker, 1968**
- 7 Setae c_1 very long, crossing the bases of d_1 , reaching to the bases of e_1
..... **S. longirostris Feres & Flechtmann, 1995**
- Setae c_1 reaching at least to the bases of d_1 , almost equal to the distance c_1-d_1 **8**
- 8 Area anterior to genital flap with longitudinal irregular striations.....
..... **S. paraelymus Feres & Flechtmann, 1995**
- Area anterior to genital flap with transverse striations..... **9**
- 9 In female: seta sc_1 much longer than sc_2 , setae d_1 and e_1 not reaching to the bases of setae next in line. Male: tarsus I with 3 solenidia and 1 tactile seta proximal to proximal duplex setae, aedeagus upturned part sigmoid without anterior projection..... **S. camur Pritchard & Baker, 1955**
- In female: setae sc_1 and sc_2 almost subequal, setae d_1 and e_1 reaching to the bases of setae next in line. Male: tarsus I with 1 solenidion and 1 tactile seta proximal to proximal duplex setae, aedeagus upturned part with anterior projection..... **S. andropogoni (Hirst, 1926)**
- 10 Dorso-central setae c_1 , d_1 , and e_1 reaching or crossing the bases of next setae in line..... **11**
- Dorso-central setae c_1 , d_1 , and e_1 not reaching behind the bases of next setae in line..... **16**
- 11 Female: tarsus I with 2 or 4 setae and 1 solenidion proximal to proximal duplex setae..... **12**
- Female: tarsus I with 1 seta and 1 solenidion proximal to proximal duplex setae..... **14**
- 12 Female: tarsus I with 4 setae and 1 solenidion proximal to proximal duplex setae..... **S. filifolius Meyer, 1974**
- Female: tarsus I with 2 setae and 1 solenidion proximal to proximal duplex setae..... **13**
- 13 Female: All hysterosomal setae longer than longitudinal interval between their bases. Male: tarsus I with 2 setae and 2 solenidia proximal to proximal duplex setae, upturned part of aedeagus making almost right angle with shaft **S. sacharum Flechtmann & Baker, 1975**
- Female: most of hysterosomal setae approximately as long as the longitudinal interval between their bases. Male: tarsus I with 3 setae and 2 solenidia proximal to proximal duplex setae, upturned part of aedeagus making acute angle with shaft..... **S. youngi Tseng, 1975**

- 14 Female: hysterosomal setae especially c_1 , d_1 , e_1 barely reaching the bases of next setae in line. Male: tarsus I with 1 solenidion and 1 tactile seta proximal to proximal duplex setae.....
**S. krungthepensis Auger & Naing, 2014 (as in Naing et al. 2014)**
- Female: hysterosomal setae especially c_1 , d_1 , e_1 longer than distance to bases of next setae in line. Male: tarsus I with 2 or 3 solenidia and 1 tactile seta proximal to proximal duplex setae **15**
- 15 Male: tibia I with 7 tactile setae and 3 solenidia, tibia II with 5 tactile setae and 1 solenidion, tarsus I with 1 tactile seta and 3 solenidia proximal to proximal duplex setae **S. arcuatus Meyer, 1974**
- Male: tibia I with 7 tactile setae and 4 solenidia, tibia II with 5 tactile setae only without solenidion, tarsus I with 1 tactile seta and 2 solenidia proximal to proximal duplex setae..... **S. rhynosperus Flechtmann & Baker, 1970**
- 16 Female: Dorsal hysterosoma medially with transverse striations except area between setae c_1 , d_1 , and e_1 forming V-shaped or longitudinal pattern.
 **17**
- Female: Dorsal hysterosoma medially with transverse striations entirely **19**
- 17 Female: Stylophore anteriorly emarginate, with notch..... **18**
- Female: Stylophore anteriorly without notch.....
 **S. sacrales Baker & Pritchard, 1960**
- 18 Female: Tarsus I with 2 solenidia and two tactile setae proximal to proximal duplex setae; striations in between setae c_1 to d_1 longitudinal
 **S. baltazarae Rimando, 1962**
- Female: Tarsus I with 1 solenidion and 2 tactile setae proximal to proximal duplex setae; striations in between setae c_1 to d_1 transverse
 **S. spiculus Baker & Pritchard, 1960**
- 19 Peritremes looped (making a loop) distally
 **S. nugax Pritchard & Baker, 1955**
- Peritremes hooked or making L-shape distally **20**
- 20 Idiosoma elongate, ratio of body length (not including rostrum): width > 2..
 **23**
- Idiosoma oval/ orbicular, ratio of body length (not including rostrum): width < 2 **21**
- 21 Female: Dorsal striations smooth without lobes. Male: aedeagus upturned part making right angle with the shaft **S. sagatus Davis, 1969**
- Female: Dorsal striations with lobes. Male: aedeagus upturned part making obtuse angle with the shaft **22**
- 22 Femur I with 7 setae, stylophore notched anteriorly, striations in pregenital area making strongly arched **S. denmarki Baker & Tuttle, 1994**
- Femur I with 9 setae, stylophore rounded anteriorly, striations in pregenital area transverse **S. pseudolycurus Ochoa, Gray & von Lindeman, 1990**
- 23 Tarsus I with 4 tactile setae proximal to proximal duplex
 **S. fluvialis McGregor, 1928**
- Tarsus I with 3 tactile setae proximal to proximal duplex **24**
- 24 Striations in pregenital area almost transverse slightly curved
 **S. freitezi Ochoa, Gray & von Lindeman, 1990**
- Striations in pregenital area longitudinal irregular
 **S. oryzae Rossi de Simons, 1966**

III- *taquarae* species subgroup (05 species)

(Female: tibia II with 5 setae, tibia I with 6 tactile setae excluding solenidion)

Key to species of *taquarae* species subgroup

- 1 Dorsal setae very short, far behind the bases of next setae in line.....2
 - Dorsal setae long, at least reaching or crossing the bases of next setae in line3
- 2 Female: peritremes hooked distally, dorsal striations without lobes, striations on pregenital area transverse; femur IV with 3 setae. Male: aedeagus upturned part sigmoid without anterior projection
 -**S. tegophallos Flechtmann & Peralta-Alba, 2012**
 - Female: peritremes simple, without hook distally, dorsal striations with lobes, striations on pregenital area longitudinal; femur IV with 2 setae. Male: aedeagus upturned part not sigmoid with anterior projection.....
 - **S. umtaliensis Meyer, 1974**
- 3 Female: tarsus I with 4 tactile setae and a solenidion proximal to proximal duplex setae. Male: aedeagus not sigmoid, shaft almost straight, narrowing toward distal end.....
 - **S. triquetrus Meyer, 1987**
 - Female: tarsus I with 2 or 3 tactile setae and a solenidion proximal to proximal duplex setae. Male: aedeagus almost sigmoid, upturned.....4
- 4 Dorsal striations with lobes, tarsus I with 2 tactile setae and a solenidion proximal to proximal duplex setae
 -**S. taquarae Paschoal, 1971**
 - Dorsal striations without lobes, tarsus I with 3 tactile setae proximal to proximal duplex setae**S. papillatus Flechtmann, 1995**

2. *asparagi* species group (20 species)

(Female: tibia II with 7 setae)

Key to species (20) of *asparagi* species group

- 1 Tibia I with 12 setae including solenidia2
 - Tibia I with 8–10 setae and 1 solenidion3
- 2 Female: femur IV with 4 setae, genua III and IV with 3 setae. Male: aedeagus downturned, with only posterior projection
 - **S. emeiensis Wang, 1983**
 - Female: femur IV with 4 setae, genua III and IV with 3 setae. Male: aedeagus upturned, with anterior and posterior projections.....
 - **S. kreiteri Flechtmann, 1999 (as in Flechtmann et al. 1999)**
- 3 Tibia I with 7 or 8 setae and a solenidion4
 - Tibia I with 9 setae and a solenidion.....7
- 4 Tibia I with 7 tactile setae and a solenidion
 -**S. lanyuensis Tseng, 1975**
 - Tibia I with 8 tactile setae and a solenidion5
- 5 Dorsal hysterosoma medially with transverse striations entirely, dorsal setae, especially c_1 , d_1 , e_1 , longer than interval between their bases
 -**S. miyatahus (Meyer, 1974)**
 - Dorsal hysterosoma medially between setae d_1 and e_1 with longitudinal irregular striations, dorsal setae shorter than interval between their bases.....6

- 6 Female: Dorsal setae serrated, tarsus I with 5 tactile setae and 1 solenidion proximal to proximal duplex setae. Male: aedeagus upturned with small anterior projection and long posterior projection..... **S. brevisetosus Ehara, 1989**
- Female: Dorsal setae nude, tarsus I with four tactile setae and a solenidion proximal to proximal duplex setae. Male: aedeagus almost straight without anterior projection **S. rhodanus Baker & Pritchard, 1960**
- 7 Femur I with 10 setae..... **8**
- Femur I with 8 or 9 setae **12**
- 8 Tibia IV with 6 setae..... **9**
- Tibia IV with 7 setae..... **10**
- 9 Peritremes hooked distally **S. lushanensis Wang, 1994**
- Peritremes simple/ straight distally **S. zhangji Wang & Cui, 1992**
- 10 Femur II with 6 setae, femur IV with 4 setae **S. kaspari Manson, 1967**
- Femur II with 7 setae, femur IV with 2 or 3 setae..... **11**
- 11 Femur III with 4 setae, femur IV with 3 setae..... **S. tuminicus Ma & Yuan, 1982**
- Femur III with 3 setae, femur IV with 2 setae
..... **S. halimodendri Wainstein, 1958**
- 12 Femur I with 8 setae..... **S. sayedi Attiah, 1967**
- Femur I with 9 setae..... **13**
- 13 Tibia III with 5 setae **14**
- Tibia III with 6 setae **15**
- 14 Female: Tibia IV with 5 setae, femur IV with 4 setae. Male: aedeagus distal part downturned, with small posterior projection
..... **S. asparagi (Oudemans, 1928)**
- Female: Tibia IV with 6 setae, femur IV with 3 setae. Male: aedeagus distal part upturned, with large posterior projection **S. tephrosiae Gutierrez, 1968**
- 15 Genu IV with 3 setae..... **S. lespedezae Beglyarov & Mitrofanov, 1973**
- Genu IV with 4 setae..... **16**
- 16 Striations on dorsal hysterosoma medially between setae e_1 forming V-shaped or irregular longitudinal patterns **17**
- Dorsal hysterosoma medially with entirely transverse striations **18**
- 17 Female. Dorsal setae c_1 , d_1 , and e_1 just reaching the bases of next consecutive setae, peritremes slightly hooked distally. Male. Aedeagus with very minute anterior projection, aedeagal knob making acute angle with shaft.....
..... **S. colocasiae Ehara, 1988 (as in Ehara and Tho 1988)**
- Female. Dorsal setae c_1 , d_1 and e_1 crossing the bases of next consecutive setae, peritremes almost straight distally. Male. Aedeagus with very prominent anterior projection, aedeagal knob making obtuse angle with shaft.....
..... **S. malodhensis Sadana et al., 1985**
- 18 Setae c_1 and d_1 reaching maximum up to 2/3 distance to setae next in line **S. protectus Meyer, 1965**
- Setae c_1 and d_1 as long as or crossing the bases of setae next in line..... **19**
- 19 Male: Eupathidium on palp tarsus absent, aedeagus knob of upturned part parallel with the shaft.....
..... **S. malayanus Ehara, 1988 (as in Ehara and Tho 1988)**
- Male: Eupathidium on palp tarsus present, aedeagus knob of upturned part making obtuse angle with the shaft.....
..... **S. bhandhufalcki Ehara & Wongsiri, 1975**

3. *bambusae* species group (22 species)

(Female: Tibia II with 8 setae)

Key to species of *bambusae* species group

- 1 Tibia I with 10 or 11 setae including solenidion 2
 - Tibia I with 9 setae including solenidion..... **S. indicus Gupta & Gupta, 1994** 3
- 2 Peritremes distally hooked, U/L-shaped 3
 - Peritremes almost straight, slightly expanded distally, not hooked/ U/L-shaped distally..... 11
- 3 Genua III and IV each with 3 setae 4
 - Genua III and IV each with 4 setae 7
- 4 Female: Dorsal setae comparatively short, far behind the bases of next setae in line. Male: aedeagus distal part upturned with anterior projection
 - **S. gilvus Ehara & Ohashi, 2005**
 - Female: Dorsal setae long, crossing the bases of next setae in line. Male: aedeagus distal part straight undulating or downturned without anterior projection 5
- 5 Female: setae c_1 just crossing setae d_1 , far behind the bases of setae e_1 , tarsus I with 2 or 3 tactile setae and a solenidion proximal to proximal duplex setae.....**S. minutus Wang, 1985 (as mentioned in Wang et al. 1985)**
 - Female: setae c_1 reaching the bases of setae e_1 , tarsus I with 4 or 5 tactile setae and 1 solenidion proximal to proximal duplex setae 6
- 6 Female: pregenital area with longitudinal striations, tarsus I with 4 tactile setae and 1 solenidion proximal to proximal duplex setae. Male: aedeagus distal part almost straight, undulating, slightly turning up
 - **S. gahniae Davis, 1969**
 - Female: pregenital area with transverse striations, tarsus I with 5 tactile setae and 1 solenidion proximal to proximal duplex setae. Male: aedeagus distal part almost straight, downturned..... **S. cercidiphylli Ehara, 1973**
- 7 Femur IV with 3 setae..... 8
 - Femur IV with 4 setae..... 9
- 8 Femur II with 6 setae, peritremes V-shaped distally
 -**S. imperatae Wang, 1983**
 - Femur II with 7 setae, peritremes L-shaped distally, slightly hooked..... **S. textor Wainstein, 1954**
- 9 Female: dorsal setae especially c_1 , d_1 , e_1 almost reaching to the bases of setae next in line. Male: aedeagus distal part downturned and sigmoid
 - **S. fauveli Gutierrez, 1978**
 - Female: dorsal setae especially c_1 , d_1 , e_1 well crossing to the bases of setae next in line. Male: aedeagus distal part not sigmoid, almost straight/ undulating..... 10
- 10 Male: aedeagus distal part very long needle-like undulating.....
 - **S. alni Beglyarov & Mitrofanov, 1973**
 - Male: aedeagus distal part downturned slightly gradually narrowing toward distal end, not needle-like..... **S. zhongdianensis Wang & Cui, 1992**
- 11 Tibia I with 10 tactile setae and 1 solenidion 12
 - Tibia I with 9 tactile setae and 1 solenidion 13

- 12 Female: femur I with 9 setae, femur II with 6 setae genu III with 3 setae.
Male: aedeagus distal part straight undulating.....
.....**S. garmani Pritchard & Baker, 1955**
- Female: femur I with 10 setae, femur II with 7 setae, genu III with 4 setae.
Male: aedeagus distal part slightly upturned, dorsally making slight knob,
then bent down distally**S. levinensis Manson, 1967**
- 13 Male: aedeagus distal part upturned **14**
- Male: aedeagus distal part, straight or downturned **18**
- 14 Male: aedeagus distal upturned part with prominent anterior projection and
long posterior projection..... **15**
- Male: aedeagus distal upturned part without anterior projection **16**
- 15 Eupathidium on male palp tarsus long, almost as long as eupathidia aedeagus
posterior projection of upturned part is 4× longer than width of aedeagus
neck and making prominent angle with neck.....
.....**S. beckeri Wainstein, 1958**
- Eupathidium on male palp tarsus minute, eupathidia 3× longer than, aedeagus
posterior projection of upturned part is 2–3× longer than width of neck
and not making angle with neck.....
.....**S. brachypodii Livshits & Mitrofanov, 1968**
- 16 Male: aedeagus distal part turn dorso-caudally, almost sigmoid in shape ...
.....**S. ibericus Reck, 1947**
- Male: aedeagus distal part turn dorsally, not sigmoid in shape..... **17**
- 17 Female: pregenital area with transverse striations, tarsus I with 4 tactile
setae and a solenidion, tarsus II with 4 setae and a solenidion proximal
to proximal duplex setae. Male: aedeagus upturned part greatly narrowing,
needle-like..... **S. floresi Rimando, 1962**
- Female: pregenital area with longitudinal striations, tarsus I with 5 tactile
setae and 1 solenidion, tarsus II with 3 setae and 1 solenidion proximal
to proximal duplex setae. Male: aedeagus upturned part blunt distally, not
narrowing **S. bambusae Reck, 1941**
- 18 Male: aedeagus distal part straight, undulating.....
.....**S. jachontovi Reck, 1953**
- Male: aedeagus distal part down turned **19**
19. Female: femur IV with 3 setae. Male: aedeagus distal part slightly down-
turned without anterior projection..... **20**
- Female: femur IV with 4 setae. Male: aedeagus distal downturned part with
distal knob, neck, and anterior projection **21**
- 20 Female: tarsus I with 19 and tarsus II with 16 setae. Male: eupathidium su
on palp tarsus long, longer than eupathidia**S. smirnovi Wainstein, 1954**
- Female: tarsus I with 18 and tarsus II with 15 setae. Male: eupathidium su
on palp tarsus almost half in length than eupathidia.....
.....**S. iraniensis Mahdavi & Asadi, 2015**
- 21 Male: aedeagus anterior and posterior projections almost equal, knob
forming obtuse angle with the shaft
.....**S. Chiangmaiensis Ehara & Wongsiri, 1975**
- Male: aedeagus posterior projections much longer (2–3×) than anterior
projection, knob forming acute angle with the shaft.....
.....**S. euphorbiae Livshitz & Mitrofanov, 1968**

4. *vermiculatus* species group (4 species)

(Female: Tibia II with 4 setae)

Key to species of *vermiculatus* species group

- 1 Tibia I with 7 setae and a solenidion, tibiae III and IV each with 4 setae.....
..... **S. *vermiculatus* Ehara & Wongsiri, 1975**
- Tibia I with 6 setae and a solenidion, tibiae III and IV each with 3 setae.....**2**
- 2 Genua III and IV each with 3 setae**S. *approximatus* Ehara, 1988**
- Genua III and IV each with 2 setae **3**
- 3 Dorsocentral area between setae c_1 , d_1 , e_1 , and f_1 smooth, without striations.....**S. *laevadorsatus* Ehara, 1988**
- Dorsocentral area between setae c_1 , d_1 , e_1 , and f_1 with transverse striations
S. *saitoi* Ehara, 1988

5. *spireafolia* species group (10 species)

(Female: Tibia II with 6 setae)

Key to species of *spireafolia* species group

- 1 Tibia I with 6 tactile setae and a solenidion
..... **S. *prosopis* Tuttle, Baker & Abbatiello, 1976**
- Tibia I with 7 tactile setae and a solenidion **2**
- Tibia I with 8 or 9 tactile setae and a solenidion **4**
- 2 Dorsal setae very long, c_1 crossing the bases of d_1 reaching up to the bases of e_1 , setae d_1 reaching up to the bases of f_1
..... **S. *parasemus* Pritchard & Baker, 1955**
- Dorsal setae, short, setae c_1 and d_1 and e_1 almost reaching up the bases of setae next in line or just crossing the bases of setae next in line..... **3**
- 3 Female: Tarsus I with 2 setae and 1 solenidion proximal to proximal duplex setae, tarsus II with 1 tactile seta and 1 solenidion proximal to duplex setae. Male aedeagus upturned distal part shorter (less than half) the length of shaft **S. *recki* Ehara, 1957**
- Female: Tarsus I with 5 tactile setae proximal to duplex setae, Tarsus II with 4 tactile setae and 1 solenidion proximal to duplex setae. Male aedeagus upturned distal part as long as the length of shaft
..... **S. *undulatus* (Beer & Lang, 1958)**
- 4 Tibia I with 9 tactile setae and a solenidion **S. *ugarovi* Wainstein, 1960**
- Tibia I with 8 tactile setae and a solenidion **5**
- 5 Peritremes hooked distally. Male aedeagus upturned part with neck and anterior projection **S. *shii* Ehara, 1965**
- Peritremes straight distally. Male aedeagus without anterior projection..... **6**
- 6 Dorsal hysterosomal setae (most of them) awl-shaped, acutely tapering from the widened proximal (basal) portion **S. *spireafolia* Garman, 1940**
- Dorsal hysterosomal setae setose **7**
- 7 Tibiae III and IV each with 6 setae..... **S. *dalbergiae* Meyer, 1974**
- Tibiae III and IV each with 5 setae..... **8**

- 8 Femur II, III, and IV with 8, 4, and 2 setae, respectively. Male aedeagus upturned part as long as the length of shaft.....**S. *elongatus* Wang & Cui, 1991**
- Femur II, III, and IV with 6, 3, and 3 setae, respectively. Male aedeagus upturned part very minute as compared to the length of shaft.....
.....**S. *avetjanae* Bagdasarian, 1954**

Acknowledgments

The authors would like to extend their sincere appreciation to Yutaka Saito (Research Faculty of Agriculture, Hokkaido University, Sapporo, Japan) for sharing the published descriptions, redescriptions, and illustrations of all the species of the genus *Stigmaeopsis*.

Additional information

Conflict of interest

The authors have declared that no competing interests exist.

Ethical statement

No ethical statement was reported.

Funding

The authors would like to extend their sincere appreciation to the Researchers Supporting Project number [RSPD2024R807], King Saud University, Riyadh, Saudi Arabia for funding this research.

Author contributions

All authors have contributed equally.

Author ORCIDs

Muhammad Kamran  <https://orcid.org/0000-0001-6084-203X>

Fahad Jaber Alatawi  <https://orcid.org/0000-0002-6824-2650>

Data availability

All of the data that support the findings of this study are available in the main text.

References

- Alvarado DG, Freitez RFP (1976) *Schizotetranychus paezi* sp. n. y *S. oryzae* (Acarina: Tetranychidae) atacando arroz en Venezuela. *Agronomía Tropical* 26: 159–165.
- Attiah HH (1967) Two new species of mites on figs, from Egypt (Acarina). *Bulletin de la Societe Entomologique D Egypte* 51: 1–24.
- Bagdasarian AT (1954) New species of tetranychid mites from Armenia *Doklady Akademii Nauk Armyanskoi SSR Erevan* 18(2): 51–56. [in Russian]
- Baker EW, Pritchard AE (1960) The tetranychoid mites of Africa. *Hilgardia* 29(11): 455–574. <https://doi.org/10.3733/hilg.v29n11p455>
- Baker EW, Tuttle DM (1994) A guide to the spider mites (Tetranychidae) of the United States, 347 pp.

- Banks N (1917) New Mites, mostly economic (Arach., Acar.). Entomological News 28: 193–199.
- Beer RE, Lang DS (1958) The Tetranychidae of Mexico. The University of Kansas Science Bulletin 38(2): 1231–1259. <https://doi.org/10.5962/bhl.part.10974>
- Beglyarov GA, Mitrofanov VI (1973) New species of the genus *Schizotetranychus* from Vladivostok area. Biological Revue. Zoology: Analysis of Complex Systems, ZACS 6: 16–22.
- Bolland R, Gutierrez J, Flechtmann CHW (1998) World Catalogue of the Spider Mite Family (Acarina: Tetranychidae). Brill, Leiden, 392 pp.
- Davis JJ (1969) Studies of Queensland Tetranychidae (Acarina: Prostigmata) 6. A new genus and five new species of spider mites from native plants. Memoirs of the Queensland Museum 15: 165–183.
- Ehara S (1957) On three spider mites of *Schizotetranychus* from Japan. Journal of the Faculty of Sciences, Hokkaido University, Series VI. Zoology: Analysis of Complex Systems, ZACS 13: 15–23.
- Ehara S (1965) Two new species of *Eotetranychus* from Shikoku, with notes on *E. kankitus* Ehara (Acarina: Tetranychidae). Journal of the Faculty of Sciences, Hokkaido University, Series VI. Zoology: Analysis of Complex Systems, ZACS 15: 618–624.
- Ehara S (1973) Three species of the genus *Schizotetranychus* (Acarina, Tetranychidae). Annotations Zoological Japanese's 46(4): 224–232.
- Ehara S (1989) Four new species of spider mites (Acarina: Tetranychidae) from Japan. Proceedings of the Japanese Society of Systematic Zoology 40: 28–38.
- Ehara S (1999) Revision of the spider mite family Tetranychidae of Japan (Acarina, Prostigmata). Species Diversity: An International Journal for Taxonomy, Systematics, Speciation, Biogeography, and Life History Research of Animals 4(1): 63–141. <https://doi.org/10.12782/specdiv.4.63>
- Ehara S, Ohashi K (2005) A new spider mite species of *Schizotetranychus* (Acarina: Prostigmata: Tetranychidae) from *Quercus gilva* in Japan. Zootaxa 884(1): 1–5. <https://doi.org/10.11646/zootaxa.884.1.1>
- Ehara S, Tho YP (1988) Spider mites of the Malay Peninsula (Acarina: Tetranychidae). The Journal of the Faculty of Education, Tottori University. Nature and Science 37: 1–24.
- Ehara S, Wongsiri T (1975) The spider mites of Thailand (Acarina: Tetranychidae). Mushi 48(13): 149–185.
- Feres RJ, Flechtmann CH (1995) Mites (Acarina) associated with bamboo (*Bambusa* sp., Poaceae) in a woody area from Northwestern São Paulo State, Brazil. Revista Brasileira de Zoologia 12(3): 533–546. <https://doi.org/10.1590/S0101-81751995000300008>
- Flechtmann CH (2012) *Schizotetranychus*-like spider mites (Acarina, Prostigmata, Tetranychidae)-revisited, new combinations and a key to groups of *Schizotetranychus* based on females. Acarologia 52(1): 87–95. <https://doi.org/10.1051/acarologia/20122039>
- Flechtmann CH, Baker EW (1970) A preliminary report on the Tetranychidae (Acarina) of Brazil. Annals of the Entomological Society of America 63(1): 156–163. <https://doi.org/10.1093/aesa/63.1.156>
- Flechtmann CHW, Baker EW (1975) A report on the Tetranychidae (Acarina) of Brazil. Revista Brasileira de Entomologia 19: 111–122.
- Flechtmann CH, Peralta-Alba LE (2012) A new species of *Schizotetranychus* (Acarina, Prostigmata, Tetranychidae) from the Chilean fauna, with a few remarkable morphological features. Systematic and Applied Acarology 17(2): 231–238. <https://doi.org/10.11158/saa.17.2.10>

- Flechtmann CHW, Kreiter S, Etienne J, De Moraes GJ (1999) Plant mites (Acari) of the French Antilles. 1. Tetranychoida (Prostigmata). *Acarologia* 40(2): 137–144.
- Garman P (1940) Tetranychidae of Connecticut. Bulletin of the Connecticut Agricultural Experimental Station 431: 67–88.
- Goux L (1949) Etude d un *Schizotetranychus* nouveau de la région Lyonnaise (Acar. Tetranychidae). Bulletin de la Société Linnéenne de Lyon 18: 100–104. <https://doi.org/10.3406/linly.1949.8556>
- Gupta YN (1980) Some spider mites (Acarina: Tetranychidae) from Andaman, Nicobar Islands with descriptions of three new species. Records of the Zoological Survey of India 77(1–4): 111–117. <https://doi.org/10.26515/rzsi/v77/i1-4/1979/161847>
- Gupta SK, Gupta YN (1994) A taxonomic review of Indian Tetranychidae (Acari: Prostigmata) with description of new species, redescription of known species, keys to genera and species. Memoirs of the Zoological Survey of India 18: 1–196.
- Gutierrez J (1968) New Tetranychidae from Madagascar (4th note). *Acarologia* 10(1): 13–28.
- Gutierrez J (1978) Five new species of Tetranychidae (mites) from New Caledonia. *Acarologia* 20(3): 351–364.
- Hirst S (1924) LV. On some new species of red spider. *Annals, Magazine of Natural History*, (ser. 9) 14: 522–527. <https://doi.org/10.1080/00222932408633151>
- Hirst S (1926) Descriptions of New Mites, including four New Species of “Red Spider.”. *Proceedings of the Zoological Society of London* 96(3): 825–841. <https://doi.org/10.1111/j.1469-7998.1926.tb07130.x>
- Hoy MA (2011) *Agricultural acarology: introduction to integrated mite management*. CRC P Inc: 1– 430.
- Jeppson LR, Keifer HH, Baker EW (1975) *Mites injurious to economic plants*. University of California Press, Berkeley, 614 pp. <https://doi.org/10.1525/9780520335431>
- Livshitz IZ, Mitrofanov VI (1968) New species of red and false spider mites (Acarina, Tetranychidae) from the Crimea. *Rev. Entomol URSS* 47(3): 671–682. [in Russian]
- Mahdavi SM, Asadi M (2015) A new species of *Schizotetranychus* (Acari, Tetranychidae) from Iran. *Systematic and Applied Acarology* 20: 674–680. <https://doi.org/10.11158/saa.20.6.9>
- Manson DCM (1967) The spider mite family Tetranychidae in New Zealand. III. The genus *Schizotetranychus*. *Acarologia* 9(4): 823–840.
- McGregor AE (1928) Descriptions of two new species of spinning mites. *Proceedings of the Entomological Society of Washington* 30(1): 11–15.
- McGregor EA (1950) Mites of the family Tetranychidae. *American Midland Naturalist* 44(2): 257–420. <https://doi.org/10.2307/2421963>
- Meyer MKPS (1965) South African Acarina I. Nine species of the subfamily Tetranychidae collected on wild plants. *Koedoe* 8(1): 82–94. <https://doi.org/10.4102/koedoe.v8i1.787>
- Meyer MKPS (1974) A revision of the Tetranychidae of Africa (Acari) with a key to the genera of the world. *Entomology Memoir, Department of Agricultural Technical Services, Republic of South Africa*, 291 pp.
- Meyer MKPS (1987) African Tetranychidae (Acari: Prostigmata) – with reference to the world genera. *Entomology Memoir, Department of Agriculture, Water Supply, Republic of South Africa* 69: 1–175.
- Migeon A, Dorkeld F (2006–2024) Spider Mites Web: a comprehensive database for the Tetranychidae. <https://www1.montpellier.inrae.fr/CBGP/spmweb> [Accessed 30/04/2024]
- Mitrofanov VI (1978) New species of *Schizotetranychus* mites (Acarina, Tetranychidae) from the Crimea. *Nauchnye Doklady Vysshei Shkoly. Biologicheskie Nauki* 6: 44–47.

- Mushtaq HMS, Alatawi FJ, Kamran M, Flechtmann CHW (2021) The genus *Oligonychus* Berlese (Acari, Prostigmata, Tetranychidae): Taxonomic assessment and a key to subgenera, species groups, and subgroups. *ZooKeys* 1079: 89–127. <https://doi.org/10.3897/zookeys.1079.75175>
- Mustafa G, Chaudhri WM, Yunus M (1972) Bionomics of a new sugarcane mite, *Schizotetranychus mustafaii* Mustafa, Chaudhri. *Sind University Research Journal (Pakistan)* 6: 107–117.
- Naing HH, Chandrapatya A, Navajas M, Auger P (2014) New species, new records of Tetranychidae (Acarina, Prostigmata) from Thailand. *Zootaxa* 3802(2): 257–275. <https://doi.org/10.11646/zootaxa.3802.2.7>
- Ochoa R, Gray B, von Lindeman G (1990) E1 Genero *Schizotetranychus* Trägårdh (Acari: Tetranychidae) en Costa Rica y Panama. *Turrialba (Costa Rica)* 40(2): 210–216.
- Oudemans AC (1928) Acarological notes. *Entomological Messages* 7(159): 285–293.
- Paschoal AD (1971) New list of plant mites from Brazil. *Peruvian Journal of Entomología* 14(1): 174–176.
- Pritchard AE, Baker EW (1955) A revision of the spider mite family Tetranychidae. *Memoirs Series, San Francisco, Pacific Coast Entomological Society*, 472 pp. <https://doi.org/10.5962/bhl.title.150852>
- Reck H (1941) Eine neue *Schizotetranychus*-Art (Tetranychida, Acari). *Soobscenija Akademii Nauk Gruzinskoj SSR* 2(5): 449–452.
- Reck GF (1947) New species of spider mites from Gruzii. *Soobscenija Akademii Nauk Gruzinskoj SSR* 8(7): 471–475. [in Russian]
- Reck GF (1948) Fauna of spider mites (Tetranychidae, Acari) from Georgia. *Trudy Zoologicheskogo Instituta Akademia Nauk Gruzinskoj SSR* 8: 175–185.
- Reck GF (1953) Research investigation on the fauna of the Tetranychidae in Georgia. *Trudy Instituta Zoologii. Akademiya Nauk Gruzinskoj SSR*. 11: 161–181. [in Russian]
- Reck GF (1956) Novye vidy tetranihovyh klescej is Vostocnoj Gruzii *Trudy Instituta Zoologii. Akademiya Nauk Gruzinskoj SSR* 15: 5–28.
- Reck GF (1959) A key to the tetranychoid mites. *Fauna Trans. Caucasia Akad Nauk Gruz Tbilissi, Akademii Nauk Gruzinskoj SSR* 1: 152.
- Rimando LC (1962) Four new species of spider mites of the genera *Eotetranychus* and *Schizotetranychus* (Tetranychidae, Acarina). *Philippine Agriculturist* 14(10): 535–544.
- Rossi De Simons NH (1966) Descripción de *Schizotetranychus oryzae* sp. n. (Acari - Tetranychidae). *Revista Investigación Agropecuaria* 3: 1–10.
- Sadana GL, Gupta BK, Goyal M (1985) Tetranychoid mites infesting vegetables in Punjab with description of two new species. *Annals of Biology* 1(2): 157–164.
- Saito Y, Mori K, Sakagami T, Lin J (2004) Reinstatement of the genus *Stigmaeopsis* Banks, with descriptions of two new species (Acari, Tetranychidae). *Annals of the Entomological Society of America* 97(4): 635–646. [https://doi.org/10.1603/0013-8746\(2004\)097\[0635:ROTGSB\]2.0.CO;2](https://doi.org/10.1603/0013-8746(2004)097[0635:ROTGSB]2.0.CO;2)
- Saito Y, Zhang YX, Mori K, Ito K, Sato Y, Chittenden AR, Lin JZ, Chae Y, Sakagami T, Sahara K (2016) Variation in nesting behavior of eight species of spider mites, *Stigmaeopsis* having sociality. *Naturwissenschaften* 103(9–10): 10. <https://doi.org/10.1007/s00114-016-1408-6>
- Saito Y, Yukie Sato AR, Chittenden JZL, Zhang YX (2018) Description of two new species of *Stigmaeopsis*, Banks 1917 (Acari, Tetranychidae) inhabiting *Miscanthus* grasses (Poaceae). *Acarologia* 58(2): 414–429. <https://doi.org/10.24349/acarologia/20184250>

- Saito Y, Sato Y, Kongchuensin M, Chao JT, Sahara K (2019) New *Stigmaeopsis* species on *Miscanthus* grasses in Taiwan and Thailand (Acari, Tetranychidae). *Systematic and Applied Acarology* 24(4): 675–682. <https://doi.org/10.11158/saa.24.4.12>
- Stoll O (1886) *Arach. Acarol. Biol. Cent. Am.*: 1–53.
- Trägårdh I (1915) Bidrag till kännedomen om spinnvalstren (*Tetranychus* Duf.). *Medd Centralanst Försöks Jordbr* 109 (Entomol. Avd. 20): 1–60.
- Tseng YH (1975) Systematics and distribution of the phytophagous mites of Taiwan, Part I. A revision of the mite family Tetranychidae, with an illustrated key to the genera of the world. *Plant Quarantine Bulletin, Bureau of Commodity Inspection and Quarantine, Ministry of Economic Affairs, Republic of China* 10: 1–132.
- Tseng YH (1990) A monograph of the mite family Tetranychidae (Acarina: Trombidiformes) from Taiwan. *Taiwan Museum Special Publication, Series 9*, 226 pp.
- Tuttle DM, Baker EW (1964) The spider mites of Arizona (Acarina: Tetranychidae). *Agricultural Experiment Station, University of Arizona, Technical Bulletin* 158: 1–41.
- Tuttle DM, Baker EW (1968) Spider mites of southwestern United States and a revision of the family Tetranychidae. *The University of Arizona Press, Tucson*, 143 pp.
- Tuttle DM, Baker EW, Abbatial MJ (1976) Spider mites of Mexico (Acari: Tetranychidae). *International Journal of Acarology* 2(2): 1–102. <https://doi.org/10.1080/01647957608683760>
- Ugarov AA, Nikolskii VV (1937) Systematic study of spider mites from Central Asia. *Trudy Uzbekistanskoi Opytnoi Stantsii Zashchity Rastenii (Tashkent)* 2: 26–64.
- Wainstein BA (1954) Fauna of spider mites injurious to orchards in South Kazakhstan. *Zoologicheskii Journal [Зоологический журнал]* 33(3): 561–564.
- Wainstein BA (1956) Material on the fauna of tetranychid mites of Kazakhstan. *Tr. Resp. St. Zashch. Rast. Kazifilial Vaskhnil* 3: 70–83.
- Wainstein BA (1958) A contribution to the knowledge of the fauna and the taxonomy of spider mites (Acariformes, Tetranychida) *Review of Entomology, URSS* 37(2): 455–459.
- Wainstein BA (1960) Tetranychoid mites of Kazakhstan (with revision of the family). *Kazakhskaja Akademiia Sel'skogo Instituta Zashchity Rastenii Trudy* 5: 1–276. [In Russian]
- Wang HF (1981) *Schizotetranychus* from China with a new species (Acarina: Tetranychidae). *Sinozoologia* 1(1): 113–116.
- Wang HF (1983) Two new species of the genus *Schizotetranychus* from Sichuan (Acarina: Tetranychidae). *Dong Wu Fen Lei Xue Bao* 8: 262–266.
- Wang HF, Cui YQ (1991) Three new species of Tetranychidae from the Hengduan Mountains, China (Acari: Tetranychidae). *Dong Wu Fen Lei Xue Bao* 16(3): 304–312.
- Wang HF, Zhang XM, Zhang KC (1985) A preliminary survey of tetranychid mites in Fujian with description of a new species (Acariformes: Tetranychoida). *Wuyi Science Journal* 5: 89–93.
- Yusof O, Zhang ZQ (2003) Discovery of *Tenuipalponychus* (Acari: Tetranychidae) in Malaysia and description of a new species. *Zootaxa* 231: 1–8. <https://doi.org/10.11646/zootaxa.231.1.1>
- Zacher (1913) Injurious status of *Schizotetranychus schizopus* (Acari: Tetranychidae) on Indian Thorny Bamboo. *Systematic and Applied Acarology* 26(2): 343–352.
- Zaher MA, Gomaa EA, El-Enany MA (1982) Spider mites of Egypt (Acari: Tetranychidae). *International Journal of Acarology* 8(2): 91–114. <https://doi.org/10.1080/01647958208683284>

New species of *Eupolyphaga* Chopard, 1929 and *Pseudoeupolyphaga* Qiu & Che, 2024 (Blattodea, Corydioidea, Corydiinae), with notes on their female genitalia

Wei Han^{1,2}, Yan-Li Che^{1,2}, Pei-Jun Zhang^{1,2}, Zong-Qing Wang^{1,2}

¹ College of Plant Protection, Southwest University, Chongqing 400715, China

² Key Laboratory of Agricultural Biosafety and Green Production of Upper Yangtze River (Ministry of Education), Southwest University, Chongqing 400715, China

Corresponding author: Zong-Qing Wang (zqwang2006@126.com)

Abstract

Two new species of *Eupolyphaga* (*E. bicolor* Han, Che & Wang, **sp. nov.** and *E. nigra* Han, Che & Wang, **sp. nov.**) and six new species of *Pseudoeupolyphaga* (*P. flava* Han, Che & Wang, **sp. nov.**, *P. deficiens* Han, Che & Wang, **sp. nov.**, *P. magna* Han, Che & Wang, **sp. nov.**, *P. longiseta* Han, Che & Wang, **sp. nov.**, *P. latizona* Han, Che & Wang, **sp. nov.**, and *P. baimaensis* Han, Che & Wang, **sp. nov.**) are described and illustrated. The female external genitalia and spermathecae of these two genera are reported and the role of these characters in species delimitation is discussed.

Key words: Cockroach, Dictyoptera, Polyphagini, spermatheca



Academic editor: Fred Legendre

Received: 1 June 2024

Accepted: 23 July 2024

Published: 4 September 2024

ZooBank: <https://zoobank.org/F918E1DE-ADA2-47B6-A711-EEA23DA861B7>

Citation: Han W, Che Y-L, Zhang P-J, Wang Z-Q (2024) New species of *Eupolyphaga* Chopard, 1929 and *Pseudoeupolyphaga* Qiu & Che, 2024 (Blattodea, Corydioidea, Corydiinae), with notes on their female genitalia. ZooKeys 1211: 151–191. <https://doi.org/10.3897/zookeys.1211.128805>

Copyright: © Wei Han et al.

This is an open access article distributed under terms of the Creative Commons Attribution License (Attribution 4.0 International – CC BY 4.0).

Introduction

Eupolyphaga was once the most diverse genus of Corydioidea in China, containing 22 species and four subspecies (Han et al. 2022). Combined with morphological characteristics and phylogenetic reconstruction results, Han et al. (2024) revised *Eupolyphaga* and transferred most of the species to *Pseudoeupolyphaga* Qiu & Che, 2024. Therefore, only seven species are now included in *Eupolyphaga*, and 15 species and four subspecies are included in *Pseudoeupolyphaga*.

For a long time, the species identification of the two genera was mainly based on some male external morphology (body color, size, maculae distribution in tegmina) and the shape of ootheca serrations (Chopard 1922, 1929; Feng and Woo 1988; Woo and Feng 1992; Qiu et al. 2018; Han et al. 2022). Female characters, such as spermatheca, basivalvula, and spermathecal plate can help to distinguish between *Pseudoeupolyphaga* from *Eupolyphaga* (Han et al. 2024). To determine whether these female characters could be used for species identification, more samples are needed to evaluate their reliability. In addition to morphological characterization, molecular data have also been used for species delimitation in the two genera and have proven to be effective and appropriate (Han et al. 2022).

Following a recent collection, we found that some specimens collected from Yunnan and Sichuan provinces showed high morphological resemblance to some of the known *Pseudoeupolyphaga* species, while also presenting subtle differences. For example, a male specimen from Guanyinqiao Township of Sichuan exhibited external morphology similar to *P. yunnanensis* (Chopard, 1922), although the former is notably larger in body size. Similarly, some male specimens from Tazigou closely resembled *P. simila* (Qiu, 2022), but the former has significantly shorter tegmina and hind wings. Whether these differences are interspecific or intraspecific variation also needed to be clarified.

Therefore, in this study, we combined morphological characters and molecular data to delimit species of *Eupolyphaga* and *Pseudoeupolyphaga*. We describe two new species of *Eupolyphaga* and six new species of *Pseudoeupolyphaga*, provide illustrations of female genitalia and spermathecae, and discuss the taxonomic significance of these female characters. This helps to explore the diversity of *Eupolyphaga* and *Pseudoeupolyphaga* and provides a basis for identifying females of these two genera.

Materials and methods

Material

All specimens studied in this article are deposited in College of Plant Protection, Southwest University, Chongqing, China (SWU). The terminology used in this article mainly follows Roth (2003) (external morphology), Klass (1997) (male genitalia) and McKittrick (1964) (female genitalia). The formulation “median sclerites” follows Qiu et al. (2018). The terminal three or four segments of the abdomen were excised and immersed in a 10% NaOH solution and heated for 30 min to eliminate fat. Subsequent procedures, including morphological dissection of males, DNA extraction, and PCR and sequencing, adhere to the methodology outlined by Han et al. (2022).

Sequence processing and phylogenetic analyses

A total of 42 sequences were analyzed, comprising 40 in-group and 2 out-group sequences [*Eucorydia dasytoides* (Walker, 1868) and *Diploptera punctata* (Eschscholtz, 1822)], as detailed in Table 1. All 21 newly acquired sequences have been submitted to GenBank (<https://www.ncbi.nlm.nih.gov/nucleotide>) with accession numbers PQ059675 to PQ059695. Alignment of all COI fragments was performed using the MUSCLE algorithm within MEGA 11 (Kumar et al. 2016), ensuring translatability into protein sequences. Genetic distances, both interspecific and intraspecific, were computed employing the Kimura 2-parameter model (Kimura 1980). PartitionFinder v. 2.1.1 (Lanfear et al. 2017) was utilized to determine the optimal partitioning scheme and substitution models with default parameters (COI_pos 1: SYM+I+G; COI_pos 2: GTR+I+G; COI_pos 3: GTR+G). Maximum-likelihood analysis involved ten independent likelihood searches, selecting the highest likelihood result. Node and branch supports were assessed via IQ-TREE v. 2.2.0 (Nguyen et al. 2015) employing 10,000 ultrafast bootstrap (UFBoot) replicates. Additionally, the “-bnni” option was employed to mitigate severe model violations.

Table 1. Samples used in species delimitation.

Species	Abbreviation	GenBank ID	Collecting information	Remark
<i>P. baimaensis</i> sp. nov.	PseuBaim	PQ059685	Baima Village, Sichuan; 4 Aug. 2019; Lu Qiu	male
<i>P. latizona</i> sp. nov.	PseuLatiSM	PQ059683	Caoke Village, Sichuan; 20 Jul. 2022; Wei Han, Xin-Xing Luo	female
	PseuLatiDB1	PQ059691	Danba County, Sichuan; 12 Jul. 2017; Jian-Yue Qiu, Hao Xu	male
	PseuLatiDB2	PQ059692	Jiaju Zangzhai, Sichuan; 12 Jul. 2017; Jian-Yue Qiu, Hao Xu	male
<i>P. longiseta</i> sp. nov.	PseuLong1	PQ059684	Baima Snow Mountain, Sichuan; 27 Jul. 2020; Wei Han, Xin-Xing Luo, Lin Guo	female
	PseuLong2	PQ059677	Baima Snow Mountain, Sichuan; 27 Jul. 2020; Wei Han, Xin-Xing Luo, Lin Guo	nymph
<i>P. flava</i> sp. nov.	PseuFlav	PQ059689	Liude Village, Yunnan; 9 Jul. 2021; Lu Qiu, Hao Xu	female
<i>P. magna</i> sp. nov.	PseuMagn	PQ059688	Jinchuan County, Sichuan; 2020; Jian-Yue Qiu	male
<i>P. deficiens</i> sp. nov.	PseuDefiHS	PQ059687	Heishui County, Sichuan; 22 Jun. 2021; Lu Qiu, Hao Xu	nymph
	PseuDefiCJS	PQ059686	Cuoji Mountain, Sichuan; 6 Aug. 2019; Lu Qiu	female
<i>P. fusca</i>	PseuFusc1	PQ059678	Cang Mountain, Yunnan; 29 Jul. 2022; Wei Han, Xin-Xing Luo	nymph
	PseuFusc2	PQ059680	Cang Mountain, Yunnan; 29 Jul. 2022; Wei Han, Xin-Xing Luo	male
<i>P. pilosa</i>	PseuPiloLDT	PQ059681	Luodatang countryside, Yunnan; 25 Jul. 2022; Wei Han, Xin-Xing Luo, Lin Guo	female
	PseuPiloWBS	PQ059690	Wenbi Mountain, Yunnan; 24 Jul. 2022; Wei Han, Lin Guo	male
	PseuPiloYL	PQ059682	Lanyue Valley, Yunnan; 24 Jul. 2022; Wei Han, Lin Guo	male
	PseuPiloWX	OP215882	/	/
<i>P. fengi fengi</i>	PseuFengZXS	PQ059693	Zixi Mountain, Yunnan; 31 Jul. 2022; Wei Han, Xin-Xing Luo	female
	PseuFengDHS	PQ059679	Dahei Mountain, Sichuan; 22 Jul. 2022; Wei Han, Xin-Xing Luo	female
	PseuFeng1	OP215870	/	/
	PseuFeng2	OP215871	/	/
<i>P. simila</i>	PseuSimiMYL	OP215883	/	/
	PseuSimiDGC	PQ059676	Dagou Village, Li County, Sichuan; 22 Apr. 2023; Wei Han	male
	PseuSimiTZG	PQ059675	Tazigou, Parktou Township, Li County, Sichuan; 18 Apr. 2023; Wei Han	male
<i>P. dongi</i>	PseuDong	OP215872	/	/
<i>P. nigrinotum</i>	PseuNigr	OP215879	/	/
<i>P. wooi</i>	PseuWooi	OP215874	/	/
<i>P. daweishana</i>	PseuDawe	OP215877	/	/
<i>P. yunnanensis</i>	PseuYunnTM	OP215869	/	/
	PseuYunnCY	OP215865	/	/
	PseuYunnBM	OP215866	/	/
<i>P. reducta</i>	PseuRedu	OP215886	/	/
<i>P. xuorum</i>	PseuXuor	OP215875	/	/
<i>E. sinensis</i>	EupoSine	OP215846	/	/
<i>E. hanae</i>	EupoHana	OP215849	/	/
<i>E. hupingensis</i>	EupoHupi	OP215854	/	/
<i>E. robusta</i>	EupoRobu	OP215856	/	/
<i>E. miracidia</i>	EupoMira	OP215878	/	/
<i>E. udenostyla</i>	EupoUden	OP215887	/	/
<i>E. bicolor</i> sp. nov.	EupoBico	PQ059694	Guiling, Guangxi; 14 Feb. 2023; Hao-Fei Fan	male
<i>E. nigra</i> sp. nov.	EupoNigr	PQ059695	Zhubu Village, Guangxi; 7 Jul. 2023; Wei Han, Xin-Ran Li	male
Outgroup				
<i>Eucoyrdia dasytoides</i>	EucoDasy	LC480880	/	/
<i>Diploptera punctata</i>	DiplPunc	MF479156	/	/

Results

Molecular analysis based on COI

The alignment of the 42 COI sequences encompasses a total of 660 nucleotide sites, with intra- and interspecific distances detailed in Suppl. material 3. The interspecific genetic distances between species in *Eupolyphaga* range from 9.8% (between *E. hanae* Qiu, Che & Wang, 2018 and *E. robusta* Qiu, Che & Wang, 2018) to 20.86% (between *E. sinensis* (Walker, 1868) and *E. nigra* sp. nov.). In *Pseudoeupolyphaga*, we found similar interspecific variations, with the largest interspecific distance recorded at 20.90% between *P. yunnanensis* and *P. latizona* sp. nov., and the smallest at 6.61% between *P. pilosa* (Qiu, Che & Wang, 2018) and *P. fusca* (Chopard, 1929). In terms of intraspecific genetic distance, a maximum of 7.54% was observed between samples from Wenbi Mountain and Luodatang countryside of *P. pilosa*.

The phylogenetic tree of *Eupolyphaga* and *Pseudoeupolyphaga*, derived from the COI sequence, is depicted in Fig. 1. The maximum likelihood (ML) tree illustrates the monophyletic nature of species distinguished by morphology, although almost all the branches exhibit low support values and a few species were represented by a single terminal, so their respective monophyly was not tested.

Taxonomy

Genus *Eupolyphaga* Chopard, 1929

Eupolyphaga Chopard, 1929: 261; Bey-Bienko 1950: 283; Princis 1962: 53; Feng et al. 1997: 165; Qiu et al. 2018: 5; Han et al. 2024: 165.

Type species. *Polyphaga sinensis* Walker, 1868, by original designation.

Supplementary diagnosis. The external structure and male genitalia characteristics have been given and discussed in Qiu et al. (2018) and Han et al. (2024). So only female characteristics are added below: Supra-anal plate (TX) distinctly pubescent, with a slightly protruded posterior margin. Paraprocts (pp.) pubescent, the inner side extending to the middle in a curved hook. The two median sclerites generally wedged. Cerci short, not exceeding the posterior margin of supra-anal plate, setose and pubescent. Paratergites (pt.) irregularly-banded. Crosspiece (cp.) nearly transparent, with a small protuberance pointing toward the posterior lobes of valvifer II (sp.pl.). The base of posterior lobes of valvifer II fused with the anterior arch (aa.), forming into a circinate structure. Posterior lobes of valvifer II curved, the terminal part generally rounded. First valvule (v.I) long, basally connected to the basivalvula (bsv.) and spermathecal plate, gradually tapering from the base to the tip. Basal part of valvifer II (v.II) and valvifer III (v.III) enlargement apparent, apex part sharp. Basivalvula symmetrical, with generally flat anterior margins, curly lateral margin, and round posterior edge. Spermathecal plate well-sclerotized, with the middle of the trailing edge folding backwards, two lobes symmetrical. Spermatheca (sp.) consists of ampulla and spermathecal duct. The ampulla mostly globular, and the spermathecal duct usually bifurcated. Vestibular sclerite (vst.s) shaped like the letter "W", with protrusions on both sides and in the middle. Subgenital plate (SVII) densely setose, posterior margin protruded and the terminal part emarginate medially.

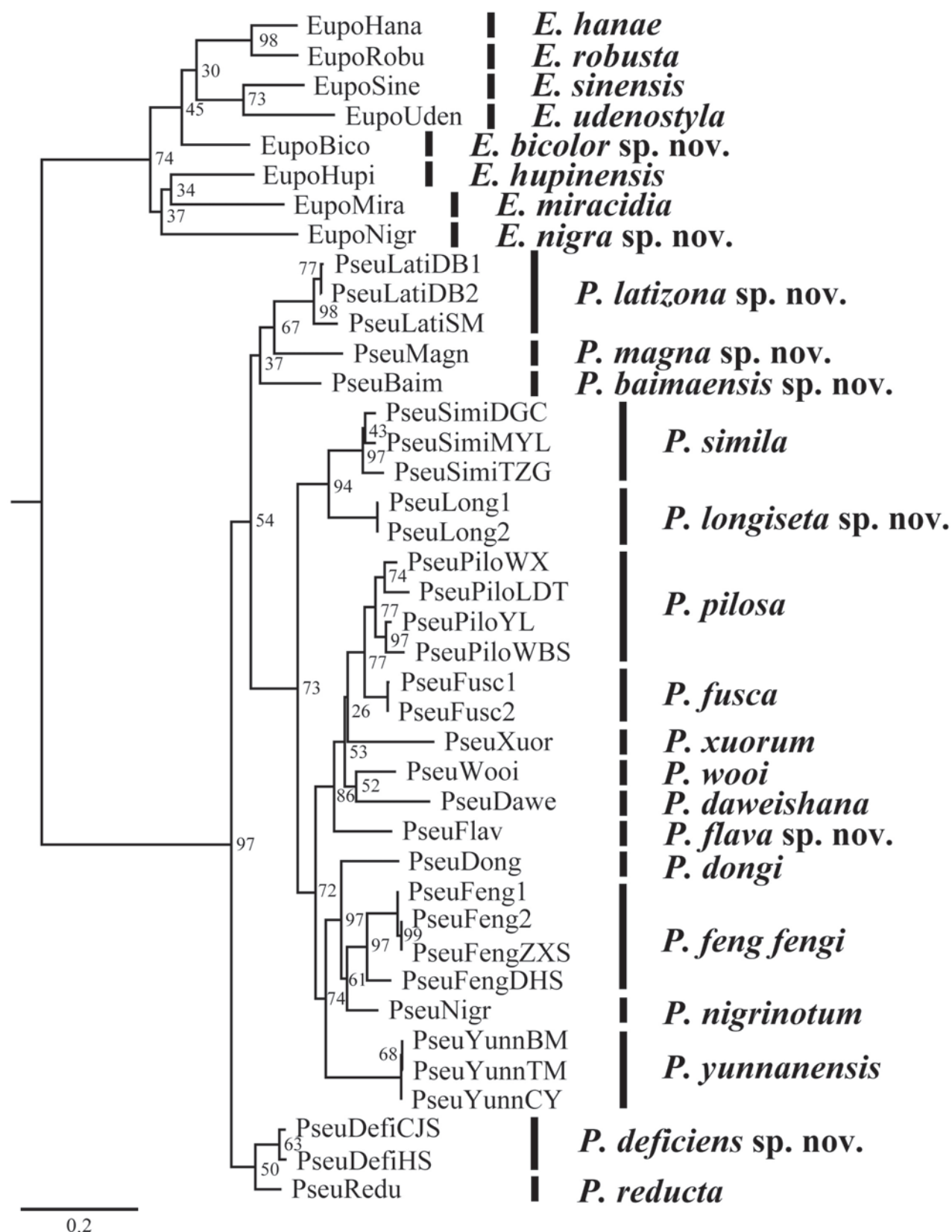


Figure 1. Phylogenetic tree of *Eupolyphaga* and *Pseudoepolyphaga* inferred by maximum-likelihood (ML) analysis of the mitochondrial COI fragment (outgroups not shown). UFBoot values are shown at the nodes.

***Eupolyphaga bicolor* Han, Che & Wang, sp. nov.**

<https://zoobank.org/34FF402F-9BF4-4C3C-8002-9D0AB626DC39>

Figs 2A–N, 4A, B, 5A, I

Type material. Holotype: CHINA • male; Guangxi Zhuang Autonomous Region, Guilin City; 14 Feb. 2023; Hao-Fei Fan leg. **Paratype:** CHINA • 1 female, same collection data as holotype.

Diagnosis. This species is smaller in male size compared to other congeneric species (body length 16.7–23.4 mm) except *E. miracidia* (12.1–12.5 mm). It resembles *E. sinensis* and *E. hanae* by its yellow abdomen, but it can be distinguished by its almost unicolored tegmina as well as black head and legs (Fig. 2A, B, G). In addition, the serrations on the keel of this species are distinctly more curved than those of *E. hanae*, and approximate those of *E. sinensis* and *E. miracidia*.

Description. Male holotype. Measurements (mm). Overall length (including tegmen): 23.51; body length: 15.96; body width (tegmina not included): 8.14; tegmen length × width: 19.66 × 7.77; pronotum length × width: 7.20 × 3.59.

Coloration. Head and face black. Ocelli pale yellowish. Antennal sockets white. Antenna blackish brown. Ante-clypeus whitish and subtransparent (Fig. 2G). Pronotum and tegmina yellowish brown. Hind wings pale brown. Legs black, coxa and trochanter slightly yellowish brown. Pulvilli and arolia white. Abdomen bright yellow (Fig. 2A, B).

Body. Head: Sub-rounded, hidden under the pronotum. Interocular space narrower than the distance between ocelli, and the latter narrower than the distance between antennal sockets. Ocelli distinct, ocelli ridge slightly curved, with a row of setae on the upper edge. Clypeus developed (Fig. 2G). **Pronotum:** Transverse oval, widest point near the middle. Anterior whitish margin indistinct. Surface covered with long setae (Fig. 2E). **Tegmina and hind wings:** Nearly unicolored, extending beyond the end of abdomen (Fig. 2A, B). **Legs:** Slender, front femur type C₁. Pulvilli and arolia present (Fig. 2B). **Abdomen:** Supra-anal plate transverse, pubescent, posterior margin protruded medially. Paraprocts simple. Cerci short. Subgenital plate densely setose along the lateral and posterior margins, the hind margin slightly concave in the middle. Styli small and short (Fig. 2I, J). **Genitalia:** Basal part of L1 prolonged, two hind lobes robust. L2 curved. Genital hook (L3) long, the hooked part curved. Right phallomere long. R1M expanded. R1L banded. R2 simple, the basis chunk rounded and the distal flat. R3 broad and concave (Fig. 2K, L).

Male paratype. Similar to the holotype, only legs slightly paler in color.

Female paratype. Body length: 22.25; body width: 15.25; pronotum length × width: 10.93 × 5.31.

Coloration. Terga reddish brown. Sterna dark reddish brown. Face black. Ocelli and ante-clypeus yellow. Antennal sockets white. The distal part of labrum pale yellow. Legs black, spines reddish black (Fig. 2C, D, F, H).

The widest point of the pronotum near the hind margin (Fig. 2F). Ocelli distinct, the interocular space larger than the distance between antennal sockets, and larger than the distance between the ocelli (Fig. 2H). Arolia and pulvilli absent. Posterior margin of the supra-anal plate (TX) protruded and emarginated medially. Cerci short, not exceeding the posterior margin of supra-anal plate. Paraprocts (pp.) pubescent, curved hook-like extensions long and robust.

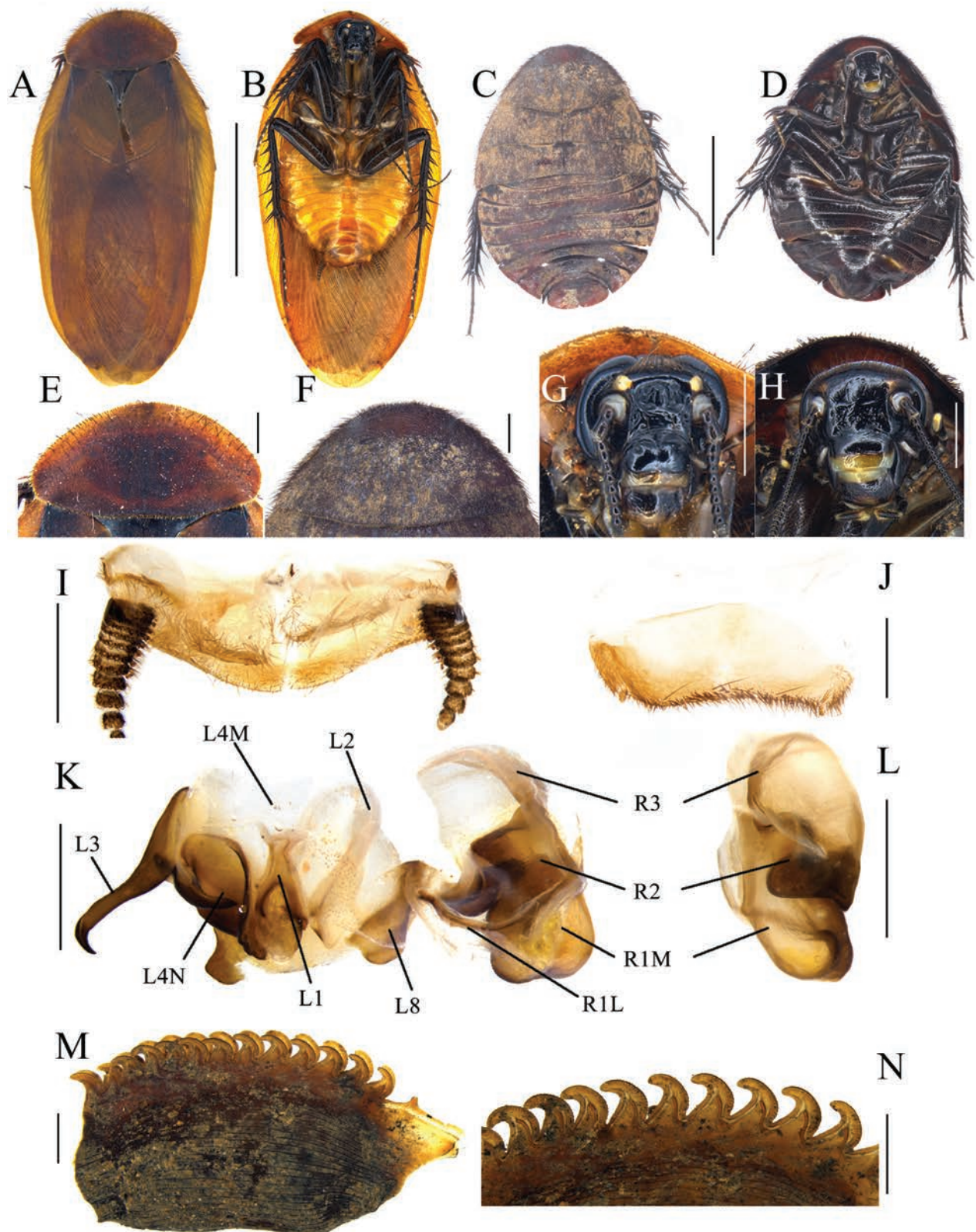


Figure 2. *Eupolyphaga bicolor* Han, Che & Wang, sp. nov. **A** male holotype, dorsal view **B** male holotype, ventral view **C** female paratype, dorsal view **D** female paratype, ventral view **E** male pronotum, dorsal view **F** female pronotum, dorsal view **G** male head, ventral view **H** female head, ventral view **I** supra-anal plate, ventral view **J** subgenital plate, ventral view **K** genitalia, dorsal view **L** right phallomere, right-ventral view **M** ootheca, lateral view **N** ootheca, close-up view to show the serration. Scale bars: 1.0 cm (**A–D**); 0.2 cm (**E–L**); 0.1 cm (**M, N**).

The two median sclerites present (Fig. 4A). Paratergites (pt.) banded, irregularly shaped. Crosspiece (cp.) weakly sclerotized, the protrusion long. Apex of posterior lobes of valvifer II (p.l.) slightly curved. Spermathecal plate (sp.pl.) narrow, concave in the middle, the two lobes each having an arch in the middle (Fig. 5A). The ampulla of spermatheca (sp.) large and spherical. The middle part and left part of spermathecal duct expanded. The right bifurcated duct expands and bifurcates again in the center, one of the bifurcated ducts connected to a small globular enlargement, while the other is curved and attached to several expansions (Fig. 5I). Basivalvula (bsv.) transverse, two lobes wide, anterior margin flat, lateral margin curly (Fig. 5A). Vestibular sclerite (vst.s.) shaped like a "W", with widened apices on both sides and a forked tip in the middle. Subgenital plate (SVII) densely setose, posterior margin protruded, slightly concave in the middle (Fig. 4B).

Nymph. Unknown.

Ootheca. Yellowish brown. The longitudinal lines distinct. Serrations on the keel large and curved. The space between the serrations of the curved portion distinct. Respiratory canals well developed (Fig. 1M, N).

Natural history. Found in the dry soil beside a cave entrance (Hao-Fei Fan pers. comm., Feb. 2023).

Etymology. The species epithet is derived from the Latin word *bicolor*, which indicates that males of this species have two distinct colors: blackish head and legs; yellowish tegmina, hind wings and abdomen.

***Eupolyphaga nigra* Han, Che & Wang, sp. nov.**

<https://zoobank.org/FE3E5490-7D2A-480C-9A25-A2A445DCADFC>

Figs 3A–N, 4C, D, 5B, J

Type material. Holotype: CHINA • male; Guangxi Zhuang Autonomous Region, Chongzuo City, Longzhou County, Zhubu Village, Buji Reservoir; 7 Jul. 2023; Wei Han, Xin-Ran Li leg. **Paratypes:** CHINA • 3 males, 1 female & 16 nymphs, same collection data as holotype.

Diagnosis. This species is almost black and is most similar to *E. robusta*. However, the abdomen of this species is unevenly scattered with some fulvous markings, whereas the abdomen of the latter is orange-yellow overall or dark yellow only on the two terminal segments. In addition, the middle part of terga of females of this species is slightly dark yellowish brown, whereas the terga of females of the latter is completely black; although serrations on the keel of both species are strongly curved, there are gaps between the serrated projections of the ootheca of this species, whereas there are almost no gaps in the latter.

Description. Male holotype. Measurements (mm). Overall length (including tegmen): 27.73; body length: 19.67; body width (tegmina not included): 10.03; tegmen length × width: 23.98 × 9.65; pronotum length × width: 8.13 × 4.79.

Coloration. Head and most of the face black. Ocelli and antennal sockets white. Antennae blackish brown. Ante-clypeus, basal part of the labrum, and a portion of the palate yellow (Fig. 3A, B, G). Pronotum, tegmina, hind wings and legs black. Pulvilli and arolia white. Abdomen black, with some fulvous markings (Fig. 3A, B).

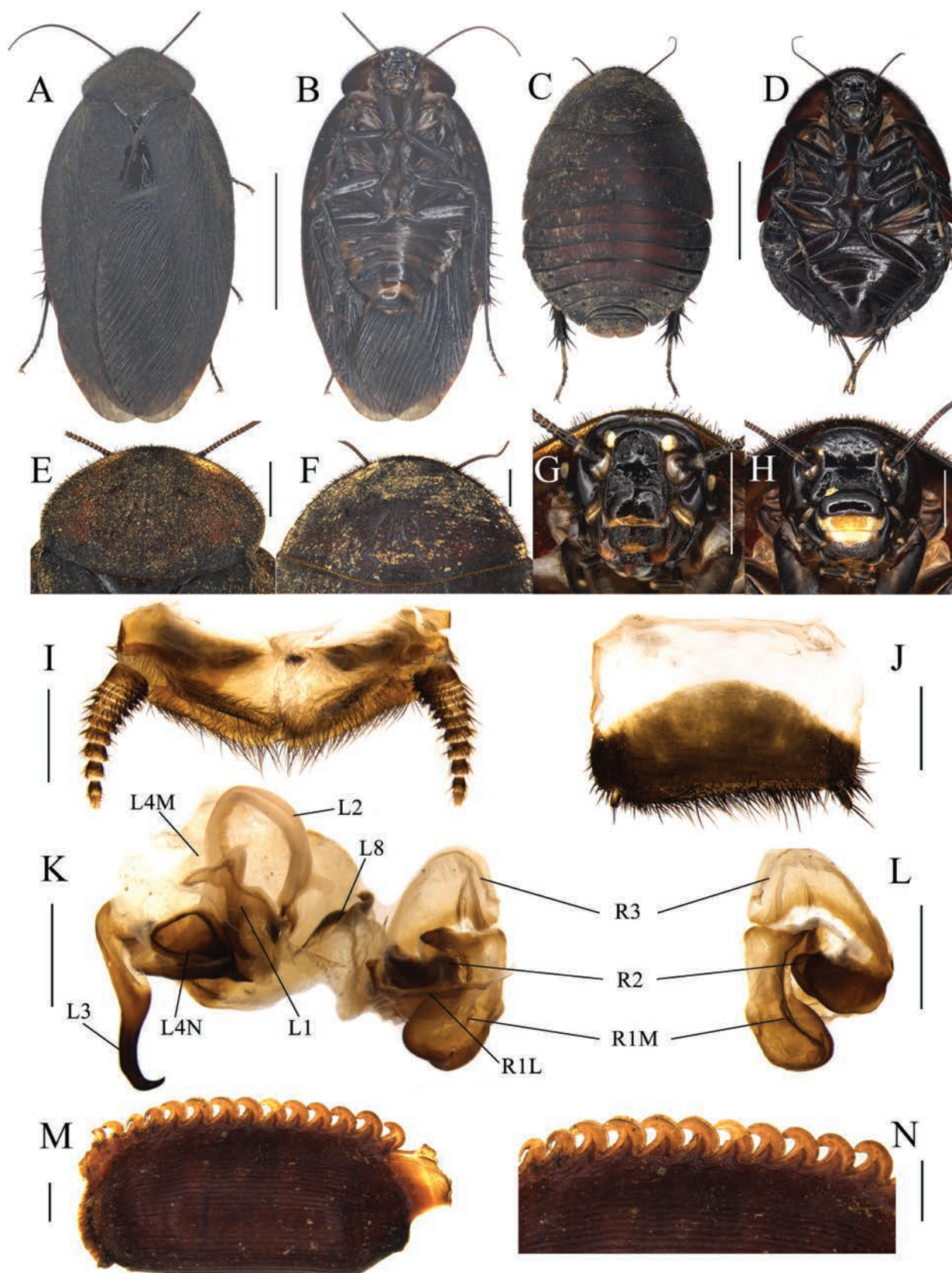


Figure 3. *Eupolyphaga nigra* Han, Che & Wang, sp. nov. **A** male holotype, dorsal view **B** male holotype, ventral view **C** female paratype, dorsal view **D** female paratype, ventral view **E** male pronotum, dorsal view **F** female pronotum, dorsal view **G** male head, ventral view **H** female head, ventral view **I** supra-anal plate, ventral view **J** subgenital plate, ventral view **K** genitalia, dorsal view **L** right phallomere, right-ventral view **M** ootheca, lateral view **N** ootheca, close-up view to show the serration. Scale bars: 1.0 cm (**A–D**); 0.2 cm (**E–L**); 0.1 cm (**M, N**).

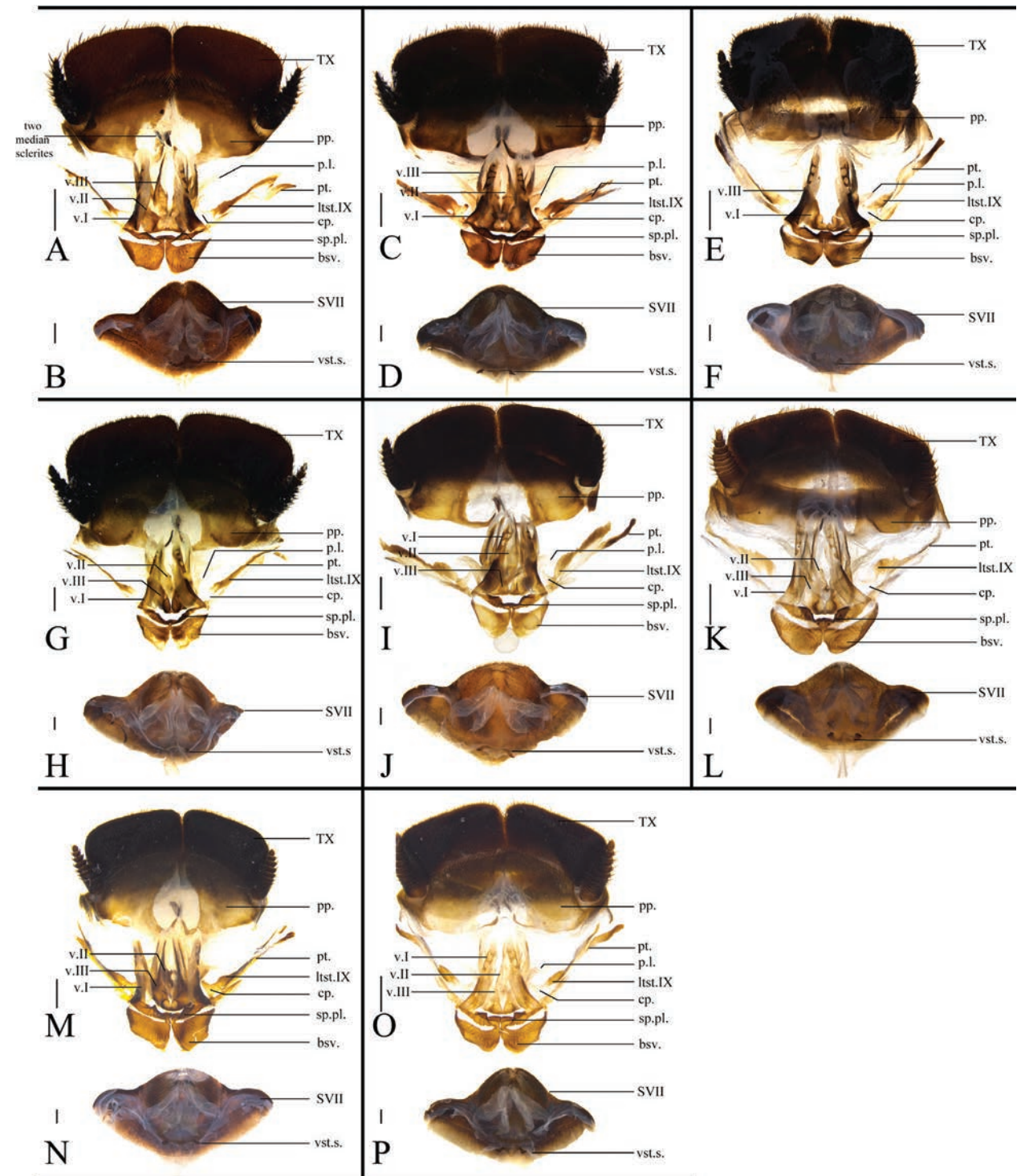


Figure 4. Female external genitalia of eight *Eupolyphaga* species (supra-anal plate and subgenital plate included) **A, B** *E. bicolor* Han, Che & Wang, sp. nov. **C, D** *E. nigra* Han, Che & Wang, sp. nov. **E, F** *E. udenostyla* Qiu, 2022 **G, H** *E. hupingensis* Qiu, Che & Wang, 2018 **I, J** *E. miracidia* Qiu, 2022 **K, L** *E. sinensis* (Walker, 1868) **M, N** *E. robusta* Qiu, Che & Wang, 2018 **O, P** *E. hanae* Qiu, Che & Wang, 2018. Abbreviations: bsv. basivalvula, cp. crosspiece, ltst. IX laterosternite IX, p.l. posterior lobes of valvifer II, pp. paraprocts, pt. paratergites, sp.pl. spermathecal plate, SVII subgenital plate, TX supra-anal plate, v.I first valvule, v.II second valve, v.III third valve, vst.s vestibular sclerite. Scale bars: 0.1 cm (**A–P**).

Body. Head: Sub-rounded, hidden under the pronotum. Interocular space narrower than the distance between the ocelli, and the latter narrower than the distance between the antennal sockets. Ocelli distinct. Ocelli ridge curved, with

a row of setae on the upper edge. Clypeus developed (Fig. 3B, G). **Pronotum:** Transverse oval, widest point near the middle. Anterior whitish margin indistinct. Surface covered with short setae (Fig. 3E). **Tegmina and hind wings:** Nearly unicolored, with a few plaques on both sides (Fig. 3A). **Legs:** Slender. Front femur type C₁. Pulvilli and arolia present (Fig. 3B). **Abdomen:** Supra-anal plate transverse, pubescent, posterior margin protruded. Paraprocts simple. Cerci pubescent. Posterior margin and lateral margins of subgenital plate densely setose, hind margin flat. Styli small, the right one bigger than the left (Fig. 3B, I–L). **Genitalia:** The basal part of L1 prolonged, and the two hind lobes robust. L2 curved. Genital hook (L3) long and robust, the hook part curved. Right phallosome smaller than the left phallosome. R2 simple, divided into two chunks. R3 broad and concave (Fig. 3K, L).

Female paratype. Body length: 27.79; body width: 19.12; pronotum length × width: 13.51 × 7.15.

Coloration. Terga dark yellowish brown to black. Sterna nearly black. Vertex and face black. Ocelli yellow. Basal part of labrum black. Distal part of labrum and ante-clypeus yellow. Legs black (Fig. 3C, D, F, H).

The widest point of pronotum near the hind margin (Fig. 3F). Ocelli distinct. Interocular space larger than the distance between antennal sockets, and the latter larger than the distance between ocelli (Fig. 3H). Arolia and pulvilli absent. Posterior margin of the supra-anal plate (TX) emarginated medially. Cerci short, not exceeding the posterior margin of supra-anal plate. Paraprocts (pp.) pubescent, curved hook-like extensions long. The two median sclerites irregularly shaped (Fig. 3C). Paratergites (pt.) banded, terminally bifurcated. Crosspiece (cp.) broad, the small protrusion short and wide. Posterior lobes of valvifer II (p.l.) short, terminal rounded. Spermathecal plate (sp.pl.) narrow and concave in the middle, the two lobes expanded in the middle (Fig. 5B). Spermatheca (sp.) consists of two distinct large ampullas, the bifurcated duct slightly expanded in the middle (Fig. 5J). Two lobes of basivalvula (bsv.) nearly triangular, with a flat anterior margin and a curly lateral margin. Vestibular sclerite (vst.s) shaped like the letter “W”, with widened apex on both sides and a robust, short protrusion in the middle. Subgenital plate (SVII) densely setose, posterior margin protruded (Fig. 3D).

Nymph. Similar to the female.

Ootheca. Yellowish brown. The longitudinal lines distinct. Serrations on the keel large and curved. The space between the serrations of the curved portion distinct. Respiratory canals well developed (Fig. 3M, N).

Natural history. Found in soft, dry soil under the cliffs near the reservoir.

Etymology. The species epithet is from the Latin *niger* indicating its black tegmina.

***Eupolyphaga udenostyla* Qiu, 2022**

Figs 4E, F, 5C, K

Eupolyphaga udenostyla Qiu in Han et al. 2022: 75.

Material examined. • 1 female; Sichuan Prov., Aba Prefecture, Wenchuan County, Keku Township; 7 Aug. 2019; Wei Han, Huan-Yu Ren leg • 1 female; same collection data as above, but 5 Oct. 2019; Lu Qiu leg • 4 females; Sichuan Prov.,

Aba Prefecture, Wenchuan County, mountains behind the 5.12 Wenchuan Earthquake Memorial Museum; Jul.–Aug. 2019; Qi Li leg.

Description on the female characters. Supra-anal plate (TX) black, densely covered with long brown setae. Paraprocts (pp.) pubescent, with thin and short curved hook-like extensions. Cerci short, not exceeding the posterior margin of the supra-anal plate. Paratergites (pt.) banded. Crosspiece (cp.) nearly transparent and the protrusion small. The first valvule (v.I) long, basal part connected to the spermathecal plate (sp.pl.). Basal of the second valvule (v.II) broad, terminal sharp. Basal part of the third valve (v.III) enlarged. Posterior lobes of valvifer II (p.I.) slightly sclerotized. The spermathecal plate narrow, arched in the middle. The anterior margin and hind margin of the two lobes have irregular protrusions. The spermatheca (sp.) consists of two distinct large ampullas. The basal ampulla connected to a long spermathecal duct; the middle part of the duct has a small globular enlargement. Basivalvula (bsv.) broad, with a flat anterior margin and a curly lateral margin. Vestibular sclerite (vst.s) shaped like the letter “W”, apically expanded in both sides, the tip of the central protuberance emarginated. The subgenital plate (SVII) densely setose, the terminal part of the posterior margin emarginated.

***Eupolyphaga hupingensis* Qiu, Che & Wang, 2018**

Figs 4G, H, 5D, L

Eupolyphaga hupingensis Qiu, Che & Wang, 2018: 18; Qiu et al. 2019: 11 (catalogue); Han et al. 2022: 88.

Material examined. • 1 female; Hunan Prov., Shaoyang City, Xinning County, Huanglong Town, Lizhu Village, Shunhuang Mountain, Zihua Ping; 24–25 May 2022; Lu Qiu leg.

Description of the female characters. Supra-anal plate (TX) black and densely covered with setae, the posterior margin slightly flat. Paraprocts (pp.) pubescent, curved hook-like extensions thin and long. The two median sclerites irregularly shaped. Cerci short, not exceeding the posterior margin of supra-anal plate. Paratergites (pt.) long and banded. Crosspiece (cp.) weakly sclerotized, barely visible. Posterior lobes of valvifer II (p.I.) short and robust. Spermathecal plate (sp.pl.) concave in the middle, with two narrow lobes. Spermatheca (sp.) consists of two distinct and large ampullas, the terminal ampulla larger. The duct bifurcated near the basal ampulla, and the bifurcated duct expands into a small ball in the middle. Basivalvula (bsv.) transverse, the two lobes nearly triangular, and the lateral margin curled. Subgenital plate (SVII) setose, the terminal part of the posterior margin flat and emarginated medially.

***Eupolyphaga miracidia* Qiu, 2022**

Figs 4I, J, 5E, M

Eupolyphaga miracidia Qiu in Han et al. 2022: 73.

Material examined. • 5 females; Hubei Prov., Xiangyang City, Maqiao Township, roadside of Ganxigou, 480–600 m; 13 Jul. 2017; Lu Qiu leg.

Description of the female characters. Supra-anal plate (TX) dark yellowish brown and densely covered with setae, posterior margin slightly protruded. Paraprocts (pp.) pubescent, curved hook-like extensions short. The two median sclerites irregularly shaped. Cerci short, not exceeding the posterior margin of supra-anal plate. Paratergites (pt.) long and banded. Crosspiece (cp.) nearly transparent, the protrusion long. Posterior lobes of valvifer II (p.l.) slightly sclerotized, two lobes long and curved. Spermathecal plate (sp.pl.) narrow, concave in the middle. The two lobes expanded, with irregular protrusions. Spermatheca (sp.) consists of two distinct, large ampullas. The basal ampulla connected to a long spermathecal duct, which is bifurcated in the middle. The terminal part of the duct slightly expanded. Basivalvula (bsv.) broad, with a relatively flat anterior margin and a curly lateral margin. Vestibular sclerite (vst.s) shaped like the letter “W”, with expanded and elongated ends on both sides. Subgenital plate densely setose, the terminal part of the posterior margin protruded and emarginated medially.

***Eupolyphaga sinensis* (Walker, 1868)**

Figs 4K, L, 5F, N

Polyphaga sinensis Walker, 1868: 14.

Homoeogamia sinensis: Saussure 1869: 282; Hollier et al. 2020: 347. Synonymized by Qiu et al. 2018.

Heterogamia sinensis: Dohrn 1888: 132.

Heterogamia dohrniana Saussure, 1893: 309; Hollier et al. 2020: 345.

Polyphaga limbata Kirby, 1903: 379.

Eupolyphaga sinensis: Chopard 1929: 262; Qiu et al. 2018: 5 (revision); Qiu et al. 2019: 11 (checklist); Han et al. 2022: 84.

Material examined. • 2 females; Beijing City, Haidian District, Beijing Xishan National Forest Park; 28 Apr. 2015; Bing–Qiang Wang leg • 1 female; Anhui Prov. Hefei City, Binhu County; 3 Oct. 2018; Lin Zhou leg • 1 female; Jiangsu Prov., Nanjing City, Xuanwu District, Zijin Mountain, Zhongshan Mausoleum; 18 Jul. 2021; Ya-Ning Sun, Yi-Fan Zhao leg.

Description on the female characters. Supra-anal plate (TX) dark yellowish brown and densely covered with setae, the posterior margin protruded medially. Paraprocts (pp.) pubescent, curved hook-like extensions thin and long. The two median sclerites irregularly-shaped. Cerci short, not exceeding the posterior margin of supra-anal plate. Paratergites (pt.) long and banded. Crosspiece (cp.) nearly transparent, the protrusion robust. Posterior lobes of valvifer II (p.l.) weakly sclerotized. Spermathecal plate (sp.pl.) broad, distinctly concave in the middle, two lobes foliated. Spermatheca (sp.) consists of four distinct, large ampullas. The terminal ampulla abnormally enlarged, with a bifurcated catheter attached to one side of the ampulla. Basivalvula (bsv.) transverse, with two long and narrow lobes, the lateral margin curly. Vestibular sclerite (vst.s) shaped like the letter “W”. The three protrusions almost identical in height. Terminal of both sides’ protrusion expanded. Subgenital plate (SVII) densely setose, posterior margin protruded and the terminal part emarginated medially.

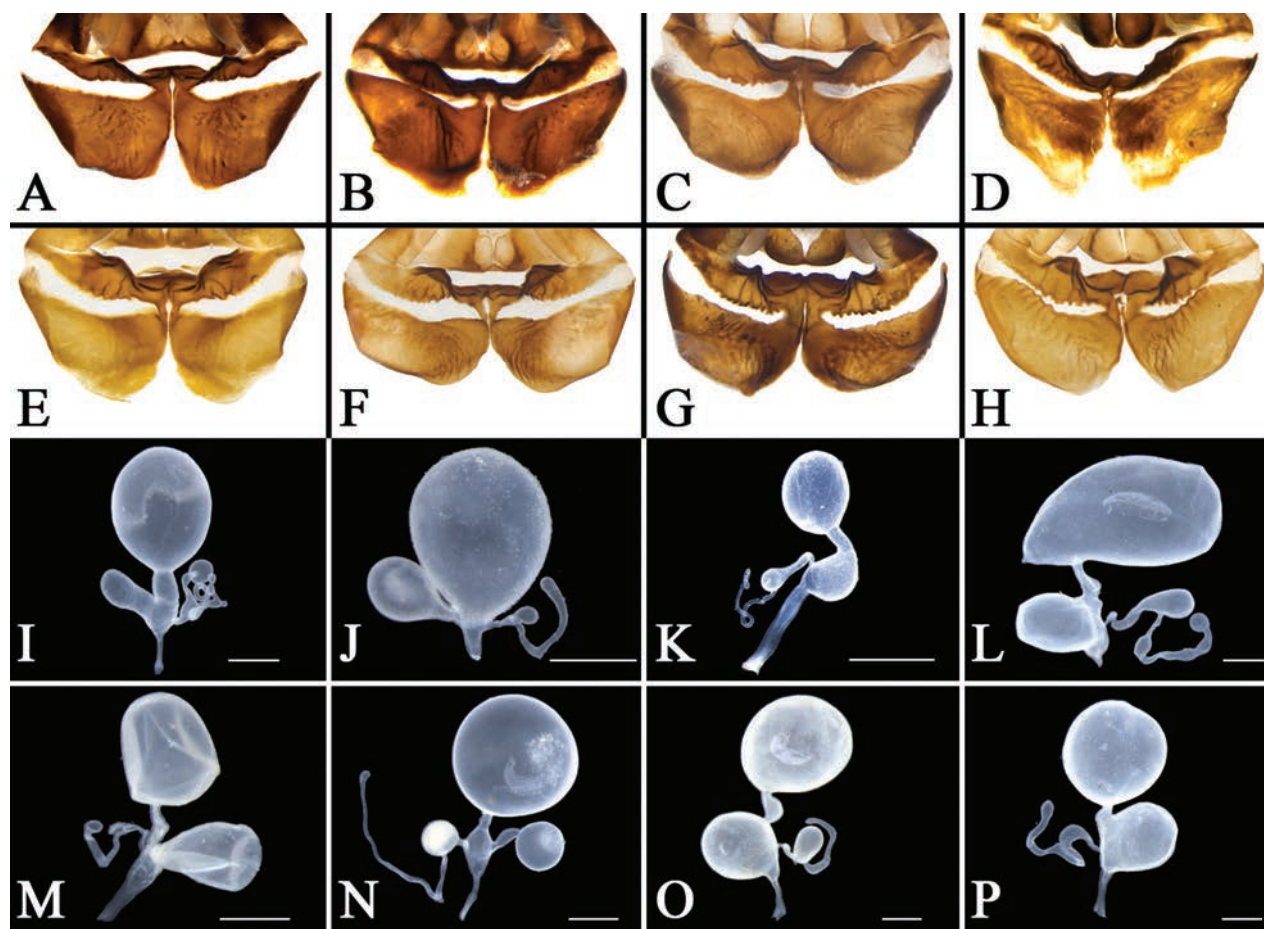


Figure 5. Basivalvula, spermathecal plate and spermatheca of eight *Eupolyphaga* species **A, I** *E. bicolor* Han, Che & Wang, sp. nov. **B, J** *E. nigra* Han, Che & Wang, sp. nov. **C, K** *E. udenostyla* Qiu, 2022 **D, L** *E. hupingensis* Qiu, Che & Wang, 2018 **E, M** *E. miracidia* Qiu, 2022 **F, N** *E. sinensis* (Walker, 1868) **G, O** *E. robusta* Qiu, Che & Wang, 2018 **H, P** *E. hanae* Qiu, Che & Wang, 2018. Scale bars: 0.05 cm (I–P).

***Eupolyphaga robusta* Qiu, Che & Wang, 2018**

Figs 4M, N, 5G, O

Eupolyphaga robusta Qiu, Che & Wang, 2018: 19; Qiu et al. 2019: 11 (catalogue); Han et al. 2022: 86.

Material examined. • 1 female; Sichuan Prov., Aba Prefecture, Wenchuan County, Miansi Town; 29 March 2020; Jian-Yue Qiu leg • 1 female; Sichuan Prov., Aba Prefecture, Maoxian County, Nanxin Town, Miancu Village; 7 Aug. 2019; Zong-Qing Wang, Lu Qiu, Wei Han, Huan-Yu Ren leg • 1 female; Sichuan Prov., Aba Prefecture, Maoxian County, Xiaomiao Mountain; 6 Aug. 2019; Lu Qiu, Wei Han, Huan-Yu Ren leg.

Description of the female characters. Supra-anal plate (TX) black and covered with setae, posterior margin slightly protruded in the middle. Paraprocts (pp.) pubescent, the curved hook-like extensions long. The two median sclerites irregularly-shaped. Cerci short, not exceeding the posterior margin of supra-anal plate. Paratergites (pt.) long and banded. Crosspiece (cp.) well-sclerotized and the protrusion robust. Posterior lobes of valvifer II (p.l.) short. Spermathecal plate (sp.pl.) narrow and slightly concave in the

middle, with two lobes that have distinct arch in the middle. Spermatheca (sp.) consists of two distinct, large ampullas, the terminal ampulla bigger, and the duct connecting the two ampullas slightly expanded. The ampulla near the base also connected to a duct that expands into a small ball in the middle. Basivalvula (bsv.) transverse, two lobes wide, lateral margins curly. Vestibular sclerite (vst.s) shaped like the letter “W”, slightly expanded at the terminal of both sides’ protrusions. The middle protrusion forked at the tip. Subgenital plate (SVII) densely setose, the posterior margin protruded and emarginated terminally.

***Eupolyphaga hanae* Qiu, Che & Wang, 2018**

Figs 40, P, 5H, P

Eupolyphaga hanae Qiu, Che & Wang, 2018: 42; Qiu et al. 2019: 11 (checklist); Han et al. 2022: 84.

Material examined. • 5 females; Chongqing City, Beibei District, Jinyun Mountain, Southwest Bureau Statue; 10 Jul. 2021; Wei Han leg • 3 females; Sichuan Prov., Suining City, Shehong County, Fuxing Town, Taixing Township, Laogangmo Village; 8 Mar. 2016; Lei Wang leg • 1 female; Sichuan Prov., Jiangjin District, Simian Mountain, Shunzigou; 6 Mar. 2016; Jian-Yue Qiu, Hao Xu leg • 1 female; Sichuan Prov., Mianyang City, Jiangyou County, Qianyuan Mountain, Jinguangdong; 16 Jan. 2022; Hao Xu, Xin-Yuan Zhang leg.

Description of the female characters. Supra-anal plate (TX) reddish brown and densely covered with setae. The posterior margin flat. Paraprocts (pp.) pubescent, curved hook-like extensions short. The two median sclerites irregularly shaped. Cerci short, not exceeding the posterior margin of supra-anal plate. Paratergites (pt.) long and banded. Crosspiece (cp.) nearly transparent, the protrusion long and robust. Posterior lobes of valvifer II (p.l.) slightly sclerotized, two lobes long and curved, with poorly-defined edges. Spermathecal plate (sp.pl.) broad and concave in the middle, two lobes with distinct cone-shaped protrusions. The posterior margin of the lobe with irregular protrusions. Spermatheca (sp.) consists of two distinct, large ampullas. The basal ampulla connected to a long spermathecal duct, the duct slightly expanded in the middle and terminal portions. Basivalvula (bsv.) transverse, anterior margin elongated terminally, the lateral margin curled. Vestibular sclerite (vst.s) shaped like the letter “W”, expanded at the terminal of both sides. Subgenital plate (SVII) densely setose, posterior margin protruded and the terminal part emarginate medially.

Genus *Pseudoeupolyphaga* Qiu & Che, 2024

Pseudoeupolyphaga Qiu & Che in Han et al. 2024: 165.

Type species. *Polyphaga yunnanensis* Chopard, 1922, by original designation.

Supplementary diagnosis. Following anatomical examination of specimens representing 15 species and subspecies, no noteworthy variations

were discerned in the sclerites of female external genitalia and the shape of spermathecae across different species within this genus. Consequently, detailed descriptions of female external genitalia and spermathecae for these species were omitted, and instead, a summary diagnosis encompassing the genus is provided (Fig. 6). Comprehensive information and illustrations of the anatomical samples are available in the supplementary material (Suppl. materials 1, 2). Paratergites (pt.) banded or lamellar. Crosspiece (cp.) indistinct or distinct, with a small protuberance that points towards the posterior lobes of valvifer II (p.l.). The posterior lobes of valvifer II fuse with the anterior arch (aa.) forming a circinate structure. Posterior lobes of valvifer II well-sclerotized or not, curved apically. The first valvule (v.I) long, slightly curved, with more pronounced lateral sclerotization. Basal part of valvifer II (v.II) and valvifer III (v.III) enlarged. The spermathecal plate (sp.pl.) well-sclerotized, narrow, depressed downward in the middle. Basivalvula (bsv.) symmetrical, with two lobes narrow. Each lobe with curved anterior margins, curly lateral margins, and round posterior margins. The spermatheca (sp.) consists of a large spherical ampulla and a short spermathecal duct. With or without a curved and elongated duct attached to the ampulla. The vestibular sclerite (vst.s) shaped like the letter “W”, with three protrusions. The subgenital plate (SVII) densely setose, posterior margin bulging and protruding, with middle part slightly concave inward or not.

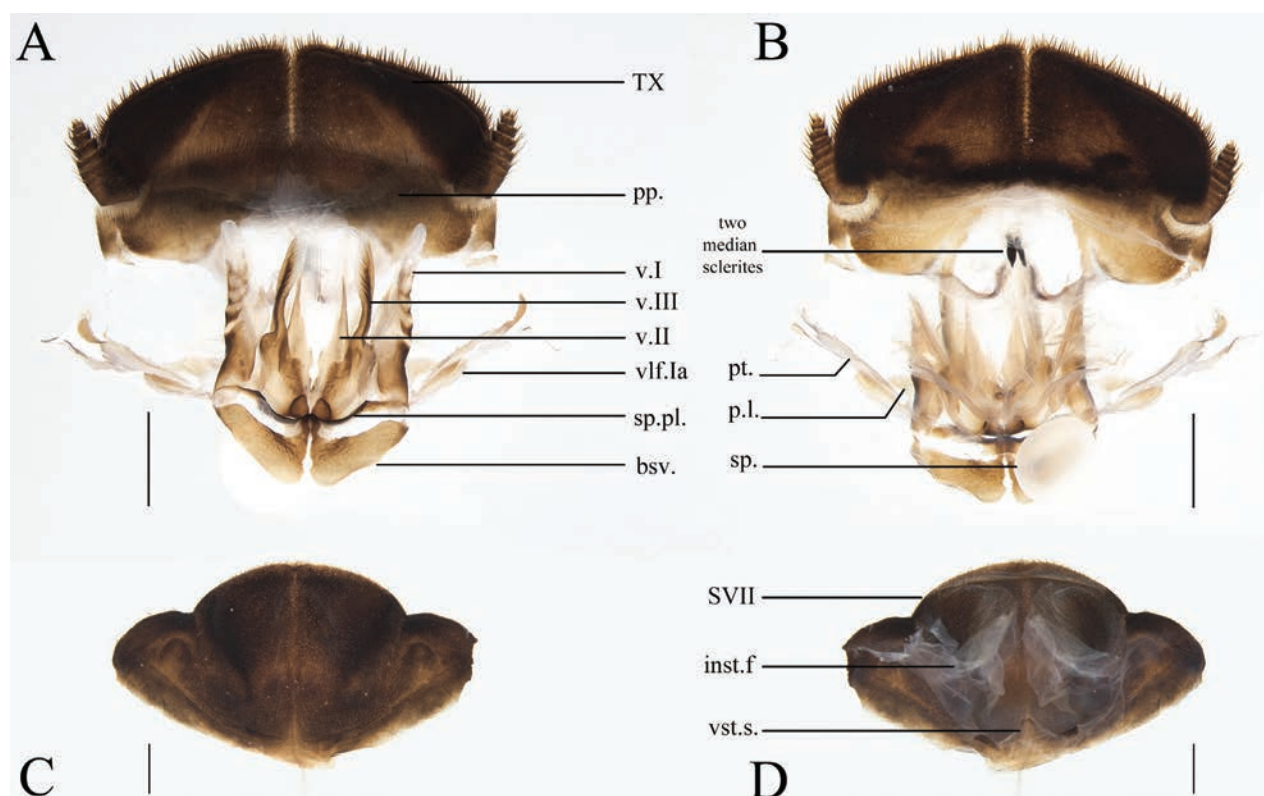


Figure 6. The supra-anal plate, subgenital plate, female external genitalia and spermatheca of the genus *Pseudoeupolyphaga*, using *P. yunnanensis* (Chopard, 1922) as an exemplar **A** supra-anal plate and female external genitalia, ventral view **B** supra-anal plate and female external genitalia, dorsal view **C** subgenital plate, ventral view **D** subgenital plate, dorsal view. Scale bars: 0.1 cm (**A–D**). Abbreviations: bsv. basivalvula, p.l. posterior lobes of valvifer II, pp. paraprocts, pt. paratergites, sp. spermatheca, sp.pl. spermathecal plate, SVII subgenital plate, TX supra-anal plate, v.I first valvule, v.II second valve, v.III third valve, vlf.la first valvifer arm, vst.s vestibular sclerite.

***Pseudoeupolyphaga flava* Han, Che & Wang, sp. nov.**

<https://zoobank.org/93E7B897-8469-4081-84B6-8D290B586FDD>

Fig. 7A–L

Type material. Holotype: CHINA • male; Yunnan Province, Lijiang City, Yongsheng County, Liude Village, G353 roadside in dry soil; 9 Jul. 2021; Lu Qiu, Hao Xu leg.

Paratypes: CHINA • 2 males, 1 female & 7 nymphs, same collection data as holotype.

Diagnosis. This species can be easily distinguished from others by its bright yellowish abdomen, present in both males and females. In addition, the males of this species have large patches in the middle of their tegmina, which is distinctly different from other congeneric species.

Description. Holotype. Measurements (mm). Overall length (including tegmen): 25.58; body length: 18.24; body width (tegmina not included): 9.21; tegmen length × width: 21.41 × 7.40; pronotum length × width: 6.95 × 3.76.

Coloration. Body mostly yellow (Fig. 7A, B). Pronotum dark yellowish brown to reddish brown, anterior margin white, with short yellow setae (Fig. 7E). Tegmina pale gray, with densely darkish brown maculae. Hind wings nearly transparent, also with densely pale-colored maculae (Fig. 7A, B). Head black. Ocelli white. Antennae brownish yellow. Forehead black. Ante-clypeus white, post-clypeus yellowish brown. Labrum pale yellowish brown (Fig. 7G). Legs yellow, tibia, tarsi, and ante-tarsi yellowish brown. Pulvilli and arolia white. Abdomen yellow, distal part slightly darker in color (Fig. 7B).

Body. Head: Sub-rounded, hidden under pronotum. Eyes developed, ocelli bulging round and protruded. Interocular space narrower than the distance between ocelli, the latter narrower than the distance between antennal sockets. Ocelli ridge indistinct, with a row of setae on the upper edge. Clypeus developed (Fig. 7G). **Pronotum:** Transverse oval, widest near the hind margin. Surface with short setae. Anterior whitish margin narrow, clearly demarcated from the yellowish-brown area, with symmetrical dark protrusions in the center (Fig. 7E). **Tegmina and hind wings:** Maculae dense and of different size. A large fused brown macula located in the center (Fig. 7A). **Legs:** Slender, front femur type C₁. Pulvilli and arolia present (Fig. 7B). **Abdomen:** Supra-anal plate transverse, pubescent, posterior margin slightly protruded medially. Paraprocts simple. Cerci long. Subgenital plate with short setae, hind margin slightly concave medially. Left stylus shorter than the right one (Fig. 7I, J). **Genitalia:** Right phallomere bigger than the left phallomere. L1 basally prolonged, two hind lobes weakly sclerotized. L2 arching, curved. Genital hook (L3) short and robust, the hook small. L4M broadly lamellate; pda subtriangular, paa broad. L5 subelliptic. L8 basally dilated, tip with a protrusion. Right phallomere long. R1M stout. R1L banded, elongate. R2 divided into two chunks, the basal one more rounded, the upper one with a flatter anterior margin and a protruded prolonged right posterior lateral angle. R3 thin, convex, and irregular (Fig. 7K, L).

Male paratypes. Similar to the holotype.

Female paratype. Body length: 20.20 mm; body width: 13.00 mm; pronotum length × width: 10.61 × 6.53 mm.

Coloration. Terga yellowish brown to reddish brown, margins with yellowish brown setae (Fig. 7C). Sterna yellow, the distal part slightly darker (Fig. 7D). Head black. Ocelli white. Ante-clypeus sub-transparent, pale gray. Post-clypeus blackish brown. Basal part of labrum pale gray (Fig. 7H). Legs yellow, tibia nearly black. Spines dark yellowish brown to black (Fig. 7C, D).

Body. The widest point of pronotum near the hind margin, anterior whitish margin indistinct (Fig. 7F). Ocelli indistinct, degraded to two small white spots. Interocular space bigger than the distance between ocelli, and almost equal to

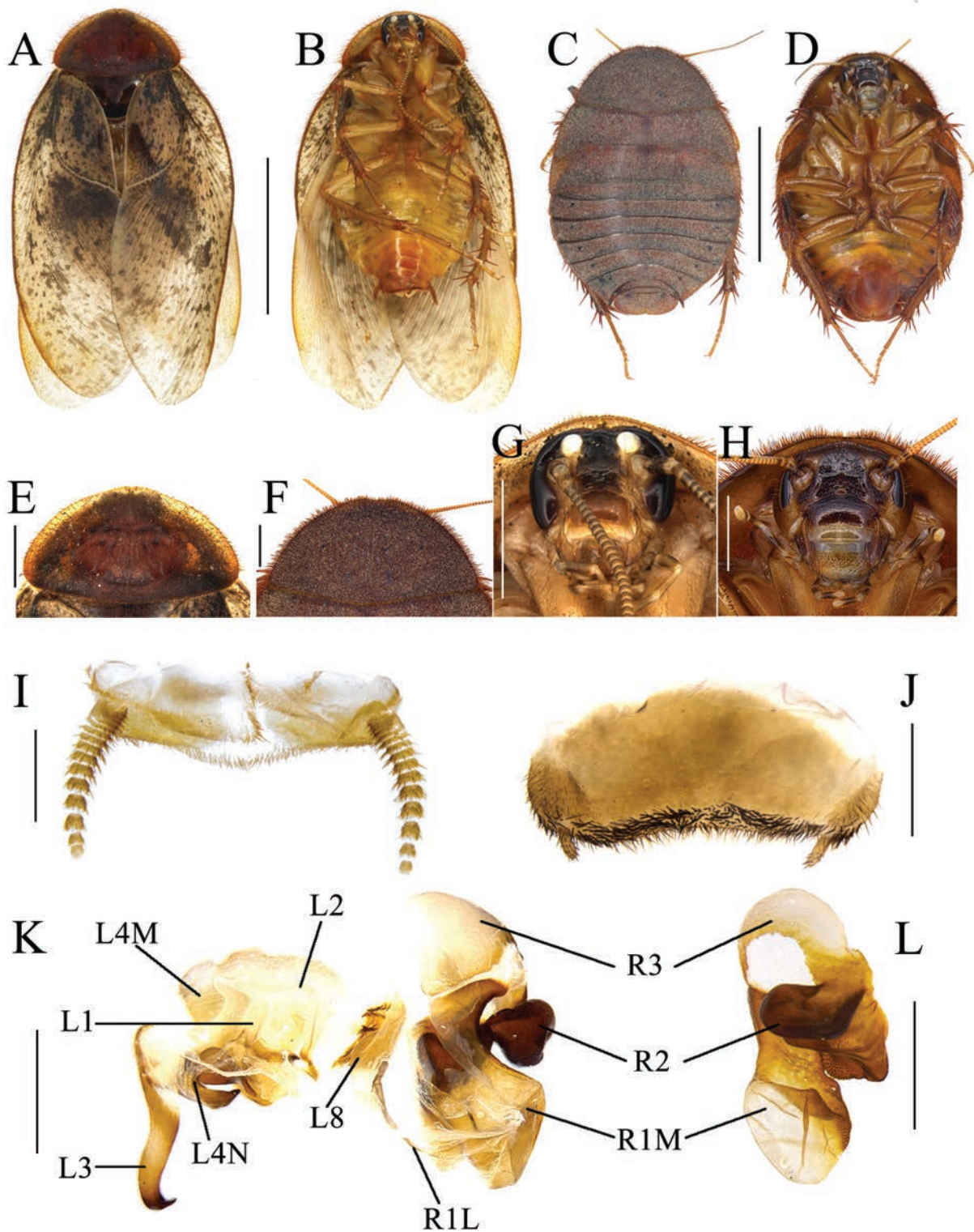


Figure 7. *Pseudoeupolyphaga flava* Han, Che & Wang, sp. nov. **A, B, E, G, I–L** male holotype **C, D, F, H** female paratype **A** habitus, dorsal view **B** habitus, ventral view **C** habitus, dorsal view **D** habitus, ventral view **E** pronotum, dorsal view **F** pronotum, dorsal view **G** head, ventral view **H** head, ventral view **I** supra-anal plate, ventral view **J** subgenital plate, ventral view **K** genitalia, dorsal view **L** right phallomere, right-ventral view. Scale bars: 1.0 cm (**A–D**); 0.2 cm (**E–H**); 0.1 cm (**I–L**).

the distance between antennal sockets (Fig. 7H). Front femur type C₁. Arolia and pulvilli absent. Supra-anal plate densely covered with long yellowish brown setae, posterior margin slightly convex, slightly emarginated medially. Cerci short and robust, not exceeding posterior margin of supra-anal plate. Posterior margin of subgenital plate protruded, emarginated medially (Suppl. material 1: fig. S1A).

Nymph. Similar to the female.

Ootheca. Unknown.

Etymology. The species epithet is derived from the Latin word *flavus*, referring to the yellowish abdomen of both males and females.

Remark. The interspecific genetic distance between this species and the other species within this genus ranges from 10.62% to 20.39%, providing support for the classification of this species as a novel taxon.

***Pseudoeupolyphaga deficiens* Han, Che & Wang, sp. nov.**

<https://zoobank.org/BC9BB5BD-69BB-4C77-82CC-2B3074E26956>

Figs 8A–L, 15A, J

Type material. Holotype: CHINA • male; Sichuan Province, Aba Prefecture, Heishui County, entrance to Dagu Glacier; 22 Jun. 2021; Lu Qiu, Hao Xu leg. **Paratypes:** CHINA • 1 female & 1 ootheca, same collection data as holotype • 1 female & 20 nymphs, Sichuan Province, Mao County, Cuoji Mountain; 6 Aug. 2019; Lu Qiu leg.

Diagnosis. This species is distinguishable from others by the broad anterior white margin of the pronotum and the absence of a distinct boundary between the markings on the tegmina in males. In addition, the surface of the ootheca of this species is unusually smooth, with serrated protuberances and blunt tips.

Description. Holotype. Measurements (mm). Overall length (including tegmen): 30.86; body length: 18.62; body width (tegmina not included): 10.34; tegmen length × width: 26.28 × 10.49; pronotum length × width: 7.51 × 3.91.

Coloration. Body yellowish brown (Fig. 8A, B). Pronotum reddish brown, covered with yellowish setae, anterior margin white (Fig. 8E). Tegmina pale yellow, with brown maculae. Wings nearly transparent (Fig. 8A, B). Face yellow. Antennae yellow. Eyes black. Ocelli white. Middle of forehead with a dark brown macula. Ante-clypeus pale yellow, post-clypeus yellowish brown. Labrum yellow (Fig. 8G). Legs yellowish brown, tibia dark yellowish brown. Pulvilli and arolia white. Abdomen yellowish brown and gradually darkening toward the distal abdomen (Fig. 8B).

Body. Head: Sub-rounded, hidden under pronotum. Eyes and ocelli developed. Ocelli ridge slightly curved, with a row of setae on the upper edge. Interocular space narrower than the distance between ocelli, the latter narrower than the distance between antennal sockets. Clypeus developed (Fig. 8G). **Pronotum:** Transverse oval, widest near the middle. Surface densely covered with short setae, center part with symmetrical black stripe. Anterior whitish margin broad, clearly delineated from reddish brown areas (Fig. 8E). **Tegmina and hind wings:** Markings varied in size and denser near the base of the tegmina (Fig. 8A, B). **Legs:** Slender, front femur type C₁. Pulvilli and arolia present (Fig. 8B). **Abdomen:** Supra-anal plate transverse, pubescent, middle part of posterior margin slightly protruded. Paraprocts simple. Subgenital plate with short setae, hind margin flat. Styli long (Fig. 8I, J). **Genitalia:** Well-sclerotized. Right phallomere bigger than the left phallomere. Anterior protrusion of L1 long and

sharp. L2 arching curved. Genital hook (L3) robust, curved hook section nearly right-angled. L4M broad lamellate. The protrusion of pda and paa broad. L7 sub-membranous, ovoid. L8 irregular, subtriangular. R1M stoutly expanded terminally, R1L elongate and banded. R2 divided into two chunks of approximate size, narrowly spaced, with rounded margins. R3 broadly concave (Fig. 8K, L).

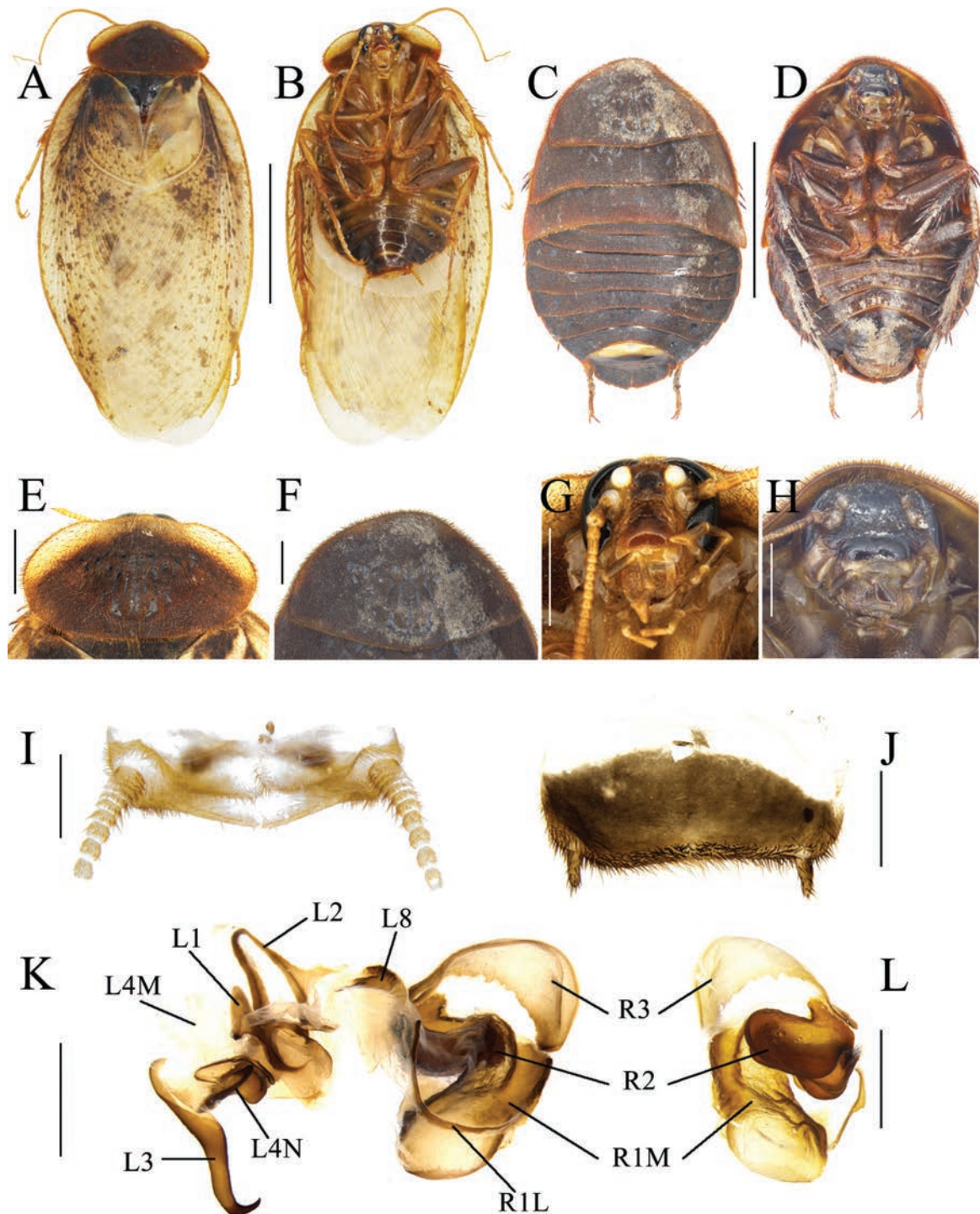


Figure 8. *Pseudoeupolyphaga deficiens* Han, Che & Wang, sp. nov. **A, B, E, G, I–L** male holotype **C, D, F, H** female paratype. **A** habitus, dorsal view **B** habitus, ventral view **C** habitus, dorsal view **D** habitus, ventral view **E** pronotum, dorsal view **F** pronotum, ventral view **G** head, ventral view **H** head, ventral view **I** supra-anal plate, ventral view **J** subgenital plate, ventral view **K** genitalia, dorsal view **L** right phallomere, right-ventral view. Scale bars: 1.0 cm (**A–D**); 0.2 cm (**E–H**); 0.1 cm (**I–L**).

Female paratype (same locality as holotype). Body length: 20.96 mm; body width: 13.82 mm; pronotum length × width: 10.75 × 6.46 mm.

Coloration. Terga dark yellowish brown (Fig. 8C). Head black. Antennae yellow. Ocelli white. Ante-clypeus yellowish white. Post-clypeus black. Labrum yellowish brown (Fig. 8H). Legs dark yellowish brown, with large dark brown patches. Spines on the leg reddish brown, terminal nearly black. Sterna dark yellowish brown, margins and both sides nearly blackish brown; middle part slightly lighter, yellowish brown (Fig. 8D).

Body. The widest point of pronotum near the hind margin, middle part with symmetrical black dark stripe, anterior whitish margin indistinct (Fig. 8F). Ocelli indistinct, degraded to two white spots. Interocular space almost equal to the distance between antennal sockets, both bigger than the distance between ocelli (Fig. 8H). Front femur type C₁. Arolia and pulvilli absent. Supra-anal plate densely covered with yellowish brown setae, posterior margin convex, middle part slightly emarginated. Cerci short and robust, not exceeding posterior margin of supra-anal plate. Posterior margin of subgenital plate protruded, emarginated medially (Suppl. material 1: fig. S1B).

Nymph. Similar to the female.

Ootheca. Reddish brown. Surface with densely parallel longitudinal lines. Ridges of serrated protuberances densely arranged with blunt tips. No respiratory canals (Fig. 15A, J).

Etymology. The species epithet is derived from the Latin word *deficiens*, to refer to the markings on the tegmina that lack distinct boundaries.

Remark. The genetic distance from other species was 8.39%–20.30%, which also provides evidence supporting the description of this new species.

***Pseudoeupolyphaga magna* Han, Che & Wang, sp. nov.**

<https://zoobank.org/72A2A7E7-49EB-442A-B2C5-121C8180C1D6>

Fig. 9A–L

Type material. Holotype: CHINA • male; Sichuan Province, Aba Prefecture, Jinchuan County, Guanyinqiao Township; 2020; Jian-Yue Qiu leg. **Paratype:** CHINA • 1 female, same collection data as holotype.

Diagnosis. The males of this species closely resemble *P. yunnanensis*, but are significantly larger than all other species in this genus as currently known, and can be distinguished accordingly.

Description. Holotype. Measurements (mm). Overall length (including tegmen): 42.44; body length: 27.56; body width (tegmina not included): 14.52; tegmen length × width: 37.40 × 12.60; pronotum length × width: 11.67 × 6.91.

Coloration. Pronotum yellowish brown, covered with yellowish setae, anterior margin white (Fig. 9A, E). Tegmina subtransparent, densely covered with blackish brown maculae (Fig. 9A). Eyes, vertex, and space between ocelli black. Face yellowish brown. Ocelli, antennal sockets, and ante-clypeus white. Antennae, post-clypeus, labrum, labial palpi and maxillary palpi yellow (Fig. 9G). Legs yellowish brown, tibia and spines dark yellowish brown to black. Pulvilli and arolia white. Sterna yellowish brown, middle and distal part nearly black (Fig. 9B).

Body. Head: Sub-rounded, hidden under pronotum. Eyes and ocelli developed. Ocelli ridge indistinct, with a row of setae on the upper edge. Interocular

space narrower than the distance between ocelli, the latter narrower than the distance between antennal sockets. Clypeus developed (Fig. 9G). **Pronotum:** Transverse oval, widest near the middle. Sparsely covered with short setae, middle part with symmetrical black stripes. Anterior whitish margin broad on

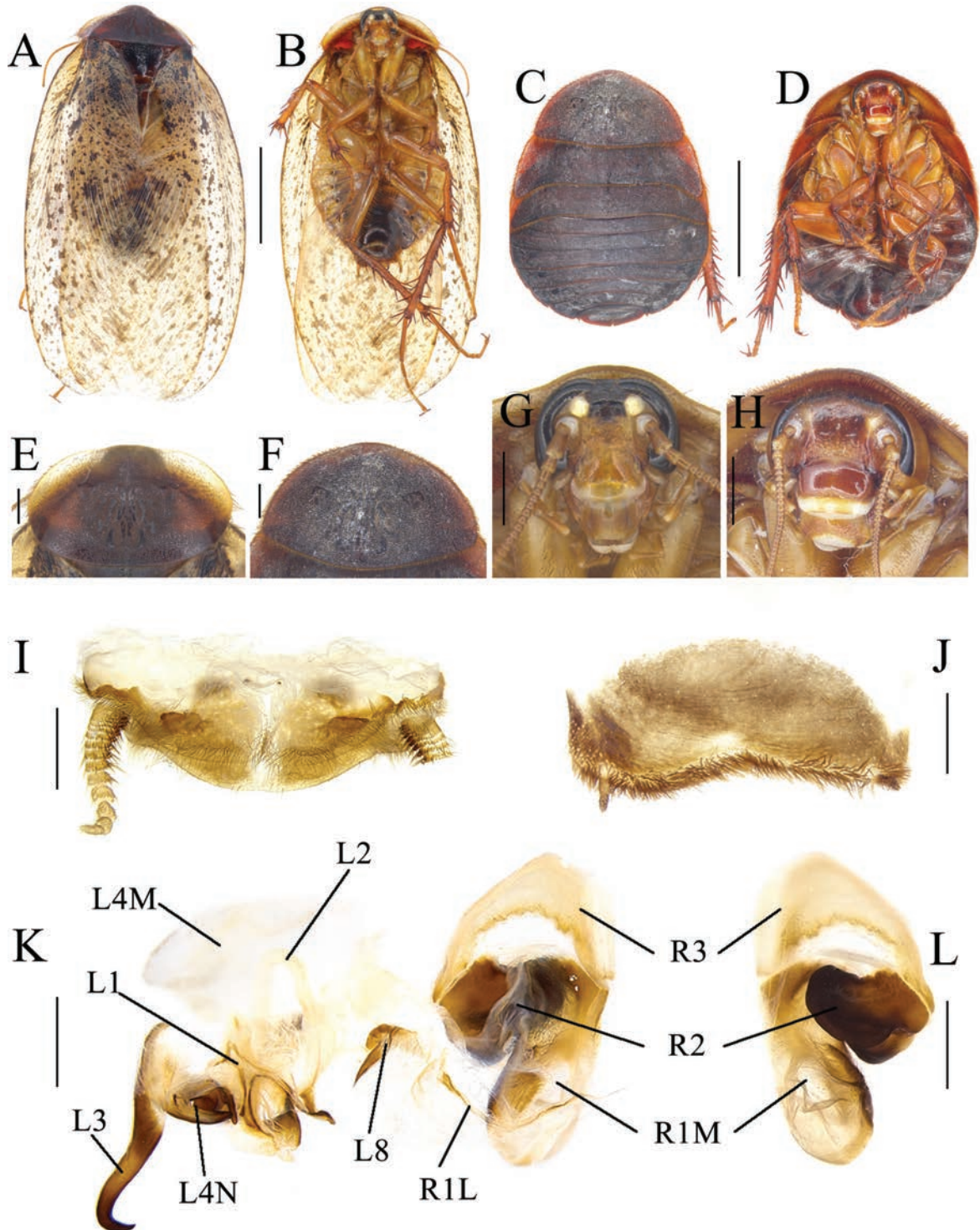


Figure 9. *Pseudoeupolyphaga magna* Han, Che & Wang, sp. nov. **A, B, E, G, I–L** male holotype **C, D, F, H** female paratype **A** habitus, dorsal view **B** habitus, ventral view **C** habitus, dorsal view **D** habitus, ventral view **E** pronotum, dorsal view **F** pronotum, dorsal view **G** head, ventral view **H** head, ventral view **I** supra-anal plate, ventral view **J** subgenital plate, ventral view **K** genitalia, dorsal view **L** right phallomere, right-ventral view. Scale bars: 1.0 cm (**A–D**); 0.2 cm (**E–H**); 0.1 cm (**I–L**).

both sides and absent in middle, unclearly delineated from the yellowish-brown areas (Fig. 9E). **Tegmina and hind wings:** Maculae uniformly distributed and of moderate size. Hind wings nearly transparent, with a few pale brown patches (Fig. 9A). **Legs:** Slender, front femur type C₁. Pulvilli and arolia present (Fig. 9B). **Abdomen:** Supra-anal plate transverse, pubescent, posterior margin slightly protruded medially. Paraprocts simple. Subgenital plate with short setae, hind margin concave in the middle. Styli long (Fig. 9I, J). **Genitalia:** L1 weakly sclerotized, two posterior lobes diverging widely. L2 arching curved, broad. Genital hook (L3) robust. L4M broad lamellate. Pda and paa developed, protrusions long. L8 irregular. R1M expanded terminally, R1L elongate and banded. R2 with two chunks. R3 broadly concave, sub-transparent (Fig. 9K, L).

Female paratype. Body length: 22.31 mm; body width: 17.27 mm; pronotum length × width: 12.88 × 6.82 mm.

Coloration. Terga reddish brown (Fig. 9C). Space between ocelli reddish brown. Antennae yellow. Ocelli, antennal sockets, ante-clypeus as well as upper and lower margins of labrum white. Middle part of labrum yellow. Post-clypeus pale reddish brown (Fig. 9H). Legs yellowish brown, tibia dark yellowish brown. Spines on foot reddish brown to black. Sterna dark reddish brown to black, darker in the middle and edges (Fig. 9D).

The widest point of pronotum near the hind margin, middle part with symmetrical black stripe, anterior whitish margin indistinct (Fig. 9F). Ocelli degraded to two white spots. Interocular space almost equal to the distance between antennal sockets, both larger than the distance between ocelli (Fig. 9H). Front femur type C₁. Arolia and pulvilli absent. Posterior margin of supra-anal plate protruded, slightly emarginated medially. Cerci short and robust, not exceeding posterior margin of supra-anal plate. Posterior margin of subgenital plate protruded and emarginated medially (Fig. 9C, D).

Nymph. Unknown.

Ootheca. Unknown.

Etymology. The species epithet is derived from the Latin word *magnus*, referring to the significantly larger male body size than is usual in the genus.

Remarks. The external morphology of this species closely resembles that of *P. yunnanensis*, particularly in the markings on the tegmina and the coloration of abdomen. However, the male of this species is significantly larger than males of the latter. The genetic distance between this species and others ranges from 13.09 to 21.97%, further supporting its status as a new species.

***Pseudoeupolyphaga longiseta* Han, Che & Wang, sp. nov.**

<https://zoobank.org/DF1330DC-C49E-4101-8984-3D8F0C3424BC>

Figs 10A–L, 15B, K

Type material. Holotype: CHINA • male; Yunnan Province, Diqing Tibetan Autonomous Prefecture, Deqin County, Baimaxueshan Nature Reserve; 27 Jul. 2020; Wei Han, Xin-Xing Luo, Lin Guo leg. **Paratypes:** CHINA • 1 female & 5 nymphs, same collection data as holotype.

Diagnosis. The male of *P. longiseta* sp. nov. shares similarities with those of *P. simila* and *P. pilosa*, yet the markings on the tegmina of this new species are more densely patterned and darker than in the latter two, particularly near the base

of the tegmina. Additionally, some maculae on the tegmina of the new species merged. Unlike males of *P. similar* and *P. pilosa*, which exhibit a yellowish longitudinal line and an interrupted longitudinal line on their abdomen, respectively, this new species lacks a longitudinal line on its abdomen. Additionally, black markings present on the female abdomen of *P. similar* are absent in the females of this new

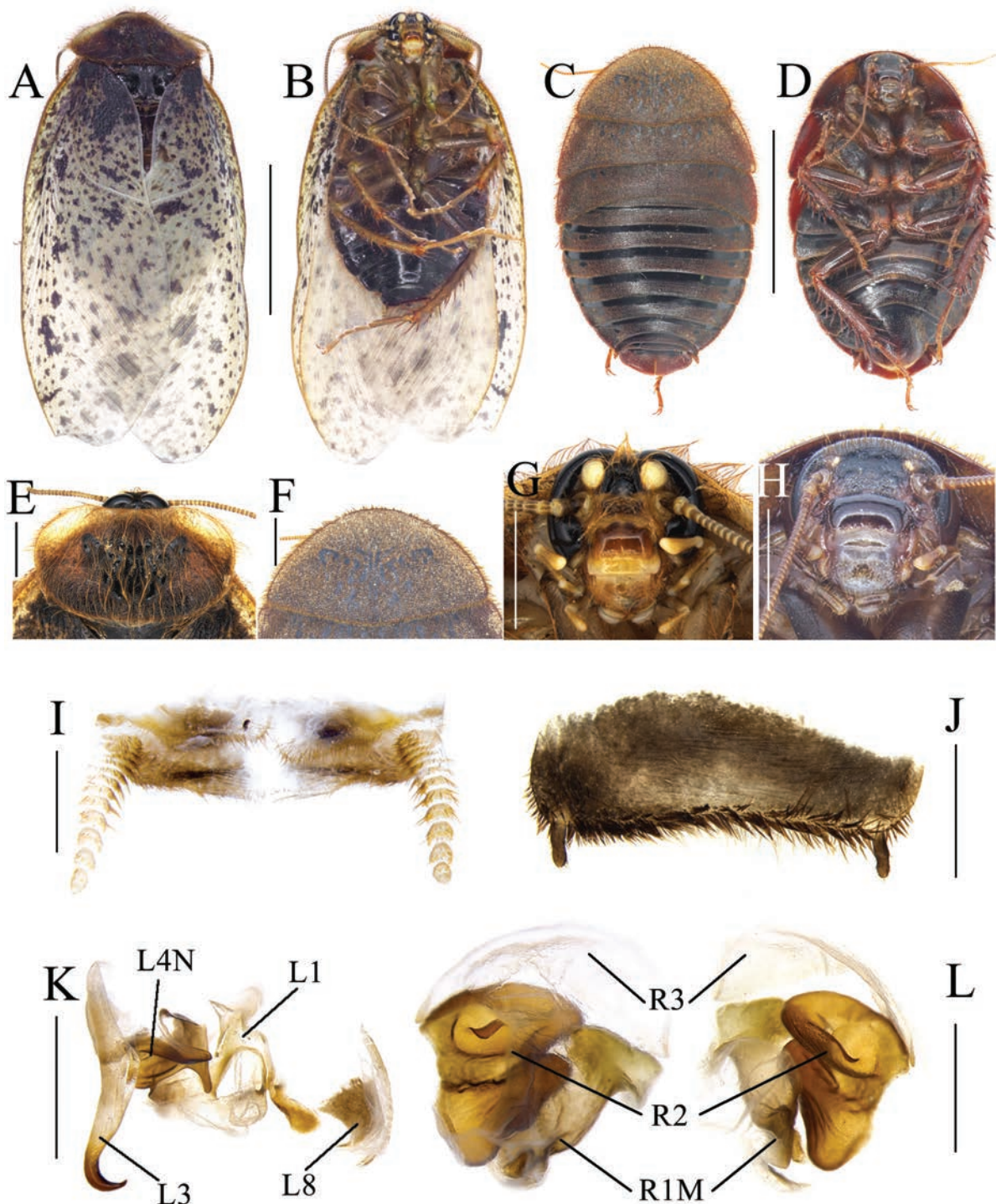


Figure 10. *Pseudoepolyphaga longiseta* Han, Che & Wang, sp. nov. **A, B, E, G, I–L** male holotype **C, D, F, H** female paratype. **A** habitus, dorsal view **B** habitus, ventral view **C** habitus, dorsal view **D** habitus, ventral view **E** pronotum, dorsal view **F** pronotum, dorsal view **G** head, ventral view **H** head, ventral view **I** supra-anal plate, ventral view **J** subgenital plate, ventral view **K** genitalia, dorsal view **L** right phallomere, right-ventral view. Scale bars: 1.0 cm (**A–D**); 0.2 cm (**E–H**); 0.1 cm (**I–L**).

species. In addition, the ootheca of this species has weak serrated protuberances and bluntly rounded tips, which are distinctly different from *P. pilosa*.

Description. Holotype. Measurements (mm). Overall length (including tegmen): 29.87; body length: 19.45; body width (tegmina not included): 10.38; tegmen length × width: 26.22 × 9.50; pronotum length × width: 7.23 × 4.10.

Coloration. Pronotum yellowish brown, covered with long yellowish setae, anterior margin white (Fig. 10A, E). Tegmina pale gray, densely covered with black maculae. Hind wings subtransparent, with pale blackish brown maculae (Fig. 10A). Eyes and space between ocelli black. Ocelli yellowish white. Antennae and labrum yellowish brown. Space between antennal sockets yellowish brown, middle with a black marking. Ante-clypeus, labial palpi and maxillary palpi yellowish white. Post-clypeus dark yellowish brown (Fig. 10B, G). Legs yellowish brown, outside of tibia nearly blackish brown. Pulvilli and arolia white. Sterna nearly black (Fig. 10B).

Body. Head: Sub-rounded, not completely hidden under pronotum. Eyes and ocelli developed. Ocelli ridge narrow, with a row of setae on the upper edge. Interocular space narrower than the distance between ocelli, the latter narrower than the distance between antennal sockets. Clypeus developed (Fig. 10G).

Pronotum: Transverse oval, widest near the anterior margin. Densely covered with long setae, central part with a symmetrical black stripe. Anterior whitish margin broad, clearly delineated from the yellowish-brown areas (Fig. 10E).

Tegmina and hind wings: Tegmina densely covered with maculae. The markings near the base of the tegmina unusually dense and continuous. Hind wing nearly transparent, with a few pale brown patches (Fig. 10B).

Legs: Slender, front femur type C₁, pulvilli and arolia present (Fig. 10B). **Abdomen:** Supra-anal plate transverse, narrow and pubescent, posterior margin slightly protruded. Paraprocts simple. Margins of subgenital plate densely covered with setae, hind margin slightly concave in the middle. Styli long (Fig. 10I, J). **Genitalia:** L1 weakly sclerotized, the left protuberance sharp, two posterior lobes diverge widely. Genital hook (L3) robust. L4M broad lamellate. Pda and paa developed, protrusions long. L8 irregular, flaky. R1M with slightly flattened posterior margin. R1L elongate and banded. One of the two R2 chunks more rounded, the other subtriangular. R3 broadly concave, subhyaline (Fig. 10K, L).

Female paratype. Body length: 20.27; body width: 12.22; pronotum length × width: 9.34 × 4.95.

Coloration. Terga yellowish brown to black (Fig. 10C). Vertex, eyes, post-clypeus and space between ocelli nearly black. Antennae yellowish brown. Ocelli and antennal sockets yellowish white. Ante-clypeus as well as upper and lower margins of labrum pale gray. Middle of labrum yellowish brown (Fig. 10H). Legs dark yellowish brown, tibia and spines dark yellowish brown to black. Sterna nearly black (Fig. 10D).

Body. The widest point of pronotum near the hind margin, middle part with symmetrical black stripes, anterior whitish margin absent (Fig. 10F). Ocelli degraded to two white spots. Interocular space almost equal to the distance between antennal sockets, both bigger than the distance between ocelli (Fig. 10H). Front femur type C₁. Arolia and pulvilli absent. Posterior margin of supra-anal plate slightly convex, emarginated medially. Cerci short and robust, not exceeding the posterior margin of supra-anal plate. Posterior margin of subgenital plate protruded and emarginated medially (Suppl. material 1: fig. S1C).

Nymph. Similar to the female, just a little paler in color.

Ootheca. Yellowish brown. Surface with densely parallel longitudinal lines. Ridges of serrated protuberances densely arranged with semicircular tips. No respiratory canals (Fig. 15B, K).

Etymology. The species epithet is derived from the Latin words *longi* and *seta*, referring to the dense, long pubescence on the pronotum and head of the species.

Remark. The genetic distance between this species and the remainder of the genus ranges from 9.18% to 18.74%, supporting it being a new species. The collection site of this species is close to the distribution site of *Epipolyphaga wukong* Qiu, Che & Wang, 2019, and there may be a sympatric distribution between them.

***Pseudoeupolyphaga latizona* Han, Che & Wang, sp. nov.**

<https://zoobank.org/6813330E-1E3B-4BBD-8189-DEBAA9C9FED4>

Figs 11A–R, 15C, D, L, M

Type material. Holotype: CHINA • male; Sichuan Province, Yaan City, Shimian County, Caoke Village; 20 Jul. 2022; Wei Han, Xin-Xing Luo leg. **Paratypes:** CHINA • 1 female, 5 nymphs & some oothecae, same collection data as holotype • 4 males; Sichuan Province, Ganzi Prefecture, Danba County; 12 Jul. 2017; Jian-Yue Qiu, Hao Xu leg • 1 male; Sichuan Province, Ganzi Prefecture, Danba County, Jiaju Zangzhai; 12 Jul. 2017; Hao Xu, Jian-Yue Qiu leg • 2 males; Sichuan Province, Ganzi Prefecture, Danba County, Zhanggu Town, Baiga Mountain; 14 Jun. 2013; Li He leg • 1 female, 3 nymphs, 3 oothecae; Sichuan Province, Ganzi Prefecture, Danba County, Zhanggu Town, Baiga Mountain; Oct. 2016; Jian-Yue Qiu leg • 1 female, 2 nymphs, 5 oothecae; Sichuan Province, Ganzi Prefecture, Danba County; 20 Feb. 2017; Jian-Yue Qiu leg • 1 male; Sichuan Province, Ganzi Prefecture, Danba County, Zhanggu Town, Baiga Mountain; 14 Jun. 2013; Li He leg • 4 nymphs, 1 ootheca; Sichuan Province, Ganzi Prefecture, Danba County, Zhanggu Town, Baiga Mountain; Feb. 2017; Lu Qiu leg.

Diagnosis. The male of this species resembles the newly described species *P. baimaensis* sp. nov., but differs in having denser markings on the tegmina, darker abdominal coloration, and more distinct boundaries of yellow-black abdominal markings. The female of this species has slightly smaller ocelli compared to the latter. Additionally, the serrations of the ootheca of this species are very weak, whereas those of *P. baimaensis* sp. nov. are slightly stronger.

Description. Holotype. Measurements (mm). Overall length (including tegmen): 33.70; body length: 20.94; body width (tegmina not included): 11.54; tegmen length × width: 29.29 × 9.91; pronotum length × width: 9.19 × 5.39.

Coloration. Pronotum dark yellowish brown, covered with short yellowish setae. Anterior margin white (Fig. 11A, K). Maculae in tegmina and hind wings blackish brown (Fig. 11A, B). Eyes, vertex, and spaces between ocelli black. Ocelli and antennal sockets white. Post-clypeus dark yellowish brown. Ante-clypeus pale yellow. Base of labrum white, rest yellowish brown. Labial palpi and maxillary palpi yellowish brown, connections white (Fig. 11B, M). Legs yellowish brown, tibia and spines dark yellowish brown. Pulvilli and arolia white. Sterna yellow, margins, middle and distal part with black markings (Fig. 11B).

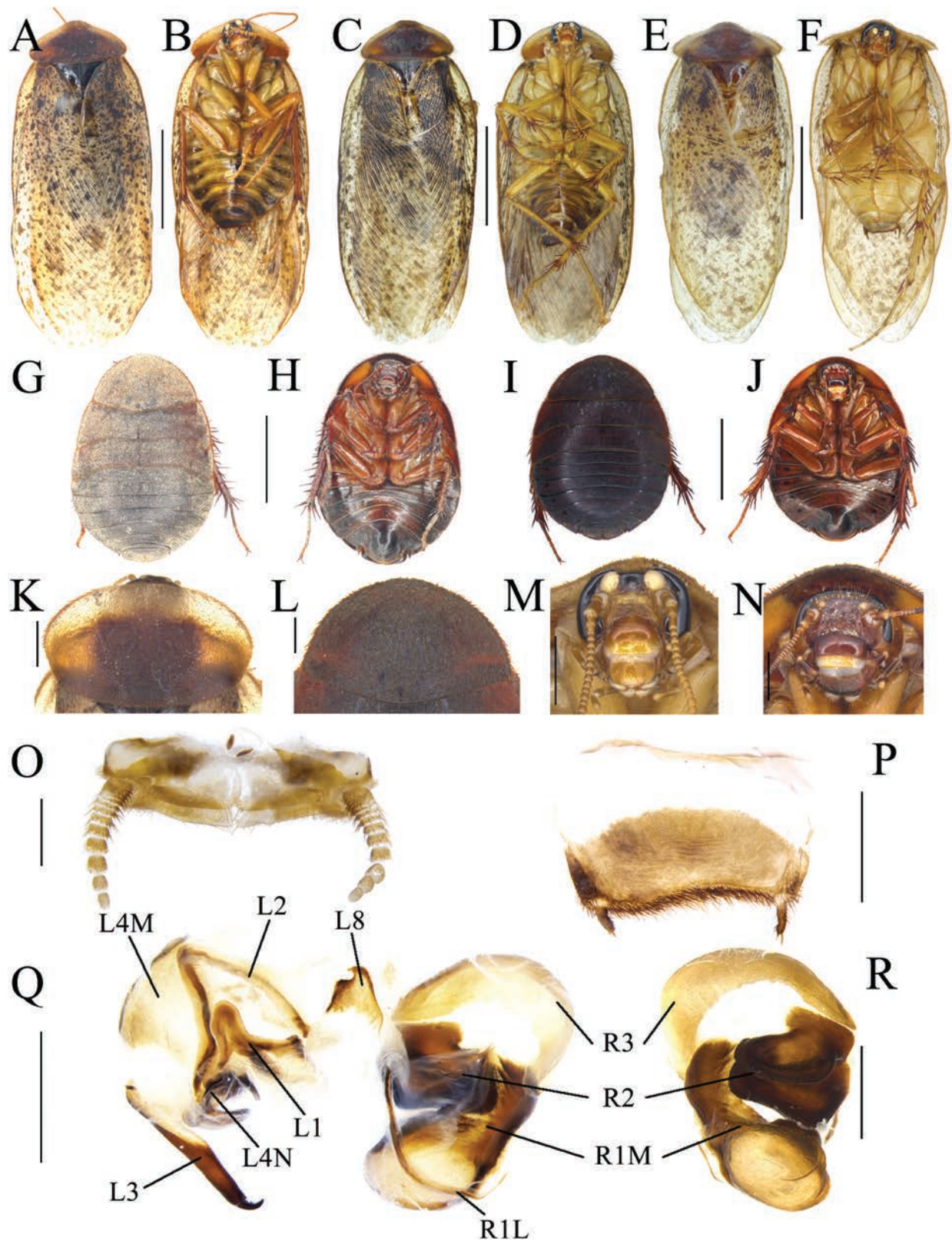


Figure 11. *Pseudoeupolyphaga latizona* Han, Che & Wang, sp. nov. **A, B, K, M, O–R** male holotype (Shimian County) **C–F** male paratype (Danba County) **G, H, L, N** female paratype (Shimian County) **I, J** female paratype (Danba County) **A** habitus, dorsal view **B** habitus, ventral view **C** habitus, dorsal view **D** habitus, ventral view **E** habitus, dorsal view **F** habitus, ventral view **G** habitus, dorsal view **H** habitus, ventral view **I** habitus, dorsal view **J** habitus, ventral view **K** pronotum, dorsal view **L** pronotum, dorsal view **M** head, ventral view **N** head, ventral view **O** supra-anal plate, ventral view **P** subgenital plate, ventral view **Q** genitalia, dorsal view **R** right phallomere, right-ventral view. Scale bars: 1.0 cm (**A–J**); 0.2 cm (**K–N**); 0.1 cm (**O–R**).

Body. Head: Sub-rounded, nearly completely hidden under pronotum. Eyes and ocelli developed. Ocelli ridge narrow, with a row of setae on the upper edge. A dimple present between the ocelli. Interocular space nearly equal to the distance between ocelli, and both narrower than the distance between antennal sockets. Clypeus developed (Fig. 11M). **Pronotum:** Transverse oval, widest near the middle. Densely covered with setae on surface, with symmetrical stripes in the middle. Anterior whitish margin greatly broad, clearly delineated from the yellowish-brown areas (Fig. 11K). **Tegmina and hind wings:** Densely covered with maculae, most of maculae small (Fig. 11A). **Legs:** Slender, front femur type C₁. Pulvilli and arolia present. **Abdomen:** Supra-anal plate transverse, narrow and pubescent, posterior margin slightly protruded medially. Paraprocts simple. Hind margin of subgenital plate densely covered with setae, slightly asymmetrical, middle part slightly concave. Styli long (Fig. 11O, P). **Genitalia:** The left protuberance of L1 robust, two posterior lobes and terminal protrusion strong. L2 arched. Genital hook (L3) straight, the hook small. L4M broad lamellate. Pda and paa developed, protrusions long. L8 irregular, subtriangular. R1M expanded terminally. R1L elongate, banded. R2 divided into two chunks. R3 broadly concave (Fig. 11Q, R).

Female paratype (same locality as holotype). Body length: 24.12 mm; body width: 16.33 mm; pronotum length × width: 11.81 × 6.85 mm.

Coloration. Terga yellowish brown to blackish brown (Fig. 11G, I). Vertex and eyes black. Ocelli yellow. Antennae yellowish brown. Antennal sockets, base of labrum and two sides of ante-clypeus white. Middle of ante-clypeus yellow. Post-clypeus and middle of labrum reddish brown. Distal part of labrum black. Legs dark yellowish brown to reddish brown, spines reddish brown to black. Sterna reddish brown to black (Fig. 11H, J).

Body. The widest point of pronotum near the hind margin, middle area with symmetrical dark stripe. Anterior whitish margin absent (Fig. 11L). Ocelli degraded to two spots. Interocular space almost equal to the distance between ocelli, both narrower than the distance between antennal sockets (Fig. 11N). Front femur type C₁. Arolia and pulvilli absent. Posterior margin of supra-anal plate protruded, slightly emarginated medially. Cerci short and robust, not exceeding posterior margin of supra-anal plate. Posterior margin of subgenital plate protruding medially (Figs 11G–J, Suppl. material 1: fig. S1D).

Nymph. Similar to the female, a little paler in color.

Ootheca. Dark reddish brown to black. Surface with densely parallel longitudinal lines. Serrations of keel very weak. No respiratory canals (Fig. 15C, D, L, M).

Etymology. The species epithet is derived from a combination of the Latin words *latus* and *zona*, which refers to the broad anterior whitish margin on the pronotum of the male.

Remark. Samples from Danba County were previously identified as *P. yunnanensis* (Qiu et al. 2018). However, their tegmina maculae are significantly denser than those of *P. yunnanensis*. There are some differences between samples from Shimian County and Danba County: the former has a darker body coloration and dense but separate tegmina maculae, while the latter has a paler body coloration and with some fused maculae in tegmina. We also found a recently emerged male individual with dense but scattered forewing maculae and a yellowish-white abdomen (Fig. 11E, F). The genetic distance between the samples from Shimian County and Danba County of this species is 4.75%,

leading to their designation as conspecific. Furthermore, the genetic distance between this species and members of the rest of the genus ranges from 12.92% to 20.90%, providing further support for its classification as a new species.

***Pseudoeupolyphaga baimaensis* Han, Che & Wang, sp. nov.**

<https://zoobank.org/74F84569-2690-4C2A-A13F-64E02FEB3CB4>

Figs 12A–L, 15E, N

Type material. Holotype: CHINA • male; Sichuan Province, Mianyang City, Pingwu County, Baima Village; 4 Aug. 2019; Lu Qiu leg. **Paratype:** CHINA • 1 female, same collection data as holotype.

Other material examined. CHINA • 10 oothecae; same collection data as holotype.

Diagnosis. The male of this species resembles *P. latizona* sp. nov., but differs in having sparser markings on the tegmina, paler abdominal coloration, and less distinct boundaries of yellow-black abdominal markings. The female of this species has slightly larger ocelli compared to the latter. Additionally, the serrations of the ootheca of this species are slightly stronger than those of *P. latizona* sp. nov.

Description. Male holotype. Measurements (mm). Overall length (including tegmen): 35.51; body length: 23.39; body width (tegmina not included): 11.53; tegmen length × width: 30.00 × 9.40; pronotum length × width: 10.28 × 5.91.

Coloration. Pronotum yellowish brown, anterior margin white. Tegmina and hind wings pale yellow, maculae blackish brown (Fig. 12A, E). Eyes, vertex, and spaces between ocelli black. Ocelli and ante-clypeus yellowish white. Antennal sockets white. Antennal sockets, post-clypeus, and labrum yellowish brown. Labial palpi and maxillary palpi yellowish brown, distal part and connections white (Fig. 12G). Legs yellowish brown, spines and outside of tibia dark yellowish brown to black. Pulvilli and arolia white. Sterna dark yellowish brown, margins and distal part black (Fig. 12B).

Body. Head: Sub-rounded, nearly completely hidden under pronotum. Eyes and ocelli developed. Ocelli ridge indistinct, with a row of setae on the upper edge. Interocular space nearly equal to the distance between ocelli, and both narrower than the distance between antennal sockets. Clypeus developed (Fig. 12G). **Pronotum:** Transverse oval, widest near the middle. Densely covered with setae and pubescence, middle part with symmetrical stripe. Anterior whitish margin greatly broad and clearly delineated from yellowish brown areas (Fig. 12E). **Tegmina and hind wings:** Densely covered with small maculae, maculae fused near the base (Fig. 12A). **Legs:** Slender, front femur type C₁. Pulvilli and arolia present (Fig. 12B). **Abdomen:** Supra-anal plate transverse, narrow and pubescent, posterior margin slightly protruded medially. Paraprocts simple. Hind margin of subgenital plate flat, densely covered with setae. Styli columnar (Fig. 12I, J). **Genitalia:** L1 weakly sclerotized, anterior protrusion round, the left protuberance robust, two posterior lobes curved. L2 arched, terminal round. Genital hook (L3) curved in the middle. L4M broad lamellate. Pda and paa developed, protrusions long. L8 long and narrow, flaky. R1M widely expanded at terminal part. R1L elongate, banded. R2 divided into two chunks. R3 broadly concave (Fig. 12K, L).

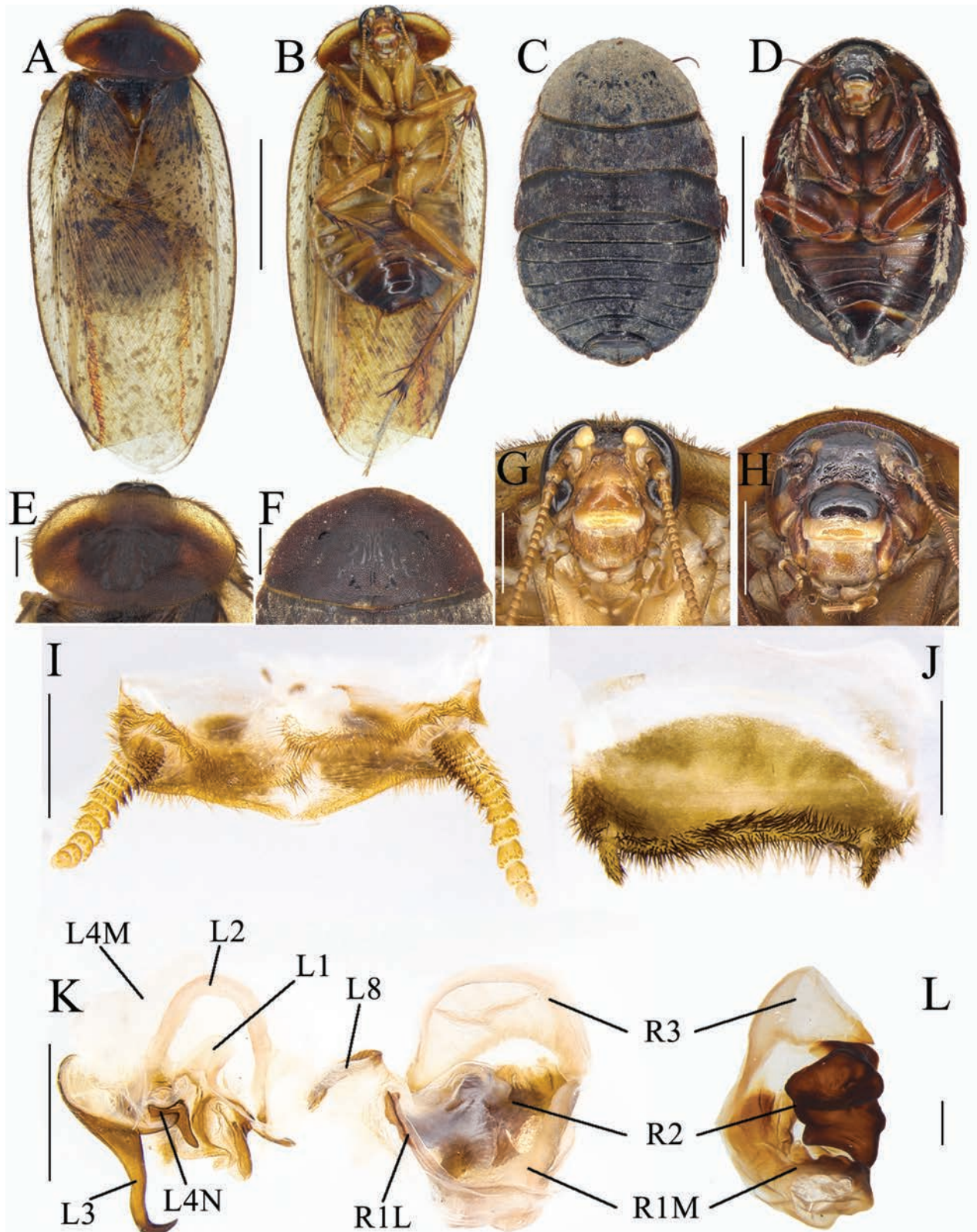


Figure 12. *Pseudoeupolyphaga baimaensis* Han, Che & Wang, sp. nov. **A, B, E, G, I–L** male holotype **C, D, F, H** female paratype. **A** habitus, dorsal view **B** habitus, ventral view **C** habitus, dorsal view **D** habitus, ventral view **E** pronotum, dorsal view **F** pronotum, dorsal view **G** head, ventral view **H** head, ventral view **I** supra-anal plate, ventral view **J** subgenital plate, ventral view **K** genitalia, dorsal view **L** right phallomere, right-ventral view. Scale bars: 1.0 cm (**A–D**); 0.2 cm (**E–H**); 0.1 cm (**I–L**).

Female paratype. Body length: 25.19 mm; body width: 16.01 mm; pronotum length × width: 9.29 × 5.09 mm.

Coloration. Terga blackish brown. Vertex, eyes, space between ocelli and post-clypeus black. Ocelli and antennae yellowish brown. Ante-clypeus and base of labrum yellowish white. Middle and distal part of labrum yellowish brown. Legs dark yellowish brown to black, spines black. Sterna nearly black, dark yellowish brown in most of central areas (Fig. 12C, D, H).

Body. The widest point of pronotum near the hind margin, middle part with symmetrical black stripe. Anterior whitish margin absent (Fig. 12F). Ocelli degraded to two spots. Interocular space almost equal to the distance between ocelli, both narrower than the distance between antennal sockets (Fig. 8H). Front femur type C₁. Arolia and pulvilli absent. Posterior margin of supra-anal plate protruded, emarginated medially. Cerci short, not exceeding posterior margin of supra-anal plate. Posterior margin of subgenital plate protruded, emarginated medially (Figs 12C, D, Suppl. material 1: fig. S1E).

Nymph. Unknown.

Ootheca. Yellowish brown. Surface with parallel longitudinal lines. Serrations of keel weak, terminal blunt. No respiratory canals (Fig. 15E, N).

Etymology. The species epithet is derived from the type locality, Baima Village, in Pingwu County, Mianyang City, Sichuan Province.

Remark. The genetic distance between this species and the remaining members of the genus ranges from 12.92% to 19.70%, providing support for its classification as a new species.

***Pseudoeupolyphaga pilosa* (Qiu, Che & Wang, 2018)**

Figs 13A–J, 15F, G, O, P

Eupolyphaga pilosa Qiu, Che & Wang, 2018: 50; Qiu et al. 2019: 11 (catalogue).
Pseudoeupolyphaga pilosa: Han et al. 2024: 166.

Type locality. “Yunnan Province, Diqing Prefecture, Weixi County, Pantiang Township, A valley Near Zhazi; 2970 m”

New material examined. CHINA • 1 male, 2 females; Yunnan Province, Lijiang City, Yulong Snow Mountain, Blue Moon Valley; 24 Jul. 2022; Wei Han, Lin Guo leg • 1 male, 1 female; Yunnan Province, Lijiang City, Wenbi Mountain; 24 Jul. 2022; Wei Han, Lin Guo leg • 1 male, 4 nymphs; Yunnan Province, Weixi County, Badi Village, Luodatang countryside; 25 Jul. 2022; Wei Han, Xin-Xing Luo, Lin Guo leg.

Remarks. This species was previously only documented in Pantiang Township, Weixi County, Yunnan Province. However, a recent collection in Yunnan has expanded its distribution range. In samples collected at various sites, the density of markings on the male tegmina varied (Fig. 13A–F). Markedly sparser markings were observed on the samples from Pantiang Township (Qiu et al. 2018: fig. 8A, B) and Luodatang countryside in Weixi County (Fig. 13A, B) compared to those from Yulong Snow Mountain (Fig. 13C, D) and Wenbi Mountain (Fig. 13E, F). Additionally, the male abdomens of samples from Pantiang Township, Yulong Snow Mountain, and Wenbi Mountain were dark brown to black, while those from Luodatang countryside were yellowish-brown.

Genetic distance analyses revealed that the genetic distance between samples from the four different collection sites ranged from 3.92% to 7.54%. Given the proximity of these new distributions to the type locality, and the absence of significant differences in oothecae (Fig. 15F, G, O, P; Qiu et al. 2018: fig. 38I, Q), the samples from the new location were temporarily classified as distinct geographic populations of *P. pilosa*.

***Pseudoeupolyphaga fengi fengi* (Qiu, Che & Wang, 2018)**

Figs 13K–N, 15H, Q

Eupolyphaga fengi fengi Qiu, Che & Wang, 2018: 42; Qiu et al. 2019: 11 (checklist).
Pseudoeupolyphaga fengi fengi: Han et al. 2024: 166.

Type locality. “Yunnan Province, Chuxiong City, Zixi Mountain; 2397 m”

New material examined. CHINA • 1 male, 2 females & 1 ootheca; Sichuan Province, Panzhihua City, Dahei Mountain, Xiaoshilin Pass; 22 Jul. 2022; Wei Han, Lin Guo leg.

Ootheca. Light reddish brown. Longitudinal lines densely arranged. Serrated protuberances sparsely arranged, tips subtriangular and slightly tilted. No respiratory ducts (Fig. 13H, Q).

Remarks. The male specimen from Zixi Mountain has pale yellowish-brown tegmina, a dark brown abdomen, and legs with yellow markings (Qiu et al. 2018: fig. 10E, F). While male samples from Dahei Mountain display pale grayish-brown tegmina, a blackish brown abdomen and legs, and yellow markings on the abdomen (Fig. 13K, L). The density of markings on tegmina is nearly identical in both location samples. Genetic distances range from 0% to 0.8% between the samples from Zixi Mountain, and from 6.6% to 7.1% between the samples from Zixi Mountain and Dahei Mountain. Since the genetic distances between the samples from Zixi Mountain and Dahei Mountain did not significantly differ, and the distribution of tegmina markings as well as the degree of density were almost identical, the differences in coloration and markings between the samples from Dahei Mountain and those from the type locality, Zixi Mountain, are temporarily considered to be intraspecific variation.

***Pseudoeupolyphaga fusca* (Chopard, 1929)**

Figs 13O–R, 15I, R

Eupolyphaga fusca Chopard, 1929: 270; Wu, 1935: 29; Princis, 1952: 35; Bey-Bienko, 1957: 896; Princis, 1962: 55; Qiu et al. 2018: 28; Qiu et al. 2019: 11 (catalogue).

Pseudoeupolyphaga fusca: Han et al. 2024: 166.

Type locality. “Yunnan Province, Kunming City”

New material examined. CHINA • 1 male, 2 females & 5 oothecae; Yunnan Province, Dali City, Cangshan National Geopark, Yudai Road; 29 Jul. 2022; Wei Han, Xin-Xing Luo leg.

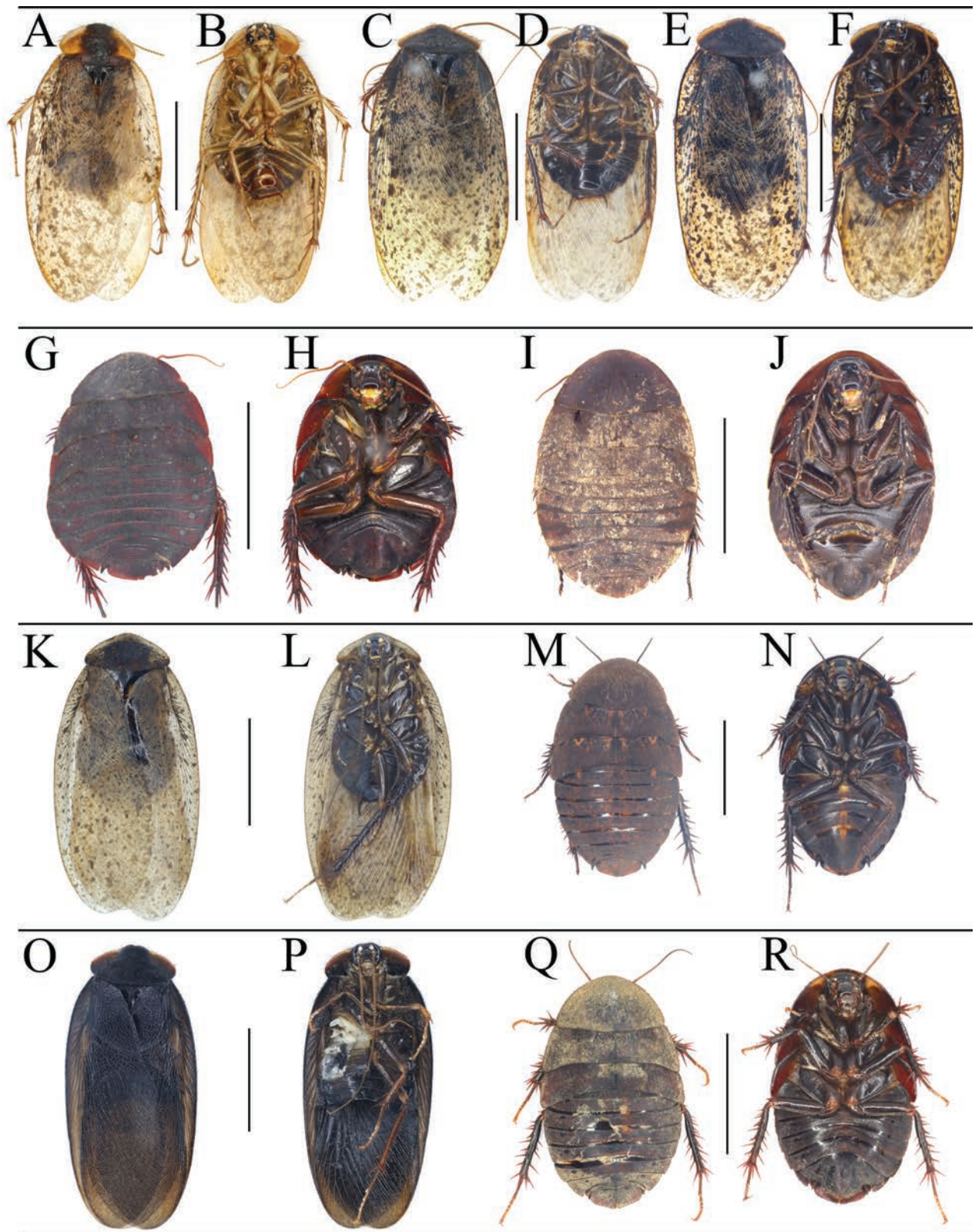


Figure 13. *Pseudoepolyphaga pilosa* (Qiu, Che & Wang, 2018) (A–J) *Pseudoepolyphaga fengi fengi* (Qiu, Che & Wang, 2018) (K–N) *Pseudoepolyphaga fusca* (Chopard, 1929) (O–R) A, B male of Luodatang countryside, C, D male of Yulong Snow Mountain, E, F male of Wenbi Mountain, G, H female of Pantiange Township, I, J female of Yulong Snow Mountain, K, L male of Dahei Mountain, M, N female of Dahei Mountain, O, P male of Cang Mountain, Q, R female of Cang Mountain. A, C, E, G, I, K, M, O, Q habitus, dorsal view B, D, F, H, J, L, N, P, R habitus, ventral view. Scale bars: 1.0 cm (A–R).

Ootheca. Light yellowish brown. Longitudinal lines densely arranged but not prominent. Serrated protuberances sparsely arranged with subtriangular tips. No respiratory ducts (Fig. 15I, R).

Remarks. This species is the only one in the genus with unicolored tegmina; the remaining species have spotted tegmina. It has the smallest interspecific genetic distance (6.61%) with *P. pilosa* in the genus. However, it can be distinguished from the latter based on tegmina coloration alone.

***Pseudoeupolyphaga simila* (Qiu, 2022)**

Fig. 14A–J

Eupolyphaga simila Qiu, 2022 in Han et al. 2022: 81.

Pseudoeupolyphaga simila: Han et al. 2024: 166.

Type locality. “Sichuan Province, Lixian County, Miyaluo Town, Siboguo Village; 2944 m”.

New material examined. CHINA • 3 males, 1 nymph; Sichuan Province, Aba Prefecture, Li County, Parktou Township, Tazigou; 22 Apr. 2023; Wei Han leg • 1 male, 1 female; Sichuan Province, Aba Prefecture, Li County, Dagou Village; 18 Apr. 2023; Wei Han leg.

Remarks. There was almost no difference in the external morphology between samples from Dagou Village (Fig. 14A, B) and the type locality Siboguo Village (Han et al. 2022: fig. 6A, B), aside from slightly denser tegmina markings in the former. The most discernible difference between Tazigou samples (Fig. 14C, D) and those from Siboguo Village was the relatively shorter and broader tegmina. Measurements for the Tazigou samples were as follows (mm): overall length: 21.87, body length: 16.71, body width (tegmina not included): 9.89, tegmen length × width: 18.44 × 8.13, and pronotum length × width: 8.37 × 3.88. Regarding genetic distance, it was 3.52% between Siboguo Village and Dagou village, 5.31% between Siboguo Village and Tazigou samples, and 5.12% between Dagou Village and Tazigou samples. Geographically, none of the three regions are more than thirty kilometers apart from each other. Hence, samples from both Dagou village and Tazigou are classified as *P. simila*.

Discussion

Incorporating molecular data could provide more reliable evidence for species identification within Corydioidea (Trotter et al. 2017; Han et al. 2022). Our results show that all morphologically identified species are supported by molecular data. However, the boundaries between interspecific and intraspecific genetic distances in *Pseudoeupolyphaga* remain unclear. The maximum intraspecific genetic distance within the genus is 7.54% (*P. pilosa*, samples from Luodatang countryside and Wenbi Mountain), while the minimum interspecific genetic distance is 6.61% (*P. pilosa* and *P. fusca*), resulting in overlapping intraspecific and interspecific genetic distances for the COI marker. This situation is detrimental to the delimitation of some morphologically similar specimens. Some studies have pointed out that the species' limited migratory capacity and substantial geographic isolation of their ranges may account for the larger intraspecific genetic distances (Qiu et

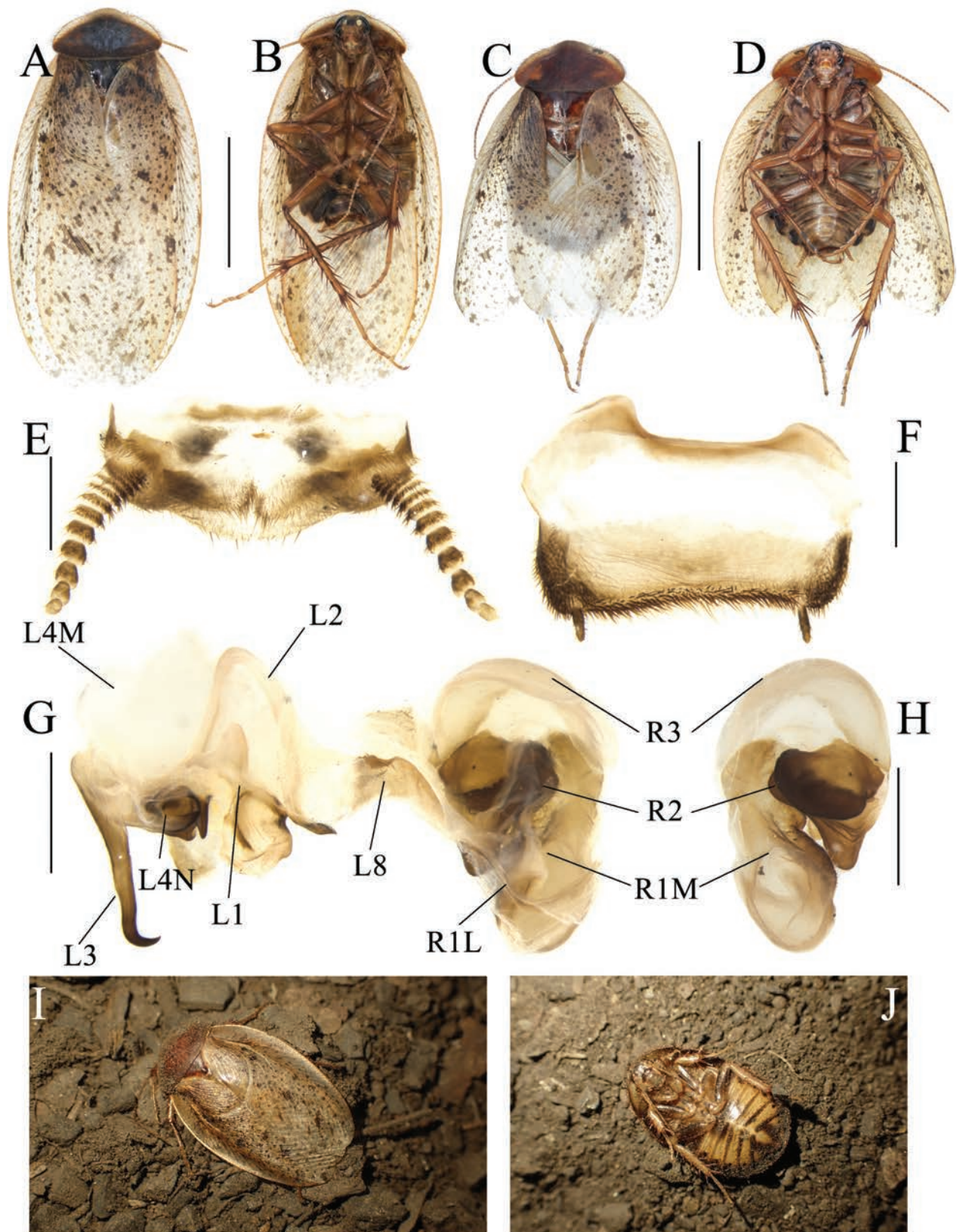


Figure 14. *Pseudoeupolyphaga simila* (Qiu, 2022) **A, B** male from Dagou Village, Li County, Aba Prefecture, Sichuan Province **C–J** male and nymph from Tazigou, Putou Township, Li County, Aba Prefecture, Sichuan Province **A** habitus, dorsal view **B** habitus, ventral view **C** habitus, dorsal view **D** habitus, ventral view **E** supra-anal plate, ventral view **F** subgenital plate, ventral view **G** genitalia, dorsal view **H** right phallomere, right-ventral view **I** a living male, dorsal view **J** a living nymph, ventral view. Scale bars: 1.0 cm (**A–D**); 0.1 cm (**E–H**).

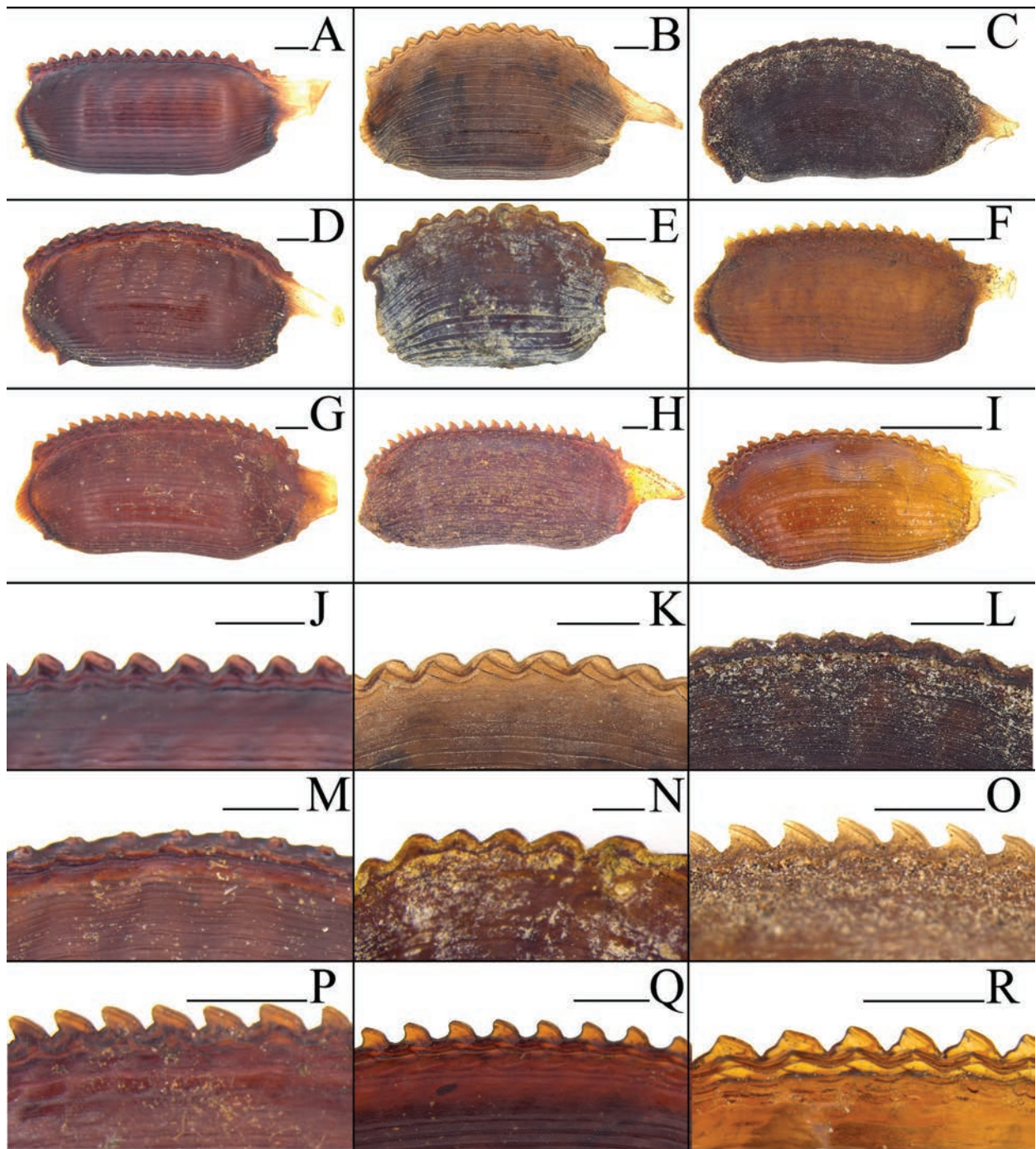


Figure 15. Oothecae of *Pseudoepolyphaga*, lateral view (A–I) and close-up view to show the serrations (J–R) A, J *P. deficiens* sp. nov. B, K *P. longiseta* sp. nov. C, D, L, M *P. latizona* sp. nov. C, L from Caoke Village D, M from Danba County E, N *P. baimaensis* sp. nov. F, G, O, P *P. pilosa* (Qiu, Che & Wang, 2018) F, O from Yulong Snow Mountain G, P from Wenbi Mountain H, Q *P. fengi fengi* (Qiu, Che & Wang, 2018) from Dahei Mountain I, R *P. fusca* (Chopard, 1929) from Cang Mountain. Scale bars: 0.1 cm (A–R).

al. 2018; Han et al. 2022). Thus, the delimitation of species in the genus should consider not only morphological and molecular differences, but also differences in geographic distance. In the future, broader sampling, more comprehensive genetic data collection, and consideration of geographic distribution or chromosome number, coupled with meticulous analyses, could facilitate comprehension of the species formation and ultimately improve species delimitation efforts.

The structure of female genitalia can serve as useful characters for species identification in Blattodea, albeit with variations in the sclerites utilized. For instance, key characters include the basivalvula, laterosternal shelf, and spermatheca in *Cryptocercus* Scudder, 1862 (Wang et al. 2015; Bai et al. 2018); and the anterior arch and basivalvula in *Anaplecta* Burmeister, 1838 (Zhu et al. 2022). Previous investigations of female genitalia within Corydioidea were limited, with descriptions available for only eight species across four genera (McKittrick 1964; Mackerras 1968; Grandcolas 1993).

In this study, we conducted a comparative analysis of the female external genitalia and spermathecae among eight species of *Eupolyphaga* and 15 species and subspecies of *Pseudoeupolyphaga*. Our findings revealed consistent structural compositions among these species, with variations observed in the degree of sclerotization in some sclerites. However, in both genera, the roles of the female external genital sclerites and spermathecae in species delimitation are not the same. Among these genital structures, the spermatheca, spermathecal plate, and basivalvula exhibited the most significant interspecific variation in *Eupolyphaga*. They can be used as reliable characters for female identification of this genus, alone or in combination. The morphology of spermatheca in *Eupolyphaga* species exhibits variability, and the females of the eight species can be distinguished based on the number, morphology, and mode of ampulla attachment (Fig. 5I–P). Additionally, the shape of the spermathecal plate varies significantly in *E. bicolor* sp. nov., *E. nigra* sp. nov., *E. hupingensis*, *E. robusta*, and *E. hanae* (Fig. 5A, B, D, G, H), distinguishing each species from the others. Furthermore, the basivalvula also serves as a distinguishing feature for species identification. For instance, in *E. hupingensis* (Fig. 5D), its shape differs distinctly from that of other species, while in *E. hanae* (Fig. 5H), the anterior margins of the two lobes are notably toothed and prominent. While most sclerites of the female genitalia in *Pseudoeupolyphaga* are poorly sclerotized and lack distinct boundaries, the other well-sclerotized sclerites (spermathecal plate and basivalvula) are almost identical in shape, as are the spermathecae. This makes them well suited as synapomorphy of the genus, but not effective for species delimitation. In the future, the study of female genitalia in more genera should be considered to reveal more about their taxonomic significance and their evolutionary patterns.

Acknowledgements

We are very grateful to all colleagues who provided specimens for this study. We thank Dr. John Richard Schrock for proofreading the draft. We also cordially thank Dr. Frédéric Legendre, Dr. Leonid N. Anisyutkin, and one anonymous reviewer for their comments and revisionary suggestions.

Additional information

Conflict of interest

The authors have declared that no competing interests exist.

Ethical statement

No ethical statement was reported.

Funding

This work was supported by National Natural Sciences Foundation of China (nos. 32070468 and 32170458) and a Program of the Ministry of Science and Technology of the People's Republic of China (2022FY202100)

Author contributions

Conceptualization: YLC, ZQW. Formal analysis: YLC, ZQW. Funding acquisition: YLC, ZQW. Investigation: WH. Methodology: ZQW. Software: YLC. Supervision: YLC. Visualization: PJZ. Writing - original draft: WH. Writing - review and editing: WH, ZQW.

Author ORCIDs

Wei Han  <https://orcid.org/0000-0002-7243-1657>

Zong-Qing Wang  <https://orcid.org/0000-0001-9413-1105>

Data availability

All of the data that support the findings of this study are available in the main text or Supplementary Information.

References

- Bai QK, Wang LL, Wang ZQ, Lo N, Che YL (2018) Exploring the diversity of Asian *Cryptocercus* (Blattodea: Cryptocercidae): species delimitation based on chromosome numbers, morphology and molecular analysis. *Invertebrate Systematics* 32: 69–91. <https://doi.org/10.1071/IS17003>
- Bey-Bienko GY (1950) Fauna of the USSR. Insects. Blattodea, 40. Institute of Zoology, Academy of Sciences of the URSS, Moscow, 343 pp.
- Bey-Bienko GY (1957) Blattoidea of Szechuan and Yunnan. Communication I. The results of the Chinese-Soviet zoologico-botanical expeditions to southwestern China 1955–1956. *Entomologicheskoe Obozrenie* 36: 895–915.
- Chopard L (1922) Les *Polyphaga* du groupe du *sinensis* Walk. (Orth. Blattidae). *Bulletin de la Société entomologique de France*: 194–196. <https://doi.org/10.3406/bsef.1922.27009>
- Chopard L (1929) Orthoptera palaeartica critica VII. Les Polyphagiens de la faune paléarctique (Orth., Blatt.). *Eos* 5: 223–358.
- Dohrn H (1888) Neue und wenig bekannte Blattiden. *Stettin Entomological Society* 49: 129–132.
- Feng PZ, Woo FC (1988) Three new species and two new records of Blattaria from Yunnan and Guizhou, China. *Entomotaxonomia* 10: 305–312.
- Feng PZ, Guo YY, Woo FC (1997) *Cockroaches of China, Species and Control*. China Science & Technology Press, 206 pp.
- Grandcolas P (1993) The genus *Therea* Billberg, 1820: phylogenetic position, new species, distribution, ecological value (Dictyoptera, Blattaria, Polyphaginae). *Canadian Journal of Zoology* 71: 1816–1822. <https://doi.org/10.1139/z93-259>
- Han W, Qiu L, Zhu J, Wang ZQ, Che YL (2022) Exploring the diversity of *Eupolyphaga* Chopard, 1929 (Blattodea, Corydioidea): species delimitation based on morphology and molecular analysis. *ZooKeys* 1120: 67–94. <https://doi.org/10.3897/zookeys.1120.87483>
- Han W, Qiu L, Zhang JW, Wang ZQ, Che YL (2024) Phylogenetic reconstruction of Corydioidea (Dictyoptera: Blattodea) provides new insights on the placement of Latindiinae

- and supports the proposal of the new subfamily Ctenoneurinae. *Systematic Entomology* 19: 156–172. <https://doi.org/10.1111/syen.12610>
- Hollier J, Marshall J, Legendre F (2020) An annotated list of the Blattodea (Insecta) described by Henri de Saussure. Part 1: The Corydiidae. *Revue Suisse de Zoologie* 127(2): 341–348. <https://doi.org/10.35929/RSZ.0023>
- Kimura M (1980) A simple method for estimating evolutionary rates of base substitutions through comparative studies of nucleotide sequences. *Journal of Molecular Evolution* 16(2): 111–120. <https://doi.org/10.1007/BF01731581>
- Kirby WF (1903) Notes on Blattidæ &c., with descriptions of new genera and species in the collection of the British Museum, South Kensington. No. II. *Annals & Magazine of Natural History* 7(70): 373–381. <https://doi.org/10.1080/00222930308678873>
- Klass KD. (1997) The external male genitalia and the phylogeny of Blattaria and Mantodea. *Bonner Zoologische Monographien* 42: 1–341.
- Kumar S, Stecher G, Tamura K (2016) MEGA7: Molecular evolutionary genetics analysis version 7.0 for bigger datasets. *Molecular Biology and Evolution* 33: 1870–1874. <https://doi.org/10.1093/molbev/msw054>
- Lanfear R, Frandsen PB, Wright AM, Senfeld T, Calcott B (2017) PartitionFinder 2: New methods for selecting partitioned models of evolution for molecular and morphological phylogenetic analyses. *Molecular Biology and Evolution* 34: 772–773. <https://doi.org/10.1093/molbev/msw260>
- Mackerras MJ (1968) Polyphagidae (Blattodea) from Eastern Australia. *Australian Journal of Entomology* 7: 147–154. <https://doi.org/10.1111/j.1440-6055.1968.tb00722.x>
- McKittrick FA. (1964) Evolutionary studies of cockroaches. *Cornell University Agricultural Experiment Station Memoir* 389: 1–197.
- Nguyen LT, Schmidt HA, von Haeseler A, Minh BQ (2015) IQ-TREE: A fast and effective stochastic algorithm for estimating maximum-likelihood phylogenies. *Molecular Biology and Evolution* 32: 268–274. <https://doi.org/10.1093/molbev/msu300>
- Princis K (1952) Kritisches verzeichnis der Blattarien Chinas und Tibets. *Opuscula Entomologica* 17: 33–43.
- Princis K (1962) Blattariae: Suborde Polyphagoidea: Fam. Polyphagidae. In: Beier M (Ed.) *Orthopterorum Catalogus. Pars 3. Uitgeverij Dr. W. Junk, 's-Gravenhage*, 3–74.
- Qiu L, Che YL, Wang ZQ (2018) A taxonomic study of *Eupolyphaga* Chopard, 1929 (Blattodea: Corydiidae: Corydiinae). *Zootaxa* 4506: 1–68. <https://doi.org/10.11646/zootaxa.4506.1.1>
- Qiu L, Yang ZB, Wang ZQ, Che YL (2019) Notes on some corydiid species from China, with the description of a new genus (Blattodea: Corydioidea: Corydiidae). *Annales de la Société Entomologique de France* 55: 261–273. <https://doi.org/10.1080/00379271.2019.1603081>
- Roth LM. (2003) Systematics and phylogeny of cockroaches (Dictyoptera: Blattaria). *Oriental Insects* 37: 1–186. <https://doi.org/10.1080/00305316.2003.10417344>
- Saussure HD (1869) *Mélanges Orthoptérologiques. Memoires de la Société de physique et d'histoire naturelle de Genève* 20: 227–328.
- Saussure HD (1893) Revision de la tribu des Hétérogamiens (Orthoptères de la Famille des Blattides). *Revue Suisse de Zoologie* 1(2): 289–318. <https://doi.org/10.5962/bhl.part.3746>
- Trotter AJ, McRAE JM, Main DC, Finston TL (2017) Speciation in fractured rock landforms: towards understanding the diversity of subterranean cockroaches (Dictyoptera: Nocticolidae: Nocticola) in Western Australia. *Zootaxa* 4250: 143–170. <https://doi.org/10.11646/zootaxa.4250.2.2>

- Walker F (1868) Catalogue of the Specimens of Blattariæ in the Collection of the British Museum. British Museum, London, 239 pp. <https://doi.org/10.5962/bhl.title.118688>
- Wang ZQ, Li Y, Che YL, Wang JJ (2015) The wood-feeding genus *Cryptocercus* (Blattoidea: Cryptocercidae), with description of two new species based on female genitalia. *Florida Entomologist* 98: 260–271. <https://doi.org/10.1653/024.098.0143>
- Woo FC, Feng PZ (1992) Blattoptera: Corydiidae, Blattidae, Epilampridae and Phyllo-dromiidae. *In*: Chinese Academy of Science (Org.), Insects of the Hengduan Mountains Region, 1. Science Press, Beijing, 865 pp.
- Wu CF (1935) *Catalogus Insectorum Sinensium*, I. The Fan Memorial Institute of Biology, Peiping, 367 pp.
- Zhu J, Zhang JW, Luo XX, Wang ZQ, Che YL (2022) Three cryptic *Anaplecta* (Blattoidea, Blattoidea, Anaplectidae) species revealed by female genitalia, plus seven new species from China. *ZooKeys* 1080: 53–97. <https://doi.org/10.3897/zookeys.1080.74286>

Supplementary material 1

Female external genitalia and spermatheca of 15 species and subspecies in *Pseudoeupolyphaga*

Authors: Wei Han, Yan-Li Che, Pei-Jun Zhang, Zong-Qing Wang

Data type: jpg

Copyright notice: This dataset is made available under the Open Database License (<http://opendatacommons.org/licenses/odbl/1.0/>). The Open Database License (ODbL) is a license agreement intended to allow users to freely share, modify, and use this Dataset while maintaining this same freedom for others, provided that the original source and author(s) are credited.

Link: <https://doi.org/10.3897/zookeys.1211.128805.suppl1>

Supplementary material 2

Collecting information for the samples included in Fig. 6 and fig. S1

Authors: Wei Han, Yan-Li Che, Pei-Jun Zhang, Zong-Qing Wang

Data type: xls

Copyright notice: This dataset is made available under the Open Database License (<http://opendatacommons.org/licenses/odbl/1.0/>). The Open Database License (ODbL) is a license agreement intended to allow users to freely share, modify, and use this Dataset while maintaining this same freedom for others, provided that the original source and author(s) are credited.

Link: <https://doi.org/10.3897/zookeys.1211.128805.suppl2>

Supplementary material 3

Genetic distances between COI genes of *Eupolyphaga* and *Pseudoeupolyphaga* species used in Fig. 1

Authors: Wei Han, Yan-Li Che, Pei-Jun Zhang, Zong-Qing Wang

Data type: xls

Copyright notice: This dataset is made available under the Open Database License (<http://opendatacommons.org/licenses/odbl/1.0/>). The Open Database License (ODbL) is a license agreement intended to allow users to freely share, modify, and use this Dataset while maintaining this same freedom for others, provided that the original source and author(s) are credited.

Link: <https://doi.org/10.3897/zookeys.1211.128805.suppl3>

Supplementary material 4

Molecular data matrix (COI genes) used in this study

Authors: Wei Han, Yan-Li Che, Pei-Jun Zhang, Zong-Qing Wang

Data type: fas

Copyright notice: This dataset is made available under the Open Database License (<http://opendatacommons.org/licenses/odbl/1.0/>). The Open Database License (ODbL) is a license agreement intended to allow users to freely share, modify, and use this Dataset while maintaining this same freedom for others, provided that the original source and author(s) are credited.

Link: <https://doi.org/10.3897/zookeys.1211.128805.suppl4>

A new southern Atlantic cryptic marine shrimp species of *Acetes* (Decapoda, Sergestidae)

Gabriel L. Bochini¹, Rogério C. Costa², Fernando L. Mantelatto¹

¹ Laboratory of Bioecology and Crustacean Systematics (LBSC), Department of Biology, Faculty of Philosophy, Science and Letters at Ribeirão Preto (FFCLRP), University of São Paulo (USP), Av. Bandeirantes 3900, 14040-901, Ribeirão Preto (SP), Brazil

² Laboratory of Biology of Marine and Freshwater Shrimp (LABCAM), Department of Biological Sciences, School of Sciences, São Paulo State University (UNESP), Av. Eng. Luiz Edmundo Carrijo Coube, 14-01, 17033-360, Bauru (SP), Brazil

Corresponding author: Fernando L. Mantelatto (flmantel@usp.br)

Abstract

A recently published molecular phylogenetic analysis, focusing on selected Western Atlantic subspecies of *Acetes americanus* Ortmann, 1893 and allies, was inconclusive about relationships among these members. This previous study found three groups that split into two distinct lineages: *Acetes americanus* (Brazil 1) (= *A. americanus* sensu stricto) and *Acetes americanus* (Brazil 2) + *A. americanus* (USA). Combined morphometry and molecular analyses applied to members of the group *Acetes americanus* (Brazil 2) revealed a new unidentified species genetically related to the *A. americanus* representatives. However, at that time, no conclusive morphological characters were found to identify it. In the present study, following an in-depth morphological analysis of specimens from the three groups, including data on the type series and consideration of the subtle distinctions of members of each lineage, morphological features of the reproductive structures (petasma and genital sternite) were found to characterize the new species, which is formally described and named herein.

Key words: *Acetes americanus*, Brazil, Cananéia, Dendrobranchiata, hidden diversity, new species, taxonomy



Academic editor: Célio Magalhães

Received: 22 May 2024

Accepted: 2 August 2024

Published: 4 September 2024

ZooBank: <https://zoobank.org/3B6C0EF3-96DA-4766-9341-C376AA94289A>

Citation: Bochini GL, Costa RC, Mantelatto FL (2024) A new southern Atlantic cryptic marine shrimp species of *Acetes* (Decapoda, Sergestidae). ZooKeys 1211: 193–209. <https://doi.org/10.3897/zookeys.1211.128059>

Copyright: © Gabriel L. Bochini et al. This is an open access article distributed under terms of the Creative Commons Attribution License (Attribution 4.0 International – CC BY 4.0).

Introduction

The genus *Acetes* H. Milne Edwards, 1830 is represented by 13 species worldwide (De Grave and Fransen 2011; DecaNet 2024). Only three species are distributed in the Western Atlantic: *Acetes americanus* Ortmann, 1893, *Acetes marinus* Omori, 1975 and *Acetes paraguayensis* Hansen, 1919 (Costa and Simões 2016; Simões et al. 2023). Historically, *Acetes americanus* has presented taxonomic instability in four subspecies (*A. americanus americanus* Ortmann, 1893; *A. a. carolinae* Hansen, 1933; *A. a. louisianensis* Burkenroad, 1934a; *A. a. limonensis* Burkenroad, 1934a), but only two of them are considered valid (Holthuis 1948) and accepted (see Simões et al. 2023 and DecaNet 2024 for review and details below), nowadays. *Acetes americanus* features a wide geographic distribution in the Western Atlantic and presents two subspecies acknowledged for their geographic separation: *Acetes americanus carolinae*

is distributed in North America and *Acetes americanus americanus*, in South America (DecaNet 2024). However, there are regions (Central America and Northern South America) where both subspecies are distributed in sympatry (Perez-Farfante and Kensley 1997). Despite the morphological similarity between these two subspecies, there are subtle morphological differences in their body and cornea lengths (Omori 1975). Yet, taxonomic inconsistencies were reported in both subspecies in the 1970s. Therefore, their geographically coexistent and subtle features make their validity doubtful and still unsolved. Accordingly, and due to pending future taxonomic rearrangements, the following nomenclature was adopted below: *A. americanus* sensu stricto - since the taxonomic status based on phylogenetic relationship, geographical distribution and morphology is clear [see lineage *A. americanus* (Brazil 1) in Simões et al. (2023); present study]; and *Acetes a. carolinae* - due to taxonomic uncertainties under this entity.

Specimens collected from the Brazilian coast were previously identified as *A. americanus* during a long-term biodiversity project focused on the Brazilian fauna, based on integrative analyses (see Mantelatto et al. 2018, 2022). These specimens showed some variability in morphological characters that have called our attention and presented some doubtful identifications. Recently, our team conducted a molecular study (Simões et al. 2023) to compare *A. americanus* specimens collected in South America to *A. a. carolinae* specimens sampled in North America. It was done using two mitochondrial markers to test the genetic validity of both subspecies and the likely existence of other entities distributed along the Western Atlantic that were not mentioned in previous investigations. This study found three strongly-supported groups divided into two different genetic lineages composed of *A. americanus* sensu stricto (Brazil 1) and *Acetes americanus* (Brazil 2) + *A. americanus* (USA) (see Simões et al. 2023; figs 3–6). The aforementioned authors used additional morphometric analysis (see Simões et al. 2023; fig. 7) to corroborate the lineages and the new unrecognized species, '*Acetes americanus* (Brazil 2)', which was genetically related to *A. americanus* representatives.

In the present study, we formally describe *Acetes americanus* (Brazil 2) based on morphology. Besides the significant support from previously developed DNA-based phylogenetic analyses, the new species was also compared to *Acetes a. americanus* and *A. a. carolinae*.

Materials and methods

Specimens were collected under field permit approval by *Instituto Chico Mendes de Biodiversidade/ICMBio*, Protocol No. 23008-1, Permanent Licenses to RCC number 23012-4 and FLM 11777-2, and SISGEN CEA7CD5 and A5845DA. Most of them were deposited at the Crustacean Collection of the Department of Biology (**CCDB**), Faculty of Philosophy, Science and Letters at Ribeirão Preto, University of São Paulo (**FFCLRP/USP**). Additional loaned specimens and the designated type series are deposited in the following scientific collections: Zoology Museum of University of São Paulo, São Paulo, Brazil (**MZUSP**); Crustacean Collection of the Laboratory of Biology of Marine and Freshwater Shrimp, São Paulo State University (UNESP), Bauru, Brazil (**CCLC**); Crustacean Collection of Federal University of Rio Grande do Sul, Brazil (**DZ/UFRGS**); Crustacean

Collection of Museu Nacional do Rio de Janeiro, Brazil (**MNRJ**); Oceanographic Museum of Federal University of Pernambuco, Brazil (**MOUFPE**); National Museum of Natural History, Smithsonian Institution, USA (**USNM**); University of Louisiana Zoological Collection, Lafayette, USA (**ULLZ**); and Natural History Museum of Denmark - University of Copenhagen, Denmark (**NHMD**).

The morphological description was based on characters and character states proposed by Omori (1975), D’Incao and Martins (2000) and Vereshchaka et al. (2016a, 2016b), which used the form of the genital area (thelycum) in females and the petasma shape in males as diagnostic characters. The phylogenetic positioning and topologies proposed by Simões et al. (2023) were followed to assess individuals’ morphology and identification.

Carapace length was measured from the rostrum tip to the carapace’s posterior margin and expressed in millimeters (mm). All measurements were taken with a calibrated ocular micrometer (+/- 0.1 mm) or digital caliper. Sex was assessed based on petasma (first pleopod) presence in males and on thelycum presence in females (Xiao and Greenwood 1993). Morphometric measurements and illustrations were carried out with the aid of a stereo microscope (Leica® M205 C) coupled with a camera (Leica® DFC 295), added with software Leica Application Suite version 3.8.0 for taking measurements. The resulting drawings were processed in Adobe Illustrator 2020®.

Molecular analyzes

The phylogenetic hypothesis was created using the same sequences produced and deposited in GenBank by Simões et al. (2023) (Suppl. material 1). Maximum likelihood phylogenetic analyzes were performed using the IQ-TREE program (Miller et al. 2010) with the mitochondrial 16S Ribosomal RNA (16S rRNA) and cytochrome c oxidase subunit I (COI) genes concatenated. Branch support was assessed by ultrafast bootstrap with 1000 replications. *Acetes paraguayensis* Hansen, 1919 was included as an outgroup following the most recent global phylogeny (Vereshchaka 2017) and Simões et al. (2023). Intra- and interspecific genetic distances were estimated using MEGA 5.0 software (Tamura et al. 2011).

Abbreviations

cl carapace length,
coll(s). collector(s),
ind. individuals,
PL. pleopods,
coord. coordinate.

Results

Taxonomy

Superfamily Sergestoidea Dana, 1852

Family Sergestidae Dana, 1852

Genus *Acetes* H. Milne Edwards, 1830

***Acetes maratayama* Bochini, Costa & Mantelatto, sp. nov.**

<https://zoobank.org/BC6949CD-ABFE-48CA-8311-ED86CC7E5B6D>

Figs 1–4

Type material. Holotype: BRAZIL: • ♂ (cl 2.94 mm); CCDB 7957; São Paulo, Cananéia, Mar Pequeno; (24°59'55"S, 47°53'49"W); 5–10 m deep; colls. Costa, R.C. et al.; 17 April 2011. **Paratypes:** • 4 ♂s and 4 ♀s (cl 2.70 – 3.93 mm); CCDB 7958 (photo available, one dissected specimen); same data as holotype • 1 ♂ and 1 ♀ (cl 2.9 and 4.04 mm, respectively); MOUFPE 22042; same data as holotype • 1 ♂ and 1 ♀ (cl 3.04 and 3.93 mm, respectively); MZUSP 45904; same data as holotype • 2 ♂s and 2 ♀s (cl 4.01 – 5.19 mm); CCDB 7959; BRAZIL, Rio de Janeiro, Macaé; (22°22'13.65"S, 41°39'9.42"W); colls. Davanso, T.M. et al.; 01 September 2013 • 2 ♂s and 2 ♀s (cl 3.25 – 5.34 mm); MNRJ 31168; BRAZIL, Rio de Janeiro, Macaé; (22°22'13.65"S, 41°39'9.42"W); colls. Davanso, T.M. et al.; 01 September 2013 • 1 ♂ and 1 ♀ (cl 4.20 and 5.53 mm, respectively); DZ/UFRGS 7089; BRAZIL, Rio de Janeiro, Macaé; (22°22'13.65"S, 41°39'9.42"W); colls. Davanso, T.M. et al.; 01 September 2013.

Additional material. • > 30 ind. (not measured); CCDB 3251; same data as holotype • > 50 ind. (not measured); CCDB 7624; BRAZIL, Rio de Janeiro, Macaé; (22°22'13.65"S, 41°39'9.42"W); colls. Davanso, T.M. et al.; 01 September 2013.

Comparative material. *Acetes a. americanus*: • 7 ind.; CCDB 6320; BRAZIL, Rio Grande do Norte, Baía Formosa; (06°21'11.6"S, 35°00'1.9"W); colls. Lopes, M., Carvalho-Batista, A.; 25 April 2014 • 2 ♀s (cl 3.6 and 5.1 mm); MZUSP 21210; BRAZIL, Alagoas, Maceió; 27/06/1989 • > 15 ind.; CCLC 258; BRAZIL, Espírito Santo, Anchieta, col. Braga, A.C.A.; 01 January 2014 • 10 ind.; CCDB 7626; BRAZIL, Rio de Janeiro, Macaé; (22°22'13.65"S, 41°39'9.42"W); colls. Davanso, T.M. et al.; 01 September 2013 • >10 ind.; CCLC 253; BRAZIL, São Paulo, Ubatuba, col. Costa, R.C.; 02 October 2014 • 10 ind.; CCDB 4939; BRAZIL, São Paulo, São Vicente, col. Castilho, A.L.; 03 September 2012 • 2 ♀s (cl 5.10 and 4.80 mm); CCLC 257; BRAZIL, Santa Catarina, Penha, coll. Davanso, T.M.; 24 June 2014.

Acetes a. carolinae: • 2 ♂s and 3 ♀s; ULLZ 3274; UNITED STATES, Gulf of Mexico, Louisiana; coll. Forman, W.W.; 31 October 1972.

Diagnosis. Rostrum acuminate, acute; median ridge with strong posterior tooth. Carapace smooth on surface, except for post-orbital and hepatic spine. Hepatic spine present in males, external part petasma not exceeding base of capitellum; inferior antennular flagellum with 10 articles. Concavity of anterior margin of genital sternite in females forming very deep arch.

Description. Male. The rostrum (Fig. 1A, B) is acuminate, acute; the median ridge has a strong posterior tooth. There is a small supraorbital spine on each side above the eyes, near the face. The hepatic spine is present (Fig. 1A). Quite large eyes do not exceed the posterior margin of the first antennular article (Fig. 1A, C). Antennule with long peduncle; very elongated third article, which is approximately three times longer than the inner margin of the second article, similar to the size of the first article (Fig. 1D); the first article in females is twice the length of the third article and approximately 4.5× longer than the second article; the inner distal lateral margin of the first article presents simple setae in the anterior half (Fig. 1G); males with inferior antennular flagellum have 10 articles; there is no clasping organ; males' thickened proximal 3-article portion

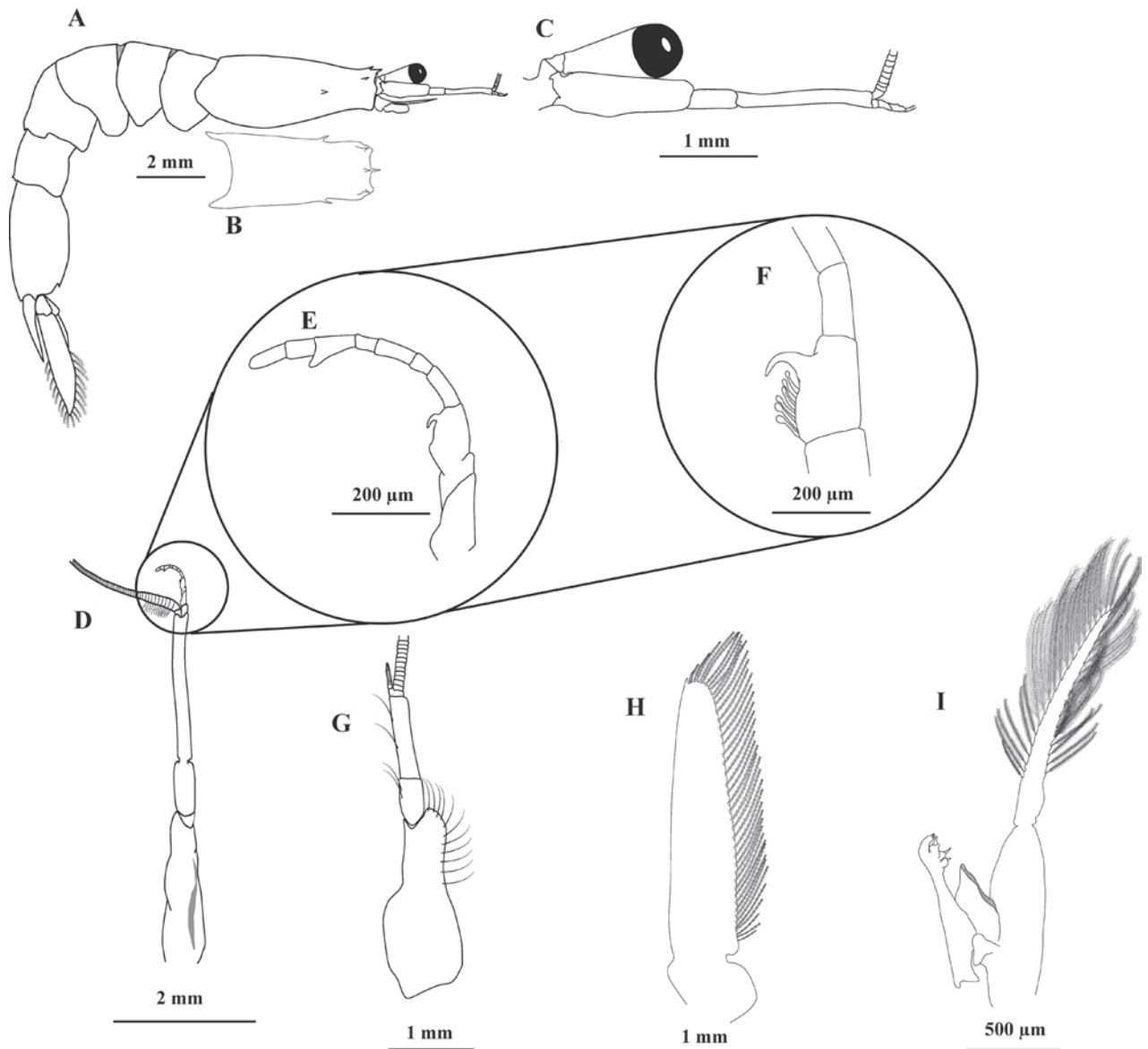


Figure 1. *Acetes maratayama* sp. nov. **A–F, H–I** male paratype, Brazil, São Paulo, Cananéia (CCDB 7958) **G** female, paratype, Brazil, São Paulo, Cananéia (CCDB 7958) **A** lateral view **B** carapace, dorsal view **C** right antennular peduncle and ocular peduncle, lateral view **D** right antennular peduncle, dorsal view **E** lower antennular flagellum, lateral view **F** proximal part of lower antennular flagellum, lateral view **G** right antennular peduncle, dorsal view **H** scaphocerite, dorsal view **I** first pleopods and petasma, lateral view.

occupies less than half of the flagellum; third article has 6 obtuse spinules similar to fingers, and 1 procurved and robust projection (Fig. 1E, F); article 8 has a projection similar to a lobe in the inner lateral part of the article's distal region (Fig. 1E). Antennal scale extending to the middle of the second antennular peduncle article with small spine on the anterior external portion (Fig. 1A, H).

Mandible with biarticulated palp; first article of the palp 3× longer than the second article (Fig. 2A); first maxilla without palp (Fig. 2B); second maxilla with one single undivided lobe (Fig. 2C); first maxilliped without palp (Fig. 2D); second maxilliped with 5 articles (Fig. 2E); third maxilliped exceeding half of the antennal scale, without reaching the distal margin of the antennal scale (Fig. 2F).

The first 3 pairs of pereopods are elongated and have a small chela (Fig. 3A–C). Fourth and fifth pereopods were completely absent, except for a pair of protuberances (genital thighs) in males. The sixth segment of the pleon is longer than the others (Fig. 1A). Slender pleopods, the hind ones, are a little stockier. First pair with one single branch, with sexual appendages in males (Fig. 3D) - the remainder has two appendages (Fig. 3E–H). Pleopods with a row of spines on the basal articles of the endopods and exopods. PL2 with 5 spines on the outer margin of the endopod basal joint and 5 spines on the inner margin of the exopod basal joint (Fig. 3E); PL3 with 12 spines on the outer margin of the endopod and with 5 ones on the outer margin of the exopod (Fig. 3F); PL4 with 7 spines on the external margin of the endopod (Fig. 3G) and PL5 with 8 spines on the external margin of the endopod (Fig. 3H). Telson shorter than the anterior segment, long triangularly truncated at the tip (Fig. 3I). Uropods significantly longer than the telson, external branch much longer than the internal one, with a thin tooth on the external edge closer to the tip (Fig. 3I). The uropod exopod is 4.5 times longer than it is wide; a small spine on the outer margin in the 1/3rd portion separates the ciliated portion from the non-ciliated portion (Fig. 3I). Telson apex is truncated; lateral margins are often curved inwards and form two short teeth between which the slightly convex posterior margin is found; there are 4 bristles between the terminal teeth, the two median ones are larger than the outer teeth, and two equal-sized bristles are external to the terminal teeth (Fig. 3J).

Males. *Acetes maratayama* sp. nov. is very similar to the other two described Atlantic species (*A. a. americanus* and *A. a. carolinae*), except for its different petasma and female genital sternite. Petasma pars externa in *A. maratayama* sp. nov. does not reach the base of the capitulum (Fig. 4B); the pars externa extends above the base of the capitulum in *A. a. carolinae* (Fig. 4C). On the other hand, it extends far beyond the capitulum base and reaches the middle portion of it in *A. americanus* (Fig. 4A). Pars externa insertion in *A. maratayama* sp. nov. is located in the middle section of the pars media (Fig. 4B, black arrow), similar to *A. a. carolinae* (Fig. 4C, black arrow). However, pars externa insertion in *A. americanus* is located close to the capitulum base (Fig. 4A, black arrow).

Female. The concave anterior margin of the genital sternite forms a very deep arch (Fig. 4E, red arrow) in comparison to *A. americanus* (Fig. 4D, red arrow), which has a shallow-arched concavity. The free sublateral projections by the margin's sides are enclosed and taper to a defined point, besides being slightly curved. *Acetes a. carolinae* shape is similar to that of *A. maratayama* sp. nov.; however, the concavity of the genital sternite is not as deep, and the arch region is straight (Fig. 4F, red arrow). The thigh of the third pair of pereopods of *A. maratayama* sp. nov. accounts for most of the inner margin convex and presents a small indentation (Fig. 4E, black arrow). No tooth was found in its distal end. However, a large, oblong, acute process projects downwards the lower side of each thigh, close to the inner margin, and far forward and somewhat outward. *Acetes a. americanus* did not have an indentation (Fig. 4D, black arrow) and *A. a. carolinae* had a small projection (Fig. 4F, black arrow).

Habitat. The species was collected by trawling in shallow waters in depths between 5 and 30 m. The bottom sediment type at the locality comprises medium and fine sand and has a salinity close to 26–28 ppt. It is considered the mesohaline area of the estuary (see Garcia et al. 2018 for environmental characterization of the Cananéia region's bottom area).

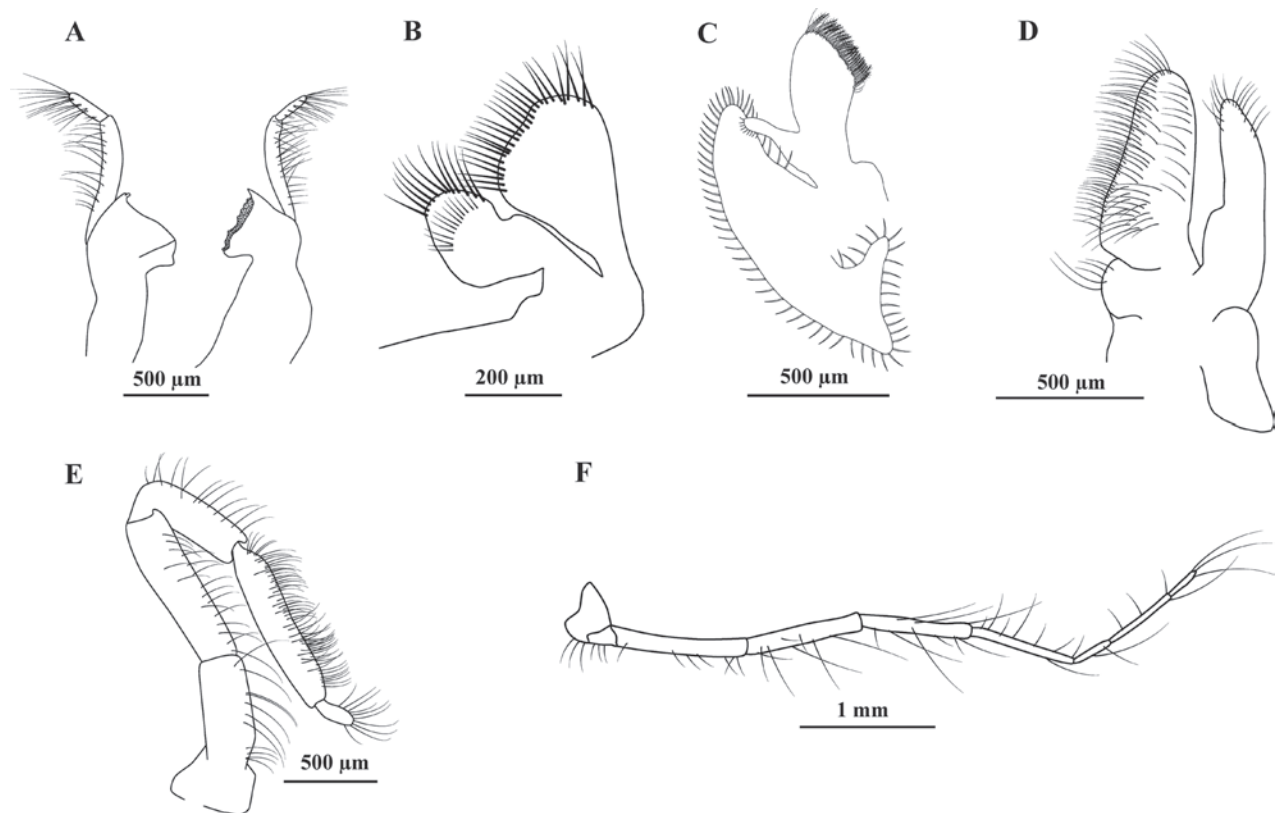


Figure 2. *Acetes maratayama* sp. nov., male paratype, Brazil, São Paulo, Cananéia (CCDB 7958) **A** right and left mandible, lateral view **B** first maxilla, dorsal view **C** second maxilla, dorsal view **D** first maxilliped, dorsal view **E** second maxilliped, lateral view **F** third maxilliped, lateral view.

Coloration in life. Translucent like other species.

Type locality. Brazil, São Paulo, Cananéia (24°59'55"S, 47°53'49"W).

Distribution. Brazil, São Paulo, Cananéia (24°59'55"S, 47°53'49"W) and Rio de Janeiro, Macaé (22°22'13.65"S, 41°39'9.42"W).

Etymology. The new species is named after the type locality, Cananéia, southern São Paulo state, Brazil. Maratayama is the old name of Cananéia recorded in the navigation log of the expedition from Portugal that arrived in the region in 1531. From the Tupi-Guarani language, Maratayama means a place where the land meets the sea or land of the sea (Mara = sea and Tayama = land).

Genetic sequences. The previous genetic characterization and generated sequences obtained by Simões et al. [2023 – as “*Acetes americanus* (Brazil 2)” - <https://peerj.com/articles/14751/#supplemental-information>] are updated and should be referred to as *Acetes maratayama* sp. nov. The data, i.e., gene marker, geographic region, voucher catalogue collection and sequence accession number (GenBank), are: 16S Ribosomal RNA (16S) – Macaé/RJ: CCLC 0261 (OP035684 to OP035686), CCLC 0267 (OP035697); Cananéia/SP: CCLC 0262 (OP035687), CCDB 3251 (OP035688, OP035698 to OP035700); cytochrome c oxidase subunit I (COI) – Macaé/RJ: CCLC 0255 (OP060472), CCLC 0261 (OP060504 to OP060507), CCLC 0267 (OP060521 to OP060523); Cananéia/SP: CCLC 0262 (OP060508), CCDB 3251 (OP060509, OP060524 to OP060528). Some of these sequences were herein used to prepare the phylogenetic tree (Suppl. material 1).

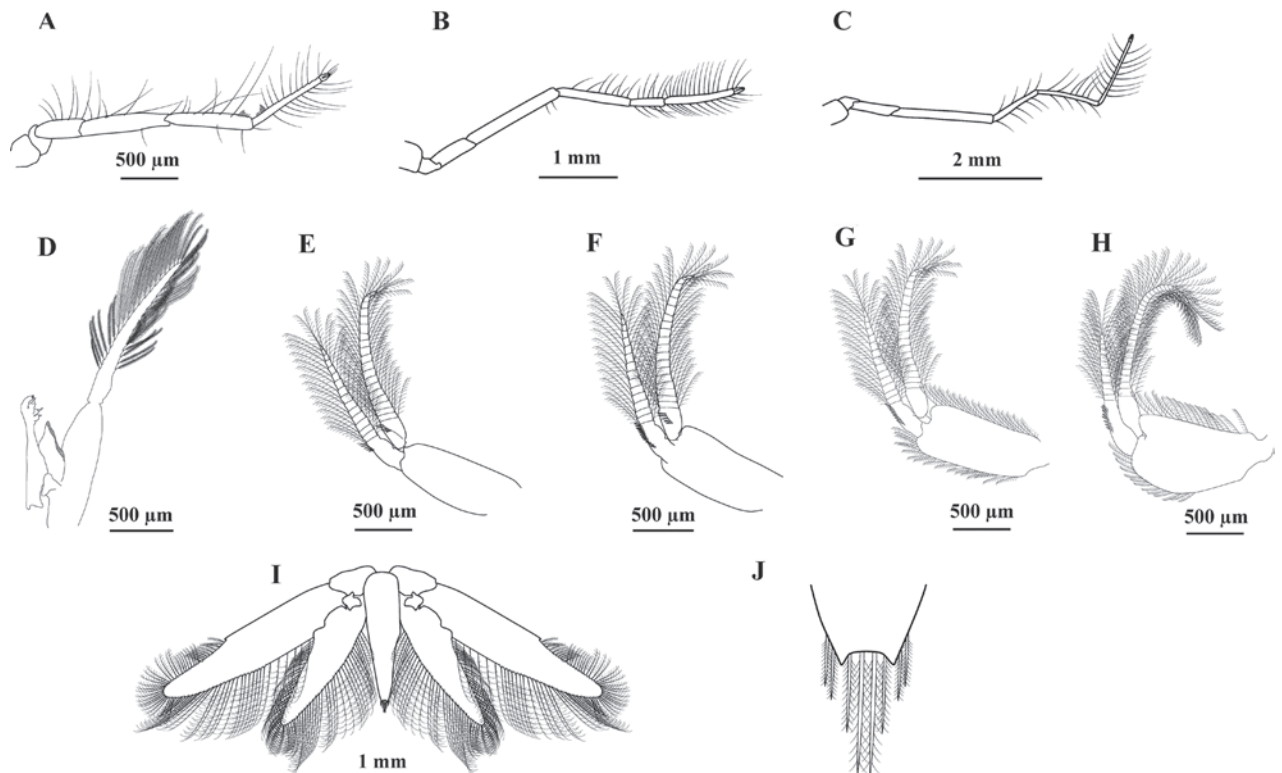


Figure 3. *Acetes maratayama* sp. nov., male paratype, Brazil, São Paulo, Cananéia (CCDB 7958) **A** first pereopod, lateral view **B** second pereopod, lateral view **C** third pereopod, lateral view **D** first pleopod with petasma, lateral view **E** second pleopod, lateral view **F** third pleopod, lateral view **G** fourth pleopod, lateral view **H** fifth pleopod, lateral view **I** uropod and telson, dorsal view **J** apex of telson, dorsal view.

Genetic distance. 16SrRNA gene: Intraspecific distances ranged from 0% (*A. americanus*, *A. maratayama* sp. nov. and *A. carolinae*) to 0.21% (*A. paraguayensis*) (Table 1). Interspecific distances between congeneric species ranged from 1.49 to 8.53% (Table 1). Regarding *A. maratayama* sp. nov., the smallest genetic distance observed was 0.85% with *A. carolinae*, 1.49% with *A. americanus* and the highest was 8.53% with *A. paraguayensis* (Table 1).

COI gene: Intraspecific distances ranged from 0 to 0.19% (*A. americanus* and *A. carolinae*), from 0 to 0.38 (*A. maratayama* sp. nov.), and from 0.57% (*A. paraguayensis*) (Table 2). Interspecific distances between congeneric species ranged from 4.78 to 19.89% (Table 2). Regarding *A. maratayama* sp. nov., the smallest genetic distance observed was with *A. americanus* (6.12–6.50%), followed by *A. carolinae* (7.65–8.63%), and the largest was with *A. paraguayensis* (19.50–19.89%) (Table 2).

Phylogenetic analyses. The phylogenetic tree based on concatenated data (16S rRNA and COI) generated a similar topology found by Simões et al. (2023), with high support values. Two distinct clades were observed, one formed by *A. americanus* and *A. carolinae* and the sister clade formed by *A. maratayama* sp. nov. (Fig. 5)

Remarks. *Acetes maratayama* sp. nov. is closely related to *A. americanus* and *A. a. carolinae*, and it presents small morphological differences, mainly in reproductive structures. Furthermore, *A. maratayama* sp. nov. has 10 articles in the antennular flagellum, whereas *A. a. carolinae* has 9 articles, *A. binghami* Burkenroad, 1934a has 7 articles and *A. intermedius* Omori, 1975 has 13–14 articles.

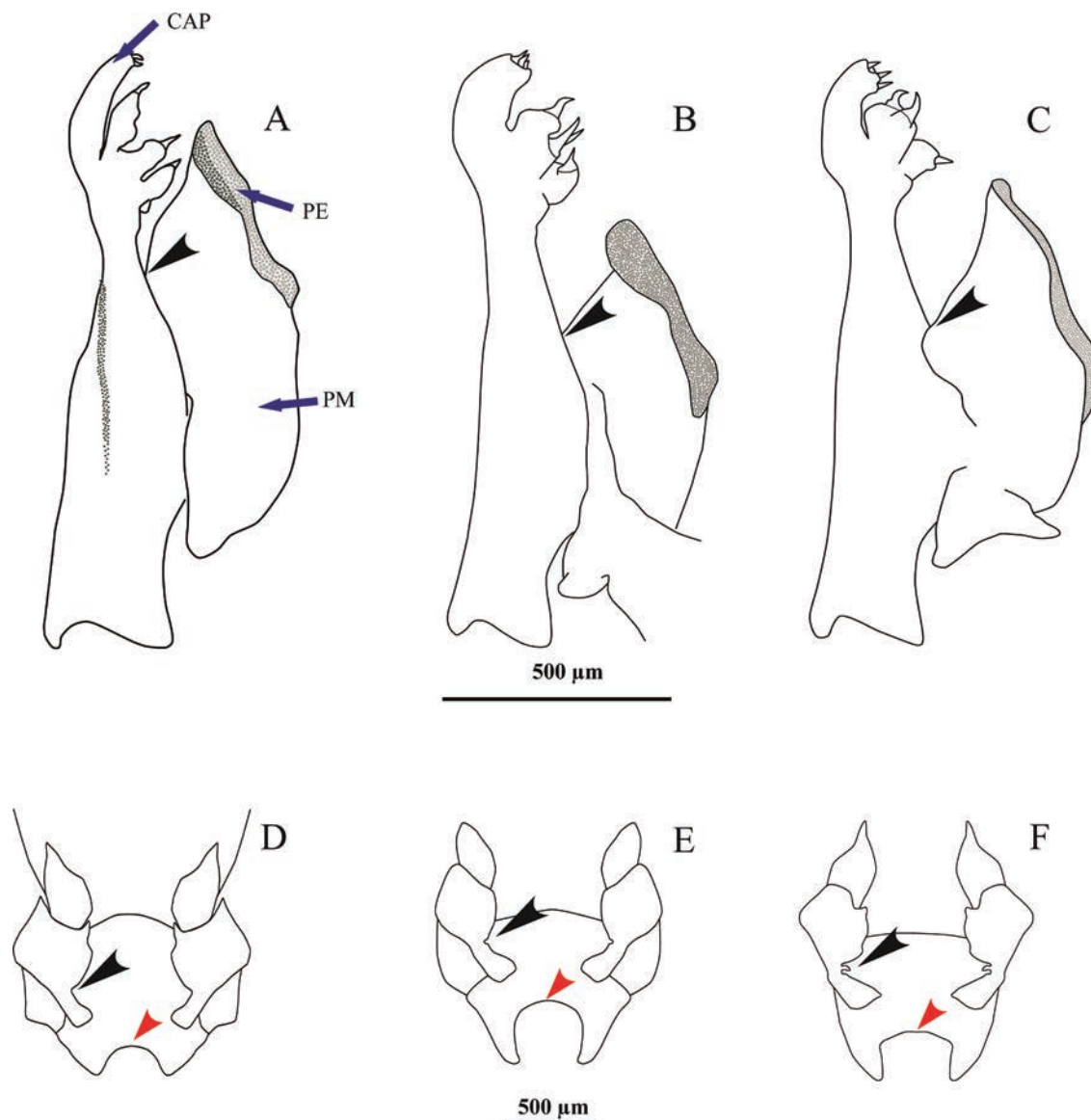


Figure 4. *Acetes americanus* **A, D**, male and female, Brazil, Rio de Janeiro, Macaé (CCDB 7626); *A. maratayama* sp. nov. **B, E**, male and female holotype, Brazil, São Paulo, Cananéia (CCDB 7957); *A. carolinae* **C, F**, male and female, United States, Gulf of Mexico, Louisiana (ULLZ 3274) **A** petasma lateral view, and **D** genital sternite ventral view **B** petasma lateral view, and **E** genital sternite, ventral view **C** petasma lateral view, and **F** genital sternite, ventral view. Cap, capitulum; PE, pars externa; PM, pars media. In males, black arrows indicate the insertion of the pars externa into the pars media of the petasma. In females, black arrows indicate the inner margin of the thigh of the third pair of pereopods, and red arrows indicate the curvature of the genital sternite.

Table 1. Genetic distance values for the 16S rRNA gene between *Acetes* species distributed in the southwest Atlantic. The comparison is made between the same individuals used to build the phylogenetic trees, and the results show the minimum and maximum genetic differences recorded intra and interspecific.

	Species	1	2	3	4
1	<i>A. americanus</i>	0%			
2	<i>A. carolinae</i>	1.92%	0%		
3	<i>A. maratayama</i>	1.49%	0.85%	0%	
4	<i>A. paraguayensis</i>	8.32–8.53%	7.89–8.10%	8.32%–8.53%	0.21%

Table 2. Genetic distance values for the COI gene between *Acetes* species distributed in the southwest Atlantic. The comparison is made between the same individuals used to build the phylogenetic trees, and the results show the minimum and maximum genetic differences recorded intra and interspecific.

	Species	1	2	3	4
1	<i>A. americanus</i>	0–0.19%			
2	<i>A. carolinae</i>	4.78–5.16%	0–0.19%		
3	<i>A. maratayama</i>	6.12–6.50%	7.65–8.63%	0–0.38%	
4	<i>A. paraguayensis</i>	19.31–19.89%	19.31–19.89%	19.50–19.89%	0.57%

Acetes maratayama sp. nov. is easily distinguishable from *A. binghami*, since the rostrum in this species does not have denticles behind the terminal tip, whereas the rostrum in *A. paraguayensis* has a strong tooth. There is a rudimentary denticle or hair minus one angular bend between this tooth and the end of the rostrum. The first article of the palp is 3 times longer than the second article. It is 5 times longer in *A. binghami*. The first article of the palp in *A. intermedius* is 2 times longer than the second article.

Historically, Burkenroad (1934b) recognized four *A. americanus* subspecies: *A. americanus carolinae* (type locality: Beaufort Inlet, North Carolina, USA), *A. a. louisianensis* (type locality: Louisiana coast, from the Mississippi River West to Timbalier Island, Gulf of Mexico, USA), *A. a. limonensis* (type locality: Sweetwater River mouth, Limon Bay, Panama) and *A. a. americanus* (type locality: mouth of Tocantins River). However, *A. a. louisianensis* was synonymized with *A. a. carolinae* and *A. a. limonensis* was synonymized with *A. a. americanus* (DecaNet 2024). Holthuis (1948) states that subspecies *A. a. louisianensis* presents intermediate characteristics of other subspecies in this genus. They are not considered valid clinal variants. Burkenroad (1934b – Penaeidae from Louisiana, p. 132) states that:

“Although I do not consider the differences here pointed out sufficiently certain or significant to require taxonomic recognition, if direct comparisons prove this to be desirable, I would suggest for Material from Louisiana with the subspecific name *Acetes carolinae louisianensis*.”

This author also added important notes to Hansen’s (1919) description of *A. carolinae* (pp. 130–132).

Thus, several records show the geographic disjunction between the Gulf of Mexico and Panama and the well-documented vicariance processes in this region, which point out speciation between these regions and Western United States Atlantic (Coates and Obando 1996; Allmon 2001; Harrison 2004; Mantelatto et al. 2023). We are still not fully convinced that *A. a. louisianensis* is synonymous with *A. a. carolinae*. Therefore, more robust morphological analyses associated with molecular analyses must be carried out to help better understand these entities.

Individuals from the Western Atlantic (North Carolina - NC) were not included in the molecular analyses carried out by Simões et al. (2023), since they focused on species distributed within Brazil. It means that doubts about *A. a. carolinae* remain unresolved. Unfortunately, we did not have the opportunity to morphologically analyze the specimens (Fig. 6) identified as the cotype of

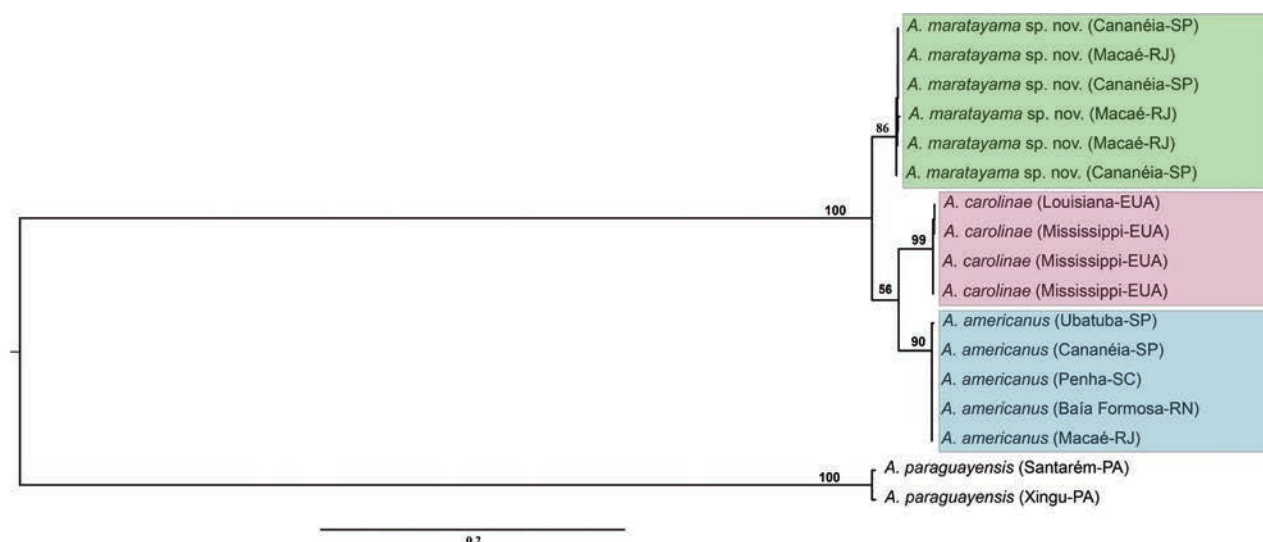


Figure 5. Phylogenetic reconstruction of *Acetes* based on concatenated markers 16S rRNA and COI. Phylogenetic tree of Bayesian inference for the *Acetes* species data with Bayesian posterior probabilities indicated (only posterior probabilities > 50% are shown).

A. a. carolinae, from USNM (74550). There is only one sequence (histone 3 gene) of *A. a. carolinae* from the North Carolina locality deposited in GenBank (KX216649) compared to our newly generated sequences of nuclear gene, histone 3 (H3), for individuals from Louisiana and Mississippi regions (ULLZ 14545 – Genbank PP816024, PP816025, PP816026). However, this gene's DNA fragment (very conserved region) is not informative enough to identify congeneric species. Simões et al. (2023) recovered the lineage identified as "*A. americanus* (USA)", which is formed by individuals from Louisiana and Mississippi, USA. Thus, doubts are raised about the likely validity/resurrection of subspecies *A. a. louisianensis*, which is strongly supported by the type locality being in the Gulf of Mexico. Further molecular analyses using other genes are necessary to elucidate the taxonomic status of *Acetes* species located in the Gulf of Mexico region and in North Carolina, named *A. a. carolinae*.

It is also important to recall that Hansen (1919) described *Acetes brasiliensis* (p. 45–46, figs 1–7) collected from the Amazon River estuary. He mentioned the similarity to *A. americanus*, as described by Ortmann (1893), for collections from the mouth of Tocantins River, Brazil (Foz do rio Pará), which is very close to Amazon River. Despite a general description and undetailed figures, he emphasized that *A. brasiliensis* presented two features (length of third joint of the antennule and exopod of the uropod) making it impossible to refer *A. brasiliensis* to the species established by Ortmann. Burkenroad (1934b, p. 130), stated that:

"The characters by which Hansen has distinguished *A. brasiliensis* from *A. americanus* seem of very uncertain importance. The differences in length of the ciliated part of the external margin of the exopod of the uropod, as those in other characters not mentioned by Hansen, are perhaps attributable to the obvious inaccuracy of Ortmann's figure. That Ortmann failed to notice the elongation of the third segment of the antennular peduncle of the male of his species is no more astonishing than that Kishinouye failed to do so for *A. japonicus*, as Kemp has shown to be the fact."



Figure 6. *Acetes a. carolinae* – type material of the original description by Hansen (1919) deposited at National Museum of Natural History, Smithsonian Institution, United States (USNM), Washington D.C., USA (USNM 74550). Photo credit: Kareen Reed and Sabrina Simões.

NHMD-83728

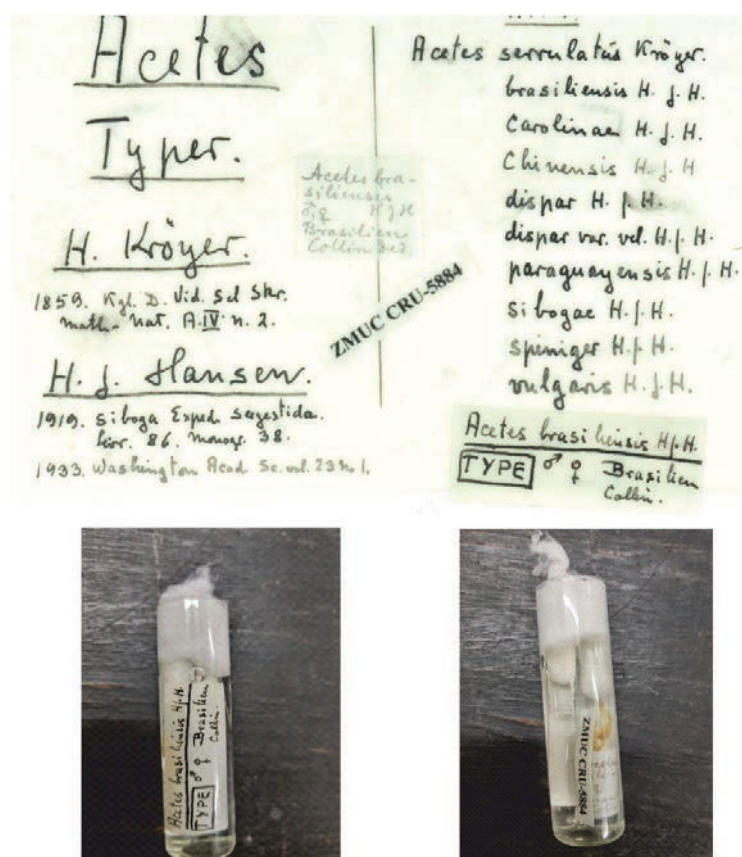


Figure 7. *Acetes brasiliensis* - Type material of the original description by Hansen (1919) deposited at Natural History Museum of Denmark - University of Copenhagen (NHMD 83728). The number ZMUC-CRU-5884 on the label is the old museum catalogue number. Photos credit: Jørgen Olesen.

We had access (by photos) to the material (one male and one female – Fig. 7) used by Hansen to describe *A. brasiliensis*, due to the great help from Dr Jørgen Olesen (curator). They are deposited at the Natural History Museum of Denmark - University of Copenhagen (NHMD 83728). We agree with Burkenroad's assertion and suggestion that *A. brasiliensis* is more likely synonymous with *A. americanus* after carefully analyzing the main characters.

Conclusions

Acetes species from the Western Atlantic are morphologically similar to each other. When we integrated more robust morphological analyses, looking in greater detail at the petasma and genital sternite, into the previous multigene molecular analysis of Simões et al. (2023), we found significant differences and described a new species, *Acetes maratayama* sp. nov. There is still taxonomic uncertainty regarding the specimens under the names *A. a. carolinae* and probably also regarding the synonymized *A. a. louisianensis*. At present, and pending future research, the name *Acetes maratayama* sp. nov. should be adopted for Macaé City, Rio de Janeiro State, and for Cananéia City, São Paulo State, Brazil. *Acetes americanus* should be adopted for Brazil (Northeastern Region: Rio Grande do Norte, Alagoas, Sergipe; Southeastern region: Espírito Santo, Rio de Janeiro, São Paulo; Southern region: Santa Catarina). *Acetes a. carolinae* is still unresolved and it most likely refers to specimens from the Western Atlantic, from North and South Carolina, given the doubts about specimens from the Gulf of Mexico and nearby areas.

Key for American species of *Acetes*

- 1 Rostrum without dorsal teeth ***Acetes binghami* Burkenroad, 1934a**
- Rostrum with one to two dorsal teeth **2**
- 2 Rostrum with two dorsal teeth ***Acetes marinus* Omori, 1975**
- Rostrum with a single dorsal tooth **3**
- 3 In males, the insertion of the pars externa is located near the base of the capitulum; the pars externa extends far beyond the base of the capitulum and reaches its middle portion. In females, the genital sternite has concavity's anterior margin forming a very shallow arch ***Acetes americanus* Ortmann, 1893**
- In males, the insertion of the pars externa is located in the middle section of the pars media. In females, the genital sternite has concavity's anterior margin forming a very deep arch **4**
- 4 In males, petasma pars externa does not reach the base of the capitulum. In females, the genital sternite with the free sublateral projections by the margin's sides are enclosed and taper to a defined point, besides being slightly curved ***Acetes maratayama* sp. nov.**
- In males, petasma pars externa extends above the base of the capitulum. In females, the concavity of the genital sternite is not so deep and the arch region is straight ***Acetes carolinae* Hansen, 1933**

Acknowledgements

We thank the LABCAM and LBSC members for their help during valuable suggestions and discussions. The authors are thankful to the curators of the following crustacean collections for providing valuable help with samplings, loans and donations samples for this work, as well many friends and colleagues for preliminary discussions: Adriane A. Braga (UFES), Célio Magalhães (INPA), Cristiana S. Serejo and Irene Cardoso (MNRJ), Darryl L. Felder (ULLZ), Dirk Brandis (ZMK), Gustavo L. Hirose (UFS), Glaucia Pontes (MCP), Inácia M. Vieira (IEPA), Jessor F. de Souza-Filho (MOUFPE), Jørgen Olesen (NHMD), Jose L. Villalobos (CNCR), Luis F. Dumont (FURG), Lourdes Rojas (YPM), Marcos Tavares (MZUSP), Mariana Terossi (UFRGS), Rafael Lemaitre (USNM), Raymond Bauer (ULL), and Sabrina M. Simões (UNESP). We are thankful to Charles Fransen, an anonymous reviewer and Christopher Glasby for the suggestions that improved the quality of the manuscript.

Additional information

Conflict of interest

The authors have declared that no competing interests exist.

Ethical statement

No ethical statement was reported.

Funding

Financial support for this project was provided by research grants from São Paulo Research Foundation - FAPESP (Temáticos Biota 2010/50188-8 and INTERCRUSTA 2018/13685-5). Additional support was provided by Coordenação de Aperfeiçoamento de Pessoal de Nível Superior - CAPES - Código de Financiamento 001 (Ciências do Mar II Proc. 2005/2014 - 23038.004308/201414) and by Conselho Nacional de Desenvolvimento Científico e Tecnológico - CNPq (PPBio 2023-07/2023 – Linha 8: Redes Costeiras Marinhas – 442421/2023-0). FLM and RCC are grateful to Research Scholarships from CNPq (PQ 302253/2019-0 and 304368/2022-9, respectively). GLB is grateful to FAPESP for ongoing post-doctoral fellowship (PD 2022/14593-2).

Author contributions

FLM conceived the main study idea, participated in its design and coordination, helped with morphology revisions, wrote the preliminary text and revised the manuscript. RCC collected most specimens, contributed to the main idea and revised the manuscript. FLM and RCC were responsible and signed for all foundation grants supporting the study, in all aspects, for all arrangements and facilities at USP and UNESP, and for obtaining the license permits for animal collections. GLB carried out the morphological analyses, prepared the results and figures, prepared the descriptions and revised the manuscript. All authors read, revised and approved the final manuscript.

Author ORCIDs

Gabriel L. Bochini  <https://orcid.org/0000-0001-9311-8419>

Rogério C. Costa  <https://orcid.org/0000-0002-1342-7340>

Fernando L. Mantelatto  <https://orcid.org/0000-0002-8497-187X>

Data availability

All of the data that support the findings of this study are available in the main text or Supplementary Information.

References

- Allmon WD (2001) Nutrients, temperature, disturbance, and evolution: A model for the late Cenozoic marine record of the western Atlantic. *Palaeogeography, Palaeoclimatology, and Palaeoecology* 166(1–2): 9–26. [https://doi.org/10.1016/S0031-0182\(00\)00199-1](https://doi.org/10.1016/S0031-0182(00)00199-1)
- Burkenroad MD (1934a) Littoral Penaeidae chiefly from the Bingham Oceanographic Collection. *Bulletin of the Bingham Oceanographic Collection* 4: 1–109.
- Burkenroad MD (1934b) The Penaeidea of Louisiana with a discussion of their world relationships. *Bulletin of the American Museum of Natural History* 68: 61–143.
- Coates AG, Obando JA (1996) *The Geologic Evolution of the Central American Isthmus. Evolution and Environment in Tropical America*. Chicago University Press, Chicago, USA, 21–56.
- Costa RC, Simões SM (2016) Avaliação dos Camarões Sergestídeos (Decapoda: Sergestidae), Chapter 29: In: Pinheiro MAA, Boos H (Org) *Livro Vermelho dos Crustáceos do Brasil: Avaliação 2010–2014*. Porto Alegre, RS, Sociedade Brasileira de Carcinologia - SBC, 466 p., 390–399.
- D’Incao F, Martins STS (2000) Brazilian species of the genera *Acetes* H. Milne Edwards, 1830 and *Peisos* Burkenroad, 1945 (Decapoda: Sergestidae). *Journal of Crustacean Biology* 20(2): 78–86. <https://doi.org/10.1163/1937240X-90000010>
- De Grave S, Fransen CHJM (2011) Carideorum catalogus: the recent species of the dendrobranchiate, stenopodidean, procarididean and caridean shrimps (Crustacea: Decapoda). *Zoologische Mededelingen* 85(9): 195–589.
- DecaNet (Eds) (2024) DecaNet. *Acetes* H. Milne Edwards, 1830. Accessed through: World Register of Marine Species. <https://www.marinespecies.org/aphia.php?p=tax-details&id=158343> [on 2024-04-13]
- Garcia JR, Lopes AEB, Silvestre AKC, Grabowski RC, Barioto JG, Costa RC, Castilho AL (2018) Environmental characterization of the Cananéia coastal area and its associated estuarine system (São Paulo state, Brazil): Considerations for three Penaeoidean shrimp species. *Regional Studies in Marine Science* 19: 9–16. <https://doi.org/10.1016/j.rsma.2018.02.010>
- Hansen HJ (1919) Sergestidae of the Siboga Expedition. *Siboga-Expeditie, XXXVIII*. Brill, Leiden, 1–65. [5 pls + 14 figs explanations] <https://doi.org/10.5962/bhl.title.10423>
- Harrison JS (2004) Evolution, biogeography, and the utility of mitochondrial 16s and COI genes in phylogenetic analysis of the crab genus *Austinia* (Decapoda: Pinnotheridae). *Molecular Phylogenetics and Evolution* 30(3): 743–754. [https://doi.org/10.1016/S1055-7903\(03\)00250-1](https://doi.org/10.1016/S1055-7903(03)00250-1)
- Holthuis LB (1948) Notes on some Crustacea Decapoda Natantia from Surinam. *Proceedings Koninklijke Nederlandsche Akademie van Wetenschappen* 51: 1104–1113.
- Mantelatto FL, Terossi M, Negri M, Buranelli RC, Robles R, Magalhães T, Tamburus AF, Rossi N, Miyazaki MJ (2018) DNA sequence database as a tool to identify decapod crustaceans on the São Paulo coastline. *Mitochondrial DNA Part A: DNA Mapping, Sequencing and Analysis* 29(5): 805–815. <https://doi.org/10.1080/24701394.2017.1365848>

- Mantelatto FL, Tamburus AF, Carvalho-Batista A, Rossi N, Buranelli RC, Pantaleão JAF, Teles JN, Zara FJ, Carvalho FL, Bochini GL, Terossi M, Robles R, Castilho AL, Costa RC (2022) Checklist of decapod crustaceans from the coast of the São Paulo state (Brazil) supported by integrative molecular and morphological data: V. Dendrobranchiata and Pleocyemata [Achelata, Astacidea, Axiidea, Caridea (Alpheoidea and Processoidea excluded), Gebiidea, Stenopodidea. *Zootaxa* 5121(1): 1–74. <https://doi.org/10.11646/zootaxa.5121.1.1>
- Mantelatto FL, Paixão JM, Robles R, Teles JN, Balbino FC (2023) Evidence using morphology, molecules, and biogeography clarifies the taxonomic status of mole crabs of the genus *Emerita* Scopoli, 1777 (Anomura, Hippidae) and reveals a new species from the western Atlantic. *Zookeys* 1161: 169–202. <https://doi.org/10.3897/zookeys.1161.99432>
- Miller MA, Pfeiffer W, Schwartz T (2010) Creating the CIPRES Science Gateway for inference of large phylogenetic trees. Gateway Computing Environments Workshop, New Orleans. <https://doi.org/10.1109/GCE.2010.5676129>
- Omori M (1975) The systematics, biogeography, and fishery of epipelagic shrimps of the genus *Acetes* (Crustacea, Decapoda, Sergestidae). *Bulletin of the Ocean Research Institute, University of Tokyo* 7: 1–91.
- Ortmann AE (1893) Decapoden und Schizopoden. In: Hensen V (Ed.) *Ergebnisse der Plankton-Expedition der Humboldt-Stiftung*. Kiel und Leipzig, Lipsius und Tischer. 2.G.b: 1–120. [pls. 1–10] <https://doi.org/10.5962/bhl.title.120070>
- Perez-Farfante I, Kensley B (1997) Penaeoid and Segestoid Shrimps and Prawns of the World. Keys and diagnoses for the families and genera. Editions du Museumnational d'Histoire naturelle, Paris, 233 pp.
- Simões SM, Costa RC, Carvalho FL, Carvalho-Batista A, Teodoro SSA, Mantelatto FL (2023) Genetic variation and cryptic lineage among the sergestid shrimp *Acetes americanus* (Decapoda). *PeerJ* 11: e14751. <https://doi.org/10.7717/peerj.14751>
- Tamura K, Peterson D, Peterson N, Stecher G, Nei M, Kumar S (2011) MEGA 5: molecular evolutionary genetics analysis using maximum likelihood, evolutionary distance, and maximum parsimony methods. *Molecular Biology and Evolution* 28: 2731–2739. <https://doi.org/10.1093/molbev/msr121>
- Vereshchaka AL (2017) The shrimp superfamily Sergestoidea: a global phylogeny with definition of new families and an assessment of the pathways into principal biotopes. *Royal Society Open Science* 4(9): 170221. <https://doi.org/10.1098/rsos.170221>
- Vereshchaka AL, Lunina AA, Olesen J (2016a) Phylogeny and classification of the shrimp genera *Acetes*, *Peisos*, and *Sicyonella* (Sergestidae: Crustacea: Decapoda). *Zoological Journal of the Linnean Society* 177(2): 353–377. <https://doi.org/10.1111/zoj.12371>
- Vereshchaka AL, Olesen J, Lunina AA (2016b) A phylogeny-based revision of the family Luciferidae (Crustacea: Decapoda). *Zoological Journal of the Linnean Society* 178: 15–32. <https://doi.org/10.1111/zoj.12398>
- Xiao Y, Greenwood JG (1993) The biology of *Acetes* (Crustacea, Sergestidae). *Oceanography and Marine Biology: An Annual Review* 31: 259–444.

Supplementary material 1

Selected species of *Acetes* and their respective localities, used in the construction of the phylogenetic hypothesis

Authors: Gabriel L. Bochini, Rogério C. Costa, Fernando L. Mantelatto

Data type: docx

Explanation note: Sequences used in genetic analyses. 16S rRNA and COI marker numbers are available from NCBI Genbank. All data used are available in the supplemental information by Simões et al. (2023). CCDB = Crustacean Collection of the Department of Biology, Faculty of Philosophy, Science and Letters at Ribeirão Preto, University of São Paulo; CCLC = Crustacean Collection of the Laboratory of Biology of Marine and Freshwater Shrimp, São Paulo State University (UNESP), Bauru, Brazil; ULLZ = University of Louisiana Zoological Collection, Lafayette, USA.

Copyright notice: This dataset is made available under the Open Database License (<http://opendatacommons.org/licenses/odbl/1.0/>). The Open Database License (ODbL) is a license agreement intended to allow users to freely share, modify, and use this Dataset while maintaining this same freedom for others, provided that the original source and author(s) are credited.

Link: <https://doi.org/10.3897/zookeys.1211.128059.suppl1>

A new species of genus *Acrossus* Mulsant, 1842 (Scarabaeidae, Aphodiinae, Aphodiini) from South Korea

Changseob Lim^{1,2}, Łukasz Minkina³

¹ Ojeong Resilience Institute, Korea University, Seoul, Republic of Korea

² Korean Entomological Institute, Korea University, Seoul, Republic of Korea

³ os. Polana Szafarska 4/39, 34-400 Nowy Targ, Poland

Corresponding author: Łukasz Minkina (klekel@interia.eu)

Abstract

A new species of the genus *Acrossus* Mulsant, 1842, *Acrossus baei* **sp. nov.** from South Korea, is described and illustrated on the basis of morphology and mitochondrial *COI* sequences. The species was compared with four related species; *Acrossus atratus* (Waterhouse, 1875), *A. humerospinosus* (Petrovitz, 1958), *A. luridus* (Fabricius, 1775), and *A. superatratus* (Nomura & Nakane, 1951). The taxonomic status and diagnostic characters of the new species are discussed. A key to species of the genus *Acrossus* in the Korean Peninsula is given.

Key words: Coleoptera, DNA barcode, Korean fauna, small dung beetles, taxonomy



Academic editor: Andrey Frolov

Received: 9 January 2024

Accepted: 5 August 2024

Published: 4 September 2024

ZooBank: <https://zoobank.org/15C1B0D4-F22B-4EC0-9B19-C60A0F5730F7>

Citation: Lim C, Minkina Ł (2024) A new species of genus *Acrossus* Mulsant, 1842 (Scarabaeidae, Aphodiinae, Aphodiini) from South Korea. ZooKeys 1211: 211–230. <https://doi.org/10.3897/zookeys.1211.118456>

Copyright: © Changseob Lim & Łukasz Minkina. This is an open access article distributed under terms of the Creative Commons Attribution License (Attribution 4.0 International – CC BY 4.0).

Introduction

Acrossus Mulsant, 1842 is a species-rich genus with 43 species known to date, one of which has two subspecies. Most of *Acrossus* species were originally described in the genus *Aphodius* Hellwig, 1798, where they have sometimes been placed in the subgenus *Acrossus*. Dellacasa et al. (2016) elevated the rank of *Acrossus* from subgenus to genus. The genus includes medium-sized to large species found mainly in the Palearctic and Oriental regions. One species is known from North America, and one from the Afro-tropical region (Dellacasa et al. 2016). Most species of this genus have a very distinctive feature: an anteriorly rounded or truncate clypeus, and, for this reason, in the past many species now belonging to other genera (such as *Paracrossidius* Balthasar, 1932 or *Odontacrossus* Dellacasa G., Král, Dellacasa M. & Bordat, 2014) were erroneously placed here in *Acrossus*. Some species (e.g. *A. devabhumi* (Mittal, 1993)) still have a questionable position within the genus. In the last 20 years, only two species have been newly described in the genus: *A. byki* Minkina, 2018 and *A. jeloneki* Minkina, 2018. The genus *Acrossus* still needs research due to the unsatisfactory level of knowledge of its species diversity.

The first author, during his study of the Aphodiinae from South Korea, found several specimens of *Acrossus* he could not identify with available literature

and which, after careful examination, proved to be an undescribed species. Here, we describe it as *Acrossus baei* sp. nov. based on a morphological comparison with the most similar species (*A. atratus* (Waterhouse, 1875), *A. humerospinosus* (Petrovitz, 1958), *A. luridus* (Fabricius, 1775), and *A. superatratus* (Nomura & Nakane, 1951)) and a phylogenetic analysis of *COI* gene sequences. A key to the genus *Acrossus* in the Korean Peninsula is also provided.

Material and methods

Specimen sampling and examination

Adult dung beetles were collected using bait-traps with various animal feces or a flight interception trap (FIT). The specimens were observed with a Nikon SMZ-U stereomicroscope. The photos were taken by a Canon EOS 5D Mark III camera equipped with a Canon MP-E 65 mm macro lens (Tokyo, Japan). Photographs were combined in Helicon Focus 7 and Adobe Photoshop Elements 2018 software. For morphological terms used in the description of species, we follow Dellacasa et al. (2001) and Dellacasa et al. (2010). The type series of the new species are indicated by a red, printed label bearing the status of the specimen, sex, name, authorship, and the year and month of the designation.

The type series and examined specimens are a part of following collections:

- KUEM** Korea University Entomological Museum (South Korea)
- NIBR** National Institute of Biological Resources (South Korea)
- SEHU** Hokkaido University Museum (Japan)
- ABCP** Axel Bellmann, private collection (Germany)
- ISEA** Łukasz Minkina and Zdzisława Stebnicka collection deposited in Institute of Systematics and Evolution of Animals Polish Academy of Sciences in Kraków (Poland)

Phylogenetic analysis

Total genomic DNA was extracted from the leg tissues of beetles using DNeasy Blood & Tissue Kit (Qiagen, Hilden, Germany) according to the manufacturer's instruction. *COI* sequences were amplified using a primer set C1-J-2183 (5' CAA CAT TTA TTT TGA TTT TTT GG 3') and TL2-N-3014 (5' TCC AAT GCA CTA ATC TGC CAT ATT A 3') (Simon et al. 1994) with AccuPower® PCR PreMix (Bioneer, Daejeon, South Korea). A new primer set Acr-L1 (5' GCC GGG ATA CCT CGA CGA TAC T 3') and Acr-R1 (5' TGC TCT GCA GGA GGC ATT TGT 3') was specifically designed to amplify sequences for old museum specimens. The polymerase chain reactions (PCR) were performed following condition: an initial denaturation for 3 min at 94 °C; followed by 36 cycles of denaturation for 30 sec at 94 °C, annealing for 30 sec at 48–50 °C and extension for 90 sec at 72 °C; and a final extension for 5 min at 72 °C. The quality of PCR amplification was verified by running the PCR products on 1.5% agarose gel electrophoresis. The verified PCR products were purified using Exonuclease I and Shrimp Alkaline Phosphatase (New England BioLabs, Ipswich, MA, USA) and then sequenced by Macrogen INC (South Korea) on an ABI Prism® 3130 Genetic Analyzer (Applied Biosystems, Foster City, CA, USA) following a standard

sequencing protocol. Sequences were aligned using the ClustalW algorithm in MEGA v. 10.2.6 (Kumar et al. 2018) and subsequently submitted to GenBank (accession numbers OR621067–OR621075, PP933827–PP933829). In total, 754 bp were obtained for the phylogenetic analysis, except for *A. atratus* and *A. humerospinosus*, which only had 220 bp available. The partial deletion method was adopted for these species in the subsequent analysis. This method allows us to retain the informative sites within the remaining 534 bp, thereby minimizing the impact of missing data on the accuracy and robustness of the phylogenetic analysis (Nei and Kumar 2000).

A total of 19 *COI* sequences were used for the phylogenetic analysis. These sequences included 12 newly obtained sequences of *A. baei* sp. nov. (seven sequences), *A. superatratus* (two sequences), *A. atratus* (two sequences) and *A. humerospinosus* (one sequence) as well as six GenBank sequences (AY132409, AY132509–AY132511, MH020527, MT872705) representing four *Acrossus* species (*A. depressus*, *A. luridus*, *A. carpetanus*, and *A. rufipes*). *Nimbus affinis* (Panzer, 1823) (AY132590) was included as the outgroup, following the phylogenetic relationships proposed by Cabrero-Sañudo and Zardoya (2004). The genetic divergence of the sequences was estimated as *p*-distance in MEGA v. 10.2.6. Maximum-likelihood (ML) and neighbor-joining (NJ) analyses were performed for the phylogenetic reconstruction. The GTR + I model was selected by the best evolutionary substitution model by jModelTest v. 2.1.7 (Darriba et al. 2012) based on Akaike information criterion (AICc). ML and NJ were performed using IQ-TREE webserver (Trifinopoulos et al. 2016) and MEGA, respectively, with 1000 bootstrap replicates.

Taxonomy

Acrossus baei sp. nov.

<https://zoobank.org/3171E85C-856D-4BE3-A5C1-B217E35ED539>

Figs 1–3, 17, 22, 23, 32, 37, 42, 47, 52, 57

Korean name: 산마루뚱뚱땡이 (San-ma-ru-ddong-pung-deng-i)

Diagnosis. The new species can be classified as *Acrossus* (following Dellacasa et al. 2001) due to: body moderately convex; head wide, eyes small, frontal suture not tuberculate; pronotum basally and laterally not serrulate, with sides always visible from above, basally and anteriorly not bordered, with posterior angles weakly obtuse-angled, with sides glabrous; scutellum small, triangular, flat, wider than two first intervals; elytra with ten distinct, impressed striae, part of them joined together before apex, humeral denticles small but distinct, intervals with distinct macrosetation; abdominal ventrites not fused each other; meso- and metatibiae apically fimbriate with spinules of unequal length .

The new species can be distinguished from all other known *Acrossus* species by the combination of the following features: moderately large body length (6.0–7.4 mm); body blackish, elytra rarely with orange spots before apex (last colour form is quite unique in the genus); head large, clypeus weakly sinuate anteriorly (only *A. humerospinosus* (Petrovitz, 1958) have that feature); pronotum wider than base of elytra; punctation of pronotum double, dense, coarser punctures with at about three times larger diameter than smaller ones (there is not to many species with so coarse and dense punctation of pronotum);



Figures 1–3. *Acrossus baei* sp. nov., ♂, holotype 1 dorsal view 2 ventral view 3 lateral view. Scale bars: 1.0 mm.

humeral denticles small but distinct (this feature helps to distinguish it from somewhat similar species: *A. atratus* and *A. luridus*); whole elytra with distinct, long macrosetation (there is no other species with so long, distinct macrosetation on whole elytral surface), intervals with very dense and coarse punctation (unique feature); elytra before apex with distinct microreticulation, matt; male's apical spur of protibiae distinctly inwardly hooked (however hook is better visible from bottom side, and in old specimens it can be wiped out, then apex of apical spur looks for widely rounded, but still inwardly curved); with two or three small teeth between first and second teeth of protibiae and three to five small teeth between second and third teeth of protibiae (this feature help to distinguish it from somewhat similar species: *A. atratus* and *A. luridus*). Aedeagus at apex with small membranous process visible only in lateral view. For more details and links to the photographs see Table 1 and Discussion.

Type locality. South Korea, Gangwon-do, Pyeongchang-gun, Jinbu-myeon, Mountain Odaesan.

Type materials. Holotype: SOUTH KOREA • ♂; Gangwon-do, Pyeongchang-gun, Jinbu-myeon, Mt. Odaesan; 37°47.23'N, 128°33.91'E; alt. 1000 m; 18 Apr.–01 May 2020; C. Lim leg.; KUEM.

Table 1. Differential characteristics of *Acrossus* species potentially confused with *A. baei* sp. nov.

Feature / species	<i>Acrossus baei</i> sp. nov.	<i>Acrossus atratus</i> (Waterhouse, 1875)	<i>Acrossus humerospinosus</i> (Petrovitz, 1958)	<i>Acrossus luridus</i> (Fabricius, 1775)	<i>Acrossus superatratus</i> (Nomura & Nakane, 1951)
Colour of elytra	Blackish, sometimes with orange-brownish spots before apex (Figs 1, 57)	Blackish (Fig. 5)	Blackish, very rarely basal half of elytra yellowish-brown (Fig. 8)	Very variable: from blackish with a lot of yellowish strips to totally blackish (Fig. 11)	Blackish (Fig. 14)
Convexity of body	Relatively least convex (Fig. 3)	Distinctly convex (Fig. 7)	Distinctly convex (Fig. 10)	Relatively less distinctly convex (Fig. 13)	Distinctly convex (Fig. 16)
Anterior part of clypeus	Weakly sinuate (Fig. 17)	Truncate (Fig. 18)	Weakly sinuate (Fig. 19)	Truncate (Fig. 20)	Truncate, sometimes weakly sinuate (Fig. 21)
Punctuation of clypeus	Very dense, punctuation double (Fig. 17)	Very dense, punctuation double (Fig. 18)	Very dense, punctuation simple (Fig. 19)	Dense, punctuation simple (Fig. 20)	Very dense, punctuation double (Fig. 21)
Apical spur of protibiae in male	Distinctly inwardly hooked before apex; when visible from above situated on inner side of protibiae, when visible anteriorly seems to be rounded at apex; in old specimens its visible only as elongate, weakly inwardly curved spur with widely rounded apex (Fig. 37)	Distinctly inwardly hooked before apex; when visible from above situated on inner side of protibiae, when visible anteriorly seems to be rounded at apex; in old specimens its visible only as elongate, weakly inwardly curved spur with widely rounded apex (Fig. 38)	When visible from above situated on upper side of protibiae and visible as acute at apex; when visible anteriorly distinctly acute at apex; in old specimens its visible as elongate, outwardly curved spur, still acute at apex (Fig. 39)	Distinctly downwardly directed, weakly inwardly hooked before apex; when visible from above situated on inner side of protibiae, when visible anteriorly seems to be rounded at apex; in old specimens its visible only as elongate, still distinctly inwardly curved spur with widely rounded apex (Fig. 40)	When visible from above situated on upper side of protibiae, and visible as acute at apex; when visible anteriorly distinctly acute at apex; in old specimens its visible as elongate, weakly outwardly curved spur, still acute at apex (Fig. 41)
Number of small teeth between first and second teeth and between second and third teeth	2–3 / 3–5 (Fig. 37)	1–2 / 1–2 (Fig. 38)	1–3 / 2–5 (Fig. 39)	0 / 0 (Fig. 40)	2–3 / 3–5 (Fig. 41)
Sides of pronotum	Widely rounded (Fig. 1)	Truncate (Fig. 5)	Widely rounded (Fig. 8)	Widely rounded (Fig. 11)	Widely rounded (Fig. 14)
Punctuation of elytra	Very dense, distinctly coarse (Fig. 47)	Very dense, moderately coarse (Fig. 48)	Very dense, moderately coarse (Fig. 49)	Very dense, moderately coarse (Fig. 50)	Very dense, moderately coarse (Fig. 51)
Humeral denticles on elytra	Small but distinct (Fig. 1)	Absent (Fig. 5)	Large, distinct (Fig. 8)	Absent (Fig. 11)	Small but distinct (Fig. 14)
Macrosetation of elytra	Long macrosetae on whole surface of elytra except disc, where are slightly shorter (Figs 1, 42)	Long macrosetae on whole surface of elytra except disc, where usually are distinctly shorter (Figs 5, 43)	Long macrosetae only on sides and before apex; very short macrosetae on whole surface of elytra (Figs 8, 44)	Long macrosetae only on sides and before apex; microsetae (visible at 200× magnification nearly on whole surface of elytra) (Figs 11, 45)	Long macrosetae on whole surface of elytra except disc, where usually are distinctly shorter (Figs 14, 46)
Apex of elytra	With relatively low preapical declivity (Fig. 3), with very distinct microreticulation (see left elytron), matt (compare with right elytron) (Fig. 42)	With relatively high preapical declivity (Fig. 7), with relatively weak microreticulation (see left elytron), shiny (compare with right elytron) (Fig. 43)	With relatively high preapical declivity (Fig. 10), without microreticulation (see left elytron), shiny (compare with right elytron) (Fig. 44)	With relatively low preapical declivity (Fig. 13), with distinct microreticulation (see left elytron), matt, (compare with right elytron) (Fig. 45)	With moderately high preapical declivity (Fig. 16), with weak microreticulation (see left elytron), matt (compare with right elytron) (Fig. 46)
Shape of metatibial claws	Moderately large, fourth metatarsomer more than two times long as their claw (Fig. 52)	Small, fourth metatarsomer nearly three times long as their claw (Fig. 53)	Moderately large, fourth metatarsomer more than two times long as their claw (Fig. 54)	Large, fourth metatarsomer less than two times longer as their claw (Fig. 55)	Small, fourth metatarsomer nearly three times long as their claw (Fig. 56)
Shape of epitorma with amount of angustofenestrae (celtes) on top	Epitorma elongate, thin, fully developed; 3 angustofenestrae on top (Fig. 32)	Epitorma elongate, relatively wide, shortened to 3/4 of length; 1 angustofenestra near top (Fig. 33)	Epitorma elongate, relatively wide, shortened to 7/8 of length; 3 angustofenestrae near top (Fig. 34)	Lack of epitorma; 1 angustofenestra at apex of row with angustofenestrae (Fig. 35)	Epitorma elongate, thin, fully developed; 2 angustofenestrae on top (Fig. 36)
Shape of aedeagus	At apex, on sides with very weak membranous process visible only in lateral view (Figs 22, 23)	At apex, on sides with very distinct, weakly sclerotized membranous process visible from above (Figs 24, 25)	At apex, on sides with distinct membranous process visible from above (Figs 26, 27)	At apex without any membranous process (Figs 28, 29)	At apex, on sides with distinct membranous process visible from above (Figs 30, 31)
Distribution	South Korea	Japan	China (Sichuan)	Europe, North Africa (Morocco), Kazakhstan, Kyrgyzstan, Russia (West Siberia), China (Xinjiang)	Russia (East Siberia and Far East), Japan, North Korea, South Korea

Paratypes (10 spm.): SOUTH KOREA • 5 spm.; same data as holotype; 2 ♂, ♀ ISEA; ♂ ABCP; ♂ NIBR • 2 ♂, ♀; Gangwon-do, Hongcheon-gun, Nae-myeon, Mt. Gyeongbansan; 37°44.78'N, 128°25.68'E; alt. 830 m; 30 Apr. 2020; C. Lim leg.; GenBank: OR621067, OR621069–OR621070; CSL-21-0013–CSL-21-0015; KUEM • ♀; Gangwon-do, Hongcheon-gun, Nae-myeon, Mt. Gyeongbansan; 37°44.78'N, 128°25.68'E; alt. 830 m; 30 Apr. 2020; C. Lim leg.; KUEM • ♀; Gyeongsangbuk-do, Youngju-si, Punggi-eup, Mt. Sobaeksan; 36°56.23'N, 128°27.6'E; alt. 856 m; 05 May 2019; C. Lim leg.; KUEM.

Additional materials. SOUTH KOREA • ♂, 2 ♀; Jeju-do, Seogwipo-si, Jungmun-dong, Youngsil trail; 33°20.2'N, 126°28.1'E; 17–27 Mar. 2021; C. Lim, J. Kim, J.M. Hwang, D. Lee legs.; GenBank: OR621071–OR621073; CSL-21-0083–CSL-21-0085; KUEM • ♀; Jeju-si, Nohyung-dong; 33°25.19.1'N, 126°29.31.6'E; 06 Jun. 2019; C. Lim leg.; GenBank: OR621068; CSL-21-0071; KUEM.

Description. Dorsum (Fig. 1). Moderately large species, relatively small as a member of the genus, body length of the holotype 6.7 mm; elongate-oval, shiny, blackish; antennae, tarsomeres, and mouth parts reddish brown.

Head (Fig. 17) large, distinctly widely trapezoidal, convex, shiny, without microreticulation. Clypeus distinctly bordered, weakly sinuate anteriorly, widely rounded laterally, not notched before genae, clypeal border without macrosetae. Genae acute-angled, very distinctly exceeding eyes, with few relatively short, thin macrosetae in basal part. Frontal suture not marked, but visible as surface without punctation, without gibbositities, epistoma without gibbosity. Punctation double, but both kinds of punctation not so clearly distinguishable due diameter of larger punctures being only two times larger than smaller ones; both kinds of punctation quite regularly, densely distributed; punctures somewhat variable in size; genae with much denser punctation.

Epipharynx (Fig. 32) transverse, with sides distinctly rounded, anterior margin of concavely arcuate, corypha not developed, zygum very narrow, with three long, thick angusto-fenestrae at apex and three additional ones arranged as row. Acanthopariae with dense, long, thin chaetae; acropariae with dense, short, thinner chaetae than on acanthopariae; chaetopariae with dense belt of quite thin, quite short chaetae; adelochaetae absent; prophobae with dense, short, thin macrosetae; chaetopediae absent. Epitorma reduced to a small, narrow triangle. Tormae relatively thin, long.

Pronotum transverse, somewhat wider than base of elytra, widest near base, moderately convex, shiny, without microreticulation, with double punctation; smaller punctures fine, with diameter about three times smaller than large punctures, quite regularly distributed, dense; larger punctures coarse, dense, not regularly distributed, much denser near base and on sides. Pronotum anteriorly and basally not bordered, distinctly bordered on sides. Borders without macrosetae. Anterior angles widely rounded; posterior angles weakly obtuse-angled, base before posterior angles truncate.

Scutellum small, triangular, with dense, irregularly sized punctation, moderately shiny, with distinct microreticulation.

Elytra (Fig. 47) elongate-oval, convex, widely rounded, weakly shiny, with weak microreticulation on disc, becoming much more distinct on sides and apex, with small but distinct humeral denticles; with ten striae and ten intervals. Striae distinctly, quite sparsely punctate with moderately large punctures; punctures weakly but clearly indenting margins of intervals. First and tenth, third and

fourth, fifth and sixth striae joined together before apex, sixth to eighth striae shortened before base, eighth distinctly; ninth and tenth striae joined before base. Intervals weakly shiny, very weakly convex, with irregularly distributed simple moderately coarse punctation, this irregular in size. Almost all punctures (on disc somewhat less frequently) bearing short, thin macrosetae.

Pygidium with similar sculpture as on abdominal ventrites.

Legs. Femora shiny, without microreticulation, quite finely and densely punctate, with punctures bearing short macrosetae. Profemora basally and apically with a belt of punctures bearing very long macrosetae; mesofemora basally with a belt of punctures bearing very long macrosetae, metafemora with much sparser than on mesofemora row of punctures bearing long macrosetae apically. Protibiae (Fig. 37) distinctly tridentate laterally, proximally serrulate; additional few (2–3) small teeth between first and second teeth, and additional few (3–5) small teeth between second and third teeth; dorsal side smooth, shiny, with a few fine punctures bearing short macrosetae; apical spur long, moderately broad, straightforward, distinctly downwardly and inwardly hooked before apex. Meso- and metatibiae with two distinct transverse carinae, fimbriate apically with row of long spinules of unequal length. Metatibiae superior apical spur very slightly longer than basimetatarsomere, latter distinctly longer than 3½ of next metatarsomeres combined. Claws (Fig. 52) moderately long, moderately thick, moderately arcuate.

Macropterous. Venter (Fig. 2). Meso-metaventral plate shiny, very slightly concave, with indistinct, quite shallow longitudinal concavity in the middle and weak longitudinal line in the middle; surface with variable in size, shallow, irregularly spaced, not so dense punctation, bearing short, thin macrosetation. Abdominal ventrites matte, with very distinct microreticulation, with quite dense, fine punctures bearing moderately long, thin macrosetae; additionally last abdominal ventrite, in the middle with row of punctures bearing very long macrosetae.

Aedeagus (Figs 22, 23) with parameres slightly shorter than phallobase. Parameres weakly but regularly downwardly bent; at apex, on sides with very weak membranous process, additionally with few very thin and very short macrosetae, which are directed inwardly and not visible due to the time when we try to separate parameres.

Etymology. The species is named in honor of Dr Yeon Jae Bae who has contributed to the conservation of dung beetles in South Korea.

Sexual dimorphism. Males with apical spur of anterior tibiae distinctly downwardly and inwardly hooked before apex, meso-metaventral very slightly concave. Females with apical spur acute at apex, meso-metaventral plate very weakly convex.

Variability. Size from 6.0 to 7.5 mm. Elytra usually blackish, sometimes with short, orange-brownish stripes before apex (Fig. 57). Punctation of head and pronotum weakly variable. Connection between elytra striae of elytra somewhat variable.

Remark. We have decided that part of the material of *A. baei* sp. nov. should be excluded from the type series. Based on a shortage of comparative material, we cannot determine the exact range of inter-individual variability of the population from Jeju Island. Therefore, in our opinion, it is better to identify type material from only one specific location (i.e. mainland South Korea)(Fig. 4).

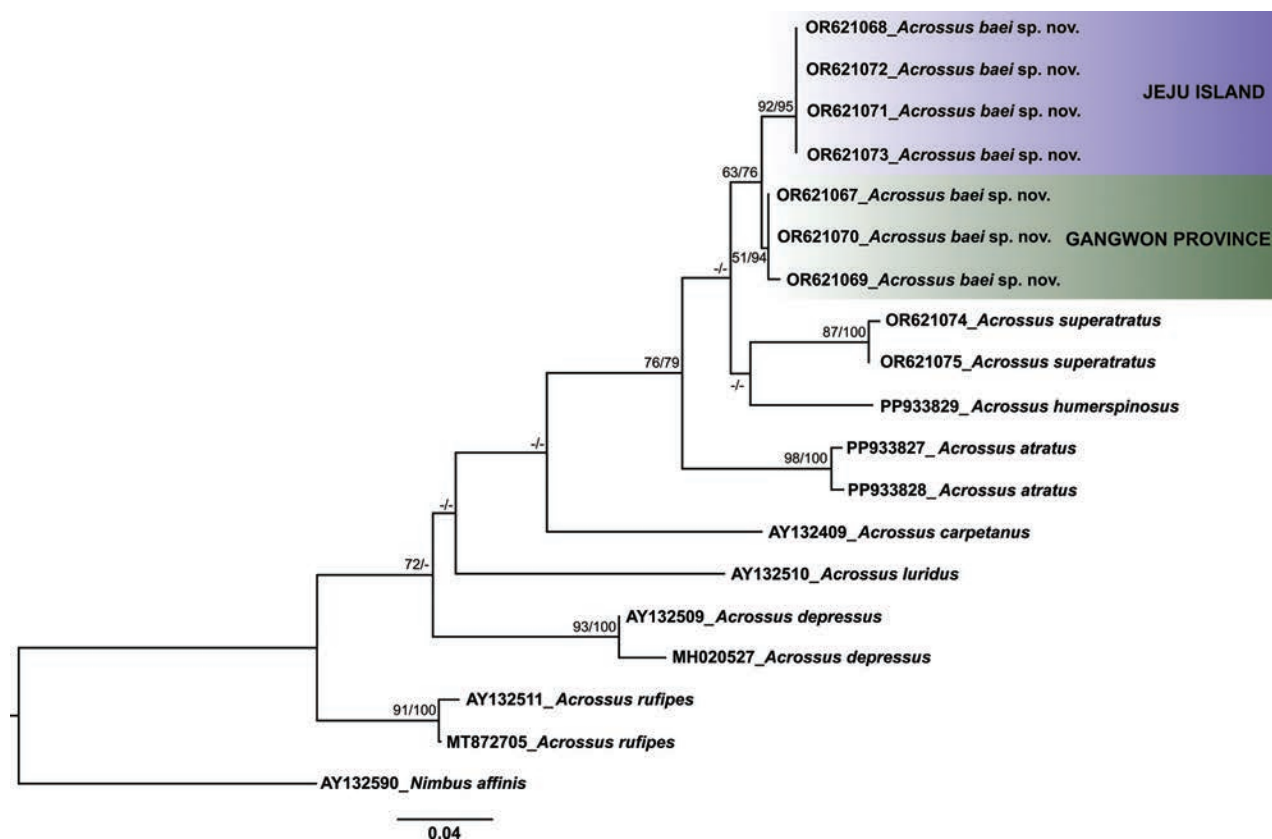


Figure 4. Phylogenetic tree based on 19 mitochondrial *COI* gene sequences of the eight *Acrossus* species and *Nimbus affinis* (outgroup). Branch values indicate bootstrap support in maximum likelihood (ML) and neighbor joining (NJ), respectively. Tree topology and branch lengths reflect the results of ML analysis. The tree is drawn to scale, with branch lengths (evolutionary distance) measured in the number of substitutions per site. Dashes (-) indicate support values of less than 50 or incongruent between ML and NJ.

***Acrossus atratus* (Waterhouse, 1875)**

Figs 5–7, 18, 24, 25, 33, 38, 43, 48, 53

Materials. JAPAN • ♂ (photographed); Saitama-ken, Asaka-shi, Adachi; 21 Apr. 1971; S. Nagao leg.; SEHU • 2 spm.; same data as photographed specimen; SEHU • 2 spm.; same data as photographed specimen; GenBank: PP933827–PP933828; CSL-21-0439–CSL-21-0440; SEHU • ♀; Kumamoto-ken, Aso-gun, Aso-shi, Mt. Oujou-dake; 26 Apr. 1999; S. Kawai leg.; ISEA.

***Acrossus humerspinosus* (Petrovitz, 1958)**

Figs 8–10, 19, 26, 27, 34, 39, 44, 49, 54

Materials. CHINA • ♂ (photographed); C Sichuan, Mt. Jinding; alt. 1500 m; 20 Jun. 2012; V. Patrikeev leg.; ISEA • 1 spm.; Yunnan, Baihanchwag, 50 km NW Lijiang; alt. 2400 m; 05 Jun. 2006; Vladimir Major leg.; ISEA • 1 spm.; Yunnan, 25 km S Zhonghian; alt. 3200 m; 14 Jun. 2006; Vladimir Major leg.; ISEA • 1 spm.; Sichuan, rd. Danba to Bomei, 35 km W Danba; alt. 2500–2700 m.; Jun.–Jul. 2007; Puchner leg.; ISEA • 1 spm.; C Sichuan, Maoxian env. Jinding Mt.; alt. 1600 m; 20 Jun. 2012; V. Patrikeev leg.; ISEA • 2 spm.; C Sichuan, Maoxian env. Jinding Mt.; alt. 1500 m; 20 Jun. 2012; V. Patrikeev leg.; ISEA • 2 spm.; NW Yunnan,



Figures 5–7. *Acrossus atratus* (Waterhouse, 1875), ♂ 5 dorsal view 6 ventral view 7 lateral view. Scale bars: 1.0 mm.

Lijang pref., S. Yulongxue Shan Mts.; alt. 3200 m.; 16 Jun. 2016; V. Patrikeev leg.; ISEA; • 1 spm.; W. Sichuan, Mt. Yadling, W of Yading vill.; alt. 3850–4650 m; 5–11 May 2012; D. Kral leg.; GenBank: PP933829; CSL-21-0459; KUEM.

***Acrossus luridus* (Fabricius, 1775)**

Figs 11–13, 20, 28, 29, 35, 40, 45, 50, 55

Materials. HUNGARY • ♂ (photographed); Csernelly; 22 Apr. 2012; Ł. Minkina leg.; ISEA • 4 spm.; same data as photographed specimen; ISEA. Ukraine • 1 spm.; płw. Tarchankut; 45°25'N, 32°32'E; 03 May 2008; C. Nowak leg.; ISEA. BULGARIA • 2 spm.; Yasna Polyana; 08 May 2013; Ł. Minkina leg.; ISEA. Iran • 1 spm.; Aarbaigan E, Sagri, 15 km W Nir; alt. 1750 m; 17 May 2002; P. Rapuzzi leg.; ISEA. Georgia • 2 spm.; Kartli Gomi; 41.905334°N, 44.380755°E, alt. 570–790 m; 5–21 May 2019; J. Klasinski leg.; ISEA. TURKEY • 2 spm.; Antalia town, near Saklikent village; alt. 200 m; 1–3 May 2019; V. Patrikeev leg.; ISEA.



Figures 8–10. *Acrossus humerospinosus* (Petrovitz, 1958), ♂ 8 dorsal view 9 ventral view 10 lateral view. Scale bars: 1.0 mm.



Figures 11–13. *Acrossus luridus* (Fabricius, 1775), ♂ 11 dorsal view 12 ventral view 13 lateral view. Scale bars: 1.0 mm.

***Acrossus superatratus* (Nomura & Nakane, 1951)**

Figs 14–16, 21, 30, 31, 36, 41, 46, 51, 56

Type materials. *Holotype*: JAPAN • ♂; Honshu, Ise, Buhei-toge; 01 Jun. 1947; S. Osawa leg.; SEHU. *Paratypes*: 2 spm.; same data as holotype; SEHU.

Additional materials. RUSSIA • ♂ (photographed); Far East, Primorskiy reg., Murav'ev-Amurskiy pen., Artem town env., Ozernyi kluch riv.; 15 May–10 Jun. 2005; A. Plutenko leg.; ISEA. NORTH KOREA • 13 spm.; Hamgjöng-punkto prov., Kvanmo-bong (Mt., 60) at human excrements; 23 May 1974; Z. Stebnicka leg.; ISEA • 3 spm.; Ryanggang-do, Samjiyon; alt. 1000 m; 26 Jun. 1988; O. Merkl, Gy. Szel legs.; NIBR. SOUTH KOREA • 1 spm.; Jeju-do, Jeju-si, Aewol-eup; 17 May. 1990; M.T. Chûjô leg.; NIBR • ♂; Gangwon-do, Hongchun-gun, Nae-myeon; 11 Jul. 1990; J.I. Kim leg.; NIBR • ♂; Yeongju-si, Mt. Sobaeksan, Huibanggyegok val.; 36°56.14'N, 128°27.37'E; 05 May. 2019; C. Lim leg.; KUEM • ♂; Pyeongchang-gun, Jinbu-myeon, Dongsan-ri, Mt. Odaesan, 1–29 May. 2020; C. Lim leg.; GenBank: OR621074; CSL-21-0429; KUEM • ♀; Seogwipo-si, Namwon-eup; 33°19.45'N, 126°36.22'E; 10 Jun. 2021; D.G. Kim leg.; GenBank: OR621075; CSL-21-0431; KUEM. JAPAN • 1 spm.; Ueno-Mura, Jukkoku-tôge Pass; 26 May 2001; S. Kawai leg.; ISEA • ♂; Kibune Yamashiro; May. 1948; K. Tsukamoto leg.; SEHU.



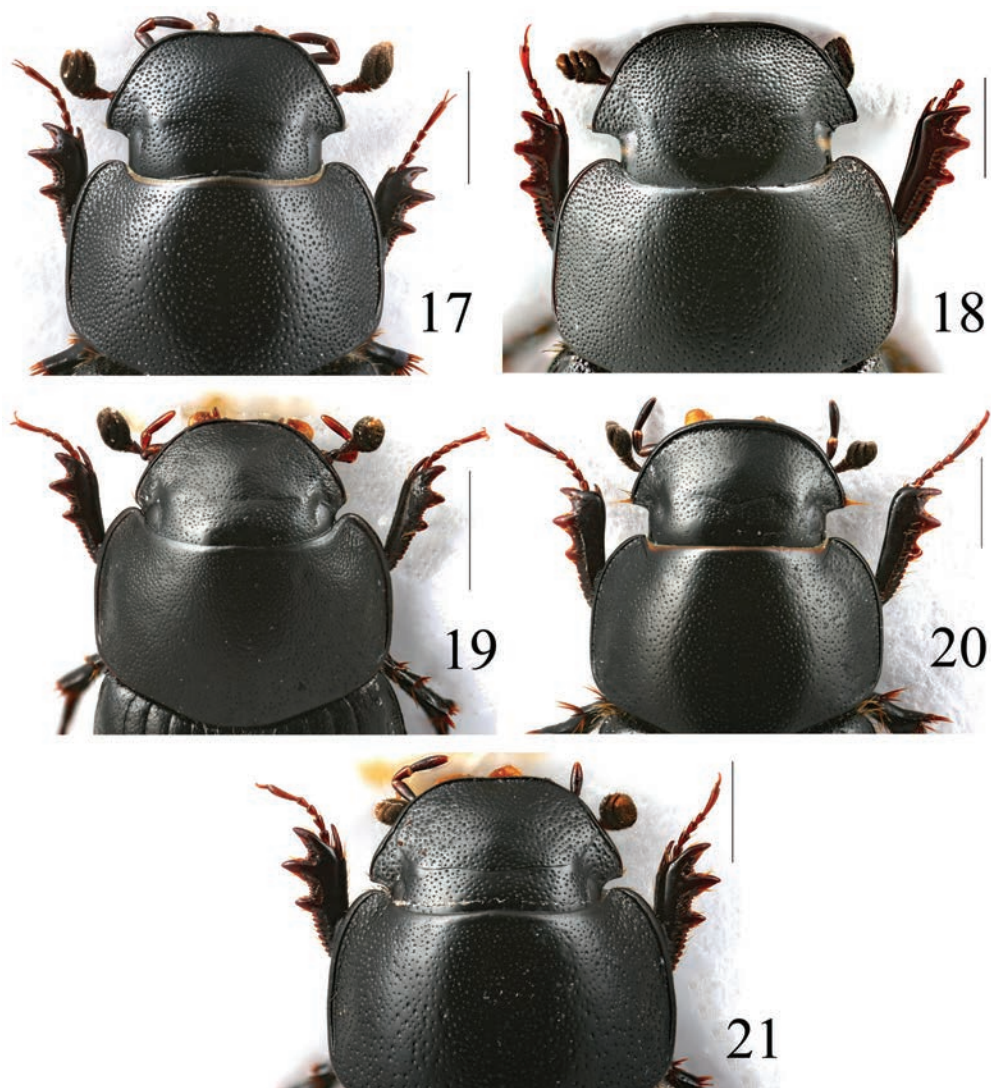
Figures 14–16. *Acrossus superatratus* (Nomura & Nakane, 1951), ♂ **14** dorsal view **15** ventral view **16** lateral view. Scale bars: 1.0 mm.

Key to the species of *Acrossus* from the Korean Peninsula

- 1 Elytra with distinct macrosetation (usually visible on sides and before apex at 50× magnification).....**2**
- Elytra at most with indistinct macrosetation or glabrous (if visible, setation can be observed only on sides and before apex at 200× magnification)... **3**
- 2 Clypeus anteriorly weakly sinuate (Fig. 17). Apical spur of protibiae in males inwardly hooked before apex (Fig. 37). Elytra with clear macrosetation on whole surface (Figs 1, 3, 42, 47). Elytra before apex with very distinct microreticulation (Fig. 42). Punctuation of body coarser
.....***Acrossus baei* sp. nov.**
- Clypeus anteriorly usually truncate, rarely weakly sinuate (Fig. 21). Apical spur of protibiae in males acute at apex (Fig. 41). Elytra with clear macrosetation on sides and before apex (Figs 14, 16, 46, 51). Elytra before apex with weak microreticulation (Fig. 46). Punctuation of body finer
.....***Acrossus superatratus* (Nomura & Nakane, 1951)**
- 3 Body brownish. Body length <6.5 mm or >10.0 mm. Elytra glabrous**4**
- Body blackish, frequently with lighter elytra. Body length 6.5–10.5 mm. Elytra with very short macrosetation before apex**5**
- 4 Body oblong ovate, length less than 6.5 mm
.....***Acrossus koreanensis* (Kim, 1986)**
- Body elongate, length more than 10.0 mm.....
.....***Acrossus rufipes* (Linnaeus, 1758)**
- 5 Body length 7.0–10.0 mm. Body more deplanate, wider. Apical spur of protibiae in males more downwardly directed. Humeral denticles indistinct. Elytral intervals slightly more convex. Elytral punctuation somewhat finer. Claws of hind legs more curved***Acrossus binaevulus* (Heyden, 1887)**
- Body length 6.0–9.5 mm. Body less deplanate, narrower. Apical spur of protibiae in males less downwardly directed. Humeral denticles very small, but distinct. Elytral intervals slightly less convex. Elytral punctuation somewhat coarser. Claws of hind legs less curved.....
.....***Acrossus depressus* (Kugelann, 1792)**

Phylogenetic analysis and discussion

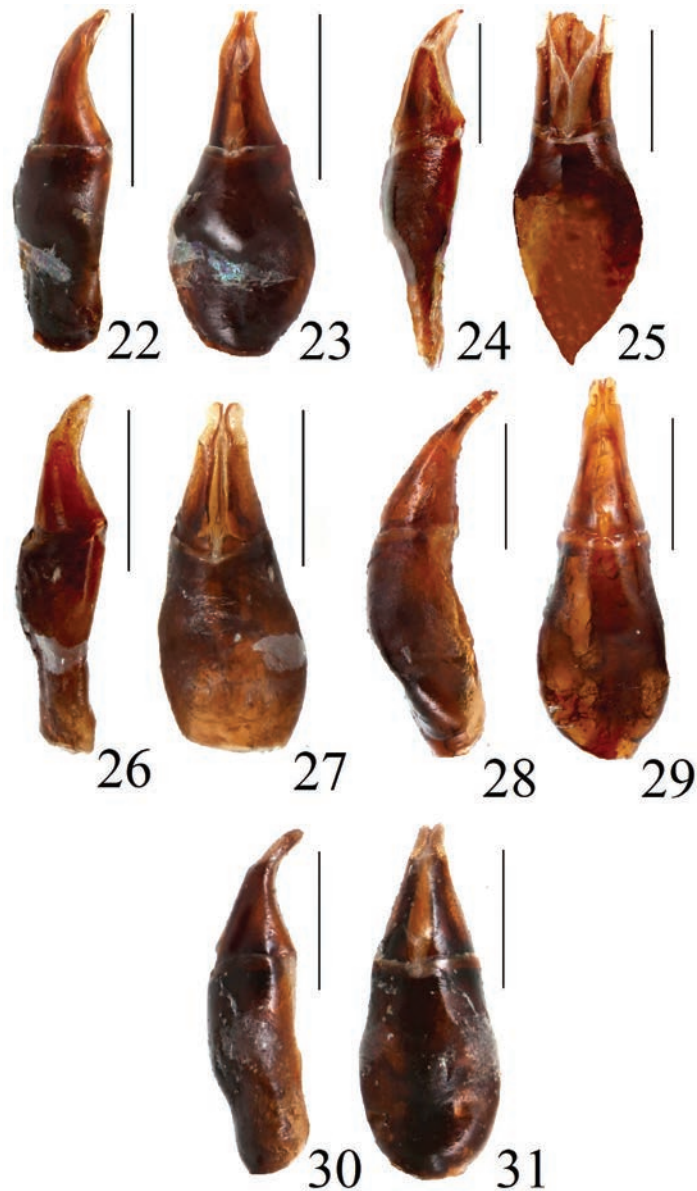
In the genus *Acrossus* Mulsant, 1842, the relations between species are still poorly known and the genus needs revision. According to our results, *A. baei* sp. nov. presents an adequately supported (63/76) monophyletic lineage (Fig. 4). Similarly, four other species—*A. rufipes*, *A. depressus*, *A. atratus*, and *A. superatratus*, each represented by at least two specimens—also present adequately supported monophyletic lineages. Among the five species we examined morphologically (excluding *A. luridus* for which only one sequence was used), four formed a monophyletic lineage (76/79). However, the phylogenetic relationships among the eight *Acrossus* species, including the relationship within the *A. baei* + *A. superatratus* + *A. humerospinosus* + *A. atratus* clade, were not well resolved in our tree. This could be attributed to the fact that our phylogenetic tree was reconstructed using only partial sequences from a single gene (*COI*). Further phylogenetic analysis, including multiple genes and a broader range of species, could offer better insights into the phylogenetic relationships within this genus.



Figures 17–21. Heads of *Acrossus* species **17** *A. baei* sp. nov., ♂, holotype **18** *A. atratus* (Waterhouse, 1875), ♂ **19** *A. humerospinosus* (Petrovitz, 1958), ♂ **20** *A. luridus* (Fabricius, 1775), ♂ **21** *A. superatratus* (Nomura & Nakane, 1951), ♂. Scale bars: 1.0 mm.

Intraspecific clades, consisting of individuals from two regions (Gangwon Province and Jeju Island) were observed in *A. baei* sp. nov. (genetic divergence: 1.42%; Table 2). The genetic divergence between *A. baei* sp. nov. and *A. superatratus*, based on individuals from the same regions, was 5.30%. This distance surpasses the typical species-level genetic divergence, indicating that they are distinct species. The other *Acrossus* species presented genetic differences ranging from 5.92% (*A. humerospinosus*) to 13.96% (*A. rufipes*) (Table 2).

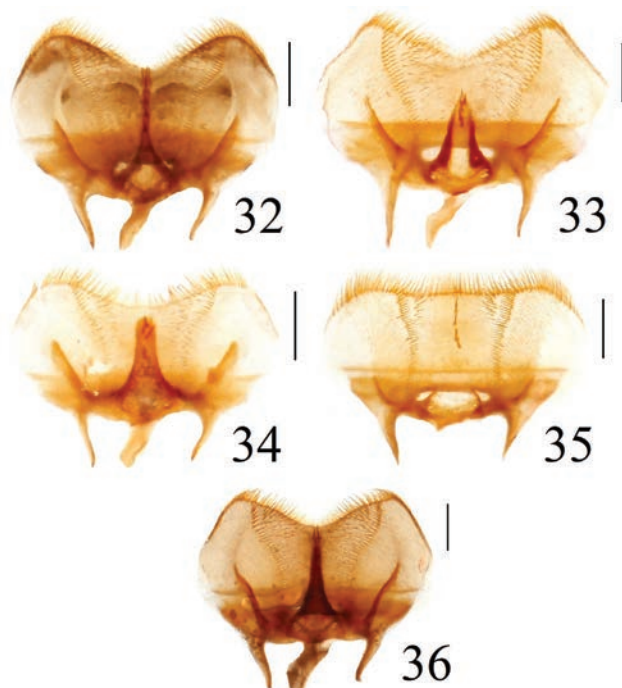
Acrossus baei sp. nov. is the third species known from South Korea (the two others are: *A. superatratus* (Nomura & Nakane, 1951) and *A. koreanensis* (Kim, 1986) (Stebnicka 1980; Kim 2012) and the sixth known from the Korean Peninsula (the three remaining are *A. binaevulus* (Heyden, 1887), *A. depressus* (Kugelann, 1792), and *A. rufipes* (Linnaeus, 1758)). Of all mentioned species, *A. baei* sp. nov. is most similar to *A. superatratus* in having distinct setation of the elytra. The other species have elytra with very short to indistinct setation (located mainly on sides of elytra or before their apices), or they are glabrous.



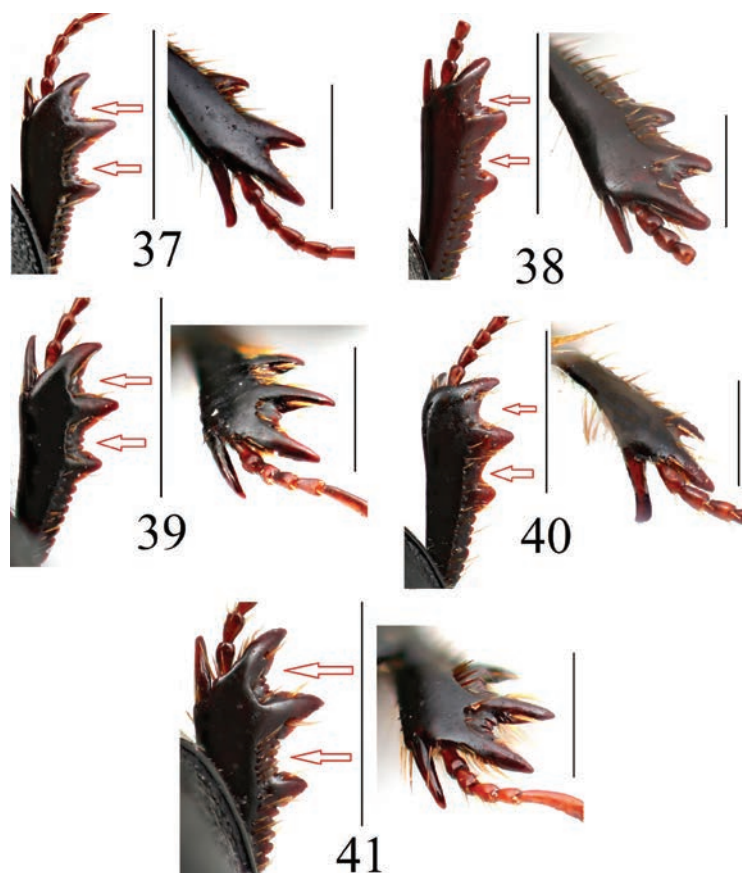
Figures 22–31. Aedeagi of *Acrossus* species **22** *A. baei* sp. nov., holotype, lateral view **23** *A. baei* sp. nov., holotype, dorsal view **24** *A. atratus* (Waterhouse, 1875), ♂, lateral view **25** *A. atratus* (Waterhouse, 1875), ♂, dorsal view **26** *A. humerospinosus* (Petrovitz, 1958), lateral view **27** *A. humerospinosus* (Petrovitz, 1958), dorsal view **28** *A. luridus* (Fabricius, 1775), ♂, lateral view **29** *A. luridus* (Fabricius, 1775), ♂, dorsal view **30** *A. superatratus* (Nomura & Nakane, 1951), ♂, lateral view **31** *A. superatratus* (Nomura & Nakane, 1951), ♂, dorsal view. Scale bars: 1.0 mm.

Table 2. Estimates of genetic divergence (ρ -distance) between intraspecific clades of *A. baei* sp. nov., and between *A. baei* sp. nov. and seven other *Acrossus* species.

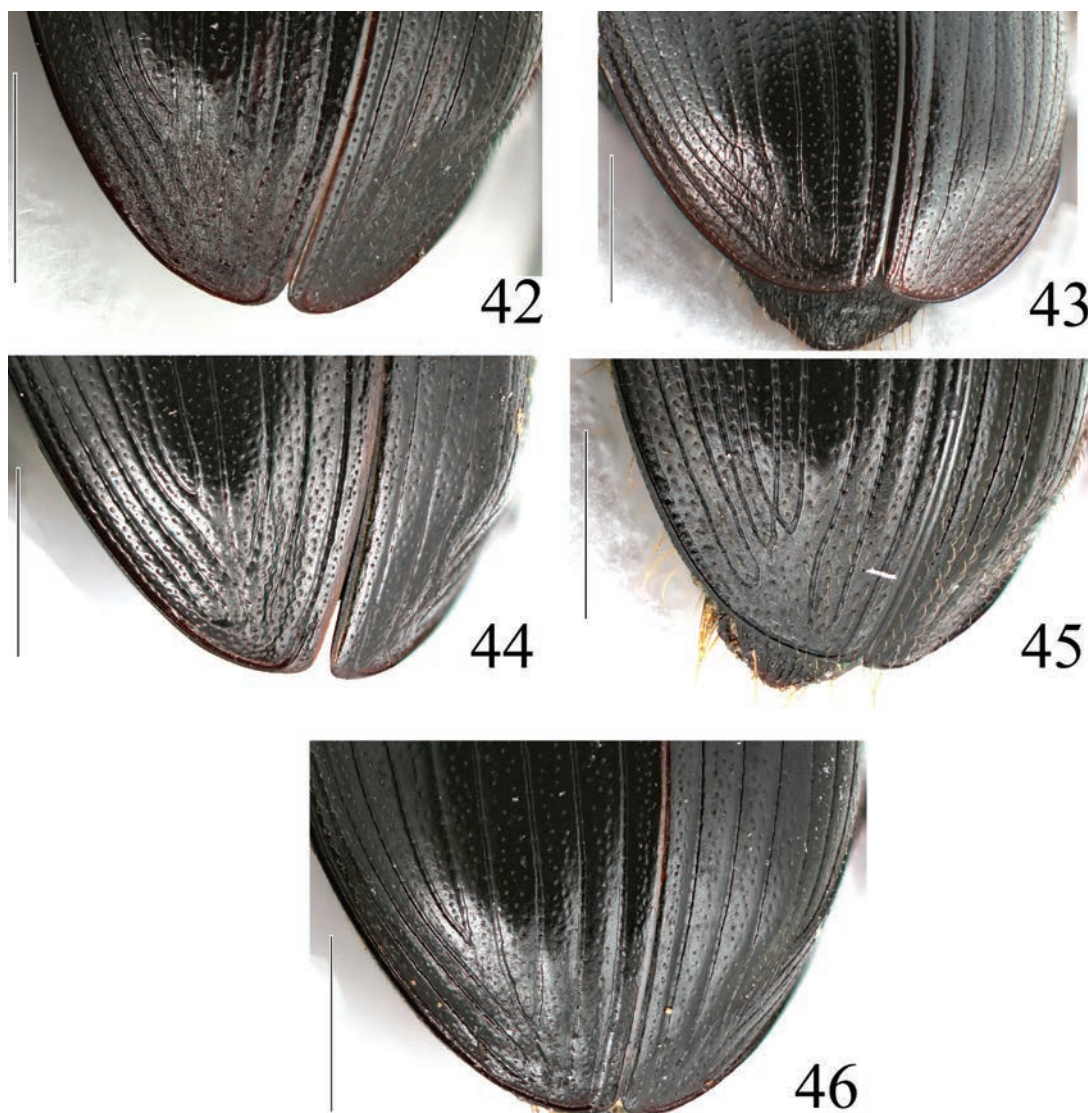
Group	Mean distance (%)	SE (%)
Between intraspecific clades of <i>A. baei</i> sp. nov. (Jeju vs Gangwon)	1.42	0.26
<i>A. superatratus</i>	5.30	1.39
<i>A. humerospinosus</i>	5.92	1.46
<i>A. atratus</i>	8.00	1.75
<i>A. luridus</i>	12.97	2.20
<i>A. depressus</i>	11.49	2.05
<i>A. rufipes</i>	13.96	2.24
<i>A. carpetanus</i>	11.06	2.06
Outgroup	15.73	2.45



Figures 32–36. Epipharingi of *Acrossus* species **32** *A. baei* sp. nov., ♂, holotype **33** *A. atratus* (Waterhouse, 1875), ♂ **34** *A. humerospinosus* (Petrovitz, 1958), ♂ **35** *A. luridus* (Fabricius, 1775), ♂ **36** *A. superatratus* (Nomura & Nakane, 1951), ♂. Scale bars: 0.5 mm.



Figures 37–41. Protibiae and their apical spurs of *Acrossus* species **37** *A. baei* sp. nov., ♂, holotype **38** *A. atratus* (Waterhouse, 1875), ♂ **39** *A. humerospinosus* (Petrovitz, 1958), ♂ **40** *A. luridus* (Fabricius, 1775), ♂ **41** *A. superatratus* (Nomura & Nakane, 1951), ♂. Scale bars: 1.0 mm.

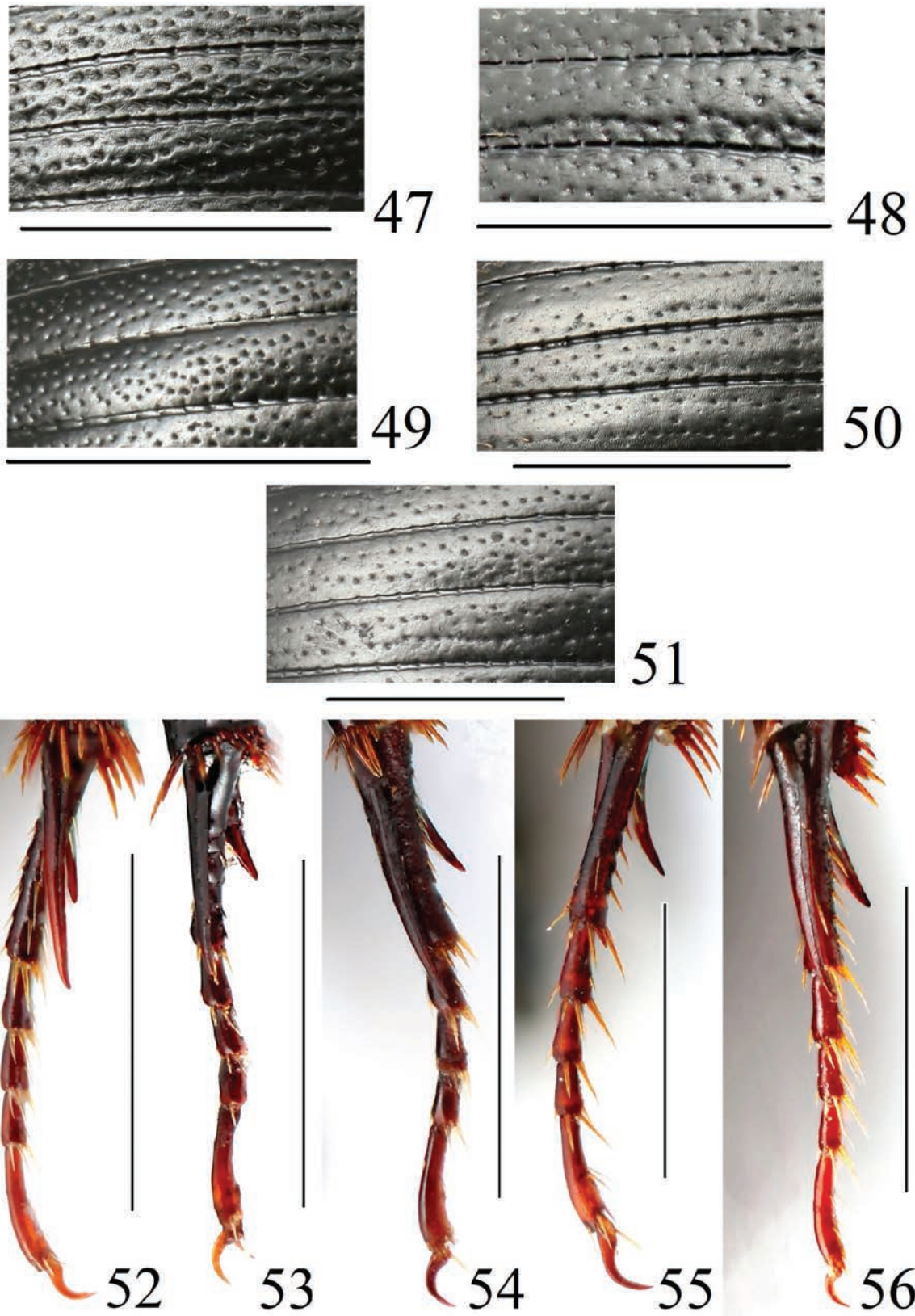


Figures 42–46. Apex of elytra of *Acrossus* species **42** *A. baei* sp. nov., ♂, holotype **43** *A. atratus* (Waterhouse, 1875), ♂ **44** *A. humerospinosus* (Petrovitz, 1958), ♂ **45** *A. luridus* (Fabricius, 1775), ♂ **46** *A. superatratus* (Nomura & Nakane, 1951), ♂. Scale bars: 1.0 mm.

To show the level of difference between them, we have proposed a key to the genus *Acrossus* from the Korean Peninsula.

In having a blackish, longitudinally oval body, the apical protibial spur of the male flattened inwards or hooked at the apex, the elytra with distinct macrosetation, and the elytral intervals flat to weakly convex, *A. baei* sp. nov. is most similar to *A. atratus* (Waterhouse, 1875) and ab. *gagates* of *A. luridus* (Fabricius, 1775), especially to the former.

To facilitate the identification of *A. baei* sp. nov. and similar species discussed above; *A. atratus*, *A. humerospinosus*, *A. luridus*, and *A. superatratus* were photographed and their characters were compared in Table 1. The drawings of the body and aedeagus of *A. luridus* has been presented many times, e.g. by Balthasar (1963), Stebnicka (1976), and Bunalski (1999), but its epipharynx was first illustrated by Dellacasa et al. (2001), and the habitus photographed by Bunalski (1999) and Rössner (2012). The photographs of the habitus and ae-



Figures 47–56. Elytra pattern and metatibiae of *Acrossus* species **47–51** elytra pattern **47** *A. baei* sp. nov., ♂, holotype **48** *A. atratus* (Waterhouse, 1875), ♂ **49** *A. humerospinosus* (Petrovitz, 1958), ♂ **50** *A. luridus* (Fabricius, 1775), ♂ **51** *A. superatratus* (Nomura & Nakane, 1951). **52–56** metatibia **52** *A. baei* sp. nov., ♂, holotype **53** *A. atratus* (Waterhouse, 1875), ♂ **54** *A. humerospinosus* (Petrovitz, 1958), ♂ **55** *A. luridus* (Fabricius, 1775), ♂ **56** *A. superatratus* (Nomura & Nakane, 1951), ♂. Scale bars: 1.0 mm.



Figure 57. *Acrossus baei* sp. nov., ♀, paratype, dorsal view. Scale bar: 1.0 mm.

deagus of *A. atratus* and *A. superatratus* were presented by Kawai et al. (2005). Here, we present, for the first time, photographs of the epipharynxes of all the species mentioned and the habitus and aedeagus of *A. humerospinosus*. We note that the shape of the aedeagi is a less distinctive character than the structure of epipharyngi, which differ considerably among species.

Acknowledgements

We are grateful to Robert Angus (London, England) for checking the English and advice. Also, we are grateful to Masahiro Ôhara (Hokkaido, Japan) for the opportunity to examine the Hokkaido University Museum collection, and members of the laboratory of Biodiversity and Ecology in Korea University for their assistance during field trips. Korean National Park Service (KNPS) provided permits to collect insects at National Park (Odaesan, Sobaeksan, and Jeju Island).

Additional information

Conflict of interest

The authors have declared that no competing interests exist.

Ethical statement

No ethical statement was reported.

Funding

This work was supported by a grant from the National Institute of Biological Resources (NIBR), which is funded by the Ministry of Environment (MOE) of the Republic of Korea (NIBR202002205), and a grant from the Core Research Institute Basic Science Research Program through the National Research Foundation of Korea (NRF) funded by the Ministry of Education (NRF-2021R1A6A1A10045235).

Author contributions

Conceptualization: ŁM. Data curation: ŁM, CL. Formal analysis: ŁM, CL. Investigation: CL. Writing - original draft: ŁM, CL. Writing - review and editing: ŁM, CL.

Author ORCIDs

Changseob Lim  <https://orcid.org/0000-0002-0565-5001>

Łukasz Minkina  <https://orcid.org/0000-0001-7056-7334>

Data availability

All of the data that support the findings of this study are available in the main text.

References

- Balthasar V (1963) Monographie der Scarabaeidae und Aphodidae der palaearktischen und Orientalischen Region. Tschechoslowakische Akademie der Wissenschaften Prag 1: 1–391.
- Bunalski M (1999) Die Blatthornkäfer Mitteleuropas. Coleoptera, Scarabaeoidea. Bestimmung - Verbreitung – Ökologie. Frantisek Slamba, Bratislava, 1–80.
- Cabrero-Sañudo FJ, Zardoya R (2004) Phylogenetic relationships of Iberian Aphodiini (Coleoptera: Scarabaeidae) based on morphological and molecular data. *Molecular Phylogenetics and Evolution* 31: 1084–1100. <https://doi.org/10.1016/j.ympev.2003.10.019>
- Darriba D, Taboada GL, Doallo R, Posada D (2012) jModelTest2: more models, new heuristic and parallel computing. *Nature Methods* 9: 772. <https://doi.org/10.1038/nmeth.2109>
- Dellacasa G, Bordat P, Dellacasa M (2001) A revisional essay of world genus-group taxa of Aphodiinae. *Memorie della Società Entomologica Italiana Genova* 79: 1–482.
- Dellacasa G, Dellacasa M, Mann DJ (2010) The morphology of the labrum (epipharynx, ikrioma and aboral surface) of adult Aphodiini, and its implications for systematics. *Insecta Mundi* 132: 1–21. <https://digitalcommons.unl.edu/insectamundi/658>
- Dellacasa M, Dellacasa G, Král D, Bezděk A (2016) Tribe Aphodiini Leach, 1816. In: Löbl I, Löbl D (Eds) *Catalogue of Palaearctic Coleoptera, Vol. 3. Scarabaeoidea - Scirtoidea - Dasciloidea - Buprestoidea - Byrrhoidea*: Brill, Leiden/Boston, 98–155.
- Kawai S, Hori S, Kawahara M, Inagaki M (2005) *Atlas of Japanese Scarabaeoidea Vol.1 Coprophagous Group*. Roppon-Ashi Entomological Books, Tokyo, 189 pp.
- Kim JI (2012) *Insect fauna of Korea. Volume 12, Number 3. Arthropoda: Insecta: Coleoptera: Scarabaeoidea. Laparosticti*. National Institute of Biological Resources Press, Incheon, 209 pp.
- Kumar S, Stecher G, Li M, Knyaz C, Tamura K (2018) MEGA X: Molecular Evolutionary Genetics Analysis across computing platforms. *Molecular Biology and Evolution* 35(6): 1547. <https://doi.org/10.1093/molbev/msy096>
- Nei M, Kumar S (2000) *Molecular Evolution and Phylogenetics*. Oxford University Press, New York, 352 pp. <https://doi.org/10.1093/oso/9780195135848.001.0001>

- Rössner E (2012) Die Hirschkäfer und Blatthornkäfer Ostdeutschland (Coleoptera: Scarabaeoidea). Verein der Freunde und Förderer des Naturkundemuseums Erfurt e.V., Erfurt, 505 pp.
- Simon C, Frati F, Beckenbach A, Crespi B, Liu H, Flook P (1994) Evolution, weighting, and phylogenetic utility of mitochondrial gene sequences and a compilation of conserved polymerase chain reaction primers. *Annals of the Entomological Society of America* 87(6): 651–701. <https://doi.org/10.1093/aesa/87.6.651>
- Stebnicka Z (1976) Żukowate – Scarabaeidae. Grupa podrodzin: Scarabaeidae laparosticti. Klucze do oznaczania owadów Polski. Część XIX. Zeszyt 28 a., 1–139.
- Stebnicka Z (1980) Scarabaeoidea of the Democratic People's Republic of Korea. *Acta zoologica cracoviensia* 24(5): 191–297.
- Trifinopoulos J, Nguyen LT, von Haeseler A, Minh BQ (2016) W-IQ-TREE: a fast online phylogenetic tool for maximum likelihood analysis. *Nucleic Acids Research* 44(W1): W232–W235. <https://doi.org/10.1093/nar/gkw256>

The redescription and complete mitogenomes of two *Oxycarenius* species (Hemiptera, Oxycarenidae) and phylogenetic implications

Changjun Meng¹, Suyan Cao¹, Wen Dong¹, Cuiqing Gao¹

¹ Co-Innovation Center for Sustainable Forestry in Southern China, College of Forestry and Grassland, Nanjing Forestry University, Nanjing, Jiangsu 210037, China
Corresponding author: Cuiqing Gao (cqgao@njfu.edu.cn)

Abstract

In this study, the two Oxycarenidae species, *O. gossypii* Horváth, 1926 and *Oxycarenius bicolor heraldus* Distant, 1904, are redescribed, and their complete mitogenomes are sequenced and analyzed. The phylogeny of Lygaeoidea is examined using 45 complete mitogenomes of lygaeoid species and four outgroup species. The gene orientation and arrangement of the two mitogenomes are found to be consistent with typical Lygaeoidea mitochondrial features, comprising 37 genes, including 13 PCGs, 22 tRNAs, 2 rRNAs, and a control region. Nucleotide composition of the species was biased towards A and T, with the gene order identical to the putative ancestral arrangement of insects. Start codons, stop codons, RNAs, relative synonymous codon usage (RSCU), and nucleotide diversity (Pi) of Oxycarenidae exhibited characteristics similar to other families in Lygaeoidea. Bayesian-inference (BI) and maximum-likelihood (ML) methods were employed to investigate phylogenetic relationships using PCG datasets from selected species. Phylogenetic analyses reveal slightly different topologies between BI and ML methods, with variation primarily concentrated in Colobathristidae and Rhyparochromidae. Our study confirms that the two sequenced Oxycarenidae species formed a single clade, and the position of Oxycarenidae remains stable in both ML and BI phylogenetic trees. These findings expand the mitochondrial genome databases of Lygaeoidea and provide valuable insights into the phylogenetic relationships within Lygaeoidea or Pentatomomorpha.

Key words: Heteroptera, Lygaeoidea, mitochondrial DNA, *Oxycarenius bicolor heraldus*, *Oxycarenius gossypii*, phylogenetic analysis



Academic editor: Natalia Golub
Received: 24 April 2024
Accepted: 29 July 2024
Published: 5 September 2024

ZooBank: <https://zoobank.org/64AB9480-1311-4322-936D-AD867F0AF71C>

Citation: Meng C, Cao S, Dong W, Gao C (2024) The redescription and complete mitogenomes of two *Oxycarenius* species (Hemiptera, Oxycarenidae) and phylogenetic implications. ZooKeys 1211: 231–250. <https://doi.org/10.3897/zookeys.1211.126013>

Copyright: © Changjun Meng et al.
This is an open access article distributed under terms of the Creative Commons Attribution License (Attribution 4.0 International – CC BY 4.0).

Introduction

Mitochondrial genome analysis is a powerful tool for elucidating the phylogeny and population genetics of insect taxa (Cameron and Whiting 2008; Li et al. 2023). Insects possess circular double-stranded mitochondrial molecules typically ranging from 14 to 20 kb in length. These genomes encode 37 genes, encompassing 13 protein-coding genes (PCGs), two ribosomal RNA genes (rRNAs), 22 transfer RNA genes (tRNAs), and a single control region. While insect mitochondria generally adhere to a conventional structure, there are exceptions, in certain species of Anoplura (Boore 1999; Shao et al. 2009). Characterized by compactness, insect mitochondrial genomes feature minimal spacer

regions or overlapping sequences between adjacent genes (Boore 1999). Notably, they exhibit small size, stable genetic composition, relatively conserved gene sequences, rapid evolutionary rates, and comprehensive molecular information. Consequently, they serve as invaluable tools for investigating molecular evolution, phylogenetics, and population genetic structure (Xue and Bu 2008; Simon and Hadrys 2013; Kocher et al. 2014).

The Lygaeoidea, the second largest superfamily in Pentatomomorpha, comprises over 4,700 described species across 16 families (Weirauch and Schuh 2011; Dellapé and Henry 2024). This widespread terrestrial superfamily primarily includes herbivorous species feeding on plant seeds or sap, with some being economically significant pests (Sweet 2000). Among them, Oxycarenidae species predominantly inhabit the plants of Malvaceae and Sterculiaceae, where they feed on seeds and can inflict substantial damage to cotton and other mallow crops (Sureshan et al. 2021). Currently, over 140 species in 27 genera have been documented worldwide (Henry and Dellapé 2009; Xiao and Gao 2022; Dellapé and Henry 2024).

Past studies investigating the phylogenetic relationships of Pentatomomorpha have relied on morphological characters for classification (Henry 1997), and more recently, they have incorporated molecular data. The increasing number of Lygaeoidea species documented in recent years underscores the importance of exploring their phylogenetic relationships using mitochondrial DNA, both to validate previous findings and to provide additional insights.

In this study, we redescribe both *O. gossypii* Horváth, 1926 and *Oxycarenius bicolor heraldus* Distant, 1904. Additionally, two misidentifications in China are rectified, and the complete mitogenomes of these species are sequenced. Subsequently, we construct phylogenetic trees using the complete mitogenomes of 45 species of Lygaeoidea and four outgroup species. These findings contribute essential data for further investigations into the phylogenetic relationships within Lygaeoidea and Pentatomomorpha.

Materials and methods

Sample collection, identification and DNA extraction

Adult specimens of *Oxycarenius bicolor heraldus* Distant, 1904 were collected from Xiangshan Park, Pukou District, Nanjing, Jiangsu Province, China, in May 2020. Adult specimens of *O. gossypii* Horváth, 1926 were collected from Phoenix Airport, Sanya City, Hainan Province, China, in March 2020.

Composite images were obtained using an M205FA Leica stereomicroscope and camera, with the Leica Application Suite v. 4.5.0. Type label data are presented verbatim, with lines on the same label separated by a slash (/), and different labels divided by double slashes (//). Texts printed [pr] and handwritten [hw] are indicated. All measurements provided in the text are expressed in millimetres.

Abbreviations

BMNH Natural History Museum, London, United Kingdom;
IZAS Institute of Zoology, Academia Sinica, Beijing, China;

MSIE Shanghai Institute of Entomology, Shanghai, China;
NKUM Institute of Entomology, Nankai University, Tianjin, China;
NJFU Nanjing Forestry University, Nanjing, Jiangsu.

Genomic DNA were extracted from adult target insects using the Rapid Animal Genomic DNA Isolation Kit (Sangon Biotech, Shanghai, China).

Sequencing, assembly, annotation, and bioinformatics analyses

The mitochondrial genomes of these two species were sequenced using an Illumina MiSeq PE300 platform (Sangon Biotech, Shanghai, China). Subsequently, Fastp v. 0.36 (Chen et al. 2018) was employed to eliminate low-quality and short reads, ensuring the integrity of the data for subsequent analysis. SPAdes v. 3.15 (Bankevich et al. 2012) facilitated the de novo assembly of the high-quality next-generation sequencing data, resulting in the generation of contigs and scaffolds. Rigorous evaluation and quality control measures were applied to the assembly results using PrInSeS-G (Massouras et al. 2010). Potential contamination originating from the host genome was meticulously identified and eliminated, retaining only the scaffolds derived from the organelle genome. Sequence similarity was assessed by comparing the scaffolds with the NCBI library using BLASTn (Ye et al. 2012). Target scaffolds were manually selected based on sequencing depth and coverage information for each scaffold. GapFiller v. 1.11 (Boetzer and Pirovano 2012) was utilized to supplement and rectify obtained alleles by correcting editing errors and filling gaps introduced during splicing, including the insertion or deletion of fragments as needed.

The two mitogenome sequences were annotated using Geneious v. 11.0.2 (Kearse et al. 2012), following the invertebrate mitochondrial genetic code. Circular maps of the mitogenomes were generated using the CGView Server (Grant and Stothard 2008). To ensure annotation accuracy, all tRNA genes were verified using the MITOS Web Server (Bernt et al. 2013), and their secondary structures were predicted using the tRNAscan-SE Server v. 1.21 (Lowe and Chan 2016). PhyloSuite v. 1.2.3 (Xiang et al. 2023) and MEGA X (Kumar et al. 2018) were employed to determine base composition and relative synonymous codon usage (RSCU) values of the two mitogenome sequences. Non-synonymous substitutions (K_a) and synonymous substitutions (K_s) of the 13 PCGs of Oxycarenidae were calculated using DnaSP5 software (Librado and Rozas 2009), and K_a/K_s values were subsequently derived. Nucleotide composition skew was computed using the formulas developed by Perna and Kocher: $AT\text{-skew} = (A - T) / (A + T)$ and $GC\text{-skew} = (G - C) / (G + C)$. This study aimed to comprehensively examine the evolutionary patterns among mitochondrial protein-coding genes (PCGs) in species of Oxycarenidae.

Phylogenetic analysis

To investigate mitogenome arrangement patterns in Lygaeoidea, we compared the gene orders of all known Lygaeoidea mitogenomes with those of closely related taxa (Table 1). For phylogenetic analyses, we examined a total of 49 mitogenomes (Table 1), which included two newly generated sequences from this study. We standardized all sequences and extracted 13 PCGs using PhyloSuite v. 1.2.2 (Perna and Kocher 1995; Xiang et al. 2023). The 13 PCGs of these species were individually

Table 1. Sequences used in this study.

Superfamily	Family	Species	Length (bp)	GenBank No.
Lygaeoidea	Berytidae	<i>Metatropis longirostris</i> Hsiao, 1974	15,744	NC_037373.1
	Berytidae	<i>Yemmalysus parallelus</i> Stusak, 1972	15,747	NC_012464.1
	Blissidae	<i>Bochrus foveatus</i> Distant, 1879	14,738	ON961018.1
	Blissidae	<i>Capodemus sinuatus</i> (Slater, Ashlock & Wilcox, 1969)	15,199	ON961019.1
	Blissidae	<i>Cavelerius yunnanensis</i> Gao & Zhou, 2021	15,330	NC_065816.1
	Blissidae	<i>Dimorphopterus gibbus</i> (Fabricius, 1794)	14,988	NC_065817.1
	Blissidae	<i>Iphicrates gressitti</i> Slate, 1966	15,288	NC_065818.1
	Blissidae	<i>Ischnodemus noctulus</i> Distant, 1901	15,291	NC_065819.1
	Blissidae	<i>Macropes dentipes</i> Motschulsky, 1859	14,923	NC_065821.1
	Blissidae	<i>Macropes harringtonae</i> Slater, Ashlock & Wilcox, 1969	15,314	OP442511.1
	Blissidae	<i>Macropes robustus</i> Zheng & Zou, 1982	15,041	NC_065822.1
	Colobathristidae	<i>Phaenacantha marcida</i> Horváth, 1914	14,540	NC_012460.1
	Geocoridae	<i>Geocoris pallidipennis</i> (Costa, 1843)	14,592	NC_012424.1
	Geocoridae	<i>Henestaris halophilus</i> (Burmeister, 1835)	14,868	MW619656.1
	Lygaeidae	<i>Arocatus melanocephalus</i> (Fabricius, 1798)	15,409	NC_063142.1
	Lygaeidae	<i>Crompus oculatus</i> Stål, 1874	15,332	MW619652.1
	Lygaeidae	<i>Kleidocerys resedae resedae</i> (Panzer, 1793)	14,688	KJ584365.1
	Lygaeidae	<i>Lygaeus</i> sp. FS-2019	15,235	MF497725.1
	Lygaeidae	<i>Nysius cymoides</i> (Spinola, 1837)	16,301	MW291653.1
	Lygaeidae	<i>Nysius fuscovittatus</i> Barber, 1958	14,575	NC_050167.1
	Lygaeidae	<i>Nysius graminicola</i> (Kolenati, 1845)	16,760	NC_073587.1
	Lygaeidae	<i>Nysius plebeius</i> Distant, 1883	17,367	MN599979.1
	Lygaeidae	<i>Nysius</i> sp.	16,330	MW465654.1
	Lygaeidae	<i>Pylorgus porrectus</i> Zheng, Zou & Hsiao, 1979	15,174	NC_080509.1
	Lygaeidae	<i>Pylorgus sordidus</i> Zheng, Zou & Hsiao, 1979	15,399	NC_084343.1
	Lygaeidae	<i>Tropidothorax cruciger</i> (Motschulsky, 1859)	15,781	NC_056293.1
	Lygaeidae	<i>Tropidothorax sinensis</i> (Reuter, 1888)	15,422	MW547017.1
	Malcidae	<i>Chauliops fallax</i> Scott, 1874	15,739	NC_020772.1
	Malcidae	<i>Chauliops</i> sp.	15,300	OP793778.1
	Malcidae	<i>Chauliops quaternaria</i> Gao & Bu, 2009	15,612	NC_087837.1
	Malcidae	<i>Chauliops zhengi</i> Xue & Bu, 2004	15,507	NC_087838.1
	Malcidae	<i>Malcus auriculatus</i> Štys, 1967	15,097	NC_063141.1
	Malcidae	<i>Malcus inconspicuus</i> Štys, 1967	15,316	OL944394.1
Malcidae	<i>Malcus setosus</i> Štys, 1967	14,894	NC_063138.1	
Ninidae	<i>Cymoninus sechellensis</i> (Bergroth, 1893)	15,962	NC_085420.1	
Ninidae	<i>Ninus insignis</i> Stål, 1860	14,632	NC_063137.1	
Oxycarenidae	<i>Oxycarenum gossypii</i> Horváth, 1926	16,144	OR_713903	
Oxycarenidae	<i>Oxycarenum bicolor heraldus</i> Distant, 1904	15,462	PP_446310	
Rhyparochromidae	<i>Bryanelllocoris orientalis</i> Hidaka, 1962	15,606	NC_063139.1	
Rhyparochromidae	<i>Eucosmetus incisus</i> (Walker, 1872)	14,562	NC_085565.1	
Rhyparochromidae	<i>Harmostica fulvicornis</i> (Horváth, 1914)	15,703	NC_063140.1	
Rhyparochromidae	<i>Ligyrocoris sylvestris</i> (Linnaeus, 1758)	16,621	PP145295.1	
Rhyparochromidae	<i>Neolethaeus assamensis</i> (Distant, 1901)	15,067	NC_037375.1	
Rhyparochromidae	<i>Panaorus albomaculatus</i> (Scott, 1874)	16,345	NC_031364.1	
Pyrrhocoroidea	Pyrrhocoridae	<i>Dysdercus evanescens</i> Distant, 1902	15,635	MW619727.1
Coreoidea	Alydidae	<i>Riptortus pedestris</i> (Fabricius, 1775)	17,191	EU427344.1
	Coreidae	<i>Hydaropsis longirostris</i> (Hsiao, 1963)	16,521	EU427337.1
	Rhopalidae	<i>Aeschyntelus notatus</i> Hsiao, 1963	14,532	EU427333.1

aligned using codon-based multiple alignments with MAFFT v. 7.313 software (Kato and Standley 2013). The concatenated PCGs were processed with PhyloSuite v. 1.2.3. PartitionFinder2 selected optimal partitioning schemes and evolutionary models for constructing Bayesian-inference (BI) and maximum-likelihood (ML) trees with confidence (Soria-Carrasco et al. 2007; Lanfear et al. 2017). Phylogenetic trees were reconstructed using IQ-TREE v. 1.6.8 (Guindon et al. 2010) and MrBayes v. 3.2.6 (Ronquist et al. 2012) with the assistance of PhyloSuite v. 1.2.2.

Results

Taxonomy

Oxycarenum gossypii Horváth, 1926

Figs 1A, 2A–C

Oxycarenum gossypii: Horváth 1926: 136; Esaki 1926: 161; Slater 1964: 673; Péricart 2001: 115.

Oxycarenum laetus: Zheng and Zou 1981: 96. Misidentification.

Material examined. CHINA • 3♂♂1♀; Yunnan, Yuanjiang; alt. 400 m; 25 Jul. 2006; Weibing Zhu leg. (NKUM) • 1♂2♀♀; Yunnan, Xishuangbanna, Mengsong; alt. 1600 m; 23 Apr. 1958; Xvwu Meng leg. (IZAS) • 1♂; Yunnan, Xishuangbanna, Damenglong; alt. 650 m; 8 Apr. 1958; Leyi Zheng leg. (IZAS) • 5♂♂6♀♀; Hainan, Sanya, Fenghuang airport; 26 Mar. 2020; Bo Cai leg. (NJFU) • 16♂♂5♀♀; Hainan, Jianfengling thermal forestry institute; 21 Apr. 1985; Leyi Zheng leg.; from capsule of *Abutilon indicum* (NKUM) • 192♂♂183♀♀; Hainan, Sanya; alt. 10 m; 5–6 Apr. 1960; Suofu Li leg. (IZAS) • 26♂♂26♀♀; Hainan, Ledong; 11 Jun. 1960; Xuezhong Zhang leg. (IZAS) • 1♂; Hainan Nada; 27 Apr. 1954; Keren Huang leg. (IZAS).

Redescription. Body brown, densely punctate, with white decumbent, erect, and apically enlarged setae. Antennae dark brown. Rostrum extends past anterior margin of abdominal sternite III, up to abdominal sternite V in females. Bucculae yellowish white. Pronotum brown, often lighter at anterior margin and posterior half, densely covered with deep, large punctures, white erect, and apically enlarged setae mixed with decumbent setae; callus area slightly elevated, densely covered with large, dark brown setae. Lateral margins of pronotum slightly sinuate. Scutellum brown, evenly punctate, flattened except basal margin concave, peripherally covered with both decumbent and erect, apically enlarged setae. Clavus brown, with both types of setae mentioned above. Corium yellowish brown, with a conspicuous black spot at distal angle; sparse erect setae, apical margin straight. Membrane smoky brown. Thoracic sternum brown, posterior margins of metapleura pale. Ostiolar peritreme of metathoracic scent gland yellow. Supracoxal lobewhite. Femora dark brown; fore femora beneath with four spines; fore tibiae yellowish brown; mid and hind tibiae pale, both ends brown. Abdominal sterna reddish brown, smooth, impunctate, without erect setae. Male sternites VI and VII with posterior margin with two transverse combs of glandular setae on either side of median line. Female abdominal sterna III to IV fused; ovipositor reaching abdominal sternites V–VII, with sternites V–VII medially strongly narrowed, pushed forward towards base of abdomen.



Figure 1. Dorsal and ventral view of *Oxycarenus* species sequenced **A** *O. gossypii* **B, C** *O. bicolor heraldus*.

Pygophore: dorsal opening narrowly triangular (Fig. 2A); lateral projections in basal one third of pygophore openings, projecting obliquely posteriorly, tips truncate; distal margin of cup-like sclerite with a narrow, deep incision (Fig. 2A). Parameres (Fig. 2B, C) with basal shank relatively broad, about twice as wide as blade; outer projection rounded, inner projection more pointed from dorsal view; another finger-like inner projection present on inner side from ventral view.

Measurements (in mm, $n = 8$). Body length 3.40–4.00, width 1.1–1.30. Head length 0.70–0.72, width across eyes 0.65–0.67; antennal segments I–IV length: 0.27–0.29: 0.56–0.58: 0.45–0.47: 0.52–0.54. Pronotum length 0.78–0.80, width of anterior margin 0.52–0.54, width of posterior margin 1.00–1.02; scutellum length 0.34–0.36, width 0.52–0.54. Distance of apex clavus–apex corium 0.60–0.62; distance of apex corium–apex membrane 0.72–0.74.

Distribution. China (Hainan, Yunnan, Taiwan); Vietnam.

Remarks. On review of descriptions and figures, we discovered that *Oxycarenus gossypii* was erroneously identified as *Oxycarenus laetus* (Kirby, 1891) in the study by Zheng and Zou (1981). However, distinct differences exist between these species: the clavus appears brown in *O. gossypii*, whereas it is pale in *O. laetus*; the membrane presents a smoky golden-brown hue in *O. gossypii* (in contrast to the colorless and hyaline membrane of *O. laetus*); and, while the corium of *O. gossypii* is pale or slightly smoky except at the base, it consistently remains pale in *O. laetus*.

***Oxycarenus bicolor heraldus* Distant, 1904**

Figs 1B, C, 2D–F

Oxycarenus heraldus: Distant 1904: 44.

Oxycarenum bicolor variety heraldus: Bergroth 1918: 73.

Oxycarenum bicolor heraldus: Slater 1964: 670.

Oxycarenum lugubris: Zheng and Zou 1981: 97. Misidentification.

Type material examined (digital photograph). **Lectotype:** BURMA • ♀; Carin Chebà [pr] / 900–1100 m [pr] / L. Fea V XII-88 [pr] // *heraldus* [hw] / Dist. [hw] // Distant Coll. / 1911–383 // Type [pr, red] // SYN/ TYPE [pr, blue] // *Oxycarenum / heraldus* / Distant, 1904: 44 [pr] / BMNH(E) / 1340705 [pr] (BMNH).

Paralectotype: same information except: BMNH(E) / 1340706 [pr].

Other material examined. CHINA • 2♀♀; Gansu, Wen county, Fanba; 30 Jul. 1988; collected from capsule of *Abutilon theophrasti* (NKUM) • 20♂♂15♀♀; Jiangsu, Nanjing, Laoshan; 20 Jun. 2021; collected from capsule of *Hibiscus mutabilis* (NJFU) • 6♂♂7♀♀; Sichuan, Qingchengshan; 16 Aug. 1956; Leyi Zheng leg. (NKUM) • 20♂♂25♀♀; Yunnan, Dali, Cangshan; 19 Aug. 2006; Zhonghua Fan leg. (NKUM) • 300♂♂242♀♀; Yunnan, Menglong, Banna,

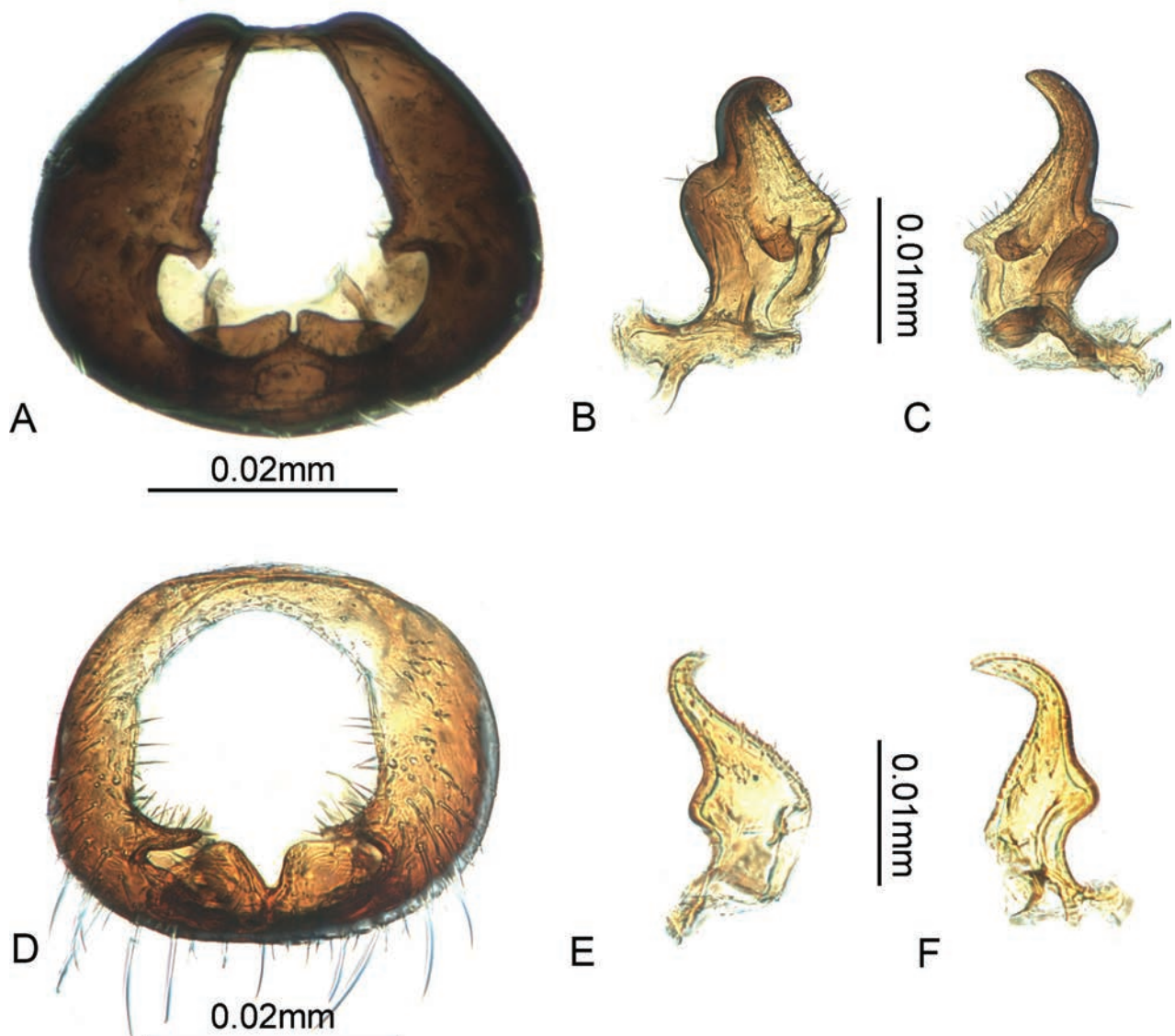


Figure 2. Genitalia of *Oxycarenum* species **A–C** *O. gossypii* **A** pygophore, posterodorsal view **B, C** left paramere, dorsal and ventral view **D–F** *O. bicolor heraldus* **D** pygophore, posterodorsal view **E, F** left paramere, dorsal and ventral view.

Mengsong, alt. 1600 m; 23 Apr. 1958; Xvwu Meng leg. (IZAS) • 40♂♂32♀♀; Yunnan, Pingbian; alt. 1300 m; 22 Jun. 1956; Keren Huang leg. (MSIE).

Redescription. Head dark, blackish brown or black, densely coarsely punctate, with white, flat, decumbent setae and sparser erect, apically enlarged, long setae. Antennae dark, blackish brown or black, with segment I extending to tip of clypeus. Head ventrally densely covered with silvery-white, flat setae. Rostrum extends to hind coxae or middle of abdominal sternite III. Bucculae dark. Pronotum brown with a black transverse stripe at callus area. Covered with coarse punctures and sparsely erect and apically enlarged long setae, with slightly sinuate lateral margins. Scutellum dark blackish brown or black, similar setae to pronotum, punctuated, with a sunken base and a slightly elevated middle. Clavus dark brown to blackish brown, possessing three lines of punctures, with middle row incomplete. Corium with exocorium, basal 1/3 of inner corium, and distal angle yellowish white, about middle 1/3 of inner corium blackish brown, not reaching exocorium; sometimes, extreme distal angles of corium slightly darkened, but not with obvious small black spots; distal margin of corium straight; clavus and corium with sparse pale erect setae. Membrane dark blackish brown, with basal margin adjoining distal margin of corium narrowly white. Head and prothorax ventrally densely covered with silvery-white, decumbent setae; thoracic sternites and pleurae black or dark blackish brown, glossy, except supracoxal lobe and posterior margin of metapleura pale; ostiolar peritreme of metathoracic scent gland strongly protruding, basally brown and distally yellow. Femora blackish brown, slightly thickened; fore femora with four spines; tibiae yellow with both ends dark blackish brown, and fore tibiae darker. Abdomen reddish brown to blackish brown. Posterior margin of sternites VI and VII in males with two conspicuous transverse combs of glandular setae on either side of median line. Female abdominal sterna III–IV fused; ovipositor reaching abdominal sternites V–VII, with sternites V–VII medially strongly narrowed and pushed forward towards abdominal sternites V.

Pygophore: dorsal opening broadly rounded; lateral projections finger-like, slightly inclined posteriorly and internally; distal margin of cup-like sclerite bifurcate (Fig. 2D). Parameres with blade falcate and curved; outer projection rounded; inner projection projecting dorsoventrally, more square (Fig. 2E, F).

Measurements (in mm, $n = 8$). Body length 3.80–4.30, width 1.10–1.40. Head length 0.71–0.73, width across eyes 0.72–0.73; antennal segments I–IV length: 0.28–0.30: 0.61–0.63: 0.47–0.49: 0.58–0.60. Pronotum length 0.83–0.85, width of anterior margin 0.58–0.60, width of posterior margin 1.10–1.11; scutellum length 0.41–0.43, width 0.54–0.55. Distance of apex clavus–apex corium 0.89–0.90; distance of apex corium–apex membrane 0.67–0.69.

Distribution. China (Gansu, Jiangsu, Hubei, Sichuan, Yunnan); Burma.

Remarks. The specific status of *Oxycarenus heraldus* Distant, 1904 was previously reduced to *Oxycarenus bicolor* var. *heraldus* by Bergroth (1918), and later treated as subspecies *Oxycarenus bicolor heraldus* by Slater (1964).

Oxycarenus bicolor heraldus shares similar coloration with *Oxycarenus bicolor bicolor*, but there are notable differences. Unlike *Oxycarenus bicolor bicolor*, the brown spots on the hemelytra of *Oxycarenus bicolor heraldus* do not reach the exocorium (the brown spots on the hemelytra extend to the lateral margin of the corium in *O. bicolor bicolor*). Furthermore, the body size of *O. bicolor heraldus* is larger (3.80–4.30 mm) compared to *O. bicolor* (which is smaller,

approximately 3.0–3.4 mm), and while the postero-lateral angles of the corium in *O. bicolor heraldus* may be slightly darkened, but they lack the distinct small black spots that are present in *O. bicolor bicolor*.

Oxycarenus bicolor heraldus is a common species in China, but it has long been misidentified as *Oxycarenus lugubris* (Motschulsky, 1859) (Zheng and Zou 1981). In comparison with *O. lugubris*, the pronotum of *O. bicolor heraldus* is brown with a black transverse stripe, whereas in *O. lugubris*, it is entirely black. Furthermore, only the middle 1/3 of the inner corium is blackish brown in *O. bicolor heraldus*, with the basal membrane narrowly white, while the distal 2/3 of the inner corium is entirely black, and the base of the membrane is also black in *O. lugubris*. Although both the species are distributed in China, *O. lugubris* has only been recorded from Taiwan and Hong Kong according to the data available on the iNaturalist website.

Genome structure and base composition

We have sequenced and annotated the complete mitogenomes of *O. gossypii* and *O. bicolor heraldus*, which were 16,144 bp and 15,462 bp in length, respectively (Table 1). These mitogenome sequences consist of the 37 typical insect mitochondrial genes, including 13 protein-coding genes (PCGs), 22 transfer RNA genes (tRNAs), and two ribosomal RNA genes (rRNAs), along with an AT-rich region known as the control region (CR), forming a double-stranded ring structure (Fig. 3). The N-strand encodes 14 genes, while the J-strand encodes 23 genes, consistent with the mitochondrial gene arrangement observed in known Lygaeoidea species and the classical insect *Drosophila yakuba* (Burla, 1954) (Clary and Wolstenholme 1985; Hua et al. 2008; Küechler et al. 2010; Cao et al. 2020).

The nucleotide composition of the *O. gossypii* mitogenome was as follows: A = 41.35%, T = 32.82%, C = 15.33%, and G = 10.50%, while that of *O. bicolor heraldus* was A = 40.86%, T = 33.11%, C = 15.68%, and G = 10.35%.

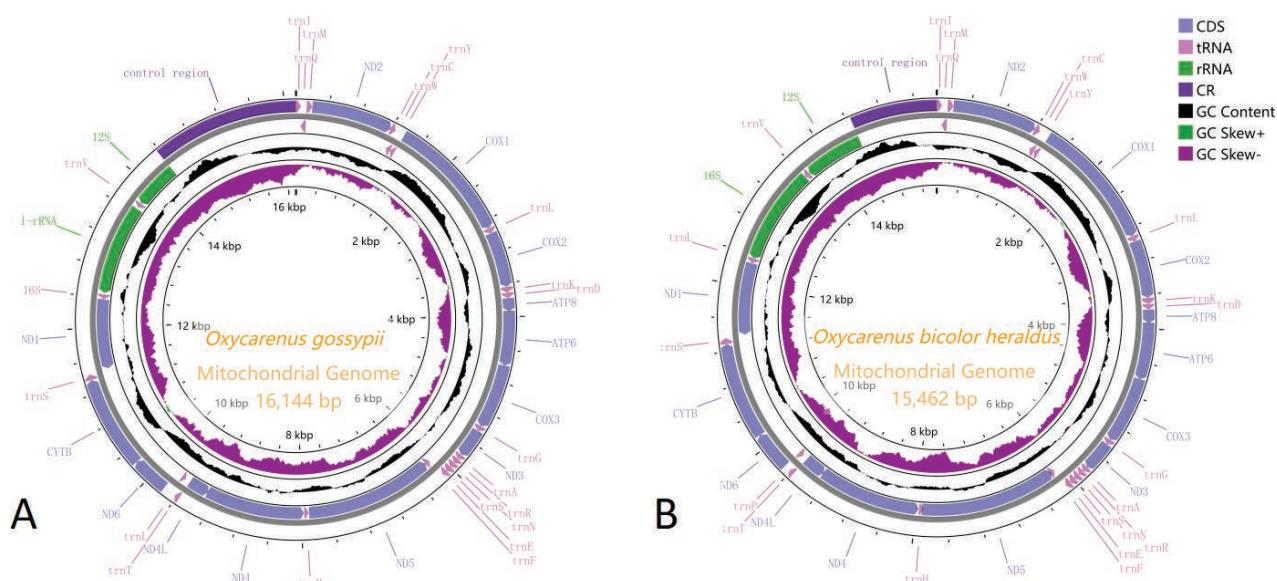


Figure 3. Circular map of the complete mitogenome of *Oxycarenus* species **A** *O. gossypii* **B** *O. bicolor heraldus*. Different colors indicate different types of genes and regions. Genes in the outer circle are located on the J-strand, and genes in the inner circle are located on the N-strand.

Both mitogenomes exhibited a high AT content, with *O. gossypii* at 74.17% and *O. bicolor heraldus* at 73.97%. Additionally, both mitogenomes displayed a slightly positive AT-skew (0.11 and 0.10) and a negative GC-skew (−0.18 and −0.20), indicating a bias towards A and T nucleotides. The study identified 15 gaps in the two mitogenome sequences, ranging from 1 bp to 22 bp, with the longest intergenic spacer being 22 bp, found between *rrnL* and *trnV* in *O. gossypii* (Table 2). Moreover, there were 25 overlapping gene regions, with lengths ranging from 1 bp to 24 bp, and the longest overlap of 24 bp was observed between *nad5* and *trnH* in *O. bicolor heraldus* (Table 3).

Table 2. Mitochondrial composition of *Oxycarenum gossypii*.

Name	Direction	Position From	Position To	Length (bp)	Intergenic nucleotides	Start/Stop Codons
<i>trnI</i>	J	1	62	62	3	
<i>trnQ</i>	N	60	128	69	-1	
<i>trnM</i>	J	130	197	68	0	
<i>nad2</i>	J	198	1187	990	2	ATA/TAA
<i>trnW</i>	J	1186	1248	63	8	
<i>trnC</i>	N	1241	1302	62	-1	
<i>trnY</i>	N	1304	1364	62	-1	
<i>cox1</i>	J	1366	2899	1534	0	TTG/T --
<i>trnL2</i>	J	2900	2964	65	0	
<i>cox2</i>	J	2965	3640	676	0	ATA/T --
<i>trnK</i>	J	3641	3711	71	0	
<i>trnD</i>	J	3712	3777	66	0	
<i>atp8</i>	J	3778	3936	159	7	ATT/TAA
<i>atp6</i>	J	3930	4595	666	1	ATG/TAA
<i>cox3</i>	J	4595	5381	787	0	ATG/TAA
<i>trnG</i>	J	5382	5447	66	0	
<i>nad3</i>	J	5448	5801	354	0	ATA/TAA
<i>trnA</i>	J	5802	5864	63	0	
<i>trnR</i>	J	5865	5927	63	0	
<i>trnN</i>	J	5928	5995	68	1	
<i>trnS1</i>	J	5995	6063	69	1	
<i>trnE</i>	J	6063	6127	65	0	
<i>trnF</i>	N	6128	6190	63	1	
<i>nad5</i>	N	6190	7899	1710	-3	ATA/TAA
<i>trnH</i>	N	7903	7964	62	-2	
<i>nad4</i>	N	7967	9286	1320	7	ATG/TAA
<i>nad4l</i>	N	9280	9558	279	-5	ATA/TAA
<i>trnT</i>	J	9564	9625	62	0	
<i>trnP</i>	N	9626	9684	59	4	
<i>nad6</i>	J	9781	10236	456	1	ATA/TAA
<i>cytb</i>	J	10236	11370	1135	0	ATG/T --
<i>trnS2</i>	J	11371	11439	69	-16	
<i>nad1</i>	N	11456	12379	924	0	ATT/TAA
<i>trnL1</i>	N	12380	12445	66	0	
<i>rrnL</i>	N	12464	13671	1208	-22	
<i>trnV</i>	N	13694	13690	67	-4	
<i>rrnS</i>	N	13765	14372	608	0	

Table 3. Mitochondrial composition of *Oxycarenum bicolor heraldus*.

Name	Direction	Position From	Position To	Length (bp)	Intergenic nucleotides	Start/Stop Codons
<i>trnI</i>	J	1	62	62	3	
<i>trnQ</i>	N	60	128	69	1	
<i>trnM</i>	J	128	195	68	0	
<i>nad2</i>	J	196	1183	988	1	ATA/TAA
<i>trnW</i>	J	1185	1246	62	8	
<i>trnC</i>	N	1239	1300	62	0	
<i>trnY</i>	N	1301	1363	63	-1	
<i>cox1</i>	J	1365	2898	1581	0	TTG/T--
<i>trnL2</i>	J	2899	2963	65	0	
<i>cox2</i>	J	2964	3639	699	0	ATA/T--
<i>trnK</i>	J	3640	3711	73	0	
<i>trnD</i>	J	3712	3774	63	0	
<i>atp8</i>	J	3775	3933	159	7	ATA/TAA
<i>atp6</i>	J	3927	4592	666	1	ATG/TAA
<i>cox3</i>	J	4592	5378	790	0	ATG/T--
<i>trnG</i>	J	5379	5443	65	0	
<i>nad3</i>	J	5444	5795	354	-1	ATT/TAG
<i>trnA</i>	J	5797	5859	63	0	
<i>trnR</i>	J	5860	5922	65	-1	
<i>trnN</i>	J	5924	5989	66	1	
<i>trnS1</i>	J	5989	6057	69	1	
<i>trnE</i>	J	6057	6122	65	0	
<i>trnF</i>	N	6123	6187	63	20	
<i>nad5</i>	N	6168	7922	1714	24	ATA/TAA
<i>trnH</i>	N	7899	7960	70	-2	
<i>nad4</i>	N	7963	9282	1320	7	ATG/TAA
<i>nad4l</i>	N	9276	9557	282	-2	ATT/TAA
<i>trnT</i>	J	9560	9621	62	0	
<i>trnP</i>	N	9622	9684	63	3	
<i>nad6</i>	J	9692	10153	462	1	ATT/TAA
<i>cytb</i>	J	10153	11289	1137	2	ATG/TAG
<i>trnS2</i>	J	11288	11358	71	-17	
<i>nad1</i>	N	11376	12298	960	0	ATA/TAA
<i>trnL1</i>	N	12299	12365	67	0	
<i>rrnL</i>	N	12366	13611	1253	0	
<i>trnV</i>	N	13612	13678	67	-1	
<i>rrnS</i>	N	13680	14453	802	0	

Protein-coding genes

The concatenated length of the 13 protein-coding genes (PCGs) of *O. gossypii* was 10,990 bp, encoding 3,663 amino acid residues. Similarly, the concatenated length of the 13 PCGs of *O. bicolor heraldus* was 11,112 bp, encoding 3,702

amino acids. Both species share the same arrangement in their mitochondrial genomes. The majority of PCGs initiate translation using the start codon ATN, except for *cox1*, which starts with TTG. There are three types of stop codons: TAA, TAG, and an incomplete stop codon T that is completed by the addition of 3'A residues to the mRNA.

The Relative Synonymous Codon Usage (RSCU) of the two Oxycarenidae species was computed and depicted in Fig. 4. Among the codons utilized, CGA-Arg, GCU-Ala, UCU-Ser, UUA-Leu, and GUU-Val were the most frequently employed. Particularly, UUA emerged as the most preferred codon. Moreover, a pronounced bias toward A/T nucleotides was evident across the Protein-Coding Genes (PCGs). Nucleotide diversity (Pi) and the ratios of Ka/Ks for the two species were calculated based on the 13 PCGs, as illustrated in Fig. 5. Pi values ranged from 0.12 to 0.26, with the highest values observed in *atp8* and the lowest in *cox3*, underscoring *cox3*'s role as the most conserved gene in Oxycarenidae. All Ka/Ks ratios were below 1, varying from 0.04 to 0.29, indicative of purifying selection acting on the genes. Particularly noteworthy was *nad6*'s highest Ka/Ks values, suggesting rapid evolution, while *cox1* and *cytb* exhibited the slowest evolution, with the lowest values.

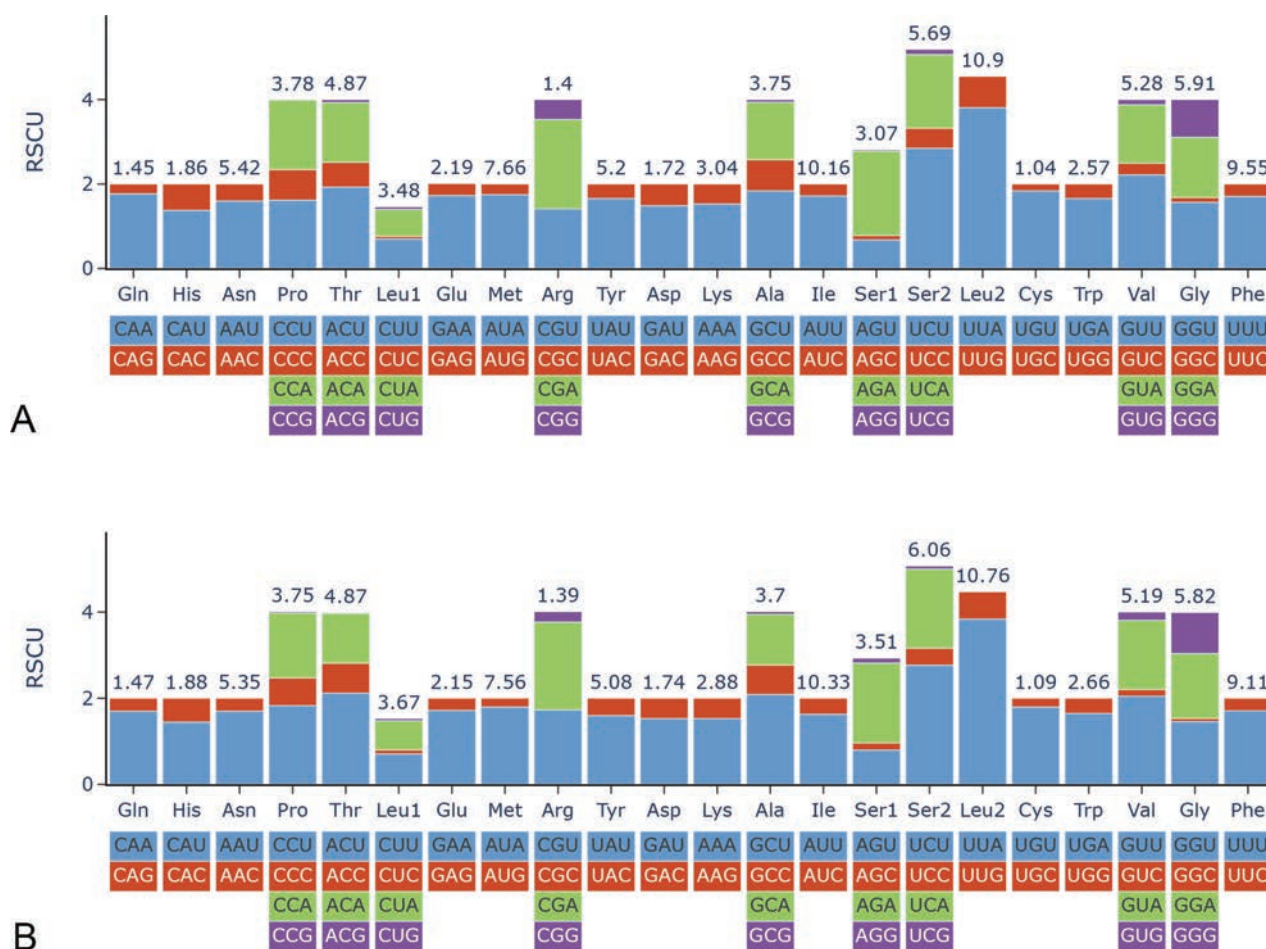


Figure 4. RSCU values of *Oxycarenus* species **A** *O. gossypii* **B** *O. bicolor heraldus*. The ordinate represents the RSCU (the number of times a certain synonymous codon is used/the average number of times that all codons encoding the amino acid are used). The abscissa represents different amino acids. The number above the bar graph represents the ratio of amino acids (number of certain amino acids/total number of all amino acids).

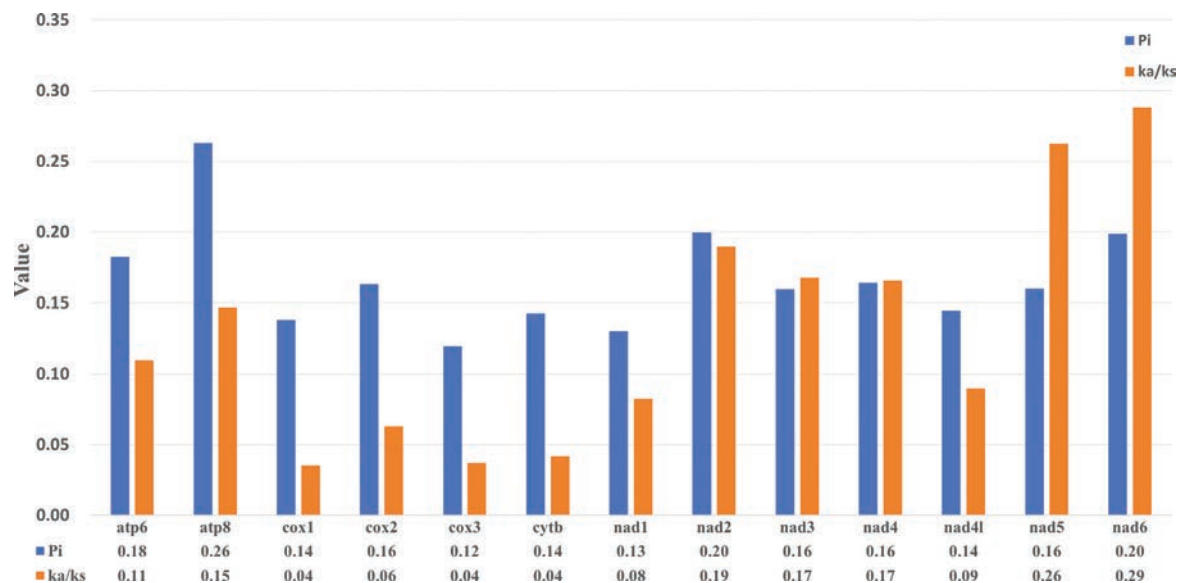


Figure 5. Nucleotide diversity (Pi) and nonsynonymous (Ka)/synonymous (Ks) mutation rate ratios of 13 PCGs of Oxycarenidae species (the Pi and Ka/Ks values of each PCG are shown under the gene name).

RNA

The rRNA genes were positioned between the AT-rich region and *trnL1*, separated by *trnV*. Their total length ranged from 1816 bp to 1840 bp. In both species, the collective length of the 22 tRNA genes was 1433 bp, with individual tRNA genes varying from 61 bp to 71 bp. Notably, eight tRNA genes were encoded on the N-strand, while the remaining 14 genes were encoded on the J-strand, consistent with previous findings (Bernt et al. 2013; Cao et al. 2020).

Most tRNA genes exhibited a typical cloverleaf secondary structure, featuring a T Ψ C arm, an amino acid acceptor arm, an anticodon arm, and a dihydrouridine arm. However, an exception was observed in *trnS1*, where the dihydrouridine arm was absent in *O. gossypii*, forming a loop. Additionally, *trnS1* of *O. bicolor heraldus* displayed an atypical cloverleaf structure, as depicted in Suppl. material 1, a pattern also observed in other species (Zhao et al. 2018).

Phylogenetic analysis

Phylogenetic relationships within Lygaeoidea were elucidated through the reconstruction of mitochondrial 13 PCGs using both BI and ML methods (Figs 6, 7). A total of 45 Lygaeoidea species were selected as the ingroup, with four species from Coreoidea and Pyrrhocoroidea serving as the outgroup. The resulting ML and BI trees exhibited slightly different topologies. Most families were consistently identified as monophyletic, except for Rhyparochromidae, which was paraphyletic. *Dysdercus evanescens* (Pyrrhocoroidea: Pyrrhocoridae) and *Neolethaeus assamensis* (Lygaeoidea: Rhyparochromidae) clustered together in both ML and BI trees (Figs 6, 7). The position of Colobathristidae proved to be unstable in the phylogenetic trees. In one instance, it clustered with Geocoridae with relatively low nodal support (Fig. 6), while another result indicated that Colobathristidae, Ninidae, and Blissidae formed a monophyletic group (Fig. 7). Furthermore, the two sequenced species of Oxycarenidae formed a single clade with a high support value.

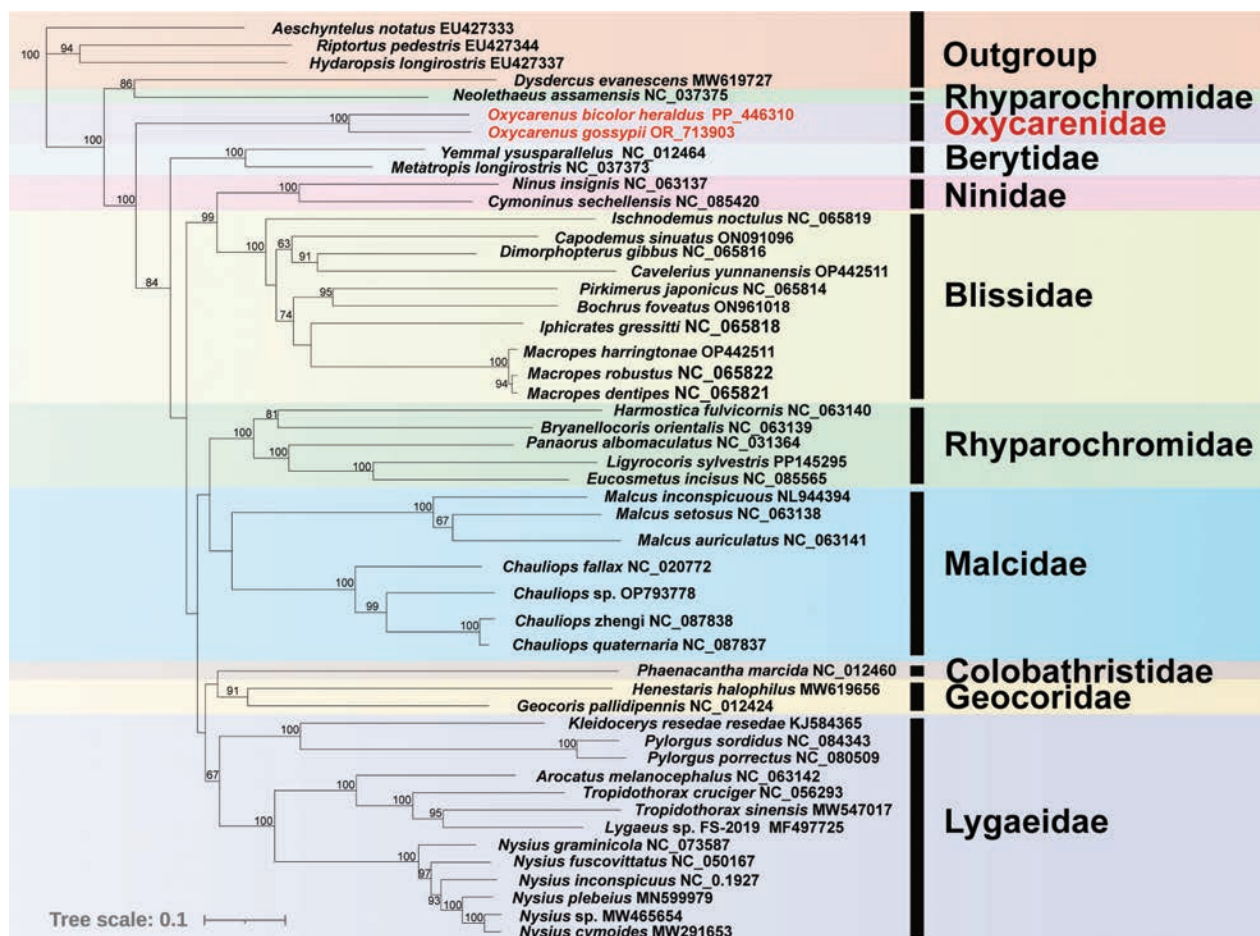


Figure 6. Phylogenetic tree of Lygaeoidea inferred from ML based on 13 PCGs. The numbers on the branches show bootstrap values (values >60% are shown). Two *Oxycarenidae* species in this study are marked in red.

Discussion and conclusion

In this study, we redescribed two *Oxycarenidae* species: *Oxycareus gossypii* and *O. bicolor heraldus*. We also detected misidentifications of two species in China. However, the sheer abundance and morphological similarities amongst oxycarenid species present challenges to providing an accurate morphology alone based classification.

The mitochondrial genomes of *O. gossypii* and *O. bicolor heraldus* were sequenced and analyzed, revealing a shared structural similarity. Both genomes exhibited a typical double-stranded ring structure housing 37 genes, including a non-coding control region. Remarkably, neither genome displayed any gene rearrangement, consistent with known genomic arrangements (Ding et al. 2023). The AT content significantly outweighed the CG content, showing a strong AT bias, a trait observed across various families within Pentatomomorpha (Guo and Yuan 2016). Our analysis of relative synonymous codon usage unveiled a prevalent preference for A/T codons, particularly at the termini of protein-coding genes, a phenomenon observed across all sequenced Pentatomomorpha (Hassanin et al. 2005; Guo and Yuan 2016). This nucleotide composition bias is believed to stem from a combination of mutational pressure and natural selection. The KA/KS analysis identified *cox1* and *cytb* as the most conserved genes, whereas *nad6* exhibited relatively higher evolutionary rates.

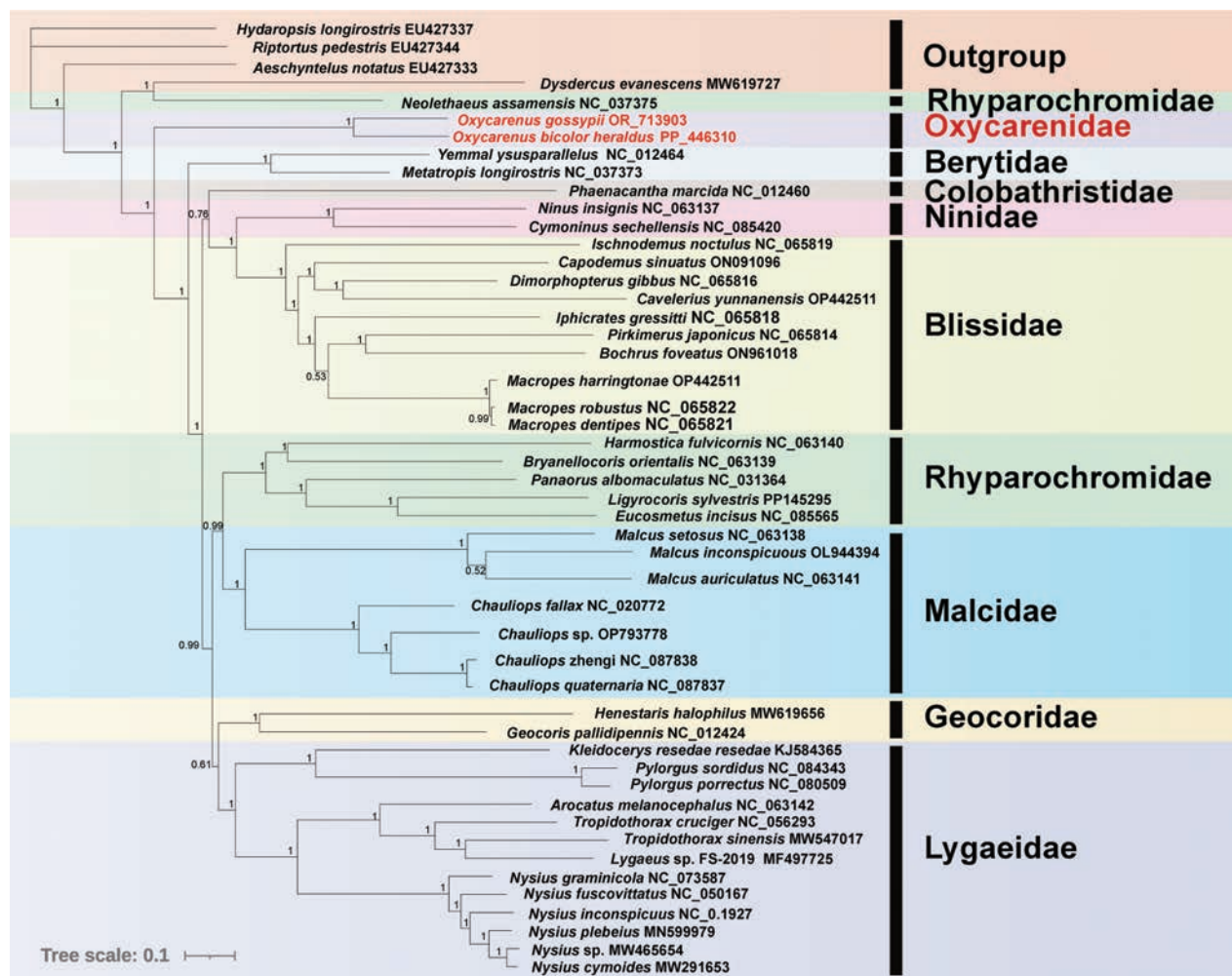


Figure 7. Phylogenetic tree of Lygaeoidea inferred from BI based on 13 PCGs. The numbers on the branches show posterior probabilities (values >0.50 are shown). Two Oxycarenidae species in this study are marked in red.

Most protein-coding genes initiated translation using the start codon ATN, with the exception of *cox1* (TTG). Additionally, three types of stop codons were identified: TAA, TAG, and an incomplete stop codon T. While most tRNA molecules exhibited a typical cloverleaf structure, *trnS1* displayed an atypical cloverleaf structure in both species.

The monophyly of most families within Lygaeoidea was strongly supported, except for Rhyparochromidae, marking a deviation from Henry's findings (1997). *Neolethaeus assamensis* (Lygaeoidea: Rhyparochromidae) clustering with *Dysdercus evanescens* (Pyrrhocoroidea: Pyrrhocoridae) in both ML and BI trees mirrored Gao and Dong's (2023) results. The branches of Ischnorhynchiinae, Lygaeinae, and Orsillinae formed a cohesive group designated as Lygaeidae, aligning with Gao and Dong's findings (Gao and Dong 2023). The sister group relationship between *Henestaris halophilus* and *Geocoris pallidipennis* supported Henry's (1997) earlier assertion. However, the phylogenetic position of Colobathristidae remained unstable in our PCG-based tree, in contrast to Ye et al.'s (2022) findings. Moreover, our results did not support the hypothesis that Colobathristidae and Berytidae formed sister groups, nor did they form the "malcid line" with Malcidae and Cymidae as proposed by Henry (1997). The formation of a monophyletic group by Blissidae and Ninidae,

excluding Berytidae, diverged from the inferred relationship based on 18S rRNA (Xie et al. 2005). However, our examination validated the hypothesis that the two sequenced Oxycarenidae species constituted a single clade, with the position of Oxycarenidae remaining stable in both ML and BI phylogenetic trees. While our findings enrich the structural information of mitochondrial genomes, a comprehensive discussion on the phylogenetic relationships within Lygaeoidea remains challenging. For a deeper understanding of their evolutionary history, it is imperative that more Lygaeoidea species are sequenced in future studies.

Acknowledgements

We extend our sincere gratitude to Professor Előd Kondorosy (Hungarian University of Agriculture and Life Sciences) for his invaluable insights and comments on the manuscript. Special thanks are also due to Shengchang Lai (Nanjing Forestry University) for assisting with data analysis. We appreciate the thoughtful feedback provided by Mallik Malipatil, Pablo Dellapé, Teng Li, which greatly contributed to the refinement of this work.

Additional information

Conflict of interest

The authors have declared that no competing interests exist.

Ethical statement

No ethical statement was reported.

Funding

This research was funded by the National Natural Science Foundation of China (grant no. 31402010), Major Project of Agricultural Biological Breeding (grant no. 2022ZD0401501), and the Highly Educated Talents Foundation in Nanjing Forestry University (grant no. G2014002).

Author contributions

Conceptualization, C.G. and C.M.; methodology, C.G., W.D. C.M.; investigation, C.G., C.M. and S.C.; funding acquisition, C.G.; writing—original draft preparation, C.M.; writing—review and editing, C.G. Both authors have read and agreed to the published version of the manuscript.

Author ORCIDs

Changjun Meng  <https://orcid.org/0009-0000-6968-8761>

Suyan Cao  <https://orcid.org/0009-0008-4432-234X>

Wen Dong  <https://orcid.org/0009-0004-6559-808X>

Cuiqing Gao  <https://orcid.org/0000-0002-0177-5161>

Data availability

All of the data that support the findings of this study are available in the main text or Supplementary Information.

References

- Bankevich A, Nurk S, Antipov D, Gurevich AA, Dvorkin M, Kulikov AS, Lesin VM, Nikolenko SI, Pham S, Prjibelski AD, Pyshkin AV, Sirotkin AV, Vyahhi N, Tesler G, Alekseyev MA, Pevzner PA (2012) SPAdes: a new genome assembly algorithm and its applications to single-cell sequencing. *Journal of Computational Biology* 19(5): 455–477. <https://doi.org/10.1089/cmb.2012.0021>
- Bergroth E (1918) Studies in Philippine Heteroptera, I. *Philippine Journal of Science* 13(2): 75–126.
- Bernt M, Donath A, Jühling F, Externbrink F, Florentz C, Fritzsich G, Pütz J, Middendorf M, Stadler PF (2013) MITOS: improved de novo metazoan mitochondrial genome annotation. *Molecular Phylogenetics and Evolution* 69(2): 313–319. <https://doi.org/10.1016/j.ympev.2012.08.023>
- Boetzer M, Pirovano W (2012) Toward almost closed genomes with GapFiller. *Genome Biology* 13(6): R56. <https://doi.org/10.1186/gb-2012-13-6-r56>
- Boore JL (1999) Animal mitochondrial genomes. *Nucleic acids research* 27(8): 1767–1780. <https://doi.org/10.1093/nar/27.8.1767>
- Cameron SL, Whiting MF (2008) The complete mitochondrial genome of the tobacco hornworm, *Manduca sexta*, (Insecta: Lepidoptera: Sphingidae), and an examination of mitochondrial gene variability within butterflies and moths. *Gene* 408(1–2): 112–123. <https://doi.org/10.1016/j.gene.2007.10.023>
- Cao Y, Wu HT, Li M, Chen WT, Yuan ML (2020) The complete mitochondrial genome of *Nysius fuscovittatus* (Hemiptera: Lygaeidae). *Mitochondrial DNA Part B* 5(3): 3483–3484. <https://doi.org/10.1080/23802359.2020.1827062>
- Chen SF, Zhou YQ, Chen YR, Gu J (2018) Fastp: an ultra-fast all-in-one FASTQ preprocessor. *Bioinformatics* 34(17): 884–890. <https://doi.org/10.1093/bioinformatics/bty560>
- Clary DO, Wolstenholme DR (1985) The mitochondrial DNA molecular of *Drosophila yakuba*: nucleotide sequence, gene organization, and genetic code. *Journal of molecular evolution* 22(3): 252–271. <https://doi.org/10.1007/BF02099755>
- Dellapé PM, Henry TJ (2024) Lygaeoidea Species File. Version 5.0/5.0. <https://lygaeoidea.speciesfile.org/> [accessed on 30 July 2024]
- Ding XF, Chen C, Wei JF, Gao XY, Zhang HF, Zhao Q (2023) Comparative mitogenomics and phylogenetic analyses of the genus *Menida* (Hemiptera, Heteroptera, Pentatomidae). *ZooKeys* 1138: 29–48. <https://doi.org/10.3897/zookeys.1138.95626>
- Distant WL (1904) Fauna of British India, including Ceylon and Burma. Rhynchota. Vol. II. (Heteroptera). Taylor and Francis, London, 503 pp.
- Esaki T (1926) Verzeichniss der Hemiptera-Heteroptera der Insel Formosa. *Annales Historico-Naturales Musei Nationalis Hungarici, Budapest*, 136–189.
- Gao CQ, Dong W (2023) Characterization of two new *Pylorgus* mitogenomes (Hemiptera, Lygaeidae, Ischnorhynchinae) and a mitochondrial phylogeny of Lygaeoidea. *ZooKeys* 1166: 141–154. <https://doi.org/10.3897/zookeys.1166.104103>
- Grant JR, Stothard P (2008) The CGView Server: a comparative genomics tool for circular genomes. *Nucleic Acids Research* 36(2): 181–184. <https://doi.org/10.1093/nar/gkn179>
- Guindon S, Dufayard JF, Lefort V, Anisimova M, Hordijk W, Gascuel O (2010) New algorithms and methods to estimate maximum-likelihood phylogenies: assessing the performance of phyML 3.0. *Systematic Biology* 59(3): 307–321. <https://doi.org/10.1093/sysbio/syq010>

- Guo ZL, Yuan ML (2016) Research progress of mitochondrial genomes of Hemiptera insects. *Scientia Sinica Vitae* 46(2): 151–166. <https://doi.org/10.1360/N052015-00229>
- Hassanin A, Léger N, Deutsch J (2005) Evidence for multiple reversals of asymmetric mutational constraints during the evolution of the mitochondrial genome of Metazoa, and consequences for phylogenetic inferences. *Systematic Biology* 54(2): 277–298. <https://doi.org/10.1080/10635150590947843>
- Henry TJ (1997) Phylogenetic analysis of family groups within the infraorder Pentatomomorpha (Hemiptera: Heteroptera), with emphasis on the Lygaeoidea. *Annals of the Entomological Society of America* 90(3): 275–301. <https://doi.org/10.1093/aesa/90.3.275>
- Henry TJ, Dellapé PM (2009) A new genus and species of Oxycarenidae (Hemiptera, Heteroptera, Lygaeoidea) from Argentina. *ZooKeys* 25: 49–59. <https://doi.org/10.3897/zookeys.25.244>
- Horváth G (1926) Sur les *Oxycarenus* nuisibles aux cotonniers, avec la description d'une espèce nouvelle (Hem. Lygaeidae). *Bulletin de la Société Entomologique de France* 31(11–12): 135–136. <https://doi.org/10.3406/bsef.1926.27678>
- Hua JM, Li M, Dong PZ, Cui Y, Xie Q, Bu WJ (2008) Comparative and phylogenomic studies on the mitochondrial genomes of Pentatomomorpha (Insecta: Hemiptera: Heteroptera). *BMC Genomics* 9: 610. <https://doi.org/10.1186/1471-2164-9-610>
- Katoh K, Standley DM (2013) MAFFT Multiple Sequence Alignment software Vvrsion 7: improvements in performance and usability. *Molecular Biology and Evolution* 30(4): 772–780. <https://doi.org/10.1093/molbev/mst010>
- Kearse M, Moir R, Wilson A, Stones-Havas S, Cheung M, Sturrock S, Buxton S, Cooper A, Markowitz S, Duran C, Thierer T, Ashton B, Meintjes P, Drummond A (2012) Geneious Basic: an integrated and extendable desktop software platform for the organization and analysis of sequence data. *Bioinformatics* 28(12): 1647–1649. <https://doi.org/10.1093/bioinformatics/bts199>
- Kirby WF (1891) Catalogue of the described Hemiptera, Heteroptera and Homoptera of Ceylon, based on the collection formed (chiefly at Pundaloya) by Mr. E. Ernest Green. *Journal of the Linnean Society of London, Zoology* 24: 72–176. <https://doi.org/10.1111/j.1096-3642.1891.tb02479.x>
- Kocher A, Kamilari M, Lhuillier E, Coissac E, Péneau J, Chave J, Murienne J (2014) Shotgun assembly of the assassin bug *Brontostoma colossus* mitochondrial genome (Heteroptera, Reduviidae). *Gene* 552(1): 184–194. <https://doi.org/10.1016/j.gene.2014.09.033>
- Küechler SM, Dettner K, Kehl S (2010) Molecular characterization and localization of the obligate endosymbiotic bacterium in the birch catkin bug *Kleidocerys resedae* (Heteroptera: Lygaeidae, Ischnorhynchinae). *FEMS Microbiology Ecology* 73(2): 408–418. <https://doi.org/10.1111/j.1574-6941.2010.00890.x>
- Kumar S, Stecher G, Li M, Knyaz C, Tamura K (2018) MEGA X: Molecular Evolutionary Genetics Analysis across computing platforms. *Molecular Biology and Evolution* 35(6): 1547–1549. <https://doi.org/10.1093/molbev/msy096>
- Lanfear R, Frandsen PB, Wright AM, Senfeld T, Calcott B (2017) PartitionFinder 2: new methods for selecting partitioned models of evolution for molecular and morphological phylogenetic analyses. *Molecular Biology and Evolution* 34(3): 772–773. <https://doi.org/10.1093/molbev/msw260>
- Li YL, Gu M, Liu XZ, Lin JN, Jiang HE, Song HY, Xiao XC, Zhou W (2023) Sequencing and analysis of the complete mitochondrial genomes of *Toona sinensis* and *Toona*

- ciliata* reveal evolutionary features of Toona. BMC Genomics 24(1): 58. <https://doi.org/10.1186/s12864-023-09150-6>
- Librado P, Rozas J (2009) DnaSP v5: a software for comprehensive analysis of DNA polymorphism data. Bioinformatics 25(11): 1451–1452. <https://doi.org/10.1093/bioinformatics/btp187>
- Lowe TM, Chan PP (2016) tRNAscan-SE On-line: integrating search and context for analysis of transfer RNA genes. Nucleic Acids Research 44(1): 54–57. <https://doi.org/10.1093/nar/gkw413>
- Massouras A, Hens K, Gubelmann C, Uplekar S, Decouttere F, Rougemont J, Cole ST, Deplancke B (2010) Primer-initiated sequence synthesis to detect and assemble structural variants. Nature Methods 7: 485–486. <https://doi.org/10.1038/nmeth.f.308>
- Péricart J (2001) Lygaeidae. In: Aukema B, Rieger C (Eds) Catalogue of the Heteroptera of the Palaearctic Region. The Netherlands Entomological Society, Amsterdam, 115 pp.
- Perna NT, Kocher TD (1995) Unequal base frequencies and the estimation of substitution rates. Molecular Biology and Evolution 12(2): 359–359. <https://doi.org/10.1093/oxfordjournals.molbev.a040211>
- Ronquist F, Teslenko M, van der Mark P, Ayres DL, Darling A, Höhna S, Larget B, Liu L, Suchard MA, Huelsenbeck JP (2012) MrBayes 3.2: efficient Bayesian phylogenetic inference and model choice across a large model space. Systematic Biology 61(3): 539–542. <https://doi.org/10.1093/sysbio/sys029>
- Shao RF, Kirkness EF, Barker SC (2009) The single mitochondrial chromosome typical of animals has evolved into 18 minichromosomes in the human body louse, *Pediculus humanus*. Genome Research 19(5): 904–912. <https://doi.org/10.1101/gr.083188.108>
- Simon S, Hadrys H (2013) A comparative analysis of complete mitochondrial genomes among Hexapoda. Molecular Phylogenetics and Evolution 69(2): 393–403. <https://doi.org/10.1016/j.ympev.2013.03.033>
- Slater JA (1964) A Catalogue of the Lygaeidae of the World: Vols. I–II. University of Connecticut, Storrs, 1668 pp.
- Soria-Carrasco V, Talavera G, Igea J, Castresana J (2007) The K tree score: quantification of differences in the relative branch length and topology of phylogenetic trees. Bioinformatics 23(21): 2954–2956. <https://doi.org/10.1093/bioinformatics/btm466>
- Sureshan SC, Tanavade RV, Ghosh S, Sella RN, Mohideen HS (2021) Complete mitochondrial genome sequencing of *Oxycarenus laetus* (Hemiptera: Lygaeidae) from two geographically distinct regions of India. Scientific Reports 11(1): 23738. <https://doi.org/10.1038/s41598-021-02881-0>
- Sweet MH (2000) Seed and chinch bugs (Lygaeoidea). In: Schaefer CW, Panizzi AR (Eds) Heteroptera of Economic Importance. CRC Press, Boca Raton, 165–286. <https://doi.org/10.1201/9781420041859>
- Weirauch C, Schuh RT (2011) Systematics and evolution of Heteroptera: 25 years of progress. In: Berenbaum MR, Carde RT, Robinson GE (Eds) Annual Review of Entomology 56: 487–510. <https://doi.org/10.1146/annurev-ento-120709-144833>
- Xiang CY, Gao FL, Jakovlić I, Lei HP, Hu Y, Zhang H, Zou H, Wang GT, Zhang D (2023) Using PhyloSuite for molecular phylogeny and tree-based analyses. iMeta 2(1): 1–42. <https://dx.doi.org/https://doi.org/10.1002/imt2.87> <https://doi.org/10.1002/imt2.87>
- Xiao SY, Gao CQ (2022) One newly-recorded genus and species of Oxycarenidae (Hemiptera: Heteroptera) from China. Journal of Nanjing Forestry University [Natural Sciences Edition] 46(3): 165–168. <https://doi.org/10.12302/j.issn.1000-2006.202104039>
- Xie Q, Bu WJ, Zheng LY (2005) The Bayesian phylogenetic analysis of the 18S rRNA sequences from the main lineages of Trichophora (Insecta: Heteroptera: Pentato-

- momorpha). *Molecular Phylogenetics and Evolution* 34(2): 448–451. <https://doi.org/10.1016/j.ympev.2004.10.015>
- Xue HJ, Bu WJ (2008) Morphology of abdominal evaporatoria in larvae of some Lygaeoidea (Insecta: Hemiptera: Heteroptera): function and bearing on classification. *Journal of Natural History* 42(1–2): 35–58. <https://doi.org/10.1080/00222930701825077>
- Ye J, Coulouris G, Zaretskaya I, Cutcutache I, Rozen, S, Madden TL (2012) Primer-BLAST: a tool to design target-specific primers for polymerase chain reaction. *BMC Bioinformatics* 13: 134. <https://doi.org/10.1186/1471-2105-13-134>
- Ye F, Kment P, Rédei D, Luo JY, Wang YH, Küechler SM, Zhang WW, Chen PP, Wu HY, Wu YZ, Sun XY, Ding L, Wang YR, Xie Q (2022) Diversification of the phytophagous lineages of true bugs (Insecta: Hemiptera: Heteroptera) shortly after that of the flowering plants. *Cladistics* 38(4): 403–428. <https://doi.org/10.1111/cla.12501>
- Zhao Q, Wang J, Wang MQ, Cai B, Zhang HF, Wei JF (2018) Complete mitochondrial genome of *Dinorhynchus dybowskyi* (Hemiptera: Pentatomidae: Asopinae) and phylogenetic analysis of Pentatomomorpha species. *Journal of Insect Science* 18(2): 44. <https://doi.org/10.1093/jisesa/iey031>
- Zheng LY, Zou HG (1981) Lygaeidae. In: Hsiao TY, Ren SZ, Zheng LY, Jing XL, Zou HG, Liu SL (Eds) *A Handbook for the Determination of the Chinese Hemiptera-Heteroptera*, Vol.2. Science Press, Beijing, 91–92. [In Chinese, with English summary]

Supplementary material 1

The predicted secondary cloverleaf structure for the *trnS1* of *Oxycarenus bicolor heraldus* and *O. gossypii*

Authors: Changjun Meng, Suyan Cao, Wen Dong, Cuiqing Gao

Data type: docx

Copyright notice: This dataset is made available under the Open Database License (<http://opendatacommons.org/licenses/odbl/1.0/>). The Open Database License (ODbL) is a license agreement intended to allow users to freely share, modify, and use this Dataset while maintaining this same freedom for others, provided that the original source and author(s) are credited.

Link: <https://doi.org/10.3897/zookeys.1211.126013.suppl1>

A checklist of the predators and parasitoids of the fall webworm *Hyphantria cunea* (Drury) (Lepidoptera, Erebidae) from around the world

Liang Ming Cao^{1,2}, Xiao Yi Wang¹, Toby R. Petrice², Therese M. Poland²

¹ Key Laboratory of Forest Protection, State Forestry and Grassland Administration, Ecology and Nature Conservation Institute, Chinese Academy of Forestry, Beijing 100091, China

² Northern Research Station, FS, USDA, 2601 Coolidge Rd, Ste 203, East Lansing, MI 48823, USA

Corresponding author: Liang Ming Cao (caolm1206@126.com)

Abstract

A checklist of 488 fall webworm *Hyphantria cunea* (Drury) natural enemies was compiled based on documentation in previous research across its world distribution, including 289 predators and 199 parasitoids. Predators in the checklist include 67 species from 17 families of Insecta, 1 species of Chilopoda, 183 species from 22 families of Arachnida, 1 species of Reptilia, 4 species from 2 families of Amphibia, 33 species from 18 families of Aves. In addition, the checklist includes fall webworm parasitoids from 18 families of Insecta. Among continents, 128 predators and 76 parasitoids were distributed in North America, 78 predators and 62 parasitoids in Asia, and 88 predators and 68 parasitoids in Europe.

Key words: China, distribution, Europe, floral differences, Natural enemy, North America



Academic editor: Reza Zahiri

Received: 2 April 2024

Accepted: 17 June 2024

Published: 9 September 2024

ZooBank: <https://zoobank.org/EF9D7289-4C8B-45BE-8BC0-2446BE33D538>

Citation: Cao LM, Wang XY, Petrice TR, Poland TM (2024) A checklist of the predators and parasitoids of the fall webworm *Hyphantria cunea* (Drury) (Lepidoptera, Erebidae) from around the world. ZooKeys 1211: 251–348. <https://doi.org/10.3897/zookeys.1211.123574>

Copyright: This is an open access article distributed under the terms of the CC0 Public Domain Dedication.

Table of contents

Introduction	254
Materials and methods.....	255
Checklist.....	256
Part I Predators.....	256
Insecta	256
Mantodea.....	256
Mantidae 螳螂科.....	256
Orthoptera	256
Tettigoniidae 螽斯科.....	256
Dermaptera.....	257
Forficulidae 球螋科.....	257
Hemiptera	257
Pentatomidae 蝽科.....	257
Anthocoridae 花蝽科.....	258
Nabidae 姬蝽科.....	258
Reduviidae 猎蝽科.....	258
Miridae 盲蝽科.....	260
Neuroptera.....	261
Chrysopidae 草蛉科.....	261
Panorpidae 蝎蛉科.....	262
Coleoptera	262
Cantharidae 花萤科.....	262
Carabidae 步甲科.....	262
Coccinellidae 瓢虫科.....	264
Silphidae 葬甲科.....	265
Staphylinidae 隐翅虫科.....	265
Hymenoptera.....	265
Formicidae 蚁科.....	265
Vespidae 胡蜂科.....	266
Chilopoda.....	267
Scutigermorpha	267
Scutigeridae 蚰蜒科.....	267
Arachnida.....	268
Araneae.....	268
Agelenidae 漏斗蛛科.....	268
Anyphaenidae 近管蛛科.....	268
Araneidae 圆蛛科.....	269
Cheiracanthiidae 红螯蛛科.....	274
Clubionidae 管巢蛛科.....	275
Dictynidae 叶蛛科.....	277
Gnaphosidae 平腹蛛科.....	278
Linyphiidae 皿蛛科.....	278
Lycosidae 狼蛛科.....	279
Mimetidae 拟态蛛科.....	280
Nephilidae 芥蛛科.....	280
Oecobiidae 壁钱科.....	280
Philodromidae 逍遥蛛科.....	281

Pisauridae 盜蛛科	283
Salticidae 跳蛛科	283
Tetragnathidae 长脚蛛科	290
Theridiidae 球腹蛛科	290
Thomisidae 蟹蛛科	292
Titanoecidae 隐石蛛科	296
Trachelidae 管蛛科	296
Uloboridae 妩蛛科	296
Trombidiformes	297
Trombidiidae 絨蟎科	297
Reptilia	297
Squamata	297
Gekkonidae 壁虎科	297
Amphibia	297
Anura	297
Bufonidae 蟾蜍科	297
Ranidae 蛙科	298
Aves	298
Bucerotiformes	298
Upupidae 戴胜科	298
Ciconiiformes	298
Ciconiidae 鸛科	298
Columbiformes	298
Columbidae 鳩鴿科	298
Cuculiformes	299
Cuculidae 杜鵑科	299
Falconiformes	299
Falconidae 隼科	299
Galliformes	299
Phasianidae 雉科	299
Passeriformes	299
Corvidae 鴉科	299
Laniidae 伯勞科	300
Muscicapidae 鶇科	300
Oriolidae 黃鶇科	301
Paridae 山雀科	301
Passeridae 雀科	302
Sturnidae 椋鳥科	302
Sylviidae 鶯科	302
Turdidae 鶇科	303
Vireonidae 綠鶇科	303
Piciformes	303
Picidae 啄木鳥科	303
Strigiformes	304
Strigidae 鴞鴞科	304
Part II Parasitoids	304
Hymenoptera	304
Ichneumonidae 姬蜂科	304
Braconidae 茧蜂科	312

Trigonalidae 钩腹蜂科	315
Chalcididae 小蜂科	316
Encyrtidae 跳小蜂科	317
Eulophidae 姬小蜂科	317
Eupelmidae 旋小蜂科	321
Eurytomidae 广肩小蜂科	322
Perilampidae 巨胸小蜂科	322
Pteromalidae 金小蜂科	322
Torymidae 长尾小蜂科	326
Trichogrammatidae 赤眼蜂科	326
Scelionidae 缘腹细蜂科	327
Diptera	328
Tachinidae 寄蝇科	328
Odiniidae 树创蝇科	338
Sarcophagidae 麻蝇科	338
Muscidae 蝇科	338
Phoridae 蚤蝇科	338
Discussion	339
Acknowledgments	339
References	340

Introduction

The fall webworm, *Hyphantria cunea* (Drury, 1773) (Lepidoptera: Erebidae), is native to North America, where it is considered to be a secondary pest (Tothill 1922). However, *H. cunea* has become a primary pest in some regions that it has invaded over the past 80 years (Edosa et al. 2019). During the 1940s, *H. cunea* invaded Hungary and Japan, and later spread to most European countries, all of East Asia, and parts of central Asia (Trajković and Žikić 2023). In 1979, *H. cunea* first invaded China where it has become a serious pest and its distribution has expanded annually (Ning et al. 2021).

Although *H. cunea* does not kill host trees in China, it causes aesthetic damage and is a nuisance pest, invading buildings, vehicles, and other structures during outbreaks (Ning et al. 2021). Also, cultural preferences in China do not tolerate the appearance of massive caterpillar nests in trees, which are much larger than those typically found in North America. It is unclear why *H. cunea* population levels are much higher in China compared to its native range; however, an important contributing factor may be a lack of natural enemies that have co-evolved with the pest in China. Therefore, it is necessary to compare the composition of *H. cunea* natural enemies in its native North American range to its invaded ranges in Europe and East Asia.

The research history on natural enemies of *H. cunea* can be divided into three stages: (1) prior to 1940 when *H. cunea* was only found in North America (Riley 1887a, b); (2) from 1940 to 1980, when *H. cunea* invaded Eastern Europe, Japan, and Korea, and natural enemy surveys were conducted in Europe, East Asia, and North America (Hasegawa and Itô 1967; Kayashima 1967; Warren and Tadić 1967; Tamura 1969; Kunimi 1983); and (3) from 1980 to present, after *H. cunea* invaded China and extensive surveys of natural enemies were conducted. During this most recent stage, numerous

Chinese parasitoids and predators that attack *H. cunea* were documented (Yang et al. 2008, 2015a, b; Li 2011). More recently, surveys of natural enemies have also been conducted in some central Asian countries, such as Turkey and Iran (Sullivan et al. 2010, 2011, 2012; Karami et al. 2023). Our objective was to compile a global checklist of known natural enemies of *H. cunea*, assemble as much information as possible about these natural enemies, and ultimately build a database for selecting candidates for use in biological control of *H. cunea*. We reviewed the available *H. cunea* natural enemy literature across all time periods and assembled a summary of this information in a species checklist.

Materials and methods

Natural enemy literature review

Our summary of *H. cunea* natural enemies is based on extensive literature searches through December 2023. A systematic literature search of CNKI (<https://www.cnki.net/index/>), Google Scholar (<https://scholar.google.com/>), Google (<https://www.google.com>), and Biodiversity Heritage Library (<https://www.biodiversitylibrary.org/>) was performed with key words, including “fall webworm”, “*Hyphantria cunea*”, “natural enemy”, “parasitoid”, “predator”. We included all literature related to predators and parasitoids of the fall webworm but did not include publications about pathogenic microorganisms of *H. cunea*. Overall, we reviewed 99 publications that reported information about natural enemies of *H. cunea*, from North America, Asia, and Europe.

Natural enemy species information collected

For each publication, we gathered relevant information about the natural enemy species reported. We compiled information into a checklist of predator and parasitoid groups, organized by Latin family name. We also included the Chinese family name. Family names were validated by checking ITIS (Integrated Taxonomic Information System; ITIS 2023). Some species names reported in the earlier literature differed from current valid names. When this occurred, we transcribed the synonym after the citation (e.g., “Oliver 1963 as *Matis carolina*”). For each species in this checklist, we summarized the following information: 1) distribution, 2) recorded interactions of predator or prey with *H. cunea*, 3) prey or host stage attacked, 4) parasitoid type, and 5) notes.

Distribution. The known geographic distribution of a given species, based on the most recent published literature or catalogue website. The level of detail about species distributions varied among publications, with some papers reporting country names (e.g., China, USA), geographical divisions or continents (e.g., North America, Asia), or zoogeographic divisions (e.g., Palearctic, Nearctic).

Recorded interactions of predator or parasitoid with *H. cunea*. The geographic distribution where each predator and parasitoid species was reported preying upon or parasitizing *H. cunea*. This information is very important for analyzing the geographical fauna of predators and parasitoids of the fall webworm

and demonstrates the species biodiversity of natural enemies among the three major regions (North America, Europe, and East Asia).

Prey stage. The *H. cunea* developmental stage preyed upon (i.e., egg, larva, pupa, or adult).

Host stage. The developmental stage of *H. cunea* that is parasitized (i.e., egg, larva, or pupa).

Parasitoid type. Parasitoids were categorized based on location of host-feeding (ectoparasitoids or endoparasitoids); brood production (solitary or gregarious); whether they parasitize hosts directly or indirectly (primary or hyperparasitoids); host specificity (monophagous, oligophagous, or polyphagous); and their impact on their host (idiobiont parasitoids that paralyze their host and koinobiont parasitoids that do not).

Notes. Biological characters of each predator or parasitoid species including any additional information or clarification about the natural enemy species.

Checklist

Part I Predators

Insecta

Mantodea

Mantidae 螳螂科

Stagmomantis carolina (Johanson, 1763)

Distribution. Trinidad, Venezuela, Guatemala, Belize, Costa Rica, Mexico, Panama, USA (Soodnarinesingh 2015).

Recorded interactions with *H. cunea*. USA [Louisiana (Oliver 1963 as *Matis carolina*)].

Prey stage. Larva (Oliver 1963).

Notes. Nymphs feed on small larva and adults feed on large larva (Oliver 1963).

Tenodera sinensis (Saussure, 1871)

Distribution. China, Japan, Micronesia, Thailand, North America, Canada (Patel and Singh 2016).

Recorded interactions with *H. cunea*. China [Beijing (Tao et al. 2008 as *Paratenodera aridifolia*)].

Orthoptera

Tettigoniidae 螞蟥科

Tettigonia viridissima (Linnaeus, 1758)

Distribution. Europe and North Africa.

Recorded interactions with *H. cunea*. Europe (Warren and Tadić 1967).

Prey stage. Larva (Warren and Tadić 1967).

Dermaptera

Forficulidae 球蝮科

***Forficula auricularia* Linnaeus, 1758**

Distribution. Europe, western Asia, North Africa, North America (Crumb et al. 1941).

Recorded interactions with *H. cunea*. Europe (Warren and Tadić 1967).

Prey stage. Egg (Warren and Tadić 1967).

Hemiptera

Pentatomidae 蝽科

***Apoecilus bracteatus* (Fitch, 1865)**

Distribution. Canada, USA (Rider and Swanson 2021).

Recorded interactions with *H. cunea*. Canada [New Brunswick, Nova Scotia (Morris 1972)].

Prey stage. Larva (Morris 1972).

***Arma custos* (Fabricius, 1794)**

Distribution. Europe, Asia (Zhao et al. 2018).

Recorded interactions with *H. cunea*. Europe (Warren and Tadić 1967), Italy (Boriani 1991). China [Shanghe County, Jinan City, Shandong Province (Wang et al. 2012 as *A. chinensis*)].

Prey stage. Egg (Boriani 1991), larva (Warren and Tadić 1967).

Notes. Found in 2.33–17.86% of *H. cunea* webs at surveyed sites in Liaoning Province (Wang et al. 2012).

***Euschistus servus* (Say, 1832)**

Distribution. Canada, USA, Mexico (EPPO 2015).

Recorded interactions with *H. cunea*. USA (Riley 1887b).

Prey stage. Larva (Warren and Tadić 1967).

***Picromerus bidens* (Linnaeus, 1758)**

Distribution. Europe, Asia (Rider 2006), North America: Canada, USA (Chordas 2015).

Recorded interactions with *H. cunea*. Europe (Warren and Tadić 1967).

Prey stage. Larva (Warren and Tadić 1967).

***Pinthaeus sanguinipes* (Fabricius, 1781)**

Distribution. Europe, Asia (Zhao et al. 2013).

Recorded interactions with *H. cunea*. Europe (Warren and Tadić 1967).

Prey stage. Larva (Warren and Tadić 1967).

***Podisus maculiventris* (Say, 1832)**

Distribution. Mexico, Bahamas, USA, Canada (De Clercq 2008).

Recorded interactions with *H. cunea*. USA [Arkansas (Tadić 1963)], Warren and Tadić (1967) also listed as *P. modestus*, a synonym of *P. maculiventris* (Phillips 1983)].

Prey stage. Larva (Warren and Tadić 1967).

***Podisus placidus* Uhler, 1870**

Distribution. USA, Canada (Phillips 1983).

Recorded interactions with *H. cunea*. USA [Arkansas (Tadić 1963)].

Prey stage. Larva (Warren and Tadić 1967).

***Podisus serieiventris* Uhler, 1871**

Distribution. USA, Canada (Phillips 1983).

Recorded interactions with *H. cunea*. USA (Warren and Tadić 1967).

Prey stage. Larva (Warren and Tadić 1967).

Anthocoridae 花蝽科

***Orius majusculus* (Reuter, 1879)**

Distribution. Europe, Canada (Henry 2008).

Recorded interactions with *H. cunea*. Europe (Warren and Tadić 1967).

Prey stage. Egg (Warren and Tadić 1967).

Nabidae 姬蝽科

***Himacerus apterus* (Fabricius, 1798)**

Distribution. China, Europe, Canada [Nova Scotia (Lartvière 1992)].

Recorded interactions with *H. cunea*. Europe (Warren and Tadić 1967 as *Nabis apterus*), China [Dandong City, Liaoning Province (Shu and Yu 1985)].

Prey stage. Egg (Shu and Yu 1985), larva (Warren and Tadić 1967; Shu and Yu 1985).

Notes. Both nymph and adult consume *H. cunea* larvae (Shu and Yu 1985).

Reduviidae 猎蝽科

***Agriosphodrus dohrni* (Signoret, 1862)**

Distribution. China, Japan, India, Vietnam.

Recorded interactions with *H. cunea*. China [Beijing, laboratory feeding and testing in 2019].

Prey stage. Larva.

Notes. Both nymph and adult consume *H. cunea* larvae in the laboratory; mature nymphs can consume 4–7 larvae per day, adults can consume 4–11 larvae per day (unpublished data, LMC).

***Arilus cristatus* (Linnaeus, 1763)**

Distribution. Canada, USA, Mexico, Guatemala (Blatchley 1926).

Recorded interactions with *H. cunea*. USA [Arkansas (Tadić 1963), Louisiana (Oliver 1963, 1964)].

Prey stage. Larva (Tadić 1963).

Notes. Both nymph and adult consume larvae of *H. cunea* (Tadić 1963; Oliver 1963), attacks second through seventh larval instars (Oliver 1964).

***Pselliopus cinctus* (Fabricius, 1776)**

Distribution. Canada, USA.

Recorded interactions with *H. cunea*. USA [Arkansas (Tadić 1963), Louisiana (Oliver 1964)].

Prey stage. Larva (Oliver 1964).

Notes. Attacks second through fifth larval instars (Oliver 1964).

***Rhynocoris iracundus* (Poda, 1761)**

Distribution. Europe, West and Middle Asia (Putshkov and Putshkov 1996).

Recorded interactions with *H. cunea*. Europe (Warren and Tadić 1967 as *Harpactor iracundus*)

Prey stage. Larva (Warren and Tadić 1967).

***Sinea spinipes* (Herrich-Schäffer, 1846)**

Distribution. USA (from New York south to Florida and west to South Dakota, Colorado, and Texas), Mexico (Froeschner 1988).

Recorded interactions with *H. cunea*. USA [Arkansas (Tadić 1963), Louisiana (Oliver 1964)].

Prey stage. Larva (Oliver 1964).

Notes. Attacks first through fourth larval instars (Oliver 1964).

***Stenopoda cinerea* Laporte, 1833**

Distribution. Canada, USA, Mexico (Froeschner 1988), Argentina (Diez and Co-scarón 2014).

Recorded interactions with *H. cunea*. USA [Arkansas (Tadić 1963)].

Prey stage. Larva (Tadić 1963).

***Yolinus albopustulatus* China, 1940**

Distribution. China, Japan, Vietnam (Lam et al. 2015).

Recorded interactions with *H. cunea*. China [Beijing, laboratory feeding and testing in 2019].

Prey stage. Larva.

Notes. Attacks *H. cunea* in the laboratory, one adult can consume 8–13 larvae per day (unpublished data, LMC).

***Zelus longipes* (Linnaeus, 1767)**

Distribution. Southern parts of USA, Mexico, Central America, the Caribbean, northern South America, Paraguay, and southern Brazil (Zhang et al. 2016).

Recorded interactions with *H. cunea*. USA [Melville (Oliver 1963 as *Z. bilobus*)].

Prey stage. Larva (Oliver 1963).

Notes. Attacks fourth through sixth larval instars (Oliver 1964).

***Zelus cervicalis* Stål, 1872**

Distribution. Belize, Colombia, Costa Rica, El Salvador, Guatemala, Honduras, Mexico, USA (Zhang et al. 2016).

Recorded interactions with *H. cunea*. USA [Lacombe (Oliver 1963)].

Prey stage. Larva (Oliver 1963).

Notes. Attacks fourth through sixth larval instars (Oliver 1964).

***Zelus luridus* Stål, 1862**

Distribution. Canada, Mexico, and USA (Zhang et al. 2016).

Recorded interactions with *H. cunea*. USA [Arkansas (Tadić 1963 as *Z. exsanguis*)].

Prey stage. Larva (Tadić 1963 as *Z. exsanguis*).

Notes. Almost all specimens collected from the US were misidentified as *Z. exsanguis* (Zhang et al. 2016).

***Zelus tetracanthus* Stål, 1862**

Distribution. Brazil, Costa Rica, Curaçao, Honduras, Mexico, Panama, Paraguay, USA and Venezuela (Zhang et al. 2016).

Recorded interactions with *H. cunea*. USA [Arkansas (Tadić 1963 as *Z. socius*)].

Prey stage. Larva (Tadić 1963 as *Z. exsanguis*).

Miridae 盲蝽科

***Deraeocoris ruber* (Linnaeus, 1758)**

Distribution. Britain, Corsica, Denmark, France, Germany, Italy, Macedonia, Moravia, Spain, Sweden, USA, Canada (Schuh 2016).

Recorded interactions with *H. cunea*. Europe (Warren and Tadić 1967).

Prey stage. Egg (Warren and Tadić 1967).

Neuroptera

Chrysopidae 草蛉科

***Chrysopa carnea* Stephens, 1836**

Distribution. Palaearctic, Afrotropical, Oriental (Oswald 2007).

Recorded interactions with *H. cunea*. Italy (Boriani 1991), Turkey [Düzce (Avci et al. 2022)].

Prey stage. Egg (Boriani 1991).

***Chrysopa formosa* Brauer, 1851**

Distribution. Palaearctic, widespread (Oswald 2007).

Recorded interactions with *H. cunea*. China [Dandong city, Liaoning province (Shu and Yu 1985)].

Prey stage. Egg and larva (Shu and Yu 1985).

***Chrysopa oculata* Say, 1839**

Distribution. Canada, USA, Mexico (Oswald 2007).

Recorded interactions with *H. cunea*. North America (Warren and Tadić 1967).

Prey stage. Egg and larva (Warren and Tadić 1967).

***Chrysopa perla* (Linnaeus, 1758)**

Distribution. Palaearctic, widespread (Oswald 2007).

Recorded interactions with *H. cunea*. Europe (Warren and Tadić 1967).

Prey stage. Egg and larva (Warren and Tadić 1967).

***Chrysopa quadripunctata* Burmeister, 1839**

Distribution. Southern Canada, eastern USA, Mexico (Oswald 2007).

Recorded interactions with *H. cunea*. USA [Arkansas (Tadić 1963)].

Prey stage. Egg and larva (Warren and Tadić 1967).

***Chrysopa pallens* (Rambur, 1838)**

Distribution. Palaearctic, widespread (Oswald 2007).

Recorded interactions with *H. cunea*. China [Dandong City, Liaoning Province (Shu and Yu 1985 as *C. septempunctata*), Liaocheng City, Shandong Province (Yue et al. 2016 as *C. septempunctata*)].

Prey stage. Egg (Shu and Yu 1985), larva (Yue et al. 2016).

***Chrysopa nipponensis* (Okamoto, 1914)**

Distribution. China, Japan, Korea, Mongolia, Philippines, eastern Russia (Oswald 2007).

Recorded interactions with *H. cunea*. China [Liaocheng City, Shandong Province (Yue et al. 2016 as *C. sinica*)].

Prey stage. Larva (Yue et al. 2016).

***Chrysopa carnea* (Stephens, 1836)**

Distribution. Palaearctic (widespread), Afrotropical (Cape Verde, Oman, United Arab Emirates, Yemen), Oriental (China, India, Nepal) (Oswald 2007).

Recorded interactions with *H. cunea*. Europe (Warren and Tadić 1967 as *C. vulgaris*).

Prey stage. Egg and larva (Warren and Tadić 1967).

Panorpidae 蝟蛉科

***Panorpa communis* Linnaeus, 1758**

Distribution. Asia, Europe (Penny and Byers 1979).

Recorded interactions with *H. cunea*. Europe (Warren and Tadić 1967).

Prey stage. Egg (Warren and Tadić 1967).

Coleoptera

Cantharidae 花萤科

***Cantharis fusca* Linnaeus, 1758**

Distribution. Western and central Europe (Kazantsev 2011).

Recorded interactions with *H. cunea*. Europe (Warren and Tadić 1967).

Prey stage. Larva (Warren and Tadić 1967).

***Cantharis rufa* (Linnaeus, 1758)**

Distribution. Europe, Canada (Pelletier and Hébert 2014).

Recorded interactions with *H. cunea*. Europe (Warren and Tadić 1967).

Prey stage. Larva (Warren and Tadić 1967).

Carabidae 步甲科

***Calosoma inquisitor* (Linnaeus, 1758)**

Distribution. Europe and part of the Mediterranean (Bruschi 2010).

Recorded interactions with *H. cunea*. Europe (Warren and Tadić 1967).

Prey stage. Egg (Warren and Tadić 1967).

***Calosoma scrutator* (Fabricius, 1775)**

Distribution. Canada, El Salvador, Guatemala, Honduras, Mexico, Nicaragua, Puerto Rico, USA, Venezuela (Bruschi 2010).

Recorded interactions with *H. cunea*. North America (Warren and Tadić 1967).

Prey stage. Larva and adult (Warren and Tadić 1967).

***Calosoma sycophanta* (Linnaeus, 1758)**

Distribution. Northern Africa and throughout Europe (Bruschi 2010).

Recorded interactions with *H. cunea*. Europe (Warren and Tadić 1967).

Prey stage. Egg and larva (Warren and Tadić 1967).

***Carabus hortensis* Linnaeus, 1758**

Distribution. Europe (Turin et al. 2003).

Recorded interactions with *H. cunea*. Europe (Warren and Tadić 1967).

Prey stage. Larva (Warren and Tadić 1967).

***Chlaenius pallipes* (Gebler, 1823)**

Distribution. China, North Korea, South Korea, Japan, Russia, Mongolia (Lorenz 2021).

Recorded interactions with *H. cunea*. China [Dandong City, Liaoning Province (Shu and Yu 1985)].

Prey stage. Pupa (Shu and Yu 1985).

***Nebria livida* (Linnaeus, 1758)**

Distribution. China, Japan, Russia, Europe (Liang and Yu 2000).

Recorded interactions with *H. cunea*. China [Liaocheng City, Shandong Province (Yue et al. 2016)].

Prey stage. Larva (Yue et al. 2016).

***Parena cavipennis* (Bates, 1873)**

Distribution. China, Japan, North Korea, South Korea, Vietnam, Nepal(?) (Shi and Liang 2023).

Recorded interactions with *H. cunea*. China [Rongcheng City, Shandong Province (Wang et al. 1999)].

Prey stage. Larva (Wang et al. 1999).

Notes. Both adults and larvae prey on *H. cunea* larvae. Adults prey at night on all instars; *P. cavipennis* larvae prey on caterpillars in webs (Wang et al. 1999).

***Parena laesipennis* (Bates, 1873)**

Distribution. China, Japan, South Korea, Vietnam, Laos, Thailand, Myanmar, Malaysia, India, Nepal (Shi and Liang 2023).

Recorded interactions with *H. cunea*. China [Dalian City, Liaoning Province (Yang et al. 2008)].

Prey stage. Larva (Yang et al. 2008).

Notes. Both adults and larvae prey on *H. cunea* and live inside the host web; consume 110–265 larvae per web; consume all larvae in 3.2% of webs in the Dalian area (Yang et al. 2008).

***Parena latecincta* (Bates, 1873)**

Distribution. Japan, South Korea, Russia, China, Vietnam, Laos, Thailand, India, Nepal, the Philippines (Shi and Liang 2023).

Recorded interactions with *H. cunea*. China [Dalian City, Liaoning Province (Yang et al. 2008)].

Prey stage. Larva (Yang et al. 2008).

Notes. Similar biology to *P. laesipennis* (Yang et al. 2008).

***Plochionus timidus* Haldeman, 1843**

Distribution. Canada, Mexico, USA (Bousquet 2012).

Recorded interactions with *H. cunea*. USA [Arkansas (Tadić 1963)].

Prey stage. Larva (Tadić 1963).

Notes. Both adult and larva prey on *H. Cunea* larvae. Adult tears larva into pieces and then consumes each piece except for the head capsule (Tadić 1963).

Coccinellidae 瓢虫科

***Coccinella septempunctata* Linnaeus, 1758**

Distribution. Native to temperate Europe, North Africa, and Asia, established in North America and South America [Brazil, Chile] (Beverley 2022).

Recorded interactions with *H. cunea*. China [Dandong City, Liaoning Province (Shu and Yu 1985), Liaocheng City, Shandong Province (Yue et al. 2016)].

Prey stage. Egg (Yue et al. 2016).

Notes. Larva of *C. septempunctata* prey on eggs (Yue et al. 2016).

***Harmonia axyridis* (Pallas, 1773)**

Distribution. Native to central and eastern Asia, introduced to Europe, North America, South America, the Middle East, South Africa, and Australia (Roy 2022).

Recorded interactions with *H. cunea*. China [Beijing (unpublished data, LMC), Liaocheng City, Shandong Province (Yue et al. 2016)].

Prey stage. Egg (Yue et al. 2016).

Notes. Larva of *H. axyridis* prey on eggs (Yue et al. 2016).

***Propylea quatuordecimpunctata* (Linnaeus, 1758)**

Distribution. Europe, North Africa, the Russian Far East, Asia, North America (Nikitsky and Ukrainsky 2016).

Recorded interactions with *H. cunea*. Europe (Warren and Tadić 1967).

Prey stage. Larva (Warren and Tadić 1967).

Silphidae 葬甲科

***Dendroxena quadrimaculata* (Scopoli, 1771)**

Distribution. Central and Southern Europe, Turkey, Iran and Kazakhstan, Northern Africa, Northern America (Stolbov and Sergeeva 2020).

Recorded interactions with *H. cunea*. Europe (Warren and Tadić 1967 as *Xylodrepa punctata*).

Prey stage. Egg and larva (Warren and Tadić 1967).

***Silpha carinata* Herbst, 1783**

Distribution. From Europe to Transbaikalia and Central Asia, including Mongolia and westernmost China (Nishikawa et al. 2010).

Recorded interactions with *H. cunea*. Europe (Warren and Tadić 1967).

Prey stage. Egg and larva (Warren and Tadić 1967).

Staphylinidae 隐翅虫科

***Quedius ochripennis* (Ménétriés, 1832)**

Distribution. West Palaearctic, Mediterranean, North Africa, Oriental (Salnitska and Solodovnikov 2019).

Recorded interactions with *H. cunea*. Europe (Warren and Tadić 1967).

Prey stage. Egg and larva (Warren and Tadić 1967).

Hymenoptera

Formicidae 蚁科

***Formica rufa* Linnaeus, 1761**

Distribution. Nearctic, Palaearctic (AntWeb, 2023).

Recorded interactions with *H. cunea*. Europe (Warren and Tadić 1967).

Prey stage. Larva (Warren and Tadić 1967).

***Linepithema humile* (Mayr, 1868)**

Distribution. Afrotropical, Australasia, Indomalaya, Nearctic, Neotropical, Oceania, Palaearctic (AntWeb 2023).

Recorded interactions with *H. cunea*. Europe (Warren and Tadić 1967 as *Iridomyrmex humilis*).

Prey stage. Larva (Warren and Tadić 1967).

***Solenopsis saevissima* (Smith, 1855)**

Distribution. Afrotropical, Neotropical (AntWeb 2023).

Recorded interactions with *H. cunea*. Europe (Warren and Tadić 1967).

Prey stage. Larva (Warren and Tadić 1967).

Vespidae 胡蜂科

***Dolichovespula arenaria* (Fabricius, 1775)**

Distribution. Abundant throughout boreal North America (Kimsey and Carpenter 2012).

Recorded interactions with *H. cunea*. Canada [New Brunswick (Morris 1972 as *Vespula arenaria*)].

Prey stage. Larva (Morris 1972).

***Dolichovespula maculate* (Linnaeus, 1763)**

Distribution. North America (Kimsey and Carpenter 2012).

Recorded interactions with *H. cunea*. Canada [New Brunswick (Morris 1972 as *Vespula maculata*)].

Prey stage. Larva (Morris 1972).

***Dolichovespula norvegicoides* (Sladen, 1918)**

Distribution. Widely throughout northern North America and further south along mountain ranges (Kimsey and Carpenter 2012).

Recorded interactions with *H. cunea*. Canada [New Brunswick (Morris 1972 as *Vespula norvegicoides*)].

Prey stage. Larva (Morris 1972).

***Polistes annularis* (Linnaeus, 1763)**

Distribution. USA (Carpenter 1996).

Recorded interactions with *H. cunea*. North America (Warren and Tadić 1967).

Prey stage. Larva and adult (Warren and Tadić 1967).

***Polistes dominulus* (Christ, 1791)**

Distribution. Central and southern Europe, Turkey, northern Africa, Israel, Syria, Afghanistan, Russia, Iran, Uzbekistan, Turkmenistan, Pakistan, India, Mongolia, China; introduced to Australia, Chile, USA (Carpenter 1996).

Recorded interactions with *H. cunea*. Europe (Warren and Tadić 1967 as *P. dominula*).

Prey stage. Larva (Warren and Tadić 1967).

***Polistes arizonensis* Snelling, 1954**

Distribution. USA (Carpenter 1996).

Recorded interactions with *H. cunea*. North America (Warren and Tadić 1967 as *P. exclamans*).

Prey stage. Larva and adult (Warren and Tadić 1967).

***Polistes aurifer* Saussure, 1853**

Distribution. Canada, Mexico, USA (Carpenter 1996).

Recorded interactions with *H. cunea*. North America (Warren and Tadić 1967 as *P. fuscatus*).

Prey stage. Larva and adult (Warren and Tadić 1967).

***Polistes metricus* Say, 1831**

Distribution. USA (Carpenter 1996).

Recorded interactions with *H. cunea*. North America (Warren and Tadić 1967).

Prey stage. Larva and adult (Warren and Tadić 1967).

***Polistes fuscatus* (Fabricius, 1793)**

Distribution. Canada, USA (Carpenter 1996).

Recorded interactions with *H. cunea*. North America (Warren and Tadić 1967 as *P. pallipes*).

Prey stage. Larva (Warren and Tadić 1967).

***Vespula alascensis* (Packard, 1870)**

Distribution. North America (Kimsey and Carpenter 2012).

Recorded interactions with *H. cunea*. Canada [New Brunswick (Morris 1972 as *V. vulgaris*)], USA [Roycefield (Smulyan 1924 as *Vespa communis*)].

Prey stage. Larva (Smulyan 1924; Morris 1972).

Notes. Preys on larvae by piercing the integument with their mandibles and consuming the liquid and softer parts (Smulyan 1924).

***Vespula maculifrons* (du Buysson, 1905)**

Distribution. Canada, USA (Kimsey and Carpenter 2012).

Recorded interactions with *H. cunea*. Canada [New Brunswick (Morris 1972 as *V. maculata*)].

Prey stage. Larva (Morris 1972).

Chilopoda

Scutigermorpha

Scutigeridae 蚰蜒科

***Thereuopoda clunifera* Wood, 1862**

Distribution. China, Japan (Würmli 1979).

Recorded interactions with *H. cunea*. Japan (Hasegawa and Itô 1967).

Prey stage. Adult (Hasegawa and Itô 1967).

Notes. Occasionally preys on *H. cunea* (Hasegawa and Itô 1967).

Arachnida

Araneae

Agelenidae 漏斗蛛科

***Agelena limbata* Thorell, 1897**

Distribution. China, Myanmar, Laos (World Spider Catalog 2023), Japan (Kunimi 1983).

Recorded interactions with *H. cunea*. Japan [Fuchu (Kunimi 1983)].

Prey stage. Larva (Kunimi 1983).

Notes. Collected from fall webworm nest (Kunimi 1983).

***Agelenopsis* sp.**

Recorded interactions with *H. cunea*. USA [Arkansas (Warren et al. 1967)].

Prey stage. Larva (Warren et al. 1967).

Notes. Collected from fall webworm nest (Warren et al. 1967).

***Allagelena difficilis* (Fox, 1936)**

Distribution. China, Korea (World Spider Catalog 2023).

Recorded interactions with *H. cunea*. China [Dandong City, Liaoning Province (Shu and Yu 1985 as *Agelena difficilis*)].

Prey stage. Larva (Shu and Yu 1985).

***Allagelena opulenta* (L. Koch, 1878)**

Distribution. Russia (Far East), Korea, Japan (World Spider Catalog 2023).

Recorded interactions with *H. cunea*. Japan [Fuchu (Kunimi 1983 as *Agelena opulenta*)].

Prey stage. Larva (Kayashima 1967; Kunimi 1983).

Notes. Collected from fall webworm nest (Kunimi 1983).

Anyphaenidae 近管蛛科

***Anyphaena celer* (Hentz, 1847)**

Distribution. Canada, USA (World Spider Catalog 2023).

Recorded interactions with *H. cunea*. USA [Arkansas (Warren et al. 1967)].

Prey stage. Larva (Warren et al. 1967).

Notes. Collected from fall webworm nest (Warren et al. 1967).

***Anyphaena maculata* (Banks, 1896)**

Distribution. USA (World Spider Catalog 2023).

Recorded interactions with *H. cunea*. USA [Arkansas (Warren et al. 1967)].

Prey stage. Larva (Warren et al. 1967).

Notes. Collected from fall webworm nest (Warren et al. 1967).

***Anyphaena* sp.**

Recorded interactions with *H. cunea*. USA [Arkansas (Warren et al. 1967)].

Prey stage. Larva (Warren et al. 1967).

Notes. Collected from fall webworm nest (Warren et al. 1967).

***Aysha* sp.**

Recorded interactions with *H. cunea*. USA [Arkansas (Warren et al. 1967)].

Prey stage. Larva (Warren et al. 1967).

Notes. Collected from fall webworm nest (Warren et al. 1967).

***Hibana gracilis* (Hentz, 1847)**

Distribution. Canada, USA, Jamaica (World Spider Catalog 2023).

Recorded interactions with *H. cunea*. USA [Arkansas (Warren et al. 1967 as *Aysha gracilis*)].

Prey stage. Larva (Warren et al. 1967).

Notes. Collected from fall webworm nest (Warren et al. 1967).

***Lupettiana mordax* (O. Pickard-Cambridge, 1896)**

Distribution. USA to Peru, Brazil (World Spider Catalog 2023).

Recorded interactions with *H. cunea*. USA [Arkansas (Warren et al. 1967 as *Anyphaena fragilis*)].

Prey stage. Larva (Warren et al. 1967).

Notes. Collected from fall webworm nest (Warren et al. 1967).

***Wulfila saltabundus* (Hentz, 1847)**

Distribution. USA, Canada (World Spider Catalog 2023).

Recorded interactions with *H. cunea*. USA [Arkansas (Warren et al. 1967 as *Anyphaenella saltabunda*)].

Prey stage. Larva (Warren et al. 1967).

Notes. Collected from fall webworm nest (Warren et al. 1967).

Araneidae 圓蛛科

***Araneus diadematus* Clerck, 1757**

Distribution. Europe, Middle East, Turkey, Caucasus, Russia (Europe to Far East), Iran, Central Asia, China, Japan. Introduced to North America (World Spider Catalog 2023).

Recorded interactions with *H. cunea*. South of the European part of former USSR (Sharov et al. 1984), Italy [Po Valley (Groppali et al. 1993), Pavia (Camerini and Groppali 1999)].

Prey stage. Larva (Groppali et al. 1993; Camerini and Groppali 1999).

***Araniella displicata* (Hentz, 1847)**

Distribution. North America, Europe, Russia (Europe to Far East), Kazakhstan, China, Korea, Japan (World Spider Catalog 2023).

Recorded interactions with *H. cunea*. USA [Arkansas (Warren et al. 1967)].

Prey stage. Larva (Warren et al. 1967).

Notes. Collected from fall webworm nest (Warren et al. 1967).

***Araneus cingulatus* (Walckenaer, 1841)**

Distribution. USA (World Spider Catalog 2023).

Recorded interactions with *H. cunea*. USA [Arkansas (Warren et al. 1967 as *Conepeira ozarkensis*)].

Prey stage. Larva (Warren et al. 1967).

Notes. Collected from fall webworm nest (Warren et al. 1967).

***Araneus circe* (Audouin, 1826)**

Distribution. Southern Europe, Egypt, Turkey, Caucasus, Iran (World Spider Catalog 2023).

Recorded interactions with *H. cunea*. USA [Arkansas (Warren et al. 1967 as *Epeira cornuta*)].

Prey stage. Larva (Warren et al. 1967).

Notes. Collected from fall webworm nest (Warren et al. 1967).

***Araneus grossus* (C. L. Koch, 1844)**

Distribution. Europe to Central Asia (World Spider Catalog 2023).

Recorded interactions with *H. cunea*. South of the European part of former USSR (Sharov et al. 1984).

Prey stage. Larva (Sharov et al. 1984).

***Araneus* sp.**

Recorded interactions with *H. cunea*. Japan [Fuchu, Akikawa (Kunimi 1983)].

Prey stage. Larva (Kunimi 1983).

Notes. Collected from fall webworm nest (Kunimi 1983).

***Araneus macacus* Uyemura, 1961**

Distribution. Russia (Far East), Japan (World Spider Catalog 2023).

Recorded interactions with *H. cunea*. Japan (Kayashima 1967 as *A. ventricosus macacus*).

Prey stage. Pupa or adult (Kayashima 1967)

***Acacesia hamata* (Hentz, 1847)**

Distribution. USA to Argentina (World Spider Catalog 2023).

Recorded interactions with *H. cunea*. USA [Arkansas (Warren et al. 1967)].

Prey stage. Larva (Warren et al. 1967).

Notes. Collected from fall webworm nest (Warren et al. 1967).

***Aoaraneus pentagrammicus* (Karsch, 1879)**

Distribution. Korea, Japan, China (World Spider Catalog 2023).

Recorded interactions with *H. cunea*. Japan (Kayashima 1967 as *Araneus pentagrammicus*).

Prey stage. Pupa or adult (Kayashima 1967).

***Argiope amoena* L. Koch, 1878**

Distribution. China, Korea, Japan (World Spider Catalog 2023).

Recorded interactions with *H. cunea*. Japan (Kayashima 1967).

Prey stage. Pupa or adult (Kayashima 1967).

***Argiope bruennichii* (Scopoli, 1772)**

Distribution. Europe, Turkey, Israel, Russia (Europe to Far East), Caucasus, Iran, Central Asia to China, Korea, Japan (World Spider Catalog 2023).

Recorded interactions with *H. cunea*. Japan (Kayashima 1967).

Prey stage. Pupa or adult (Kayashima 1967).

***Argiope* sp.**

Recorded interactions with *H. cunea*. China [Liaocheng, Shandong Province (Yue et al. 2016)].

Prey stage. Larva (Yue et al. 2016).

***Bijoaraneus mitificus* (Simon, 1886)**

Distribution. Pakistan, India, Bangladesh, China, Thailand, Cambodia, Singapore, Philippines, New Guinea (World Spider Catalog 2023).

Recorded interactions with *H. cunea*. Japan [Akikawa (Kunimi 1983 as *Araneus mitificus*)].

Prey stage. Larva (Kunimi 1983).

Notes. Collected from fall webworm nest (Kunimi 1983).

***Cyclosa atrata* Bösenberg & Strand, 1906**

Distribution. China, Korea, Japan, Russia (World Spider Catalog 2023).

Recorded interactions with *H. cunea*. Japan (Kayashima 1967).

Prey stage. Pupa or adult (Kayashima 1967).

***Cyclosa* sp.**

Recorded interactions with *H. cunea*. China [Liaocheng, Shandong Province (Yue et al. 2016)].

Prey stage. Larva (Yue et al. 2016).

***Epeira* sp.**

Recorded interactions with *H. cunea*. USA [Arkansas (Warren et al. 1967)].

Prey stage. Larva (Warren et al. 1967).

Notes. Collected from fall webworm nest (Warren et al. 1967).

***Eustala anastera* (Walckenaer, 1841)**

Distribution. North and Central America (World Spider Catalog 2023).

Recorded interactions with *H. cunea*. USA [Arkansas (Warren et al. 1967)].

Prey stage. Larva (Warren et al. 1967).

Notes. Collected from fall webworm nest (Warren et al. 1967).

***Eustala* sp.**

Recorded interactions with *H. cunea*. USA [Arkansas (Warren et al. 1967)].

Prey stage. Larva (Warren et al. 1967).

Notes. Collected from fall webworm nest (Warren et al. 1967).

***Gibbaranea bituberculata* (Walckenaer, 1802)**

Distribution. North Africa, Europe, Turkey, Israel, Russia (Europe to Far East), Caucasus, Iran, Central Asia to China, Japan, India (World Spider Catalog 2023).

Recorded interactions with *H. cunea*. Italy [Italy [Po Valley (Groppali et al. 1993 as *Araneus bituberculatus*), Pavia (Camerini and Groppali 1999)].

Prey stage. Larva (Groppali et al. 1993; Camerini and Groppali 1999).

***Larinioides cornutus* (Clerck, 1757)**

Distribution. North America, Europe, Turkey, Israel, Caucasus, Russia (Europe to Far East), Iran, China, Korea, Japan (World Spider Catalog 2023).

Recorded interactions with *H. cunea*. South of the European part of former USSR (Sharov et al. 1984 as *Nuctenea cornuta*), Italy [Po Valley (Groppali et al. 1993)].

Prey stage. Larva (Sharov et al. 1984; Groppali et al. 1993).

***Larinioides patagiatus* (Clerck, 1757)**

Distribution. North America, Europe, Turkey, Caucasus, Russia (Europe to Far East), Central Asia, China, Mongolia, Japan (World Spider Catalog 2023).

Recorded interactions with *H. cunea*. South of the European part of former USSR (Sharov et al. 1984 as *Nuctenea patagiata*).

Prey stage. Larva (Sharov et al. 1984).

***Micrathena gracilis* (Walckenaer, 1805)**

Distribution. North and Central America (World Spider Catalog 2023).

Recorded interactions with *H. cunea*. USA [Arkansas (Warren et al. 1967)].

Prey stage. Larva (Warren et al. 1967).

Notes. Collected from fall webworm nest (Warren et al. 1967).

***Neoscona arabesca* (Walckenaer, 1841)**

Distribution. North, Central America, Caribbean. Introduced to Nepal, China (World Spider Catalog 2023).

Recorded interactions with *H. cunea*. USA [Arkansas (Warren et al. 1967)].

Prey stage. Larva (Warren et al. 1967).

Notes. Collected from fall webworm nest (Warren et al. 1967).

***Neoscona crucifera benjamina* (Lucas, 1838)**

Distribution. North America. Introduced to Hawaii, Canary Is., Madeira (World Spider Catalog 2023).

Recorded interactions with *H. cunea*. USA [Arkansas (Warren et al. 1967 as *N. sacra*)].

Prey stage. Larva (Warren et al. 1967).

Notes. Collected from fall webworm nest (Warren et al. 1967).

***Neoscona pratensis* (Hentz, 1847)**

Distribution. Canada, USA (World Spider Catalog 2023).

Recorded interactions with *H. cunea*. USA [Arkansas (Warren et al. 1967)].

Prey stage. Larva (Warren et al. 1967).

Notes. Collected from fall webworm nest (Warren et al. 1967).

***Neoscona scylloides* (Bösenberg & Strand, 1906)**

Distribution. Russia (Far East), Korea, Japan, China (World Spider Catalog 2023).

Recorded interactions with *H. cunea*. Japan (Kayashima 1967).

Prey stage. Pupa or adult (Kayashima 1967).

***Ocrepeira ectypa* (Walckenaer, 1841)**

Distribution. USA (World Spider Catalog 2023).

Recorded interactions with *H. cunea*. USA [Arkansas (Warren et al. 1967 as *Wixia ectypa*)].

Prey stage. Larva (Warren et al. 1967).

Notes. Collected from fall webworm nest (Warren et al. 1967).

***Singa hamata* (Clerck, 1757)**

Distribution. Europe, Turkey, Russia (Europe to Far East), Caucasus to Central Asia, China, Korea, Japan (World Spider Catalog 2023).

Recorded interactions with *H. cunea*. Italy [Central Padana Plain (Groppali et al. 1994)].

Prey stage. Larva (Groppali et al. 1994).

***Singa* sp.**

Recorded interactions with *H. cunea*. USA [Arkansas (Warren et al. 1967)].

Prey stage. Larva (Warren et al. 1967).

Notes. Collected from fall webworm nest (Warren et al. 1967).

***Yaginumia sia* (Strand, 1906)**

Distribution. China, Korea, Japan (World Spider Catalog 2023).

Recorded interactions with *H. cunea*. Japan [Akikawa (Kunimi 1983 as *Y. zea*)].

Prey stage. Larva (Kunimi 1983).

Notes. Collected from fall webworm nest (Kunimi 1983).

Cheiracanthiidae 红螯蛛科

***Cheiracanthium erraticum* (Walckenaer, 1802)**

Distribution. Azores, Europe, Turkey, Caucasus, Russia (Europe to Far East), Iran, Central Asia, China, Korea, Japan (World Spider Catalog 2023).

Recorded interactions with *H. cunea*. South of the European part of former USSR (Sharov et al. 1984).

Prey stage. Larva (Sharov et al. 1984).

***Cheiracanthium eutittha* Bösenberg & Strand, 1906**

Distribution. China (Taiwan), Japan (World Spider Catalog 2023).

Recorded interactions with *H. cunea*. Japan [Fuchu, Akikawa (Kunimi 1983 as *Chiracanthium eutittha*)].

Prey stage. Larva (Kunimi 1983).

Notes. Collected from fall webworm nest (Kunimi 1983).

***Cheiracanthium inclusum* (Hentz, 1847)**

Distribution. North America, Central America, Caribbean, South America. Introduced to Réunion (World Spider Catalog 2023).

Recorded interactions with *H. cunea*. USA [Arkansas (Warren et al. 1967 as *Chiracanthium inclusum*)].

Prey stage. Larva (Warren et al. 1967).

Notes. Collected from fall webworm nest (Warren et al. 1967).

***Cheiracanthium lascivum* Karsch, 1879**

Distribution. Russia (Sakhalin), China, Korea, Japan (World Spider Catalog 2023).

Recorded interactions with *H. cunea*. Japan [Akikawa (Kunimi 1983 as *Chiracanthium lascivum*)].

Prey stage. Larva (Kunimi 1983).

Notes. Collected from fall webworm nest (Kunimi 1983).

***Cheiracanthium mildei* L. Koch, 1864**

Distribution. Azores, Europe, North Africa, Turkey, Middle East, Caucasus, Russia (Europe) to Central Asia. Introduced to North America, Argentina (World Spider Catalog 2023).

Recorded interactions with *H. cunea*. Italy [Po Valley (Groppali et al. 1993)].

Prey stage. Larva (Groppali et al. 1993).

***Cheiracanthium japonicum* Bösenberg & Strand, 1906**

Distribution. Russia (Far East), Mongolia, China, Korea, Japan (World Spider Catalog 2023).

Recorded interactions with *H. cunea*. Japan [Fuchu (Kunimi 1983 as *Chiracanthium japonicum*)].

Prey stage. Larva (Kunimi 1983).

Notes. Collected from fall webworm nest (Kunimi 1983).

***Chieracanthium* sp.**

Recorded interactions with *H. cunea*. Italy [Po Valley (Groppali et al. 1993)].

Prey stage. Larva (Groppali et al. 1993).

***Cheiracanthium unicum* Bösenberg & Strand, 1906**

Distribution. Korea, Japan, China, Laos (World Spider Catalog 2023).

Recorded interactions with *H. cunea*. Japan [Akikawa (Kunimi 1983 as *Chiracanthium unicum*)].

Prey stage. Larva (Kunimi 1983).

Notes. Collected from fall webworm nest (Kunimi 1983).

Clubionidae 管巢蛛科

***Bucliona jucunda* (Karsch, 1879)**

Distribution. Russia (Far East), Korea, Japan, China (World Spider Catalog 2023).

Recorded interactions with *H. cunea*. Japan [Fuchu (Kunimi 1983 as *Clubiona jucunda*)].

Prey stage. Larva (Kunimi 1983).

Notes. Collected from fall webworm nest (Kunimi 1983).

***Clubiona abboti* L. Koch, 1866**

Distribution. Canada, USA (World Spider Catalog 2023).

Recorded interactions with *H. cunea*. USA [Arkansas (Warren et al. 1967)].

Prey stage. Larva (Warren et al. 1967).

Notes. Collected from fall webworm nest (Warren et al. 1967).

***Clubiona corrugata* Bösenberg & Strand, 1906**

Distribution. Russia (Far East), China, Korea, Japan, Thailand (World Spider Catalog 2023).

Recorded interactions with *H. cunea*. Japan [Fuchu (Kunimi 1983)].

Prey stage. Larva (Kunimi 1983).

Notes. Collected from fall webworm nest (Kunimi 1983).

***Clubiona diversa* O. Pickard-Cambridge, 1862**

Distribution. Europe, Caucasus, Russia (Europe to Far East), Kazakhstan, Pakistan, Korea, Japan (World Spider Catalog 2023).

Recorded interactions with *H. cunea*. USA [Arkansas (Warren et al. 1967 as *Clubiona pallens*)].

Prey stage. Larva (Warren et al. 1967).

Notes. Collected from fall webworm nest (Warren et al. 1967).

***Clubiona lutescens* Westring, 1851**

Distribution. Europe, Turkey, Caucasus, Russia (Europe to Far East), Iran, Kazakhstan, Korea, Japan. Introduced to North America (World Spider Catalog 2023).

Recorded interactions with *H. cunea*. Japan [Akikawa (Kunimi 1983)].

Prey stage. Larva (Kunimi 1983).

Notes. Collected from fall webworm nest (Kunimi 1983).

***Clubiona marmorata* L. Koch, 1866**

Distribution. France to Ukraine and Turkey (World Spider Catalog 2023).

Recorded interactions with *H. cunea*. South of the European part of former USSR (Sharov et al. 1984).

Prey stage. Larva (Sharov et al. 1984).

***Clubiona moesta* Banks, 1896**

Distribution. USA, Canada, China (World Spider Catalog 2023).

Recorded interactions with *H. cunea*. USA [Arkansas (Warren et al. 1967)].

Prey stage. Larva (Warren et al. 1967).

Notes. Collected from fall webworm nest (Warren et al. 1967).

***Clubiona obesa* Hentz, 1847**

Distribution. USA, Canada (World Spider Catalog 2023).

Recorded interactions with *H. cunea*. USA [Arkansas (Warren et al. 1967)].

Prey stage. Larva (Warren et al. 1967).

Notes. Collected from fall webworm nest (Warren et al. 1967).

***Clubiona pallidula* (Clerck, 1757)**

Distribution. Europe, Caucasus, Russia (Europe to Far East), Central Asia. Introduced to North America (World Spider Catalog 2023).

Recorded interactions with *H. cunea*. South of the European part of former USSR (Sharov et al. 1984).

Prey stage. Larva (Sharov et al. 1984).

***Clubiona* sp.**

Recorded interactions with *H. cunea*. USA [Arkansas (Warren et al. 1967)].

Prey stage. Larva (Warren et al. 1967).

Notes. Collected from fall webworm nest (Warren et al. 1967).

***Clubiona vigil* Karsch, 1879**

Distribution. Russia (Kurile Is.), Korea, Japan, China (World Spider Catalog 2023).

Recorded interactions with *H. cunea*. Japan [Fuchu, Akikawa (Kunimi 1983)].

Prey stage. Larva (Kunimi 1983).

Notes. Collected from fall webworm nest (Kunimi 1983).

***Elaver excepta* (L. Koch, 1866)**

Distribution. Canada, USA, Caribbean (World Spider Catalog 2023).

Recorded interactions with *H. cunea*. USA [Arkansas (Warren et al. 1967 as *Clubionides excepta*)].

Prey stage. Larva (Warren et al. 1967).

Notes. Collected from fall webworm nest (Warren et al. 1967).

Dictynidae 叶蛛科

***Dictyna arundinacea* (Linnaeus, 1758)**

Distribution. North America, Europe, Turkey, Caucasus, Russia (Europe to Far East), Iran, Central Asia, China, Korea, Japan (World Spider Catalog 2023).

Recorded interactions with *H. cunea*. Moldova (Sharov et al. 1984).

Prey stage. Larva (Sharov et al. 1984).

***Dictyna foliicola* Bösenberg & Strand, 1906**

Distribution. Russia (Far East), China, Korea, Japan (World Spider Catalog 2023).

Recorded interactions with *H. cunea*. Japan (Kayashima 1967).

Prey stage. Larva (Kayashima 1967).

***Dictyna pusilla* Thorell, 1856**

Distribution. Europe, Turkey, Caucasus, Russia (Europe to Far East), Central Asia (World Spider Catalog 2023).

Recorded interactions with *H. cunea*. Italy [Po Valley (Groppali et al. 1993), Central Padana Plain (Groppali et al. 1994)].

Prey stage. Larva (Groppali et al. 1994).

***Dictyna* sp.**

Recorded interactions with *H. cunea*. USA [Arkansas (Warren et al. 1967)].

Prey stage. Larva (Warren et al. 1967).

Notes. Collected from fall webworm nest (Warren et al. 1967).

***Phantyna segregata* (Gertsch & Mulaik, 1936)**

Distribution. USA, Mexico (World Spider Catalog 2023).

Recorded interactions with *H. cunea*. USA [Arkansas (Warren et al. 1967 as *Dictyna* aff *segregata*)].

Prey stage. Larva (Warren et al. 1967).

Notes. Collected from fall webworm nest (Warren et al. 1967).

Gnaphosidae 平腹蛛科

***Cesonia bilineata* (Hentz, 1847)**

Distribution. Canada, USA, Mexico (World Spider Catalog 2023).

Recorded interactions with *H. cunea*. USA [Arkansas (Warren et al. 1967)].

Prey stage. Larva (Warren et al. 1967).

Notes. Collected from fall webworm nest (Warren et al. 1967).

***Drassyllus* sp.**

Recorded interactions with *H. cunea*. USA [Arkansas (Warren et al. 1967)].

Prey stage. Larva (Warren et al. 1967).

Notes. Collected from fall webworm nest (Warren et al. 1967).

***Zelotes* sp.**

Recorded interactions with *H. cunea*. USA [Arkansas (Warren et al. 1967)].

Prey stage. Larva (Warren et al. 1967).

Notes. Collected from fall webworm nest (Warren et al. 1967).

Linyphiidae 皿蛛科

***Frontinellina frutetorum* (C. L. Koch, 1835)**

Distribution. Europe, North Africa, Turkey, Caucasus, Russia (Europe to south Siberia), Iran, Kazakhstan, Central Asia (World Spider Catalog 2023).

Recorded interactions with *H. cunea*. Italy [Po Valley (Groppali et al. 1993)].

Prey stage. Larva (Groppali et al. 1993).

***Grammonota maculata* Banks, 1896**

Distribution. USA, Costa Rica (World Spider Catalog 2023).

Recorded interactions with *H. cunea*. USA [Arkansas (Warren et al. 1967)].

Prey stage. Larva (Warren et al. 1967).

Notes. Collected from fall webworm nest (Warren et al. 1967).

***Linyphia* sp.**

Recorded interactions with *H. cunea*. South of the European part of former USSR (Sharov et al. 1984).

Prey stage. Larva (Sharov et al. 1984).

***Oedothorax retusus* (Westring, 1851)**

Distribution. Europe, Turkey, Caucasus, Russia (Europe to north-eastern Siberia), Kazakhstan, China (World Spider Catalog 2023).

Recorded interactions with *H. cunea*. China [Dandong City, Liaoning Province (Shu and Yu 1985)].

Prey stage. Larva (Shu and Yu 1985).

***Strandella quadrimaculata* (Uyemura, 1937)**

Distribution. Japan (World Spider Catalog 2023).

Recorded interactions with *H. cunea*. Japan [Fuchu (Kunimi 1983)].

Prey stage. Larva (Kunimi 1983).

Notes. Collected from fall webworm nest (Kunimi 1983).

Lycosidae 狼蛛科

***Arctosa cinerea* (Fabricius, 1777)**

Distribution. Europe, North Africa, Congo, Caucasus, Russia (Europe to Far East), Middle East, Kazakhstan, China, Korea, Japan (World Spider Catalog 2023).

Recorded interactions with *H. cunea*. South of the European part of former USSR (Sharov et al. 1984).

Prey stage. Larva (Sharov et al. 1984).

***Pardosa astrigera* L. Koch, 1878**

Distribution. Russia (Far East), Korea, Japan, China (World Spider Catalog 2023).

Recorded interactions with *H. cunea*. Japan (Kayashima 1967 as *Lycosa t-insignita*).

Prey stage. Larva and adult (Kayashima 1967).

Mimetidae 拟态蛛科

***Mimetus puritanus* Chamberlin, 1923**

Distribution. USA, Jamaica (World Spider Catalog 2023).

Recorded interactions with *H. cunea*. USA [Arkansas (Warren et al. 1967)].

Prey stage. Larva (Warren et al. 1967).

Notes. Collected from fall webworm nest (Warren et al. 1967).

***Mimetus syllepsicus* Hentz, 1832**

Distribution. USA, Mexico (World Spider Catalog 2023).

Recorded interactions with *H. cunea*. USA [Arkansas (Warren et al. 1967 as *M. interfactor*)].

Prey stage. Larva (Warren et al. 1967).

Notes. Collected from fall webworm nest (Warren et al. 1967).

Nephilidae 芥蛛科

***Trichonephila clavata* (L. Koch, 1878)**

Distribution. China, Korea, Japan (World Spider Catalog 2023).

Recorded interactions with *H. cunea*. Japan (Kayashima 1967 as *Nephila clavata*), Japan [Akikawa (Kunimi 1983 as *Nephila clavata*)].

Prey stage. Larva (Kunimi 1983) pupa or adult (Kayashima 1967).

Notes. Collected from fall webworm nest (Kunimi 1983).

Oecobiidae 壁钱科

***Oecobius cellariorum* (Dugès, 1836)**

Distribution. Mediterranean, Russia (Europe), Azerbaijan, Jordan, Iran; introduced to USA, China, Japan (World Spider Catalog 2023).

Recorded interactions with *H. cunea*. USA [Arkansas (Warren et al. 1967 as *Oecobius texanus*)].

Prey stage. Larva (Warren et al. 1967).

Notes. Collected from fall webworm nest (Warren et al. 1967).

***Uroctea lesserti* Schenkel, 1936**

Distribution. China, Korea (World Spider Catalog 2023).

Recorded interactions with *H. cunea*. China [Dandong City, Liaoning Province (Shu and Yu 1985)].

Prey stage. Larva (Shu and Yu 1985).

Philodromidae 逍遥蛛科

***Philodromus abbotii* Walckenaer, 1837, nomen dubium**

Distribution. USA (World Spider Catalog 2023).

Recorded interactions with *H. cunea*. USA [Arkansas (Warren et al. 1967)].

Prey stage. Larva (Warren et al. 1967).

Notes. Collected from fall webworm nest (Warren et al. 1967).

***Philodromus aureolus* (Clerck, 1757)**

Distribution. Europe, Turkey, Caucasus, Russia (Europe to Central Asia and Middle Siberia), Kazakhstan, Iran, Central Asia, Mongolia, China, Korea, Japan (World Spider Catalog 2023).

Recorded interactions with *H. cunea*. South of the European part of former USSR (Sharov et al. 1984), Italy [Po Valley (Groppali et al. 1993), Central Padana Plain (Groppali et al. 1994)].

Prey stage. Larva (Sharov et al. 1984; Groppali et al. 1994).

***Philodromus cespitum* (Walckenaer, 1802)**

Distribution. North America, Europe, North Africa, Turkey, Caucasus, Russia (Europe to Far East), Kazakhstan, Iran, Mongolia, China, Korea, Japan (World Spider Catalog 2023).

Recorded interactions with *H. cunea*. Italy [Po Valley (Groppali et al. 1993 as *P. caespitum*)].

Prey stage. Larva (Groppali et al. 1993).

***Philodromus keyserlingi* Marx, 1890**

Distribution. USA, Canada (World Spider Catalog 2023).

Recorded interactions with *H. cunea*. USA [Arkansas (Warren et al. 1967)].

Prey stage. Larva (Warren et al. 1967).

Notes. Collected from fall webworm nest (Warren et al. 1967).

***Philodromus marxii* Keyserling, 1884**

Distribution. USA (World Spider Catalog 2023).

Recorded interactions with *H. cunea*. USA [Arkansas (Warren et al. 1967)].

Prey stage. Larva (Warren et al. 1967).

Notes. Collected from fall webworm nest (Warren et al. 1967).

***Philodromus pernix* Blackwall, 1846**

Distribution. USA, Canada (World Spider Catalog 2023).

Recorded interactions with *H. cunea*. USA [Arkansas (Warren et al. 1967)].

Prey stage. Larva (Warren et al. 1967).

Notes. Collected from fall webworm nest (Warren et al. 1967).

***Philodromus rufus* Walckenaer, 1826**

Distribution. North America, Europe, Turkey, Caucasus, Russia (Europe to Far East), Kazakhstan, Iran, Central Asia, Mongolia, China, Korea, Japan (World Spider Catalog 2023).

Recorded interactions with *H. cunea*. USA [Arkansas (Warren et al. 1967)].

Prey stage. Larva (Warren et al. 1967).

Notes. Collected from fall webworm nest (Warren et al. 1967).

***Philodromus* sp.**

Recorded interactions with *H. cunea*. USA [Arkansas (Warren et al. 1967)].

Prey stage. Larva (Warren et al. 1967).

Notes. Collected from fall webworm nest (Warren et al. 1967).

***Philodromus* sp.**

Recorded interactions with *H. cunea*. Italy [Po Valley (Groppali et al. 1993)].

Prey stage. Larva (Groppali et al. 1993).

***Philodromus spinitarsis* Simon, 1895**

Distribution. Russia (south Siberia, Far East), China, Korea, Japan (World Spider Catalog 2023).

Recorded interactions with *H. cunea*. China [Dandong City, Liaoning Province (Shu and Yu 1985)].

Prey stage. Larva (Shu and Yu 1985).

***Philodromus vulgaris* (Hentz, 1847)**

Distribution. USA, Canada (World Spider Catalog 2023).

Recorded interactions with *H. cunea*. USA [Arkansas (Warren et al. 1967)].

Prey stage. Larva (Warren et al. 1967).

Notes. Collected from fall webworm nest (Warren et al. 1967).

***Thanatus formicinus* (Clerck, 1757)**

Distribution. North America, Europe, North Africa, Turkey, Caucasus, Russia (Europe to Far East), Iraq, Iran, Kazakhstan, Central Asia, China, Japan (World Spider Catalog 2023).

Recorded interactions with *H. cunea*. USA [Arkansas (Tadić 1963 as *Philodromus formicinus*)].

Prey stage. Larva (Tadić 1963).

Pisauridae 盜蛛科

***Pisaura mirabilis* (Clerck, 1757)**

Distribution. Europe, Turkey, Middle East, Caucasus, Russia (Europe to Middle Siberia), Central Asia, China (World Spider Catalog 2023).

Recorded interactions with *H. cunea*. South of the European part of former USSR (Sharov et al. 1984).

Prey stage. Larva (Sharov et al. 1984).

***Pisaura lama* Bösenberg & Strand, 1906**

Distribution. Russia (Far East), China, Korea, Japan (World Spider Catalog 2023).

Recorded interactions with *H. cunea*. Japan (Kayashima 1967).

Prey stage. Pupa or adult (Kayashima 1967).

***Pisaurina mira* (Walckenaer, 1837)**

Distribution. Canada, USA (World Spider Catalog 2023).

Recorded interactions with *H. cunea*. USA [Arkansas (Warren et al. 1967 as *Dapanus mirus*)].

Prey stage. Larva (Warren et al. 1967).

Notes. Collected from fall webworm nest (Warren et al. 1967).

Salticidae 跳蛛科

***Aelurillus v-insignitus* (Clerck, 1757)**

Distribution. Europe, Turkey, Caucasus, Russia (Europe to Far East), Kazakhstan, Central Asia, China (World Spider Catalog 2023).

Recorded interactions with *H. cunea*. Italy [Central Padana Plain (Groppali et al. 1994)].

Prey stage. Larva (Groppali et al. 1994).

***Carrhotus xanthogramma* (Latreille, 1819)**

Distribution. Europe, Turkey, Caucasus, Russia (Europe to Far East), China, Korea, Japan (World Spider Catalog 2023).

Recorded interactions with *H. cunea*. Japan [Akikawa (Kunimi 1983)].

Prey stage. Larva (Kunimi 1983).

Notes. Collected from fall webworm nest (Kunimi 1983).

***Colonus sylvanus* (Hentz, 1846)**

Distribution. USA to Panama (World Spider Catalog 2023).

Recorded interactions with *H. cunea*. USA [Arkansas (Warren et al. 1967 as *Thiodina sylvana*)].

Prey stage. Larva (Warren et al. 1967).

Notes. Collected from fall webworm nest (Warren et al. 1967).

***Eris militaris* (Hentz, 1845)**

Distribution. USA, Canada (World Spider Catalog 2023).

Recorded interactions with *H. cunea*. USA [Arkansas (Warren et al. 1967 as *E. marginatus*)].

Prey stage. Larva (Warren et al. 1967).

Notes. Collected from fall webworm nest (Warren et al. 1967).

***Eris rufa* (C. L. Koch, 1846)**

Distribution. USA (World Spider Catalog 2023).

Recorded interactions with *H. cunea*. USA [Arkansas (Warren et al. 1967 as *E. pineus*)].

Prey stage. Larva (Warren et al. 1967).

Notes. Collected from fall webworm nest (Warren et al. 1967).

***Eris* sp.**

Recorded interactions with *H. cunea*. USA [Arkansas (Warren et al. 1967)].

Prey stage. Larva (Warren et al. 1967).

Notes. Collected from fall webworm nest (Warren et al. 1967).

***Evarcha arcuata* (Clerck, 1757)**

Distribution. Europe, Turkey, Caucasus, Russia (Europe to Far East), Kazakhstan, Iran, Central Asia, China, Japan (World Spider Catalog 2023).

Recorded interactions with *H. cunea*. South of the European part of former USSR (Sharov et al. 1984).

Prey stage. Larva (Sharov et al. 1984).

***Evarcha falcata* (Clerck, 1757)**

Distribution. Europe, Turkey, Caucasus, Russia (Europe to south Siberia), Kazakhstan, Afghanistan, China (World Spider Catalog 2023).

Recorded interactions with *H. cunea*. South of the European part of former USSR (Sharov et al. 1984).

Prey stage. Larva (Sharov et al. 1984).

***Heliophanus auratus* C. L. Koch, 1835**

Distribution. Europe, Turkey, Caucasus, Russia (Europe to south Siberia), Kazakhstan, Central Asia, China (World Spider Catalog 2023).

Recorded interactions with *H. cunea*. South of the European part of former USSR (Sharov et al. 1984).

Prey stage. Larva (Sharov et al. 1984).

***Hentzia mitrata* (Hentz, 1846)**

Distribution. USA, Canada, Bahama Is. (World Spider Catalog 2023).

Recorded interactions with *H. cunea*. USA [Arkansas (Warren et al. 1967)].
Prey stage. Larva (Warren et al. 1967).
Notes. Collected from fall webworm nest (Warren et al. 1967).

***Hentzia palmarum* (Hentz, 1832)**

Distribution. North America, Bermuda, Bahama Is., Cuba (World Spider Catalog 2023).

Recorded interactions with *H. cunea*. USA [Arkansas (Warren et al. 1967)].
Prey stage. Larva (Warren et al. 1967).
Notes. Collected from fall webworm nest (Warren et al. 1967).

***Hentzia* sp.**

Recorded interactions with *H. cunea*. USA [Arkansas (Warren et al. 1967)].
Prey stage. Larva (Warren et al. 1967).
Notes. Collected from fall webworm nest (Warren et al. 1967).

***Icius* sp.**

Recorded interactions with *H. cunea*. USA [Arkansas (Warren et al. 1967)].
Prey stage. Larva (Warren et al. 1967).
Notes. Collected from fall webworm nest (Warren et al. 1967).

***Jotus* sp.**

Recorded interactions with *H. cunea*. Japan [Fuchu, Akikawa (Kunimi 1983)].
Prey stage. Larva (Kunimi 1983).
Notes. Collected from fall webworm nest (Kunimi 1983).

***Macaroeris nidicolens* (Walckenaer, 1802)**

Distribution. Macaronesia, Europe, North Africa to Turkey, Caucasus, Turkmenistan, Iran; introduced to Sri Lanka (World Spider Catalog 2023).

Recorded interactions with *H. cunea*. Italy [Po Valley (Groppali et al. 1993 as *Eris nidicolens*), Central Padana Plain (Groppali et al. 1994 as *Eris nidicolens*)].
Prey stage. Larva (Groppali et al. 1994).

***Maevia inclemens* (Walckenaer, 1837)**

Distribution. USA, Canada (World Spider Catalog 2023).

Recorded interactions with *H. cunea*. USA [Arkansas (Warren et al. 1967 as *M. vittata*)].
Prey stage. Larva (Warren et al. 1967).
Notes. Collected from fall webworm nest (Warren et al. 1967).

***Metacyrba taeniola* (Hentz, 1846)**

Distribution. USA, Mexico (World Spider Catalog 2023).

Recorded interactions with *H. cunea*. USA [Arkansas (Warren et al. 1967)].
Prey stage. Larva (Warren et al. 1967).
Notes. Collected from fall webworm nest (Warren et al. 1967).

***Metaphidippus* sp.**

Recorded interactions with *H. cunea*. USA [Arkansas (Warren et al. 1967)].
Prey stage. Larva (Warren et al. 1967).
Notes. Collected from fall webworm nest (Warren et al. 1967).

***Myrmarachne japonica* (Karsch, 1879)**

Distribution. Russia (Far East), China, Korea, Japan (World Spider Catalog 2023).
Recorded interactions with *H. cunea*. Japan [Akikawa (Kunimi 1983)].
Prey stage. Larva (Kunimi 1983).
Notes. Collected from fall webworm nest (Kunimi 1983).

***Orienticius vulpes* (Grube, 1861)**

Distribution. Russia (south Siberia to Far East), China, Korea, Japan (World Spider Catalog 2023).
Recorded interactions with *H. cunea*. Japan [Akikawa (Kunimi 1983 as *Dendryphantès atratus*)].
Prey stage. Larva (Kunimi 1983).
Notes. Collected from fall webworm nest (Kunimi 1983).

***Paraphidippus aurantius* (Lucas, 1833)**

Distribution. USA to Panama, Greater Antilles (World Spider Catalog 2023).
Recorded interactions with *H. cunea*. USA [Arkansas (Warren et al. 1967 as *Eris aurantia*)].
Prey stage. Larva (Warren et al. 1967).
Notes. Collected from fall webworm nest (Warren et al. 1967).

***Peckhamia picata* (Hentz, 1846)**

Distribution. North America (World Spider Catalog 2023).
Recorded interactions with *H. cunea*. USA [Arkansas (Warren et al. 1967)].
Prey stage. Larva (Warren et al. 1967).
Notes. Collected from fall webworm nest (Warren et al. 1967).

***Pelegrina galathea* (Walckenaer, 1837)**

Distribution. Canada to Costa Rica, Bermuda (World Spider Catalog 2023).
Recorded interactions with *H. cunea*. USA [Arkansas (Warren et al. 1967 as *Metaphidippus galathea*)].
Prey stage. Larva (Warren et al. 1967).
Notes. Collected from fall webworm nest (Warren et al. 1967).

***Pelegrina insignis* (Banks, 1892)**

Distribution. USA, Canada (World Spider Catalog 2023).

Recorded interactions with *H. cunea*. USA [Arkansas (Warren et al. 1967 as *Metaphidippus insignis*)].

Prey stage. Larva (Warren et al. 1967).

Notes. Collected from fall webworm nest (Warren et al. 1967).

***Pelegrina proterva* (Walckenaer, 1837)**

Distribution. USA, Canada (World Spider Catalog 2023).

Recorded interactions with *H. cunea*. USA [Arkansas (Warren et al. 1967 as *Metaphidippus protervus*)].

Prey stage. Larva (Warren et al. 1967).

Notes. Collected from fall webworm nest (Warren et al. 1967).

***Phintella castrisiana* (Grube, 1861)**

Distribution. Canary Is., Southern Europe, North Africa, Middle East, Turkey, Caucasus, Iran, Russia (Far East), Korea, Japan (World Spider Catalog 2023).

Recorded interactions with *H. cunea*. South of the European part of former USSR (Sharov et al. 1984 as *Icius castrisianus*).

Prey stage. Larva (Sharov et al. 1984).

***Platycryptus undatus* (De Geer, 1778)**

Distribution. North America (World Spider Catalog 2023).

Recorded interactions with *H. cunea*. USA [Arkansas (Warren et al. 1967 as *Metacyrba undata*)].

Prey stage. Larva (Warren et al. 1967).

Notes. Collected from fall webworm nest (Warren et al. 1967).

***Plexippoides doenitzi* (Karsch, 1879)**

Distribution. China, Korea, Japan (World Spider Catalog 2023).

Recorded interactions with *H. cunea*. Japan (Kayashima 1967 as *Hasarius doenitzi*).

Prey stage. Larva (Kayashima 1967).

***Plexippus paykulli* (Audouin, 1826)**

Distribution. Africa. Introduced to both Americas, Europe, Middle East, Nepal, southern Asia, Australia, Pacific Is. (World Spider Catalog 2023).

Recorded interactions with *H. cunea*. Japan (Kayashima 1967).

Prey stage. Larva (Kayashima 1967).

***Plexippus* sp.**

Recorded interactions with *H. cunea*. USA [Arkansas (Warren et al. 1967)].

Prey stage. Larva (Warren et al. 1967).

Notes. Collected from fall webworm nest (Warren et al. 1967).

***Phidippus audax* (Hentz, 1845)**

Distribution. North America; introduced to Hawaii, Azores, India (World Spider Catalog 2023).

Recorded interactions with *H. cunea*. USA [Arkansas (Warren et al. 1967)].

Prey stage. Larva (Warren et al. 1967).

Notes. Collected from fall webworm nest (Warren et al. 1967).

***Phidippus carolinensis* G. W. Peckham & E. G. Peckham, 1909**

Distribution. USA, Mexico (World Spider Catalog 2023).

Recorded interactions with *H. cunea*. USA [Arkansas (Warren et al. 1967)].

Prey stage. Larva (Warren et al. 1967).

Notes. Collected from fall webworm nest (Warren et al. 1967).

***Phidippus clarus* Keyserling, 1885**

Distribution. North America (World Spider Catalog 2023).

Recorded interactions with *H. cunea*. USA [Arkansas (Warren et al. 1967)].

Prey stage. Larva (Warren et al. 1967).

Notes. Collected from fall webworm nest (Warren et al. 1967).

***Phidippus insignarius* C. L. Koch, 1846**

Distribution. USA (World Spider Catalog 2023).

Recorded interactions with *H. cunea*. USA [Arkansas (Warren et al. 1967)].

Prey stage. Larva (Warren et al. 1967).

Notes. Collected from fall webworm nest (Warren et al. 1967).

***Phidippus mystaceus* (Hentz, 1846)**

Distribution. USA (World Spider Catalog 2023).

Recorded interactions with *H. cunea*. USA [Arkansas (Warren et al. 1967 as *P. incertus*)].

Prey stage. Larva (Warren et al. 1967).

Notes. Collected from fall webworm nest (Warren et al. 1967).

***Phidippus princeps* (G. W. Peckham & E. G. Peckham, 1883)**

Distribution. USA, Canada (World Spider Catalog 2023).

Recorded interactions with *H. cunea*. USA [Arkansas (Warren et al. 1967)].

Prey stage. Larva (Warren et al. 1967).

Notes. Collected from fall webworm nest (Warren et al. 1967).

***Phidippus putnami* (G. W. Peckham & E. G. Peckham, 1883)**

Distribution. USA (World Spider Catalog 2023).

Recorded interactions with *H. cunea*. USA [Arkansas (Warren et al. 1967)].

Prey stage. Larva (Warren et al. 1967).

Notes. Collected from fall webworm nest (Warren et al. 1967).

***Phidippus whitmani* G. W. Peckham & E. G. Peckham, 1909**

Distribution. USA, Canada (World Spider Catalog 2023).

Recorded interactions with *H. cunea*. USA [Arkansas (Warren et al. 1967)].

Prey stage. Larva (Warren et al. 1967).

Notes. Collected from fall webworm nest (Warren et al. 1967).

***Rhene atrata* (Karsch, 1881)**

Distribution. Russia (south Siberia, Far East), China, Korea, Japan (World Spider Catalog 2023).

Recorded interactions with *H. cunea*. Japan [Fuchu, Akikawa (Kunimi 1983 as *Dendryphantes atratus*)].

Prey stage. Larva (Kunimi 1983).

Notes. Collected from fall webworm nest (Kunimi 1983).

***Salticus zebraneus* (C. L. Koch, 1837)**

Distribution. Europe, Turkey, Russia (Europe, Caucasus), Iran (World Spider Catalog 2023).

Recorded interactions with *H. cunea*. South of the European part of former USSR (Sharov et al. 1984), Italy [Central Padana Plain (Groppali et al. 1994)].

Prey stage. Larva (Sharov et al. 1984; Groppali et al. 1994).

***Sassacus cyaneus* (Hentz, 1846)**

Distribution. USA (World Spider Catalog 2023).

Recorded interactions with *H. cunea*. USA [Arkansas (Warren et al. 1967 as *Agassa cyanea*)].

Prey stage. Larva (Warren et al. 1967).

Notes. Collected from fall webworm nest (Warren et al. 1967).

***Sibianor pullus* (Bösenberg & Strand, 1906)**

Distribution. Russia (Far East), Korea, Japan, China (World Spider Catalog 2023).

Recorded interactions with *H. cunea*. Japan [Akikawa (Kunimi 1983 as *Bianor pullus*)].

Prey stage. Larva (Kunimi 1983).

Notes. Collected from fall webworm nest (Kunimi 1983).

***Thiodina* sp.**

Recorded interactions with *H. cunea*. USA [Arkansas (Warren et al. 1967)].

Prey stage. Larva (Warren et al. 1967).

Notes. Collected from fall webworm nest (Warren et al. 1967).

***Zygoballus sexpunctatus* (Hentz, 1845)**

Distribution. USA (World Spider Catalog 2023).

Recorded interactions with *H. cunea*. USA [Arkansas (Warren et al. 1967)].

Prey stage. Larva (Warren et al. 1967).

Notes. Collected from fall webworm nest (Warren et al. 1967).

Tetragnathidae 长脚蛛科

***Tetragnatha laboriosa* Hentz, 1850**

Distribution. Alaska to Chile, Argentina, Falkland Is. (World Spider Catalog 2023).

Recorded interactions with *H. cunea*. USA [Arkansas (Warren et al. 1967)].

Prey stage. Larva (Warren et al. 1967).

Notes. Collected from fall webworm nest (Warren et al. 1967).

***Tetragnatha* sp.**

Recorded interactions with *H. cunea*. South of the European part of former USSR (Sharov et al. 1984).

Prey stage. Larva (Sharov et al. 1984).

***Tetragnatha squamata* Karsch, 1879**

Distribution. Russia (Far East), China, Korea, Japan (World Spider Catalog 2023).

Recorded interactions with *H. cunea*. Japan [Fuchu, Akikawa (Kunimi 1983)].

Prey stage. Larva (Kunimi 1983).

Notes. Collected from fall webworm nest (Kunimi 1983).

Theridiidae 球腹蛛科

***Enoplognatha ovata* (Clerck, 1757)**

Distribution. Europe, Turkey, Caucasus, Russia (Europe to Middle Siberia), Kazakhstan, Iran, Central Asia, Korea, Japan. Introduced to North America (World Spider Catalog 2023).

Recorded interactions with *H. cunea*. South of the European part of former USSR (Sharov et al. 1984).

Prey stage. Larva (Sharov et al. 1984).

***Euryopsis funebris* (Hentz, 1850)**

Distribution. Canada, USA. Introduced to South Africa (World Spider Catalog 2023).

Recorded interactions with *H. cunea*. USA [Arkansas (Warren et al. 1967 as *Euryopsis funebris*)].

Prey stage. Larva (Warren et al. 1967).

Notes. Collected from fall webworm nest (Warren et al. 1967).

***Euryopsis* sp.**

Recorded interactions with *H. cunea*. USA [Arkansas (Warren et al. 1967)].

Prey stage. Larva (Warren et al. 1967).

Notes. Collected from fall webworm nest (Warren et al. 1967).

***Heterotheridion nigrovariegatum* (Simon, 1873)**

Distribution. Europe, Turkey, Caucasus, Russia (Europe) to Central Asia, Iran, China (World Spider Catalog 2023).

Recorded interactions with *H. cunea*. South of the European part of former USSR (Sharov et al. 1984 as *Theridion nigrovariegatum*).

Prey stage. Larva (Sharov et al. 1984).

***Neospintharus trigonum* (Hentz, 1850)**

Distribution. USA, Canada (World Spider Catalog 2023).

Recorded interactions with *H. cunea*. USA [Arkansas (Warren et al. 1967 as *Argyrodes trigonum*)].

Prey stage. Larva (Warren et al. 1967).

Notes. Collected from fall webworm nest (Warren et al. 1967).

***Parasteatoda tepidariorum* (C. L. Koch, 1841)**

Distribution. Asia; introduced to Canada, USA, South America, Europe, Turkey, Caucasus, Russia (Europe to Far East), South Africa, Seychelles, New Zealand, Hawaii (World Spider Catalog 2023).

Recorded interactions with *H. cunea*. USA [Arkansas (Warren et al. 1967 as *Achaeearanea tepidariorum*)], Japan (Kayashima 1967 as *Theridion tepidariorum*), Japan [Fuchu, Akikawa (Kunimi 1983 as *Achaeearanea tepidariorum*)], China [Dandong City, Liaoning Province (Shu and Yu 1985 as *Theridion tepidariorum*)].

Prey stage. Larva (Warren et al. 1967; Kunimi 1983; Shu and Yu 1985), adult (Kayashima 1967).

Notes. Collected from fall webworm nest (Warren et al. 1967; Kunimi 1983).

***Phylloneta sisypchia* (Clerck, 1757)**

Distribution. Europe, Turkey, Caucasus, Russia (Europe to south Siberia), Kazakhstan, Central Asia, China (World Spider Catalog 2023).

Recorded interactions with *H. cunea*. Italy [Po Valley (Groppali et al. 1993 as *Theridion sisypchium*)].

Prey stage. Larva (Groppali et al. 1993).

***Takayus takayensis* (Saito, 1939)**

Distribution. China, Korea, Japan (World Spider Catalog 2023).

Recorded interactions with *H. cunea*. Japan [Fuchu (Kunimi 1983 as *Theridion takayense*)].

Prey stage. Larva (Kunimi 1983).

Notes. Collected from fall webworm nest (Kunimi 1983).

***Teutana* sp.**

Recorded interactions with *H. cunea*. USA [Arkansas (Warren et al. 1967)].

Prey stage. Larva (Warren et al. 1967).

Notes. Collected from fall webworm nest (Warren et al. 1967).

***Theridion differens* Emerton, 1882**

Distribution. USA, Canada (World Spider Catalog 2023).

Recorded interactions with *H. cunea*. USA [Arkansas (Warren et al. 1967)].

Prey stage. Larva (Warren et al. 1967).

Notes. Collected from fall webworm nest (Warren et al. 1967).

***Theridion varians* Hahn, 1833**

Distribution. Europe, North Africa, Turkey, Caucasus, Russia (Europe to Far East), Kazakhstan, Iran, Central Asia, China. Introduced to Canada, USA (World Spider Catalog 2023).

Recorded interactions with *H. cunea*. South of the European part of former USSR [Moldova, Russia (Sharov et al. 1984)].

Prey stage. Larva (Sharov et al. 1984).

***Theridion* sp.**

Recorded interactions with *H. cunea*. Japan [Akikawa (Kunimi 1983)].

Prey stage. Larva (Kunimi 1983).

Notes. Collected from fall webworm nest (Kunimi 1983).

***Yunohamella yunohamensis* (Bösenberg & Strand, 1906)**

Distribution. Russia (Sakhalin, Kurile Is.), Korea, Japan (World Spider Catalog 2023).

Recorded interactions with *H. cunea*. Japan [Akikawa (Kunimi 1983 as *Theridion yunohamense*)].

Prey stage. Larva (Kunimi 1983).

Notes. Collected from fall webworm nest (Kunimi 1983).

Thomisidae 蟹蛛科

***Bassaniana decorata* (Karsch, 1879)**

Distribution. Russia (Far East), China, Korea, Japan (World Spider Catalog 2023).

Recorded interactions with *H. cunea*. Japan [Fuchu, Akikawa (Kunimi 1983 as *Oxyptila decorata*)].

Prey stage. Larva (Kunimi 1983).

Notes. Collected from fall webworm nest (Kunimi 1983).

***Diaea subdola* O. Pickard-Cambridge, 1885**

Distribution. Pakistan, India, China, Russia (Far East), Korea, Japan (World Spider Catalog 2023).

Recorded interactions with *H. cunea*. Japan [Fuchu, Akikawa (Kunimi 1983 as *Misumenops japonicus*)].

Prey stage. Larva (Kunimi 1983).

Notes. Collected from fall webworm nest (Kunimi 1983).

***Ebrechtella tricuspidata* (Fabricius, 1775)**

Distribution. Europe, Turkey, Caucasus, Russia (Europe to Far East), Kazakhstan, Iran, Central Asia, China, Korea, Japan (World Spider Catalog 2023).

Recorded interactions with *H. cunea*. South of the European part of former USSR (Sharov et al. 1984, name as *Misumenops tricuspιδatus*), Japan [Fuchu, Akikawa (Kunimi 1983 as *Misumenops tricuspιδatus*)], China [Dandong City, Liaoning Province (Shu and Yu 1985 as *Misumena tricuspιδatus*)].

Prey stage. Larva (Kunimi 1983; Sharov et al. 1984; Shu and Yu 1985).

Notes. Collected from fall webworm nest (Kunimi 1983).

***Mecaphesa asperata* (Hentz, 1847)**

Distribution. North, Central America, Caribbean (World Spider Catalog 2023).

Recorded interactions with *H. cunea*. USA [Arkansas (Warren et al. 1967 as *Misumenops asperatus*)].

Prey stage. Larva (Warren et al. 1967).

Notes. Collected from fall webworm nest (Warren et al. 1967).

***Mecaphesa celer* (Hentz, 1847)**

Distribution. North, Central America (World Spider Catalog 2023).

Recorded interactions with *H. cunea*. USA [Arkansas (Warren et al. 1967 as *Misumenops celer*)].

Prey stage. Larva (Warren et al. 1967).

Notes. Collected from fall webworm nest (Warren et al. 1967).

***Misumessus oblongus* (Keyserling, 1880)**

Distribution. Canada, USA (World Spider Catalog 2023).

Recorded interactions with *H. cunea*. USA [Arkansas (Warren et al. 1967 as *Misumenops oblongus*)].

Prey stage. Larva (Warren et al. 1967).

Notes. Collected from fall webworm nest (Warren et al. 1967).

***Misumenops* sp.**

Recorded interactions with *H. cunea*. USA [Arkansas (Warren et al. 1967)].

Prey stage. Larva (Warren et al. 1967).

Notes. Collected from fall webworm nest (Warren et al. 1967).

***Oxytate striatipes* L. Koch, 1878**

Distribution. Russia (Far East), China, Korea, Japan (World Spider Catalog 2023).

Recorded interactions with *H. cunea*. Japan [Fuchu, Akikawa (Kunimi 1983)].

Prey stage. Larva (Kunimi 1983; Shu and Yu 1985).

Notes. Collected from fall webworm nest (Kunimi 1983).

***Pistius truncatus* (Pallas, 1772)**

Distribution. Europe, Turkey, Caucasus, Russia (Europe to Far East), Iran, China (World Spider Catalog 2023).

Recorded interactions with *H. cunea*. Japan [Akikawa (Kunimi 1983)].

Prey stage. Larva (Kunimi 1983).

Notes. Collected from fall webworm nest (Kunimi 1983).

***Spiracme striatipes* (L. Koch, 1870)**

Distribution. Europe, Turkey, Caucasus, Russia (Europe) to Central Asia, Iran, China (World Spider Catalog 2023).

Recorded interactions with *H. cunea*. China [Dandong City, Liaoning Province (Shu and Yu 1985 as *Xysticus striatipes*)].

Prey stage. Larva (Shu and Yu 1985).

***Synema globosum* (Fabricius, 1775)**

Distribution. Europe, Turkey, Caucasus, Russia (Europe to Far East), Israel, Iran, Central Asia, China, Korea, Japan (World Spider Catalog 2023).

Recorded interactions with *H. cunea*. South of the European part of former USSR (Sharov et al. 1984).

Prey stage. Larva (Sharov et al. 1984).

***Synema parvulum* (Hentz, 1847)**

Distribution. USA, Mexico (World Spider Catalog 2023).

Recorded interactions with *H. cunea*. USA [Arkansas (Warren et al. 1967)].

Prey stage. Larva (Warren et al. 1967).

Notes. Collected from fall webworm nest (Warren et al. 1967).

***Tmarus* sp.**

Recorded interactions with *H. cunea*. USA [Arkansas (Warren et al. 1967)].

Prey stage. Larva (Warren et al. 1967).

Notes. Collected from fall webworm nest (Warren et al. 1967).

***Thomisus labefactus* Karsch, 1881**

Distribution. Korea, Japan, China, Thailand (World Spider Catalog 2023).

Recorded interactions with *H. cunea*. Japan [Akikawa (Kunimi 1983)].

Prey stage. Larva (Kunimi 1983).

Notes. Collected from fall webworm nest (Kunimi 1983).

***Thomisus onustus* Walckenaer, 1805**

Distribution. Selvagens Is. (Portugal), Europe, North Africa, Turkey, Caucasus, Russia (Europe to south Siberia), Israel, Central Asia, Iran, China, Korea, Japan (World Spider Catalog 2023).

Recorded interactions with *H. cunea*. South of the European part of former USSR (Sharov et al. 1984).

Prey stage. Larva (Sharov et al. 1984).

***Xysticus ferox* (Hentz, 1847)**

Distribution. USA, Canada (World Spider Catalog 2023).

Recorded interactions with *H. cunea*. USA [Arkansas (Warren et al. 1967)].

Prey stage. Larva (Warren et al. 1967).

Notes. Collected from fall webworm nest (Warren et al. 1967).

***Xysticus funestus* Keyserling, 1880**

Distribution. North America (World Spider Catalog 2023).

Recorded interactions with *H. cunea*. USA [Arkansas (Warren et al. 1967)].

Prey stage. Larva (Warren et al. 1967).

Notes. Collected from fall webworm nest (Warren et al. 1967).

***Xysticus lanio* C. L. Koch, 1835**

Distribution. Europe, Turkey, Caucasus, Russia (Europe to Middle and south Siberia), Turkmenistan (World Spider Catalog 2023).

Recorded interactions with *H. cunea*. South of the European part of former USSR (Sharov et al. 1984).

Prey stage. Larva (Sharov et al. 1984).

***Xysticus* sp.**

Recorded interactions with *H. cunea*. USA [Arkansas (Warren et al. 1967)].

Prey stage. Larva (Warren et al. 1967).

Notes. Collected from fall webworm nest (Warren et al. 1967).

***Xysticus* sp.**

Recorded interactions with *H. cunea*. Italy [Po Valley (Groppali et al. 1993)].

Prey stage. Larva (Groppali et al. 1993).

Titanoecidae 隐石蛛科

***Nurscia albofasciata* (Strand, 1907)**

Distribution. Russia (Far East), Korea, Japan, China; introduced to Britain (World Spider Catalog 2023).

Recorded interactions with *H. cunea*. Japan [Akikawa (Kunimi 1983)].

Prey stage. Larva (Kunimi 1983).

Notes. Collected from fall webworm nest (Kunimi 1983).

Trachelidae 管蛛科

***Trachelas japonicus* Bösenberg & Strand, 1906**

Distribution. Russia (Kurile Is.), Korea, Japan, China (World Spider Catalog 2023).

Recorded interactions with *H. cunea*. Japan [Fuchu, Akikawa (Kunimi 1983)].

Prey stage. Larva (Kunimi 1983).

Notes. Collected from fall webworm nest (Kunimi 1983).

***Trachelas similis* F. O. Pickard-Cambridge, 1899**

Distribution. Canada, USA (World Spider Catalog 2023).

Recorded interactions with *H. cunea*. USA [Arkansas (Warren et al. 1967 as *T. aff. laticeps*)].

Prey stage. Larva (Warren et al. 1967).

Notes. Collected from fall webworm nest (Warren et al. 1967).

***Trachelas* sp.**

Recorded interactions with *H. cunea*. USA [Arkansas (Warren et al. 1967)].

Prey stage. Larva (Warren et al. 1967).

Notes. Collected from fall webworm nest (Warren et al. 1967).

***Trachelas tranquillus* (Hentz, 1847)**

Distribution. Canada, USA (World Spider Catalog 2023).

Recorded interactions with *H. cunea*. USA [Arkansas (Warren et al. 1967)].

Prey stage. Larva (Warren et al. 1967).

Notes. Collected from fall webworm nest (Warren et al. 1967).

Uloboridae 妩蛛科

***Octonoba varians* (Bösenberg & Strand, 1906)**

Distribution. China, Korea, Japan (World Spider Catalog 2023).

Recorded interactions with *H. cunea*. Japan [Fuchu (Kunimi 1983 as *Uloborus varians*)].

Prey stage. Larva (Kunimi 1983).

Notes. Collected from fall webworm nest (Kunimi 1983).

Trombidiformes

Trombidiidae 絨蟎科

***Allothrombidium fuliginosum* (Hermann, 1804)**

Distribution. Asia, Europe (CABI Compendium 2022).

Recorded interactions with *H. cunea*. Italy (Boriani 1991).

Prey stage. Egg (Boriani 1991).

Reptilia

Squamata

Gekkonidae 壁虎科

***Gecko japonicus* (Schlegel, 1836)**

Distribution. China, South Korea, Japan (Uetz et al. 2023).

Recorded interactions with *H. cunea*. Japan (Hasegawa and Itô 1967).

Prey stage. Adult (Hasegawa and Itô 1967).

Notes. Occasionally preys on *H. cunea* (Hasegawa and Itô 1967).

Amphibia

Anura

Bufo 蟾蜍科

***Anaxyrus americanus* (Holbrook, 1836)**

Distribution. Canada, USA (Frost 2023).

Recorded interactions with *H. cunea*. Europe (Warren and Tadić 1967 as *Bufo americanus*).

Prey stage. Larva (Warren and Tadić 1967).

***Bufo bufo* (Linnaeus, 1758)**

Distribution. Albania, Austria, Belarus, Belgium, Bosnia and Herzegovina, Bulgaria, China, Croatia, Czech Republic, Denmark, Estonia, Finland, France, Germany, Greece, Hungary, Italy, Jersey, Kazakhstan, Kosovo, Latvia, Liechtenstein, Lithuania, Luxembourg, Moldova, Montenegro, Netherlands, North Macedonia, Norway, Poland, Romania, Russia, San Marino, Serbia, Slovakia, Slovenia, Sweden, Switzerland, Turkey, Ukraine, United Kingdom (Frost 2023).

Recorded interactions with *H. cunea*. Europe (Warren and Tadić 1967).

Prey stage. Larva (Warren and Tadić 1967).

***Bufo gargarizans* Cantor, 1842**

Distribution. China, India, North Korea, South Korea, Russia, Vietnam (Frost 2023).

Recorded interactions with *H. cunea*. China [Dandong City, Liaoning Province (Shu and Yu 1985)].

Prey stage. Larva (Shu and Yu 1985).

Ranidae 蛙科

***Pelophylax nigromaculatus* (Hallowell, 1861)**

Distribution. China, Japan, Korea, North Korea, South Korea, Mongolia, Russia (Frost 2023).

Recorded interactions with *H. cunea*. China [Dandong City, Liaoning Province (Shu and Yu 1985 as *Rana nigromaculatus*)].

Prey stage. Larva (Shu and Yu 1985).

Aves

Bucerotiformes

Upupidae 戴胜科

***Upupa epops* Linnaeus, 1758**

Distribution. Breeds in northwestern Africa (east to northwestern Libya), Canary Islands, and central and southern Europe south to Israel, and east to southeastern Siberia and northern Korea, south to northwestern India and China; mostly migratory, winters to Africa and South Asia (Avibase 2023).

Recorded interactions with *H. cunea*. Italy (Camerini 1994).

Prey stage. Larva (Camerini 1994).

Ciconiiformes

Ciconiidae 鸬鹚科

***Ciconia ciconia* (Linnaeus, 1758)**

Distribution. West Palearctic and West Asia: overwinters in tropical and South Africa (Avibase 2023).

Recorded interactions with *H. cunea*. Europe (Warren and Tadić 1967).

Prey stage. Larva (Warren and Tadić 1967).

Columbiformes

Columbidae 鸠鸽科

***Streptopelia decaocto* (Frivaldszky, 1838)**

Distribution. Europe to Middle East, India, Sri Lanka, China, and Korea; introduced to North America and Mexico (Avibase 2023).

Recorded interactions with *H. cunea*. Italy (Camerini 1994).

Prey stage. Larva (Camerini 1994).

***Streptopelia turtur* (Linnaeus, 1758)**

Distribution. Azores, Canary Is., and Europe to West Siberia and Kazakhstan (Avibase 2023).

Recorded interactions with *H. cunea*. Italy (Camerini 1994).

Prey stage. Larva (Camerini 1994).

Notes. Actively prey on the *H. cunea* in September (Camerini 1994).

Cuculiformes

Cuculidae 杜鹃科

***Coccyzus americanus* (Linnaeus, 1758)**

Distribution. Canada to Mexico and West Indies; overwinters in Argentina (Avibase 2023).

Recorded interactions with *H. cunea*. North America (Warren and Tadić 1967).

Prey stage. Larva (Warren and Tadić 1967).

***Cuculus canorus* Linnaeus, 1758**

Distribution. Europe, Siberia to Kamchatka and Japan; overwinters in Africa (Avibase 2023).

Recorded interactions with *H. cunea*. North America (Warren and Tadić 1967).

Prey stage. Larva (Warren and Tadić 1967).

Falconiformes

Falconidae 隼科

***Falco tinnunculus* Linnaeus, 1758**

Distribution. Europe, northwest Africa, and the Middle East to east central Siberia, Afghanistan, and western and northern Pakistan east in the Himalayas to Nepal and Bhutan; overwinters in eastern Africa and southern and southern Asia (Avibase 2023).

Recorded interactions with *H. cunea*. Italy (Camerini 1994).

Prey stage. Larva (Camerini 1994).

Galliformes

Phasianidae 雉科

***Gallus gallus* (Linnaeus, 1758)**

Distribution. Palaearctic, Oriental (Avibase 2023).

Recorded interactions with *H. cunea*. Europe (Warren and Tadić 1967).

Prey stage. Larva (Warren and Tadić 1967).

Passeriformes

Corvidae 鸦科

***Corvus corone* Linnaeus, 1758**

Distribution. West Europe (Avibase 2023).

Recorded interactions with *H. cunea*. Europe (Warren and Tadić 1967).

Prey stage. Larva (Warren and Tadić 1967).

***Cyanopica cyanus* (Pallas, 1776)**

Distribution. East central Asia (Avibase 2023).

Recorded interactions with *H. cunea*. China [Dandong City, Liaoning Province] (Shu and Yu 1985).

Prey stage. Larva (Shu and Yu 1985).

Notes. Prey heavily on *H. cunea* from early May to early June (Shu and Yu 1985).

***Pica pica* (Linnaeus, 1758)**

Distribution. Europe, from the British Isles, France, and southern Scandinavia to eastern Europe and Asia Minor (Avibase 2023).

Recorded interactions with *H. cunea*. China [Dandong City, Liaoning Province] (Shu and Yu 1985), Europe (Warren and Tadić 1967).

Prey stage. Larva (Shu and Yu 1985; Warren and Tadić 1967), adult (Camerini 1994).

Notes. Preys heavily on *H. cunea* from early May to early June (Shu and Yu 1985).

Laniidae 伯劳科

***Lanius collurio* Linnaeus, 1758**

Distribution. Widespread in the Palearctic region, South Africa (Avibase 2023).

Recorded interactions with *H. cunea*. Europe (Warren and Tadić 1967).

Prey stage. Larva (Warren and Tadić 1967).

***Lanius minor* Gmelin, 1788**

Distribution. Iberian Peninsula to Siberia and central Asia, south Africa (Avibase 2023).

Recorded interactions with *H. cunea*. Europe (Warren and Tadić 1967).

Prey stage. Larva (Warren and Tadić 1967).

Muscicapidae 鹟科

***Luscinia luscinia* (Linnaeus, 1758)**

Distribution. North Eurasia, overwinters in east and south Africa (Avibase 2023).

Recorded interactions with *H. cunea*. Europe (Warren and Tadić 1967).

Prey stage. Larva (Warren and Tadić 1967).

***Luscinia megarhynchos* Brehm, 1831**

Distribution. West Europe, North Africa, and Asia Minor; tropical Africa (Avibase 2023).

Recorded interactions with *H. cunea*. Italy (Camerini 1994).

Prey stage. Adult (Camerini 1994).

***Muscicapa striata* (Pallas, 1764)**

Distribution. Europe to North Africa, Siberia, and Asia Minor (Avibase 2023).

Recorded interactions with *H. cunea*. Europe (Warren and Tadić 1967).

Prey stage. Larva (Warren and Tadić 1967).

***Oenanthe oenanthe* (Linnaeus, 1758)**

Distribution. British Isles to Mediterranean, and east to Siberia, Alaska, and northwest Canada (Yukon); winter to central Africa (Avibase 2023).

Recorded interactions with *H. cunea*. Italy (Camerini 1994).

Prey stage. Larva (Camerini 1994).

Notes. Preys on *H. cunea* during migration (Camerini 1994).

Oriolidae 黄鹂科

***Oriolus oriolus* (Linnaeus, 1758)**

Distribution. West Palearctic to east Siberia; winter to Africa and northwest India (Avibase 2023).

Recorded interactions with *H. cunea*. Europe (Warren and Tadić 1967).

Prey stage. Larva (Warren and Tadić 1967).

Paridae 山雀科

***Cyanistes caeruleus* (Linnaeus, 1758)**

Distribution. Continental Europe to north Spain, Sicily, north Turkey, and north Urals (Avibase 2023).

Recorded interactions with *H. cunea*. Europe (Warren and Tadić 1967).

Prey stage. Larva (Warren and Tadić 1967).

***Parus major* Linnaeus, 1758**

Distribution. Palaearctic, Mediterranean, Ethiopian, Nearctic, Neotropical, Oriental (Avibase 2023).

Recorded interactions with *H. cunea*. China [Dandong City, Liaoning Province] (Shu and Yu 1985), Europe (Warren and Tadić 1967).

Prey stage. Larva (Warren and Tadić 1967), Adult (Shu and Yu 1985; Camerini 1994).

Notes. Actively preys on *H. cunea* larvae (Camerini 1994); preys heavily from early May to early June in Liaoning Province, China (Shu and Yu 1985); may be used as a biocontrol agent by augmenting its population using artificial broods (Camerini 1994).

Passeridae 雀科

Passer domesticus (Linnaeus, 1758)

Distribution. Palaearctic, Mediterranean, Ethiopian, Nearctic, Neotropical, Oriental, Australian (Avibase 2023).

Recorded interactions with *H. cunea*. China [Dandong City, Liaoning Province] (Shu and Yu 1985), Europe (Warren and Tadić 1967).

Prey stage. Adult (Warren and Tadić 1967), larva (Shu and Yu 1985).

Notes. Preys heavily from early May to early June (Shu and Yu 1985).

Passer montanus (Linnaeus, 1758)

Distribution. Palaearctic, Mediterranean, Ethiopian, Nearctic, Neotropical, Oriental, Australian (Avibase 2023).

Recorded interactions with *H. cunea*. China [Dandong City, Liaoning Province] (Shu and Yu 1985), Japan [Hiratsuka Shrine] (Hasegawa and Itô 1967). Europe (Warren and Tadić 1967).

Prey stage. Adult (Warren and Tadić 1967; Hasegawa and Itô 1967; Camerini 1994), larva (Shu and Yu 1985).

Notes. Preys heavily from early May to early June (Shu and Yu 1985), played an important role in suppressing the reproduction of *H. cunea* (Hasegawa and Itô 1967).

Sturnidae 椋鸟科

Sturnus vulgaris Linnaeus, 1758

Distribution. Canary Is. and Iceland to Ural Mts., north Ukraine, and southeast Europe (Avibase 2023).

Recorded interactions with *H. cunea*. Italy (Camerini 1994).

Prey stage. Larva (Warren and Tadić 1967), pupa and adult (Camerini 1994).

Spodiopsar cineraceus (Temminck, 1835)

Distribution. Northeast Asia; winters in south China and Philippines (Avibase 2023).

Recorded interactions with *H. cunea*. Japan [Hiratsuka Shrine] (Hasegawa and Itô 1967).

Prey stage. Adult (Hasegawa and Itô 1967; Camerini 1994).

Notes. Played an important role in suppressing the reproduction of *H. cunea* (Hasegawa and Itô 1967).

Sylviidae 莺科

Curruca curruca (Linnaeus, 1758)

Distribution. East Siberia to north Altai and north Mongolia (Avibase 2023).

Recorded interactions with *H. cunea*. Europe (Warren and Tadić 1967).

Prey stage. Larva (Warren and Tadić 1967).

Turdidae 鶇科

***Saxicola rubetra* (Linnaeus, 1758)**

Distribution. West Palearctic; tropical and south Africa (Avibase 2023).

Recorded interactions with *H. cunea*. Italy (Camerini 1994).

Prey stage. Larva (Camerini 1994).

Notes. Preys on *H. cunea* during migrations (Camerini 1994).

***Turdus merula* Linnaeus, 1758**

Distribution. West Europe; introduced Southeast Australia, Tasmania, Norfolk, Lord Howe Is. (Avibase 2023).

Recorded interactions with *H. cunea*. Europe (Warren and Tadić 1967).

Prey stage. Larva (Warren and Tadić 1967).

***Turdus philomelos* Brehm, 1831**

Distribution. North and east Europe to central Asia; winters to North Africa and Iran (Avibase 2023).

Recorded interactions with *H. cunea*. Europe (Warren and Tadić 1967).

Prey stage. Larva (Warren and Tadić 1967).

Vireonidae 绿鹟科

***Vireo olivaceus* (Linnaeus, 1766)**

Distribution. West-central and Eastern US; overwinters in Cuba and central South America (Avibase 2023).

Recorded interactions with *H. cunea*. North America (Warren and Tadić 1967).

Prey stage. Larva (Warren and Tadić 1967).

Piciformes

Picidae 啄木鸟科

***Dendrocopos major* (Linnaeus, 1758)**

Distribution. Palaearctic, Mediterranean, Oriental (Avibase 2023).

Recorded interactions with *H. cunea*. Italy (Camerini 1994).

Prey stage. Larva (Warren and Tadić 1967), pupa (Camerini 1994).

***Dendrocopos medius* (Linnaeus, 1758)**

Distribution. Northwest Spain to France, Estonia, West Russia, Ukraine, Italy, Balkans (Avibase 2023).

Recorded interactions with *H. cunea*. Europe (Warren and Tadić 1967).

Prey stage. Larva (Warren and Tadić 1967).

***Dendrocopos syriacus* (Hemprich & Ehrenberg, 1833)**

Distribution. Southeast Europe, Transcaucasia, Turkey, and Iran to Israel and Jordan (Avibase 2023).

Recorded interactions with *H. cunea*. Europe (Warren and Tadić 1967).

Prey stage. Larva (Warren and Tadić 1967).

Strigiformes

Strigidae 鸱鹞科

***Asio otus* (Linnaeus, 1758)**

Distribution. Europe, Asia, North Africa, North America (Avibase 2023).

Recorded interactions with *H. cunea*. North America (Warren and Tadić 1967).

Prey stage. Larva (Warren and Tadić 1967).

Part II Parasitoids

Hymenoptera

Ichneumonidae 姬蜂科

***Apechthis compunctor* (Linnaeus, 1758)**

Distribution. Asia, Europe, USA (Yu et al. 2016).

Recorded interactions with *H. cunea*. Former USSR (Yu et al. 2016).

Host stage. Prepupa (Yu et al. 2016).

Parasitoid type. Endoparasitoid, solitary, koinobiont (Yu et al. 2016).

***Casitaria genuina* (Norton, 1863)**

Distribution. Canada, USA (Yu et al. 2016).

Recorded interactions with *H. cunea*. USA [New England or New York or New Jersey (Schaffner and Griswold 1934 as *Neonortonia major*); Colorado (Swain 1937 as *Neonortonia major*)].

Host stage. Larva (Warren and Tadić 1967).

Parasitoid type. Endoparasitoid (Yu et al. 2016).

***Casitaria limenitidis* (Howard, 1889)**

Distribution. Canada, USA (Yu et al. 2016).

Recorded interactions with *H. cunea*. USA [New England or New York or New Jersey (Schaffner and Griswold 1934 as *C. orgyiae*); Colorado (Swain 1937 as *C. orgyiae*)].

Host stage. Larva (Warren and Tadić 1967).

Parasitoid type. Endoparasitoid (Yu et al. 2016).

***Casitaria ischnogaster* Thomson, 1887**

Distribution. Europe, Palaeartic (Yu et al. 2016).

Recorded interactions with *H. cunea*. Former USSR (Yu et al. 2016).

Host stage. Larva (Yu et al. 2016).

Parasitoid type. Endoparasitoid, solitary (Yu et al. 2016).

***Casinarina nigripes* (Gravenhorst, 1829)**

Distribution. Europe, Palaeartic, Oriental (Yu et al. 2016).

Recorded interactions with *H. cunea*. China [Dandong City, Liaoning Province (Shu and Yu 1985 as *Apanteles ardimarium*)].

Host stage. Larva (Shu and Yu 1985).

Parasitoid type. Endoparasitoid, solitary (Shu and Yu 1985).

***Cratichneumon culex* (Müller, 1776)**

Distribution. Europe, Palaeartic (Yu et al. 2016).

Recorded interactions with *H. cunea*. Former USSR (Yu et al. 2016).

Host stage. Larva, pupa (Yu et al. 2016).

Parasitoid type. Endoparasitoid, solitary, polyphagous (Yu et al. 2016).

***Cratichneumon luteiventris* (Gravenhorst, 1820)**

Distribution. Europe, Palaeartic (Yu et al. 2016).

Recorded interactions with *H. cunea*. Former USSR (Yu et al. 2016).

Host stage. Larva, emerge from pupa (Yu et al. 2016).

Parasitoid type. Endoparasitoid, polyphagous (Yu et al. 2016).

***Diradops hyphantriae* Kasparyan & Pinson, 2007**

Distribution. Mexico (Yu et al. 2016).

Recorded interactions with *H. cunea*. Mexico (Kasparyan and Pinson 2007).

Host stage. Larva (Kasparyan and Pinson 2007).

Parasitoid type. Koinobiont endoparasitoid (Kasparyan and Pinson 2007).

***Enicospilus lineolatus* (Roman, 1913)**

Distribution. Brunei, China, India, Indonesia, Japan, Korea, Malaysia, Nepal, New Caledonia, Papua New Guinea, Philippines, Sri Lanka (Yu et al. 2016).

Recorded interactions with *H. cunea*. China (Yang et al. 2008).

Host stage. Larva-prepupa (Yang et al. 2008).

Parasitoid type. Solitary (Yang et al. 2008).

Notes. Parasitoid female to male ratio 1.8 (Yang et al. 2008); parasitism rate 1.5% (Yang et al. 2008).

***Enicospilus ramidulus* (Linnaeus, 1758)**

Distribution. Europe, Asia (Yu et al. 2016).

Recorded interactions with *H. cunea*. Turkey [Samsun Province (Sullivan et al. 2010)].

Host stage. Pupa (Sullivan et al. 2010).

Parasitoid type. Endoparasitoid, solitary (Sullivan et al. 2010), polyphagous (Yu et al. 2016).

***Enicospilus glabratus* (Say, 1835)**

Distribution. North America, South America (Yu et al. 2016).

Recorded interactions with *H. cunea*. USA [Colorado (Swain 1937 as *Eremotylus glabratus*)].

Host stage. Larva (Warren and Tadić 1967).

Parasitoid type. Polyphagous (Yu et al. 2016).

***Gelis* sp.**

Recorded interactions with *H. cunea*. Turkey [Samsun Province (Sullivan et al. 2010)].

Host stage. Pupa (Sullivan et al. 2010).

Parasitoid type. Endoparasitoid, solitary (Sullivan et al. 2010), polyphagous (Yu et al. 2016).

***Gotra octocincta* (Ashmead, 1906)**

Distribution. China, Japan, Korea (Yu et al. 2016).

Recorded interactions with *H. cunea*. China [Binzhou City, Shandong Province (Li 2011)].

Host stage. Larva-pupa (Li 2011).

Parasitoid type. Polyphagous (Yu et al. 2016).

Notes. Parasitism rate 0.2% (Li 2011).

***Gregopimpla inquisitor* (Scopoli, 1763)**

Distribution. Palaearctic, Europe, Canada (Yu et al. 2016).

Recorded interactions with *H. cunea*. Former USSR, South Korea (Yu et al. 2016).

Host stage. Larva, emerge from pupa (Yu et al. 2016).

Parasitoid type. Endoparasitoid, polyphagous (Yu et al. 2016).

***Gregopimpla kuwanae* (Viereck, 1912)**

Distribution. Palaearctic, Oriental (Yu et al. 2016).

Recorded interactions with *H. cunea*. China [Tai'an City, Shandong Province (Li 2011)].

Host stage. Larva-pupa (Li 2011).

Parasitoid type. Polyphagous (Yu et al. 2016).

Notes. Parasitism rate 1.3% (Li 2011).

***Gregopimpla malacosomae* (Seyrig, 1927)**

Distribution. Palaearctic, Europe (Yu et al. 2016).

Recorded interactions with *H. cunea*. Europe (Sullivan et al. 2010).

Host stage. Larva (Sullivan et al. 2010).

Parasitoid type. Polyphagous (Yu et al. 2016).

***Heterischnus truncator* (Fabricius, 1798)**

Distribution. Palaearctic, Europe (Yu et al. 2016).

Recorded interactions with *H. cunea*. Former USSR (Yu et al. 2016).

Host stage. Larva, emerged from pupa (Yu et al. 2016).

Parasitoid type. Endoparasitoid, polyphagous (Yu et al. 2016).

***Hyposoter fugitivus* (Say, 1835)**

Distribution. Brazil, Canada, USA (Yu et al. 2016).

Recorded interactions with *H. cunea*. USA [Colorado (Swain 1937)], Canada (Morris 1976b).

Host stage. Early instar larvae (Morris 1976b).

Parasitoid type. Solitary, endoparasitoid, koinobiont (Morris 1976b), polyphagous (Yu et al. 2016).

Notes. Parasitoid female to male ratio 0.67 (Morris 1976b).

***Hyposoter rivalis* (Cresson, 1872)**

Distribution. China, Canada, USA (Yu et al. 2016).

Recorded interactions with *H. cunea*. USA [Colorado (Swain 1937 as *H. pilosulus*)], Canada (Morris 1976b as *H. pilosulus*).

Host stage. Early instar larvae (Morris 1976b).

Parasitoid type. Solitary, endoparasitoid, koinobiont (Morris 1976b), polyphagous (Yu et al. 2016).

Notes. Parasitoid female to male ratio 1.27 (Morris 1976b).

***Ichneumon deliratorius* Linnaeus, 1758**

Distribution. Europe, Palaearctic, Nearctic (Yu et al. 2016).

Recorded interactions with *H. cunea*. North America (Townes 1944 as *Pterocormus cinctitarsis*).

Host stage. Larva (Warren and Tadić 1967).

Parasitoid type. Endoparasitoid, polyphagous (Yu et al. 2016).

***Iseropus stercorator* (Fabricius, 1793)**

Distribution. Europe, Palaearctic, Nearctic (Yu et al. 2016).

Recorded interactions with *H. cunea*. Former USSR (Yu et al. 2016).

Host stage. Larva, emerged from pupa (Yu et al. 2016).

Parasitoid type. Endoparasitoid, polyphagous (Yu et al. 2016).

***Itoplectis alternans* (Gravenhorst, 1829)**

Distribution. Europe, Palaearctic, USA (Yu et al. 2016).

Recorded interactions with *H. cunea*. Former USSR (Yu et al. 2016).

Host stage. Larva (Yu et al. 2016).
Parasitoid type. Polyphagous (Yu et al. 2016).

***Itopectis conquisitor* (Say, 1835)**

Distribution. Nearctic, Neotropical, Oceanic (Yu et al. 2016).
Recorded interactions with *H. cunea*. USA [Colorado (Swain 1937)], North America (Townes 1944).
Host stage. Larva (Warren and Tadić 1967).
Parasitoid type. Polyphagous (Yu et al. 2016).

***Itopectis maculator* (Fabricius, 1775)**

Distribution. Europe, Palaeartic, Oriental (Yu et al. 2016).
Recorded interactions with *H. cunea*. Europe (Sullivan et al. 2010).
Host stage. Larva, emerged from pupa (Sullivan et al. 2010).
Parasitoid type. Polyphagous (Yu et al. 2016).

***Itopectis viduata* (Gravenhorst, 1829)**

Distribution. Europe, Palaeartic, Nearctic (Yu et al. 2016).
Recorded interactions with *H. cunea*. Europe (Sullivan et al. 2010).
Host stage. Larva, emerged from pupa (Sullivan et al. 2010).
Parasitoid type. Polyphagous (Yu et al. 2016).

***Netelia (Netelia) testacea* (Gravenhorst, 1829)**

Distribution. Afrotropical, Australasian, Europe, Neotropical, Palaeartic, Oceanic, Oriental (Yu et al. 2016).
Recorded interactions with *H. cunea*. Europe (Warren and Tadić 1967).
Host stage. Pupa (Warren and Tadić 1967).
Parasitoid type. Polyphagous (Yu et al. 2016).

***Phobocampe pallipes* (Provancher, 1875)**

Distribution. Canada, USA (Yu et al. 2016).
Recorded interactions with *H. cunea*. USA [Colorado (Swain 1937 as *Hyposoter pallipes*)].
Host stage. Larva (Warren and Tadić 1967).
Parasitoid type. Polyphagous (Yu et al. 2016).

***Phygadeuon variabilis* Gravenhorst, 1829**

Distribution. Europe, Palaeartic, Oriental (Yu et al. 2016).
Recorded interactions with *H. cunea*. Former USSR (Yu et al. 2016).
Host stage. Larva, emerged from pupa (Yu et al. 2016).
Parasitoid type. Endoparasitoid, polyphagous (Yu et al. 2016).

***Pimpla aethiops* Curtis, 1828**

Distribution. Europe, East Asia (Yu et al. 2016).

Recorded interactions with *H. cunea*. China (Yang et al. 2008 as *Coccygomimus parnarae*).

Host stage. Pupa (Yang et al. 2008).

Parasitoid type. Solitary (Yang et al. 2008).

Notes. Parasitoid female to male ratio 2 (Yang et al. 2008); parasitism rate 0.34% (Yang et al. 2008).

***Pimpla aterrima* Gravenhorst, 1829**

Distribution. Europe, Palaeartic (Yu et al. 2016).

Recorded interactions with *H. cunea*. Asia (Warren and Tadić 1967).

Host stage. Pupa (Warren and Tadić 1967).

Parasitoid type. Polyphagous (Yu et al. 2016).

***Pimpla disparis* Viereck, 1911**

Distribution. East Asia, USA (Yu et al. 2016).

Recorded interactions with *H. cunea*. Japan [Tokyo (Tamura 1969 as *Coccygomimus disparis*)], China [Dandong City, Liaoning Province (Shu and Yu 1985 as *Coccygomimus disparis*)], Wugong Conty, Shaanxi Province (Ran and Zhao 1989 as *Coccygomimus disparis*)], China (Yang et al. 2008 as *Coccygomimus disparis*).

Host stage. Pupa (Ran and Zhao 1989; Yang et al. 2008).

Parasitoid type. Solitary (Yang et al. 2008), koinobiont (Ran and Zhao 1989).

Notes. Parasitoid female to male ratio 2.78 (Yang et al. 2008); parasitism rate 10% (Yang et al. 2008).

***Pimpla luctuosa* Smith, 1874**

Distribution. East Asia (Yu et al. 2016).

Recorded interactions with *H. cunea*. China [Wugong Conty, Shaanxi Province (Ran and Zhao 1989 as *Coccygomimus luctuosus*)], Dandong City, Liaoning Province (Shu and Yu 1985 as *Coccygomimus luctuosus*)].

Host stage. Pupa (Ran and Zhao 1989), mature larva and pupa (Shu and Yu 1985).

Parasitoid type. Solitary, koinobiont (Ran and Zhao 1989).

Notes. Parasitism rate 4–6% (Shu and Yu 1985).

***Pimpla pedalis* Cresson, 1865**

Distribution. Canada, USA (Yu et al. 2016).

Recorded interactions with *H. cunea*. North America (Warren and Tadić 1967).

Host stage. Larva (Warren and Tadić 1967).

Parasitoid type. Polyphagous (Yu et al. 2016).

***Pimpla rufipes* (Miller, 1759)**

Distribution. Europe, Asia, Oceanic (Yu et al. 2016).

Recorded interactions with *H. cunea*. Europe (Warren and Tadić 1967 as *P. instigator*), Turkey [Samsun Province (Sullivan et al. 2010)], Iran [Guilan province (Karami et al. 2023)].

Host stage. Pupa (Sullivan et al. 2010).

Parasitoid type. Endoparasitoid, solitary (Sullivan et al. 2010), polyphagous (Yu et al. 2016).

***Pimpla spuria* Gravenhorst, 1829**

Distribution. Europe, Asia (Yu et al. 2016).

Recorded interactions with *H. cunea*. Europe (Warren and Tadić 1967).

Host stage. Pupa (Warren and Tadić 1967).

Parasitoid type. Polyphagous (Yu et al. 2016).

***Pimpla turionellae* (Linnaeus, 1758)**

Distribution. Europe, Nearctic, Asia (Yu et al. 2016).

Recorded interactions with *H. cunea*. China (Yang et al. 2008 as *Coccygomyia turionellae*).

Host stage. Pupa (Yang et al. 2008).

Parasitoid type. Solitary parasitism (Yang et al. 2008).

Notes. Parasitoid female to male ratio 1.6 (Yang et al. 2008); parasitism rate 0.12% (Yang et al. 2008).

***Rhimphoctona (Xylophylax) megacephalus* (Gravenhorst, 1829)**

Distribution. Europe, Palaearctic, Oriental (Yu et al. 2016).

Recorded interactions with *H. cunea*. Europe (Warren and Tadić 1967 as *Pyraconon austriacus*).

Host stage. Pupa (Warren and Tadić 1967).

Parasitoid type. Polyphagous (Yu et al. 2016).

***Sinophorus validus* (Cresson, 1864)**

Distribution. Canada, USA (Yu et al. 2016).

Recorded interactions with *H. cunea*. USA [Colorado (Swain 1937 as *Eulimneria valida*)], Canada (Morris 1976b).

Host stage. First instar larvae (Morris 1976b).

Parasitoid type. Solitary parasitism, endoparasitoid, koinobiont (Morris 1976b), polyphagous (Yu et al. 2016).

Notes. Adults of *S. validus* emerge a week or two later than those of *H. cunea* and attack first-instar larvae (Morris 1976b). Parasitoid female to male ratio 0.92 (Morris 1976b).

***Therion morio* (Fabricius, 1781)**

Distribution. Canada, Mexico, Panama, USA (Yu et al. 2016).

Recorded interactions with *H. cunea*. USA [Colorado (Swain 1937)], North America (Warren and Tadić 1967).

Host stage. Pupa (Warren and Tadić 1967).

Parasitoid type. Polyphagous (Yu et al. 2016).

***Therion sassacus* Viereck, 1917**

Distribution. Canada, Mexico, USA (Yu et al. 2016).

Recorded interactions with *H. cunea*. USA [Colorado (Swain 1937)], Canada (Morris 1976b).

Host stage. Larva of late instar (Morris 1976b).

Parasitoid type. Solitary, endoparasitoid, koinobiont (Morris 1976b), polyphagous (Yu et al. 2016).

Notes. Parasitoid female to male ratio 0.89 (Morris 1976b).

***Theronia atalantae* (Poda, 1761)**

Distribution. Europe, Palaeartic, Oriental, USA (Yu et al. 2016).

Recorded interactions with *H. cunea*. Europe (Warren and Tadić 1967).

Host stage. Pupa (Warren and Tadić 1967).

Parasitoid type. Polyphagous (Yu et al. 2016).

***Theroscopus esenbeckii* (Gravenhorst, 1815)**

Distribution. Europe, West Palaeartic (Yu et al. 2016).

Recorded interactions with *H. cunea*. Europe (Warren and Tadić 1967 as *Hemiteles inaequalis* and *H. subzonatus*).

Host stage. Pupa (Warren and Tadić 1967).

Parasitoid type. Polyphagous (Yu et al. 2016).

***Trychosis legator* (Thunberg, 1822)**

Distribution. Palaeartic (Yu et al. 2016).

Recorded interactions with *H. cunea*. Europe (Warren and Tadić 1967 as *T. ingratus*).

Host stage. Pupa (Warren and Tadić 1967).

Parasitoid type. Polyphagous (Yu et al. 2016).

***Virgichneumon albilineatus* (Gravenhorst, 1820)**

Distribution. Europe, Asia (Yu et al. 2016).

Recorded interactions with *H. cunea*. Turkey [Samsun Province (Sullivan et al. 2010)].

Host stage. Pupa (Sullivan et al. 2010).

Parasitoid type. Endoparasitoid, solitary (Sullivan et al. 2010), polyphagous (Yu et al. 2016).

***Virgichneumon dumeticola* (Gravenhorst, 1829)**

Distribution. Europe, Asia (Yu et al. 2016).

Recorded interactions with *H. cunea*. Turkey [Samsun Province (Sullivan et al. 2010)], Iran [Guilan province (Karami et al. 2023)].

Host stage. Pupa (Sullivan et al. 2010).

Parasitoid type. Endoparasitoid, solitary (Sullivan et al. 2010), polyphagous (Yu et al. 2016).

Notes. Parasitoid female to male ratio 2.16 (Sullivan et al. 2010).

***Virgichneumon subcyaneus* (Cresson, 1864)**

Distribution. Canada, USA (Yu et al. 2016).

Recorded interactions with *H. cunea*. USA [New England or New York or New Jersey (Schaffner and Griswold 1934 as *Amblyteles pullatus*), Colorado (Swain 1937 as *Amblyteles subcyaneus*)], North America (Warren and Tadić 1967 as *Vulgichneumon subcyaneus*).

Host stage. Larva (Warren and Tadić 1967).

Parasitoid type. Polyphagous (Yu et al. 2016).

***Vulgichneumon brevicinctor* (Say, 1825)**

Distribution. Canada, USA (Yu et al. 2016).

Recorded interactions with *H. cunea*. USA [New England or New York or New Jersey (Schaffner and Griswold 1934 as *Amblyteles brevicinctor*), Colorado (Swain 1937 as *Amblyteles brevicinctor*)].

Host stage. Larva (Warren and Tadić 1967).

Parasitoid type. Solitary, polyphagous (Yu et al. 2016).

***Vulgichneumon leucaniae* (Uchida, 1924)**

Distribution. China, Japan, Russia (Yu et al. 2016).

Recorded interactions with *H. cunea*. China [Dandong City, Liaoning Province (Shu and Yu 1985); Wugong Conty, Shaanxi Province (Ran and Zhao 1989)].

Host stage. Pupa (Ran and Zhao 1989).

Parasitoid type. Solitary, koinobiont (Ran and Zhao 1989).

Braconidae 茧蜂科

***Aleiodes sanctihyacinthi* (Provancher, 1880)**

Distribution. Canada, USA, Serbia (Yu et al. 2016).

Recorded interactions with *H. cunea*. USA [Colorado (Swain 1937 as *Rogas hyphantriae*)].

Host stage. Larva (Warren and Tadić 1967).

Parasitoid type. Polyphagous (Yu et al. 2016).

***Apanteles (Dolichogenidea) lacteicolor* Viereck, 1911**

Distribution. Europe, Asia, North America (Yu et al. 2016).

Recorded interactions with *H. cunea*. USA [Colorado (Swain 1937 as *Apanteles lacteicolor*), New England (Marsh 1979)].

Host stage. Larva (Warren and Tadić 1967).

Parasitoid type. Polyphagous (Yu et al. 2016).

***Apanteles (Pholetesor) glacialis* (Ashmead, 1902)**

Distribution. North America (Yu et al. 2016).

Recorded interactions with *H. cunea*. USA [Alaska (Marsh 1979)].

***Apanteles singularis* (Yang & You, 2002)**

Distribution. China (Yu et al. 2016).

Recorded interactions with *H. cunea*. China [Yangling City, Shaanxi Province; Yantai City, Shandong Province (Yang et al. 2002 as *Dolichogenidea singularis*)].

Host stage. Larva 1–3 instar (Yang et al. 2002).

Parasitoid type. Koinobiont, primary, solitary, endoparasitoid, polyphagous (Yang et al. 2002).

Notes. 5–6% parasitism (Yang et al. 2002).

***Cotesia diacrisiae* (Gahan, 1917)**

Distribution. Canada, USA (Yu et al. 2016).

Recorded interactions with *H. cunea*. USA [Colorado (Swain 1937 as *Apanteles diacrisiae*)].

Host stage. Larva (Warren and Tadić 1967).

Parasitoid type. Polyphagous (Yu et al. 2016).

***Cotesia gregalis* Yang & Wei, 2002**

Distribution. China (Yu et al. 2016).

Recorded interactions with *H. cunea*. China [Tianjin City; Qinhuangdao City, Hebei Province; Dalian City, Liaoning Province; Yantai City, Shandong Province (Yang et al. 2002)].

Host stage. Larva (Yang et al. 2002).

Parasitoid type. Koinobiont, primary, gregarious, endoparasitoid (Yang et al. 2002).

Notes. Parasitism rate 6% (Yang et al. 2002).

***Cotesia hyphantriae* (Riley, 1887)**

Distribution. Bulgaria, Canada, China, Czech, Czechoslovakia, Germany, Greece, Hungary, Iran, Japan, Korea, Mexico, Moldova, Netherlands, Poland, Romania, Russia, Slovakia, Switzerland, Turkey, USA, Ukraine, UK, Yugoslavia (Yu et al. 2016).

Recorded interactions with *H. cunea*. USA [Colorado (Swain 1937 as *Apanteles hyphantriae*)], Turkey [Düzce (Avci et al. 2022 as *Apanteles hyphantriae*)]. Canada (Morris 1976b as *Apanteles hyphantriae*).

Host stage. Larva (Morris 1976b), egg and larva (Warren and Tadić 1967).

Parasitoid type. Solitary, endoparasitoid, koinobiont (Morris 1976b), polyphagous parasitism (Yu et al. 2016).

Notes. Parasitoid female to male ratio 1.38 (Morris 1976b).

***Cotesia ordinaria* (Ratzeburg, 1844)**

Distribution. Asia, Europe (Yu et al. 2016).

Recorded interactions with *H. cunea*. China [Dandong City, Liaoning Province (Shu and Yu 1985 as *Apanteles ardimarium*)].

Host stage. Larva (Shu and Yu 1985).

Parasitoid type. Endoparasitoid, gregarious parasitism (Shu and Yu 1985).

***Cotesia plutellae* (Kurdjumov, 1912)**

Distribution. Widespread all over the world (Yu et al. 2016).

Recorded interactions with *H. cunea*. Hungary [Hédervár (Papp 1988 as *Apanteles plutellae*)], Europe (Warren and Tadić 1967 as *Apanteles plutellae*).

Host stage. Larva (Warren and Tadić 1967).

Parasitoid type. Polyphagous (Yu et al. 2016).

***Cotesia ruficrus* (Haliday, 1834)**

Distribution. Widespread all over the world (Yu et al. 2016).

Recorded interactions with *H. cunea*. Hungary [Újszentmargita (Papp 1988 as *Apanteles ruficrus*)], Europe (Warren and Tadić 1967 as *Apanteles ruficrus*).

Host stage. Larva (Warren and Tadić 1967).

Parasitoid type. Polyphagous (Yu et al. 2016).

***Cotesia vanessae* (Reinhard, 1880)**

Distribution. Asia, North Africa, North America, Europe (Yu et al. 2016).

Recorded interactions with *H. cunea*. Europe (Warren and Tadić 1967 as *Apanteles vanessae*).

Host stage. Larva (Warren and Tadić 1967).

Parasitoid type. Polyphagous (Yu et al. 2016).

***Meteorus acronyctae* Muesebeck, 1923**

Distribution. USA (Yu et al. 2016).

Recorded interactions with *H. cunea*. USA [Colorado (Swain 1937)].

Host stage. Larva (Warren and Tadić 1967).

Parasitoid type. Polyphagous (Yu et al. 2016).

***Meteorus bakeri* Cook & Davis, 1891**

Distribution. Canada, USA (Yu et al. 2016).

Recorded interactions with *H. cunea*. USA [Colorado (Swain 1937)].

Host stage. Larva (Warren and Tadić 1967).

Parasitoid type. Polyphagous (Yu et al. 2016).

***Meteorus hyphantriae* Riley, 1887**

Distribution. Canada, USA (Yu et al. 2016).

Recorded interactions with *H. cunea*. USA [Washington DC (Riley 1887b), Colorado (Swain 1937)].

Host stage. Larva (Riley 1887b; Warren and Tadić 1967).

Parasitoid type. Polyphagous (Yu et al. 2016).

Notes. Performed well as natural enemy during outbreak and prevented further increase in *H. cunea* populations (Riley 1887b). The parasitism rate 0.08–3.94% of black fall webworm race, and 0.24–5.71% of orange race (Oliver 1964).

***Meteorus pendulus* (Müller, 1776)**

Distribution. Asia, North America, Europe (Yu et al. 2016).

Recorded interactions with *H. cunea*. USA [Colorado (Swain 1937 as *M. communis*)].

Host stage. Larva (Warren and Tadić 1967 as *M. communis*).

Parasitoid type. Polyphagous (Yu et al. 2016).

***Meteorus versicolor* (Wesmael, 1835)**

Distribution. Canada, USA (Yu et al. 2016).

Recorded interactions with *H. cunea*. USA [Colorado (Swain 1937)], Canada [New Brunswick and Nova Scotia (Morris 1976c)].

Host stage. Larva (Warren and Tadić 1967).

Parasitoid type. Polyphagous (Yu et al. 2016).

***Microplitis hyphantriae* Ashmead, 1898**

Distribution. Canada, USA (Yu et al. 2016).

Recorded interactions with *H. cunea*. USA [Washington DC (Ashmead 1898)].

Host stage. Larva (Warren and Tadić 1967).

Parasitoid type. Polyphagous (Yu et al. 2016).

Trigonalidae 钩腹蜂科

***Lycogaster pullata nevadensis* (Cresson, 1879)**

Distribution. Nearctic (Townes 1956).

Recorded interactions with *H. cunea*. USA [Boulder, Colorado (Townes 1956)], North America (Warren and Tadić 1967).

Host stage. Larva (Warren and Tadić 1967).

Parasitoid type. Probably a hyperparasitoid (Townes 1956).

Chalcididae 小蜂科

***Brachymeria femorata* (Panzer, 1801)**

Distribution. Europe, Asia (Noyes 2019).

Recorded interactions with *H. cunea*. Europe (Warren and Tadić 1967).

Host stage. Pupa (Warren and Tadić 1967).

Parasitoid type. Endoparasitoid, polyphagous (Noyes 2019).

***Brachymeria lasus* (Walker, 1841)**

Distribution. Australian, Europe, Asia, North Africa, USA (Noyes 2019).

Recorded interactions with *H. cunea*. Japan [Tokyo (Tamura 1969 as *B. obscurata*), China [Wugong Conty, Shaanxi Province (Ran and Zhao 1989)], China (Yang et al. 2008), Iran [Guilan province (Karami et al. 2023)].

Host stage. Larva (Ran and Zhao 1989), Pupa only in summer generations (Yang et al. 2008).

Parasitoid type. Solitary, polyphagous (Ran and Zhao 1989), gregarious parasitism (Yang et al. 2008).

Notes. Parasitoid female to male ratio 6.4 (Yang et al. 2008); parasitism rate 6.6–16.7% (Yang et al. 2008).

***Brachymeria ovata* (Say, 1824)**

Distribution. Nearctic, Neotropical (Noyes 2019).

Recorded interactions with *H. cunea*. North America (Peck 1963).

Host stage. Pupa (McDermott 1911; Burks 1936).

Parasitoid type. Polyphagous (Noyes 2019).

***Brachymeria tibialis* (Walker, 1834)**

Distribution. Europe, North Africa, East Asia, South Asia, USA (Noyes 2019).

Recorded interactions with *H. cunea*. Europe (Warren and Tadić 1967 as *B. intermedia*), Italy (Borioni 1991 as *B. intermedia*).

Host stage. Pupa (Warren and Tadić 1967).

Parasitoid type. Endoparasitoid, polyphagous (Noyes 2019).

***Brachymeria subconica* Boucek, 1992**

Distribution. Nearctic, Neotropical (Noyes 2019).

Recorded interactions with *H. cunea*. Mexico [Nuevo Leon (Noyes 2019)].

Host stage. Larva (Noyes 2019).

Parasitoid type. Primary, polyphagous (Noyes 2019).

***Conura meteori* Burks, 1940**

Distribution. Canada, USA, Mexico (Noyes 2019).

Recorded interactions with *H. cunea*. North America (Peck 1963 as *Cerastonicra meteori*).

Host stage. Cocoon (Riley 1888).

Parasitoid type. Hyperparasitoid (Riley 1888), polyphagous (Noyes 2019).

***Dirhinus himalayanus* Westwood, 1836**

Distribution. India, Iran, Japan, Malaysia, Pakistan, Philippines, Thailand, Turkmenistan, former USSR (Noyes 2019).

Recorded interactions with *H. cunea*. Japan (Habu 1960 as *D. luzonensis*).

Host stage. Pupa (Habu 1960).

Parasitoid type. Hyperparasitoid of tachinid, polyphagous (Habu 1960).

Encyrtidae 跳小蜂科

***Exoristobia klinoclavata* Xu, 2000**

Distribution. China (Noyes 2019).

Recorded interactions with *H. cunea*. China (Yang et al. 2008).

Host stage. Larva or pupa (Yang et al. 2008).

Parasitoid type. Hyperparasitoid, endoparasitoid, gregarious (Yang et al. 2008).

Notes. 47 wasps were reared on average from 1 host puparium, parasitoid female to male ratio 6.2, parasitism rate 1.6% (Yang et al. 2008).

Eulophidae 姬小蜂科

***Aprostocetus esurus* Riley, 1879**

Distribution. Canada, USA (Noyes 2019).

Recorded interactions with *H. cunea*. USA [Washington DC (Marlatt 1903; Peck 1963 as *Syntomosphyrum esurus*).

Host stage. Pupa (Marlatt 1903), larva (Warren and Tadić 1967).

Parasitoid type. Hyperparasitoid (Marlatt 1903), polyphagous (Peck 1963).

***Aprostocetus magniventer* Yang, 2003**

Distribution. China (Noyes 2019).

Recorded interactions with *H. cunea*. China [Yantai City, Shandong Province] (Yang et al. 2003b).

Host stage. Pupa (Yang et al. 2003b).

Parasitoid type. Endoparasitoid, gregarious parasitism (Yang et al. 2003b).

Notes. Parasitoid female to male ratio 2.6, highest parasitism rate 3.5% (Yang et al. 2003b).

***Baryscapus coerulescens* Ashmead, 1898**

Distribution. Canada, USA (Noyes 2019).

Recorded interactions with *H. cunea*. USA (Swain 1937 as *Tctrasticlms dotcni*), North America (Peck 1963 as *Tetrastinhus coerulescens*).

Host stage. Pupa (Swain 1937).

Parasitoid type. Hyperparasitoid (Swain 1937; Noyes 2019).

***Chouioia cunea* Yang, 1989**

Distribution. China, Iran, Italy, Japan, Korea (Noyes 2019).

Recorded interactions with *H. cunea*. China [Wugong County, Shaanxi Province (types); Beijing City (Yang 1989)], Italy [Cremona, Mantova, Pumenengo Bergamo (Boriani 1991), Pontirolo Nuovo, Bergamo; Eraclea, Venezia (Boriani 1994b)], Iran [Guilan province (Karami et al. 2023)], South Korea (Kim et al. 2011), Turkey [Samsun region (Sullivan et al. 2011); Düzce (Avci et al. 2022)].

Host stage. Pupa (Yang 1989).

Parasitoid type. Endoparasitoid, gregarious parasitism, polyphagous, hyperparasitoid of tachinids (Yang 1989).

Notes. Parasitoid female to male ratio 68, the highest parasitism rate 83.2% (in lab) (Yang 1989). Average parasitism 1.9%, average clutch size 117, average parasitoid female to male ratio 44.5 (Sullivan et al. 2011).

***Elachertus cacoeciae* Howard, 1885**

Distribution. Canada, USA (Noyes 2019).

Recorded interactions with *H. cunea*. USA [Washington DC (Howard 1885), North America (Peck 1963)].

Host stage. Larva (Warren and Tadić 1967).

Parasitoid type. Primary (Howard 1885).

***Elachertus cidariae* Ashmead, 1898**

Distribution. Bermuda, Canada, USA; induced to former Yugoslavia (Noyes 2019).

Recorded interactions with *H. cunea*. USA [New England or New York or New Jersey (Schaffner and Griswold 1934 as *E. hyphantriae* and *E. marylandicus*), North America (Warren and Tadić 1967 as *E. hyphantriae*; Burks 1979 as *E. hyphantriae* and *E. marylandicus*), USA [West Virginia (Butler 1993)].

Host stage. Larva (Warren and Tadić 1967 as *E. hyphantriae*).

Parasitoid type. Polyphagous, ectoparasitoid (Noyes 2019).

Notes. Parasitism rate 0.2% (Nordin et al. 1972 as *E. hyphantriae*).

***Elasmus atratus* Howard, 1897**

Distribution. Canada, USA (Noyes 2019).

Recorded interactions with *H. cunea*. Canada [New Brunswick; Nova Scotia] (Morris 1976a).

Host stage. Cocoon (Morris 1976a).

Parasitoid type. Hyperparasitoid (Morris 1976a), polyphagous (Noyes 2019).
Notes. Most prevalent hyperparasitoid (Morris 1976a).

***Elasmus nigrescens* Ashmead, 1895**

Unavailable name, determinations made by Mr. W. H. Ashmead (Webster 1895).

Distribution. USA (Webster 1895).

Recorded interactions with *H. cunea*. USA [Warren County, Southern Ohio (Webster 1895)].

Host stage. Cocoon (Webster 1895).

Parasitoid type. Hyperparasitoid (Webster 1895).

***Elasmus pullatus* Howard, 1885**

Distribution. USA (Noyes 2019).

Recorded interactions with *H. cunea*. USA [Ohio, Missouri, Kans (Peck 1963)].

***Elasmus varius* Howard, 1885**

Distribution. USA (Noyes 2019).

Recorded interactions with *H. cunea*. USA (Peck 1963).

***Neochrysocharis hyphantriae* Yoshimoto, 1978**

Distribution. Mexico, USA (Noyes 2019).

Recorded interactions with *H. cunea*. Mexico (Yoshimoto 1978).

Host stage. Pupa (Yoshimoto 1978).

Parasitoid type. Hyperparasitoid (Yoshimoto 1978).

***Pediobius bruchicida* Rondani, 1872**

Distribution. Afrotropical, Australia, Europe, Palaearctic, West Asia (Noyes 2019).

Recorded interactions with *H. cunea*. Europe (Noyes 2019).

Host stage. Pupa (Noyes 2019).

Parasitoid type. Facultative hyperparasitoid, endoparasitoid, gregarious (Noyes 2019).

***Pediobius elasmii* (Ashmead, 1904)**

Distribution. Australia, India, Indonesia, Malaysia, Papua New Guinea, China, Philippines, Sri Lanka (Noyes 2019).

Recorded interactions with *H. cunea*. China (Yang et al. 2008).

Host stage. Pupa (Yang et al. 2008).

Parasitoid type. Gregarious parasitism (Yang et al. 2008).

Notes. Parasitoid female to male ratio 2.8–13.6 (Yang et al. 2008); parasitism rate 2.6% (Yang et al. 2008).

***Pediobius pupariae* Yang, 2015**

Distribution. China (Noyes 2019).

Recorded interactions with *H. cunea*. China (Yang et al. 2015b).

Host stage. Pupa (Yang et al. 2015b).

Parasitoid type. Gregarious parasitism (Yang et al. 2015b).

***Pediobius pyrgo* Walker, 1839**

Distribution. Europe, Nearctic, Oriental, Palearctic (Noyes 2019).

Recorded interactions with *H. cunea*. Europe (Noyes 2019).

Host stage. Pupa (Noyes 2019).

Parasitoid type. Primary, hyperparasitoid (Noyes 2019).

***Rhichnopelte crassicornis* Nees, 1834**

Distribution. Palearctic, Europe, West Asia (Noyes 2019).

Recorded interactions with *H. cunea*. Iran [Gilan, Rezvanshahr (Yefremova et al. 2007)].

Host stage. Larva (Yefremova et al. 2007)

Parasitoid type. Gregarious parasitism, ectoparasitoid (Yefremova et al. 2007)

***Tetrastichomyia clisiocampae* (Ashmead, 1894)**

Distribution. Italy, USA (Noyes 2019).

Recorded interactions with *H. cunea*. Italy [Pontirolo Nuovo, Bergamo (Boriani 1994b)] (Boriani 1991 as *Tetrastichus goidanichi*).

Host stage. Pupa (Boriani 1994b).

Parasitoid type. Endoparasitoid, hyperparasitoid (Boriani 1994b).

***Tetrastichus litoreus* Yang, Qiao & Han, 2003**

Distribution. China (Noyes 2019).

Recorded interactions with *H. cunea*. China [Qinhuangdao City, Hebei Province (Yang et al. 2003a)].

Host stage. Pupa (Yang et al. 2003a).

Parasitoid type. Endoparasitoid, gregarious parasitism (Yang et al. 2003a).

Notes. Parasitoid female to male ratio 5 (Yang et al. 2003a) and 3 (Yang et al. 2008); parasitism rate 0.1% (Yang et al. 2008).

***Tetrastichus nigricoxae* Yang, 2003**

Distribution. China (Noyes 2019).

Recorded interactions with *H. cunea*. China [Yangling City, Shaanxi Province; Xuzhou City, Jiangsu Province (Yang and Wei 2003)].

Host stage. Pupa (Yang and Wei 2003).

Parasitoid type. Endoparasitoid, gregarious, oligophagous parasitism (Yang and Wei 2003).

Notes. Parasitoid female to male ratio 1.9, parasitism rate 6.2–13.4% (Yang and Wei 2003).

***Tetrastichus septentrionalis* Yang, 2001**

Distribution. China, South Korea (Noyes 2019).

Recorded interactions with *H. cunea*. China [Tianjin City; Dalian City, Liaoning Province; Qinhuangdao City, Hebei Province; Yantai City, Shandong Province], South Korea [Seoul] (Yang et al. 2001; Kim et al. 2011).

Host stage. Pupa (Yang et al. 2001).

Parasitoid type. Endoparasitoid, gregarious, oligophagous (Yang et al. 2001).

Notes. Parasitoid female to male ratio 10, the highest parasitism rate 24% (Yang et al. 2001), 3.2% (Yang et al. 2008).

***Tetrastichus shandongensis* Yang, 2003**

Distribution. China (Noyes 2019).

Recorded interactions with *H. cunea*. China [Yantai City, Shandong Province (Yang and Wei 2003)].

Host stage. Pupa (Yang and Wei 2003).

Parasitoid type. Endoparasitoid, gregarious (Yang and Wei 2003).

Notes. Parasitoid female to male ratio 3.2, the parasitism rate 6.2% (Yang and Wei 2003), 3.6% (Yang et al. 2008).

***Trichospilus albiflagellatus* Yang & Wang, 2015**

Distribution. China (Noyes 2019).

Recorded interactions with *H. cunea*. China [Yantai City, Shandong Province (Yang et al. 2015a)].

Host stage. Pupa (Yang et al. 2015a).

Parasitoid type. Endoparasitoid, gregarious (Yang et al. 2015a).

Notes. Average parasitoid female to male ratio 58.56, highest parasitism rate 28.6% (Yang et al. 2001).

Eupelmidae 旋小蜂科

***Eupelmus fulvipes* Förster, 1860**

Distribution. Austria, Azerbaijan, China, France, Georgia, Germany, Hungary, Iran, Italy, Montenegro, Poland, Romania, Russia, Serbia, Spain, Turkey (Gibson and Fusu 2016; Noyes 2019; Yang et al. 2008).

Recorded interactions with *H. cunea*. China [Qinhuangdao City, Hebei Province (Yang et al. 2008)].

Host stage. Pupa (Yang et al. 2008).

Parasitoid type. Gregarious, endoparasitoid (Yang et al. 2008).

Notes. Parasitism rates 0.1%, 3 females were reared from a single pupa (Yang et al. 2008).

Eurytomidae 广肩小蜂科

***Eurytoma appendigaster* Swederus, 1795**

Distribution. Europe, North Africa, North America, China (Noyes 2019).

Recorded interactions with *H. cunea*. Europe (Noyes 2019).

Host stage. Pupa (Noyes 2019).

Parasitoid type. Primary, polyphagous (Noyes 2019).

***Eurytoma goidanichi* Boucek, 1970**

Distribution. Europe, Iran (Noyes 2019), China (Yang et al. 2008).

Recorded interactions with *H. cunea*. China (Yang et al. 2008).

Host stage. Pupa (Yang et al. 2008)

Parasitoid type. Gregarious, hyperparasitoid (Yang et al. 2008).

Notes. Parasitoid female to male ratio 2.2, parasitism rate 22% (Yang et al. 2008).

***Eurytoma rosae* Nees, 1834**

Distribution. Europe, Asia, North Africa, Argentina (Noyes 2019).

Recorded interactions with *H. cunea*. Romania [Piatra Craiului National Park (Popescu 2006)].

Host stage. Pupa (Noyes 2019).

Parasitoid type. Primary, polyphagous (Noyes 2019).

***Eurytoma verticillata* (Fabricius, 1798)**

Distribution. Europe, East Asia, North America (Noyes 2019).

Recorded interactions with *H. cunea*. Italy [Eraclea, Venezia (Boriani 1994b)].

Host stage. Pupa (Boriani 1994b).

Parasitoid type. Endoparasitoid, hyperparasitoid, polyphagous (Boriani 1994b).

Perilampidae 巨胸小蜂科

***Perilampus hyalinus* Say, 1929**

Distribution. Canada, Cuba, Mexico, Peru, Puerto Rico, USA (Noyes 2019).

Recorded interactions with *H. cunea*. Canada, USA (Peck 1963).

Host stage. Pupa or cocoon (Smith 1912).

Parasitoid type. Hyperparasitoid (Smith 1912; Tripp 1962).

Pteromalidae 金小蜂科

***Catolaccus aeneoviridis* Girault, 1911**

Distribution. Bermuda, Canada, Mexico, USA, Nearctic (Noyes 2019).

Recorded interactions with *H. cunea*. USA [Colorado (Swain 1937)].

Host stage. Cocoon (Swain 1937).

Parasitoid type. Hyperparasitoid (Swain 1937).

***Coelopisthia extenta* (Walker, 1835)**

Distribution. Europe, Kazakhstan, Uzbekistan, USA (Noyes 2019).

Recorded interactions with *H. cunea*. Italy [Pontirolo Nuovo, Bergamo; Eraclea, Venezia (Borioni 1994b)].

Host stage. Pupa (Borioni 1994b).

Parasitoid type. Endoparasitoid, gregarious, hyperparasitoid (Borioni 1994b).

***Conomorium amplum* (Walker, 1835)**

Distribution. Belgium, Canary Islands, Czech, France, Germany, Greece, Hungary, Italy, Kazakhstan, Madeira, Netherlands, China, Romania, Spain, Sweden, Switzerland, Tselinograd Obl., UK, Uzbekistan (Noyes 2019).

Recorded interactions with *H. cunea*. Italy [Pianengo, Cremona; Bisnate, Milano, Pontirolo Nuovo, Bergamo (Borioni 1991 as *C. patulum*; Borioni 1994a)], Turkey [Samsun region (Sullivan et al. 2011)].

Host stage. Pupa (Borioni 1994a).

Parasitoid type. Endoparasitoid, gregarious (Borioni 1994a).

Notes. Average parasitism 0.047%, average clutch size 1.5, average parasitoid female to male ratio 0.5 (Sullivan et al. 2011).

***Conomorium cuneae* Yang & Baur, 2004**

Distribution. China (Noyes 2019).

Recorded interactions with *H. cunea*. China [Tianjin City; Yantai City, Shandong Province; Wugong City, Shaanxi Province, Dalian City, Liaoning Province; Qinhuangdao City, Hebei Province (Yang and Baur 2004)].

Host stage. Pupa (Yang and Baur 2004).

Parasitoid type. Endoparasitoid, gregarious (Yang and Baur 2004).

Notes. Parasitoid female to male ratio 7.5, highest parasitism rate 3.6–12.2% (Yang and Baur 2004), 1.2% (Yang et al. 2008).

***Dibrachys maculipennis* Szelenyi, 1957**

Distribution. Canada, Hungary, Kirgizia, Slovakia, Sweden (Noyes 2019).

Recorded interactions with *H. cunea*. Europe (Noyes 2019).

Host stage. Cocoon (Noyes 2019).

Parasitoid type. Hyperparasitoid (Noyes 2019).

***Dibrachys microgastri* (Bouche, 1834)**

Distribution. Europe, Asia, North America (Noyes 2019).

Recorded interactions with *H. cunea*. Italy [Pontirolo Nuovo, Bergamo (Borioni 1994b as *D. boarmiae*)], China (Yang et al. 2008 as *D. cavus*), Turkey [Samsun region (Sullivan et al. 2011 as *D. boarmiae*)], North America (Warren and Tadić 1967).

Host stage. Pupa (Borioni 1994b), larva-pupa (Yang et al. 2008).

Parasitoid type. Endoparasitoid, gregarious, hyperparasitoid, polyphagous (Borioni 1994b), gregarious, hyperparasitoid (Yang et al. 2008).

Notes. Parasitoid female to male ratio 8.0, highest parasitism rate 0.15% (Yang et al. 2008). Average parasitism 1.2%, average clutch size 10, average female to male ratio 24 (Sullivan et al. 2011).

***Dirhinus anthracia* Walker, 1846**

Distribution. Australia, India, Philippines, South Africa, China, Vietnam, Zambia (Noyes 2019).

Recorded interactions with *H. cunea*. South Korea (Kim et al. 2011).

Host stage. Pupa (Kim et al. 2011).

Parasitoid type. polyphagous (Noyes 2019).

***Hypopteromalus inimicus* Muesebeck, 1927**

Distribution. Canada, USA (Noyes 2019).

Recorded interactions with *H. cunea*. Canada [New Brunswick, Nova Scotia (Morris 1976a)].

Host stage. Cocoon (Morris 1976a).

Parasitoid type. Hyperparasitoid (Morris 1976a).

***Hypopteromalus percussor* Girault, 1917**

Distribution. Canada, USA (Noyes 2019).

Recorded interactions with *H. cunea*. USA Colorado (Swain 1937)].

Host stage. Cocoon (Swain 1937).

Parasitoid type. Hyperparasitoid (Swain 1937).

***Hypopteromalus tabacum* Fitch, 1864**

Distribution. Canada, USA (Noyes 2019).

Recorded interactions with *H. cunea*. USA (Peck 1951).

***Psychophagus omnivorus* (Walker, 1835)**

Distribution. Europe, West Asia, North Africa, North America (Noyes 2019).

Recorded interactions with *H. cunea*. Turkey [Samsun region (Sullivan et al. 2011), Italy (Borioni 1991), Iran [Guilan province (Karami et al. 2023)]

Host stage. Pupa (Sullivan et al. 2011).

Parasitoid type. Gregarious, polyphagous (Noyes 2019).

Notes. Average parasitism 6.7%, average clutch size 60, average parasitoid female to male ratio 0.92 (Sullivan et al. 2011).

***Pteromalus apum* Retzius, 1783**

Distribution. Argentina, Canada, Russia, USA, Europe (Noyes 2019).

Recorded interactions with *H. cunea*. Europe (Warren and Tadić 1967 as *Pteromalus planiscuta*).

Host stage. Pupa (Warren and Tadić 1967).

***Pteromalus bifoveolatus* Foerster, 1861**

Distribution. Europe (Noyes 2019), China (Yang et al. 2008).

Recorded interactions with *H. cunea*. China (Yang et al. 2008).

Host stage. Pupa (Yang et al. 2008).

Parasitoid type. Gregarious parasitism (Yang et al. 2008), polyphagous (Noyes 2019).

Notes. Parasitoid female to male ratio 5.5, highest parasitism rate 0.2% (Yang et al. 2008).

***Pteromalus egregious* Foerster, 1841**

Distribution. Canada, Germany, Hungary, USA (Noyes 2019).

Recorded interactions with *H. cunea*. Europe (Noyes 2019).

***Pteromalus phycidis* Ashmead, 1898**

Distribution. Canada, USA (Noyes 2019).

Recorded interactions with *H. cunea*. North America (Noyes 2019).

Parasitoid type. Hyperparasitoid (Noyes 2019).

***Trichomalopsis cotesiae* Yang, 2015**

Distribution. China (Noyes 2019).

Recorded interactions with *H. cunea*. China (Yang et al. 2015b).

Host stage. Larva (Yang et al. 2015b).

Parasitoid type. Hyperparasitoid (Yang et al. 2015b).

***Trichomalopsis genalis* (Graham, 1969)**

Distribution. Europe (Noyes 2019), China (Yang et al. 2008).

Recorded interactions with *H. cunea*. China (Yang et al. 2008).

Host stage. 4th instar larva (Yang et al. 2008).

Parasitoid type. Gregarious, polyphagous (Yang et al. 2008).

Notes. Parasitoid female to male ratio 1.6, parasitism rate 0.2% (Yang et al. 2008).

***Trichomalopsis germanica* (Graham, 1969)**

Distribution. Germany, Sweden (Noyes 2019), China (Yang et al. 2008).

Recorded interactions with *H. cunea*. China (Yang et al. 2008 as *T. germanicus*).

Host stage. Pupa (Yang et al. 2008)

Parasitoid type. Gregarious, hyperparasitoid (Yang et al. 2008).

Notes. Parasitoid female to male ratio 2, highest parasitism rate 15% (Yang et al. 2008).

***Trichomalopsis hemiptera* Walker, 1835**

Distribution. Europe, North America, East Asia (Noyes 2019).

Recorded interactions with *H. cunea*. USA [New England (Peck 1963 as *Eupterotnalus hernipterus*, laboratory rearing)].

Parasitoid type. Hyperparasitoid (Noyes 2019).

Torymidae 长尾小蜂科

***Monodontomerus aeneus* Fonscolombe, 1832**

Distribution. Europe, Iran, Kazakhstan, China, USA, Chile (Noyes 2019).

Recorded interactions with *H. cunea*. Europe (Noyes 2019).

Parasitoid type. Polyphagous (Noyes 2019).

***Monodontomerus aereus* Walker, 1834**

Distribution. Europe, Asia, North Africa, North America (Noyes 2019).

Recorded interactions with *H. cunea*. North America, Europe (Warren and Tadić 1967).

Host stage. Larva (Warren and Tadić 1967).

Parasitoid type. Polyphagous (Noyes 2019).

***Monodontomerus dentipes* Dalman, 1820**

Distribution. Europe, Asia, North America (Noyes 2019).

Recorded interactions with *H. cunea*. Europe (Noyes 2019).

Parasitoid type. Polyphagous (Noyes 2019).

***Monodontomerus minor* (Ratzeburg, 1848)**

Distribution. Europe, Asia, North America (Noyes 2019).

Recorded interactions with *H. cunea*. Italy [Eraclea, Venezia (Boriani 1994b)], China (Yang et al. 2008).

Host stage. Pupa (Boriani 1994b), larva-pupa (Yang et al. 2008).

Parasitoid type. Endoparasitoid, gregarious, hyperparasitoid, polyphagous (Boriani 1994b), hyperparasitoid (Yang et al. 2008).

Notes. Parasitoid female to male ratio 1.4, highest parasitism rate 0.15% (Yang et al. 2008).

Trichogrammatidae 赤眼蜂科

***Trichogramma brassicae* Bezdenko, 1968**

Distribution. Europe, Asia, Australia, North America (Noyes 2019).

Recorded interactions with *H. cunea*. Turkey [Düzce (Avci et al. 2022)].

Host stage. Egg (Avci et al. 2022).

Parasitoid type. Polyphagous (Noyes 2019).

***Trichogramma cacaeciae* Marchal, 1927**

Distribution. Europe, Asia, North America, South America (Noyes 2019).

Recorded interactions with *H. cunea*. Moldova (Plugaru 1979).

Host stage. Egg (Plugaru 1979).

Parasitoid type. Polyphagous (Noyes 2019).

***Trichogramma dendrolimi* Matsumura, 1926**

Distribution. Europe, Asia, Chile (Noyes 2019).

Recorded interactions with *H. cunea*. Asia (Warren and Tadić 1967), South Korea (Noyes 2019), China [Beijing, tested in lab, unpublished data, CLM].

Host stage. Egg (Warren and Tadić 1967; Noyes 2019).

Parasitoid type. Polyphagous, primary (Noyes 2019).

***Trichogramma evanescens* Westwood, 1833**

Distribution. Europe, Asia, North America, South America (Noyes 2019).

Recorded interactions with *H. cunea*. Europe (Warren and Tadić 1967).

Host stage. Egg (Warren and Tadić 1967).

Parasitoid type. Polyphagous (Noyes 2019).

***Trichogramma minutum* Riley, 1871**

Distribution. Europe, Asia, Africa, North America, South America (Noyes 2019).

Recorded interactions with *H. cunea*. Europe (Warren and Tadić 1967), Italy (Viggiani and Laudonia 1989).

Host stage. Egg (Warren and Tadić 1967).

Parasitoid type. Polyphagous (Noyes 2019).

***Trichogramma ostriniae* Pang & Chen, 1974**

Distribution. China, Japan, South Korea, South Africa, USA (Noyes 2019).

Recorded interactions with *H. cunea*. China [Beijing, tested in lab, unpublished data, CLM].

Host stage. Egg (unpublished data).

Parasitoid type. Polyphagous (Noyes 2019).

***Trichogramma piceum* Dyurich, 1987**

Distribution. Italy, Moldova (Noyes 2019).

Recorded interactions with *H. cunea*. Italy (Noyes 2019).

Host stage. Egg (Noyes 2019).

Parasitoid type. Polyphagous (Noyes 2019).

Scelionidae 缘腹细蜂科

***Telenomus chloropus* (Thomson, 1861)**

Distribution. Ukraine, Turkey, UK, Russia, Moldavia, Kazakhstan, Georgia, Kazakhstan, Far East, France, Hungary, Japan, Spain, Sweden, USA, Ireland, Iran (Samin et al. 2010).

Recorded interactions with *H. cunea*. Europe (Warren and Tadić 1970 as *Telenomus mayri*).

Host stage. Egg (Warren and Tadić 1970).

***Telenomus bifidus* Riley, 1887**

Distribution. USA (Riley 1887a).

Recorded interactions with *H. cunea*. USA [Washington, D.C. (Riley 1887a)].

Host stage. Egg (Riley 1887a).

Parasitoid type. Endoparasitoid, oligophagous (Riley 1887b),

Notes. Parasitize eggs of first and second generations of fall webworm. Useful natural enemy (Riley 1887a).

Diptera

Tachinidae 寄蝇科

***Archytas (Nemochaeta) aterrimus* (Robineau-Desvoidy, 1830)**

Distribution. Canada, USA, Mexico (O'Hara et al. 2020).

Recorded interactions with *H. cunea*. North America (Sullivan and Ozman-Sullivan 2012).

***Bactromyia aurulenta* (Meigen, 1824)**

Distribution. China, Europe, Japan, South Korea, Russia, Transcaucasia (O'Hara et al. 2020).

Recorded interactions with *H. cunea*. Japan [Honshu, Ibaraki (Tschorsnig 2017)].

***Bessa parallela* (Meigen, 1824)**

Distribution. China, Europe, Japan, Mongolia, Russia, Armenia (O'Hara et al. 2020).

Recorded interactions with *H. cunea*. Japan [Tsukuba (Watanabe 2005)], Serbia, Hungary, Japan, Montenegro, Moldova [Kishinev], Russia [European part], Japan [Honshu, Tokyo, Fuchu, Nara] (Tschorsnig 2017). Asia, Europe (Sullivan and Ozman-Sullivan 2012 as *Bessa selecta*, *Ptychomyia selecta*).

Host stage. Pupa (Warren and Tadić 1967 as *B. fugax* and *B. selecta*).

***Blepharipa sericariae* (Rondani, 1870)**

Distribution. Palaearctic: China, Japan (O'Hara et al. 2020).

Recorded interactions with *H. cunea*. Japan [Honshu, Tokyo] (Tschorsnig 2017).

***Blepharipa zebina* (Walker, 1849)**

Distribution. China, Japan, North Korea, South Korea, Russia, India, Myanmar, Nepal, Sri Lanka, Thailand (O'Hara et al. 2020).

Recorded interactions with *H. cunea*. China [Wugong County, Shaanxi Province (Ran and Zhao 1989)].

Host stage. Pupa (Ran and Zhao 1989).

Parasitoid type. Solitary, polyphagous (Ran and Zhao 1989).

***Blondelia eufitchiae* (Townsend, 1892)**

Distribution. Canada, USA (O'Hara et al. 2020).

Recorded interactions with *H. cunea*. USA [Colorado (Swain 1937 as *Masicera eufitchiae*)], North America (Sullivan and Ozman-Sullivan 2012).

Host stage. Larva (Warren and Tadić 1967).

***Blondelia hyphantria* (Tothill, 1922)**

Distribution. Canada, USA, China (O'Hara et al. 2020).

Recorded interactions with *H. cunea*. Canada (Tothill 1922 as *Lydella hyphanthrae*), USA [Colorado] (Swain 1937 as *Anetia hyphanthrae* and *Lydella hyphanthrae*), North America (Sullivan and Ozman-Sullivan 2012).

Host stage. Larva-pupa (Tothill 1922), larva (Warren and Tadić 1967).

Parasitoid type. Solitary (Tothill 1922).

Notes. Maggot travels from one feeding area to another (Tothill 1922).

***Blondelia nigripes* (Fallén, 1810)**

Distribution. Central Asia, China, Japan, South Korea, Iran, Mongolia, Russia, Transcaucasia, Europe (O'Hara et al. 2020).

Recorded interactions with *H. cunea*. Europe (Sullivan and Ozman-Sullivan 2012), Hungary, Russia (Tschorsnig 2017).

***Blondelia obconica* (Walker, 1853)**

Distribution. USA (O'Hara et al. 2020).

Recorded interactions with *H. cunea*. North America (Sullivan and Ozman-Sullivan 2012 as *Tachina obconica*).

***Cadurcia* sp.**

Distribution. Europe (Sullivan and Ozman-Sullivan 2012).

Recorded interactions with *H. cunea*. Europe (Sullivan and Ozman-Sullivan 2012).

***Carcelia bombylans* Robineau-Desvoidy, 1830**

Distribution. China, Europe, Japan, Russia, Azerbaijan (O'Hara et al. 2020).

Recorded interactions with *H. cunea*. Italy (Boriani 1991). Serbia, Italy [Lombardia, Mantua] (Tschorsnig 2017).

***Carcelia gnava* (Meigen, 1824)**

Distribution. China, Europe, Japan, South Korea, Russia, Armenia (O'Hara et al. 2020).

Recorded interactions with *H. cunea*. South Korea (Tschorsnig 2017).

***Carcelia kockiana* (Townsend, 1927)**

Distribution. China (Ran and Zhao 1989), India, Indonesia, Malaysia, Philippines, Papua New Guinea (O'Hara et al. 2020).

Recorded interactions with *H. cunea*. China [Wugong County, Shaanxi Province (Ran and Zhao 1989)].

Host stage. Pupa (Ran and Zhao 1989).

Parasitoid type. Solitary, polyphagous (Ran and Zhao 1989).

***Carcelia matsukarehae* (Shima, 1969)**

Distribution. China, Japan, Russia (O'Hara et al. 2020).

Recorded interactions with *H. cunea*. China [Shandong (Tschorsnig 2017)].

***Carcelia protuberans* (Aldrich & Webber, 1924)**

Distribution. Canada, USA (O'Hara et al. 2020).

Recorded interactions with *H. cunea*. USA [Colorado (Swain 1937 as *Zenillia protuberans*)], North America (Sullivan and Ozman-Sullivan 2012).

Host stage. Larva (Warren and Tadić 1967).

***Carcelia sumatrana* Townsend, 1927**

Distribution. China, Japan, Russia, Indonesia, Malaysia, Sri Lanka (O'Hara et al. 2020).

Recorded interactions with *H. cunea*. Japan [Honshu, Tokyo, Fuchu City (Tschorsnig 2017)].

***Ceromasia auricaudata* Townsend, 1908**

Distribution. Canada, USA (O'Hara et al. 2020).

Recorded interactions with *H. cunea*. North America (Sullivan and Ozman-Sullivan 2012).

***Ceromasia rubrifrons* (Macquart, 1834)**

Distribution. Uzbekistan, China, Europe, Japan, Israel, Mongolia, Morocco, Russia, Transcaucasia (O'Hara et al. 2020).

Recorded interactions with *H. cunea*. Moldova (Tschorsnig 2017).

***Chetogena claripennis* (Macquart, 1848)**

Distribution. Canada, USA, Puerto Rico, Mexico, Venezuela (O'Hara et al. 2020).

Recorded interactions with *H. cunea*. USA [Colorado (Swain 1937 as *Phorocera claripennis*)], North America (Warren and Tadić 1967 as *Euphorocera claripenn*, Sullivan and Ozman-Sullivan 2012).

Host stage. Larva (Warren and Tadić 1967).

***Chetogena scutellaris* (van der Wulp, 1890)**

Distribution. USA, Venezuela (O'Hara et al. 2020).

Recorded interactions with *H. cunea*. USA [Colorado (Swain 1937 as *Phorocera floridensis*)], North America (Warren and Tadić 1967 as *Euphorocera floridensis*, Sullivan and Ozman-Sullivan 2012), Mexico [Tamaulipas (Kasparyan and Pinson 2007)].

***Clemelis pullata* (Meigen, 1824)**

Distribution. China, Europe, Israel, Mongolia, Morocco, Russia, Armenia (O'Hara et al. 2020).

Recorded interactions with *H. cunea*. Moldova [Cahul (Tschorsnig 2017)].

***Compsilura concinnata* (Meigen, 1824)**

Distribution. Canada, USA, China, Europe, Japan, Kazakhstan, North Korea, South Korea, Iran, Israel, Lebanon, Algeria, Egypt, Morocco, Russia, Armenia, Azerbaijan, Nigeria, South Africa, India, Indonesia, Malaysia, Australia, Papua New Guinea (O'Hara et al. 2020).

Recorded interactions with *H. cunea*. Canada (Morris 1976b), Italy (Borini 1991), Turkey [Samsun Province (Sullivan et al. 2012)], Iran [Guilan province (Karami et al. 2023)], Japan [Tsukuba (Watanabe 2005)], China (Yang et al. 2008). Austria [Burgenland, Weiden], Serbia [Vojvodina], Hungary, Romania [Bukarest], Ukraine [Transcarpathia], Slovakia [Gabčíkovo, Nitra env.], Japan [Honshu, Gunma], France [Gironde and/or Landes], Bulgaria [Silistra], Turkey [Samsun], Moldova, Italy [Lombardia, Ponte Merlano, Emilia-Romagna, Mantova], Russia, [Voronezh Region], Azerbaijan [Guba-Khachmaz Region], China [Shangdong, Hebei, Liaoning] (Tschorsnig 2017).

Host stage. Pupa and larva (Warren and Tadić 1967), pupa (Sullivan et al. 2012).

Parasitoid type. Endoparasitoid, solitary or gregarious, polyphagous (Yang et al. 2008).

Notes. Parasitism rate is higher for wandering *H. cunea* larvae than in feeding larvae (Watanabe 2005). Parasitoid female to male ratio 1.5 (Yang et al. 2008); parasitism rate 2% (Yang et al. 2008). Female injects fully incubated eggs directly into the host haemocoel. Parasitism 0.14% in Samsun (Sullivan et al. 2012).

***Drino facialis* (Townsend, 1928)**

Distribution. China, India, Indonesia, Malaysia, Philippines, Sri Lanka, Thailand (O'Hara et al. 2020).

Recorded interactions with *H. cunea*. China [Wugong Conty, Shaanxi Province (Ran and Zhao 1989)].

Host stage. Pupa (Ran and Zhao 1989).

Parasitoid type. Solitary, polyphagous (Ran and Zhao 1989).

***Drino inconspicua* (Meigen, 1830)**

Distribution. China, Europe, Algeria, Egypt, Russia, Armenia, Azerbaijan, Georgia (O'Hara et al. 2020).

Recorded interactions with *H. cunea*. Europe (Sullivan and Ozman-Sullivan 2012 as *Drina incospicua*, *Sturmia inconspicua*), Serbia [Vojvodina], Hungary (Tschorsnig 2017).

Host stage. Larva (Warren and Tadić 1967).

***Drino inconspicuoides* (Baranov, 1932)**

Distribution. China, Japan (O'Hara et al. 2020).

Recorded interactions with *H. cunea*. Japan [Tsukuba (Watanabe 2005)].

Notes. Parasitism rate is higher in wandering *H. cunea* larvae than in feeding larvae (Watanabe 2005).

***Eurysthaea scutellaris* (Robineau-Desvoidy, 1849)**

Distribution. China, Europe, Japan, Russia, Armenia, Azerbaijan (O'Hara et al. 2020).

Recorded interactions with *H. cunea*. Serbia (Tschorsnig 2017).

***Exorista fasciata* (Fallén, 1820)**

Distribution. China, Europe, Mongolia, Egypt, Russia, Transcaucasia (O'Hara et al. 2020).

Recorded interactions with *H. cunea*. China [Wugong County, Shaanxi Province (Ran and Zhao 1989); Dandong City, Liaoning Province (Shu and Yu 1985)].

Host stage. Pupa and larva (Warren and Tadić 1967), Pupa (Ran and Zhao 1989).

Parasitoid type. Solitary, polyphagous (Ran and Zhao 1989).

***Exorista japonica* (Townsend, 1909)**

Distribution. China, Japan, North Korea, South Korea, India, Nepal, Vietnam (O'Hara et al. 2020).

Recorded interactions with *H. cunea*. China [Dandong City, Liaoning Province (Shi 1981); Wugong County, Shaanxi Province (Ran and Zhao 1989)], China (Yang et al. 2008), Japan [Tsukuba (Watanabe 2005)]. Japan [Honshu, Saitama, Tokyo, Kanazawa], South Korea (Tschorsnig 2017).

Host stage. Larva to pupa (Ran and Zhao 1989).

Parasitoid type. Solitary, polyphagous (Ran and Zhao 1989; Yang et al. 2008).

Notes. Female oviposits on surface of host. Parasitism rate is higher for wandering *H. cunea* larvae than in feeding larvae (Watanabe 2005); parasitoid female to male ratio 1.5 (Yang et al. 2008); parasitism rate 10% (Shu and Yu 1985), 4–15.7% (Yang et al. 2008).

***Exorista larvarum* (Linnaeus, 1758)**

Distribution. Canada, USA, Tajikistan, Turkmenistan, China, Europe, Japan, North Korea, Iran, Israel, Saudi Arabia, Mongolia, Egypt, Russia, India (O'Hara et al. 2020).

Recorded interactions with *H. cunea*. Italy (Boriani 1991), Iran [Guilan province (Karami et al. 2023)], Turkey [Düzce (Avci et al. 2022)]. Austria [Burgenland, Weiden], Serbia [Vojvodina], Hungary, Romania, Turkey, Moldova, Italy [Lombardia, Ponte Merlano], Russia, Azerbaijan (Tschorsnig 2017).

Host stage. Pupa (Warren and Tadić 1967).

***Exorista rustica* (Fallén, 1810)**

Distribution. China, Europe, Kazakhstan, North Korea, South Korea, Israel, Mongolia, Egypt, Russia, Transcaucasia, Thailand (O'Hara et al. 2020).

Recorded interactions with *H. cunea*. Hungary (Tschorsnig 2017).

***Exorista segregata* (Rondani, 1859)**

Distribution. Turkmenistan, Uzbekistan, Europe, Iran, Israel, Lebanon, Mongolia, Algeria, Canary Islands, Egypt, Morocco, Tunisia, Russia, Armenia, Azerbaijan, Georgia (O'Hara et al. 2020).

Recorded interactions with *H. cunea*. Serbia, Hungary (Tschorsnig 2017).

***Exorista sorbillans* (Wiedemann, 1830)**

Distribution. Tajikistan, China, Hungary, Romania, Ukraine, Bulgaria, Greece, Italy, Serbia, Spain, Turkey, Austria, France, Japan, South Korea, Iran, Israel, Mongolia, Canary Islands, Egypt, Russia, Cameroon, D.R. Congo, Kenya, Malawi, Nigeria, Sierra Leone, Uganda, India, Australia, Lord Howe Island, Papua New Guinea (O'Hara et al. 2020).

Recorded interactions with *H. cunea*. China [Shandong (Tschorsnig 2017)].

***Exorista xanthaspis* (Wiedemann, 1830)**

Distribution. Tajikistan, Turkmenistan, Uzbekistan, China, Europe, Kazakhstan, South Korea, Israel, Saudi Arabia, Mongolia, Egypt, Russia, Transcaucasia, Africa, U.A. Emirates, Yemen, India, Indonesia, Japan, Thailand (O'Hara et al. 2020).

Recorded interactions with *H. cunea*. Serbia [Vojvodina], Serbia, Hungary, Romania, Bulgaria [Silistra region], Russia (Tschorsnig 2017).

Host stage. Pupa and larva (Warren and Tadić 1967 as *E. fallax*).

***Gonia bimaculata* Wiedemann, 1819**

Distribution. Tajikistan, Turkmenistan, Uzbekistan, China, Europe, Iran, Israel, "Palestine", Saudi Arabia, Algeria, Canary Islands, Egypt, Tunisia, Azerbaijan (O'Hara et al. 2020).

Recorded interactions with *H. cunea*. Serbia [Vojvodina (Tschorsnig 2017)].

Host stage. Larva (Warren and Tadić 1967).

***Hyphantrophaga blanda* (Osten Sacken, 1887)**

Distribution. Canada, USA (O'Hara et al. 2020).

Recorded interactions with *H. cunea*. Canada [Quebec (Beaulne 1939 as *Zenilla blanda*)], Canada (Morris 1976b as *Eusisyropa blanda*).

Host stage. Larva (Warren and Tadić 1967), larva of later instar (Morris 1976b).

Parasitoid type. Solitary, endoparasitoid, koinobiont (Morris 1976b).

***Hyphantrophaga hyphantriae* (Townsend, 1891)**

Distribution. Canada, USA (O'Hara et al. 2020).

Recorded interactions with *H. cunea*. USA [Colorado (Swain 1937 as *Hyphantrophaga desmiae*)], North America (Warren and Tadić 1967 as *Hyphantrophaga desmiae*, Sullivan and Ozman-Sullivan 2012).

Host stage. Larva (Warren and Tadić 1967).

***Hyphantrophaga virilis* (Aldrich & Webber, 1924)**

Distribution. Canada, USA, Costa Rica, Mexico (O'Hara et al. 2020).

Recorded interactions with *H. cunea*. USA [Colorado (Swain 1937 as *Zenilla virilis*)], North America (Warren and Tadić 1967 as *Eusisyropa virilis*, Sullivan and Ozman-Sullivan 2012).

Host stage. Larva (Warren and Tadić 1967).

***Hystricia abrupta* (Wiedemann, 1830)**

Distribution. Canada, USA, Mexico (O'Hara et al. 2020).

Recorded interactions with *H. cunea*. USA [Colorado (Swain 1937 as *Bombyliopsis abrupta*)], North America (Warren and Tadić 1967 as *Bombyliopsis abrupta*, Sullivan and Ozman-Sullivan 2012).

Host stage. Larva (Warren and Tadić 1967).

***Isosturmia picta* (Baranov, 1932)**

Distribution. China, Japan, South Korea, India, Malaysia, Nepal, Sri Lanka (O'Hara et al. 2020).

Recorded interactions with *H. cunea*. South Korea (Tschorsnig 2017).

***Kuwanimyia conspersa* Townsend, 1916**

Distribution. China, Japan (O'Hara et al. 2020).

Recorded interactions with *H. cunea*. Japan [Honshu, Tokyo, Asukayama (Tschorsnig 2017)].

***Lespesia aletiae* (Riley, 1879)**

Distribution. Canada, USA, Puerto Rico, Costa Rica, Honduras, Mexico, Argentina, Brazil,

Uruguay (O'Hara et al. 2020).

Recorded interactions with *H. cunea*. USA [Colorado (Swain 1937 as *Achaetoneura aletia*)], North America (Warren and Tadić 1967; Sullivan and Ozman-Sullivan 2012).

Host stage. Larva (Swain 1937; Warren and Tadić 1967).

Parasitoid type. Solitary, endoparasitoid.

***Lespesia archippivora* (Riley, 1871)**

Distribution. Canada, USA, Cuba, Puerto Rico, Guadeloupe, Trinidad and Tobago, Guatemala, Honduras, Mexico, Nicaragua, Panama, Argentina, Brazil, Colombia, Peru, Uruguay, Venezuela (O'Hara et al. 2020).

Recorded interactions with *H. cunea*. North America (Sullivan and Ozman-Sullivan 2012).

***Lespesia frenchii* (Williston, 1889)**

Distribution. Canada, USA (O'Hara et al. 2020).

Recorded interactions with *H. cunea*. USA [Colorado (Swain 1937 as *Achaetoneura frenchii*)].

Host stage. Larva (Swain 1937; Warren and Tadić 1967).

Parasitoid type. Solitary, endoparasitoid.

***Myiopharus floridensis* (Townsend, 1892)**

Distribution. USA, Jamaica, Puerto Rico, Mexico (O'Hara et al. 2020).

Recorded interactions with *H. cunea*. North America (Warren and Tadić 1967 as *Euphorocero floridensis*).

Host stage. Larva (Warren and Tadić 1967).

***Nemoraea pellucida* (Meigen, 1824)**

Distribution. China, Europe, Japan, Kazakhstan, South Korea, Iran, Algeria, Russia, Georgia (O'Hara et al. 2020).

Recorded interactions with *H. cunea*. Italy (Boriani 1991), Turkey [Samsun Province (Sullivan et al. 2012)]. France [Gironde and/or Landes], Turkey [Tekirdağ, Samsun, Saricakaya, Adapazari], Italy [Emilia-Romagna, Mantova, Lombardia, Mantua, Veneto, Pavia], Romania [Bukarest] (Tschorsnig 2017).

Host stage. Pupa (Sullivan et al. 2012).

Parasitoid type. Endoparasitoid, solitary, polyphagous.

Notes. Female deposits fully developed eggs near hosts, and eggs develop into planidium-type larvae that mount and enter the hosts. Parasitism rate 2.4–19.4% in Samsun (Sullivan et al. 2012).

***Nilea hortulana* (Meigen, 1824)**

Distribution. China, Europe, Japan, Russia (O'Hara et al. 2020).

Recorded interactions with *H. cunea*. Japan (Tschorsnig 2017).

***Pales pavida* (Meigen, 1824)**

Distribution. Turkmenistan, China, Europe, Japan, Kazakhstan, Iran, Israel, Mongolia, Morocco, Russia, Armenia, Azerbaijan, Georgia (O'Hara et al. 2020).

Recorded interactions with *H. cunea*. China [Dandong City, Liaoning Province (Shu and Yu 1985 as *Centophorocera pavida*); Wugong County, Shaanxi Province (Ran and Zhao 1989)], Japan [Tsukuba (Watanabe 2005)], Turkey [Düzce (Avci et al. 2022)]. Japan [Tokyo, Koto, Tachikawa, Honshu], Serbia [Vojvodina], Hungary, Montenegro, Moldova, China [Liaoning], Russia, Ukraine [Crimea, Yarkoe Pole], Turkey [Samsun], Italy [Pavia, Emilia-Romagna, Bologna, Lombardia] (Tschorsnig 2017).

Host stage. Larva (Warren and Tadić 1967), pupa (Ran and Zhao 1989).

Parasitoid type. Solitary, polyphagous (Ran and Zhao 1989).

***Panzeria aldrichi* (Townsend, 1892)**

Distribution. Canada, USA (O'Hara et al. 2020).

Recorded interactions with *H. cunea*. USA [Colorado (Swain 1937 as *Varichaeta aldrichi*)], North America (Warren and Tadić 1967 as *Mericia aldrichi*, Sullivan and Ozman-Sullivan 2012).

Host stage. Larva (Warren and Tadić 1967).

***Panzeria ampelus* (Walker, 1849)**

Distribution. Canada, USA (O'Hara et al. 2020).

Recorded interactions with *H. cunea*. USA [Colorado (Swain 1937 as *Panzeria radicum*, *Ernestia ampelus*)], North America (Warren and Tadić 1967 as *Ernestia ampelus*, Sullivan and Ozman-Sullivan 2012), Canada (Morris 1976b as *Mericia ampelus*).

Host stage. Larva (Warren and Tadić 1967), Later instar larvae (Morris 1976b).

Parasitoid type. Solitary, endoparasitoid, koinobiont (Morris 1976b).

Notes. Univoltine in Canada, female deposits larvae on foliage near *H. cunea* colonies, parasitoid larvae attack host larvae they contact (Morris 1976b).

***Panzeria arcuata* (Tothill, 1921)**

Distribution. Canada, USA (O'Hara et al. 2020).

Recorded interactions with *H. cunea*. North America (Sullivan and Ozman-Sullivan 2012).

***Panzeria johnsoni* (Tothill, 1921)**

Distribution. Canada, USA (O'Hara et al. 2020).

Recorded interactions with *H. cunea*. USA [Colorado (Swain 1937 as *Ernestia johnsoni*)], North America (Warren and Tadić 1967 as *Mericia johnsoni*, Sullivan and Ozman-Sullivan 2012).

Host stage. Larva (Warren and Tadić 1967).

***Patelloa leucaniae* (Coquillett, 1897)**

Distribution. Canada, USA (O'Hara et al. 2020).

Recorded interactions with *H. cunea*. North America (Warren and Tadić 1967; Sullivan and Ozman-Sullivan 2012).

Host stage. Larva (Warren and Tadić 1967).

***Pseudogonia parisiaca* (Robineau-Desvoidy, 1851)**

Distribution. China, Europe, Kazakhstan, Russia, Transcaucasia (O'Hara et al. 2020).

Recorded interactions with *H. cunea*. Italy (Tschorsnig 2017).

***Senometopia prima* (Baranov, 1931)**

Distribution. China, Japan, India, Indonesia (O'Hara et al. 2020).

Recorded interactions with *H. cunea*. Japan (Tschorsnig 2017).

***Sturmia bella* (Meigen, 1824)**

Distribution. Central Asia, China, Europe, Japan, South Korea, Middle East, Morocco, Russia, Armenia, Georgia, Nepal, New Caledonia, Solomon Islands (O'Hara et al. 2020).

Recorded interactions with *H. cunea*. Japan (Tschorsnig 2017).

***Tachina praeceps* Meigen, 1824**

Distribution. Kyrgyzstan, Turkmenistan, Uzbekistan, China, Europe, Kazakhstan, Iran, Israel, Mongolia, North Africa, Russia, Armenia, Azerbaijan (O'Hara et al. 2020).

Recorded interactions with *H. cunea*. Moldova (Tschorsnig 2017).

***Thelaira nigripes* (Fabricius, 1794)**

Distribution. China, Europe, Japan, North Korea, South Korea, Iran, Russia (O'Hara et al. 2020).

Recorded interactions with *H. cunea*. Russia, Serbia (Tschorsnig 2017).

Host stage. Larva (Warren and Tadić 1967).

***Winthemia* sp.**

Distribution. North America.

Recorded interactions with *H. cunea*. USA [Colorado (Swain 1937)], North America (Sullivan and Ozman-Sullivan 2012).

***Zenillia dolosa* (Meigen, 1824)**

Distribution. China, Europe, Japan, South Korea, Russia (O'Hara et al. 2020).

Recorded interactions with *H. cunea*. Japan [Tsukuba (Watanabe 2005)].

***Zenillia libatrix* (Panzer, 1797)**

Distribution. China, Europe, Japan, Iran, Russia, Armenia (O'Hara et al. 2020).

Recorded interactions with *H. cunea*. Italy (Boriani 1991). Italy, Japan (Tschorsnig 2017).

Host stage. Larva (Warren and Tadić 1967).

Oдиниidae 树创蝇科

? *Odinia maculata* (Meigen, 1830)

Distribution. North America.

Recorded interactions with *H. cunea*. Canada [Quebec (Beaulne 1939)].

Notes. Gaimari and Mathis (2011) cataloged *O. maculata* as a synonym of *O. trinotata* Robineau-Desvoidy, 1830, but the latter is only distributed in Europe in their catalogue; Beaulne (1939) noted *O. maculata* was a parasitoid of *H. cunea*, which may be a misidentification.

Sarcophagidae 麻蝇科

***Sarcophaga carnaria* (Linnaeus, 1758)**

Distribution. Palaearctic (Pape 1996).

Recorded interactions with *H. cunea*. Europe (Warren and Tadić 1967).

Host stage. Pupa (Warren and Tadić 1967).

Parasitoid type. Polyphagous.

Muscidae 蝇科

***Musca domestica* Linnaeus, 1758**

Distribution. Originated from central Asia, but now occurs on all inhabited continents, Europe, Asia, Africa, Australasia, Arctic, Americas (Hewitt 2011).

Recorded interactions with *H. cunea*. Europe (Warren and Tadić 1967).

Host stage. Pupa and Larva (Warren and Tadić 1967).

Parasitoid type. Polyphagous.

***Muscina stabulans* (Fallén, 1817)**

Distribution. Cosmopolitan (de Carvalho et al. 2005).

Recorded interactions with *H. cunea*. Europe (Warren and Tadić 1967).

Host stage. Larva (Warren and Tadić 1967).

Parasitoid type. Polyphagous.

Phoridae 蚤蝇科

***Megaselia scalaris* (Loew, 1866)**

Distribution. Europe, Africa, Asia, Americas (Karami et al. 2023).

Recorded interactions with *H. cunea*. Iran [Guilan province (Karami et al. 2023)].

Host stage. Pupa (Karami et al. 2023).

Parasitoid type. Polyphagous (Karami et al. 2023).

Discussion

The diversity of *H. cunea* predators and parasitoids differs among its native and invaded ranges. In North America, where *H. cunea* is native, 128 predators and 76 parasitoids have been reported. *Hyphantria cunea* is not considered a major pest in North America, which is likely attributed, in part, to its long co-evolutionary history with its natural enemies such as birds, spiders, and insects (Schowalter and Ring 2017). In the Eastern Hemisphere, 78 predators and 62 parasitoids have been reported in Asia, and 88 predators and 68 parasitoids have been reported in Europe. Currently, *H. cunea* is rarely reported as causing significant damage in some countries such as Hungary, Italy, and Japan: *H. cunea* was introduced into these countries in the 1940's, and it is possible that native enemies have had sufficient time to adapt to *H. cunea* and help control its outbreaks. However, in newly invaded countries such as China, Iran, and Turkey, *H. cunea* outbreaks frequently occur, possibly because native natural predators in these countries are still adapting to *H. cunea*.

Acknowledgments

We sincerely thank Dr Reza Zahiri (Staatliches Museum für Naturkunde Karlsruhe, Karlsruhe, Baden-Württemberg, Germany), Dr James K. Adams (Department of Biology, Dalton State College, Dalton, Georgia, USA), and Dr Hui-lin Han (Northeast Forestry University, Harbin, Heilongjiang, China) for their critical reading of and helpful comments on the manuscript.

Additional information

Conflict of interest

The authors have declared that no competing interests exist.

Ethical statement

No ethical statement was reported.

Funding

The National Key R&D Program of China (2021YFD1400300); Development Funding from Ecology and Nature Conservation Institute, Chinese Academy of Forestry (99801-2023).

Author contributions

Funding acquisition: XYW. Methodology: LMC, TMP. Resources: TRP. Writing - original draft: LMC. Writing - review and editing: XYW, LMC, TRP, TMP.

Author ORCIDs

Liang Ming Cao  <https://orcid.org/0000-0002-6581-6719>

Xiao Yi Wang  <https://orcid.org/0000-0001-8136-6642>

Toby R. Petrice  <https://orcid.org/0000-0003-3764-577X>

Therese M. Poland  <https://orcid.org/0000-0001-7684-1306>

Data availability

All of the data that support the findings of this study are available in the main text.

References

- AntWeb [Version 8.101] (2023) California Academy of Science. [Online at] <https://www.antweb.org> [accessed 29 November 2023]
- Ashmead WH (1898) Part 2. Descriptions of new parasitic Hymenoptera. *Proceedings of the Entomological Society of Washington* 4: 155–171.
- Avci O, Öztemiz S, Ciner İ (2022) Amerikan beyaz kelebeği, *Hyphantria cunea* (Drury) (Lepidoptera: Arctiidae)'nin ergin popülasyon takibi ile biyolojik mücadelede parazitoit ve predatörlerinin belirlenmesi. *Türkiye Biyolojik Mücadele Dergisi* 13(2): 128–137. <https://doi.org/10.31019/tbmd.1149134>
- Avibase (2023) The World Bird Database. [Online at] <https://avibase.bsc-eoc.org/avibase.jsp?lang=EN> [accessed 12 December 2023]
- Beaulne JI (1939) Parasites and predators reared at Quebec. *Canadian Entomologist* 71(5): 120. <https://doi.org/10.4039/Ent71120-5>
- Beverley C (2022) *Coccinella septempunctata* (seven-spot ladybird). CABI Compendium, CABI. <https://doi.org/10.1079/cabicompendium.11733> [Accessed 12 December 2023]
- Blatchley WS (1926) Heteroptera or true bugs of eastern North America, with especial reference to the faunas of Indiana and Florida. Nature Publishing Company, Indianapolis, IN, 1116 pp. <https://doi.org/10.5962/bhl.title.6871>
- Boriani M (1991) *Chouioia cunea* Yang (Hymenoptera, Eulophidae), parasitoid of *Hyphantria cunea* (Drury) (Lepidoptera Arctiidae), new for Europe. *Bollettino di Zoologia Agraria e Bachicoltura* 23(2): 193–196.
- Boriani M (1994a) *Conomorium amplum* (Walker, 1835): Correct name of a parasitoid from *Hyphantria cunea* (Drury, 1773) in Italy (Hymenoptera, Pteromalidae-Lepidoptera, Arctiidae). *Entomofauna* 15(37): 431–432.
- Boriani M (1994b) New records of parasitoids from *Hyphantria cunea* (Drury, 1883) in Italy (Lepidoptera, Arctiidae). *Entomofauna* 15(37): 425–430.
- Bousquet Y (2012) Catalogue of Geadephaga (Coleoptera, Adephaga) of America, north of Mexico. *ZooKeys* 245: 1–1722. <https://zookeys.pensoft.net/article/4003/>
- Bruschi S (2010) *Calosoma* of the World. <https://www.calosomas.com/index.html> [Accessed 29 November 2023]
- Burks BD (1936) The Illinois Species of *Brachymeria* (Hymenoptera, Chalcididae). *Transactions of the Illinois State Academy of Science, Illinois State Academy of Science* 29: 251–253.
- Burks BD (1979) Eulophidae. In: Krombein KV, Hurd Jr PD, Smith DR, Burks BD (Eds) *Catalog of Hymenoptera in America North of Mexico, Volume 1, Symphyta and Apocrita (Parasitica)*. Smithsonian Institution Press, Washington DC, 967–1021.
- Butler L (1993) Parasitoids associated with the macrolepidoptera community at Cooper's Rock State Forest, West Virginia: A baseline study. *Proceedings of the Entomological Society of Washington* 95(3): 504–510.
- Camerini G (1994) Gli uccelli predatori (Birds as predators of *Hyphantria cunea* in Italy) In: book: *L'ifantria in Italia (Hyphantria cunea in Italy)*. Parte Seconda Publisher: Edagricole-Bologna Editors, Anselmo Montermini, 139–154.
- Camerini G, Groppali R (1999) Predatori e parassitoidi di *Hyphantria cunea* in provincia di Pavia. *Informatore Fitopatologico* 10: 19–28.

- Carpenter JM (1996) Distributional checklist of species of the genus *Polistes* (Hymenoptera: Vespidae, Polistinae, Polistini). *American Museum Novitates* 3188: 1–39.
- Chordas III SW (2015) *Picromerus bidens* (Hemiptera: Pentatomidae) new for Ohio, USA. *Entomological News* 125(3): 217–219. <https://doi.org/10.3157/021.125.0311>
- CABI Compendium (2022) *Allothrombium fuliginosum* (velvet, mite, red (England)). CABI. [Accessed 29 November 2023]
- Crumb SE, Eide PM, Bonn AE (1941) The European earwig. *Technical Bulletin United States Department of Agriculture Washington D.C.* 766: 1–76.
- de Carvalho CJB, Couri MS, Pont AC, Pamplona D, Lopes SM (2005) A catalogue of the Muscidae (Diptera) of the Neotropical Region. *Zootaxa* 860(1): 1–282. <https://doi.org/10.11646/zootaxa.860.1.1>
- De Clercq P (2008) Spined soldier bug, *Podisus maculiventris* Say (Hemiptera: Pentatomidae: Asopinae). In: Capinera JL (Ed.) *Encyclopedia of Entomology*, Vol 4. Springer, Heidelberg, 3508–3510.
- Diez F, Coscarón MC (2014) The Stenopodainae (Hemiptera, Heteroptera) of Argentina. *ZooKeys* 452: 51–77. <https://doi.org/10.3897/zookeys.452.6519>
- Edosa TT, Jo YH, Keshavarz M, Anh YS, Noh MY, Han YS (2019) Current status of the management of fall webworm, *Hyphantria cunea*: Towards the integrated pest management development. *Journal of Applied Entomology* 143(1–2): 1–10. <https://doi.org/10.1111/jen.12562>
- EPPO (2015) EPPO technical document No. 1068, EPPO study on pest risks associated with the import of tomato fruit. EPPO Paris. https://www.eppo.int/media/uploaded_images/RESOURCES/eppo_publications/td_1068_tomato_study.pdf [Accessed 22 November 2023]
- Froeschner RC (1988) Family Reduviidae Latreille, 1807. The assassin bugs. In: Henry TJ, Froeschner RC (Eds) *Catalog of the Heteroptera, or true bugs, of Canada and the continental United States*. CRC Press, New York, 616–651. https://doi.org/10.1163/9789004590601_038
- Frost DR (2023) Amphibian species of the World: an online reference. Version 6.2. <https://amphibiansoftheworld.amnh.org/index.php> [Accessed 02 December 2023]
- Gaimari SD, Mathis WN (2011) World catalog and conspectus on the family Odiniidae (Diptera: Schizophora). *Myia* 12: 291–339.
- Gibson GAP, Fusu L (2016) Revision of the Palaearctic species of *Eupelmus* (*Eupelmus*) Dalman (Hymenoptera: Chalcidoidea: Eupelmidae). *Zootaxa* 4081(1): 001–331. <https://doi.org/10.11646/zootaxa.4081.1.1>
- Groppali R, Priano M, Camerini G, Pesarini C (1993) Ragni (Araneae) in nidi larvali di *Hyphantria cunea* Drury (Lepidoptera Arctiidae) nella Pianura Padana Centrale. *Bollettino di Zoologia Agraria e Bachicoltura* 25: 153–160.
- Groppali R, Priano M, Camerini G, Pesarini C (1994) Predazione di larve di *Hyphantria cunea* Drury (Lepidoptera Arctiidae) su Acero negundo da parte di ragni (Araneae). *Bollettino di Zoologia Agraria e Bachicoltura* 2: 151–156.
- Habu A (1960) A revision of the Chalcididae (Hymenoptera) of Japan with descriptions of sixteen new species. *Bulletin of the National Institute of Agricultural Sciences, Series C* 11: 131–363. [Plant Pathology and Entomology]
- Hasegawa H, Itô Y (1967) Biology of *Hyphantria cunea* Drury (Lepidoptera: Arctiidae) in Japan. I. notes on adult biology with reference to the predation by birds. *Applied Entomology and Zoology* 2(2): 100–110. <https://doi.org/10.1303/aez.2.100>
- Henry TJ (2008) First North American records for the palearctic *Orius majusculus* (Reuter) (Hemiptera: Heteroptera: Anthracoridae). *Proceedings of the Entomolog-*

- ical Society of Washington 110(4): 953–959. <https://doi.org/10.4289/0013-8797-110.4.953>
- Hewitt CG (2011) The house-fly: *Musca domestica* Linn: its structure, habits, development, relation to disease and control. Cambridge University Press, London, 404 pp.
- Howard LO (1885) Descriptions of North American Chalcididae. U.S. Department of Agriculture. Bureau of Entomology, Bulletin No. 5: 28.
- ITIS (2023) the Integrated Taxonomic Information System (ITIS) on-line database, www.itis.gov, CC0. <https://doi.org/10.5066/F7KH0KBK> [Accessed 06 December 2023]
- Karami A, Talebi AA, Gilasian E, Fathipour Y, Mehrabadi M (2023) Native parasitoids of the fall webworm, *Hyphantria cunea* (Drury, 1773) (Lepidoptera, Erebidae), an invasive alien pest in northern Iran. *Journal of Insect Biodiversity and Systematics* 9(1): 81–101. <https://doi.org/10.52547/jibs.9.1.81>
- Kasparyan DR, Pinson DO (2007) A new species of *Diradops* Townes from Mexico (Hymenoptera: Ichneumonidae: Banchinae), a parasitoid of *Hyphantria cunea* (Drury) (Lepidoptera: Arctiidae), with notes on *Diradops mexicanus* (Cresson). *Zoosystematica Rossica* 16(1): 39–42. <https://doi.org/10.31610/zsr/2007.16.1.39>
- Kayashima I (1967) Study on spiders (particularly referring to grass-spiders) to prey upon fallweb worms (*Hyphantria cunea* Drury). *Acta Arachnologica* 21(1): 1–31. <https://doi.org/10.2476/asjaa.21.1>
- Kazantsev SV (2011) An annotated checklist of Cantharoidea (Coleoptera) of Russia and adjacent territories. *Russian Entomological Journal* 20(4): 387–410. <https://doi.org/10.15298/rusentj.20.4.05>
- Kim IK, Park Y, Koh SH (2011) Chalcidoid wasps parasitizing pupae of fall webworm, *Hyphantria cunea* (Drury), in South Korea. *Entomological Research* 41(6): 278. <https://doi.org/10.1111/j.1748-5967.2011.00373.x>
- Kimsey LS, Carpenter JM (2012) The Vespinae of North America (Vespidae, Hymenoptera). *Journal of Hymenoptera Research* 28: 37–65. <https://doi.org/10.3897/jhr.28.3514>
- Kunimi Y (1983) Spiders inhabiting the colonial-webs of the fall webworm, *Hyphantria cunea* Drury (Lepidoptera Arctiidae). *Applied Entomology and Zoology* 18(1): 81–89. <https://doi.org/10.1303/aez.18.81>
- Lam TX, Cai WZ, Tomokuni M, Ishikawa T (2015) The assassin bug subfamily Harpactorinae (Hemiptera: Reduviidae) from Vietnam: an annotated checklist of species. *Zootaxa* 3931(1): 101–116. <https://doi.org/10.11646/zootaxa.3931.1.7>
- Lartvière M (1992) *Himacerus apterus* (Fabricius), a Eurasian Nabidae (Hemiptera) new to North America: Diagnosis, geographical distribution, and bionomics. *Canadian Entomologist* 124(4): 725–728. <https://doi.org/10.4039/Ent124725-4>
- Li Y (2011) Investigation on natural enemy insect resources of *Hyphantria cunea* (Drury) in Shandong and biology of *Exorista japonica* Townsend. Master thesis of Shandong Agricultural University, 50 pp. [In Chinese with English abstract]
- Liang HB, Yu PY (2000) Species of ground beetles (Coleoptera: Carabidae) predating oriental armyworm (Lepidoptera: Notuidae) in China. *Natural Enemies of Insects* 22(4): 160–167. [In Chinese with English abstract]
- Lorenz W (2021) Carabcat database. In: Bánki O, Roskov Y, Döring M et al. (Eds) *Catalogue of life checklist (v.03 (08/2021))*. <https://doi.org/10.48580/dfqf-3dk> [Accessed on 04 December 2023]
- Marlatt CL (1903) A chalcidid parasite of the asiatic lady-bird. *Proceedings of the Entomological Society of Washington* 5: 138–139.

- Marsh PM (1979) Braconidae. Aphidiidae. Hybrizontidae. In: Krombein KV, Hurd Jr PD, Smith DR, Burks BD (Eds) Catalog of Hymenoptera in America north of Mexico. Smithsonian Institution Press, Washington D.C., 144–313.
- McDermott FA (1911) The attack of a larval hemipter upon a caterpillar. Proceedings of the Entomological Society of Washington 13: 90–91.
- Morris RF (1972) Predation by wasps, birds, and mammals on *Hyphantria cunea*. Canadian Entomologist 104(10): 1581–1591. <https://doi.org/10.4039/Ent1041581-10>
- Morris RF (1976a) Hyperparasitism in populations of *Hyphantria cunea*. Canadian Entomologist 108(7): 685–687. <https://doi.org/10.4039/Ent108685-7>
- Morris RF (1976b) Influence of genetic changes and other variables on the encapsulation of parasites by *Hyphantria cunea*. Canadian Entomologist 108(7): 673–684. <https://doi.org/10.4039/Ent108673-7>
- Morris RF (1976c) Relation of mortality caused by parasites to the population density of *Hyphantria cunea*. Canadian Entomologist 108(11): 1291–1294. <https://doi.org/10.4039/Ent1081291-11>
- Nikitsky NB, Ukrainsky AS (2016) The ladybird beetles (Coleoptera, Coccinellidae) of Moscow Province. Entomological Review 96(6): 710–735. <https://doi.org/10.1134/S0013873816060051>
- Ning J, Lu PF, Fan J, Ren LL, Zhao LL (2021) American fall webworm in China: A new case of global biological invasions. Innovation (Cambridge (Mass.)) 3(1): 100201. <https://doi.org/10.1016/j.xinn.2021.100201>
- Nishikawa M, Ikeda H, Kubota K, Sota T (2010) Taxonomic redefinition and natural history of the endemic silphid beetle *Silpha longicornis* (Coleoptera: Silphidae) of Japan, with an analysis of its geographic variation. Zootaxa 2648(1): 1–31. <https://doi.org/10.11646/zootaxa.2648.1.1>
- Nordin GL, Rennels RG, Maddox JV (1972) Parasites and pathogens of the fall webworm in Illinois. Environmental Entomology 1(3): 351–354. <https://doi.org/10.1093/ee/1.3.351>
- Noyes JS (2019) Universal Chalcidoidea database. World wide web electronic publication. <http://www.nhm.ac.uk/chalcidoids> [Accessed 4 May 2023]
- O'Hara JE, Henderson SJ, Wood DM (2020) Preliminary checklist of the Tachinidae (Diptera) of the world. Version 2.1. PDF document, 1039 pp. http://www.nadsdiptera.org/Tach/WorldTachs/Checklist/Tachchlist_ver2.1.pdf [Accessed 5 November 2023]
- Oliver AD (1963) An ecological study of the fall webworm, *Hyphantria cunea* (Drury), in Louisiana. LSU Historical Dissertations and Theses, 820 pp. https://repository.lsu.edu/gradschool_disstheses/820
- Oliver AD (1964) Studies on the biological control of the fall webworm, *Hyphantria cunea*, in Louisiana. Journal of Economic Entomology 57(3): 314–318. <https://doi.org/10.1093/jee/57.3.314>
- Oswald JD (2007) Lacewing digital library. <https://lacewing.tamu.edu> [Accessed on 28 November 2023]
- Pape T (1996) Catalogue of the Sarcophagidae of the world (Insecta: Diptera). Memoirs of Entomology International 8: 1–558.
- Papp J (1988) Contributions to the Braconid fauna of Hungary, VIII. Microgasterinae (Hymenoptera: Braconidae). Folia Entomologica Hungarica 49: 167–184.
- Patel S, Singh RP (2016) Updated checklist and distribution of Mantidae (Mantodea: Insecta) of the world. International Journal of Research 2(4): 17–54. <https://doi.org/10.20431/2454-941X.0204003>

- Peck O (1951) Superfamily Chalcidoidea. In: Muesebeck CFW, Krombein KV, Townes H (Eds) Hymenoptera of America North of Mexico Synoptic Catalog, United States Government Printing Office, Washington, 565 pp.
- Peck O (1963) A catalogue of the Nearctic Chalcidoidea (Insecta; Hymenoptera). Canadian Entomologist 30(Supplement): 1–1088. <https://doi.org/10.4039/entm9530fv>
- Pelletier G, Hébert C (2014) The Cantharidae of eastern Canada and northeastern United States. Canadian Journal of Arthropod Identification 25: 1–246. <https://doi.org/10.3752/cjai.2014.25>
- Penny ND, Byers GW (1979) A check-list of the Mecoptera of the world. Acta Amazonica 9(2): 365–388. <https://doi.org/10.1590/1809-43921979092365>
- Phillips KA (1983) A taxonomic revision of the Nearctic species of *Apateticus* Dallas and *Podisus* Herrich-Schäffer (Heteroptera: Pentatomidae: Asopinae). Ph.D. dissertation, Oregon State University, Corvallis, 275 pp.
- Plugaru SG (1979) Removal of a *Trichogramma* from the eggs of the fall webworm moth in the Moldavian SSR, USSR. Izvestiya Akademii Nauk Moldavskoy SSR 1979(4): 87–88. [Seriya Biologicheskikh i Khimicheskikh Nauk]
- Popescu IE (2006) Torymid and eurytomid wasps (Hymenoptera, Chalcidoidea: Torymidae, Eurytomidae) of Piatra Craiului National Park (Brasov, Romania). Research in Piatra Craiului National Park 2: 170–177.
- Putshkov PV, Putshkov VG (1996) Family Reduviidae Latreille, 1807 – assassin-bugs. In: Aukema B, Rieger C (Eds) Catalogue of the Heteroptera of the Palaearctic Region: Chimicomorpha I. Vol. 2. Netherlands Entomological Society, Amsterdam, 361 pp.
- Ran RB, Zhao DJ (1989) Parasitic natural enemies insects of *Hyphantria cunea* Drury in Shaanxi. Acta University Septentrionali Occident Agriculture 17(3): 93–95. [In Chinese]
- Rider DA (2006) Family Pentatomidae. In: Aukema B, Rieger C (Eds) Catalogue of the Heteroptera of the Palaearctic Region, Pentatomomorpha II. Vol. 5. Netherlands Entomological Society, Amsterdam, 233–403.
- Rider DA, Swanson DR (2021) A distributional synopsis of the Pentatomidae (Heteroptera) north of Mexico, including new state and provincial records. Zootaxa 5015(1): 1–69. <https://doi.org/10.11646/zootaxa.5015.1.1>
- Riley CV (1887a) The fall web-worm, (*Hyphantria cunea* Drury). In: Riley CV (Ed.) Report of the Commissioner of Agriculture 1886. Washington Government Printing Office, 531 pp.
- Riley CV (1887b) Our shade trees and their insect defoliators. United States Department of Agriculture, Division of Entomology Bulletin. No.10: 33–52.
- Riley CV (1888) Our shade trees and their insect defoliators. United States Department of Agriculture, Division of Entomology Bulletin (Second, Revised Edition), No. 10: 36–58.
- Roy H (2022) *Harmonia axyridis* (harlequin ladybird). CABI Compendium. CABI. <https://doi.org/10.1079/cabicompndium.26515> [Accessed 29 November 2023]
- Salnitska M, Solodovnikov A (2019) Rove beetles of the genus *Quedius* (Coleoptera, Staphylinidae) of Russia: A key to species and annotated catalogue. ZooKeys 847: 1–100. <https://doi.org/10.3897/zookeys.847.34049>
- Samin N, Kocak E, Ghahari H, Shojai M (2010) A checklist of Iranian *Telenomus* Haliday (Hymenoptera: Platygastroidae: Scelionidae: Telenominae). Linzer biologische Beiträge 42(2): 1437–1444. <https://zenodo.org/records/5323940>
- Schaffner JV, Griswold CL (1934) Macrolepidoptera and their parasites reared from field collections in the northeastern part of the United States. United States Department of Agriculture, no. 188. Miscellaneous publication, 160 pp. <https://doi.org/10.5962/bhl.title.65414>

- Schowalter TD, Ring DR (2017) Biology and management of the fall webworm, *Hyphantria cunea* (Lepidoptera: Erebididae). *Journal of Integrated Pest Management* 8(1): 7. <https://doi.org/10.1093/jipm/pmw019>
- Schuh RT (2016). On-line systematic catalog of plant bugs (Insecta: Heteroptera: Miridae). In: Bánki O, Roskov Y, Döring M et al. (Eds) *Catalogue of life checklist* (v.03 (08/2021)). *Catalogue of Life Checklist*. <https://doi.org/https://doi.org/10.48580/dfp3-3ff> [Accessed on 04 December 2023]
- Sharov AA, Izhevskiy SS, Prokovjeva EA, Mikhailov KG (1984) Spiders as predators of *Hyphantria cunea* in the south of USSR European part. *Zoologicheskii jurnal* 63(3): 392–398.
- Shi YS (1981) *Exorista japonica*—A natural enemy of the fall webworm *Hyphantria cunea* (Drury). *Acta Entomologica Sinica* 24(3): 342. [In Chinese]
- Shi HL, Liang HB (2023) Taxonomic revision of the genus *Parena* Motschulsky, 1860 (Coleoptera, Carabidae, Lebiini, Metallicina). *Zootaxa* 5286(1): 1–144. <https://doi.org/10.11646/zootaxa.5286.1.1>
- Shu CR, Yu CY (1985) Natural enemies' investigation of *Hyphantria cunea*. *Natural Enemies of Insects* 7(2): 91–94. [In Chinese]
- Smith HS (1912) Technical results from the gypsy moth parasite laboratory. V. The chalcidoid genus *Perilampus* and its relations to the problem of parasite introduction. Technical Series, Bureau of Entomology. United States Department of Agriculture 19(4): 34–63.
- Smulyan MT (1924) Attacks of *Vespa communis* De Saussure on *Hyphantria cunea* Drury. *Psyche* (Cambridge, Massachusetts) 31(3–4): 138–139. <https://doi.org/10.1155/1924/24278>
- Soodnarinesingh C (2015) The online guide to the animals of Trinidad and Tobago—*Stagmomantis carolina* (Carolina Mantis). https://sta.uwi.edu/fst/lifesciences/sites/default/files/lifesciences/documents/ogatt/Stagmomantis_carolina%20-%20Carolina%20Mantis.pdf [Accessed on 24 November 2023]
- Stolbov VA, Sergeeva EV (2020) First records of the *Dendroxena quadrimaculata* (Scopoli, 1771) (Coleoptera, Silphidae) in Tyumen region and possible reasons for its range expansion in western Siberia. *Acta Biologica Sibirica* 6: 369–374. <https://doi.org/10.3897/abs.6.e53528>
- Sullivan GT, Ozman-Sullivan SK (2012) Tachinid (Diptera) parasitoids of *Hyphantria cunea* (Lepidoptera: Arctiidae) in its native North America and in Europe and Asia - A literature review. *Entomologica Fennica* 23(4): 181–192. <https://doi.org/10.33338/ef.7384>
- Sullivan GT, Karaca I, Ozman-Sullivan SK, Kolarov J (2010) Ichneumonid (Hymenoptera) parasitoids of overwintering *Hyphantria cunea* (Drury) (Lepidoptera: Arctiidae) pupae in hazelnut plantations of the central Black Sea region of Turkey. *Zootaxa* 2608(1): 63–68. <https://doi.org/10.11646/zootaxa.2608.1.5>
- Sullivan GT, Karaca I, Ozman-Sullivan SK, Yang ZQ (2011) Chalcidoid parasitoids of overwintered pupae of *Hyphantria cunea* (Lepidoptera: Arctiidae) in hazelnut plantations of Turkey's central Black Sea region. *Canadian Entomologist* 143(4): 411–414. <https://doi.org/10.4039/n11-014>
- Sullivan GT, Karaca I, Ozman-Sullivan SK, Kara K (2012) Tachinid (Diptera: Tachinidae) parasitoids of overwintered *Hyphantria cunea* (Drury) (Lepidoptera: Arctiidae) pupae in Hazelnut Plantations in Samsun Province, Turkey. *Journal of Entomological Research Society* 14: 21–30.
- Swain RB (1937) The parasites of the fall webworm *Hyphantria cunea* Dr. (Lep.: Arctiidae). *Entomological News* 48(9): 244–248.

- Tadić MD (1963) Natural enemies of fall webworm (*Hyphantria cunea* Dr.) in North America. *Entomophaga* 8(4): 245–252. <https://doi.org/10.1007/BF02377530>
- Tamura M (1969) Notes on the parasitic insects of the fall webworm, *Hyphantria cunea* Drury. *Proceedings of the Kanto-Tosan Plant Protection Society* 16: 136–137.
- Tao WQ, Xue Y, Chen FW, Wang H, Guo YM, Zhao HL (2008) Bionomics of *Hyphantria cunea* in Beijing. *Forest Pest and Disease* 27(2): 9–11. [In Chinese with English abstract]
- Tothill JD (1922) The natural control of the fall webworm (*Hyphantria cunea*) in Canada, together with an account of several parasites. *Bulletin, New series (Technical) No. 3*, 107 pp. <https://doi.org/10.5962/bhl.title.63051>
- Townes HK (1944) A catalogue and reclassification of the Nearctic Ichneumonidae (Hymenoptera). Part I. The subfamilies Ichneumoninae, Tryphoninae, Cryptinae, Phaeogeninae and Lissonotinae. *Memoirs of the American Entomological Society* 11: 1–477.
- Townes H (1956) The Nearctic species of trigonalid wasps. *Proceedings of the United States National Museum* 106(3367): 295–304. <https://doi.org/10.5479/si.00963801.106-3367.295>
- Trajković A, Žikić V (2023) Stuck in the caterpillars' web: A half-century of biocontrol research and application on gregarious lepidopteran pests in Europe. *Sustainability (Basel)* 15(4): 2881. <https://doi.org/10.3390/su15042881>
- Tripp HA (1962) The biology of *Perilampus hyalinus* Say (Hymenoptera: Perilampidae), a primary parasite of *Neodiprion swainei* Midd. (Hymenoptera: Diprionidae) in Quebec, with descriptions of the egg and larval stages. *Canadian Entomologist* 94(12): 1250–1270. <https://doi.org/10.4039/Ent941250-12>
- Tschorsnig HP (2017) Preliminary host catalogue of Palaearctic Tachinidae (Diptera). [Provided online on] http://www.nadsdiptera.org/Tach/WorldTachs/CatPalHosts/Cat_Pal_tach_hosts_Ver1.pdf [Accessed on 22 November 2023]
- Turin H, Penev L, Casale A, Arndt E, Assmann T, Makarov K, Mossakowski D (2003) Species accounts. In: Turin H et al. (Eds) *The genus Carabus in Europe - A synthesis*. Pensoft Publisher, Sofia, Moscow, 511 pp.
- Uetz P, Freed P, Aguilar R, Reyes F, Kudera J, Hošek J (2023) The reptile database. <http://www.reptile-database.org> [Accessed on 02 December 2023]
- Viggiani G, Laudonia S (1989) Le specie italiane di *Trichogramma* Westwood (Hymenoptera: Trichogrammatidae), con un commento sullo stato della tassonomia del genere. *Bollettino del Laboratorio di Entomologia Agraria. Filippo Silvestri* 46: 107–124.
- Wang JS, Zhang YH, Jiang SP, Wang JB, Zhang XB, Sun JY (1999) Preliminary study on the bionomics of *Parena cavipennis*, a predator of *Hyphantria cunea*. *Zhongguo Shengwu Fangzhi Xuebao* 15(4): 183–184. [In Chinese with English abstract]
- Wang WL, Sun YL, Liu Q, Yan JH, Kang Z, Lin ZQ (2012) Preliminary observation of preyed ability of *Arma chinensis* (Fallou), a new natural enemy of *Hyphantria cunea* (Drury). *Shandong Forestry Science and Technology* 42(1): 11–14. <https://doi.org/10.3969/j.issn.1002-2724.2012.01.004> [In Chinese with English abstract]
- Warren LO, Tadić M (1967) The fall webworm, *Hyphantria cunea*, its distribution and natural enemies: a world list (Lepidoptera: Arctiidae). *Journal of the Kansas Entomological Society* 40(2): 194–202. <http://www.jstor.org/stable/25083620>
- Warren LO, Tadić M (1970) The fall webworm, *Hyphantria cunea* (Drury). *Agricultural Experiment Station, Division of Agriculture, Bulletin 759*, University of Arkansas, Fayetteville, 108 pp.
- Warren LO, Peck WB, Tadić M (1967) Spiders associated with the fall webworm, *Hyphantria cunea* (Lepidoptera: Arctiidae). *Journal of the Kansas Entomological Society* 40(3): 382–395. <http://www.jstor.org/stable/25083645>

- Watanabe M (2005) Parasitism and over-wintering status of tachinids (Diptera) on larvae of the fall webworm, *Hyphantria cunea* Drury (Lepidoptera: Arctiidae), in the Kanto Region of Japan. *Applied Entomology and Zoology* 40(2): 293–301. <https://doi.org/10.1303/aez.2005.293> [<http://odokon.ac.affrc.go.jp/>]
- Webster FM (1895) Notes on some reared Hymenoptera, largely parasitic, and chiefly from Ohio. *Canadian Entomologist* 27(3): 67–68. <https://doi.org/10.4039/Ent2767-3>
- World Spider Catalog (2023) World spider catalog. Version 24.5. Natural History Museum Bern, online at <http://wsc.nmbe.ch>. [Accessed on 28 November 2023] <https://doi.org/10.24436/2>
- Würmli M (1979) Taxonomic problems in the genus *Thereuopoda* (Chilopoda Scutigero-morpha: Scutigerae): the role of postmaturational moultings. In: Camatini M (Ed.) *Myriapod biology*. Academy Press, London, 39–48.
- Yang ZQ (1989) A new genus and species of Eulophidae (Hymenoptera: Chalcidoidea) parasitizing *Hyphantria cunea* (Drury) (Lepidoptera: Arctiidae) in China. *Entomotaxonomia* 11(1–2): 117–123, 129. [In Chinese with English abstract]
- Yang ZQ, Baur H (2004) A new species of *Conomorium* Masi (Hymenoptera: Pteromalidae), parasitizing the fall webworm *Hyphantria cunea* (Drury) (Lepidoptera: Arctiidae) in China. *Mitteilungen der Schweizerischen Entomologischen Gesellschaft* 77(3/4): 214–218, 219.
- Yang ZQ, Wei JR (2003) Two new species of *howardi* species group in the genus *Tetrastichus* (Hymenoptera: Eulophidae) parasitizing fall webworm from China. *Linye Kexue* 39(5): 39, 67–73. [In Chinese with English abstract]
- Yang ZQ, Wang BH, Wei JR (2001) A new species of Eulophidae (Hymenoptera: Chalcidoidea) parasitizing fall webworm in China and Korea. *Acta Entomologica Sinica* 44(1): 98–102.
- Yang ZQ, Wei JR, You LS (2002) Two new braconid species parasitizing larva of fall webworm from China (Hymenoptera: Braconidae). *Dong Wu Fen Lei Xue Bao* 27(3): 608–615. [In Chinese with English abstract]
- Yang ZQ, Qiao XR, Han YS (2003a) A new species of the genus *Tetrastichus* (Hymenoptera, Eulophidae) parasitizing fall webworm in Qinhuangdao, Hebei Province, China. *Dong Wu Fen Lei Xue Bao* 28(4): 733–736. [In Chinese with English abstract]
- Yang ZQ, Wang CZ, Liu YM (2003b) A new species in the genus *Aprostocetus* (Hymenoptera: Eulophidae) parasitizing pupa of fall webworm from Yantai, Shandong Province, China. *Linye Kexue* 39(6): 87–89. [In Chinese with English abstract]
- Yang ZQ, Wang XY, Wei JR, Qu HR, Qiao XR (2008) Survey of the native insect natural enemies of *Hyphantria cunea* (Drury) (Lepidoptera: Arctiidae) in China. *Bulletin of Entomological Research* 98(3): 293–302. <https://doi.org/10.1017/S0007485308005609>
- Yang ZQ, Cao LM, Wang CZ, Wang XY, Song LW (2015a) *Trichospilus albiflagellatus* (Hymenoptera: Eulophidae), a new species parasitizing pupa of *Hyphantria cunea* (Lepidoptera: Arctiidae) in China. *Annals of the Entomological Society of America* 108(4): 641–647. <https://doi.org/10.1093/aesa/sav044>
- Yang ZQ, Yao YX, Cao LM (2015b) Chalcidoidea parasitizing forest defoliators (Hymenoptera) Science Press, Beijing, China, 72, 235–236.
- Yefremova Z, Ebrahimi E, Yegorenkova E (2007) The subfamilies Eulophinae, Entedoninae and Tetrastichinae in Iran, with description of new species (Hymenoptera, Eulophidae). *Entomofauna* 28(30): 332–333.
- Yoshimoto CM (1978) Revision of the subgenus *Achrysocharella* Girault of America north of Mexico (Chalcidoidea, Eulophidae: Chrysonotomyia Ashmead). *Canadian Entomologist* 110(7): 708–710. <https://doi.org/10.4039/Ent110697-7>

- Yu DS, van Achterberg C, Horstmann K (2016) Taxapad 2015: World Ichneumonoidea, taxonomy, biology, morphology and distribution. Taxapad Interactive Catalogue on Flash Drive. Nepean.
- Yue XQ, Zhang GM, Jiang XQ, Liu XH (2016) Study on species and parasitism of natural enemies to *Hyphantria cunea* (Drury) in Liaocheng City. Shandong Nongye Kexue 48(6): 95–98. [In Chinese with English abstract]
- Zhang G, Hart E, Weirauch C (2016) A taxonomic monograph of the assassin bug genus *Zelus* Fabricius (Hemiptera: Reduviidae): 71 species based on 10,000 specimens. Biodiversity Data Journal 4: e8150. <https://doi.org/10.3897/BDJ.4.e8150>
- Zhao Q, Rédei D, Bu WJ (2013) A revision of the genus *Pinthaeus* (Hemiptera: Heteroptera: Pentatomidae). Zootaxa 3636: 59–84. <https://doi.org/10.11646/zootaxa.3636.1.3>
- Zhao Q, Wei JF, Bu WJ, Liu GQ, Zhang HF (2018) Synonymize *Arma chinensis* as *Arma custos* based on morphological, molecular and geographical data. Zootaxa 4455: 161–176. <https://doi.org/10.11646/zootaxa.4455.1.7>

New faunistic records of chironomids and phantom midges (Diptera, Chironomidae and Chaoboridae) from Ukraine indicate recent climatic refugia in the Eastern Carpathians

Peter Bitušík¹, Milan Novikmec², Marek Svitok^{2,3}, Ladislav Hamerlík^{1,4}

¹ Faculty of Natural Sciences, Matej Bel University, Tajovského 40, SK-974 01 Banská Bystrica, Slovakia

² Faculty of Ecology and Environmental Sciences, Technical University in Zvolen, T. G. Masaryka 24, SK-960 53 Zvolen, Slovakia

³ Department of Forest Ecology, Faculty of Forestry and Wood Sciences, Czech University of Life Sciences Prague, Kamýcka 129, CZ-165 21 Prague, Czech Republic

⁴ Institute of Zoology, Slovak Academy of Sciences, Dúbravská cesta 9, SK-845 06 Bratislava, Slovakia

Corresponding author: Peter Bitušík (peter.bitušik@umb.sk)

Abstract

The aquatic insect fauna of the Eastern Carpathians is poorly known, especially in Ukraine. To address this knowledge gap, we conducted faunistic surveys of Chironomidae and Chaoboridae in 2018 and 2021. The study involved sampling of 11 watercourses and 10 mountain lakes situated in the Ukrainian part of the Eastern Carpathians. A total of 101 taxa were identified, including 40 chironomid species and one genus that have been recorded for the first time from Ukraine. The occurrence of one species previously considered as “doubtfully present” in Ukraine was confirmed by this study. One of the two identified phantom midge species, *Chaoborus* (s. str.) *obscuripes* (van der Wulp, 1859), is recorded for the first time from Ukraine. The most intriguing records are chironomid species *Cricotopus* (s. str.) *beckeri* Hirvenoja, 1973, *Eukiefferiella bedmari* Vilchez-Quero & Laville, 1987, and *Pseudorthocladius* (s. str.) *berthelemyi* Moubayed, 1990. These species have Mediterranean distribution and their occurrence in the Eastern Carpathians could be remains of once-widespread populations that currently survive in the Carpathian refugia due to adverse climatic conditions in the former distribution area. The high number of first records from a relatively small number of sites indicates a great gap in the knowledge of the Ukrainian chironomid fauna.

Key words: climatic relicts, mountain lakes, pupal exuvia, submontane rivers



Academic editor: Viktor Baranov

Received: 15 April 2024

Accepted: 28 June 2024

Published: 9 September 2024

ZooBank: <https://zoobank.org/E6BB88C5-5795-4E80-9888-82146DD4CE9C>

Citation: Bitušík P, Novikmec M, Svitok M, Hamerlík L (2024) New faunistic records of chironomids and phantom midges (Diptera, Chironomidae and Chaoboridae) from Ukraine indicate recent climatic refugia in the Eastern Carpathians. ZooKeys 1211: 349–367. <https://doi.org/10.3897/zookeys.1211.125436>

Copyright: © Peter Bitušík et al.
This is an open access article distributed under terms of the Creative Commons Attribution License (Attribution 4.0 International – CC BY 4.0).

Introduction

Chironomids are the most ubiquitous free-living holometabolous insects known from all zoogeographic regions, and all climatic zones from the tropics to the polar regions, including Antarctica (Ashe and O'Connor 2009). Recently, 7290 species belonging to nearly 440 genera and 11 subfamilies have been described worldwide (Ferrington 2007; Pape et al. 2011). In immature stages, most species inhabit various types of freshwaters although some species thrive in brackish water and intertidal pools, and few are truly marine. Finally, semi-terrestrial and fully terrestrial species are also known (Sæther et al. 2000). Among aquatic insects, Chironomidae is the most species-rich insect family

found in freshwater ecosystems (Cranston 1995; Ferrington 2007). The species richness of the family recorded from only one stream locality is often astonishing. In some cases, the number of chironomid species recorded is higher than the diversity of all the other benthic macroinvertebrates (own observations).

Chironomidae can withstand an extremely wide range of environmental conditions in terms of water column depth, temperature, pH, dissolved oxygen, habitat drying and, finally, the gradient of human impacts such as pollution, habitat modification, and changes in watersheds (Ferrington 2007 and references therein). Consequently, chironomids have attracted the attention of researchers around the world as biological indicators for environmental impact assessments, ecosystem health, palaeolimnological reconstructions, and climate change (Resh and Rosenberg 2008; Eggermont and Heiri 2012; Nicacio and Juen 2015 and references therein). Compared to chironomids, the global diversity of phantom midges is low. The Chaoboridae family consists of about 51 extant species in six genera and two subfamilies (Borkent 2014). The immature stages usually live in standing waters, in some cases in small, temporary ponds. Larvae are predators and mostly planktonic; they are often considered keystone species that can eliminate or strongly suppress other invertebrates in the community (MacKay et al. 1990). Subfossil remains of the *Chaoborus* genus have been used in palaeoenvironmental research but also in contemporary ecological studies (e.g., Luoto and Nevalainen 2009; Tolonen et al. 2012). Despite the indisputable importance of both the chaoborids and chironomids and the rapid progress in the knowledge of their distribution, there are still areas that are “terra incognita”. The Eastern Carpathians are undoubtedly one of them.

Here, we present results from an ongoing faunistic inventory of chironomids and chaoborids from Ukrainian Carpathian Mountain lakes, which are supplemented by results from earlier investigations of the flowing waters in this territory.

Materials and methods

Study area

This study was conducted in the Ukrainian Carpathians located in the northern part of the Eastern Carpathians, extending through the western part of Ukraine (Fig. 1). The total length of this mountain range is approximately 240 km with total area of ca 24,000 km². The Ukrainian Carpathians are medium-high mountains with the highest elevation slightly exceeding 2000 m a.s.l. (Novikoff and Hurdu 2015; Vyshnevskiy and Donich 2021). The studied area is characterised by complex geology consisting mostly of flysch with different constituents. Only small areas are formed by limestone, shales, and volcanic rocks, predominantly andesites and gneisses (Ivanik et al. 2019). We sampled 11 streams and 10 mountain lakes (Table 1). Except for lakes Sinevir and Dragobratske located in deciduous and coniferous forests, respectively, all studied lakes are situated above 1500 m a.s.l., i.e., above formerly accepted climatic tree line (Kobiv 2017). The semi-natural meadows and pastures (so-called *polonynas* in the vernacular) dominate the catchment vegetation. The proportion of dwarf pine (*Pinus mugo*), dwarf juniper (*Juniperus communis* subsp. *nana*), green alder (*Alnus viridis*), and scattered Norway spruce (*Picea abies*) is different in individual catchments.

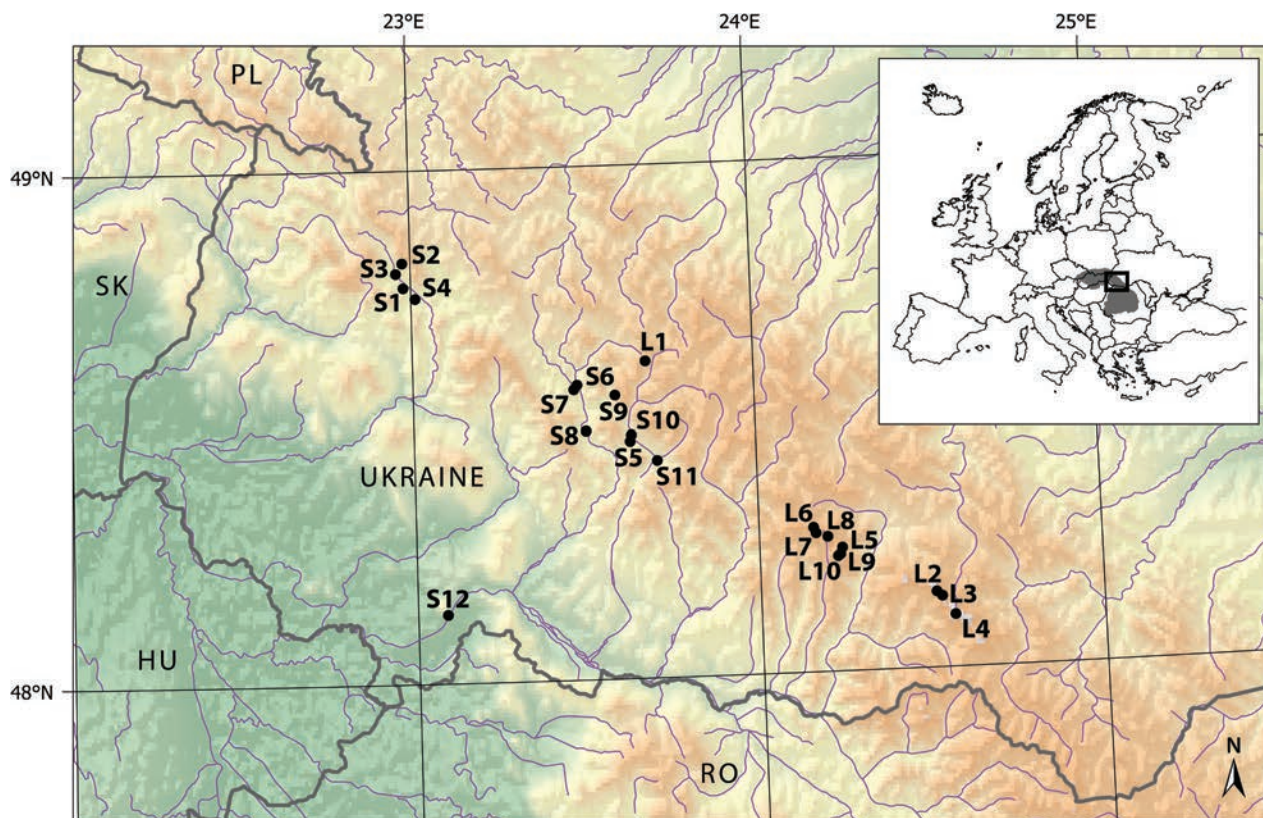


Figure 1. Map showing of sampling localities of Chironomidae and Chaoboridae in the Ukrainian part of the Eastern Carpathians. The site abbreviations correspond to the Table 1. Inset shows location of the investigated territory within the Carpathian Mountains (grey area).

Table 1. Basic characteristics of the sampling sites. Strahler stream order was estimated from Google Earth Pro. Stream width, depth and lake depth were estimated in the field. Lake area was derived from Google Earth Pro using Polygon tool.

Stream/Lake name	Code	Latitude, Longitude	Elevation (m)	Stream order	Av. width (m)	Av. depth (m)
Zhdenivka River	S1	48°46.29'N, 22°58.68'E	409	IV.	6	0.30
Nameless headwater stream	S2	48°49.19'N, 22°58.58'E	777	II.	2	0.15
Tributary of the Zhdenivka River	S3	48°47.98'N, 22°57.41'E	454	III.	3	0.20
Latoricja River	S4	48°45.00'N, 23°00.75'E	360	IV.	20	0.30
Gluhana peat bog channel	S5	48°27.94'N, 23°37.94'E	596	I.	0.4	0.10
Rika River (village Soimy)	S6	48°34.00'N, 23°28.53'E	449	IV.	35	0.15
Rypenka River (village Soimy)	S7	48°33.92'N, 23°28.29'E	448	IV.	25	0.30
Rika River (above Zaperedillia village)	S8	48°29.08'N, 23°30.24'E	382	V.	30	0.50
Nameless tributary of the Volovets River	S9	48°33.14'N, 23°35.51'E	725	II.	2	0.15
Tereblia River (village Sinevyr)	S10	48°28.25'N, 23°38.16'E	573	IV.	18	0.30
Sukhar brook (village Kolochava)	S11	48°25.40'N, 23°42.58'E	580	III.	10	0.30
Tisa River (Vinohradiv)	S12	48°08.06'N, 23°05.15'E	124	VII.	120	–
				Area (ha)	Max. depth (m)	
Sinevir Lake	L1	48°37.01'N, 23°41.04'E	989	4.20	22	
Brespo Lake	L2	48°08.62'N, 24°30.94'E	1627	0.03	0.4	
Bolotnoe ozerce	L3	48°08.55'N, 24°31.25'E	1695	0.01	0.9	
Brebeneskul Lake	L4	48°06.10'N, 24°33.74'E	1793	0.60	3.2	
Dragobratske Lake	L5	48°14.45'N, 24°14.45'E	1382	0.07	1.5	
Apshynets Lake	L6	48°16.91'N, 24°09.53'E	1491	2.97	1.8	
Geryshaska (Dohiaska) Lake	L7	48°16.25'N, 24°09.93'E	1585	2.58	2	
Kosivske Lake	L8	48°15.78'N, 24°11.96'E	1614	0.13	1	
Ivor Lake	L9	48°13.70'N, 24°14.10'E	1606	0.04	2	
Small Ivor Lake	L10	48°13.69'N, 24°14.07'E	1602	0.04	0.6	

All the studied flowing water sites except the Tisa River were located in the Carpathians. Most of the sampling sites were situated in valleys of the submontane belt up to 550–600 m a.s.l. (established according to climate and vegetation characteristics; Golubets 1977), only two sites (S2, S9) were situated in the lower montane belt above 700 m a.s.l. Stream bottom substrates were mostly dominated by cobbles with an admixture of finer components such as gravel and sand. The bottom habitats of both mountain brooks were more complex due to the presence of boulders and a considerable proportion of woody debris. Because of the bed surface roughness and shallow depth, turbulent flow is generally prevailing. Even though most sites were located near roads and often in settlements, the channels, banks, and riparian vegetation were visibly well preserved, without the signs of artificial modifications.

The above characteristics mostly do not apply to the Upper Tisa River. The river stretch close to the town of Vinohradiv flows in a lowland landscape (the Hungarian lowland ecoregion; Afanasyev et al. 2020). The floodplain is covered with alluvial forests containing willow and poplar. In the studied section, the low slope and high discharge altered the river channel morphology significantly, forming a high degree of channel sinuosity. The basic characteristics of the sampling sites are summarised in Table 1.

Sampling and identification

Chironomids and chaoborids were collected during the sampling campaigns in May 2018 (flowing waters and Sinevir Lake) and in August 2021 (mountain lakes in the Chornohora and Svidovets Massifs). A hand net attached to a telescopic handle (mesh size 250 µm, frame diameter 25 cm) was used to skim the water surface and collect floating material along the shores of streams and lakes. In lakes, the material was collected at the leeward shore; in flowing waters, the floating material was collected along an ~ 100-meter-long stretch while moving upstream.

On the shore, the netted sample was placed in a labelled 100-ml plastic bottle and preserved with 75% ethanol. In the laboratory, the samples were placed in a Petri dish and all chironomid material was picked up under a stereomicroscope (7.5–50×). Sorted exuvia, pupae, and adults were mounted on microscopic slides and identified following the keys of Langton and Visser (2003), Ekrem (2004), Stur and Ekrem (2006), and Langton et al. (2013) for pupal exuvia and Langton and Pinder (2007a, 2007b) for adults under high magnification (400×) using phase contrast. Chaoborid larvae, which were collected accidentally during the chironomid sampling of lakes, were identified using Parma (1969) and Sæther (1997).

The nomenclature and distribution of species are consistent with Fauna Europaea (de Jong 2016), and Ashe and O'Connor (2009, 2012). Voucher specimens are deposited in the collections of the Dept. of Biology and Environmental Studies, Faculty of Natural Sciences, Matej Bel University in Banská Bystrica.

Results and discussion

A total of 2088 specimens were collected and identified as 99 chironomid species/taxa (belonging to 43 genera from 5 subfamilies) and two chaoborid species of the same subfamily and genus. Altogether, 40 species and one genus

of Chironomidae, and one species of Chaoboridae were recorded for the first time in Ukraine. The occurrence of one chironomid species, *Nilotanypus dubius* (Meigen, 1804), previously considered as “doubtfully present” in Ukraine (Spies and Sæther 2013) was finally confirmed. A list of all species/ taxa recorded is given below (sampling site codes refer to Table 1; **Pe** after the genus name refers to a morphotype not associated with an adult by Langton (1991); # – previously doubtfully present in Ukraine, * – first record of species/ genus from Ukraine). For detailed information on the abundance and life stages of collected specimens see Supplementary file 1.

CHIRONOMIDAE

Tanypodinae

Procladius (Holotanypus) choreus (Meigen, 1804): L5, L6, L9

Nilotanypus dubius (Meigen, 1804)#: S1, S6, S7, S8

Thienemannimyia carnea (Fabricius, 1805)*: S7

Zavrelimyia barbatipes (Kieffer, 1911): L6

Diamesinae

Diamesa (Diamesa) cinerella Meigen, 1835*: S8

Diamesa (Diamesa) cf. tonsa (Haliday, 1856): S6

Diamesa (Diamesa) vaillanti Serra-Tosio, 1972*: S7

Potthastia Pe1 Langton, 1991: S4, S7, S8

Sympotthastia macrocera Serra-Tosio, 1973*: S6

Prodiamesinae

Prodiamesa olivacea (Meigen, 1818): L1

Orthoclaadiinae

Brillia bifida (Kieffer, 1909): S3

Brillia flavifrons (Johannsen, 1905)*: S7

Corynoneura celtica Edwards, 1924*: S1, S3, S10

Corynoneura cf. scutellata Winnertz, 1846: L1, L6

Corynoneura Pe2a Langton, 1991: S1, S4, S5, S6, S7, S8

Corynoneura Pe4 Langton, 1991: S1

Cricotopus (Cricotopus) annulator Goetghebuer, 1927: S1, S4, S5, S6, S7

Cricotopus (Cricotopus) beckeri Hirvenoja, 1973*: S4, S6, S8

Cricotopus (Cricotopus) curtus Hirvenoja, 1973*: S6

Cricotopus (Cricotopus) fuscus (Kieffer, 1909): S1, S11

Cricotopus (Cricotopus) pallidipes Edwards, 1929*: S8

Cricotopus (Cricotopus) similis Goetghebuer, 1921*: S1, S7, S8

Cricotopus (Cricotopus) tremulus (Linnaeus, 1758)*: S1, S3, S6, S8

Cricotopus (Cricotopus) trifascia Edwards, 1929: S4, S11

Cricotopus (Cricotopus) vierriensis Goetghebuer, 1935: S1, S4, S6, S7, S8

Cricotopus Pe 17 Langton, 1991: S4, S8

Cricotopus (Isocladius) reversus Hirvenoja, 1973*: L1
Cricotopus (Isocladius) sylvestris (Fabricius, 1794): L6, L7
Cricotopus (Isocladius) Pe 5 Langton, 1991: L6, L7
Cricotopus (Paratrichocladius) rufiventris (Meigen, 1830): S4, S7, S10
Eukiefferiella bedmari Vilchez-Quero & Laville, 1987*: S4
Eukiefferiella brevicar (Kieffer, 1911): S2, S3
Eukiefferiella clypeata (Thienemann, 1919)*: S6, S7, S11
Eukiefferiella coerulescens (Kieffer, 1926): S3, S8
Eukiefferiella devonica (Edwards, 1929): S9
Eukiefferiella fuldensis Lehmann, 1972: S10
Eukiefferiella ilkleyensis (Edwards, 1929): S4, S6, S7, S8, S10
Euryhapsis Pe1 Langton, 1991: S11
Heleniella serratosioi Ringe, 1976*: S1, S4, S6, S7, S8, S9, S10, S11
Krenosmittia boreoalpina (Goetghebuer, 1944)*: S1, S3, S6, S7, S8, S10
Krenosmittia camptophleps (Edwards, 1929)*: S10
Limnophyes cf. asquamatus Andersen, 1937: L3
Nanocladius (Nanocladius) parvulus (Kieffer, 1909): S3, S4, S6, S8
Nanocladius (Nanocladius) rectinervis (Kieffer, 1911)*: S6, S7, S8, S10, S11
Orthocladius (Orthocladius) dentifer Brundin, 1947: L7
Orthocladius (Orthocladius) excavatus Brundin, 1947*: S7, S8, S11
Orthocladius (Orthocladius) oblidens (Walker, 1856)*: S11
Orthocladius (Orthocladius) pedestris Kieffer, 1909*: S1, S3, S4, S7, S8, S11
Orthocladius (Orthocladius) rivinus Potthast, 1914*: S3
Orthocladius (Orthocladius) rubicundus (Meigen, 1818): S1, S3, S4, S7, S8, S10
Orthocladius (Euorthocladius) ashei Sponis, 1990*: S4, S7, S8, S11
Orthocladius (Euorthocladius) rivicola Kieffer, 1911: S3, S6, S8, S10, S11
Orthocladius (Euorthocladius) rivulorum Kieffer, 1909: S4, S6, S7, S8
Paracricotopus niger (Kieffer, 1913)*: S4, S6, S7, S8, S11
Parakiefferiella bathophila (Kieffer, 1912)*: S4, S7, S8
Parametricnemus stylatus (Spaerck, 1923): S1, S3, S4, S6, S7, S8, S9, S10, S11
Psectrocladius (Psectrocladius) limbatellus (Holmgren, 1869): S11
Psectrocladius (Psectrocladius) oligosetus Wuelker, 1956: L2, L3, L9, L10
Psectrocladius (Psectrocladius) schlienzi Wuelker, 1956*: L1
Pseudorthocladius (Pseudorthocladius) berthelemyi Moubayed, 1990*: S6
Rheocricotopus (Psilocricotopus) chalybeatus (Edwards, 1929): S1, S4, S6, S7, S8
Rheocricotopus (Rheocricotopus) fuscipes (Kieffer, 1909): S1, S3, S7, S8
Rheosmittia spinicornis (Brundin, 1956)*: S2, S3, S10
Symbiocladius rhithrogenae (Zavrel, 1924): S11
Synorthocladius semivirens (Kieffer, 1909): S3, S10
Thienemanniella majuscula (Edwards, 1924): S1
Thienemanniella Pe 1b Langton, 1991: S3
Thienemanniella Pe 2 Langton, 1991: S10
Tvetenia verralli (Edwards, 1929)*: S6

Chironominae

Benthalia sp.: L7
Demicryptochironomus Pe1 Langton, 1991: S11
Microtendipes chloris (Meigen, 1818): S5, S7

Microtendipes pedellus (De Geer, 1776): L6
Paracladopelma mikianum (Goetghebuer, 1937)*: S6, S11
Phaenopsectra flavipes (Meigen, 1818): S5, L1, L2, L6, L7
Polypedilum (*Polypedilum*) *albicorne* (Meigen, 1838)*: S4, S6, S7, S11
Polypedilum (*Polypedilum*) *laetum* (Meigen, 1818): S11
Polypedilum (*Polypedilum*) *nubeculosum* (Meigen, 1804): S11
Polypedilum (*Pentapedilum*) *sordens* (van der Wulp, 1875): S7
Polypedilum (*Pentapedilum*) cf. *uncinatum* (Goetghebuer, 1921): L2, L5, L7
Polypedilum (*Tripodura*) cf. *apfelbecki* (Strobl, 1900): S6
Polypedilum (*Uresipedilum*) *convictum* (Walker, 1856): S4, S11
Cladotanytarsus (*Cladotanytarsus*) *atridorsum* Kieffer, 1924: L6, L7, L8
Cladotanytarsus (*Cladotanytarsus*) *vanderwulpi* (Edwards, 1929): S6, S7, S8
Micropsectra atrofasciata (Kieffer, 1911): S6, S7
Micropsectra lindrothi Goetghebuer, 1931*: L7
Micropsectra lindebergi Saewedal, 1976/ *insignilobus* Kieffer, 1924: S5
Neozavrelia Pe1 Langton, 1991*: S1, S4, S5, S6, S7, S8
Paratanytarsus austriacus (Kieffer, 1924): L6
Paratanytarsus dissimilis (Johannsen, 1905)*: S5
Paratanytarsus laccophilus (Edwards, 1929): L2, L5, L7, L8, L9, L10
Rheotanytarsus pentapoda (Kieffer, 1909)*: S6, S7
Rheotanytarsus rhenanus Klink, 1983*: S1, S6, S7
Stempellinella flavidula (Edwards, 1929)*: S8
Tanytarsus aberrans Lindeberg, 1970*: L6
Tanytarsus debilis (Meigen, 1830)*: L5, L7
Tanytarsus gregarius Kieffer, 1909: L2, L4
Tanytarsus heusdensis Goetghebuer, 1923*: S6, S7
Virgatanytarsus Pe1 Langton, 1991: S4

CHAOBORIDAE

Chaoborinae

Chaoborus (*Chaoborus*) *crystallinus* (De Geer, 1776): L3
Chaoborus (*Chaoborus*) *obscuripes* (van der Wulp, 1859)*: L7

Of the 99 recorded chironomid taxa, 22 were found exclusively in lakes, and 20 of them only in alpine lakes. Fourteen lacustrine species/ taxa (i.e., 70%) were also found in lakes during our previous research (Bitušík et al. 2020) indicating a similar species composition of all the studied lakes. Phantom midges were not deliberately targeted since the larvae recorded were caught by chance while collecting pupal exuvia. However, one of the species recorded, *Chaoborus* (s. str.) *obscuripes* (van der Wulp, 1859), appears to be the first record in the Ukrainian Carpathian alpine lakes. Most chironomid species have been found in flowing waters. Overall, they are considered typical for streams and rivers of Western and Central Europe (e.g., Caspers 1991; Laville and Vinçon 1991; Ruse 1995; Orendt 2002a, 2002b; Schöll and Haybach 2004; Bitušík et al. 2006; Calle-Martínez and Casas 2006; Prat et al. 2016 and citation therein). Because most of the newly recorded species are widespread in stagnant and flowing waters in Europe and the Palaearctic Region, and do not increase our

knowledge on their ecology, only species with restricted distributions and rarely collected elsewhere are discussed further in more detail. Regarding the common species not discussed further in the text, their geographical distribution is documented in Ashe and O'Connor (2009, 2012) and de Jong (2016), while their ecology is summarised in Moller Pillot (2009, 2013) and Vallenduuk and Moller Pillot (2007).

Family Chironomidae
Subfamily Diamesinae
Tribe Diamesini

***Diamesa (Diamesa) vaillanti* Serra-Tosio, 1972**

Material examined. 1 pupal exuvium, Rypenka river (S7), 7 May 2018.

Distribution. Palaearctic: Germany, Switzerland, France, Italy, Austria, Slovakia, Poland, Russia, Spain, Turkey, Morocco (Ashe and O'Connor 2009), and Azerbaijan (Kownacki 1985).

Habitat. Rheophilic species inhabiting high-altitude springs, streams (including glacier-fed), and rivers with rocky bottoms, but also alpine lakes (Bitušik 2004; Lencioni et al. 2011; Rossaro and Lencioni 2015). The species is cold-stenothermal (e.g., Rossaro 1991) although the findings from streams in the High Atlas indicate that it can tolerate relatively high temperatures of up to 22 °C (Azzouzi et al. 1992).

Remarks. The occurrence of the species is limited to waters at high altitudes. Since our record is from 448 m a.s.l., our finding is exceptional.

***Sympotthastia macrocera* Serra-Tosio, 1973**

Material examined. 2 pupal exuvia, Rika River (S6) in Soimy village, 7 May 2018.

Distribution. Palaearctic. For a long time, known only from Western Europe (France, Germany; Ashe and O'Connor 2009). More recent data comes from the Drava River in Croatia (Kresonja 2018). Our record is evidence for the current easternmost occurrence in Europe, but there are indications that the distribution of this species may extend as far as the Ural Mountains (Krasheninnikov 2012).

Habitat. Generally, larvae of the genus *Sympotthastia* inhabit cold running waters and springs (Sæther and Andersen 2013). A few data indicate that *S. macrocera* is probably a rheophilic species.

Remarks. *Sympotthastia macrocera* appears to be a relatively rare species with little known ecology.

Subfamily Orthoclaadiinae

***Cricotopus (Cricotopus) beckeri* Hirvenoja, 1973**

Material examined. 1 pupal exuvium, Latoricja River (S4), 5 May 2018; 1 pupal exuvium, Rika River (S6); 2 pupal exuvia, Rika River (S8) above Zaperedillia village, 7 May 2018.

Distribution. Palaearctic. France, Spain, Greece, Madeira, Corsica, Turkey, Algeria, Morocco, Slovakia. Its questionable occurrence in Finland (Ashe and O'Connor 2012) was not accepted later Paasivirta (2014).

Habitat. Principally inhabits the rhithral zone of streams at lower altitudes (Hirvenoja and Moubayed 1989; Kettani and Langton 2012; Moubayed-Breil and Ashe 2016).

Remarks. *Cricotopus beckeri* has been considered an exclusively Mediterranean species (Laville and Reiss 1992). Our record is the second reliable finding in the Carpathians (Bitušík and Langton 1994) far from its continuous distribution. We assume that the isolated populations in the Carpathians could be remnants of once widespread populations, which currently survive in refugia due to adverse climatic conditions. Thus, they could be considered a climatic relict, as customary for some plant species (Molnár et al. 2017). Interestingly, Reiss (1986) already hypothesised that the extra-Mediterranean occurrence of another Mediterranean chironomid, *Paratanytarsus mediterraneus* Reiss, 1981, could have a relict character in the Middle Rhine.

***Cricotopus (Cricotopus) pallidipes* Edwards, 1929**

Material examined. 1 pupal exuvium, Rika River (S8), 7 May 2018.

Distribution. Palaearctic. Finland, Norway, France, Portugal, Spain, Germany, Great Britain, Ireland, Romania, Hungary, Russia, Lebanon, and Morocco (Cobo et al. 2002; Soriano and Cobo 2006; Móra et al. 2006; Ashe and O'Connor 2012).

Habitat. The ecological requirements of this species are still unclear. It has been found in flowing and stagnant waters in cold climatic zones (Aagaard et al. 1997; Pozdeev 2012) to warm rivers, canals, lakes, and marshes in central and southern Europe, and North Africa (e.g., Laville and Tourenq 1968; Móra et al. 2006; Abbou and Fahde 2017; Moubayed et al. 2019). French authors (Tourenq 1976; Moubayed et al. 2019) consider it a lacustrine species, tolerant of low oxygen content.

Remarks. Currently known only from few European countries. It does not seem to be abundant anywhere. In Bavaria and the Sauerland Mountains (Germany), it is listed among possibly endangered species; however, its status is unknown (Orendt and Reiff 2003; Dittmar 2012).

***Eukiefferiella bedmari* Vilchez-Quero & Laville, 1987**

Material examined. 3 pupal exuvia, Latoricja River (S4), 5 May 2018.

Distribution. Palaearctic. France, Spain, Greece, Corsica, Turkey, Lebanon, Algeria, and Morocco (Ashe and O'Connor 2012).

Habitat. Streams and rivers (Laville and Langton 2002; Chaib et al. 2013; Moubayed-Breil and Ashe 2016).

Remarks. *E. bedmari* is a circum-mediterranean faunistic element (Laville and Reiss 1992; Moubayed-Breil 2008). Our unexpected extra-Mediterranean finding suggests the relict character of its population in the Carpathians (see comments to *Cricotopus beckeri*).

***Orthocladius (Orthocladius) rivinus* Potthast, 1914**

Material examined. 1 pupal exuvium, left-hand tributary of Zhdnivka River (S3), 7 May 2018.

Distribution. Palaearctic. Norway, Great Britain, Ireland, Austria, Slovakia, Hungary, Poland, Belarus, Germany, Switzerland, France, Italy, Spain, Canary Islands, and Portugal (Cobo et al. 2002; Ashe and O'Connor 2012; Moller Pillot 2013; Móra et al. 2013; Sołtys-Lelek et al. 2014).

Habitat. Rheophilic species inhabiting springs and flowing waters from small streams to large rivers, although it has been reported also from lakes (Langton and Visser 2003). Rossaro et al. (2003) underline its preference for cold waters, but some findings question this (e.g., Langton and Orendt 1996; Móra et al. 2013).

Remarks. The species is known from a few European countries and is generally considered rare. Like the ambiguous data on its ecology, this may also be the result of misidentification.

***Psectrocladius (Psectrocladius) schlienzi* Wuelker, 1956**

Material examined. 1 pupal exuvium, Lake Sinevir (L1), 7 May 2018.

Distribution. Palaearctic? In addition to some European countries (Austria, Denmark, Finland, Germany, Great Britain, Italy, Moldova, Netherlands, Norway, Portugal, Slovakia, Czech Republic, Spain, Sweden, Switzerland; Ashe and O'Connor 2012; Syrovátka and Langton 2015), it was also recorded in Mongolia (Hayford 2005). However, the species may have a Holarctic distribution, provided that its presence in North America can be confirmed (Sealock and Ferrington 2008). Baranov et al. (2024) found a species resembling *P. schlienzi* in Namibia, but it is possible that the specimen belongs to a yet undescribed species of *Psectrocladius* related to *P. schlienzi*.

Habitat. Different types of stagnant waters from lakes to pools. For example, the only record from the Carpathians comes from a shallow pond in an exploited part of an alkaline fen (Bitušik and Illéšová 1998). Its occurrence in slowly flowing waters is exceptional (de Beauvesère-Storm and Tempelman 2009).

Remarks. The records are scattered across Europe, and it seems that the species is not abundant anywhere (Moller Pillot 2013).

***Pseudorthocladius (Pseudorthocladius) berthelemyi* Moubayed, 1990**

Material examined. 11 pupal exuvia, Rika River (S6), 7 May 2018.

Distribution. Palaearctic. Austria, Bulgaria, Corsica, France, Germany, Portugal, Slovakia, Spain, Turkey, and Morocco (Ashe and O'Connor 2012).

Habitat. Mountain streams and rivers with stony bottoms. The species is rheophilic, cold-stenothermal with high demand for dissolved oxygen (Martínez et al 1995; Moubayed-Breil et al. 2012). It can also inhabit hygropetric sites (Moubayed-Breil 2008).

Remarks. The species is considered a Mediterranean element (Moubayed-Breil 2008) with an originally circum-mediterranean distribution

(Laville and Langton 2002). The extra-Mediterranean occurrence in more northerly countries indicates its relict character (see comments to *Cricotopus beckeri*).

Subfamily Chironominae

Tribe Chironomini

Paracladopelma mikianum (Goetghebuer, 1937)

Material examined. 2 pupal exuvia, Rika River (S6), 7 May 2018; 1 pupal exuvium, Tisa River (S12), 8 May 2018.

Distribution. Palaearctic. The species was recorded only from a few countries in Europe (e.g., Spain, Hungary, Slovakia, Portugal, France, Germany, Romania) and North Africa (Morocco, Lebanon).

Habitat. It is a rheophilic species inhabiting fast-flowing streams and rivers (Moller Pillot 2009). Although Calle-Martínez and Casas (2006) listed the species in a chironomid community usually associated with low-temperature or torrential mountain streams, our finding from Tisa River and other records from large lowland rivers (Gandouin et al. 2006; Klink 2010) indicate that the species does not have as strict cold temperature preferences as though previously (Ringe 1974).

Remarks. Laville and Vinçon (1986) considered the species to be a Mediterranean-Palaearctic element whose northern limit is located in the Pyrenees, the Alps, and the Carpathians.

Tribe Tanytarsini

Neozavrelia Goetghebuer, 1941

Material examined. 11 pupal exuvia, Zhdenivka River (S1), 5 May 2018; 17 pupal exuvia, Latoricja River (S4), 5 May 2018; 1 pupal exuvium, Rika River (S6), 7 May 2018; 18 pupal exuvia Rika River (S8), 7 May 2018; 19 pupal exuvium, Rypenka River (S7), 7 May 2018; 1 pupal exuvium, channel at Gluhana peat bog (S5), 7 May 2018.

Distribution. Species-rich genus (38 valid species, de Jong 2016) with a worldwide distribution except for Africa and Neotropics (Epler et al. 2013). Five species have been recorded in Europe, three of which are reliably confirmed in the Carpathians: *N. improvisa* Fittkau, 1954, *N. luteola* Goetghebuer, 1941 (Gilka 2007), and *N. cuneipennis* (Edwards, 1929) (Tatole 2023).

Habitat. Larvae of *Neozavrelia* inhabit streams, rivers, lakes, and ponds in peat bogs; they are also known from hygropetric sites, and one species lives in a hot spring (Epler et al. 2013).

Remarks. Except for *N. cuneipennis* (= *N. longappendiculata* Albu, 1980), the morphological characteristics of the pupae do not yet allow for distinguishing the European species (Langton and Visser 2003). The morphotype *Neozavrelia* Pe1 Langton, 1991 includes four species: *N. bernensis* Reiss, 1968, *N. fuldensis* Fittkau, 1954, *N. improvisa*, and *N. luteola*.

Family Chaoboridae

Chaoborus (Chaoborus) obscuripes (van der Wulp, 1859)

Material examined. 1 larva, Lake Geryshaska (L7), 15 September 2021.

Distribution. Palaearctic. The species is widespread mainly in Northern and Western Europe, but also in Poland and the European part of Russia (Borkent 1981; de Jong 2016).

Habitat. Small, shallow nutrient-poor, meso- and polyhumic ponds with pH 4.5–5.5 (Nilssen 1974; Joniak and Domek 2006; Kuper and Verberk 2011), often fishless. Larger larvae with darker pigmentation are more sensitive to visually dependent predators (Stenson 1981).

Remarks. The species seems to occur sporadically and mostly in small numbers (Borkent 1981), which is probably related to its ecological requirements for water chemistry and the absence of fish.

The first annotated checklist of Ukrainian Chironomidae consists of 302 species (Baranov 2011a). However, this list requires revision because it contains invalid species identified solely on the basis of larvae using outdated identification keys. In recent decades, the study of taxonomy, ecology, and biogeography of chironomids in Ukraine has intensified (Baranov 2011b, 2013, 2014; Baranov and Przhiboro 2014; Baranov and Ferrington 2013; Moubayed-Breil and Baranov 2018; Didenko et al. 2021). Our survey revealed a significant gap in the taxonomic knowledge of Ukrainian chironomids. The high number of new records suggests that the chironomid fauna, especially from flowing waters is far from being fully discovered. Undoubtedly, it is necessary to continue the study of the chironomid fauna of the Eastern Carpathians. Particularly, the collection of the pupal exuvia could be a very useful tool in studying species richness, ecology, and distribution, but also for water quality assessment and monitoring purposes.

Acknowledgements

We gratefully acknowledge the support of the Carpathian Biosphere Reserve Administration. We are indebted to Mykola M. Voloshchuk, Peter Turis, and Milan Valachovič for providing field collection assistance. We are grateful to the reviewer and subject editor for their valuable comments to the previous version of the manuscript.

Additional information

Conflict of interest

The authors have declared that no competing interests exist.

Ethical statement

No ethical statement was reported.

Funding

The study of mountain lakes in the Carpathians was supported by the Slovak Research and Development Agency (project No. APVV-20-0358) and Grant Agency VEGA (project No. 1/0400/21).

Author contributions

PB identified Chironomidae pupal exuviae and adults and wrote the text, MN and MS collected the data, prepared the map, tables and wrote part of the text, LH wrote part of the text.

Author ORCIDs

Milan Novikmec  <https://orcid.org/0000-0002-5192-4575>

Marek Svitok  <https://orcid.org/0000-0003-2710-8102>

Data availability

All of the data that support the findings of this study are available in the main text or Supplementary Information.

References

- Aagaard K, Solem JO, Nøst T, Hanssen O (1997) The macrobenthos of the pristine stream, Skiftesåa, Høylandet, Norway. *Hydrobiologia* 348(1/2/3): 81–94. <https://doi.org/10.1023/A:1003037200703>
- Abbou F, Fahde A (2017) Structure et diversité taxonomique des peuplements de macroinvertébrés benthiques du réseau hydrographique du bassin du Sebou (Maroc). *International Journal of Biological and Chemical Sciences* 11(4): 1785–1806. <https://doi.org/10.4314/ijbcs.v11i4.29>
- Afanasyev S, Lyashenko A, Iarochevitch A, Lietytska O, Zorina-Sakharova K, Marushevska O (2020) Pressures and impacts on ecological status of surface water bodies in Ukrainian part of the Danube River basin. In: Bănăduc D, Curtean-Bănăduc A, Pedrotti F, Cianfaglione K, Akeroyd JR (Eds) *Human Impact on Danube Watershed Biodiversity in the XXI Century*. Geobotany Studies. Springer Nature, Switzerland, 327–358. https://doi.org/10.1007/978-3-030-37242-2_16
- Ashe P, O'Connor JP (2009) *A World Catalogue of Chironomidae (Diptera)*. Part 1. Buchonomyiinae, Chilenomyiinae, Podonominae, Aphroteniinae, Tanypodinae, Usambaromyiinae, Diamesinae, Prodiamesinae and Telmatogetoninae. Irish Biogeographical Society and National Museum of Ireland, Dublin, 445 pp.
- Ashe P, O'Connor JP (2012) *A World Catalogue of Chironomidae (Diptera)*. Part 2. Orthocladiinae. Irish Biogeographical Society and National Museum of Ireland, Dublin, 968 pp.
- Azzouzi A, Laville H, Reiss F (1992) Nouvelles récoltes de Chironomidés (Diptera) du Maroc. *Annales de Limnologie* 28(3): 225–232. <https://doi.org/10.1051/limn/1992019>
- Baranov VA (2011a) A preliminary annotated checklist of non-biting midges (Diptera, Chironomidae) of Ukraine. *Ukrainska Entomofaunistyka* 2: 7–24. <https://doi.org/10.5281/zenodo.5565484>
- Baranov VA (2011b) New and rare species of Orthocladiinae (Diptera, Chironomidae) from the Crimea, Ukraine. *Vestnik Zoologii* 45(5): 405–410. <https://doi.org/10.2478/v10058-011-0026-1>
- Baranov VA (2013) First records of several Tanypodinae species (Diptera, Chironomidae) from Ukraine. *Vestnik Zoologii* 47(3): 59–62. <https://doi.org/10.2478/vzoo-2013-0027>
- Baranov VA (2014) Adult female of *Chaetocladius insolitus* Caspers, 1987 (Diptera: Chironomidae) with notes on species distribution. *Aquatic Insects* 36(1): 9–14. <https://doi.org/10.1080/01650424.2015.1007071>

- Baranov VA, Ferrington Jr LC (2013) Hibernial emergence of Chironomidae in Ukraine. *Chironomus* 26(26): 33–40. <https://doi.org/10.5324/cjcr.v0i26.1616>
- Baranov VA, Przhiboro AA (2014) New records of non-biting midges (Diptera: Chironomidae) from springs and streams of the Ukrainian Carpathians (Gorgany Massif). *Zoosystematica Rossica* 23(1): 150–157. <https://doi.org/10.31610/zsr/2014.23.1.150>
- Baranov V, Lin X, Hübner J, Chimeno C (2024) Uncovering the hidden diversity of non-biting midges (Diptera, Chironomidae) from central Namibia, using morphology and DNA barcodes. *African Invertebrates* 65(1): 13–36. <https://doi.org/10.3897/afrinvertebr.65.111920>
- Bitušík P (2004) Chironomids (Diptera, Chironomidae) of the mountain lakes in the Tatra Mts. (Slovakia). A review. *Dipterologica bohemoslovaca* 12: 25–53.
- Bitušík P, Illéšová D (1998) New records of Chironomidae (Diptera, Nematocera) from Slovakia. *Biologia* 53: 238–238.
- Bitušík P, Langton PH (1994) Further new records of chironomids (Diptera, Chironomidae) from Slovakia. *Biologia* 49: 235–237.
- Bitušík P, Svitok M, Dragúňová M (2006) The actual longitudinal zonation of the river Hron (Slovakia) based on chironomid assemblages (Diptera: Chironomidae). *Acta Universitatis Carolinae. Biologica* 50: 5–17.
- Bitušík P, Novikmec M, Hamerlik L (2020) Chironomids (Insecta, Diptera, Chironomidae) from alpine lakes in the Eastern Carpathians with comments on newly-recorded species from Ukraine. *Biodiversity Data Journal* 8: e49378. <https://doi.org/10.3897/BDJ.8.e49378>
- Borkent A (1981) The distribution and habitat preferences of the Chaoboridae (Culicomorpha: Diptera) of the Holarctic region. *Canadian Journal of Zoology* 59(1): 122–133. <https://doi.org/10.1139/z81-019>
- Borkent A (2014) World catalog of extant and fossil Chaoboridae (Diptera). *Zootaxa* 3796(3): 469–493. <https://doi.org/10.11646/zootaxa.3796.3.4>
- Calle-Martínez D, Casas JJ (2006) Chironomid species, stream classification, and water-quality assessment: The case of 2 Iberian Mediterranean mountain regions. *Journal of the North American Benthological Society* 25(2): 465–476. [https://doi.org/10.1899/0887-3593\(2006\)25\[465:CSSCAW\]2.0.CO;2](https://doi.org/10.1899/0887-3593(2006)25[465:CSSCAW]2.0.CO;2)
- Caspers N (1991) The actual biocoenotic zonation of the River Rhine exemplified by the chironomid midges (Insecta, Diptera). *Internationale Vereinigung für theoretische und angewandte Limnologie. Verhandlungen - Internationale Vereinigung für Theoretische und Angewandte Limnologie* 24(3): 1829–1834. <https://doi.org/10.1080/03680770.1989.11899080>
- Chaib N, Bouhala Z, Fouzari L, Marziali L, Samraoui B, Rossaro B (2013) Environmental factors affecting the distribution of chironomid larvae of the Seybouse wadi, North-eastern Algeria. *Journal of Limnology* 72(2): 203–214. <https://doi.org/10.4081/jlimnol.2013.e16>
- Cobo F, Soriano Ó, Báez M (2002) Chironomidae. In: Hjorth-Andersen MC-T (Ed.) *Catálogo de los Diptera de España, Portugal y Andorra*. Sociedad Entomológica Aragonesa (SEA), Zaragoza, 35–44.
- Cranston PS (1995) Introduction. In: Armitage PD, Cranston PS, Pinder LCV (Eds) *The Chironomidae: Biology and ecology of non-biting midges*. Chapman & Hall, London, 7 pp. https://doi.org/10.1007/978-94-011-0715-0_1
- de Beauvesère-Storm A, Tempelman D (2009) De dansmug *Psectrocladius schlienzi* nieuw voor Nederland, met een beschrijving van de larve (Diptera: Chironomidae). *Nederlandse Faunistische Mededelingen* 30: 17–22.

- de Jong Y (2016). Fauna Europaea. Fauna Europaea Consortium. Checklist dataset. <https://doi.org/10.15468/ymk1bx> [GBIF.org on 2024-03-21]
- Didenko A, Volikov Y, Baranov V, Kruzhylina S, Gurbyk A, Bielikova O (2021) Chironomid diversity in the diets of Ponto-Caspian gobiids in a freshwater habitat: Implications for resource partitioning. *Limnologica* 89: 125890. <https://doi.org/10.1016/j.limno.2021.125890>
- Dittmar H (2012) Beiträge zur aquatischen Insektenfauna des Sauerlandes. *Abhandlungen aus dem Westfälischen Museum für Naturkunde* 74: 3–41.
- Eggermont H, Heiri O (2012) The chironomid-temperature relationship: Expression in nature and palaeoenvironmental implications. *Biological Reviews of the Cambridge Philosophical Society* 87(2): 430–456. <https://doi.org/10.1111/j.1469-185X.2011.00206.x>
- Ekrem T (2004) Immature stages of European *Tanytarsus* species I. The *eminulus*-, *gregarius*-, *lugens*- and *mendax* species groups (Diptera, Chironomidae). *Deutsche Entomologische Zeitschrift*. *Deutsche Entomologische Zeitschrift* 51(1): 97–146. <https://doi.org/10.1002/mmnd.20040510110>
- Epler JH, Ekrem T, Cranston PS (2013) 10. The larvae of Chironominae (Diptera: Chironomidae) of the Holarctic Region – Keys and diagnoses. In: Andersen T, Sæther OA, Cranston PS & Epler JH (Eds) *Chironomidae of the Holarctic Region. Keys and diagnoses. Larvae*. *Insect Systematics & Evolution, Suppl.* 66: 387–556.
- Ferrington Jr LC (2007) Global diversity of non-biting midges (Chironomidae; Insecta-Diptera) in freshwater. *Hydrobiologia* 595(1): 447–455. <https://doi.org/10.1007/s10750-007-9130-1>
- Gandouin E, Maasri A, Van Vliet-Lanoe B, Franquet E (2006) Chironomid (Insecta: Diptera) assemblages from a gradient of lotic and lentic waterbodies in river floodplains of France: a methodological tool for paleoecological applications. *Journal of Paleolimnology* 35(1): 149–166. <https://doi.org/10.1007/s10933-005-8149-4>
- Gitka W (2007) A faunistic review of chironomids of the tribe Tanytarsini (Diptera: Chironomidae) of the Tatra National Park. *Dipteron* 23: 11–17.
- Golubets MA (1977) Eastern-Carpathian Mountain subprovince. In: Barbarych AI (Ed.) *Geobotanical regionalization of Ukrainian SSR*. Naukova dumka, Kyiv, 18–44.
- Hayford B (2005) New records of Chironomidae (Insecta: Diptera) from Mongolia with review of distribution and biogeography of Mongolian Chironomidae. *Journal of the Kansas Entomological Society* 78(2): 192–200. <https://doi.org/10.2317/0406.24.1>
- Hirvenoja M, Moubayed J (1989) The adults and preimaginal stages of continental populations of *Cricotopus (Cricotopus) beckeri* Hirvenoja (Diptera, Chironomidae). *Annales de Limnologie* 25(3): 251–254. <https://doi.org/10.1051/limn/1989027>
- Ivanik O, Shevchuk V, Kravchenko D, Shpyrko S, Yanchenko V, Gadiatska K (2019) Geological and geomorphological factors of natural hazards in Ukrainian Carpathians. *Journal of Ecological Engineering* 20(4): 177–186. <https://doi.org/10.12911/22998993/102964>
- Joniak T, Domek P (2006) Influence of humification on biodiversity of lake benthic macroinvertebrates. *Acta Agrophysica* 7: 3636–368.
- Kettani K, Langton PH (2012) Les Chironomidae du Maroc (Diptera, Nematocera). *Bulletin de la Société Entomologique de France* 117(4): 411–424. <https://doi.org/10.3406/bsef.2012.3065>
- Klink A (2010) Macroinvertebrates of the Seine basin. *Hydrobiologisch Adviesburo Klink Rapporten en Mededelingen* 108, Wageningen, 71 pp.
- Kobiv Y (2017) Response of rare alpine plant species to climate change in the Ukrainian Carpathians. *Folia Geobotanica* 52(2): 217–226. <https://doi.org/10.1007/s12224-016-9270-z>

- Kownacki A (1985) Spring benthic macroinvertebrate communities of selected streams in the High Caucasus (Azerbaijan SSR). *Hydrobiologia* 123(2): 137–144. <https://doi.org/10.1007/BF00018975>
- Krasheninnikov AB (2012) Phenology of some chironomid species (Diptera, Chironomidae) of the Middle Urals. *Fauna Norvegica* 31: 55–55. <https://doi.org/10.5324/fn.v31i0.1371>
- Kresonja M (2018) Urban aquatic habitats, neglected sources of biodiversity. Comparison of chironomid communities (Chironomidae, Diptera) in fountains, artificial lakes and the River Drava. PhD Thesis, University Josip Juraj Strossmayer in Osijek, Osijek, Croatia.
- Kuper JT, Verberk WCEP (2011) Fenologie, habitat en verspreiding van Pluimmuggen in Nederlandse hoogvenen (Diptera: Chaoboridae). *Nederlandse Faunistische Mededelingen* 35: 73–82.
- Langton PH (1991) A key to pupal exuviae of West Palaearctic Chironomidae. Privately published. Huntington, Cambridgeshire, England, 368 pp.
- Langton PH, Orendt C (1996) A collection of Chironomidae from La Gomera, Canary Islands. *Entomologist's Gazette* 47: 279–281.
- Langton PH, Pinder LCV (2007a) Keys to the adult male Chironomidae of Britain and Ireland 1. Scientific Publication - Freshwater Biological Association 64: 1–239.
- Langton PH, Pinder LCV (2007b) Keys to the adult male Chironomidae of Britain and Ireland 2. Scientific Publication - Freshwater Biological Association 64: 1–168.
- Langton PH, Visser H (2003) Chironomidae exuvia. A key to pupal exuvia of the West Palaearctic Region. Interactive Identification System for the European Limnofauna (IISEL), World Biodiversity Database, CD-ROM Series.
- Langton PH, Bitušik P, Mitterova J (2013) A contribution towards a revision of West Palaearctic *Procladius* Skuse (Diptera: Chironomidae). *Chironomus* 26(26): 41–44. <https://doi.org/10.5324/cjcr.v0i26.1620>
- Laville H, Langton P (2002) The lotic Chironomidae (Diptera) of Corsica (France). *Annales de Limnologie* 38(1): 53–64. <https://doi.org/10.1051/limn/2002006>
- Laville H, Reiss F (1992) The chironomid fauna of the Mediterranean region reviewed. *Netherlands Journal of Aquatic Ecology* 26(2–4): 239–245. <https://doi.org/10.1007/BF02255247>
- Laville H, Tourenq JN (1968) Nouvelles récoltes de chironomides en Camargue et dans les Marismas du Guadalquivir (Diptères). *Annales de Limnologie* 4(1): 73–80. <https://doi.org/10.1051/limn/1968010>
- Laville H, Vinçon G (1986) Inventaire 1986 des Chironomidés (Diptera) connus des Pyrénées. *Annales de Limnologie* 22(3): 239–251. <https://doi.org/10.1051/limn/1986022>
- Laville H, Vinçon G (1991) A typological study of Pyrenean streams: Comparative analysis of the Chironomidae (Diptera) communities in the Ossau and Aure Valleys. *Internationale Vereinigung für theoretische und angewandte Limnologie. Verhandlungen - Internationale Vereinigung für Theoretische und Angewandte Limnologie* 24(3): 1775–1784. <https://doi.org/10.1080/03680770.1989.11899070>
- Lencioni V, Marziali L, Rossaro B (2011) Diversity and distribution of chironomids (Diptera, Chironomidae) in pristine Alpine and pre-Alpine springs (Northern Italy). *Journal of Limnology* 70(1s): 106–121. <https://doi.org/10.4081/jlimnol.2011.s1.106>
- Luoto T, Nevalainen L (2009) Larval chaoborid mandibles in surface sediments of small shallow lakes in Finland: Implications for palaeolimnology. *Hydrobiologia* 631(1): 185–195. <https://doi.org/10.1007/s10750-009-9810-0>

- MacKay NA, Carpenter SR, Soranno PA, Vanni MJ (1990) The impact of two *Chaoborus* species on a zooplankton community. *Canadian Journal of Zoology* 68(5): 981–985. <https://doi.org/10.1139/z90-141>
- Martínez DC, Quero AV, Jiménez JC (1995) Les chironomidés (Diptera) du bassin du Haut-Guadalquivir (Sierra de Cazorla, sud de l'Espagne). *Annales de Limnologie* 31(3): 201–213. <https://doi.org/10.1051/limn/1995018>
- Moller Pillot HKM (2009) Chironomidae larvae of the Netherlands and adjacent lowlands: biology and ecology of the Chironomini. KNNV Publishing, Zeist, 270 pp.
- Moller Pillot HKM (2013) Chironomidae Larvae of the Netherlands and Adjacent Lowlands. Biology and Ecology of the aquatic Orhocladiinae. KNNV Publishing, Zeist, 312 pp.
- Molnár A, Végvári Z, Tóthmérész B (2017) Identification of floral relicts based on spatial distance of isolation. *Forests* 8(11): 459. <https://doi.org/10.3390/f8110459>
- Móra A, Tóth M, Debreceni Á, Csépes E (2006) Contribution to the chironomid fauna (Diptera: Chironomidae) of the Upper-Tisza, NE Hungary. *Folia Historico-naturalia Musei Matraensis* 30: 253–261.
- Móra A, Polyák L, Farkas A (2013) Contribution to the Chironomidae (Diptera) fauna of the Sajó/Slaná River, Hungary and Slovakia. *Acta Biologica Debrecina-Supplementum Oecologica Hungarica* 31: 69–81.
- Moubayed J, Bernard A, Claude J, Decoin R, Tissot B (2019) Inventaire des Chironomidae de la réserve naturelle nationale du Lac de Remoray. II. Liste des espèces recensées en 2019 avec commentaires sur leur écologie et leur distribution géographique (Diptera). *Ephemera* 20: 113–131.
- Moubayed-Breil J (2008) Non-biting midges from Continental France: New records, faunal and biogeographical outline (Diptera, Chironomidae). *Ephemera* 9: 17–32.
- Moubayed-Breil J, Ashe P (2016) New records and additions to the database on the geographical distribution of some threatened chironomid species from continental France (Diptera, Chironomidae). *Ephemera* 16: 93–108.
- Moubayed-Breil J, Baranov VA (2018) Taxonomic notes on the genus *Hydrobaenus* with description of *H. simferopolus* sp. nov. from Crimea (Diptera: Chironomidae). *Acta Entomologica Musei Nationalis Pragae* 58(2): 347–355. <https://doi.org/10.2478/aemnp-2018-0029>
- Moubayed-Breil J, Langton PH, Ashe P (2012) *Rheotanytarsus dactylophoreus*, a new mountain species from streams in the Eastern Pyrenees and Corsica (Diptera: Chironomidae). *Fauna Norvegica* 31: 167–167. <https://doi.org/10.5324/fn.v31i0.1375>
- Nicacio G, Juen L (2015) Chironomids as indicators in freshwater ecosystems: An assessment of the literature. *Insect Conservation and Diversity* 8(5): 393–403. <https://doi.org/10.1111/icad.12123>
- Nilssen JP (1974) On the ecology and distribution of the Norwegian larvae of *Chaoborus* (Diptera, Chaoboridae). *Norsk Entomologisk Tidsskrift* 1: 37–44.
- Novikoff A, Hurdu BI (2015) A critical list of endemic vascular plants in the Ukrainian Carpathians. *Contributii Botanice* 50: 43–91.
- Orendt C (2002a) Die Chironomidenfauna des Inns bei Mühlendorf (Oberbayern). *Lauterbornia* 44: 109–120.
- Orendt C (2002b) Biozönotische Klassifizierung naturnaher Flussabschnitte des nördlichen Alpenvorlandes auf der Grundlage der Zuckmücken-Lebensgemeinschaften (Diptera: Chironomidae). *Lauterbornia* 44: 121–146.
- Orendt C, Reiff N (2003) Rote Liste gefährdeter Zuckmücken (Diptera: Chironomidae) Bayerns. *Bayerisches Landesamt für Umweltschutz* 166: 301–304.

- Paasivirta L (2014) Checklist of the family Chironomidae (Diptera) of Finland. *ZooKeys* 441: 63–90. <https://doi.org/10.3897/zookeys.441.7461>
- Pape T, Blagoderov V, Mostovski MB (2011) Order Diptera Linnaeus, 1758. In: Zhang ZO (Ed.) *Animal biodiversity: an outline of higher-level classification and survey of taxonomic richness*. *Zootaxa* 3148: 222–229. <https://doi.org/10.11646/zootaxa.3148.1.42>
- Parma S (1969) Notes on the larval taxonomy, ecology, and distribution of the Dutch *Chaoborus* species (Diptera, Chaoboridae). *Beaufortia* 17: 21–50.
- Pozdeev IV (2012) A new data on Chironomid fauna (Diptera, Chironomidae) of the Upper and Middle Kama River basin. *Evraziatskii Entomologicheskii Zhurnal* 11: 87–90.
- Prat N, Puntí T, Rieradevall M (2016) The use of larvae and pupal exuviae to study the biodiversity of Chironomidae in Mediterranean streams. *Journal of Entomological and Acarological Research* 48 (1): 29–36. <https://doi.org/10.4081/jear.2016.5529>
- Reiss F (1986) A contribution to the zoogeography of the Turkish Chironomidae (Diptera). *Israel Journal of Entomology* 19: 161–170.
- Resh V, Rosenberg D (2008) Water pollution and insects. In: Capinera J (Ed.) *Encyclopedia of Entomology*, Springer Science+Business Media B.V., Dordrecht, 4158–4168.
- Ringe F (1974) Chironomiden-Emergenz 1970 in Breitenbach und Rohrwiesbach. *Schlitzer Produktionsbiologische Studien* (10). *Archiv für Hydrobiologie (Supplementband 45)*: 212–304.
- Rossaro B (1991) Chironomids and water temperature. *Aquatic Insects* 13(2): 87–98. <https://doi.org/10.1080/01650429109361428>
- Rossaro B, Lencioni V (2015) A key to larvae of *Diamesa* Meigen, 1835 (Diptera, Chironomidae), well known as adult males and pupae from Alps (Europe). *Journal of Entomological and Acarological Research* 47(3): 123–138. <https://doi.org/10.4081/jear.2015.5516>
- Rossaro B, Lencioni V, Casalegno C (2003) Revision of West Palaearctic species of *Orthocladius* s. str. van der Wulp, 1874 (Diptera: Chironomidae: Orthoclaudiinae), with a new key to species. *Studi Trentini di Scienze Naturali. Acta Biologica* 79: 213–241.
- Ruse LP (1995) Chironomid community structure deduced from larvae and pupal exuvia of a chalk stream. *Hydrobiologia* 315(2): 135–142. <https://doi.org/10.1007/BF00033625>
- Sæther OA (1997) Family Chaoboridae. In: Papp L, Darvas B (Eds) *Contributions to a Manual of Palaearctic Diptera 2. Nematocera and Lower Brachycera*. Science Herald, Budapest, 305–323.
- Sæther OA, Andersen T (2013) 7. The larvae of Diamesinae (Diptera: Chironomidae) of the Holarctic Region – Keys and diagnoses. In: Andersen T, Sæther OA, Cranston PS, Epler JH (Eds) *Chironomidae of the Holarctic Region. Keys and diagnoses. Larvae*. *Insect Systematics & Evolution, Suppl.* 66: 145–178.
- Sæther OA, Ashe P, Murray DA (2000) Family Chironomidae. In: Papp L, Darvas B (Eds) *Contribution to a Manual of Palaearctic Diptera (with special reference to flies of economic importance)*. Appendix. Science Herald, Budapest, 113–334.
- Schöll F, Haybach A (2004) Typology of large European rivers according to their Chironomidae communities (Insecta: Diptera). *Annales de Limnologie-International Journal of Limnology* 40: 309–316). <https://doi.org/https://doi.org/10.1051/limn/2004028>
- Sealock AW, Ferrington LC (2008) Key and descriptions of the Chironomidae pupal exuvia of Hardwood Creek, near Hugo, Minnesota. Chironomidae Research Group, University of Minnesota, St. Paul, 86 pp.
- Sołtys-Lelek A, Barabasz-Krasny B, Możdżeń K (2014) Selected aspects of the protection of biotopes on the example of the Ojców National Park (Southern Poland). *Annales Universitatis Paedagogicae Cracoviensis* 174: 98–117.

- Soriano O, Cobo F (2006) Lista faunística de los quironómidos (Diptera, Chironomidae) de Madrid (España). *Graellsia* 62(Extra): 7–20. <https://doi.org/10.3989/graellsia.2006.v62.iExtra.107>
- Spies M, Sæther OA (2013) Fauna Europaea: Chironomidae. In: Pape T, Beuk P (Eds) Fauna Europaea: Diptera. Fauna Europaea version 2017.06. <https://www.faunaeur.org> [accessed 12 September 2019]
- Stenson JA (1981) The role of predation in the evolution of morphology, behaviour and life history of two species of *Chaoborus*. *Oikos* 37(3): 323–327. <https://doi.org/10.2307/3544123>
- Stur E, Ekrem T (2006) A revision of West Palaearctic species of the *Micropsectra atrofasciata* group (Diptera: Chironomidae). *Zoological Journal of the Linnean Society* 146(2): 165–225. <https://doi.org/10.1111/j.1096-3642.2006.00198.x>
- Syrovátka V, Langton PH (2015) First records of *Lasiodiamesa gracilis* (Kieffer, 1924), *Parochlus kiefferi* (Garrett, 1925) and several other Chironomidae from the Czech Republic and Slovakia. *Chironomus* 28(28): 45–56. <https://doi.org/10.5324/cjcr.v0i28.1953>
- Tatole V (2023) An updated checklist of chironomid species (Diptera, Chironomidae) from Romania. *Travaux du Museum National d'Histoire Naturelle "Grigore Antipa" / Muzeul National de Istorie Naturala "Grigore Antipa"* 66(1): 17–105. <https://doi.org/10.3897/travaux.66.e102065>
- Tolonen KT, Brodersen KP, Kleisborg TA, Holmgren K, Dahlberg M, Hamerlik L, Hämäläinen H (2012) Phantom midge-based models for inferring past fish abundances. *Journal of Paleolimnology* 47(4): 531–547. <https://doi.org/10.1007/s10933-012-9579-4>
- Tourenq JN (1976) Recherches écologiques sur les chironomides (Diptera) de Camargue. I. Etude faunistique et biogéographique. *Annales de Limnologie* 12(1): 17–74. <https://doi.org/10.1051/limn/1976009>
- Vallenduuk HJ, Moller Pillot HKM (2007) Chironomidae larvae of the Netherlands and adjacent lowlands. General ecology and Tanypodinae. KNNV Publishing, Zeist, 144 pp.
- Vyshnevskiy VI, Donich OA (2021) Climate change in the Ukrainian Carpathians and its possible impact on river runoff. *Acta Hydrologica Slovaca* 22(1): 3–14. <https://doi.org/10.31577/ahs-2021-0022.01.0001>

Supplementary material 1

Checklist of chironomid and chaoborid taxa recorded in studied streams and lakes of the Ukrainian part of the Eastern Carpathians

Authors: Peter Bitušik, Milan Novikmec, Marek Svitok, Ladislav Hamerlik

Data type: xlsx

Copyright notice: This dataset is made available under the Open Database License (<http://opendatacommons.org/licenses/odbl/1.0/>). The Open Database License (ODbL) is a license agreement intended to allow users to freely share, modify, and use this Dataset while maintaining this same freedom for others, provided that the original source and author(s) are credited.

Link: <https://doi.org/10.3897/zookeys.1211.125436.suppl1>

